ASSESSMENT OF WASTE ROCK WEATHERING CHARACTERISTICS AT THE ANTAMINA MINE BASED ON FIELD CELLS EXPERIMENT

by

CELEDONIO ARANDA CLEMENTE

B.A.Sc. Universidad Nacional Santiago Antúnez de Mayolo, 2000

A THESIS SUBMITTED IN PARTIAL FULFILLMENT OF
THE REQUIREMENTS FOR THE DEGREE OF
MASTER OF APPLIED SCIENCE

in

THE FACULTY OF GRADUATE STUDIES

(Mining Engineering)

THE UNIVERSITY OF BRITISH COLUMBIA

(Vancouver)

March 2010

ABSTRACT

The weathering behaviour of waste rock is being evaluated using field cell experiments at the Antamina Mine. The results presented here are a component of a larger study that is being conducted in Antamina, whose objective is to understand the geochemical and hydrological behaviour exhibited by different waste rock types, and their potential operational and post-closure impacts on the environment, in order to identify and implement prevention/mitigation measures.

The waste rock is currently classified into three classes based on metal (zinc, arsenic) and sulfide contents: reactive (A), slightly reactive (B), and non-reactive (C). This thesis presents the analysis only of Class B marble and hornfels material. Particle size was measured through the standard sieving method and Elutriation techniques, and surface area through geometrical estimation and the BET methods. The data gathered was correlated with chemical assay results and complemented with the mineralogical and mineral availability for leaching data obtained using a Mineral Liberation Analyzer. Minerals containing copper, lead, and zinc, and all sulfide minerals were examined.

Seven field kinetic cells were installed with samples having particles of less than 10 cm in diameter. Metal leaching, elemental production rates and release rate trends from two years of data are presented. The relationship between mineral availability and field cells drainage data was investigated. A refined waste rock classification system for Class B was recommended including the incorporation of lithology, mineralogy, mineral availability for leaching, and sulfur-sulfide content.

The diopside marble samples were found to be coarser than the black marble and gray hornfels samples. Large surface were reported in the black marble, this was because a relatively higher proportion of clay minerals were found in this sample.

Acid-base accounting testing reported that all samples were non-acid generating. However, Cu, Pb, Zn, and Sb were reported in higher concentrations in the leachate from the field cells. Solid phase concentrations of these elements were found to increase as the size fractions decreased, but in two diopside samples, Cu, Pb and Zn minerals were available for leaching in high proportion from the coarse particles. The main sources of these elements were chalcopyrite, galena, and sphalerite.

TABLE OF CONTENTS

LIST OF TABLES

LIST OF FIGURES

ACKNOWLEDGEMENTS

I would like to acknowledge Compañía Minera Antamina S.A., the Natural Sciences and Engineering Research Council of Canada (NSERC), and ART group of Teck Company for their financial support and for providing data.

I would like to offer my enduring gratitude to Dr. Bern Klein, my supervisor, who expanded my vision of the science and patiently provided me with superior guidelines through which to conduct my research. I would also like to thank Dr. Roger Beckie and Dr. Ulrich Mayer for always providing me with valuable support and for answering my endless questions.

I would like to offer a special thank you to Henri Letient from Teck Cominco Ltd., who was the initiator of this entire research project, and who also inspired me to begin my studies in this field.

I would like to express my appreciation to Dr. Ward Wilson, Dr. Marcelo Veiga, and to give a special thanks to Charlene Haupt from the University of British Columbia. I thank Dr. Stephane Brienne, Randy Blaskovich from ART group, Antonio Mendoza, Fabiola Sifuentes, James Jackson, Jéssica Flores, Angélica Lagos, Raul Parra, as well as all the personnel from the Antamina mine for their collaboration.

I would especially like to express my deep gratitude to my parents, my siblings, and to Vivi, who all provided me with enduring and unconditional moral support.

Cele.

DEDICATION

I present this thesis with a special dedication to my dear parents, Nishi and Hilda, the authors of my existence, and I would like to thank them profusely for their eternal patience and love. I am also grateful to my brother Grover and my sisters Roxi and Mery, the long-time witnesses of my efforts and dedication. I would like to acknowledge my grandparents Fide(†), Facu(†), and Uficha, for always offering me wise advises.

I offer a special dedication to my daughter Stefy, the love of my life who, through her charisma and tenderness, brings me a very special joy and who has inspired me to achieve many goals, including this Masters degree. I would also like to express great gratitude and appreciation to Vivi, who is so important in my life, and the witness of many of my triumphs and failures.

Finally, I want to offer a heartfelt thank you to my friends Jessy, Amedsy, Ronald, Ernesto, Henri, and Jorge, who have motivated me throughout this process and who have contributed so much to my personal development.

Cele

1 INTRODUCTION

1.1 Description of Research Project

In 2005, the Norman B. Keevil Institute of Mining Engineering and the Earth and Ocean Sciences Department of the University of British Columbia (UBC) in collaboration with Teck's Applied Research & Technology (ART) group, the Natural Sciences and Engineering Research Council of Canada (NSERC) and Compañía Minera Antamina S.A. (Antamina) began an integrated project to improve the understanding of the geochemical and hydrogeological behaviour of different waste rock classes and to estimate the potential operational and post-closure impacts on the environment. Therefore, an extensive neutral drainage research project consisting of several waste rock classes and types is currently being conducted at the Antamina Mine in Peru. The Antamina deposit is a polymetallic copper-zinc-molybdenum skarn hosted in a limestone matrix. The drainage from the Antamina mine waste rock is occurring under circumneutral pH conditions, and the duration and intensity of the drainage is not well understood.

The five-year project has four components: the construction of five experimental instrumented piles, (Corazao Gallegos, 2007), the installation of field kinetic cells (Aranda et al., 2009), the installation of five lysimeters for a cover study, and a detailed mineralogical characterization of the waste rock material. The results will assist with the identification and implementation of prevention/mitigation measures, as well as a refinement of the current waste rock management program at the mine.

Approximately 1539 millions tonnes (Mt) of waste rock will be moved and placed in different dumps at Antamina. This will be achieved by end dumping into dumps of between 200 and 300 m high on steep mountain faces. In addition, the medium/low/marginal grade (MG/LG/ML) material will be stockpiled until close to the end of the mine's life (Golder Associates, 2007a). Five major waste rock types, namely limestone, marble, hornfels, skarn (endoskarn and exoskarn), and intrusive have been identified at the deposit. Marble and hornfels contribute the largest amount (by weight) to the waste rock at 86% (Antamina, 2004). However, intrusive and endoskarn are the most reactive rock types fond at the site (Golder Associates, 2004).

The Antamina mine presents an excellent opportunity to study neutral drainage from waste rock. The polymetallic skarn consists of not only one of the largest combined copper-zinc deposits in the world, but also contains molybdenum, lead, bismuth and a number of minor and trace elements of concern.

It is believed that the climate and elevation of the site will not significantly impact the processes being studied. In fact, the average yearly precipitation (1100 – 1300 mm) and temperature (~8 C) are similar to those in many Canadian locations although, due to its tropical latitude and high elevation, winters are warmer and summers are cooler at the Antamina site. The site's moderate winter climate has the significant advantage that field work can be conducted throughout the year, and the seasonal nature of precipitation allows for the investigation of drainage water quantity and quality in response to both dry and wet periods.

Based upon the rock types and the content of zinc, arsenic and sulfide, waste rock is classified into three categories: reactive (Class A), slightly reactive (Class B), and non-reactive (Class C) (Antamina, 2007). While the reactive material will likely produce low-quality drainage, it is not clear how to evaluate the risk

of low-quality drainage from slightly reactive, neutral drainage material, particularly over the long term and over the larger spatial scales of full-scale dumps. Class B marble and hornfels waste rock were selected for study in this thesis due to uncertainty about their reactivity levels. Furthermore, as there are variations in mineralogy for different rock types, chemical composition does not provide sufficient information for use as the only criterion on which to base a classification scheme. Therefore, the need exists to either carry out additional tests or to develop other procedures that include mineralogy in order to improve the current classification system.

In 2006, seven field kinetic tests (field cells) were installed using waste rock material whose particles were less than 10 cm (4 inches) in diameter, from each tipping phase during the construction of the first 30,000 tonne experimental waste rock pile (Corazao Gallegos, 2007). The focus of the field cell program will be on assessing mineralogical and microbiological controls for metal release and attenuation. A generally applicable waste rock classification will be developed by including quantitative mineralogical information and correlating this with observed leaching characteristics. The field cell data will also be essential to interpreting and scaling-up the pile experiment results.

Indeed, unlike the piles, the smaller-scale field cells are not strongly influenced by preferential flow or gas-transport limitations. These experiments will allow us to observe the geochemical responses of individual material types contained in the experimental piles in isolation of these physical processes and other material types.

The field cells were constructed in ~1.5 m tall (200 L) polyethylene barrels, placed outdoors, with their tops being open to natural precipitation, and draining at the bottom into individual leachate-collection tanks which will be monitored for flow volume and geochemistry on a weekly basis. Although Antamina's ongoing waste management program includes a number of field cells of similar design, it was essential to conduct field cell experiments using materials representative of those present in the experimental piles.

Subsequently, the material was characterized through standard particle size analysis, with specific surface area determined by geometrical estimation for coarse material, and using the Brunauer, Emmett and Teller (BET) method for fine particles. This data was correlated with whole-rock chemistry ICP-MS (Inductively Coupled Plasma Mass Spectrometry) results and complemented by an extensive mineralogical study which used a Mineral Liberation Analyzer (MLA). MLA included bulk mineralogy and liberation which was aimed to obtaining exposure or availability for the leaching of sulfides and some of the metals and minerals of interest. The study focused on minerals containing elements such as antimony, arsenic, calcium, copper, lead, molybdenum, zinc, and sulfur-sulfide. Metal leaching concentrations and metal release rates from two years of drainage data were processed and are presented as part of this study.

Some geochemical processes, including sulfide weathering, heavy metal release (Sb, As, Cu, Pb and Zn), and neutralization potential by carbonate and silicate mineral dissolution in waste rock are part of this study as well. Finally, the relationship between the mineral availability and field cell drainage data was investigated, yielding results that allowed for the refinement of the classification of Class B waste rock produced at the Antamina operation.

1.2 Research Objectives

1.2.1 General

The main objective is to understand the geochemical behaviour of Class B waste rock from the Antamina mine through the operation of field kinetic cells. The results of waste rock characterization, whole-rock chemistry, mineralogy, and the availability for leaching of sulfide minerals were key components of the drainage quality interpretation. The combination of all these aspects allowed for a refinement of the current waste rock classification system. The conclusions of this research will provide information that will allow for the design of additional control techniques for drainage from waste rock dumps in order to minimize long-term environmental impacts.

1.2.2 Specifics

- This study will carry out a waste rock characterization, whole-rock chemistry and mineralogy of several samples of Class B material placed in the field cells. The availability for leaching of some elements of concern such as zinc, copper, lead, and sulfur-sulfide will also be established.
- The relationship between mineral availability and field cell drainage data will be verified and explained.
- Finally this study will establish a correlation between the conclusions found and current waste rock management at Antamina.

1.3 Study Site Description

The Antamina mine, the largest mining industrial project that has ever been undertaken in Peru, is a copper-zinc-molybdenum deposit located in the North Central Peruvian Andes, approximately 270 km north of Lima and 50 km west of Huaraz (the closest large city), and is at an elevation of between 4,100 and 4,700 meters above sea level. Access to the mine is by a 3.5-hour drive on 200 km of paved road from Huaraz (Figure 1.1).

Currently, the ownership of Antamina is divided as follows: 33.75% BHP Billiton, 33.75% Xstrata Limited, 22.50% Teck Cominco Ltd., and 10% Mitsubishi Corporation. The investment for the construction phase was 2.3 billion US dollars, covering the mine site, port facilities and the 320 km pipeline which carries copper and zinc concentrates from the mine to the coast. Construction began in 1999 and the first concentrate was shipped from the Pacific coast (Punta Lobitos Port) on July 11th, 2001. Commercial production began in October 2001, and the current anticipated mine life is 23 years, i.e. until 2024 (Golder Associates, 2007a).

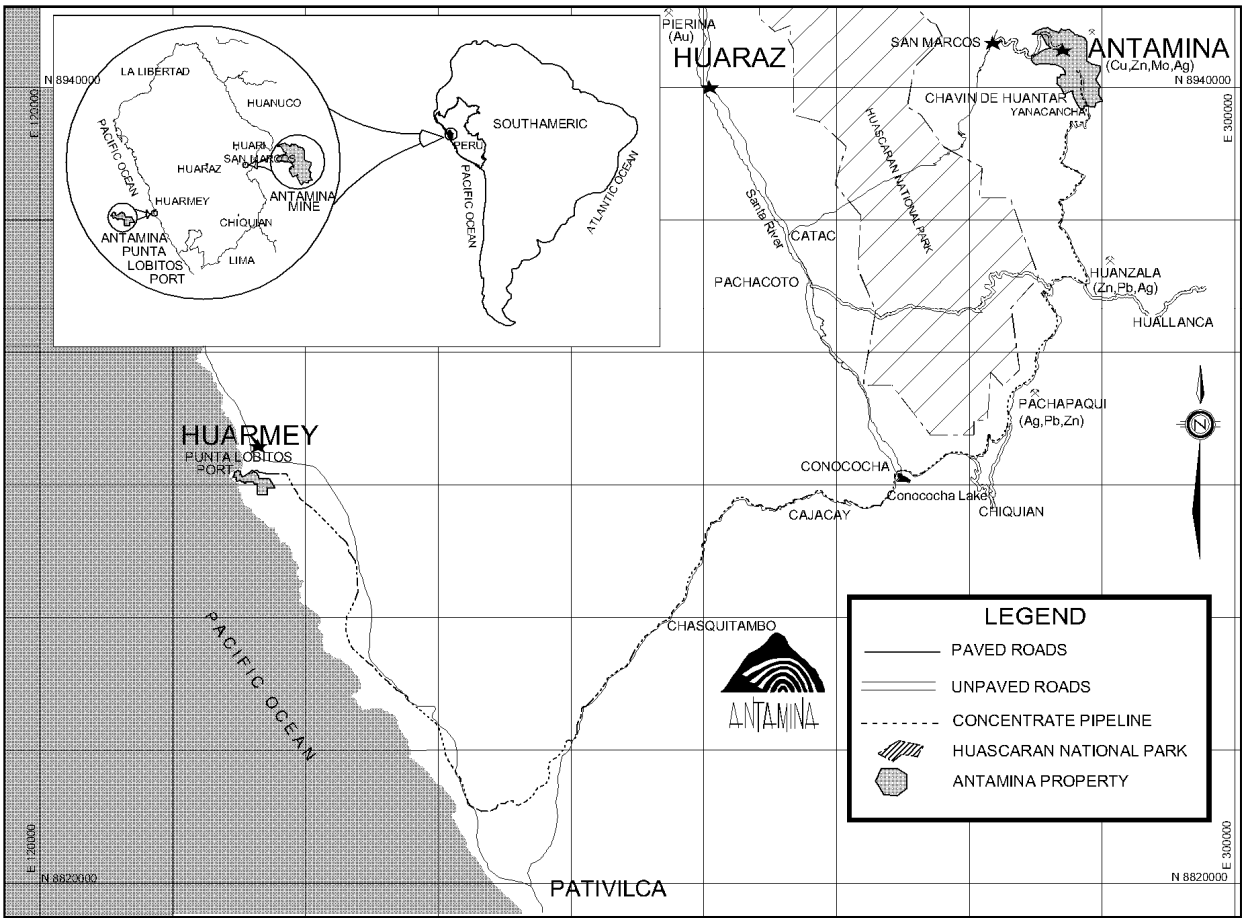

Figure 1.1 The Antamina mine location

Antamina is one of the larger known copper-zinc skarn (>3000 Mt @ 1.1% Cu and 1.3% Zn) deposits in the world with silver, molybdenum, lead and bismuth formed by the intrusion of a quartz monzonite body into limestone (Lipten and Smith, 2004).

Antamina is an open pit mine which processes 87,000 to 104,000 tonnes of ore per day, and excavates between 231,000 to 252,000 tonnes of waste rock per day. Depending on its classification, waste rock is either used as construction material or placed in the appropriate waste rock dump (East and/or Tucush). Most of the “dirty” or reactive waste rock is placed in the East Dump and the “clean” material is sent to the Tucush and South Dumps (Golder Associates, 2007a).

1.4 Background

1.4.1 Geology of the Deposit

Currently 156 rock/sub-rock types have been identified and logged within the Antamina deposit through a rigorous application of the Antamina core logging manual. The general skarn zoning from the intrusive core outwards is as follows: brown garnet endoskarn, mixed brown and green garnet indeterminate skarn, mixed brown and green garnet exoskarn, green garnet exoskarn, diopside exoskarn, wollastonite exoskarn, hornfels, marble, and limestone. Heterolithic breccia composed of all skarn types can occur in

any lithology type (Figure 1.2) (Lipten and Smith, 2004). Some of the rock types investigated in this study are described below.

Silty limestone, variously hornfelsed and marbleized, is commonly barren. Weak mineralization with veins, and less predominately galena [PbS], with minor pyrite [FeS_2], chalcopyrite [$CuFeS_2$], sphalerite [(Zn,Fe)S] and pyrrhotite [$Fe_{(1-x)}S$ (0<x<0.2)] can also be present in the waste rock (Antamina, 2001).

a. Diopside exoskarn

Diopside is a magnesium calcium silicate mineral [$MgCaSi_2O_6$], and is common in metamorphic rocks (Dana et al., 1993).

Diopside characterizes the outermost zone of exoskarn. This unit is located predominantly on the northern and eastern flanks of the deposit, and comprises a pale green diopside with calcite, quartz and wollastonite. This generally presents weak mineralization occasionally reaching levels which are sufficient to be considered as ore grade (Lipten and Smith, 2004). However, diopside material with low grades that are disposed as waste rock can contain elements that are of concern to the environment, and which can be mobilised in the leachates.

b. Hornfels

Hornfels is a metamorphic rock commonly composed of quartz, mica, feldspar, garnet, andalusite and/or cordierite (Dana et al., 1993; Klein et al., 2002). Hornfels is hard, dense, and nearly homogeneous with microcrystalline to fine-grained rock. Its colour may occur as anywhere black, gray, and greenish or nearly white (Dietrich and Skinner, 1979).

At the Antamina deposit, hornfels can be found as pale-brown, pale-green, gray, or yellowish-gray, and varies from fine-grained to aphanitic. It ranges from massive to laminated, with fine, wavy, compositional banding, and generally consists of a very fine-grained aggregate of garnet, phlogopite and diopside, with minor traces of wollastonite. This rock presents very low porosity or permeability, only contains rare, minor sulfides, and almost never reaches ore grade. Where these layers occur on the margins of the intrusion, they appear to limit development of the ore. In contrast to the diopside skarn described above, they are thought to be of thermal metamorphic origin, which in turn is metasomatic in origin (Lipten and Smith, 2004).

c. Limestone/Marble

Limestone/marble is composed mostly of calcite [$CaCO_3$] and/or rarely of dolomite [$CaMg(CO_3)_2$]. Marble is a metamorphic rock (metamorphosed limestone) and may be snow white, gray, black, yellowish, chocolate, pink, mahogany-red, bluish, lavender, or greenish in color. Marble may be essentially pure carbonate rock or contain one or more of a great variety of disseminated minerals. Typical impurities include brucite, diopside, epidote, feldspars, forsterite, graphite, grossular, pyrite, quartz, among others. Marble can range in grain size from very fine to coarse-grained (Dana et al., 1993; Dietrich and Skinner, 1979; Klein et al., 2002).

At the Antamina mine, most limestone/marble cut by drilling at the margins of the skarn is light grey, very fine grained and micritic, with parallel bedding on a scale of several centimetres, and contains no fossils,

shell fragments or other biogenic or sedimentary structures. In outcrops found on the upper valley slopes, this limestone/marble is thickly bedded (1 to 3 m) and light grey, and on cliff faces it weathers to a white or creamy color. Limestone/marble is interpreted as belonging to the Jumasha Formation that is anomalously thick as a result of structural thickening by thrust faulting at Antamina. At the head of the Antamina valley, interbedded (2 to 3 m beds) micritic and stromatolitic limestone can be found (Lipten and Smith, 2004).

d. Intrusive

Intrusive is an igneous rock formed by magma (molten rock) being cooled and becoming solid. It may form with or without crystallization.

The Antamina intrusion was previously divided into Earlymineral, Inter-mineral, Late-mineral and Post-mineral phases, each of which was divided into several sub-phases which were classified primarily according to their degree of alteration, intensity, type of veining, associated mineralization, and location. Currently, an empirical classification of intrusive rocks, based on their petrography rather than on time inferences, is being used (Lipten and Smith, 2004).

e. Endoskarn

Two widespread types of endoskarn are recognized at Antamina. The first is a coarse-grained pink garnet variety, which consists of a milky-white plagioclase-rich matrix (distinguishable from the pale-grey, translucent matrix of un-skarned porphyry). It further encloses large pink garnets and more sparse maroon garnets, and displays relict porphyritic texture. Significant mineralization does not appear to be associated paragenetically with the development of coarse grained endoskarn, which, although commonly containing disseminated molybdenite, only rarely hosts blebs and/or veinlets of chalcopyrite, which are associated with epidote. Narrow intervals of plagioclase endoskarn commonly occur between porphyry and coarse-grained pink-garnet endoskarn. Plagioclase endoskarn rarely contains ore-grade copper, and entirely lacks zinc, but is a useful indicator of proximity to ore.

The second major type of endoskarn is a fine-grained darkpink garnet variety that commonly hosts crackle or mosaic breccia, and constitutes many of the fragments in heterolithic breccia bodies cutting intrusive rock. Fine-grained pink endoskarn is distinguishable from coarser-grained plagioclase - or pink-garnet endoskarn, on the basis of colour, grain-size, mineralogy and relict porphyritic textures (Lipten and Smith, 2004).

f. Exoskarn

In much of the deposit, the skarn facies adjacent to marble or hornfels is a green garnet skarn. In this facies, garnet commonly appears to replace calcite directly, i.e., there is no evidence that garnet replaced wollastonite. It is believed that green garnet exoskarn in different parts of the deposit is formed by two different reaction paths, one, mentioned above, via wollastonite skarn, and the other, directly from marble. The two types are texturally indistinguishable.

Green garnet skarn contains either chalcopyrite-sphalerite ore or sphalerite alone, with the sulfides ranging from disseminated to massive and interbanded with green garnet. Sphalerite typically averages

3-5% in green-garnet exoskarn. However, it is erratically distributed, commonly occurring as rich bands separated by relatively barren sections (Lipten and Smith, 2004).

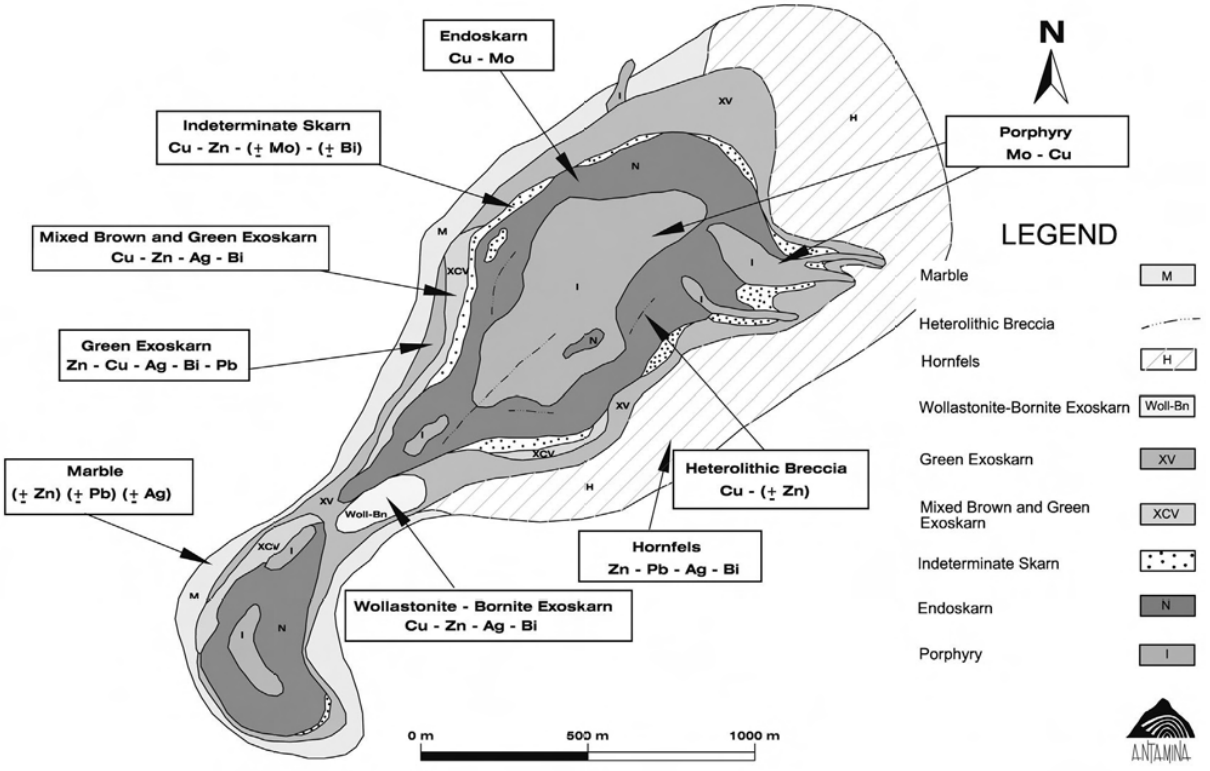

Figure 1.2 Lithology and metal zoning of Antamina deposit (Antamina, 2001)

1.4.2 Waste Rock Classification

The initial Environmental Impact Assessment (EIA) of Antamina defined the geochemical characterization of four major rock types: intrusive, endoskarn, exoskarn and mineralized limestone (Golder Associates, 2007a; Klohn-Crippen, 1998).

In order to select “clean” or non-reactive waste rock material which was used as rock-fill in the tailings dam construction, Antamina developed a procedure for waste rock characterization during the initial stages of development. This procedure was refined as mine development proceeded. Antamina found that high zinc concentrations occur in skarn and diopside material, ranging from <100 mg/kg to 16,000 mg/kg (1.6%) and an average of 1,700 mg/kg. However, solid phase zinc concentrations of 1,000 mg/kg (0.1%) were found in gray and pale-brown hornfels. The highest zinc concentrations were observed in hornfels which was in contact with skarn and diopside. The clean waste rock was defined for material containing less than 0.07% zinc and 2% sulfides (Antamina, 2000). As a result, the current waste rock classification system was established. Subsequently, some modifications have been incorporated. This classification scheme is referred to daily in mine development processes and forms the basis for on-site material placement. The current classification system (Table 1.1) was extracted from the “Material Classification for Dispatch Polygons and Field Stakes – March 2007” (Antamina, 2007), which is shown in full in Appendix A1.

Table 1.1 Current waste rock classification system at the Antamina Mine

Class	Waste rock classification	Metal limits / Restrictions *	Destination
A	**(Reactive)** Skarn (endoskarn/exoskarn), Limestone, Intrusive, Hornfels, or Marble with high zinc, arsenic and sulfides	• > 1500 mg/kg (0.15%) Zn • > 400 mg/kg (0.04%) As • > 3 % visual sulfides; • Visual Oxide > 10%	Within Pit Limits East Dump
B	**(Slightly reactive)** Limestone, Hornfels, or Marble with moderate zinc, arsenic and sulfides	• 700 – 1500 mg/kg Zn • < 400 mg/kg (0.04%) As • 2-3 % visual sulfides • Visual Oxide < 10%	Stockpiles Pads Construction Material Tucush or East Dumps
C	**(Non-reactive)** Limestone, Hornfels, or Marble with low zinc, arsenic and sulfides	• < 700 mg/kg (0.07%) Zn • < 400 mg/kg (0.04%) As • < 2% visual sulfides • Minimal oxides	Wherever Needed East or Tucush Dumps Tailings Dam

Source: Antamina, 2007
* Visual oxidation criteria is applicable only during the tailings dam construction

The classification system presented above does not include molybdenum as a criterion, because high levels of molybdenum are typically more associated with intrusives or endoskarn, which are classified as Class A material regardless of their molybdenum content. During mining, waste rock designation is performed by the Antamina's Geology Department. Geological maps are created using drill-hole logs. Block model maps, including chemical distributions, are created based on the lithology and the chemical assay results of samples collected from the bore holes. Subsequently, geological contacts are outlined in the field using geological maps of an active bench with an active dig face (Golder Associates, 2007b).

1.5 Waste Rock Sampling

While the experimental instrumented Class B marble and hornfels waste rock pile was constructed through four tipping phases using material that came from the Antamina open pit (Corazao Gallegos, 2007), representative portions of waste rock were sampled from each phase. These samples were collected in order to carry out different tests which have been described in Chapter 3 and Chapter 4.

The sampling process followed the procedures outlined below:

- The end-dumping into the pile was conducted in three to four tipping phases. Previously, a second protective layer was also conformed in the pile using Class B material. In addition, to avoid cracking the geomembrane placed as part of the lysimeters, a first protective layer of 2B Marble, which is crushed Class C material was installed (Corazao Gallegos, 2007).
- 26 tips of 240-tonne haul trucks (CAT 793C) were stockpiled next to the area where the pile was built, eventually making up the second protective layer. In order to obtain a representative sample, eight shovels of 16-tonne excavator (CAT 330D L) of material were collected randomly from the stockpile and filled a small dump truck. This material was flattened on a clean area next to the stockpiles, where it was carefully mixed, homogenized and quartered into four 4-tonne portions. The two

opposite portions were again combined and mixed generating two 8-tonne portions. One of these portions was selected and split into two 4-tonne portions and finally one small portion was chosen for sampling. The remaining material was returned to the stockpiles, although a batch was also used for particle size analysis.

- Cobbles and boulders (material above 50 cm in diameter) were removed from the portion chosen by using an excavator, while the material from 10 cm to 50 cm was removed by hand to avoid the disintegration of the coarser into the finer material. Then, approximately 1200 kg in all was taken from random locations of the portion. The sample was placed in 25-kg plastic bags and sent to the field cells area for sorting for different tests. In order to understand the geochemical behaviour of the waste rock at field scale using field kinetic cells, and for practical reasons, only material with particles less than 10 cm (4 inches) in diameter was sampled. Material greater than this size was discarded.
- The first tipping phase was completed after 27 tips of 240-tonne haul trucks (CAT 793C) had been placed onto the protected lysimeter. The second phase required 26 tips and the third/fourth phase was made up of 41 tips. During each tipping phase, approximately 10% of the material was selected and placed on the top platform next to the ramp near the pile. For example, the first tipping phase consisted of 27 tips, 3 tips were collected in a distributed manner, and every ninth haul truck was selected for the sampling process. Therefore, 3 tips were selected in each of the first and second phases.
- In the last phase (third/fourth), approximately 30 tips were required, but during the night shift, the mine's operators mistakenly end-dumped 41 tips, therefore some material had to be removed. The next day, based on the texture and color of the material, Antamina's geologists suspected a possible mixing with Class C material. Because of this, another sample was taken, and was denominated as part of the fourth tipping phase. One year later, based upon the chemical assay results and the block model (locations from which the material came); Antamina's Geology and Short-term Planning Departments confirmed that material placed into the pile was Class B gray hornfels.
- Once the tips were stockpiled, eight shovels of 16-tonne excavator (CAT 300D L) were randomly collected from the corresponding stockpiles. Subsequently, these were also carefully mixed, homogenized and separated into four 4-tonne portions, and then the same procedure described above for material placed as the secondary protective layer, was followed. Figure 1.3 shows the locations of the Class B waste rock samples taken during the construction of the experimental pile (Corazao Gallegos, 2007), which represent different zones of the whole pile. These are also summarized in Table 1.2.

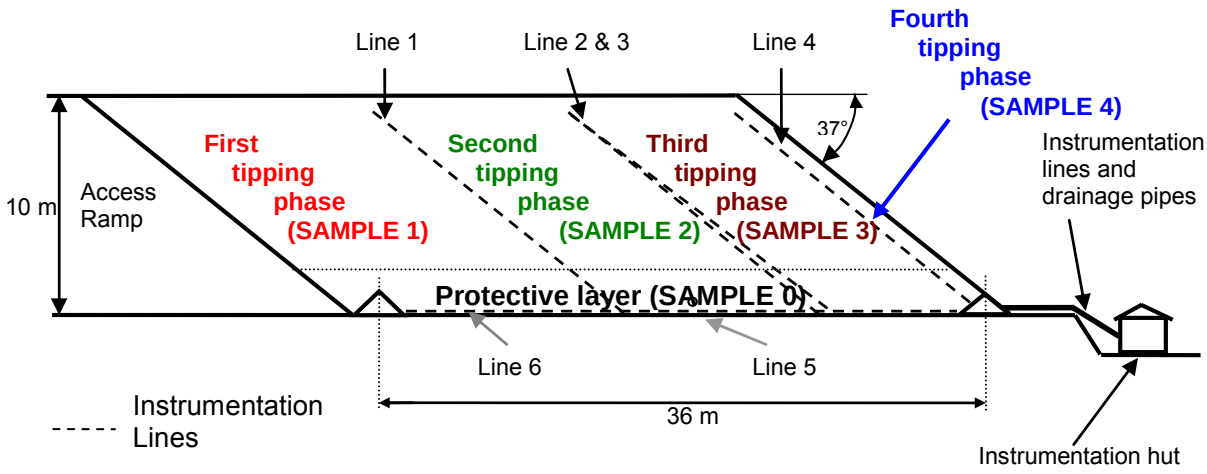

Figure 1.3 Locations in the pile of Class B waste rock samples

Table 1.2 Summary of Class B waste rock samples collected from the experimental pile

Sample	Lab code	Field cell	Location in the pile
SAMPLE 0	FC-0	UBC-1-0A and UBC-1-0B	Protective layer
SAMPLE 1	FC-1	UBC-1-1A	First tipping phase
SAMPLE 2	FC-2	UBC-1-2A and UBC-1-2B	Second tipping phase
SAMPLE 3	FC-3	UBC-1-3A	Third tipping phase
SAMPLE 4	FC-4	UBC-1-4A	Fourth tipping phase

Once in the field cells area, the 1200 kg sample was flattened on a sheet of geomembrane to keep it separated from the underlying material. In order to obtain representative samples, the material was carefully mixed and homogenized.

Finally, by using the coning and quartering method (Figure 1.4), 300 kg samples were obtained. A brief description of this method is given below.

- The 1200 kg portion was arranged by hand into a conical pile. The conical pile was then flattened and split into four quarters (1 to 4).
- The opposite corners (1 & 3 and 2 & 4) were removed from the original conical pile and combined to form two separate small conical piles of 600 kg each.
- Each 600 kg conical pile was again flattened and split into four quarters. As before, opposite quarters were mixed to form two smaller 300 kg conical piles.
- When there were four 300 kg conical piles, these were recombined again into one large conical pile and the process was repeated three times. Once three iterations were completed, samples of approximately 300 kg (A, B, C and D conical piles) became considered as the representative portions

of the original sample and were deemed suitable for using in the different tests (Figure 1.5). When duplicate field cells were required, approximately 1500 kg of material was sampled.

Figure 1.4 Coning and quartering of Class B black marble waste rock material

Table 1.3 Summary of material quantities required for different tests

Test type	Waste rock mass (kg)	Small conical pile
Field cell	300	A
PSA, SAD, assay and mineralogical characterization by size fractions	150	B
Sequential leach testing	50	
Extra	100	
Assay for head samples	50	C
ABA analysis	50	
Moisture content	20	
Extra	180	
Extra material	300	D
Total	1200	

As is described in Table 1.3, material from conical pile A was used for installing the field cell (Chapter 4). The material from conical pile B was sent to UBC for conducting particle size analysis, surface area determination, particle or true density determination and chemistry assay by size fractions, and

mineralogical characterization (Chapter 3). Conical pile C was sent to ALS laboratories to carry out chemistry assay for bulk sample, acid-base accounting (ABA) analysis, and moisture content (Chapter 3). Finally, conical pile D was retained as excess or extra material for repeat testing, if required, and was stored in plastic bags to minimize weathering effects.

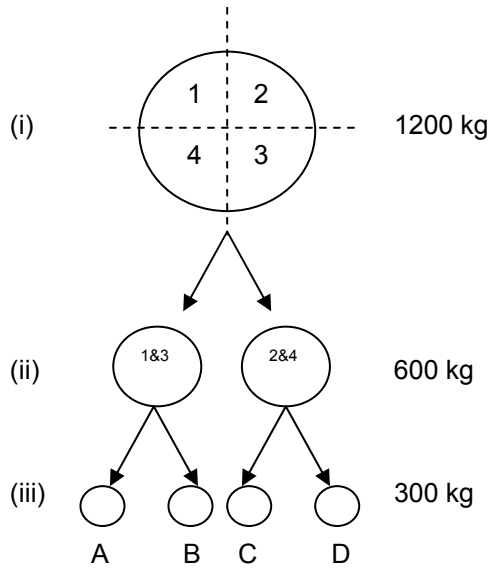

Figure 1.5 Coning and quartering process

1.6 Thesis Components

This thesis was written in the Manuscript-Based format and its body is divided into six chapters:

Chapter One provides an introduction to the research and includes the objectives, the site description of where the research was conducted, previous work done at the site relating to this study, the waste rock classification system, and how the samples were taken. A literature review was defined in **Chapter Two**. All tests carried out as part of the characterization of the different waste rocks (marble and hornfels) are presented in **Chapter Three**. **Chapter Four** details the description and behaviour, as well as the geochemical speciation and a simple water balance of field kinetic cells (field cells). **Chapter Five** provides a discussion and integration of the laboratory and field results. Finally, the conclusions and recommendations are described in **Charter Six**. Appendices A, B, C, D and E related to Chapters One, Two, Three, Four and Five, respectively, have been included at the end of this thesis.

2 LITERATURE REVIEW

2.1 Acid Rock Drainage and Metal Leaching (ARD/ML)

ARD/ML is produced when sulfide material is exposed to oxygen (air) and water (rain) (Akcil and Koldas, 2006). Therefore, ARD/ML is generated at mine sites when sulfide minerals are oxidized. Sulfide minerals are present in the host rock associated with most types of metal mining activity. Prior to mining, oxidation of these minerals and the formation of sulfuric acid is a function of natural weathering processes (USEPA, 1994). Commonly releases of ARD/ML have low pH, high electrical conductivity, high concentrations of metals and salts such as Al, Fe, Mn, Ca, Mg, K, Na (Akcil and Koldas, 2006) as well as trace elements such as Zn, Cu, Cd, Pb, Co, Ni, As, Sb and Se (MEND (Canada), 2000).

The oxidation of sulfide minerals is made up of several reactions, and each sulfide has a different oxidation rate. For example, marcasite and framboidal pyrite will oxidize quickly, while crystalline pyrite will oxidize slowly. The reactions of acid generation are best illustrated by examining the oxidation of pyrite [FeS_2], which is one of the most common sulfide minerals (Akcil and Koldas, 2006; British Columbia Acid Mine Drainage Task Force, 1990; Gormely Process Engineering, 1989; Manahan, 2005; USEPA, 1994).

The first important reaction is the oxidation of the sulfide mineral [S_2^{2-}] into dissolved iron, sulphate and hydrogen ions:

$$2FeS_{2(s)} + 2H_2O_{(l)} + 7O_{2(g)} \rightarrow 2Fe^{2+}_{(aq)} + 4SO_4^{2-}{}_{(aq)} + 4H^{+}_{(aq)} \qquad \text{Eq. 2.1}$$

The dissolved Fe^{2+}, SO_4^{2-} and H^+ represent an increase in the total dissolved solids (TDS) and acidity of the water and, unless neutralized, induce a decrease in pH. If the surrounding environment is sufficiently oxidizing (dependent on O_2 concentration and bacterial activity), much of the ferrous iron [Fe^{2+}] will be slowly oxidized to ferric iron [Fe^{3+}] at lower pH values, according to Eq. 2.2:

$$4Fe^{2+}_{(aq)} + O_{2(g)} + 4H^{+}_{(aq)} \rightarrow 4Fe^{3+}_{(aq)} + 2H_2O_{(l)} \qquad \text{Eq. 2.2}$$

At pH levels between 3.5 and 4.5, iron oxidation is catalyzed by a variety of bacterium. Below a pH of 3.5, the same reaction is catalyzed by the iron bacterium *Acidithiobacillus ferrooxidans*. At pH values between 2.3 and 3.5, ferric iron precipitates as hydrated iron oxide [$Fe(OH)_3$] and jarosite, remaining little Fe^{3+} from solution (Eq. 2.3) while simultaneously lowering pH. $Fe(OH)_3$ precipitates and is identifiable as the deposit of amorphous, yellow, orange, or red deposit on stream bottoms ("yellow boy").

$$Fe^{3+}_{(aq)} + 3H_2O_{(l)} \leftrightarrow Fe(OH)_{3(s)} + 3H^{+}_{(aq)} \qquad \text{Eq. 2.3}$$

Any Fe^{3+} from Eq. 2.2 that does not precipitate from solution through Eq. 2.3 may react in contact with pyrite and dissolve it. So, the reaction shown in Eq. 2.4 can occur:

$$FeS_{2(s)} + 14Fe^{3+}_{(aq)} + 8H_2O_{(l)} \rightarrow 15Fe^{2+}_{(aq)} + 2SO_4^{2-}{}_{(aq)} + 16H^{+}_{(aq)} \qquad \text{Eq. 2.4}$$

This reaction generates more acid. The dissolution of pyrite by ferric iron (Fe^{3+}), in conjunction with the oxidation of the ferrous ion constitutes a cycle of dissolution of pyrite. Based on these simplified basic reactions, acid generation that produces iron, and which eventually precipitates as $Fe(OH)_3$, may be represented by a combination of Eq. 2.1 – Eq. 2.3:

$$4FeS_{2(s)} + 14H_2O_{(l)} + 15O_{2(g)} \rightarrow 4Fe(OH)_{3(s)} + 8SO_4^{2-}{}_{(aq)} + 16H^+{}_{(aq)} \quad \text{Eq. 2.5}$$

On the other hand, the overall equation for stable ferric iron that is used to oxidize additional pyrite (combinations of Eq. 2.1 – Eq. 2.3) is:

$$8FeS_{2(s)} + 34H_2O_{(l)} + 15O_{2(g)} + 52Fe^{3+}{}_{(aq)} \rightarrow 60Fe^{2+}{}_{(aq)} + 16SO_4^{2-}{}_{(aq)} + 68H^+{}_{(aq)} \quad \text{Eq. 2.6}$$

The oxidation of other sulfide minerals is different. Some of them are able to leach high quantities of their constituents elements under acid conditions, but their elements could also be mobilized under circumneutral pH conditions (Blowes et al., 2003).

2.2 Neutral Rock Drainage and Metal Leaching (NRD/ML)

NRD/ML is produced when any acid generated after sulfide oxidation is neutralized by the available neutralization capacity of the material, usually due to the dissolution of carbonates and silicates (Bay et al., 2009).

Soluble metal contaminants depend critically on sulfide weathering and heavy metal mobility, which are both to a large extent determined by pH and redox conditions. The contaminants Cu and Zn are essentially conserved in the aqueous phase at the lower pH levels (Stromberg and Banwart, 1999b). Although, for many rock types and environmental conditions, metal leaching is significant only if drainage pH decreases to less than 6 or 5.5. However, neutral-pH drainage does not necessarily prevent metal leaching from occurring in sufficient quantities to cause negative impacts. Whereas the solubility of Al, Fe, and Cu are greatly reduced at circumneutral pH drainage, elements such as Sb, As, Cd, Mo, Se and Zn remain relatively soluble and can occur in significantly high concentrations. Even though there is insufficient attenuation or dilution prior to a sensitive receptor, neutral pH metal leaching of Al, Fe and Cu can cause negative impacts (Price, 2003; Price et al., 1998). Iron is produced in low concentrations under circumneutral pH conditions.

Indications of acid generation and neutralization are (Robertson and Broughton, 1992)

- increasing or constant sulphate production
- decreasing alkalinity;
- rate of sulphate production exceeding availability of alkalinity (as indicated by Ca and Mg in solution) or
- release of “indicator” metals such as Zn, Al, or Fe.

Even though the *Acidithiobacillus ferrooxidans* are the most commonly known bacteria which accelerate acid drainage generation by catalyzing iron oxidation, there are other sulfide ore bacteria which can act

under circumneutral pH conditions. *Acidithiobacillus thioparus, A. neapolitanus* or *A. denitrificants* are able to grow and act when the pH ranges from 4 to 10 (USEPA, 1994).

Naturally occurring alkalinity, such as carbonate minerals, can partially or even completely neutralize acidity *in situ*. When this situation occurs, the resulting non-acidic leachate is likely to have low iron concentrations but may contain elevated concentrations of sulphate, calcium and magnesium. Natural neutralization through reactions with acid-consuming minerals (carbonate minerals in particular) may result in low concentrations of dissolved metals due to the low solubility of metal carbonates, hydroxides and oxyhydroxides in the pH range of 6 to 7. A few days following exposure, acid may be generated and released by high sulfur wastes which have small amounts of carbonate minerals. In contrast, wastes with low sulfur (<2%) and some carbonate may not release acid for year or decades (MEND (Canada), 2000). In an open system, the complete oxidation of pyrite and neutralization of all generated acidity is given by:

$$FeS_{2(s)} + 2CaCO_{3(s)} + 3.75H_2O_{(l)} + 1.5O_{2(g)} \rightarrow Fe(OH)_{3(s)} + 2SO_4^{2-}{}_{(aq)} + 2Ca^{2+}{}_{(aq)} + 2CO_{2(g)} \quad \text{Eq. 2.7}$$

where 1 mole of FeS_2 (64 g of sulfur) is neutralized by 2 moles of $CaCO_3$ (200 g of $CaCO_3$). Therefore, the constant is 31.25, which means that it takes 31.35 mg of $CaCO_3$ to neutralize 1000 mg of rock containing 1% pyritic sulfur.

Following the oxidation of a sulfide mineral, the resulting acid/neutral products may either be immediately flushed by water moving over the rock. However, if there is no water movement, these then can accumulate in rock and be flushed afterwards. If the acid products are flushed from the sulfide mineral, they may eventually encounter an acid-consuming mineral; the resulting neutralization will remove a portion of the acidity and iron from solution and will neutralize the pH. Sulphate concentrations are usually not affected by neutralization (Akcil and Koldas, 2006).

In the case of weathering of waste rock, the pH regime is determined by the pH-buffering properties of the groundmass minerals (e.g. carbonates and silicates). Where carbonate minerals are present, the reaction shown in Eq. 2.8 will occur at circumneutral-pH for as long as carbonate minerals remain to neutralise the acid produced through pyrite oxidation (Alarcón et al., 2004).

$$2H^{+}_{(aq)} + SO_4^{2-}{}_{(aq)} + CaCO_{3(s)} <--> SO_4^{2-}{}_{(aq)} + Ca^{2+}{}_{(aq)} + H_2CO_3^{0}{}_{(s)} \quad \text{Eq. 2.8}$$

The acidity produced when the sulfides are oxidized may be partially or completely consumed by dissolution of carbonate and/or silicate minerals. Primary silicate minerals dissolve more slowly than sulfides. However, the rate at which primary silicates dissolve is still important since they are abundant in waste rock and represent the largest capacity for acid consumption (Stromberg and Banwart, 1999b).

2.3 Prediction of Acid Rock Drainage / Metal Leaching

There are two important points that must be considered when evaluating the acid generation potential of a waste rock material

1. How to collect samples from the field which will be used in analytical testing

2. How to define available and optimal analytical test methods.

Factors affecting the selection of the sampling system and analytical methods include an existing knowledge of the geology, costs, and length of time available to conduct the test. The following list of components describes the solid phase composition and reaction environment of sulfide minerals (USEPA, 1994).

a. Components affecting the total capacity to generate acid are characterized by:
   - Amount of acid generating (sulfide) minerals present, assuming total reaction of sulfide minerals
   - Amount of acid neutralizing minerals present
   - Amount and type of potential contaminants present.

b. Components affecting the rate of acid generation include:
   - Type of sulfide mineral present
   - Type of carbonate mineral (and other neutralizing minerals) present
   - Mineral surface area available for reaction, therefore availability for leaching
   - Occurrence of the mineral grains in the waste (i.e., included, locked, liberated)
   - Particle size and surface area of the waste
   - Texture and association of the minerals
   - Available water and oxygen
   - Bacteria

However, choosing geological factors for sample selection most importantly involves a good understanding of the local geology. This information is important to both the sampling system and application of test results. Environmental factors include consideration of the potential environmental contaminants in the rock and climatic variables. A quality assurance/quality control program should be carried out and coordinated with the Mine Planning Department for sample collection and acid/neutral prediction testing.

2.3.1 Sampling

The selection of samples has important implications for subsequent acid/neutral prediction testing. The main purpose of testing rock material is to allow classification and planning for waste disposal based on the predicted drainage quality from that material. Samples must be selected to characterize both the type and volume of rock materials, as well as to account for the variability of materials that will be exposed during mining. Sampling techniques used to evaluate recoverable mineral resources (assay samples) are similar to those required for prediction of acid/neutral generation potential.

The first two stages of an acid prediction analysis for either new or existing mines are (1) to review the geology and mineralogy and (2) to classify the rock and collect samples (Broughton and Robertson, 1992; Robertson and Broughton, 1992).

There are reservations to prescribing a number of samples for collection per volume of material. This is particularly true in the case of existing mines, when collecting samples from waste rock dumps for acid generation potential tests. Waste rock dumps are usually constructed by end-dumping process by using haul trucks, creating heterogeneous deposits that are very difficult to sample with confidence.

Factors to consider in a sampling program for existing or new mines include the method of sample collection, sample storage time and environment. Each of these factors can affect the physical and chemical characteristics of a sample, which later on should be described. Samples collected from cores exposed to the environment may be physically and/or chemically altered. Sometimes, when samples are collected from a drill core, this can be contaminated with the lubricant used for drilling, it can be problematic. Collecting samples of waste rock is difficult because of the variability inherent in these waste units. Drilling is considered to be the preferred method for collecting samples from waste rock piles (Ferguson and Morin, 1991).

However, sampling from an open pit where mining is taking place is also allowed. At this time, the current waste rock may be characterized and assessed. Since individual samples will be used to test and classify larger volumes of waste, it is important to consider how representative samples are to be collected. Compositing is a common practice used to sample large volumes of material. Typically, composite samples are collected from drill-hole cuttings on benches prior to blasting, but compositing samples from the open pit during the mining process can be also considered to be suitable.

2.3.2 Analytical Test Methods

Either static or kinetic analytical tests are commonly used to assess or predict the acid generation potential of the waste material. A static test determines the amount of both the total acid generating, and total acid neutralizing potential of a sample. The capacity of the sample to generate acidic drainage is calculated as either the difference of the values, or as a ratio of the values. These tests do not attempt to predict the rate of acid generation, only the potential to produce acid. Static tests can be conducted quickly, and are cheap compared to kinetic tests. Kinetic tests are usually used to simulate the geochemical processes found at mining sites. These tests require more time and are considerably more expensive than static tests.

Static tests

Static tests predict the drainage quality of the waste material by comparing its maximum acid production potential with its maximum neutralization potential.

Acid-Base Accounting (ABA)

The acid-base accounting test was developed in 1974 to evaluate coal mine waste, and was modified in 1978 (Sobek et al., 1978). The acid production potential (AP) is the maximum amount of sulfuric acid that can be produced from the oxidation of sulfide minerals in the material (Skousen et al., 2002), and is determined by multiplying the percent of sulfur-total or sulfur- sulfide content (depending on the test) in the sample by a conversion factor (Eq. 2.9), and assumes that two moles of acid will be produced for each mole of sulfur. Units for AP are tons of acidity per tonne of rock.

AP = 31.25 x percent S Eq. 2.9

Neutralization Potential (NP) is a measure of the maximum neutralization potential available to neutralize acid, fundamentally carbonate material. NP is determined first by a simple fizz test to select the acid strength to use in the next step. Based on this information, two methods can be followed: i) adding hydrochloric acid to a sample and boiling the sample until the reaction stops; then the resulting solution is back titrated to pH 7 with sodium hydroxide to determine the amount of acid consumed in the reaction between HCl and the sample; and ii) direct hydrochloric acid titration of the sample; with the endpoint pH usually being 3.5 (Ferguson and Morin, 1991).

The net neutralizing potential (NNP) is determined by the difference between the neutralizing (NP) and acid forming potentials (AP), i.e. subtracting the AP from the NP (Eq. 2.10), resulting in values that are either positive or negative.

NNP = NP – AP Eq. 2.10

The results of AP, NP, and NNP are typically expressed in mass (kg, metric tonne, etc.) of calcium carbonate ($CaCO_3$) per 1000 metric tonne of rock, parts per thousand.

Tests conducted by Ferguson indicate that NNP values of less than -20 (kg $CaCO_3$/tonne) are likely potentially acid generating (PAG). Those with NNP values greater than +20 were likely non-acid generating (NAG). Therefore, if the difference between NP and AP is negative, then the potential exists for the waste to form acid, and if it is positive then there may be lower risk. Prediction of the acid potential when the NNP is between -20 and +20 is more difficult, and an uncertain potentially acid generating (UPAG) designation is given (Lapakko, 1993; Robertson and Broughton, 1992). It then becomes necessary to conduct additional tests to resolve the uncertainty.

The other typical parameter, the Neutralization Potential Ratio (NPR), which is the ratio of NP to AP (Eq. 2.11), is also used in the assessment. An NNP of 0 is equivalent to an NPR of 1 (Ferguson and Morin, 1991). When the NPR is greater than 3:1, experience indicates that there is a lower risk for acidic drainage to develop. However, for NPRs between 3:1 and 1:1, referred to as the zone of uncertainty, additional kinetic testing is usually recommended. Finally, samples with a NPR of 1:1 or less are more likely to generate acid (Brodie et al., 1991; Robertson and Broughton, 1992).

In 1997, similar ARD screening criteria, based on the results of ABA tests, were published. When NPR is less than 1, it is likely ARD generation can occur, unless sulfide minerals are non-reactive. If NPR is between 1 and 2, ARD generation is possible, and will occur if NP is insufficiently reactive or is depleted at a faster rate than sulfides. However, when NPR is between 2 and 4, potential acid generation will not occur unless there is significant preferential exposure of sulfides along fracture planes, or extremely reactive sulfides are present in combination with insufficiently reactive NP. Finally, if NPR is greater than 4, NAG will be expected (Price, 1997). The screening criteria to predict ARD, based on different ABA tests results, are summarized in Table 2.1.

$$NPR = NP / AP \quad \text{Eq. 2.11}$$

Prediction of drainage quality for a sample based on these values requires assumptions that reaction rates are similar, and that the acid consuming minerals will dissolve. When reviewing data on static tests, an important consideration is the particle size of the sample material, and how it is different from the waste, or unit, being characterized. Assumptions of the test are that all the sulfur in the sample is reactive. This assumption does not take into account the presence of gypsum and other non-reactive sulfur minerals. A shortcoming of this technique is the potential to overestimate NP in one or more of the following ways: i) the use of strong acid may dissolve minerals that would not otherwise react to maintain drainage pH within an environmentally acceptable range; ii) the use of boiling acid may cause an overestimation of NP by reacting with iron and manganese carbonates, which would not otherwise factor in the natural NP (this observation is problematic with samples that contain large quantities of these carbonates; iii) the NP may be underestimated as a result of the contribution from metal hydroxides that precipitate during the titration with sodium hydroxide. Due to the factors mentioned above, the method was modified, and is described below (USEPA, 1994).

Modified Acid-Base Accounting

The Modified Acid-Base Accounting method is similar to the previous method, with some exceptions. This method calculates AP based only on sulfur-sulfide content. This is different from the sulfur-total calculation used in the regular ABA testing. The modified method assumes that sulfur present as sulphate is not acid producing, and therefore may underestimate available AP if jarosite, or other acid producing sulphate minerals, are present.

Determination of NP uses a longer (24-hour) acid digestion process at ambient temperature, rather than boiling hydrochloric acid, as is done in the ABA method. When back titrating with sodium hydroxide to determine the acid consumed in the digestion, an endpoint of 8.3 is used rather than 7. Conducting the acid digestion at standard temperature may reduce the contribution of iron carbonate minerals when determining the NP.

Table 2.1 Screening criteria to predict the PAG based on the Standard ABA testing results

Potential for ARD	NNP (kg $CaCO_3$/tonne)	NPR*	NPR**
Potentially Acid Generating (PAG)	< -20	< 1	< 1
Uncertain Potentially Acid Generating (UPAG)	-20 – +20	1 – 3	1 – 2 (possibly) 2 – 4 (low)
Non-acid Generating (NAG)	> +20	> 3	> 4

* Brodie et al., 1991
** (Price, 1997)

Kinetic Tests

Kinetic tests attempt to simulate the natural oxidation reactions of the field conditions. The tests typically use a larger sample volume and require a much longer time for completion than do static tests. These tests provide information on the rate of sulfide mineral oxidation, and therefore acid production, as well as an indication of drainage water quality. Preference for tests tends to change with time as experience and understanding increase. However, the humidity cells are the kinetic tests that are most commonly used.

Kinetic tests can be used to assess the impact of different variables on the potential to generate acid. For example, samples may be inoculated with bacteria (a requirement for some tests); temperature of the sample environment may also be controlled during the test. Most tests require the sample particle size to be less than a specified sieve size (e.g., minus 200 mesh). Larger sample volumes and test equipment may examine acid potential from coarse particles. Acid drainage control mechanisms, such as through increasing alkalinity by adding lime, may also be examined using kinetic tests.

Humidity Cell Tests

Both Standard and Modified Humidity Cell Tests are used to determine the rate of acid/neutral drainage. Tests are conducted in a chamber resembling a box with ports for air input and output. The modified humidity cell test uses crushed samples and resembles a column.

The standard humidity cell test leaches a 200 g sample crushed to minus 2.38 mm in an enclosed plastic container. The test is typically run for ten weeks and follows a seven day cycle. The sample may be inoculated with bacteria. During the seven day cycle, dry air is passed through the sample container for the first three days, and humidified air is passed through for the next three days. On the seventh day, the sample is rinsed with 200 mL of distilled water, and the leachate is collected (Sobek et al., 1978). The modified humidity cell test uses 1 kg of sample and is rinsed with 750 mL of distilled water, running for twenty weeks in seven day cycles as well (Price, 1997). However, some other modifications, for which 25 to 50 kg of sample is required (SRK cell), have been presented. This involves adding an equivalent amount to specific site rainfall on the top area of the cell in the order of 0.01 L/kg/week or less; the test runs continuously (Brodie et al., 1991; Robertson and Broughton, 1992). Parameters such as pH, acidity, alkalinity, EC, redox potential (the oxidation-reduction potential of an environment), sulphate, and dissolved metals may be analyzed.

Depending on the sample, the test duration may need to be extended. Monitoring sulphate and dissolved metal loads is important to track both oxidation reaction and metal mobility. Two points are important when using this and other kinetic tests: i) if the sample was allowed to begin reacting before testing began (e.g., in storage) there may be a build-up of oxidation products in the sample, and this would be flushed out in the early water rinses, and ii) neutral drainage may lead to an incorrect prediction of acid potential if the test period is not long enough.

Column Tests

Column Tests are very similar to the humidity cell test method described above. These are conducted by stacking the waste or material in a cylinder or similar device. Wetting and drying cycles are created by adding water to the column and then allowing the column it to dry. Each of the cycles may occur over a

period from several days to a week or more, though they typically last for three days each. Care must be taken to avoid piping along the sample-wall interface when packing the column. Water added to the column is collected and analyzed to determine the oxidation rate, sulphate production, metal release, and other parameters.

Column test equipment, like humidity cells are relatively simple forms of apparatus. They are easily modified to test control options, such as through the addition of limestone, the influence of bacteria, and water saturation. However, despite the fact that some conditions can be controlled using the humidity or column tests, actual site-conditions are impossible to reproduce using these tests.

Field Scale Test

Field scale testing, such as through the use of on-site waste rock piles (Corazao Gallegos, 2007), use large volumes of material to construct test cells in ambient environmental conditions, typically at the mine site. These tests are very different from laboratory tests, where experiments are conducted under controlled conditions. Sample size varies, and may be as much as 1000 metric tonnes or more, depending on space availability. Particle size of the test material is not usually reduced in order to better approximate field conditions. The sample is loaded onto an impervious liner to catch solutions, and a vessel is used to collect the leachate. The volume of solution is determined, and an aliquot is analyzed for pH, sulphate, dissolved metals, and other parameters.

A consideration of climatic conditions is important when evaluating results from field scale tests. Climatic effects must be distinguished from the rate of sulfide oxidation, acid generation, neutralization, and metal dissolution, as determined by the analysis of the leach solution. This is necessary because climatic effects, especially precipitation, determine the rate of flushing. While colder weather will slow oxidation down, it is well known that heating increases reaction rates and the subsequent chemical composition of the leachate.

However, it is helpful to supplement kinetic tests with an understanding of the empirical data which characterizes the specific sample, including an analysis of specific surface area, mineralogy, particle size distribution, availability of metals, etc. Such information may affect the interpretation of test data and is important when making spatial and temporal comparisons between samples based on the test data.

2.3.3 Application of Different Tests for Acid/Neutral Rock Drainage Prediction

While ABA is the most commonly used method for predicting pre and post-mining water quality, kinetic or leaching tests have also been widely used. Initially, results from static and laboratory kinetic tests can be used to classify mine wastes on the basis of their potential to generate acid. The difference, or ratio of NP and AP, determined after ABA testing, becomes the initial basis of the classification; however, it is not a suitable indicator to predict either acid or neutral drainage (Skousen et al., 2002).

The determination of AP based on estimated or reactive sulfur content in the sample has some inherent limitations. When total sulfur is used as the basis for estimating sulfide content, this uncertainty may be attributable to possible errors in: i) assessment of true acidity and neutralization in the sample; ii) calculated acidity based on total sulfur conversion value; and iii) analytical error. Similar errors exist for

static tests that determine reactive sulfide mineral concentrations. Estimating long-term reactive sulfide based on short-term tests may result in uncertainty due to difficulties in predicting oxidation rates.

ABA tests conducted on an iterative basis, where the initial sample set is small, are helpful when establishing boundaries between lithologic units. The goal of sampling is to collect representative samples that define the variability of the lithologies present. If significant variability in the acid generation or neutralization potential is identified in the initial sample test results, additional sampling to refine lithologic boundaries is warranted. Waste rock data from static tests are very limited and demonstrate the variability expected within these waste units (USEPA, 1994). Therefore, based on the interpretation of the static test data, the next phase of prediction is to verify the ARD/ML potential and rate with kinetic tests, which certainly provide more information than the ABA data, and indicate water quality trends as a result of weathering.

As a background, present methods of assessing drainage quality from waste rock tend to focus on relatively rapid, small scale tests which may have limited predictive ability on the field scale. Acid-base accounting and various laboratory leaching procedures such as humidity cells can provide useful information, but fail to represent the larger scale physical and geochemical processes. Indeed, studies at several sites have shown that the rate of chemical weathering in waste rock piles can be many times faster in smaller-scale experiments than is inferred from observations of outflow in larger-scale piles (Frostad et al., 2002; Frostad et al., 2005).

Kinetic tests are often conducted to confirm results from static tests and estimate when and how fast acid generation can occur. These tests provide insight regarding the rate of acid production and the water quality potentially produced, and are used to evaluate treatment and control measures. Unlike for static tests, there is no standardized method for evaluating test results. Data are examined for changes through time and for water quality characteristics. Laboratory kinetic tests tend to accelerate the natural oxidation rate over tests which are observed in the field. This may be advantageous in terms of condensing time, and providing earlier insight into the potential for acid generation.

Generally, kinetic tests are evaluated for changes in pH, sulphate, acidity and a host of potential metals. Samples with pH values of less than 3 are considered strongly acidic; between 3 and 5 the sample is acid generating, and there may be some neutralization occurring; at pH values >5, the sample is not considered to be significantly acidic, or an alkaline source is believed to be neutralizing the acid; therefore the solution is occurring under circumneutral pH conditions. Sulphate is a product of sulfide oxidation and can be used as a measure of the rate of oxidation and acid production. When evaluating test data, in addition to other parameters, it is important to examine the cumulative sulphate production curve as an indicator of sulfide oxidation. An analysis of metals in the leachate is not necessarily a good indicator of acid generation (Robertson and Broughton, 1992). However, release rates in the sample solution serve as indicators of the presence of contaminants which can impact the environment.

Although results of laboratory kinetic tests are routinely used to predict the long-term weathering rates of a waste rock dump, the field kinetic tests, which are less commonly conducted, are operated to incorporate site-specific conditions that are difficult to account for in laboratory kinetic tests. Therefore, field tests are better tools through which to predict ARD/NRD/ML generation. Relevant factors to consider between field and laboratory conditions include particle size distribution, surface area, mineral availability,

flush volumes, air movement, and temperature, among others. The field rates of weathering can be in an order of magnitude greater than the adjusted laboratory results (Frostad et al., 2005), or in contrast, in an order of magnitude lower in the field (Malmstrom et al., 2000). Whichever the result; this must be corrected for, taking into account surface area, availability of minerals as well as other factors present in the waste rock. Additionally, mineral weathering occurs more rapidly at higher temperatures, typically resulting in an overestimate of reaction rates in lab rates. Therefore, field test experiments are considered to be useful for validating sulphate and metal release rates, and are more accurate for predictions of leaching quality than are humidity cells or laboratory column tests.

One of the kinetic field tests consists of field cells (barrels) which are commonly operated under site-specific conditions. They are small enough to allow individual tests to be conducted on several types of material in order to provide information on rates of sulfide oxidation, metal leaching and neutralization potential (NP) depletion. Nevertheless, even though field tests provide site-specific weathering conditions, their results are difficult to interpret if some characteristics, such as mineralogy and reaction kinetics, are not taken into account. These characteristics should be determined in the laboratory, which could help during the interpretation phase and for making final predictions.

The field cells allow for the collection of representative sub-samples prior to, and following, tests for mineralogical characterization. Furthermore, the study of the material placed in field cells can allow for the refinement of the waste rock classification system by including quantitative mineralogical information. Likewise, the results from field cells can support the results of large scale tests such as those done on experimental piles, by demonstrating the weathering characteristics of the constituent materials. In addition, the results can also assist with scale-up by first relating the field cell results with test piles, and then with the full scale waste rock dumps.

On the other hand, Canadian Mine Environment Neutral Drainage (MEND) recommends that long-term predictions of water chemistry from waste rock dumps must be made using empirical/engineering models based on laboratory tests and field cells (MEND (Canada), 1996; MEND (Canada), 2000).

Finally, whichever test is selected, evaluation of data should be conducted throughout the project. The aim of this testing is to determine if the results are useful, if changes should be made to the schedule of sample analysis, or if the tests can be concluded. As soon as the tests indicate that the material does generate unacceptable drainage water, the focus of the prediction program should change to the evaluation of control measures (Robertson and Broughton, 1992).

2.4 Waste Rock Characterization

The potential for a mine (open pit, waste rock dumps, tailings impoundment) to generate acid/neutral drainage and release contaminants is dependent on many factors, and is site specific (USEPA, 1994). Chemical, biological and physical factors, classified into three categories (Table 2.2), are important for determining the rate of acid/neutral drainage generation. Physical factors, particularly waste rock dump permeability, are important. Dumps with high permeability have high oxygen circulation, which contributes to higher oxidation rates, hence, higher temperatures and increased oxygen ingress through convection (Akcil and Koldas, 2006). In reality, the factors affecting acid generation and neutralization are

considerably more numerous and complex. In large part, for both the acid-producing and acid-consuming minerals, mineralogical and environmental factors are extremely important (Sherlock et al., 1995).

a. **Primary** factors of acid/neutral drainage generation include sulfide minerals, water, oxygen, ferric iron, bacteria to catalyze the oxidation reaction and generated heat. Some sulfide minerals are more easily oxidized (e.g. pyrite and pyrrhotite) and hence, may have a greater impact on timing and magnitude during acid prediction analysis compared to other metal sulfides. Also important is the physical occurrence of the sulfide mineral. Well crystallized minerals will have smaller exposed surface areas than those that are disseminated.

   Both water and oxygen are necessary to generate sulfide oxidation or acid drainage. Water serves as both a reactant and a medium for bacteria in the oxidation process. Water also transports the oxidation products. A ready supply of atmospheric oxygen is required to drive the oxidation reaction. Oxygen is particularly important to maintain the rapid bacterially catalyzed oxidation at pH values below 3.5. Oxidation of sulfide minerals is significantly reduced when the concentration of oxygen in the pore spaces of mining waste units is less than 1 or 2 percent. Different bacteria are better suited to different pH levels. The type of bacteria and their population sizes change as their growth conditions are optimized. The *Acidithiobacillus ferrooxidans* has involved oxidation of pyrite; however, the bacterium may accelerate the oxidation of sulfides of antimony, gallium, molybdenum, arsenic, copper, cadmium, cobalt, nickel, lead and zinc. Environmental conditions must be favourable for bacterial growth. For example, *A. ferrooxidans* is most active in water with a pH of less than 3.2. If conditions are not favourable, the bacterial influence on acid generation will be minimal (Akcil and Koldas, 2006).

   The oxidation reaction is exothermic, with the potential to generate a large amount of heat, and therefore thermal gradients within the unit. Heat from the reaction is dissipated by thermal conduction or convection. The maximum temperature depends on the ambient atmospheric temperature, strength of the heat source, and the nature of the upper boundary. If the sulfide waste is concentrated in one area, as is the case with encapsulation, the heat source may be very strong.

b. **Secondary** factors act to either neutralize the acid produced by sulfide oxidation or may change the effluent character by adding metals ions mobilized by residual acid. Neutralization of acid by the alkalinity released when acid reacts with carbonate or silicate minerals is an important means of moderating acid production. The most common neutralizing minerals are calcite and dolomite. Products from the oxidation reaction (hydrogen ions, metal ions, etc.) may also react with other non-neutralizing constituents. Possible reactions include ion exchange on clay particles, gypsum precipitation, and the dissolution of other minerals. Dissolution of other minerals contributes to the contaminant load in the acid/neutral drainage. Examples of metals occurring in the dissolved load include aluminum, manganese, copper, lead, zinc, among others.

Table 2.2 Factors for determining the rate of acid/neutral drainage generation

Category	Factors	Description
Primary	Sulfide minerals	Oxidation reaction and rates. Physical occurrence (texture, grain size, association)
	Water	Oxidation reaction. Transport of oxidation products. Atmospheric oxygen supplier
	Oxygen content in the gas and the water	Create oxic environment
	Bacterial activity	Heat generation, increases oxidation reaction
	Ferric iron, pH, temperature	
Secondary	Carbonate minerals	Neutralization potential
Tertiary	Physical properties of material (particle size, permeability, surface area, density, specific gravity)	Weathering and breakdown processes.
	Chemical properties of material (metal content, mineralogy, liberation, association)	Oxidation reaction, oxidation rates, speciation, solubility or dissolution
	Hydrology (saturation, flowrate, hydraulic head and gradient)	Flows displacement

c. **Tertiary** factors affecting acid/neutral drainage are the physical characteristics of the material, the placement method of acid generating and acid neutralizing materials, and the hydrologic regime in the vicinity. The physical characteristics of the material, including particle size, permeability, and physical weathering characteristics, are important to the acid/neutral drainage. Particle size is a fundamental concern since it affects the surface area exposed to weathering and oxidation. Very coarse grain material, as is found in waste dumps, exposes less surface area but may allow air and water to penetrate deeper into the unit, exposing more material to oxidation and ultimately producing more acid/neutral drainage. Air circulation in coarse material is aided by wind, changes in barometric pressure, and possibly convective gas flow caused by heat generated by the oxidation reaction. In contrast, fine-grain material may retard air and very fine material may limit water flow; however, finer grains expose more surface area to oxidation. The relationships between particle size, surface area, and oxidation play a prominent role in acid/neutral rock drainage prediction methods. As materials weather with time, particle size is reduced, exposing larger amounts of surface area and changing the physical characteristics of the unit.

All these factors act mostly in conjunction, and each of them influences the potential for acid generation. They are therefore important considerations for the long-term (USEPA, 1994).

Particle size distribution (PSD) is generally used for defining the fine and coarse size fractions where weathering processes can occur. In waste rock, where only a small proportion of the whole is physically available to react, greater prediction accuracy will be achieved by selectively analyzing the “reactive” size fraction. This is particularly important for a waste rock such as marble or hornfels, where most of the mass occurs in coarse particles (Price, 1997).

Since the surface area (SA) of exposed sulfide minerals is directly proportional to mineral-water reaction rates, it is necessary to determine the specific surface area (SSA) to understand weathering at the field scales. Surface area increases exponentially as particle size decreases, such that finer particles have a

higher SA. As a consequence, fines particles contribute most to metal leaching, and are the focus of studies on weathering processes. Even though the concept that surface area is inversely proportional to particle size is well known; for porous materials such as limestone or marble, surface area can be even higher in their coarse particles because of the surface area of the pores, which greatly increases the total surface area of the particles.

While in principle, all solid surfaces in soils and waste rock can act as adsorbers, solid phases with a large specific surface area (SSA) will adsorb most, and the adsorption capacity therefore depends of the grain size. Solids with large SSA reside in the clay fraction (<2 μm), but coarser grains in a sediment are often coated with organic matter and iron oxyhydroxides. The adsorption capacity is therefore linked to the clay content (fraction <2 μm), clay minerals, organic matter (%C), and oxide or hydroxide content.

Most sorption is connected with the specific binding of heavy metals to the variable charge surfaces of oxides and organic matter. Their surface charge can be positive or negative depending on the pH and the solution composition. Variable charge solids are important in regulating the mobility of both positively charged heavy metals such as Pb^{2+} and Zn^{2+}. At circumneutral pH, the heavy metals remain fixed by sorption or soil equilibriums (Appelo and Postma, 2005).

Some studies assume that most of the weatherable primary silicates are in the coarse size fractions (White and Brantley, 2003)

2.5 Weathering of Neutralizing Minerals

The dissolution and alteration of various minerals can contribute to the neutralization of acid. Neutralizing minerals include: (1) calcium and magnesium-bearing carbonates; (2) oxides and hydroxides of calcium, magnesium, and aluminum; (3) soluble, non-resistant silicate minerals; and (4) phosphates (primarily apatite). The primary sink for acidity is silicate weathering and, as a consequence, chemical weathering results in the dissolution of species that determine the alkalinity of water.

The dissolved carbonate system is also an important factor in determining the neutralizing capacity of water. Depending on the pH of the solution, the carbonic acid will tend to dissociate to hydrogen [H^+], bicarbonate (HCO_3^-) and carbonate (CO_3^{2-}) ions. The dominant species in solution are: H_2CO_3 at pH < 6.3; HCO_3^- at 6.3 < pH < 10.3; and CO_3^{2-} at pH > 10.3. In general, the role of carbonates is important because of the reactivity of the minerals and their resultant neutralizing capacity. The role of silicates in this process is, however, poorly understood. Some silicate neutralization capacity can be identified based on elevated concentrations of silica and aluminum in tailings water and within waste rock drainage. If calculations of the buffer intensity and neutralizing capacity of simple carbonate and silicate systems would be carried out, it would be indicated that the acid-neutralizing capacity of silicate minerals is greater than the carbonates and thermodynamically possible. However, the weathering of silicate minerals occurs more slowly (except with regard to the clays) than it does for the more reactive carbonate minerals (Langmuir, 1997). It is for this reason that the most important buffering that occurs within or near surface natural waters is by the carbonate system (Sherlock et al., 1995).

2.5.1 Mineral Solubility

Each mineral has a different dissolution rate; therefore not all minerals weather at the same rate.

Carbonates

Calcite dissolution can occur in open or closed systems depending on whether carbon dioxide is available for gas exchange. At neutral pH, the two types of dissolution may be represented by Equations 2.12 and 2.13:

Open sytem: $CaCO_{3(S)} + CO_{2(g)} + H_2O_{(l)} = Ca^{2+}_{(aq)} + 2HCO_3^-{}_{(aq)}$ Eq. 2.12

Closed system: $CaCO_{3(S)} + H^+_{(aq)} = Ca^{2+}_{(aq)} + HCO_3^-{}_{(aq)}$ Eq. 2.13

Open systems have a greater solubility of calcite than do closed systems. Eq. 2.12 also indicates that within an open system, half the dissolved carbonate within solution is from calcite dissolution and half is from carbon dioxide dissolution. These equations have been used to describe acid neutralization within tailings and waste rock piles (Ferguson and Morin, 1991).

Silicates

Silicate minerals are composed of silicon atoms coordinated with four oxygen atoms in a regular tetrahedron. In general, there is an increase in silicate stability and resistance to weathering with increasing bonding between the silica tetrahedral. For example, the dissolution of the end-member of plagioclase feldspar, anorthite, may be presented as congruent (Eq. 2.14) or incongruent (Eq. 2.15):

$CaAl_2Si_2O_{8(S)} + 2H^+_{(aq)} + 6H_2O_{(l)} = Ca^{2+}_{(aq)} + 2Al^{3+}_{(aq)} + 2H_4SiO_{4(s)} + 6OH^-_{(aq)}$ Eq. 2.14

$CaAl_2Si_2O_{8(S)} + 2H^+_{(aq)} + H_2O_{(l)} = Ca^{2+}_{(aq)} + Al_2Si_2O_5(OH)_{4(s)}$ Eq. 2.15

Factors determining whether dissolution is congruent or incongruent include mineral structure and composition, as well as external environmental factors. Common end products of chemical weathering and alteration processes of many silicates are clay minerals.

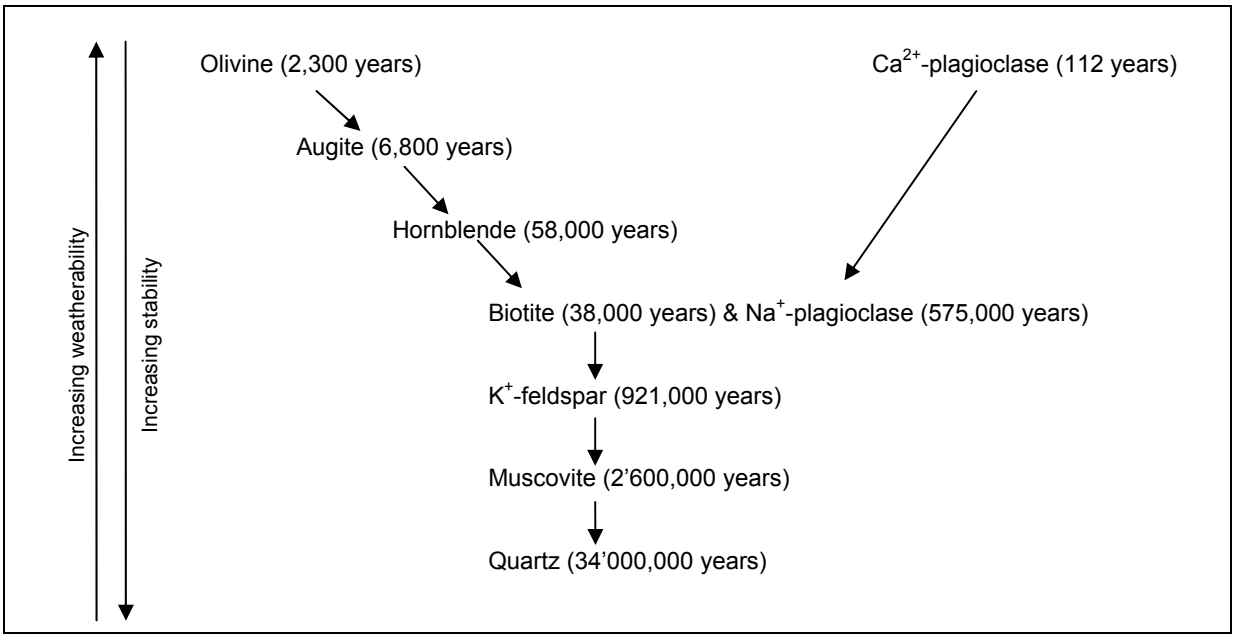

Figure 2.1 Goldich's sequence of increasing weatherability and/or stability of main silicate minerals

Figure 2.1 shows the weatherability of common silicate minerals for a certain particle size. Assuming olivine = forsterite, augite = diopside, hornblende = tremolite, Ca-plagioclase = anorthite, Na-plagioclase = albite, K-feldspar = microline, and muscovite is comparable with clay minerals such as illite, then olivine and Ca-plagioclase are listed as the most easily weatherable minerals, and quartz as the mineral most resistant to weathering (Appelo and Postma, 2005; Langmuir, 1997).

2.5.2 Comparison of Dissolution Rates

Temperature is an important factor that controlling the dissolution rate of carbonates and silicates, as well as the sulfide minerals oxidation. Furthermore, mineral solubility also increases with temperature. However, both calcite and gypsum are the exceptions to this rule since their solubility decreases if temperature increases. Therefore, in mining wastes containing carbonate and sulfide minerals, if temperatures are increased due to exothemic oxidation-reactions given by bacteria for instance, then the oxidation rate will increase as well. However, carbonate mineral solubility could decrease, resulting in reduced neutralization potential (Langmuir, 1997; Sherlock et al., 1995).

Other factors influencing the dissolution rate of both calcite and silicate, but which are not included in the rate equation, are mineral composition and structure (texture, liberation, association), and these determine the number of reactive sites. The more complex the bonding within the mineral, the more stable and insoluble it will be. A combination of different factors may origin a reactivity index, which may be used to classify the material.

2.5.3 Rates of Rock Weathering

For rocks such as calcite which contain carbonate minerals, weathering and dissolution rates can be of the same order of magnitude as the redox reaction rates responsible for acid generation in sulfidic mining wastes. However, for many other carbonate and silicate minerals, weathering rates are usually in orders of magnitude lower than sulfide mineral oxidation (e.g. pyrite), even though these minerals often contribute to the neutralization potential measured through ABA testing. Therefore, it is important to recognize that if calcite or other carbonate minerals coexist with silicate minerals, the calcite will pre-empt the role of acid neutralization through its dissolution, even though the silicate minerals may potentially have a greater neutralization capacity through alteration processes (Sherlock et al., 1995).

In addition, sulfide minerals such as pyrite can oxidize at various rates, but in most cases the resulting acid-production rates will exceed the specific dissolution rates of the neutralizing minerals. For reactive carbonate minerals such as calcite, rates can be of the same order as acid-production rates. However, in an oxic environment and at circumneutral, laboratory studies suggest that calcite can dissolve up to 4 orders of magnitude faster than pyrite (Stromberg and Banwart, 1999b). On the other hand, other carbonates and the silicate minerals can weather at orders of magnitude which are slower than sulfide mineral oxidation, leading to acidic drainage and unacceptable water quality.

Factors mentioned earlier, including individual chemical reactions, secondary alteration and precipitation processes, ion exchange and adsorption, and biological processes will affect the element release or rock weathering rates in the field because these factors act according to processes that are site-specific. In addition to factors that control mineral weathering rates, there are other factors that contribute to the

overall rate of chemical rock weathering; these include temperature, mineral composition (texture, association), solid solution, particle size, and surface area. Climate (rainfall) and local redox conditions also influence mineral and rock dissolution rates. As such, with increased flushing, the dissolution rate also increases.

2.6 Mineralogical Characterization

Although static tests and chemical assays can provide a measure of the concentrations of various elements in a bulk sample or its specific size fractions, these tests do not identify the contributing mineral phases, leading to a significant limitation for prediction, and therefore waste management. The mineralogical forms determine drainage chemistry quality. For example, total iron identified by whole-rock analysis may occur in acid-generating pyrite, acid-neutralizing calcium-iron carbonate, and/or some for iron oxides/hydroxides. Identification of the participating mineral phases is therefore necessary for interpreting kinetic test (e.g. field cells) results and most other aspects involved in predicting drainage chemistry. However, some omissions in mineralogy measurements are due to a the following factors (Price, 1997):

- Mineralogy includes a wide range of factors and properties beyond the already very difficult task of assigning a mineral name; critical parameters include grain size, elemental composition and elemental distribution.
- Mineralogy terminology is often imprecise for the purpose of metal leaching prediction. For example, the term “plagioclase” covers a range of minerals which differ greatly in their weathering capability and consequent effective field neutralization potential. Minerals can be very difficult to identify by conventional techniques. For specific mineral identification, more sophisticated techniques are recommended.
- All available mineralogical procedures have major flaws or limitations when these are used as a tool for prediction.
- More accurate and comprehensive methods are expensive.

Although it has rarely been investigated in any detail, mineralogy plays a great role in determining the rates of elemental release, as well as acid generation and neutralization. However, it must be complemented with site-specific information for a better prediction of drainage chemistry.

Even though initial comprehensive mineralogical information is usually obtained by visual rock description, this procedure is subjective and its accuracy of identification depends largely on the experience of practitioners and their familiarity with the local geology, contributing to the prediction of drainage quality.

In as much as the mineral constituents of a geological sample ultimately determine its overall acid/neutral generation potential, the next step in predicting the metal leaching potential of a sample or interpreting its static and kinetic tests, should include an accurate measurement of mineral abundance. The most common techniques to acquire mineral abundance data are: petrographic analysis through optical microscopy, X-ray diffraction (XRD) analysis and scanning electron microscopy (SEM).

A **petrographic examination** is a microscopic examination of thin sections, or polished thin sections, preferably of sized fractions. This technique allows for the identification of minerals and their specific features including alteration, grain size, associations and estimations of modal analysis. These can be obtained either by a visual scan (which takes almost 30 minutes) or through a more tedious point-counting procedure. However, some disadvantages include: subsampling errors may be large for coarse fragments; thin sections are very small and may not be representative; minerals at levels less than roughly 0.5 wt. % will not normally be detected. Furthermore, this method is not used to detect features smaller than 100 μm. Quantitative analysis is labour-intensive with results that are somewhat subjective. Even though the point counting procedure can be used to make accurate estimations of mineral percentages, it is very time consuming. Therefore, it is better to carry out analyses using submicroscopic procedures such as SEM.

X-ray diffraction (XRD) can be used for a general mineralogical assessment or to identify specific silicate minerals and for modal analysis. Semi-quantitative mineralogical data can be derived through a direct comparison of reflection peak sizes. Unlike petrographic techniques, XRD detection is not limited to grains larger than 100 μm, and is generally carried out on a pulverized sample. Disadvantages with XRD are that it has a poor precision rate, it is unable to detect minor or trace mineral constituents (e.g. sulfide minerals with less than 1 wt.%), some minerals cannot be distinguished, and mineral identification is often operator-dependent.

More sophisticated investigative procedures can be used to identify fine-grained minerals, to describe small, potentially important, mineral alteration features, and to identify the elemental composition of specific minerals. The general availability of **scanning electron microscope** (SEM) instrumentation makes point-counting using a SEM-EDS setup an increasingly attractive option if it can be run automatically.

On the other hand, further important information for the prediction of drainage chemistry involves the availability of the mineral for leaching. This can be obtained through liberation by free surface, and mineral association combined with modal mineralogy data by using a SEM.

Nevertheless, in the last two decades, a new and sophisticated technique has been developed for modern digital mine planning, plant design and mineral processing operations. Traditionally, the measurement of these ore characteristics employed the tools of an optical microscope and/or a semi-automated SEM. These methods are time consuming, costly and frequently produce semi-quantitative results from data sets that are too small to be statistically valid.

Recently, modern SEM-based quantitative mineralogy tools have advanced rapidly. These have increasing computer power, improved SEM hardware and sophisticated image analysis methods. Texture resolutions can now be submicron. SEM measurement times have been reduced to less than an hour for simple analyses, where they previously required many hours. Through image analysis, particle sections are recognized and separated, and the mineral grains within are delineated for discrete X-ray analysis to determine mineralogy. The modern tools do not only increase the speed and accuracy of liberation analysis, but also enhance measurement automation. The instruments that allow for the gathering of

these types of results are the QEM*SCAM or QEM*SEM (Automated-Scanning electron microscopy) and MLA (Mineral Liberation Analyzer).

2.6.1 Mineral Liberation Analyzer (MLA)

The MLA (Figure 2.2) was first presented as a new development in the field of SEM-based automated mineral measurement tools in 1997. It is an automated mineral analysis system that can identify minerals in polished sections of drill core, particulate or waste rock materials, and quantify a wide range of mineral characteristics, such as mineral abundance, type, grain size, liberation, and association, among others. Mineral texture and liberation potential are fundamental properties of ore, and they drive its economic treatment; the same concept can be used to evaluate the weathering process in a waste rock and as such to anticipate the occurrence of negative environmental impacts. MLA uses back-scattered electron (BSE) image analysis, which is fundamental to mineral liberation analysis. The principal image analysis functions used by the MLA are known as particle de-agglomeration (which detects agglomerates and separates them according a set of predetermined parameters) and phase segmentation (which identifies all distinct mineral phases (or grains) and defines their boundaries accurately). For best MLA analysis results, typical particle sizes mounted in polished sections should range from 10 μm to 1 mm, and should preferably be of a defined narrow size fraction. MLA performs measurements according to several X-ray analyses including point X-ray analysis (typically >2000 counts), area X-ray analysis, and X-ray mapping.

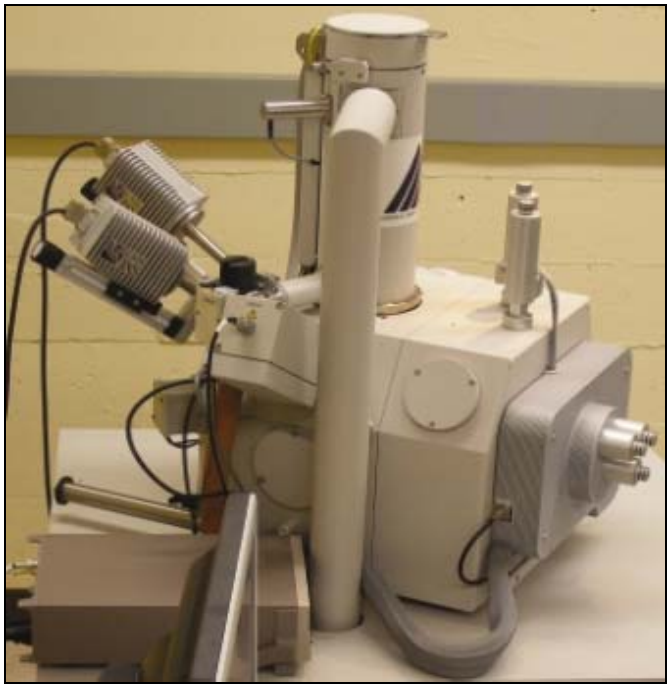

Figure 2.2 Mineral Liberation Analyzer (MLA) at JKTech's property (http://www.jktech.com.au)

MLA analyses can be carried out through many measurement modes combining the fundamental BSE image and the various X-ray analyses. The principal modes include: X-ray modal analysis (XMOD), standard BSE liberation analysis (BSE), extended BSE liberation analysis (XBSE), Ford analysis or grain-based X-ray mapping (GXMAP), sparse phase liberation analysis (SPL), rare phase search (RPS), Latti

analysis (SXBSE), Schouwstra analysis (SPL-dual zoom). These measurement modes are designed to accommodate many different mineralogical information requirements (Fandrich et al., 2006). However, as a tool to support the prediction of drainage chemistry during waste management, XMOD and XBSE modes would be preferred for the analysis of mineral phases, liberation, association, and grain sizes.

XMOD is the classical point counting method in which mineral identification is determined by one X-ray analysis at each counting point. This mode uses BSE imaging to discriminate particle matter from its background and then collects one X-ray spectrum from each grid point across the particle. The X-ray spectra are saved for off-line classification. This method only produces modal mineralogy information, i.e. percentages of the mineral phases present in the sample.

XBSE implements area X-ray analysis to efficiently and effectively analyze ore or waste rock samples containing mineral phases with sufficient BSE contrast to ensure effective segmentation. The high resolution of BSE imaging for grain boundary definition, and the speed of single X-ray mineral identification make this method ideal for a great majority of mineralogical samples. This mode is used fundamentally to identify liberation by particle composition or by free surface of the mineral.

3 WASTE ROCK CHARACTERIZATION

3.1 Introduction

As was indicated in Chapter 1, material from conical pile B was used to determine the physical and chemical characterization of the waste rock, which includes a particle size analysis, surface area and particle density determination, chemistry assay by size fractions and mineralogy, and liberation using the Mineral Liberation Analyzer (MLA). Furthermore, conical pile C was used to carry out chemistry assay for the bulk or head sample, acid-base accounting (ABA) analysis, and moisture content. The different tests are described below.

3.2 Preparation of Sample

Five samples (Figure 3.1) which all came from conical pile B: FC-0 (black marble), FC-1 (diopside marble), FC-2 (diopside marble), FC-3 (diopside marble), and FC-4 (gray hornfels) were processed and prepared at the University of British Columbia in Canada using the following procedure:

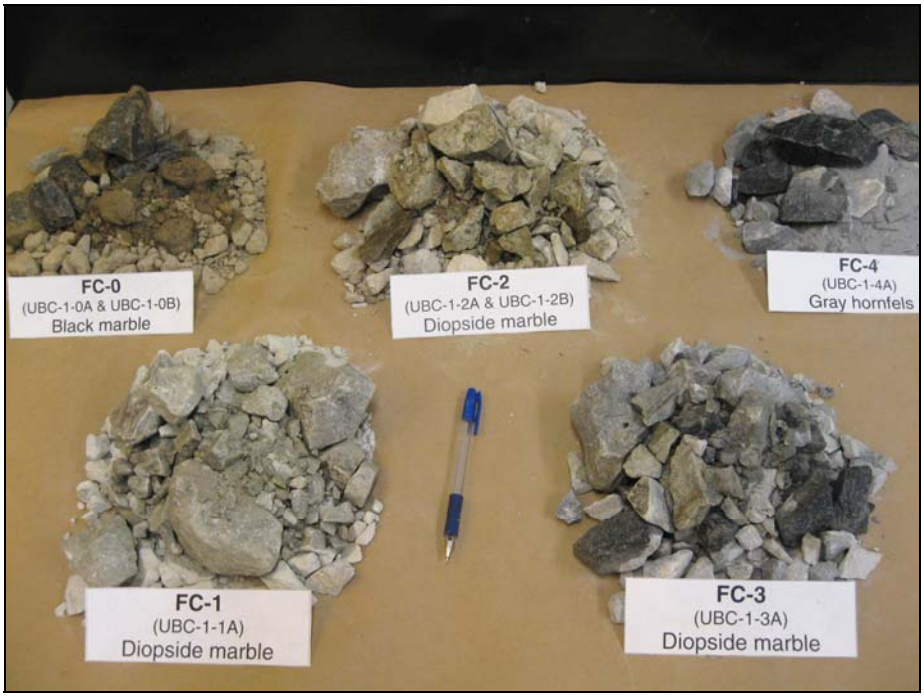

Figure 3.1 Bulk Class B wet/dry waste rock samples used in different tests

- Each sample was spread out, homogenized and mixed with a shovel over a clean, dry plastic cloth; they were then were coned, quartered and riffled several times using a clean Gilson Splitter Model SP-1, P-500 (Figure 3.2).
- Subsequently, each sample was separated into two portions (Table 3.1). Only the first portion was used to carry out the different tests which are outlined below.

Figure 3.2 Riffling by using the Gilson Splitter Model SP-1of Class B waste rock samples before starting the laboratory testing

Table 3.1 Waste rock sample portions after riffling the Conical Pile B

Sample code	Wet waste rock mass (kg)		
	P-1	P-2	Total
FC-0	133.7	137.0	270.7
FC-1	156.4	156.3	312.7
FC-2	160.1	173.5	333.6
FC-3	141.5	135.5	277.0
FC-4	141.1	140.9	282.0

Seven samples in all (including two duplicates) from conical pile C: UBC-1-0A/0B (black marble), UBC-1-1A (diopside marble), UBC-1-2A/2B (diopside marble), UBC-1-3A (diopside marble), and UBC-1-4A (gray hornfels) were sent to ALS Environmental Laboratory in Lima, Peru to determine the solid phase element content. The procedure used is described later.

3.3 Particle Size Analysis

Since only relatively small amounts of material were used in the sizing process, it is essential that the sample be representative of the bulk material; therefore portion C-1 (approximately 150 kg) indicated in Table 3.1 was used to conduct a particle size analysis. A good analysis of the different size fractions will be useful for beginning the understanding of the geochemical behaviour in the field cells. Size analysis is of great importance in establishing the degree of liberation of the values from the sulfide minerals at various particle sizes (Wills et al., 2006). Two methods of size analysis were utilized, the wet/dry sieving method and the Elutriation technique.

3.3.1 Sieving Method

The sieving method was conducted following the distinguished standard methods. Two stainless steel cloth sieve types were used: The US Standard Sieve Trays (45 cm x 65 cm) and 8 inch standard round Gilson sieves. By following the standard square root of 2 ($\sqrt{2}$ = 1.414) series, twenty size fractions were selected: 100 mm (4”), 75 mm (3”), 50 mm (2”), 37.5 mm (1.5”), 25 mm (1”), 19 mm (3/4”), 12.5 mm (1/2”), 9.5 mm (3/8”), 6.3 mm (1/4”), 4.75 mm (#4), 3.35 mm (#6), 2.36 mm (#8), 1.18 mm (#16), 600 μm (#30), 300 μm (#50), 150 μm (#100), 106 μm (#140), 75 μm (#200), 53 μm (#270) and <53 μm. Cobble and coarse materials (>6.3 mm) were wet sieved by hand using screen trays; whereas the sand and fine sizes (until <53 μm) were wet and dry sieved by round sieves with a vibrating sieve shaker (ro-tap). The finest size was filtered with a pressure filter using a 0.45 μm paper filter. The samples were dried at 45 – 50°C in an oven (Estrin, model 100-DO) which was controlled by a portable thermometer. Figure 3.3 shows the screening process that was followed.

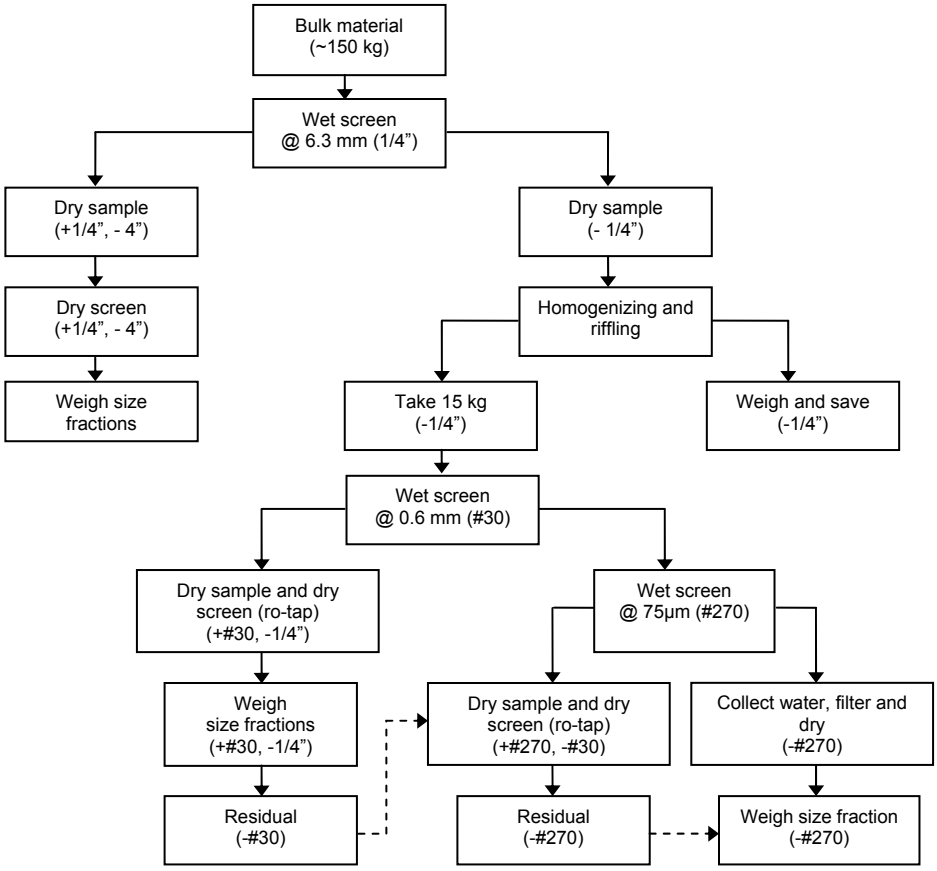

Figure 3.3 Wet and dry sieving process of Class B waste rock material

3.3.2 Elutriation Technique

As sieving is rarely carried out on a routine basis below 38 μm, a sub-sieving elutriation technique was used, although at the fine end of the scale, separation becomes impractical below 10 μm (Wills et al., 2006). The Warman cyclosizer, Model No M4 (Warman International, Australia) was utilized as an

elutriator. It is a laboratory precision apparatus used for the rapid and accurate determination of particle size distribution within the sub-sieve range, and consists of five 3 inches diameter cyclones arranged in series such that the overflow of one unit is the feed to the next unit (Figure 3.4). Fines particles (<53 μm) were separated according to their Stokesian settling characteristics by a principle based on the well known hydraulic cyclone principle. The cyclosizer collected all particles into a single cyclone. The individual units are inverted in relation to conventional cyclone arrangements, and at the apex of each, a chamber is situated so that the discharge is effectively closed. Water was pumped through the units at a controlled rate (11.6 L/min), and a waste rock sample of 100 grams was introduced ahead of the cyclones. The tangential entry into the cyclones induced the liquid to spin, resulting in a portion of the liquid, together with the faster-setting particles, reporting to the apex opening, while the remainder of the liquid, together with the slower settling particles, was discharged through the vortex outlet and into the next cyclone in the series.

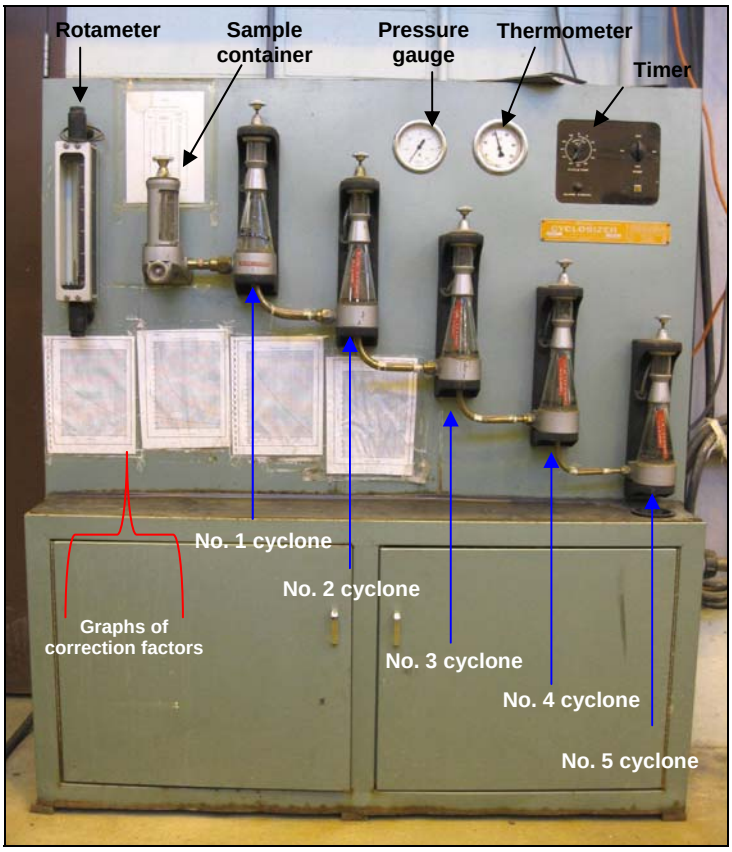

Figure 3.4 The Warman cyclosizer used as an elutriator during the particle size analysis

The cyclosizer has clearly defined Limiting Particle Separation Size (LPSS) at standard values of the operating variables: water flow rate (11.6 L/min), water temperature (20°C), specific gravity of the material (2.65), and elutriation time (infinite). If these values differ, the Effective Particle Separation Size (EPSS) needs to be computed. During the test, only the flow rate was kept as a standard variable, while the others variables were specified for each material. To correct for practical operation at other levels of these variables, a set of correction graphs were employed. These graphs provide a correction factor for each

variable within the specified operation range. The relationship between LPSS and EPSS for any cyclone is given by:

$$d_e = d_l . f_1 . f_2 . f_3 . f_4 \qquad \text{Eq. 3.1}$$

where d_e = effective particle separation size of cyclone

d_l = limiting particle separation size of the same cyclone, and

f_1, f_2, f_3, f_4 are the separate correction factors for water flow rate, water temperature, specific gravity and time, respectively.

Thus, the particle size analysis adjusted for EPSS of five samples was obtained. Its calculations are summarized in Appendix C1 (Table C1.1). Considering that the size fractions for all samples were close to each other, for practical purposes, especially for plotting, the average EPSS fractions were determined as 38 μm, 28 μm, 20 μm, 15 μm, 10 μm and <10 μm for all samples. In order to plot weight proportions, the size fractions N_i, given with their representative sizes d_{pi}, were obtained by using Eq. 3.2, which shows the geometric mean of the upper and lower boundaries of the representative size (King, 2001).

$$d_{pi} = (D_i . D_{i-1})^{1/2} \qquad \text{Eq. 3.2}$$

where d_{pi} = representative size of each size fraction i (m)

D_i = upper mesh size of each size fraction i (m)

D_{i-1} = lower mesh size of each size fraction i (m)

However, since $D_N = 0$ and D_0 is undefined, Eq. 3.2 cannot be used to calculate the representative sizes in the two extreme size fractions. These sizes are calculated using

$$d_{p1} = \frac{d_{p2}^2}{d_{p3}} \qquad \text{Eq. 3.3}$$

$$d_{pN} = \frac{d_{pN-1}^2}{d_{pN-2}} \qquad \text{Eq. 3.4}$$

where d_{p1} = the upper extreme representative size of sample (m)

d_{pN} = the lowest extreme representative size of sample (m)

These equations project the sequence d_{pi} as a geometric progression into the two extreme size fractions.

In the next phase, both sieving and elutriation method results were combined and the particle size distribution of the five rock samples was plotted in a semi-log diagram shown in Figure 3.5 and Appendix C1 (Table C1.2). The diopside marble samples were coarser than the black marble and gray hornfels samples. The particle mass that was coarser than 2 mm was 73 wt.%, 82 wt.%, 90 wt.%, 82 wt.% and 72 wt.% for samples FC-0, FC-1, FC-2, FC-3 and FC-4, respectively. Therefore, sandy silt material (below 2 mm) was present between 10 – 30 wt.% in most of the samples. The D_{50} (median particle size) ranged from approximately 12 to 32 mm for all samples. The P80 ranged between below 35 and 75 mm for all samples. Likewise, the black marble sample contained almost 8 wt.% of the finest size material (below 0.01 mm), mostly as clay mineral mixed with hydrous ferric oxides (HFO) or iron oxyhydroxides. Results were higher in this sample than in other samples, where the finest size fraction amounts ranged between 1.6 – 2.6 wt.%. Lithology dependence is the main reason for the difference in particle size distribution in the waste rock samples. The diopside marble samples have a uniform particle size distribution, suggesting that the minerals are distributed over all size fractions. In contrast, the black marble and gray hornfels samples have irregular mass distribution, indicating that some mineral phases are present in specific size fractions.

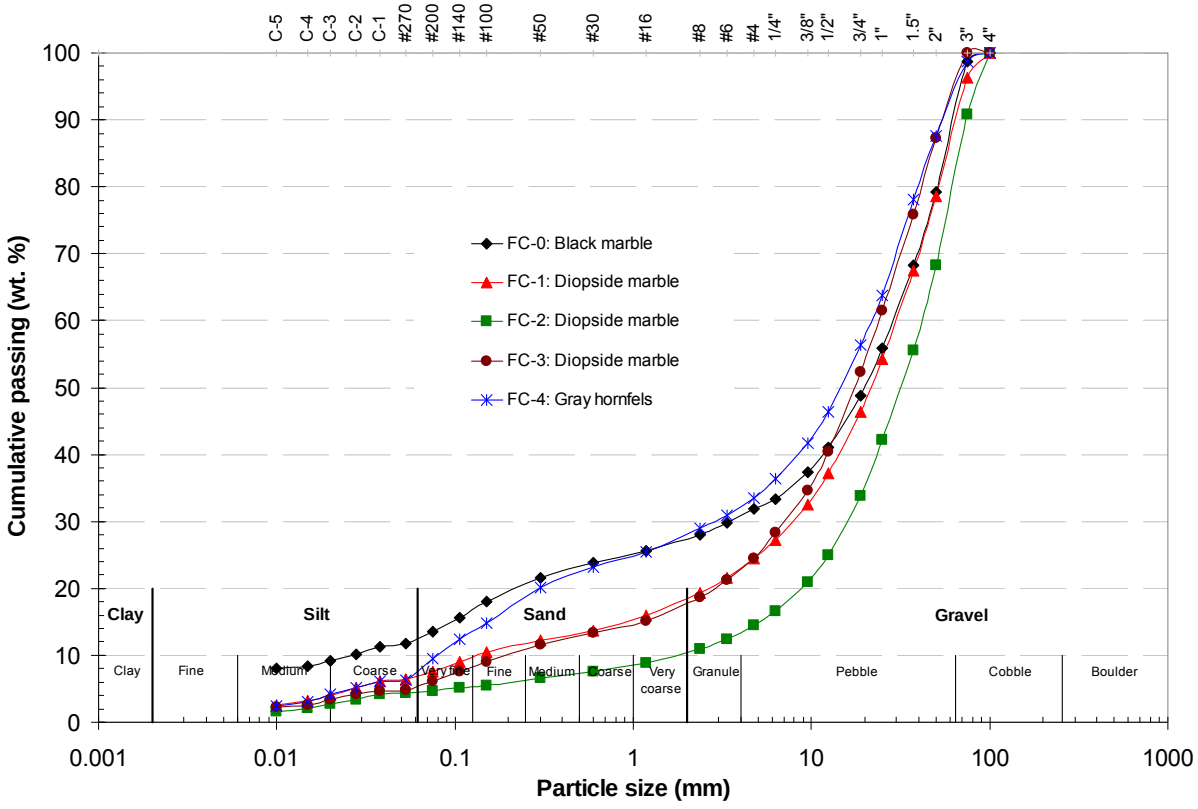

Figure 3.5 Particle size distribution of Class B waste rock samples

An assessment was done at the finest size fraction (<53 μm). Approximately 12 wt.% of the whole-rock was present in this size fraction in the black marble (FC-0) sample. This amount was found to be higher when compared to the other four samples, whose amounts ranged from 1.6 to 3.3 wt.%. Therefore, if an

average of 2.5 wt.% is considered as a typical distribution at the finest size fraction (<53 μm), independently of their properties, then approximately 80% (9.5 wt.% of 12 wt.%) can be considered as clayey silt particles. However, according to the soil classification system, between 6 – 8 wt.% (approximately 50 – 67% in amount of the <53 μm size fraction) of FC-0 sample is considered to be clay particles, which can be fully conformed by clay minerals mixed with HFO or iron oxyhydroxide minerals (Figure 3.5). This amount could contribute to the high surface area at the finest size fraction. Furthermore, the clay minerals, HFO and iron oxyhydroxides could play an important role in geochemical processes.

Gravel, sand, silt and clay, and their sub-classifications were taken from the soil classification system (Bartram et al., 1996; Carter et al., 2008; Dana et al., 1993; Klein et al., 2002; Morris and Johnson, 1967).

3.4 Density Determination

Particle, true or real density is defined as the ratio of the mass to the volume occupied by that mass. Therefore, the contribution to the volume made by pores or internal voids must be subtracted when measuring the true density. If the powder or material has no porosity, true density can be measured by displacement on any fluid in which the solid remains inert (Lowell, 2004). Usually, however, the solid particles contain pores, cracks, or crevices such as in the marble and hornfels waste rock which was studied, where the rock could not easily be completely penetrated by a displaced liquid. In these instances, the particle or true density can be measured by using a gas or air in place of the displaced liquid. Thus, the air-comparison pycnometer was selected for measuring the volume of each size fraction for all samples.

The air-comparison pycnometer consists of two chambers (reference=A, measuring=B), two handwheels, a coupling valve connecting the two chambers, a differential pressure indicator (scale), and a counter calibrated in cubic centimetres (Figure 3.6). When the coupling valve is closed, any change in position of the sample handwheel must be offset by a change in the reference handwheel in order to maintain equal pressure on each side of the differential pressure indicator. When the reference handwheel reaches its final stop (part 2 on Figure 3.6), the counter reads the volume of the sample (V_x) which is proportional to the difference in distance (d_x) each handwheel has moved. Thus, volumes of Class B waste rock were measured with a Beckman Model 930 Air Comparison Pycnometer (Beckman Instruments, Fullerton, CA, 92634).

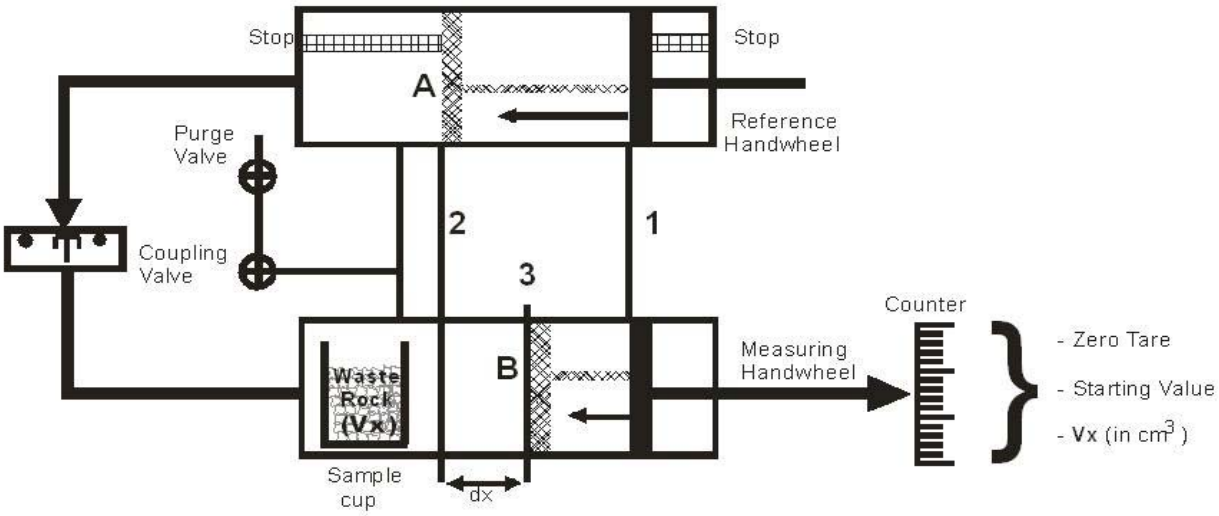

Figure 3.6 Diagram of an air-comparison pycnometer

Dry particles above 6.3 mm (1/4 inch) were crushed, following which a representative sample was taken. Samples below 6.3 mm were measured keeping their own size fraction. The steel sample cup was filled up to 95%, and following the procedure explained above (Treat et al., 1987), the volume was obtained. Samples were then weighed. The volume and weight of each sample was measured twice or three times. Once these were determined, the particle or true density (ρ) was readily calculated by using Eq. 3.5.

$$\rho = \frac{w_d}{V_x} \qquad \text{Eq. 3.5}$$

where ρ = particle or true density (kg/m^3)

w_d = dry weight of the sample (kg), and

V_x = volume of the sample (m^3).

Previously, ball bearings with known volumes were used for calibrating the air pycnometer. A calibration curve (Appendix C2, Figure C2.1) was used to adjust the volume values measured with the instrument.
In order to validate the density values obtained with the air pycnometer, these were compared with the values obtained by using the standard traditional displacement method (Carter et al., 2008; Figura and Teixeira, 2007), determining difference errors of less than 2%. For the displacement method procedure, the same sample measured with the air pycnometer was placed within a 200 mL volumetric flask. The flask then filled up with water. The samples inside and outside the flasks were weighed, and by the differences of volumes and masses found, the densities were obtained. Table 3.2 and Table C2.8 show the particle density values obtained through both methods.

Table 3.2 Waste rock volume values obtained by using the air pycnometer and water displacement method for determining particle density

Sample code	Representative size (mm)	Volume (g/cm^3)		
		Air pycnometer	Water displacement	Error
FC-0-E	30.6	2.75	2.74	0.01
FC-0-I	7.7	2.74	2.71	0.01
FC-0-N	0.8	2.80	2.77	0.01
FC-0-S	0.063	2.75	2.71	0.02
FC-2-E	30.6	3.12	3.09	0.01
FC-2-I	7.7	3.15	3.12	0.01
FC-2-N	0.8	3.13	3.11	0.01
FC-2-R	0.089	3.03	2.93	0.02

Consequently, average particle density values for all size fractions were computed for final results (Figure 3.7 and Appendix C2, Table C2.3 to Table C2.7). In most of the samples, particles below 0.3 mm were found to be slightly less dense than the coarse material, except in the gray hornfels sample where the density values were similar in all size fractions. The diopside marble samples were denser than the black marble and gray hornfels samples, because diopside mineral has a high density (3200 kg/m^3) when compared to calcite (2710 kg/m^3)(Dana et al., 1993).

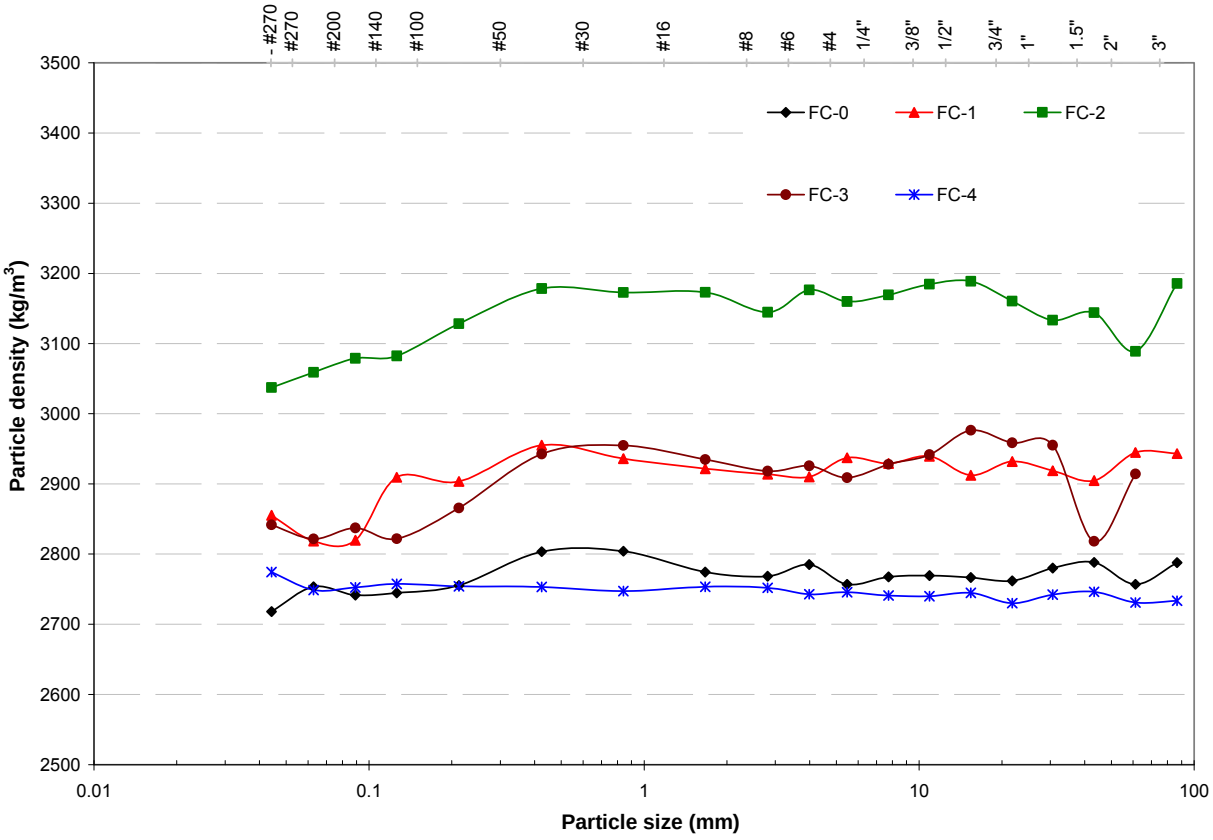

Figure 3.7 Particle density for all size fractions in Class B samples placed in the field cells

In addition, particle density per sample was computed averaging all size fractions results (Table 3.3). Since particle density should be higher than whole-core (host-rock units) density, this was verified. Most of the samples have a relatively higher particle density than the whole-core density which was reported by Antamina; although the diopside marble samples were found to have much higher particle density ranging from 2,900 to 3,140 kg/m^3. This result is due to the diopside content, as was mentioned above.
Finally, particle density results were used to obtain specific surface area through geometrical estimation.

3.5 Surface Area Determination

Real surface area is affected by particle size, shape, voids, porosity and roughness. Samples from each size fraction were analyzed to determine their specific surface area (SSA). SSA for samples above 6.3 mm (1/4 inch) was determined by Geometrical Estimation (SSA_{GE}) and the BET method (SSA_{BET}) was used for samples below 6.3 mm.

Table 3.3 Average particle density results compared with whole-host density given by Antamina for Class B material

Sample code	Rock type	Particle density	Whole-core density
		(kg/m^3)	(kg/m^3)
FC-0	Black marble	2,770	2,710
FC-1	Diopside marble	2,910	2,710
FC-2	Diopside marble	3,140	2,770
FC-3	Diopside marble	2,900	2,770
FC-4	Gray hornfels	2,750	2,780

3.5.1 The Geometrical Estimation (GE) Method

SSA_{GE} results were estimated based on the particle geometric diameter and particle density results. These results do not take into account the surface area in the pore spaces and the surface area that results from the surface roughness. Also, a specific shape factor should be considered for irregular particles such as for waste rocks (Brantley and Mellott, 2000; Figura and Teixeira, 2007; Lowell, 2004). Nevertheless, the estimation was determined, as is outlined below:

Specific surface area based on volume (A_v) was calculated as:

$$A_v = \frac{A}{V} \qquad \text{Eq. 3.6}$$

where, A_v = specific surface area based on volume (m^{-1})

A = sectional area of the specific solid (m^2)

V = volume of the specific solid (m^3)

SSA_{GE} were estimated using equivalent diameters for individual particles with irregular shapes, where the shape factor of a sphere was assumed. Thus, Eq. 3.6 was noted as:

$$A_v = \frac{\pi . d_A^2}{\frac{\pi}{6} . d_V^3} \qquad \text{Eq. 3.7}$$

where, d_A, d_V diameter of a sphere (m)

Then with $d_A = d_V = d$, Eq. 3.7 is simplified to:

$$A_v = \frac{6}{d} \qquad \text{Eq. 3.8}$$

where, d is the geometric diameter of the particle (m) and was obtained by measuring samples sides as is shown in Figure 3.8.

Twenty particles in all for nine coarse size fractions (3", 2", 1.5", 1", ¾", ½", 3/8", ¼" and #4 mesh) of 5 samples were measured, and using Eq. 3.9, a geometrical average diameter was obtained. Subsequently, an arithmetic average of the geometrical diameters was computed as the diameter for each size fraction (Eq. 3.10).

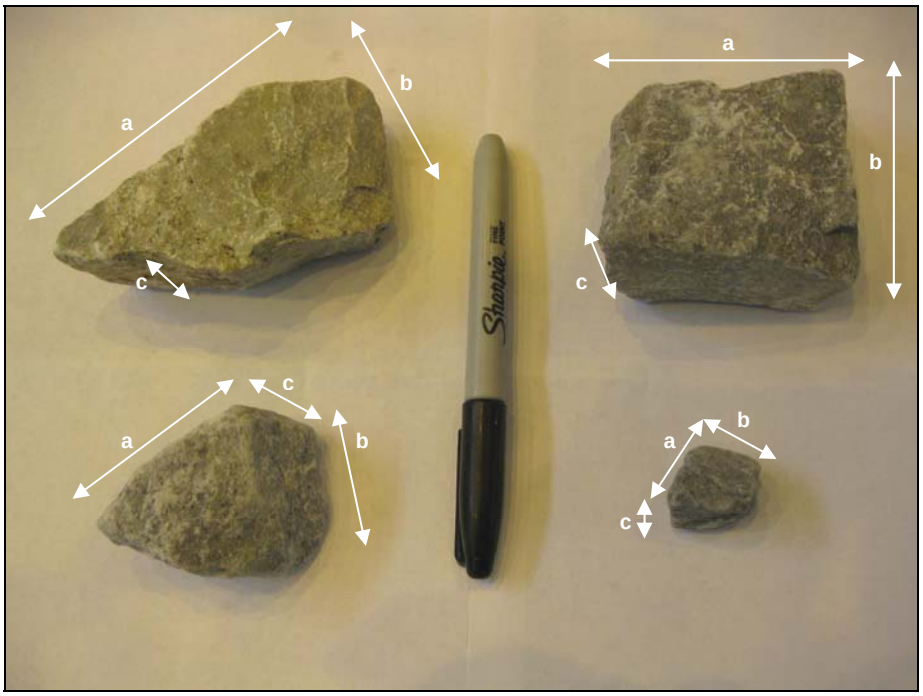

Figure 3.8 Sides of an irregular solid (waste rock particles)

$$d_i = (a_i.b_i.c_i)^{1/3} \quad \text{Eq. 3.9}$$

where, d_i = geometrical diameter of a particle i (m)

a_i = length of a particle i (m)

b_i = breadth of a particle i (m)

c_i = thickness of a particle i (m)

$$d = \frac{1}{n}\sum_{i=1}^{n=20} d_i \quad \text{Eq. 3.10}$$

where, n = number of particles measured

The particle density results obtained previously were taken to calculate the specific surface area based on mass ($SSA_{GE} = A_m$) for each size fraction using Eq. 3.11. These have been summarized in Table 3.4. All calculations are shown in Appendix C3 (Table C3.1 to Table C3.5).

$$A_m = \frac{A_v}{\rho} \quad \text{Eq. 3.11}$$

where A_m = specific surface area based on mass (m^2/kg)

ρ = particle or true density (kg/m^3)

Table 3.4 Specific surface area results obtained by the GE method

Size		Specific surface area (m^2/kg)				
mesh	(mm)*	**FC-0**	**FC-1**	**FC-2**	**FC-3**	**FC-4**
4”	122.5	NS	NS	NS	NS	NS
3”	86.6	0.029	0.026	0.024	NS	0.024
2”	61.2	0.037	0.033	0.032	0.036	0.038
1.5”	43.3	0.052	0.046	0.043	0.049	0.054
1”	30.6	0.075	0.069	0.062	0.069	0.071
¾”	21.8	0.105	0.092	0.086	0.090	0.099
½”	15.4	0.146	0.143	0.128	0.137	0.140
3/8”	10.9	0.196	0.191	0.173	0.191	0.208
¼”	7.7	0.268	0.266	0.245	0.266	0.283
#4	5.5	0.362	0.383	0.337	0.388	0.400

NS: No sample

* Representative particle size of the size fraction

The results followed the trend of lower specific surface areas with increasing particle size. No significant difference exists between SSA_{GE} for all samples at the same size fraction.

3.5.2 The Brunauer, Emmett, and Teller (BET) Method

BET is one of the gas adsorption experimental methods available for the surface area and pore size characterization of porous material such as marble and hornfels waste rock (Lowell, 2004). The BET method measures surface area such that specific surface area (SSA_{BET}) was initially measured with a "ruler" equivalent to the area of the adsorbate molecule.

The SSA_{BET} was determined using the multi-point (eleven points) method. Nitrogen was used as the inert adsorbate gas and its vapour adsorption data (77K) were obtained for relative vapour pressure (P/P_o) of 0.05, 0.10, 0.15, 0.20, 0.25 and 0.30. The SSA was calculated for relative pressures, through adsorption isotherms, which were drawn using the BET method.

The cross-sectional area of a nitrogen molecule (N_2) was assumed to be 16.2 $Å^2$. The SSA_{BET} were determined from the estimated amount of nitrogen required for monolayer coverage, the cross-sectional area of a nitrogen molecule, and the sample weight. Nitrogen was selected since it has a higher cross-sectional area than an oxygen molecule (O_2), assumed to be 14.3 $Å^2$. The premise was demonstrated by measurements of the specific surface area and pore volumes of a carbon molecular sieve, whose measurements using O_2 were higher than with N_2 (Zhonghua and Vansant, 1995). Therefore, if O_2 has a smaller cross-sectional area, then the surface area measured using N_2 as adsorbate gas is available for the weathering process. However, O_2 can be used directly as an adsorbate gas as well.

Furthermore, krypton (Kr) and argon (Ar) can also be used as adsorbate gases. However, since their molecule diameters are smaller than N_2 (Kr: 15.2 $Å^2$ and Ar: 10.3 $Å^2$ at 78 K), these yield different values for the SSA_{BET}, with Kr < N_2 and with Ar < N_2 for most materials.

Samples were wet screened and dried at 50°C in an oven (Despatch ranging from 0 - 550°C) for ~24 hours. After that, samples of 5 - 8 grams were outgassed with nitrogen at room temperature (25°C) for between 8 to 24 hours. The complete outgassing was tested until it reached a differential pressure from 20 to 50 micron/minute. After outgassing, nitrogen adsorption was determined for every sample over the relative equilibrium adsorption pressure (P/P_o) range of 0.05 – 0.30, as explained above. In the expression (P/P_o), P is the absolute adsorption equilibrium pressure and P_o is the condensation pressure of nitrogen under laboratory conditions (Brantley and Mellott, 2000; Dogan et al., 2006; Dogan et al., 2007).

The experiments were conducted using an Autosorb-1 Surface Area Analyzer (Quantachrome Instruments Corporation, Boynton Beach, Florida), and 55 readings (5 samples x 11 size fractions) were performed. Table 3.5 summarizes the SSA_{BET} results obtained by the BET method. The entire calculations of the SSA_{BET} results are shown in Appendix C3 (Table C3.1 to Table C3.5).

Table 3.5 Specific surface area results obtained by the BET method

Size		Specific surface area (m^2/kg)				
mesh	(mm)*	**FC-0**	**FC-1**	**FC-2**	**FC-3**	**FC-4**
#4	5.5	921	651	1050	880	350
#6	4.0	1269	696	1355	804	530
#8	2.8	1440	737	1486	488	563
#16	1.7	1912	927	882	583	677
#30	0.84	2243	816	1078	711	672
#50	0.42	2067	890	1295	711	609
#100	0.21	1291	698	1645	504	216
#140	0.13	1308	488	2014	491	237
#200	0.089	1425	435	2203	471	236
#270	0.063	1675	456	1989	544	218
-#270	0.045	11730	3328	5851	2697	1513

* Representative particle size of the size fraction

The results shown in Table 3.5 are not consistent with the pattern, in which large size fractions should have low specific surface areas, suggesting that the results are dependent upon the properties of each material. Several factors such as porosity and roughness, which are taken into account by BET, can originate different SSA_{BET} results regardless of the size fraction.

Widely different results of SSA were obtained for size fraction US Std. No 4 mesh (4.75 mm) by using the both the GE and BET methods for all samples. SSA_{BET} were significantly higher than SSA_{GE} (Table 3.4 and Table 3.5). As previously mentioned, the roughness and porosity of the samples were the main reasons of this difference (Brantley and Mellott, 2000). The BET method considers the measurements of surface area within the macropores as pores with diameters >50 nm, mesopores as pores with diameters of 2 - 50 nm, and micropores as pores with diameters 0.02 – 2 nm (Dogan et al., 2006), contributing tremendously in high SSA results. Therefore, in order to adjust the SSA_{GE} results of the coarse size fractions, and taking into account the roughness and porosity, the surface roughness and porosity factor (lamda= λ) was calculated (Helgeson et al., 1984).

$$\lambda = \frac{SSA_{BET}}{SSA_{GE}} \qquad \text{Eq. 3.12}$$

Lamda was computed for ten (#4, #6, #8, #16, #30, #50, #100, #140, #200 and #270 mesh) size fractions in each specific sample (Table 3.6). The SSA_{GE} results for these size fractions were obtained according to Eq. 3.13. Sphere shape factors were assumed and their diameters (d_{mean}) were estimated based on particle size (geometrical average of the upper and lower value of the size fraction). The minus St. US

No. 270 mesh (<53 μm) size fraction was not considered useful for this purpose because the range and distribution of particle sizes in this specific size fraction was not well defined for each sample.

$$SSA_{GE} = \frac{6/d_{mean}}{\rho} \qquad \text{Eq. 3.13}$$

where d_{mean} = particle mean diameter based on particle size (m)

ρ = particle or true density (kg/m^3)

Following this, λ results were plotted according to geometrical diameter (representative particle size of each size fraction) for all samples. Several regression types were fitted, and finally logarithmic trendlines including their equations and coefficient of determination (R^2) for each were obtained (Table 3.7 and Appendix C3, Figure C3.1). Logarithmic trends were selected because these provide more consistent results for this type of sample (Brantley and Mellott, 2000). These results were much higher than those obtained by the GE method.

Table 3.6 Specific surface area based on geometrical estimation and lamda values for all samples

Size		Specific surface area (m^2/kg)									
		FC-0		FC-1		FC-2		FC-3		FC-4	
mesh	(mm)*	SSA_{GE}	λ	SSA_{GE}	λ	SSA_{GE}	λ	SSA_{GE}	λ	SSA_{GE}	λ
#4	5.5	0.36	2543	0.38	1700	0.34	3118	0.39	2266	0.40	875
#6	4.0	0.54	2350	0.52	1346	0.47	2862	0.51	1563	0.55	966
#8	2.8	0.77	1868	0.73	1007	0.68	2190	0.73	667	0.78	726
#16	1.7	1.30	1475	1.23	753	1.13	778	1.23	476	1.31	518
#30	0.84	2.54	882	2.43	336	2.25	480	2.41	295	2.60	259
#50	0.42	5.04	410	4.79	186	4.45	291	4.81	148	5.14	119
#100	0.21	10.27	126	9.74	72	9.04	182	9.87	51	10.27	21
#140	0.13	17.34	75	16.35	30	15.44	130	16.86	29	17.26	14
#200	0.089	24.55	58	23.87	18	21.86	101	23.72	20	24.45	10
#270	0.063	34.69	48	33.89	13	31.23	64	33.85	16	34.75	6

* Representative particle size of the size fraction

Consequently, the equations shown in Table 3.7 were found and used to calculate lamda ($\lambda = m.Ln(d) + b$). Following this and taking into account the roughness and porosity for the coarse size fractions, including size fraction of US Std. No 4 mesh for some samples, the SSA was calculated

according to Eq. 3.14, which was derived from Eq. 3.12. The results are shown in Figure 3.9 and Table 3.8.

$$SSA_{BET} = [m.Ln(d) + b].SSA_{GE} \qquad \text{Eq. 3.14}$$

where $d =$ particle geometrical diameter based on the size fraction (m)

$m =$ slope of the trend (m^{-1})

$b =$ interception, is a constant

Table 3.7 Regression trends and equations for lamda according to size fraction

Sample code	Equation	R^2	Type
Pattern	$\lambda = m\ Ln\ (d) + b$		
FC-0	Lamda (FC-0) = 584.59*Ln(d) + 1288	0.93	Logarithmic
FC-1	Lamda (FC-1) = 350.65*Ln(d) + 728.67	0.87	Logarithmic
FC-2	Lamda (FC-2) = 653.15*Ln(d) + 1359.6	0.78	Logarithmic
FC-3	Lamda (FC-3) = 386.21*Ln(d) + 754.12	0.68	Logarithmic
FC-4	Lamda (FC-4) = 222.31*Ln(d) + 467.1	0.90	Logarithmic

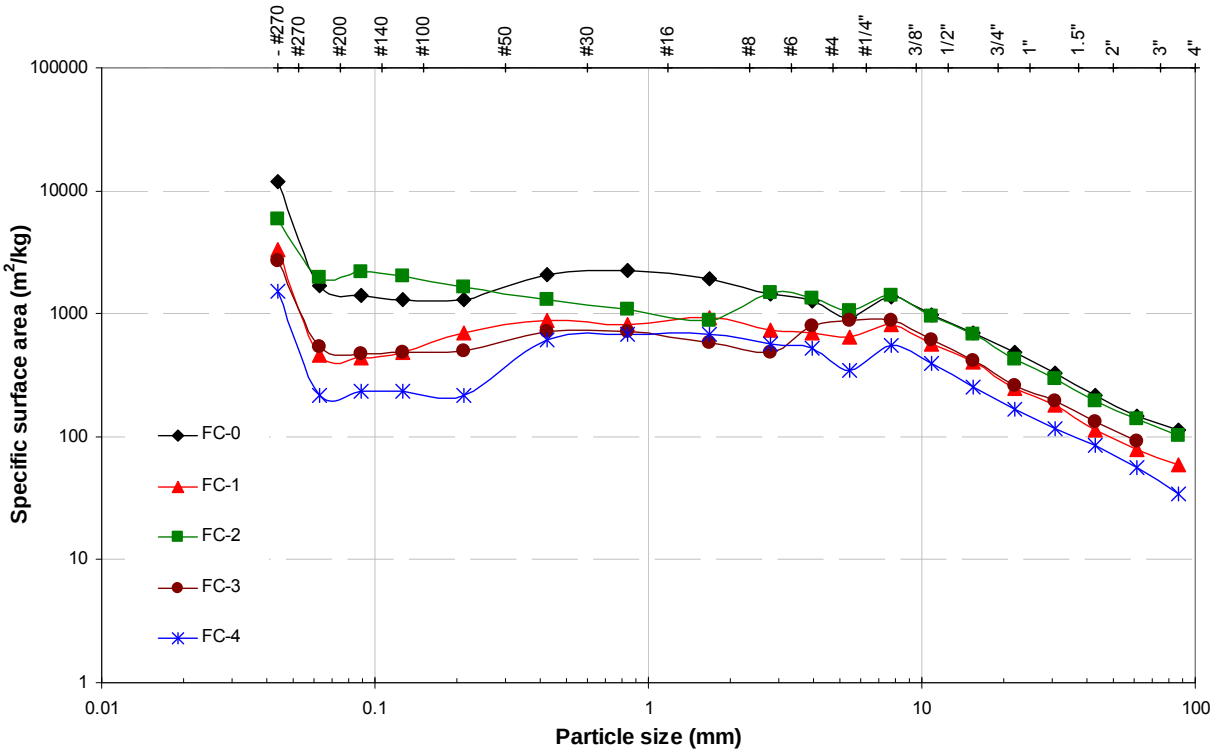

Figure 3.9 Specific surface area for all Class B waste rock samples

The specific surface area for the coarse size fractions was higher, particularly in the black marble and one of the diopside marble (FC-2) samples (Figure C3.2), suggesting that high weathering rates can occur in these samples; whereas the gray hornfels sample showed the lowest SSA.

Table 3.8 Final specific surface area for all Class B waste rock samples

Size fraction		Specific surface area (m^2/kg)				
mesh	(mm)*	FC-0	FC-1	FC-2	FC-3	FC-4
4"	122.5	NS	NS	NS	NS	NS
3”	86.6	112	60	103	NS	34
2”	61.2	148	78	138	92	57
1.5”	43.3	219	113	195	132	85
1”	30.6	331	179	300	193	117
¾”	21.8	485	248	429	261	169
½”	15.4	702	406	678	420	251
3/8”	10.9	973	565	950	609	392
¼”	7.7	1378	814	1400	884	552
#4	5.5	921	651	1050	880	350
#6	4.0	1269	696	1355	804	530
#8	2.8	1440	737	1486	488	563
#16	1.7	1912	927	882	583	677
#30	0.84	2243	816	1078	711	672
#50	0.42	2067	890	1295	711	609
#100	0.21	1291	698	1645	504	216
#140	0.13	1308	488	2014	491	237
#200	0.089	1425	435	2203	471	236
#270	0.063	1675	456	1989	544	218
-#270	0.045	11730	3328	5851	2697	1513

NS: No sample
* Representative particle size of the size fraction

The SSA results were verified through the porosity measurements (Table 3.9), which were obtained for all samples at the same size fraction of US Std. No 8 mesh (representative particle size of 2.81 mm). Only the specific surface area and volumes in micropores were measured using the full isotherm micro-pore analysis method with the Autosorb-1 Surface Area Analyzer. Thus, five samples were measured using the adsorption-desorption multi-points (40 points) method with nitrogen as adsorbate gas and oxygen as adsorbent gas.

Micropores with pore diameters below 0.8 nm were found in most of the samples. Approximately, 90% of the SSA_{BET} corresponded to the SSA present in the pores spaces (SSA_{PORES}). Nevertheless, if the

SSA_{PORES} is subtracted from the original SSA_{BET}, the results continue still being significantly higher than the SSA_{GE}. This suggests that the SSA of the mesopores, macropores and roughness continue being part of the effective SSA (Table 3.9).

Table 3.9 Pores SSA and volume by using adsorption method in comparison with SSA_{GE} for all Class B waste rock samples (@ US Std. No 8 mesh)

Parameter	unit	FC-0	FC-1	FC-2	FC-3	FC-4
SSA_{BET}	m^2/kg	1440.0	737.3	1486.0	487.5	563.0
SSA_{PORES} +	m^2/kg	1288.4	685.4	1343.0	429.5	484.0
SSA_{PORES} in SSA_{BET}	%	89	93	90	90	86
Effective SSA †	m^2/kg	151.6	51.9	143.0	49.0	79.0
SSA_{GE} ‡	m^2/kg	0.76	0.72	0.67	0.72	0.76
Pore volume	cm^3/kg	3.16	1.84	2.87	1.21	1.23
Ranking		I	III	II	V	IV

+ SSA by using the full isotherm method. Only the micropores were considered (< 20 nm of the instrument)
† Different SSA results at same size fraction because these have different particle density results
‡ Surface area determined by adsorption, in which the SA of mesopores and macropores is still present

The pore volumes and their specific surface areas were higher in the black marble and one of the diopside marble (FC-2) samples, which were related to their respective SSA_{BET}. Despite the fact that sample FC-3 had the lowest pore volume and SSA_{PORES}; it was not found to be significantly different from that of sample FC-4, whose SSA, was the lowest for all the samples, and is shown in Table 3.8.
Once the specific surface areas for each size fraction were obtained, the surface area (SA) for each size fraction was obtained according to Eq. 3.15, which allowed for obtaining the surface area distribution of each sample (Figure C3.3).

$$SA_i = SSA_i \quad x \quad wt_i \qquad \text{Eq. 3.15}$$

where SA_i = surface area for each size fraction i (m^2)

SSA_i = specific surface area for each size fraction i (m^2/kg)

wt_i = weight of each size fraction i (kg)

The weight surface area distributions for all samples shown in Figure 3.10 indicate that the black marble (FC-0) sample reports higher SA (72 wt.%) in the fine material (below 0.2 mm). This is because high SSA was found in the finest size fraction (<53 μm), which is almost seven times higher than in other samples (Table 3.8 and Figure 3.9). As previously mentioned, the 6 – 8 wt.% (Figure 3.5) of mass present as clays minerals mixed with hydrous ferric oxides (HFO) or iron oxyhydroxides in sample FC-0 has contributed to the highest specific surface area. Therefore, the distribution of the surface area in the fine particles becomes high. It is important to note that weathering, or some other geochemical processes, could occur

particularly at this size fraction, altering the geochemical behaviour of the whole sample. On the other hand, the distribution of the SA is higher in the coarse particles of other samples (55 – 60 wt.% above 0.2 mm), indicating that high weathering rates could occur from large particles of the diopside marble and gray hornfels samples.

The weight average specific surface areas for each sample were estimated according to Eq. 3.16. These were then extrapolated to whole-rock material placed in the field cells through Eq. 3.17 and the results are discussed in Chapter 5.

$$SSA_s = \frac{\sum_{i=1}^{N} SSA_i \ . \ wt_i}{\sum_{i=1}^{N} wt_i} \qquad \text{Eq. 3.16}$$

where SSA_s = weight average specific surface area for each sample (m^2)

SSA_i = specific surface area for each size fraction i (m^2/kg)

wt_i = weight of each size fraction i (kg)

N = number of size fractions i

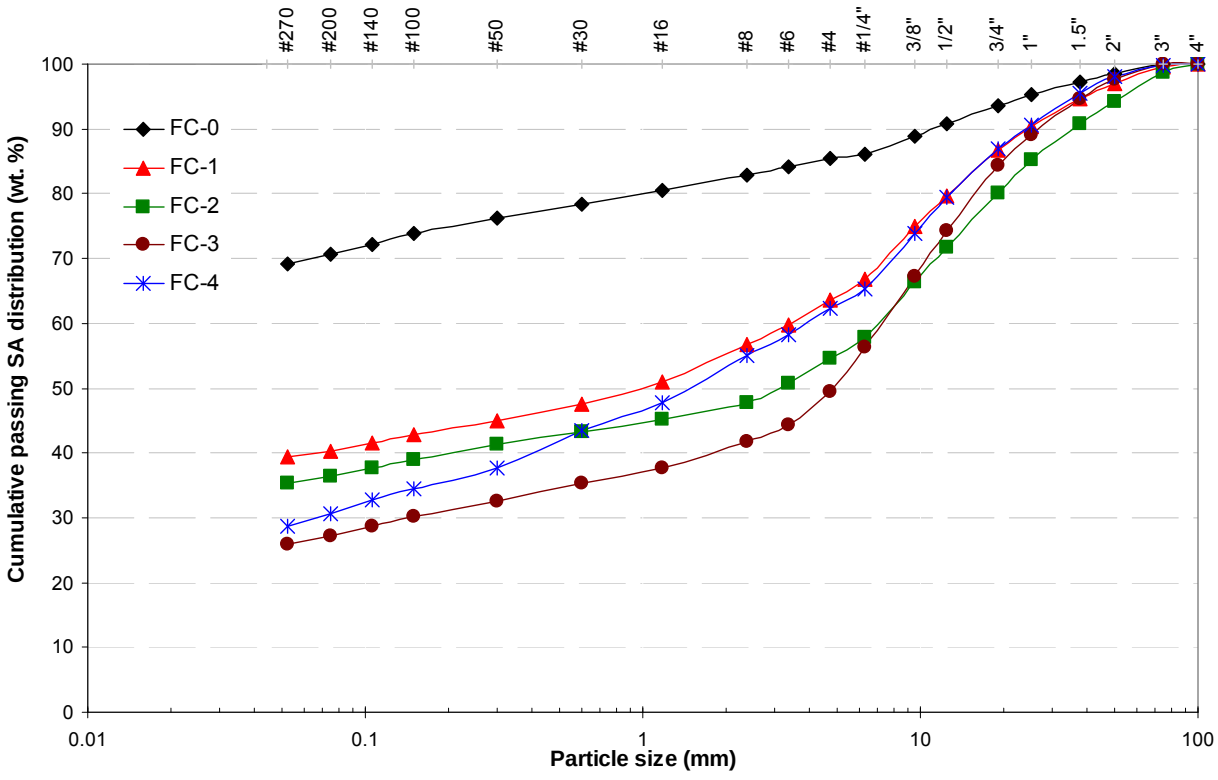

Figure 3.10 Cumulative passing weight surface area distribution for all Class B waste rock samples

Thus, the weight average specific surface areas of 1984 m^2/kg for FC-0, 539 m^2/kg for FC-1, 712 m^2/kg for FC-2, 501 m^2/kg for FC-3, and 336 m^2/kg for FC-4 were obtained (Appendix C3, Table C3.1 to Table C3.5). The weight average SSA in sample FC-0 is higher than for the other samples due to the reasons explained previously.

$$SA_s = SSA_s \,.\, m \,.(1-\omega) \qquad \text{Eq. 3.17}$$

where SA_s = surface area for each whole-waste rock placed in the field cell (m^2)

m = total mass or weight of the whole-rock placed in the field cell (kg)

ω = moisture content of waste rock (%)

3.6 Mineral Assay

Metals in the bulk and size fraction sub-samples for all Class B waste rock samples were determined. Some were done through Inductively Coupled Plasma Mass Spectrometry (ICP-MS) while others were arrived at through Optical Emission Spectrometer (ICP-OES).

Initially, only seven bulk or head samples (25 kg each), which included two duplicates, were sent to ALS Laboratory Group in Lima, Peru for analysis. Twenty-nine main metals were analyzed by ICP-OES using two digesting strong acids. The analysis was carried out using procedures adapted from "Test Methods for Evaluating Solid Waste" SW-846 Method 3050B, published by the United States Environmental Protection Agency (US-EPA). The sample was manually homogenized and a representative subsample (50 g) of the wet material was weighed. The sample was then digested by hotplate using a 1:1 ratio of nitric acid and hydrochloric acid. Instrumental analysis was by ICP-OES. This method is not a total digestion technique. It involves a very strong acid digestion process that is intended to dissolve those metals that could potentially become "environmentally available." By design, elements bound in silicate structures are not normally dissolved by this procedure as they are not usually mobile in the environment.

Later on, the sample preparation was considered the most critical step in the entire laboratory operation. This procedure involved obtaining representative sub-samples for 95 size fractions (19 size fractions x 5 samples) and was based on the homogenizing and riffling. Coarse size fractions (above 2 mm) were crushed until achieving 70% passing 1.18 mm (US Std. 8 mesh) screen, using primary (Jaw), secondary (Massco cone) and tertiary (cone) crushers, depending on the size of the material. A split of up to 250 g was taken and pulverized with a ring mill pulveriser using a carbon steel (chrome free) ring set (TM Engineering Ltd.) up to better than 85% passing a 75 micron (US Std. No. 200 mesh) screen. Fine size fractions (below 2 mm) were directly pulverized. Thus, 105 (21 size fractions x 5 samples) samples weighing approximately 50 g including duplicates as part of the QA/QC were delivered to ALS Chemex Laboratory in Vancouver, Canada and 47 (Ag, Al, As, Ba, Be, Bi, Ca, Cd, Ce, Co, Cr, Cs, Cu, Fe, Ga, Ge, Hf, In, K, La, Li, Mg, Mn, Mo, Na, Nb, Ni, P, Pb, Rb, Re, Sb, Sc, Se, Sn, Sr, Ta, Te, Th, Ti, Tl, U, V, W, Y, Zn, Zr) metals were analyzed by ICP-MS using the ME-MS61 (Ultra-Trace Level) internal method. A prepared sample (0.25 g) was digested with perchloric, nitric, hydrofluoric and hydrochloric acids. Four acid digestions are able to dissolve most minerals; however, although the term “near-total” is used, depending on the sample matrix, not all elements are quantitatively extracted. Total sulfur contents were

also obtained by ICP-MS and the Leco methods (see laboratory procedures at ALS Chemex web page http://www.alsglobal.com/mineral). The results of duplicate samples were compared, and for most of the parameters, no significant differences were found. However, some parameters were repeated since, for them, some relatively great differences were observed.

The assay result for head samples using the results of the size fractions was back calculated through Eq. 3.18, and these are reported in Appendix C4 (Table C4.1 to Table C4.5).

$$[Xe_{hs}] = \frac{1}{100}\sum_{i=1}^{N}[Xe_i].wt_i\% \qquad \text{Eq. 3.18}$$

where $[Xe_{hs}]$ = solid concentration of specific element for head sample (mg/kg or %)

$[Xe_i]$ = solid concentration of specific element for each size fraction i (mg/kg or %)

$wt_i\%$ = weight percent of each size fraction i

N = number of size fractions i

In order to compare the results using the ICP-MS method, an analysis of the head samples using the same method (ME-MS61) were obtained from the ALS Laboratory Group in Lima, Peru and are reported in Appendix C4 (Table C4.6).

The samples obtained directly from the bore holes by geologists were delivered to the Antamina internal laboratory. Only nine (Ag, As, Bi, Co, Cu, Fe, Mo, Pb and Zn) metals of interest were evaluated by ICP-OES following the same procedure indicated above.

Table 3.10 Assay results of main metals of solid phase for all samples

Parameter	Metals and total sulfur by ICP-MS								
	S-total	Fe	Ca	Cu	Pb	Zn	Sb	As	Mo
	%	%	%	mg/kg	mg/kg	mg/kg	mg/kg	mg/kg	mg/kg
FC-0 - Black marble									
Average	0.23	0.81	30.6	526	542	1358	11.04	120	5.0
Minimum	0.22	0.67	27.0	331	255	525	9.63	74	1.6
Maximum	0.25	1.06	33.1	845	852	2220	12.55	194	9.8
FC-1 - Diopside marble									
Average	0.29	1.27	26.7	819	309	649	16.54	68	92.5
Minimum	0.26	1.21	24.4	761	252	645	13.59	63	81.1
Maximum	0.32	1.33	29.1	878	366	653	19.50	73	104.0
FC-2 - Diopside marble									
Average	1.17	3.48	18.4	680	840	479	3.84	44	43.8
Minimum	1.05	3.34	16.9	606	634	406	3.62	41	35.8
Maximum	1.37	3.58	19.5	824	1010	590	4.18	47	52.6

Parameter	Metals and total sulfur by ICP-MS								
	S-total	Fe	Ca	Cu	Pb	Zn	Sb	As	Mo
	%	%	%	mg/kg	mg/kg	mg/kg	mg/kg	mg/kg	mg/kg
FC-3 - Diopside marble									
Average	0.72	1.55	31.4	532	622	1271	3.59	36	66.4
Minimum	0.67	1.53	30.3	423	514	1183	3.50	34	62.8
Maximum	0.78	1.57	32.6	642	730	1360	3.68	37	70.0
FC-4 - Gray hornfels									
Average	0.24	0.29	35.3	162	160	401	5.95	20	5.5
Minimum	0.24	0.29	34.6	121	150	274	5.71	18	5.4
Maximum	0.25	0.30	36.1	203	170	528	6.19	23	5.7

All results obtained by different methods and laboratories were compared, with no significant differences found between them (Appendix C4, Table C4.6). However, since the ICP-MS results were found to be greater than the ICP-OES values, and because the digestions were different for both methods, allowing for more species to be available (trace levels) for detection, the ICP-MS results were selected and averaged (Table 3.10). Likewise, total sulphur results by the ICP-MS method were chosen because they reported higher concentrations than did the Leco method results.

3.7 Acid-base Accounting (ABA) Testing

The ABA testing was carried out at ALS Chemex Laboratory in Vancouver, Canada by using the Modified Sobek (1978) method. Initially, seven head samples were sent to ALS Laboratory Group in Lima, Peru, who then delivered the samples to Canada. The inorganic carbon (CO_2) was determined using the C-GAS05 method. Table 3.11 summaries the ABA testing results. Some parameters have been calculated based on Eq. 2.9, 2.10, and 2.11, and the acid generation screening criteria were done based on Table 2.1.

As is shown in Table 3.11, all Class B materials placed in the field cells are non-acid generating. Their paste pH indicates that they are under circumneutral pH conditions. According to this, higher neutralization potential is present in all samples in Figure 3.11a. In the duplicates of the black marble (FC-0) and gray hornfels (FC-4) samples, most of the sulfur content is present as sulphate ($S\text{-}SO_4$), which may mean that the source of sulphate in the leachate from these samples is most likely due to sulphate mineral dissolution rather than sulfide mineral oxidation. The likely source of sulphate could be iron sulphate in black marble (probably as a secondary mineral because this sample was slightly weathered after sampling). However, its presence is uncertain in gray hornfels because mineralogy data does not report any form of sulphate mineral in this sample. This is in agreement with Antamina's geology reports, in which no significant abundance of sulphate primary minerals such as barite or gypsum were reported.

Table 3.11 ABA testing results for Class B material placed into the field cells

Parameter	Units	FC-0	Duplicate of FC-0	FC-1	FC-2	Duplicate of FC-2	FC-3	FC-4
Efferve.		4	4	4	4	4	4	4
Paste pH		7.3	7.7	7.9	7.6	7.6	7.9	8.1
S-total	%	0.15	0.13	0.26	1.11	0.98	0.65	0.12
S-S_2	%	0.13	0.01	0.24	1.03	0.93	0.64	0.01
S-SO_4	%	0.02	0.12	0.02	0.08	0.05	0.01	0.11
AP	kg $CaCO_3$/t	4.1	0.3	7.5	32.2	29.1	20.0	0.3
NP	kg $CaCO_3$/t	769	838	605	184	175	707	990
NNP	kg $CaCO_3$/t	764.9	837.7	597.5	151.8	145.9	687.0	989.7
NPR		189.3	2681.6	80.7	5.7	6.0	35.4	3168.0
Ca	%	30.6	30.6	26.7	18.4	18.4	31.4	35.3
Mg	%	0.4	0.3	0.4	0.2	0.2	0.4	0.5
CO_2	%	31.9	33.5	24.6	5.8	5.9	29	40.6
AG criteria		**NAG**	**NAG**	**NAG**	**NAG**	**NAG**	**NAG**	**NAG**
Moisture content								
ω	%	**0.51**		**0.05**	**0.21**		**0.29**	**0.05**

In others samples, leachate sulphate concentrations will result from the sulfide mineral oxidation because most of the sulfur is present as sulfide (S-S_2) and is evidenced by a straight trendline between AP and S-S_2 in Figure 3.11b.

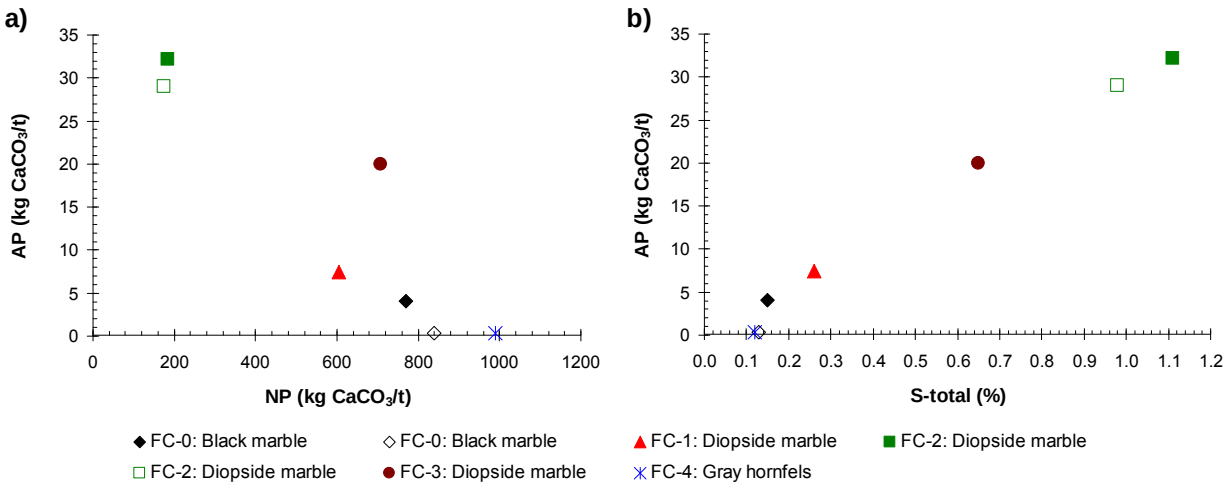

Figure 3.11 a) Acid potential and neutralization potential, b) acid potential generation in function of S-total for all Class B waste rock samples

3.8 Moisture Content

Moisture contents (ω) of waste rock samples placed in the field cells were determined using the gravimetric method (ASTM-Method D2794-00) and Eq. 3.19 (Table 3.11). A representative 5 kg of bulk sample as initial sample (wet weight) was dried at 105°C for a minimum of six hours. Most of the samples placed in the field cells were almost dry (<1%).

$$\omega(\%) = \frac{wet\ \ weight - dry\ \ weight}{wet\ \ weight}\ \ x\ \ 100 \qquad \text{Eq. 3.19}$$

3.9 Mineralogical Evaluation by the Mineral Liberation Analyzer (MLA)

An evaluation of mineral abundance and liberation by free surface (exposure or availability) of 45 (5 samples x 9 size fractions) samples was conducted using MLA at ART of Teck in Trail, B.C., Canada. Samples below US Std. 16 mesh (1.18 mm) were prepared, and were analyzed according to the following size fractions: +600 μm, +300 μm, +150 μm, +106 μm, +75 μm, +53 μm, 38 μm (C-1), 28 μm (C-2), 20 μm (C-3), 15 μm (C-4), 10 μm (C-5) and <10 μm (C-6). As previously mentioned, the size fractions from C-1 to C-6 were obtained by cyclosizing. These were combined or blended as C-1/C-2, C-3/C-4, C-5/C-6, and finally nine subsamples (size fractions) per sample were mounted in polished sections. Bulk samples of approximately 100 g for each size fraction were split after the particle size analysis.

At the beginning, accurate split sub-samples of 1-1.5 g were obtained in equivalent portions using a rotary micro riffler with a 3 inch turntable, and 15mm OD x 8 tubes (*Quantachrome* Instruments Corporation, Boynton Beach, Florida). This was considered to be a crucial step in sample preparation because very small samples are made into polished grain mounts for MLA examination.

In order to produce a sample for MLA analysis that could show a representative sample for a single polishing area as completely as possible, grain single and double mounts containing 1.5 g of sample were prepared. Samples were encased in Epoxy resin (pucks) of 30 mm diameter by 15 to 17 mm in height, providing a mineral mount that was as close as possible to being one layer of particles in thickness. The smaller the particles, the more difficult it becomes to produce a "monolayer." Once the Epoxy resins were prepared, they were cured by being placed in a Leco pressure vessel and left inside the vessel at 42 psi of air pressure during the 24 hours which had been set as the curing time.

Subsequently, the mounts were converted in high quality polished sections. This process was considered to be another crucial step in the preparation of polished grain mounts. This was done by using a Struers Tegra polisher system with force/pressure between 10 and 30 N as maximum, and at a 150 RPM speed rate. Mounts were polished with Silicon Carbide, PLAN and/or DAC polishing surface/cloths which were previously primed or wetted with extra lubricant (water, green and oil) and abrasives (320 or 500 grit, 9, 6, 3 and 1 μm diamond suspensions). A silicone carbide cloth was only used during the face bevelling process, and the removal of most silicon grease lines was accomplished using 320 and 500 grit abrasives and water as lubricant for 5-10 seconds. In order to remove some scratches from the previous step and to

start to generate particle faces, the PLAN cloth was used for coarse and fine grinding with 9 and 6 μm as diamond suspension abrasives and green lubricant during ~3 minutes. As the final quality was almost met, and in order to clean up the particle faces, coarse and fine polishing was done with TEXMET and DAC cloths with minimal amounts (2 - 3 squirts) of 3 and 1 μm diamond pulp, respectively, as well as green lubricant for between 1 and 5 minutes. To finish the polishing and to remove any surface scratches and clean up small surface pluck-outs, DAC cloth with an abrasive/lubricant of silica gel 0.04 μm was used for 2 - 3 minutes. Finally, to remove any residual colloidal silica that had crystallized and scratch the final surface, 30 seconds of water washing with the same DAC cloth used in the previous step was done. After each step, the sections were cleaned with soap/water and the level/parallel with the front face was inspected with a microscope at 200X as part of the QA/QC. Finally, the polished sections were cleaned with denatured ethanol and blow dried, applying a protective plastic cap. Consequently, the sections were ready to be carbon coated.

Samples were run in double (transverse) and single mounts by using different magnifications according to the size fractions. These ranged from 150 to 1,200. The Extended BSE liberation analysis (XBSE) mode was performed to determine the liberation. This mode is also able to report mineral phases because it incorporates X-ray analysis. The BSE gray level was conducted to identify the different mineral phases present in the polished sections. Analytical running time ranged from 30 to 200 minutes. The analyses of the finest size fractions which had been mounted as double required a longer time; whereas for the single mounts required a shorter time for analysis.

3.9.1 Determining Mineral Phases

Mineral abundance, also called modal mineralogy, was determined by using the X-ray fluorescence mapping feature and image analysis, which can identify the mineral phases in a number of points (some examples are shown in Figure 3.12 and Figure 3.13). Bulk mineral phases for all samples were calculated on a mass basis through Eq. 3.20. The bulk mineralogy shown in Table 3.12 was calculated by taking into account only the size fractions below 1.18 mm. These represent the bulk mineralogy of the whole waste rock samples placed in the field cells. All mineral phases by mineral groups and metal by mineral phases found by MLA analysis are shown in Appendix C5 (Table C5.1 to Table C5.7 and Figure C5.1).

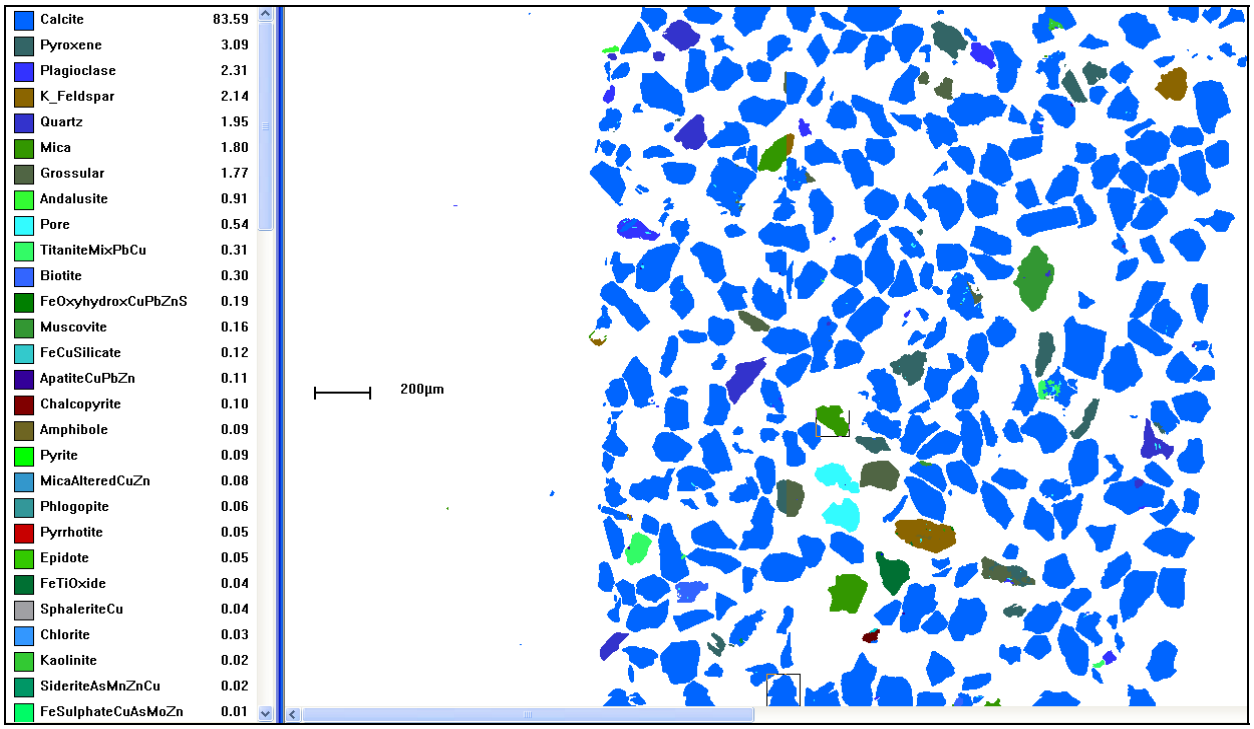

Figure 3.12 View of mineral abundance using MLA in black marble (FC-0) at 0.1 – 0.15 mm size fraction

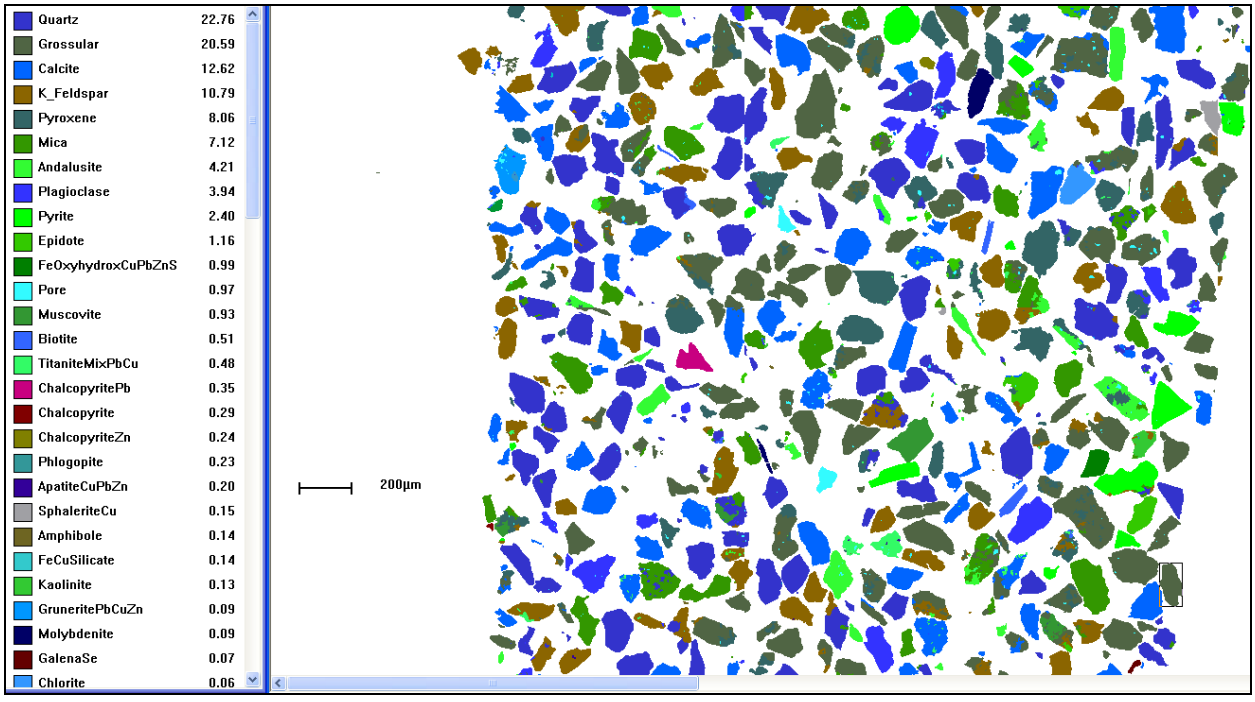

Figure 3.13 View of mineral abundance using MLA in diopside marble (FC-2) at 0.1 – 0.15 mm size fraction

Table 3.12 Bulk mineralogy of Class B waste rock samples placed in the field cells

Mineral group	Mineral phases	Mineral phase abundance (wt.%)				
		FC-0	FC-1	FC-2	FC-3	FC-4
Sulfide	Bornite	0.00	0.02	0.00	0.00	0.00
	Galena	0.03	0.08	0.08	0.06	0.01
	Sphalerite	0.05	0.26	0.15	0.24	0.04
	Chalcopyrite	0.11	0.65	0.79	0.38	0.07
	Pyrrhotite	0.11	0.15	0.02	0.25	0.03
	Realgar-Orpiment	0.00	0.00	0.00	0.00	0.00
	Watanabeite	0.00	0.01	0.00	0.00	0.01
	Pyrite	0.19	0.72	3.42	1.49	0.49
	Molybdenite	0.00	0.04	0.05	0.01	0.00
	Others	0.00	0.03	0.01	0.00	0.01
	Total sulfides	**0.48**	**1.98**	**4.53**	**2.44**	**0.67**
Carbonate	Calcite	55.22	47.47	10.51	65.50	90.61
	Otavite	0.00	0.00	0.00	0.00	0.03
	Siderite	0.01	0.00	0.04	0.02	0.00
	Dolomite	0.04	0.03	0.01	0.06	0.12
	Others	0.36	0.05	0.48	0.09	0.02
	Total carbonates	**55.63**	**47.54**	**11.04**	**65.67**	**90.78**
Silicate	Biotite	1.60	1.50	0.54	1.42	1.32
	Chlorite	0.30	0.04	0.06	0.04	0.11
	K_Feldspar	5.66	7.06	13.86	2.50	0.36
	Kaolinite	0.53	0.23	0.28	0.06	0.04
	Muscovite	1.01	0.77	0.83	0.17	0.04
	Plagioclase	5.21	3.06	3.33	3.78	1.99
	Pyroxene	7.94	7.63	15.43	5.52	1.43
	Quartz	8.30	8.73	9.78	2.91	1.27
	Mica	4.06	3.12	5.16	1.31	0.42
	Titanite	0.49	0.36	0.88	0.34	0.15
	Others	5.89	17.05	32.09	12.92	0.87
	Total silicates	**41.00**	**49.57**	**82.23**	**30.96**	**8.01**
Phosphates		**1.04**	**0.35**	**0.43**	**0.30**	**0.09**
Oxides/Hydroxides	FeOxyhydroxides	1.09	0.35	1.21	0.25	0.33
	Others	0.10	0.04	0.08	0.03	0.01
	Total oxi/hydroxides	**1.19**	**0.39**	**1.29**	**0.28**	**0.34**
Sulphates	FeSulphate	0.32	0.06	0.35	0.17	0.04
	Gypsum	0.01	0.00	0.00	0.01	0.00
	Others	0.00	0.00	0.00	0.00	0.00
	Total sulphates	**0.33**	**0.07**	**0.35**	**0.18**	**0.05**
Others		**0.35**	**0.13**	**0.14**	**0.17**	**0.07**
	Total	**100.0**	**100.0**	**100.0**	**100.0**	**100.0**

NOTE: A value of ZERO means that there is "trace" (i.e. <0.01 wt.%)

- **Other sulfide minerals:** Chalcocite, AgSulphosalt, Arsenopyrite, Enargite, EnargiteZn, Galenobismutite, LinnaeiteNiCuZn, SieginiteCuFe, TennantiteZnFe, and Stibnite.
- **Other carbonate minerals:** Smithsonite, Ankerite, GruneritePbCuZn, Malachite, and Rhodochrosite.
- **Other silicate minerals:** Amphibole, Andalusite, Apophyllite, CaMoSilicate, Epidote, Fayalite, FeCuSilicate, Grossular, MoSilicate, Phlogopite, Pyroxene, Sericite, TalcFe, Willemite, and Zircon.
- **Phosphate minerals:** Apatite, ApatiteCuPbZn, FornaciteCa, Goyazite, MonaziteCe, and TyrolitePb.
- **Other Oxide/hydroxide minerals:** Cassiterite, Cuprite, FeTiOxide, Paratacamite, PbMoOxide, PbOxideZn, Portlandite, Spinel, Srebrodolskite, and Wulfingite.
- **Other sulphate minerals:** Alunite, Barite, Celestine, JarositeCu, and MoCaSulphate.
- **Other minerals:** ChloroOrganic, Fluorite, MolybdofornaciteZn, Powellite_trans, Wulfenite-trans, Scheelite, and TrampMetal.

$$MP_{bulk} = \frac{\sum_{i=1}^{N} MP_i . wt_i\%}{\sum_{i=1}^{N} wt_i\%} \quad \text{Eq. 3.20}$$

where MP_{bulk} = mineral phase of bulk sample (wt. %)

MP_i = mineral phase at each size fraction i (%)

$wt_i\%$ = weight percentage of each size fraction i

N = number of size fractions i

Several mineral phases were identified. Large amounts of sulfide minerals were present in the diopside marble samples, particularly in samples FC-2 and FC-3, which increased the possibility of the occurrence of high sulfide oxidation and therefore a release of the elements that constituted these minerals. Iron sulfide minerals (i.e. pyrite and pyrrhotite) were identified as the most abundant sulfide minerals in all the samples. However, galena, sphalerite and chalcopyrite were also identified in relatively high proportions, particularly in the diopside marble samples, suggesting that these minerals are the primary source of Pb, Zn and Cu, which may be mobilized in the drainage water after oxidation. Sb, As and Mo sulfide minerals were present in trace amounts, indicating that after their oxidation, very low leachate concentrations of these elements are likely to be observed.

Calcite was found to be the most abundant carbonate mineral (~99%). Some other carbonate minerals such as dolomite were also identified in low proportions. The greatest amounts of carbonate minerals were present in the gray hornfels sample (FC-4), whereas the lowest amounts were present in one of the diopside marble samples (FC-2).

High amounts of silicate minerals such as andalusite, biotite, chlorite, epidote, K-feldspar, muscovite, plagioclase, pyroxene, quartz, sericite, and zircon, among others, were found in sample FC-2. In contrast, sample FC-4 contained low levels of silicate minerals.

Other minerals such as phosphates, oxides, hydroxides and sulphates were also identified in low quantities. However, in the black marble sample (FC-0), relatively high amounts of phosphate (principally apatite) and oxide/hydroxide minerals (ferric oxyhydroxides or HFO, and Fe oxides) were also reported.

3.9.2 Determining Mineral Availability for Leaching

Mineral availability was determined based on mineral liberation by free surface data (Appendix C5, Table C5.8 to Table C5.12), which can be defined by the composition of the particle surface to categorise the liberation of the mineral grain (Figure 3.14).

In order to calculate the liberation of specific minerals such as sulfides, the surface areas of the samples were initially calculated. Straightforward line scan measurements (LSM), which are defined by the transition along the line scan from the mineral of concern to any other mineral, are widely used to estimate the size of the mineral grain, giving as result an average intercept length (L). This length is used to calculate the mineral surface area that can later on be expressed as an average volume. Thus, to

overcome problems which can arise after line scan measurements, the phase-specific surface area (PSSA), which is the mineral surface area per unit volume, was estimated through an indirect measurement from an LSM. PSSA is inversely proportional to L, as is indicated in Eq. 3.21 (Sutherland, 2007).

$$PSSA = 4 / L \qquad \text{Eq. 3.21}$$

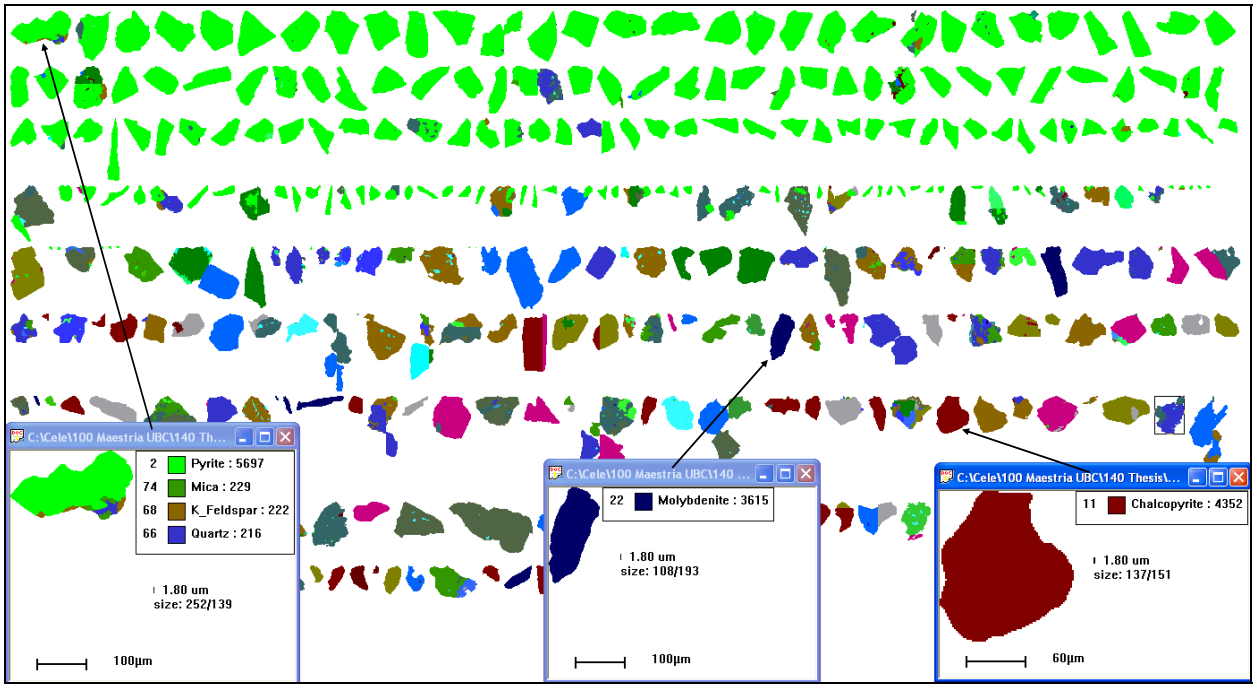

Figure 3.14 View of mineral liberation by free surface area using MLA in diopside marble (FC-2) at 0.1 – 0.15 mm size fraction

This is commonly used in the measurements; however it is also used for particles with regular shapes such as a cubes or spheres. Therefore, if the PSSA of a cube or sphere is 6, then the size of mineral grains are reported by assuming that the grains are cubes or spheres. This is given by:

$$D_{Mineral} = 6 / PSSA \qquad \text{Eq. 3.22}$$

where $D_{(Mineral)}$ = size of the mineral grain present in a specific particle (m)

$D_{(Mineral)}$ is valid only for simple shapes (cubes and spheres), using this result and the equation of surface area or volume of a cube or sphere, the surface area or volume of the mineral grains was estimated.

After that, the total minerals present in a particle (sum of mineral grains) were obtained through Eq. 3.23.

$$Mineral_{(Total)} = Mineral_{(Exposed)} + Mineral_{(Inclusion)} \quad \text{Eq. 3.23}$$

where $M_{(Total)}$ = total mineral volume present in a specific particle

$M_{(Exposed)}$ = total mineral volume exposed, free or fully liberated from a specific particle

$M_{(Inclusion)}$ = total mineral volume not exposed from the particle, either fully locked or enclosed in another mineral

Thus, the availability of the specific mineral phase or mineral group was determined as a fraction of the mineral exposed of the total mineral present in the particle (Eq. 3.24). These values were sorted by middling classes to provide a better understanding.

$$Mineral_{(Avail.)} = \frac{Mineral_{(Exposed)}}{Mineral_{(Total)}} x100 \quad \text{Eq. 3.24}$$

where $Mineral_{(Avail.)}$ = mineral availability of one particle (%)

Figure 3.15 shows the different possible middling classes of mineral availability results. The exposure or availability of the mineral of concern was defined for all grains whose surface was exposed on the particle. The 0% of middling class means that the mineral grains were not exposed (locked), therefore they were almost impermeable because they were fully encapsulated within another mineral and were not available for leaching. The exposure middling classes greater than zero and less than 100% only occur if some mineral or inclusion grains are exposed in a particle. However, if the mineral grains are fully liberated (free of the liberation definition), or the binary or tertiary attachment grains or inclusions have a portion of their edges exposed (Figure 3.16), then they will be available for leaching (100%).

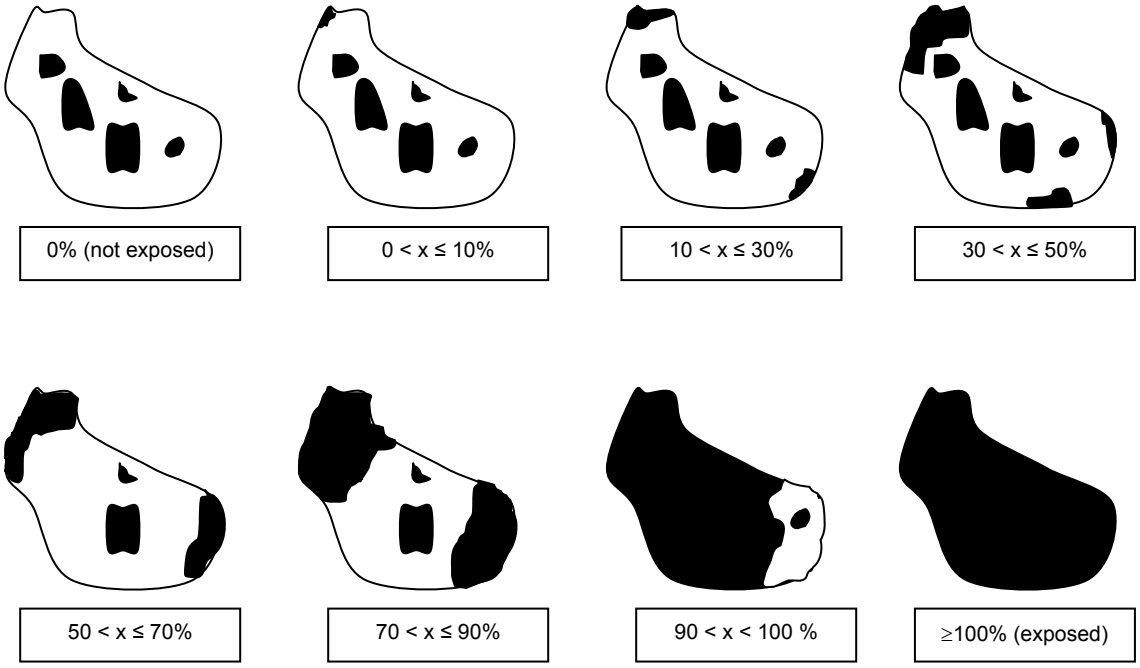

Figure 3.15 Mineral (black grains) exposure or availability at different middling classes in cross section particles

Therefore, the total mineral exposed or available for each size fraction (Table 3.13) was obtained by summing the availability proportions reported in middling classes greater than 0%.

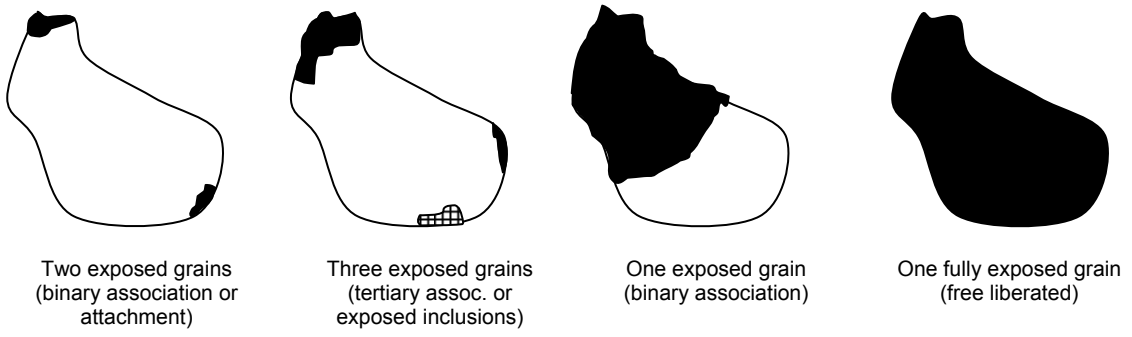

Figure 3.16 Different forms with full exposure or availability mineral grains (100 % of middling class)

The values shown in Table 3.13 were plotted as a function of their representative particle sizes and then an extrapolation was performed to determine the availability of minerals for leaching in the coarse particle sizes. Almost all mineral types from all the samples fitted with exponential regression lines (Eq. 3.25), which were the same as those used in the liberation concept. However, the availability of Cu, Pb and Zn minerals in the coarse size fractions of samples FC-2 and FC-3 were given by logarithmic trendlines (Eq. 3.26), suggesting that in the coarse size fractions, Cu, Pb, and Zn were still available for leaching in

relatively high proportions. Logarithmic trendlines were selected rather than exponential ones because these reported better coefficients of determination.

Table 3.13 Mineral availability per size fractions of Class B waste rock samples placed in the field cells

Size fraction		Mineral availability (wt. %)																					
		FC-0					FC-1					FC-2					FC-3					FC-4				
mesh	(mm)*	S_2	Cu	Pb	Zn	Sb	S_2	Cu	Pb	Zn	Sb	S_2	Cu	Pb	Zn	Sb	S_2	Cu	Pb	Zn	Sb	S_2	Cu	Pb	Zn	Sb
#30	0.84	97.1	93.0	91.9	96.1	0	89.0	94.7	93.1	94.4	100	96.3	96.2	95.2	97.3	0	94.4	96.1	95.9	20.6	0	91.9	91.3	82.9	92.8	0
#50	0.42	99.3	96.9	94.7	96.5	0	98.2	96.2	93.6	96.2	50.0	99.7	93.8	84.4	91.8	0	98.4	91.6	87.3	88.1	0	95.9	96.1	96.9	90.6	0
#100	0.21	97.8	97.2	96.1	96.2	0	98.4	98.0	97.6	98.1	76.7	99.8	96.7	95.9	97.8	0	98.4	95.7	93.7	95.5	0	91.0	94.9	95.5	95.8	0
#140	0.13	99.9	98.2	96.9	97.0	0	99.4	97.1	96.0	96.0	0	99.8	98.2	97.5	98.8	0	99.6	98.1	96.7	97.2	0	99.8	97.5	95.2	96.1	100
#200	0.089	99.7	98.7	98.2	97.5	0	99.5	95.8	94.0	94.6	99.7	99.9	98.7	98.1	98.9	0	99.7	98.7	96.5	98.6	0	97.8	97.4	96.3	96.5	100
#270	0.063	99.3	99.2	98.6	98.9	0	99.5	97.4	93.0	95.1	97.4	99.9	98.9	98.4	99.0	0	99.4	98.6	97.5	98.3	0	98.8	97.1	95.6	96.8	100
-#270	0.045	99.7	99.9	99.8	99.8	0	99.4	99.4	99.2	99.6	100	99.9	99.5	99.3	99.4	68	99.6	99.6	99.2	99.3	0	99.9	99.4	98.3	99.1	100

Table 3.14 summarizes the values used to calculate the availability in the coarse size fractions, which are also shown in Figure 3.17.

Table 3.14 Values used in the trendlines to calculate availability of minerals at coarse particles

Minerals	FC-0		FC-1		FC-2		FC-3		FC-4	
	m	B	m	B	m	b	m	b	m	b
Sulfide	-0.03	99.7	-0.13	99.99	-0.04	99.99	-0.06	99.99	-0.09	98.62
Cu	-0.08	99.58	-0.04	97.93	**-1.61**	**94.4**	**-1.99**	**93.2**	-0.08	98.34
Pb	-0.09	98.87	-0.04	96.16	**-3.11**	**89.8**	**-2.30**	**91.01**	-0.17	98.61
Zn	-0.03	98.26	-0.03	96.97	**-1.61**	**94.6**	**-2.65**	**91.07**	-0.08	97.26
R^2	44 – 60%		18 – 88%		41 – 84%		39 – 93%		46 – 77%	

Bold numbers correspond to variables of logarithmic equations

$$Mineral_{(Avail.)i} = b \,.\, e^{m.d_i} \qquad \text{Eq. 3.25}$$

$$Mineral_{(Avail.)i} = m \,.\, Ln(d_i) + b \qquad \text{Eq. 3.26}$$

where $Mineral_{(Avail.)i}$ = mineral availability at each size fraction i (%)

d_i = geometrical diameter, which is the representative size of size fraction i (mm)

b = mineral availability intersection, is a constant (%)

m = slope of the curve

The extrapolation through exponential regression lines in samples FC-2 and FC-3 showed a low sulfide mineral availability for leaching in the coarse particles. The opposite is true for Cu, Pb and Zn minerals, which had a high availability for leaching (Figure 3.18).

The availability of the whole sample was obtained as an average weight through Eq. 3.27. These results represent the bulk availability of the minerals for leaching in the waste rock samples which were placed in the field cells.

$$Mineral_{(Avail.-bulk)} = \frac{\sum_{i=1}^{N} Mineral_{(Avail.)i}.wt_i\%}{\sum_{i=1}^{N} wt_i\%} \qquad \text{Eq. 3.27}$$

where $Mineral_{(Avail.-bulk)}$ = mineral availability of bulk or whole sample (wt.%)

The Reactivity Index (RI) and Net Reactivity Potential (NRP) were established and computed as new indicators of mineral weathering based on availability and solid phase concentration. The reactivity index, calculated according to Eq. 3.28, is the proportion of a mineral or element present in the sample that could be accessibly released (only through exposed mineral grains). The *RI* takes into account mineral availability based on elemental distribution rather than bulk sample obtained by average weight through Eq. 3.27, being the elemental distribution the most representative.

Finally, the *RI* result was used to calculate the NRP, which is the proportion of the initial concentration (solid phase) of the mineral or element that will leach from the waste rock.

$$RI = \frac{\sum_{i=1}^{N} Mineral_{(Avail.)i}.[Xe_i].wt_i\%}{\sum_{i=1}^{N} [Xe_i].wt_i\%} \qquad \text{Eq. 3.28}$$

$$NRP = RI.[Xe_{hs}] \qquad \text{Eq. 3.29}$$

where RI = reactivity index given by cumulative elemental availability at size fraction (wt. %)

NRP = net reactivity potential available for leaching (mg/kg or %)

$[Xe_{hs}]$ = solid concentration of specific element for head or bulk sample (mg/kg or %)

$[Xe_i]$ = solid concentration of specific element for each size fraction i (mg/kg or %)

$wt_i\%$ = weight percent of each size fraction i

N = number of size fractions i

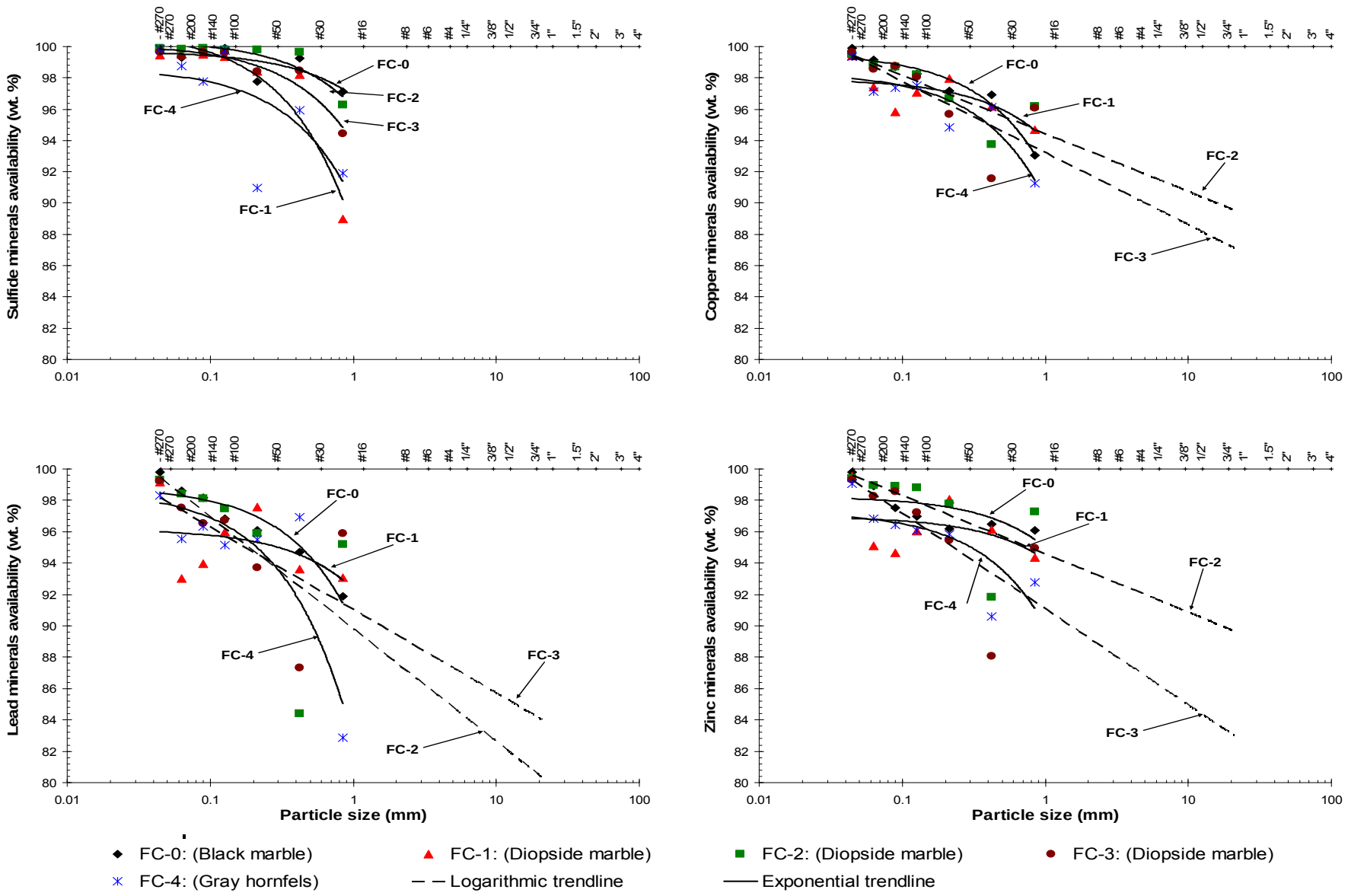

Figure 3.17 Regression lines to be used in determining mineral availability for leaching in all Class B waste rock samples

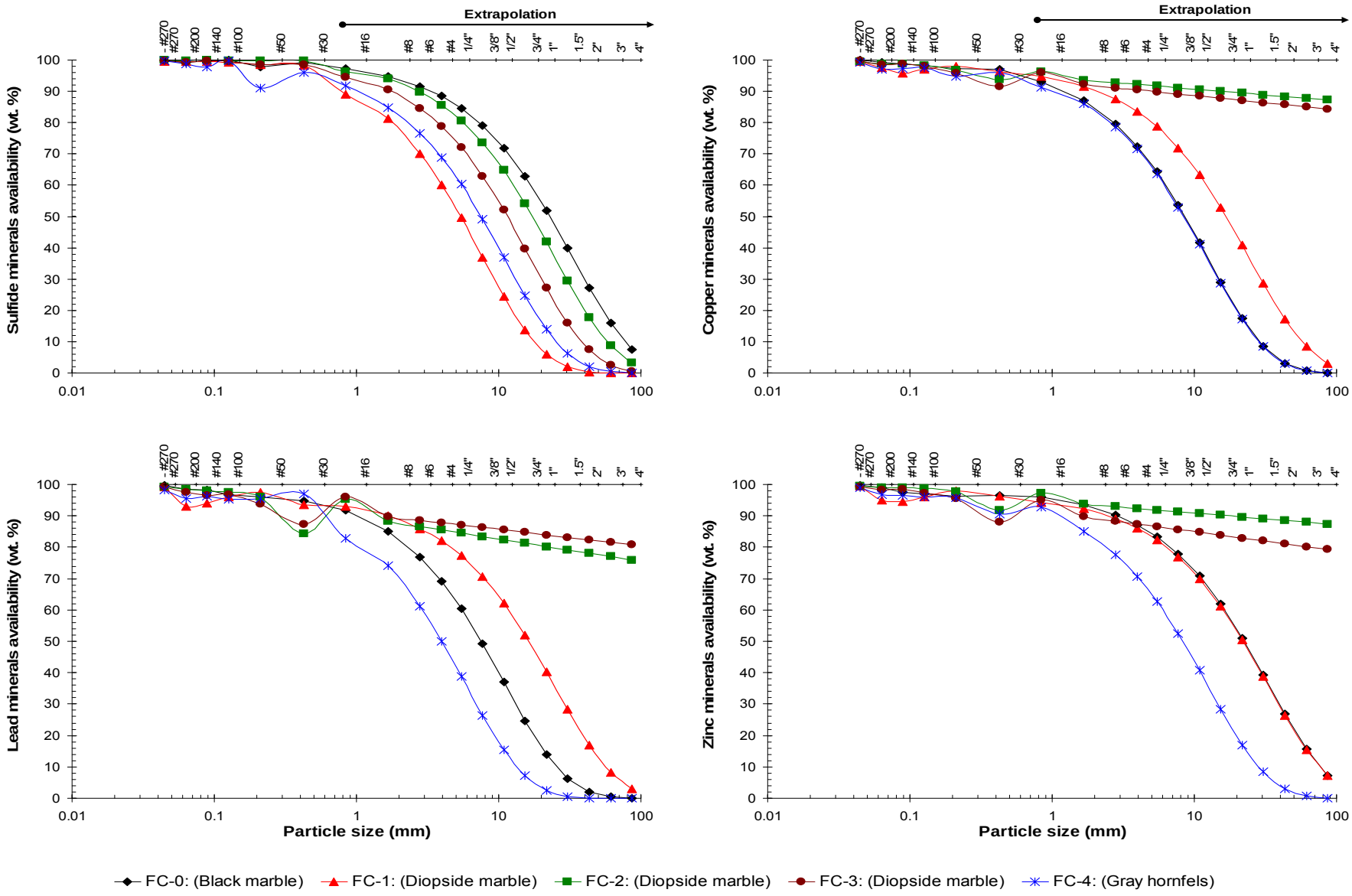

Figure 3.18 Mineral availability for leaching present in all Class B waste rock samples

4 FIELD CELLS EXPERIMENT

4.1 Introduction

Between March and August 2006, eight field cells were installed using waste rock material from the first 30,000 tonne experimental waste rock pile (Corazao Gallegos, 2007). The waste rock was taken from each tipping phase during the pile construction as is detailed in Section 1.5, providing two cells of black marble (UBC-1-0A/B corresponding to FC-0 lab code), four of diopside marble (UBC-1-1A, UBC-1-2A/B and UBC-1-3A corresponding to FC-1, FC-2, and FC-3 lab codes, respectively) and one of gray hornfels (UBC-1-4A corresponding to FC-4 lab code). All were composed of Class B material. One cell was also installed using Class C construction material black marble (UBC-1-XA) and was used in a protective layer at the base of the pile (Table 4.1). Details regarding the installation and operation of the field cells are described below.

4.2 Field Cell Installation

As was mentioned in Chapter 1, once a suitable sample was obtained, the material from conical pile A was selected to place into the field cells based on the following procedures:

- The lid was cut off or removed from a new 205-Litre (55-gallon) plastic drum;
- The inside of each drum was inspected, any dirt was removed and the inside was wiped dry;
- A ¾ inch PVC male adaptor as outlet fitting was installed in the lower portion of each drum (as close to the bottom as possible) and tightened with a ¾ inch PVC threaded hexagonal washer and sealed with silicone (Figure 4.1);
- A piece of geotextile (filter fabric) was taped over the outlet fitting at the base to prevent silica sand grains from migrating out of each drum;
- Four 2.5 cm (one-inch) diameter aeration holes were drilled into the rear-side of each drum, opposite from the leachate collection system. These holes were located at a higher level to avoid loss of drainage water (Appendix D1, Figure D1.1);
- Each empty field cell was placed on the support berm prepared with a 5% slope (Appendix D1, Figure D1.2). The installation took place in the designated area to place the field cells;
- The drums were sloped slightly towards the leachate collection system in order to drain as much water as possible into the sample collection bucket;
- A bottom drainage layer, consisting of approximately 15 cm height of 30 mesh silica sand (75 kg), was placed in each drum and overlaid by a geotextile which was also taped and used as a separation layer;
- Approximately 300 kg of waste rock from each conical pile A was placed in each field cell in several batches; these were weighted with a 25-kg spring scale to determine the total mass of waste rock placed in the cell. In some field cells, more than 300 kg were used. This additional material was taken from conical pile D. The drum was not filled fully, and as such the top 10 to 15 cm was kept empty.
- One-inch diameter reinforced PVC tubing was connected to the outlet fitting at the base of each drum and directed towards a sample collection bucket.

- A 20-L transparent plastic graduated sample collection bucket, placed at the front-bottom of each drum, was fitted with a lid into which a one-inch diameter hole was drilled. The PVC tubing was passed through this hole and sealed with silicone. A plastic pipe was installed at the bottom of the bucket to allow the drainage sampling.
- A rock sample plastic bag was placed over the sample bucket to prevent dirt and precipitation from entering the sample;
- A permanent label, which included a field cell code, information on the origin and location of the waste rock collected, its rock type and class, the date it was constructed or installed, and the mass of the rock, was affixed to the drum and sample bucket.

Some aspects of the procedure were adopted from the Antamina reports (Golder Associates, 2003; Golder Associates, 2004) and other work using similar kinetic cells (Broughton and Robertson, 1992; Robertson and Broughton, 1992). Figure 4.1 shows some of the steps followed during the installation of each field cell until to complete the construction of the eight cells (Figure 4.2).

Figure 4.1 Some accessories used for field cell installation

The field cells were then left exposed to the atmosphere and subjected to on-site weather conditions such as precipitation, evaporation and fluctuating temperatures. Furthermore, the details of field cell construction and installation are shown in the drawings and picture contents in Appendix D1 (Figure D1.1 and Figure D1.2) and in Appendix D2 (Figure D2.1 to Figure D2.8).

Figure 4.2 Field cells installed with Class B marble and hornfels waste rock material

4.2.1 Description of Waste Rock Samples

The solid phase assays (Zn and As only for field cells FC-1-0A/0B as example) and the geological information from each sample was obtained from the block model of Antamina's Geology Department (Appendix D3, Figure D3.1 to Figure D3.10).

In order to confirm the geological description of the material, Antamina's geologists assisted with an on-site examination of the material at the field cell location, and the results were compared with the initial geological description obtained from the block model (Table 4.2).

The waste rock classification and rock types mentioned in Table 4.1 did correspond to the block model description. However, the geologists described the material content in six of the field cells as being of Class C and only two as being of Class B (Table 4.2). Whereas the examination in the field was conducted only based on visual criteria, the block model takes into account the average of the metal content (chemical assay) in order to classify the material according to established criteria shown in Table 1.1, indicating that the classification based on the assay is more consistent and precise.

The rock lithology varied between what was indicated in the field cell and in the polygons of the block model. Several rock types and/or sub-types occurred in each polygon. The groups that determined waste rock class are shown in Figure D3.2, Figure D3.6 and Figure D3.8. However, the predominant rock type was determined as the most abundant and therefore the most representative of the polygon. The lithology of five field cells (UBC-1-0A/B, -1A, -3A and -XA) described in the block model was found to be consistent with the geologists' descriptions (Table 4.2). The only variety was in the sub-type description, for instance, where gray marble was described instead of diopside marble. In field cells UBC-1-2A and -2B, the geologists described the material as diopside exoskarn, which was therefore classified as Class A based on the classification criteria indicated in Table 1.1. However, diopside marble was present as the

most abundant rock type in the polygon, and therefore was considered to be the most representative. In addition, the gray hornfels sample described within the block model was seen as gray marble by geologists, and this variation may have been due to the reasons mentioned previously.

The “dirtiest” samples containing visually 2 - 3% sulfides (pyrite) were found in field cells UBC-1-2A and -2B. The other samples contained less than 1% sulfides. The black marble and gray hornfels seemed to contain the lowest amounts of very finely disseminated sulfide content. The black marble particles were coated by a relatively high content of smooth red-brownish clay minerals mixed with HFO or iron oxyhydroxide minerals. Particles of the diopside marble sample placed in the UBC-1-1A field cell were brownish, mixed with few pale-green and gray particles. In field cells -2A/2B particles were greenish, dense, hard, and striated, whereas field cell -3A was black, bluish with few pale-green particles. Hornfels particles in field cell -4A were mostly gray with some fine-grained pinkish.

4.2.2 Monitoring Program for Field Cells

After field cell installation, a long-term monitoring program that included sampling frequency and parameters to be measured was established. As part of Antamina’s monitoring program, the procedure described below was followed in the collection and shipping of the samples to the external laboratory:

- New clean plastic and glass bottles, coolers, preservers and other sampling equipment were prepared prior to the beginning of the sampling.
- Water drainage was sampled only when a sufficient amount of drainage (~4 Litre) had been collected in the sample collection buckets. Meanwhile, only field parameters were recorded.
- The sample bottles were labelled with station code, sampling date, parameter, sample class, sampling frequency, preserver, and sampling time. The sample class was used to identify the samples within the database system. Sample class “M”, which meant that samples were to be sent to an external laboratory, was always used. A weekly sampling (“S” for “semanal” in Spanish) routine was determined. This practice was adopted from Antamina mine’s Water Quality Monitoring Program.
- Before sampling, the bottles were rinsed three times with liquid from the same sample, to avoid contamination. This was considered to be part of the QA/QC program as well. Additional aspects of sample conservation for later analysis in the laboratory which was also part of the QA/QC are described later on.
- Electrical conductivity, pH, and temperature were recorded using calibrated MULTILINE P4 WTW Multi-parameter equipment. Other pertinent observations such as discoloration, mineral precipitate and algal growth were also recorded.
- The drainage water volume, which was recorded, and an average flow rate passing through the field cell, was computed. Once the volume record was complete, the water was discarded or was used for extra sample.
- Water samples were submitted to an external laboratory, Environmental Laboratories Peru S.A.C. (Envirolab) in Lima, Peru for analysis. The following analyzed parameters are summarized in Table 4.3: electrical conductivity, pH, alkalinity (as total, as CO_3^{2-} and as HCO_3^-), total suspended solids, total dissolved solids, hardness, total acidity, sulphate, chloride, fluoride, nitrate and ammonia

as N, and total and dissolved metals (Ag, Al, As, B, Ba, Be, Bi, Ca, Cd, Co, Cr. Cu, Fe, Hg, K, Mg, Mn, Mo, Na, Ni, Pb, Sb, Se, Si, Sn, Sr, Ti, Th, V, and Zn) by ICP-MS.

Table 4.1 Description of the field cells containing Class B waste rock material

N°	Field cell code	Waste rock class	Rock type (Lithology)	Sampling date* (mm/dd/yy)	Installation date (mm/dd/yy)	Waste rock mass - *m*** (kg)	Pile location†	Initial source‡
1	**UBC-1-0A**	B	Black marble	03/15/2006	03/21/2006	275	Protective layer	Open pit, Mesh: 3-SP-4358-12, Polygon: 02 **(3-SP-4358-12-02)**
2	**UBC-1-0B (duplicate)**	B	Black marble	03/15/2006	03/21/2006	275	Protective layer	Open pit, Mesh: 3-SP-4358-12, Polygon: 02 **(3-SP-4358-12-02)**
3	**UBC-1-1A**	B	Diopside marble	05/12/2006	06/14/2006	290	First tipping phase	Open pit, Mesh: 3-SP-4343-22, Polygon: 02 **(3-SP-4343-22-02)**
4	**UBC-1-2A**	B	Diopside marble	06/29/2006	08/13/2006	325	Second tipping phase	Open pit, Mesh: 3-NP-4373-29, Polygon: 02 **(3-NP-4373-29-02)**
5	**UBC-1-2B (duplicate)**	B	Diopside marble	06/29/2006	08/13/2006	325	Second tipping phase	Open pit, Mesh: 3-NP-4373-29, Polygon: 02 **(3-NP-4373-29-02)**
6	**UBC-1-3A**	B	Diopside marble	07/07/2006	08/13/2006	325	Third tipping phase	Open pit, Mesh: 3-SP-4328-21, Polygons: 01 and 06 **(3-SP-4328-21-01)** **(3-SP-4328-21-06)**
7	**UBC-1-4A**	B	Gray hornfels	07/07/2006	08/13/2006	325	Third/fourth tipping phase	Open pit, Mesh: 3-SP-4328-21, Polygons: 08 **(3-SP-4328-21-08)**
8	**UBC-1-XA**	C	Black marble	03/15/2006	03/21/2006	284	Base of the pile	Third crusher

***** Refers to sampling date done at each tipping phase event.
****** Fresh sample, after that, the moisture content was dropped for further calculations
† Refers to where the waste rock was sampled within the pile during the end-dumping.
‡ Initial location from which the waste rock came when moved from the open pit to its place into the pile

Table 4.2 Comparison between the block model and the geological field description of the samples

Block model			On-site examination			
Field cell code	**Waste rock class**	**Rock type†**	**Waste rock class**	**Rock type**	**Alteration / Veins**	**Mineralization**
UBC-1-0A	B	• Marble • **Black marble**	C	Marble	• 1% oxidation on the surface • <1% calcite veins	• 0.5% traces of very fine disseminated pyrite
UBC-1-0B	B	• Marble • **Black marble**	C	Marble	• 1% oxidation on the surface • <1% calcite veins	• 0.5% traces of very fine disseminated pyrite
UBC-1-1A	B	• Marble • Black marble • **Diopside marble**	C	Diopside marble	• 1% oxidation. • <1% secondary copper mineral (malachite)	• <1% fine disseminated pyrite
UBC-1-2A	B	• **Diopside marble** • Diopside hornfels • Diopside exoskarn	B	Green garnet diopside exoskarn	• 2% oxidation on the surface • <1% secondary copper mineral (chrysocolla) • <1% calcite veins with pyrite	• 2 - 3% coarse disseminated cubic pyrite • Traces of chalcopyrite, sphalerite, and galena • Contains 10% of fragments of green garnet wollastonite
UBC-1-2B	B	• **Diopside marble** • Diopside hornfels • Diopside exoskarn	B	Green garnet diopside exoskarn	• 2% oxidation on the surface • <1% calcite veins with pyrite	• 2 - 3% coarse disseminated cubic pyrite • Traces of chalcopyrite, sphalerite, and galena • Contains 10% of fragments of green garnet wollastonite
UBC-1-3A	B	• Black marble • Diopside marble	C	Gray marble	• <1% oxidation on the surface • <1% calcite veins with pyrite	• <1% fine disseminated pyrite • Traces of chalcopyrite and sphalerite Contains 10% of fragments of diopside marble
UBC-1-4A	B	• Diopside marble • **Gray hornfels** • Diopside exoskarn	C	Gray marble	• <1% oxidation on the surface • <1% calcite veins	• 1% very fine disseminated pyrite • Fine to medium particles
UBC-1-XA+	C	Black marble	C	Marble		

+ Not conducted by onsite examinee

† Highlighted and underlined rock types exist as the most abundant; therefore the most representative of the polygon

Table 4.3 Parameters and sampling frequency of field cell monitoring

Laboratories and field	Field cell codes / Parameters	UBC-1-0A	UBC-1-0B	UBC-1-1A	UBC-1-2A	UBC-1-2B	UBC-1-3A	UBC-1-4A	UBC-1-XA
Field	pH	S	S	S	S	S	S	S	S
	Electrical Conductivity	S	S	S	S	S	S	S	S
	Temperature	S	S	S	S	S	S	S	S
	Turbidity	S	S	S	S	S	S	S	S
	Volume+	S	S	S	S	S	S	S	S
Envirolab	Generals*	S	S	S	S	S	S	S	S
	Total Hardness	S	S	S	S	S	S	S	S
	Fluoride	S	S	S	S	S	S	S	S
	Total Metals**	S	S	S	S	S	S	S	S
	Dissolved Metals**	S	S	S	S	S	S	S	S
	Ammonia as N	S	S	S	S	S	S	S	S
	Nitrate as N	S	S	S	S	S	S	S	S
ALS	Similar to Envirolab	Temporary, for Quality Assurance and Quality Control (QA/QC) only							

S : Weekly "Semanal"
\+ Volume recording frequency depended on the seasons on-site. Sometimes, during a heavy rain, the recording was done only every two weeks
* Generals contains: pH, electrical conductivity, and alkalinity (as total, as carbonate and as bicarbonate), total suspended solids, total dissolved solids, total acidity, sulphate, chloride
** Metals by ICP-MS: Ag, Al, As, B, Ba, Be, Bi, Ca, Cd, Co, Cr. Cu, Fe, Hg, K, Mg, Mn, Mo, Na, Ni, Pb, Sb, Se, Si, Sn, Sr, Ti, Th, V, and Zn

4.3 Field Cell Water Drainage Results

Field cell installation began in March 2006, and the first sample was collected in April 2006. During two dry seasons (May-October of 2006 and 2007), no drainage water was collected from the field cells. After two wet seasons of collected data, the chemical analysis carried out by routine procedures was revised and used to make the interpretations regarding the field cells. This report presents two years' worth of data; however, the monitoring is on-going and future updates will be required.

4.3.1 Quality Assurance and Quality Control (QA/QC)

The water analyses were carried out by standard procedures, such as those described in "Standard methods for the examination of water and wastewater" (American Public Health Association. et al., 1998; Eaton et al., 2005; Greenberg et al., 1992). However, some aspects regarding the collection and conservation of the water samples, as well as the quality evaluation of chemical analysis were given special attention.

a. Field analyses and sample conservation

In order to remove some suspended solids and/or colloids that needed to be taken out before the analysis of real ions content, the samples for dissolved metal constituent analysis were filtered through 0.45 μm membrane filters.

Precautions to avoid changes in the chemical composition of the sample before analysis consisted of both measuring sensitive components in the field (pH, EC, temperature and turbidity) and the conservation of the samples for later analysis in the laboratory; for instance, samples for metals were preserved with nitric acid to pH <2, the nutrients (nitrate and ammonia) were acidified with sulphuric acid to pH <2. The non-metal samples were not preserved; these were only kept refrigerated at 4°C. Acidification stops most bacterial growth, blocks oxidation reactions, and prevents adsorption or precipitation of cations.

b. Chemical analysis errors

There are two types of errors in chemical analyses: errors of precision and errors of accuracy.

The **precision** was initially calculated by repeating the analysis of the same sample in order to confirm its result. In addition, in the field cells, duplicate samples were collected and were sent to the laboratory in the same batch with the other samples. The results obtained by using the Eq 4.1, show good relative range value (R) between the parameters of comparison; they lie within the acceptable range (0 – 0.2). However, some results exceeded the acceptable range, in which case the samples were reanalysed.

$$R = \frac{(X_1 - X_{2)}}{(X_1 + X_2)/2} \qquad \text{Eq. 4.1}$$

where X_1 and X_2 are the duplicates result from an individual sample and $X_1 - X_2$ is the absolute difference between X_1 and X_2 (Bartram et al., 1996).

The **accuracy** of the analysis for major ions was estimated through the **charge-balance error (*CBE*)**, for which the sum of positive and negative charges in the water should be equal.

$$CBE = \frac{(\sum cations - \sum anions)}{(\sum cations + \sum anions)} x100 \qquad \text{Eq. 4.2}$$

Where cations and anions were expressed as meq/L, the sums were taken for the cations Ca^{2+}, Mg^{2+}, Na^{+}, K^{+} and NH_4^{+}, and the anions Cl^{-}, HCO_3^{-}, CO_3^{2-}, SO_4^{2-} and NO_3^{-}. Differences in CBE of up to $\pm$2% are inevitable in almost all laboratories. However, larger errors of up to $\pm$5% may be accepted for groundwater, and of up to $\pm$10% are acceptable for surface water (Appelo and Postma, 2005; Bartram et al., 1996; Fritz, 1994; Murray and Wade, 1996). After the evaluation of 188 samples from 8 field cells, 98.4% of the data were found to be within the acceptable range ($\pm$10%). Thus, three samples of the three field cells on the same day were over-range. The sulphate results were identified as a erroneous data; these were iterated in order to obtain an acceptable charge balance error. The values were very close to others reported under different field cell codes. Therefore, a transcription fault of sulphate data related to the erroneous sample was detected. These values were changed to the correct position, and their charge balance gave a result that was within the acceptable range. Consequently, 100% of the samples were verified within $\pm$10% of error (Table 4.4 and Figure 4.3).

Table 4.4 Charge-Balance errors of water drainage data from the field cells

Field cell code	Sampling period (dd/mm/yy)	Charge-Balance Error (%)							
		# of samples	Min	Max	Average	St. Dev.	Av. ±St. Dev.	# > (± 10%)*	# > (± 10%)**
UBC-1-0A	06/04/2006 --> 02/05/2005	22	-5.3	5.4	0.2	3.4	0.2 ± 3.4	0	0
UBC-1-0B	06/04/2006 --> 02/05/2005	22	-5.1	4.9	-0.5	3.1	-0.5 ± 3.1	0	0
UBC-1-1A	26/10/2006 --> 02/05/2005	29	-5.1	6.8	-0.2	3.3	-0.2 ± 3.3	0	0
UBC-1-2A	26/10/2006 --> 02/05/2005	25	-4.3	4.8	1.4	2.9	1.4 ± 2.9	0	0
UBC-1-2B	12/10/2006 --> 02/05/2005	25	-5.5	8.3	0.7	3.5	0.7 ± 3.5	0	0
UBC-1-3A	26/10/2006 --> 02/05/2005	21	-5.7	5.8	0.7	3.7	0.8 ± 3.7	1	0
UBC-1-4A	02/11/2006 --> 02/05/2005	26	-3.2	5.8	1.7	2.8	1.7 ± 2.8	1	0
UBC-1-XA	16/11/2006 --> 02/05/2005	18	-4.4	5.8	1.0	3.6	1.0 ± 3.6	1	0
Total		188						3	0
Performance (%)								98.4	100.0

* A number of initial over-range samples (±10%). CBE of for (-21.5% for UBC-1-3A, 44.4% for UBC1-4A and -21.4% for UBC-1-XA were obtained. All samples were taken on January 11th, 2007

** Number of final over-range samples (±10%), after sulphate results relocation.

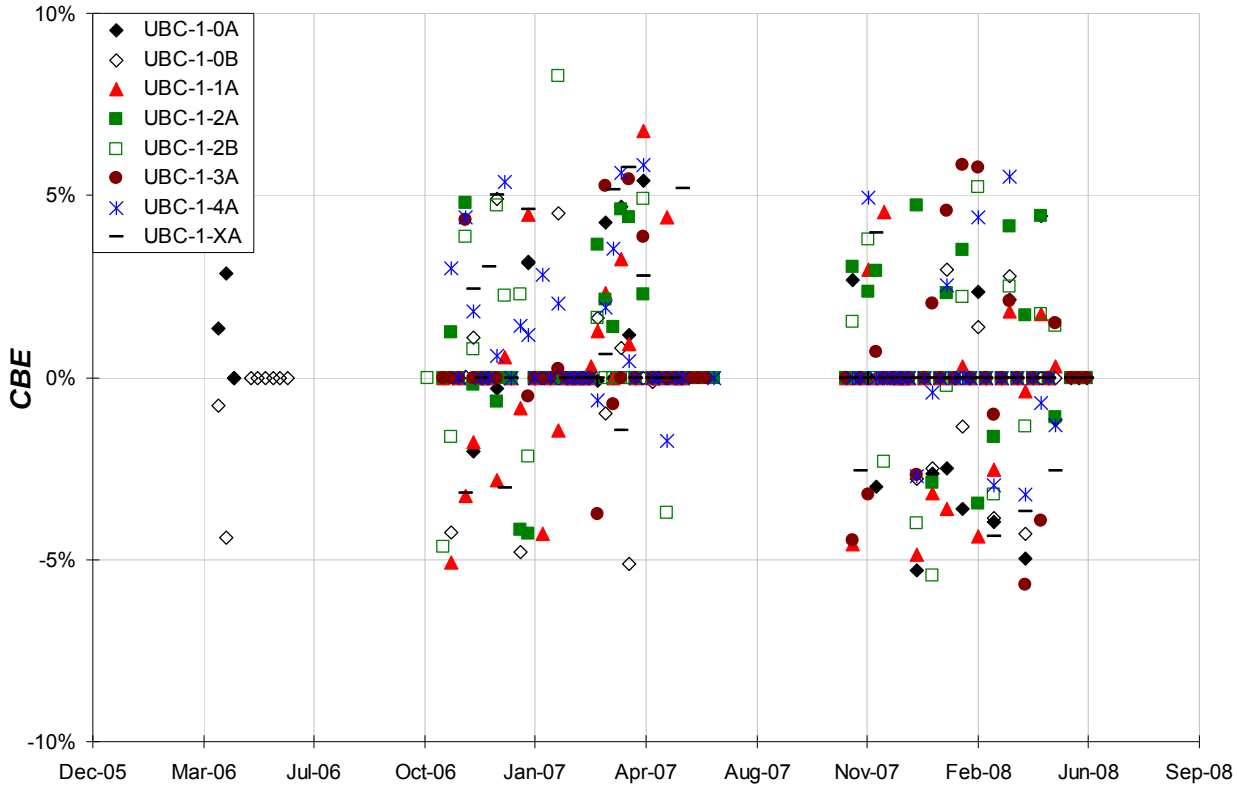

Figure 4.3 Charge balance error of the drainage data of the samples placed into the field cells

The other accuracy method used was the relationship between the **total dissolved solids (TDS)** and **electrical conductivity (EC)**. The value of TDS (mg/L) should not exceed the numerical value of

electrical conductivity (μS/cm). The relationship between the two variables is often described by a constant, commonly 0.65, but in most water a range from 0.55 to 0.80 is considered acceptable (Eq. 4.3). This relationship varies according to chemical composition (Bartram et al., 1996). 91.2% of the drainage data were found to be within the acceptable range (Table 4.5).

$$0.55 \leq \frac{TDS}{EC} \leq 0.80 \qquad \text{Eq. 4.3}$$

In addition, since the totals of any variable must be greater than its component parts, the metals were evaluated. Then, 100% of total metals were verified as being greater than their dissolved constituents.

Table 4.5 Relationship between the total dissolved solids and electrical conductivity of water drainage from the field cells

Field cell code	Sampling period (dd/mm/yy)	TDS/EC						
		# of samples	Min	Max	Average	St. Dev.	Av. ±St. Dev.	# <0.55, >0.80*
UBC-1-0A	06/04/2006 --> 02/05/2005	11	0.52	0.87	0.70	0.11	0.70 ± 0.11	3
UBC-1-0B	06/04/2006 --> 02/05/2005	15	0.59	0.87	0.71	0.08	0.71 ± 0.08	2
UBC-1-1A	26/10/2006 --> 02/05/2005	18	0.57	0.80	0.71	0.07	0.71 ± 0.07	0
UBC-1-2A	26/10/2006 --> 02/05/2005	14	0.59	0.82	0.71	0.07	0.71 ± 0.07	1
UBC-1-2B	12/10/2006 --> 02/05/2005	14	0.59	0.81	0.73	0.07	0.73 ± 0.07	2
UBC-1-3A	26/10/2006 --> 02/05/2005	10	0.68	0.79	0.74	0.03	0.74 ± 0.03	0
UBC-1-4A	02/11/2006 --> 02/05/2005	18	0.59	0.80	0.71	0.06	0.71 ± 0.06	0
UBC-1-XA	16/11/2006 --> 02/05/2005	13	0.65	0.85	0.74	0.06	0.74 ± 0.06	2
Total		113						10
Performance (%)								91.2

* A number of samples over-range of the relationship between TDS and EC (0.55 ≤ TDS/EC ≤ 0.80)

c. Comparison between duplicate field cells

As part of the QA/QC program, two field cells were installed as duplicates, UBC-1-0B of UBC-1-10A and UBC-1-2B of UBC-1-2A. During the evaluation of the sampling period, the frequency of the water drainage collection was kept similar to the original field cell, which generated a great deal of data from which to make a comparison between the results. Since there were several parameters measured, comparisons using Eq. 4.1 were only done for some of them. Most of the results were found to be within the acceptable range. However, the comparison was more consistent in the concentration plots of the main selected parameters, which were shown to be in the same order of magnitude (Chapter 5).

4.3.2 Data Analysis

The water drainage data collected between October 2006 and May 2008 (two rainy seasons) is summarized in Appendix D4, Table D4.1. After a QA/QC review, the laboratory results, in conjunction with the field data, were input into EQWin Database Manager.

In the following section, the analyzed parameters are briefly interpreted. However, only some of the selected parameters were considered to be highly important and relevant in terms of their long-term environmental impacts. These will be discussed in Chapter 5.

a. pH

In general, all the drainage from the field cells occurs under circumneutral pH conditions, and pH varies between 6.8 and 9.0 (Figure 4.4 and Table 4.6). Despite this, one of the diopside marble samples (UBC-1-1A) showed relatively alkaline conditions (i.e., pH between 8.0 and 9.5).

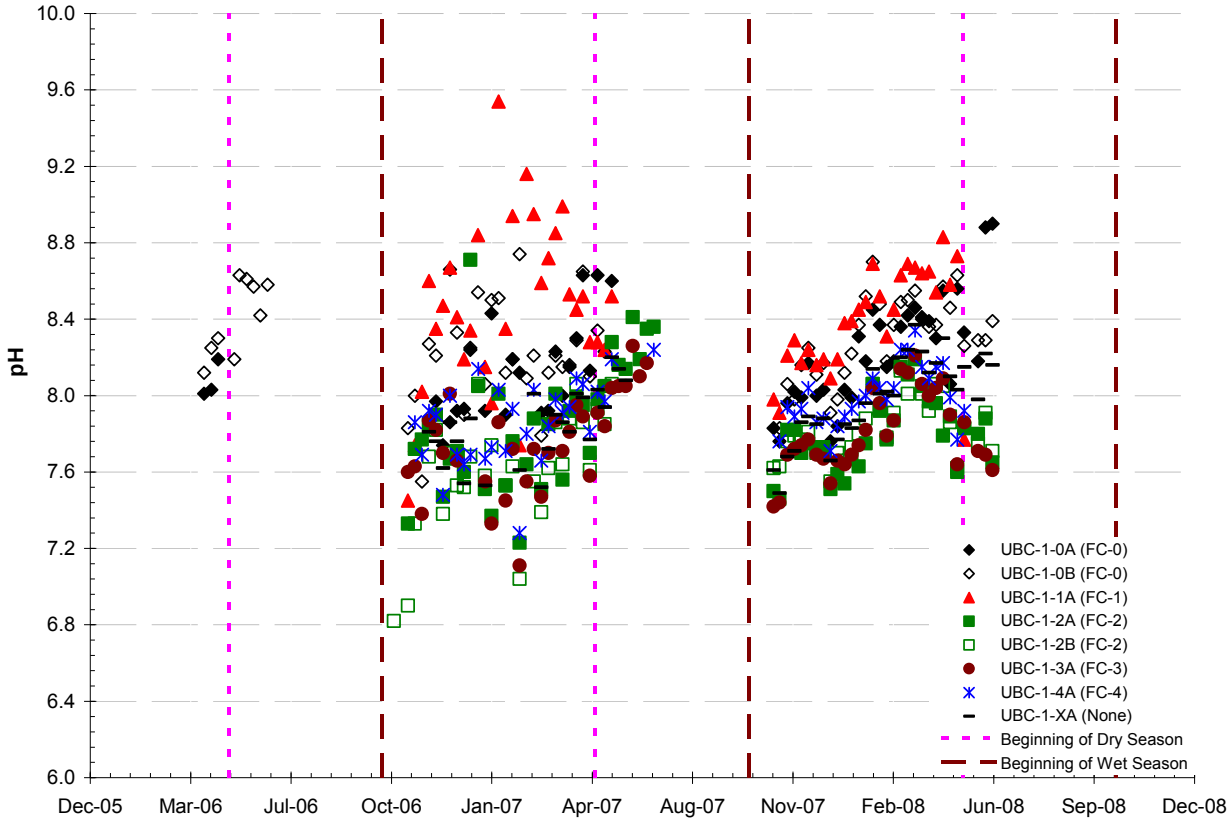

Figure 4.4 pH variation in the leachate from the field cells

b. Temperature

The temperatures of the leachates from the field cells ranged between 5 and 15°C for all samples. During the wet season, some water samples of diopside marble material reached temperatures of up to 25°C, indicating that the weathering of minerals in this rock type at this temperature may occur faster than at lower temperatures. However, the temperature variation within the whole-waste rock should be more

important to analyze because of its effect on the weathering process. This data is not available for this report.

c. Electrical conductivity (EC)

The results of EC ranged from 200 to 1,000 μS/cm. At the beginning of the wet season, high EC values (1,000 – 2,000 μS/cm) were reported, but these subsequently decreased. Higher EC results corresponded to the black and diopside marble samples.

d. Nitrate (NO_3) and ammonia (NH_3)

Both NO_3 and NH_3 were reported as nitrogen. These were only present in the initial samples (130 mg/L NO_3 and 9 mg/L NH_3) and were rapidly flushed out. Both originated from explosives (ammonia nitrate in conjunction with diesel) used during the mining process.

e. Sodium (Na), Potassium (K), and Magnesium (Mg)

The concentrations found in the initial samples in all the field cells (4 - 55 mg/L Na, 3 - 27 mg/L K, and 5 - 27 mg/L Mg) were rapidly depleted up to 1 - 3 mg/L Na, K and Mg. This suggests that the minerals containing these elements, such as silicate or carbonate mineral, were not weathering rapidly. However, calcium concentrations were found in high ranges. These are discussed further on.

f. Aluminum (Al), Manganese (Mn), and Iron (Fe)

Very low concentrations of Al and Mn were reported, with concentrations from 0.1 to <0.02 mg/L Al, and from 1 to <0.1 mg/L Mn. Therefore, there was no issue with respect to these parameters in the leachate from the field cells. Low aluminum and manganese concentrations would suggest that very slow weathering of silicate minerals such as plagioclase [$NaAlSi_3O_8$] or carbonate minerals such as ankerite [$Ca(Fe,Mg,Mn)(CO_3)_2$] were taking place. However, under circumneutral pH conditions, the amorphous hydroxide aluminum [$Al(OH)_3(am)$] formation may control the release of aluminum.

Very low dissolved iron concentrations (<0.01 mg/L), most of them below the analytical detection limit (0.001 mg/L), were detected in the leachates from all the field cells, suggesting that the formation and precipitation of secondary iron minerals such as iron oxide or hydroxide minerals is probably taking place.

g. Selenium (Se), Cadmium (Cd), and Nickel (Ni)

Although Se and Cd are soluble under circumneutral pH conditions, these were found in low concentrations (<0.002 – 0.012 mg/L Se and <0.003 – 0.06 mg/L Cd), suggesting that either Se and Cd minerals are present in very low proportions and are unavailable for leaching from the waste rock samples, or that they occur in insoluble mineral phases. On the other hand, very low concentrations of below 0.01 mg/L were found for Ni, indicating that there is no environmental concern for this element.

h. Silicon (Si)

Silicon concentrations were stable for the evaluated period for all samples. Concentrations ranged from 2 to 5 mg/L in black marble and gray hornfels samples, but were relatively higher (4 – 9 mg/L) in the diopside marbles samples. Higher Si concentrations (7 - 9 mg/L) were identified in one of the diopside samples UBC-1-2A/2B, indicating that weathering of silicate minerals was occurring rapidly for this particular sample.

i. Other elements

As was mentioned, some element indicators of metal leaching under circumneutral pH conditions which are of environmental concern, including sulphate (SO_4), calcium (Ca), total alkalinity, copper (Cu), lead (Pb), zinc (Zn), antimony (Sb), arsenic (As), molybdenum (Mo), and fluoride (F) were observed. The concentrations of these elements are presented in Table 4.6, and will be widely discussed in Chapter 5.

4.3.3 Loading and Release Rates

Leachate data (i.e. element concentrations and drained volume), sampling period time, moisture content, and mass and surface area of waste rock placed in the field cells were used to calculate loading and release rates. The results are discussed in the next chapter and are shown in Appendix E2 (Figure E2.1 to Figure E.10).

Initially, elemental production (mg/kg) was calculated by multiplying the elemental concentration (mg/L) by the drained volume (L) and dividing by mass of the waste rock (kg) and moisture content (ω), as is shown in Eq. 4.4. Later on, the total mass elemental released (mg) in the leachate was calculated through Eq. 4.5 by multiplying the cumulative elemental production by the mass of waste rock.

$$EP_t = \frac{[Xe].V}{m.(1-\omega)} \qquad \text{Eq. 4.4}$$

$$TEP = CEP \,.\, m \,.(1-\omega) \qquad \text{Eq. 4.5}$$

where EP = elemental production (mg/kg of waste rock),

TEP = total elemental production to date (mg of element),

CEP = cumulative elemental production to date (mg/kg of waste rock),

$[Xe]$ = concentration of specific element from the field cell drainage data (mg/L),

V = effluent volume recorded from the field cell (L),

m = total mass of whole-waste rock placed in the field cell (kg),

ω = moisture content of waste rock (%)

Table 4.6 Summary of concentrations of key selected parameters found in the leachate from the field cells

Parameter	pH	SO_4	Ca	Alk.	Cu	Pb	Zn	Sb	As	Mo	F	SO_4	Ca	Alk.	Cu	Pb	Zn	Sb	As	Mo	F
Aspect	s.u.	mg/L										mmol/L									
UBC-1-0A: From 06/04/06 to 02/05/08 (22)*																					
Average	8.63	240.0	137.9	45.2	0.003	0.01	0.06	0.01	0.007	0.025	1.1	2.5	3.4	0.45	4.0E-05	4.8E-05	9.8E-04	1.1E-04	9.8E-05	2.7E-04	0.06
Maximum	8.15	739.7	373.5	59.2	0.011	0.01	0.17	0.04	0.022	0.04	3.1	7.7	9.3	0.59	1.7E-04	4.8E-05	2.6E-03	3.4E-04	2.9E-04	4.2E-04	0.16
Minimum	7.74	53.2	62.8	35.2	0.001	0.01	0.02	0.01	0.001	0.02	0.5	0.6	1.6	0.35	1.6E-05	4.8E-05	3.5E-04	8.2E-05	1.3E-05	2.1E-04	0.03
UBC-1-0B (Duplicate: From 06/04/06 to 02/05/08 (22)																					
Average	8.74	251.9	122.3	45.8	0.001	0.01	0.02	0.05	0.017	0.028	0.9	2.6	3.1	0.46	2.3E-05	4.8E-05	3.7E-04	3.9E-04	2.3E-04	2.9E-04	0.05
Maximum	8.28	694.2	323.8	61.2	0.008	0.01	0.10	0.07	0.026	0.03	1.2	7.2	8.1	0.61	1.3E-04	4.8E-05	1.6E-03	5.5E-04	3.5E-04	3.1E-04	0.06
Minimum	7.55	111.3	63.5	39.0	0.001	0.01	0.01	0.01	0.001	0.02	0.6	1.2	1.6	0.39	1.6E-05	4.8E-05	1.4E-04	8.2E-05	1.3E-05	2.1E-04	0.03
UBC-1-1A: From 26/10/06 to 02/05/08 (29)																					
Average	9.54	67.4	47.6	50.3	0.002	0.01	0.04	0.19	0.024	0.04	1.3	0.7	1.2	0.50	3.0E-05	5.1E-05	6.3E-04	1.5E-03	3.2E-04	4.1E-04	0.07
Maximum	8.43	192.2	103.0	62.2	0.009	0.02	0.12	0.25	0.035	0.06	1.6	2.0	2.6	0.62	1.4E-04	7.7E-05	1.8E-03	2.1E-03	4.7E-04	6.3E-04	0.08
Minimum	7.45	25.7	29.8	39.0	0.001	0.01	0.004	0.02	0.012	0.01	1.0	0.3	0.7	0.39	1.6E-05	4.8E-05	6.1E-05	1.6E-04	1.6E-04	1.0E-04	0.05
UBC-1-2A: From 26/10/06 to 02/05/08 (25)																					
Average	8.71	162.6	78.4	40.1	0.10	0.45	4.4	0.05	0.020	0.03	1.4	1.7	2.0	0.40	1.5E-03	2.2E-03	6.7E-02	4.4E-04	2.6E-04	3.2E-04	0.07
Maximum	7.84	395.5	158.1	50.2	0.21	1.15	16.9	0.11	0.036	0.05	2.2	4.1	3.9	0.50	3.3E-03	5.6E-03	2.6E-01	8.7E-04	4.8E-04	5.2E-04	0.11
Minimum	7.23	77.6	49.9	30.1	0.03	0.18	0.9	0.02	0.001	0.01	0.3	0.8	1.2	0.30	5.0E-04	8.6E-04	1.4E-02	1.7E-04	1.3E-05	1.0E-04	0.02
UBC-1-2B (Duplicate): From 12/10/06 to 02/05/08 (25)																					
Average	8.19	231.7	108.9	35.5	0.14	0.65	4.1	0.05	0.014	0.03	1.5	2.4	2.7	0.35	2.2E-03	3.1E-03	6.3E-02	3.9E-04	1.9E-04	2.9E-04	0.08
Maximum	7.73	863.1	434.5	49.1	0.26	3.99	9.6	0.09	0.028	0.04	2.2	9.0	10.8	0.49	4.0E-03	1.9E-02	1.5E-01	7.2E-04	3.7E-04	4.2E-04	0.12
Minimum	6.82	96.9	59.7	7.5	0.08	0.16	2.2	0.02	0.001	0.01	1.0	1.0	1.5	0.07	1.3E-03	7.7E-04	3.4E-02	1.4E-04	1.3E-05	1.0E-04	0.05
UBC-1-3A: From 26/10/06 to 02/05/08 (21)																					
Average	8.26	238.5	110.3	42.8	0.15	0.39	4.7	0.05	0.012	0.02	1.5	2.5	2.8	0.43	2.4E-03	1.9E-03	7.2E-02	4.5E-04	1.6E-04	2.3E-04	0.08
Maximum	7.79	410	194.3	56.2	0.31	0.88	13.9	0.08	0.022	0.03	1.9	4.3	4.8	0.56	4.8E-03	4.2E-03	2.1E-01	6.5E-04	2.9E-04	3.1E-04	0.10
Minimum	7.11	102.8	54.9	32.0	0.04	0.01	1.3	0.04	0.001	0.01	1.1	1.1	1.4	0.32	5.8E-04	4.8E-05	2.0E-02	3.1E-04	1.3E-05	1.0E-04	0.06
UBC-1-4A: From 02/11/06 to 02/05/08 (26)																					
Average	8.34	126.3	59.1	50.4	0.035	0.24	1.8	0.13	0.008	0.019	1.5	1.3	1.5	0.50	5.6E-04	1.2E-03	2.7E-02	1.0E-03	1.1E-04	2.0E-04	0.08
Maximum	7.93	467.4	161.9	60.2	0.072	0.64	4.4	0.17	0.016	0.03	1.9	4.9	4.0	0.60	1.1E-03	3.1E-03	6.8E-02	1.4E-03	2.1E-04	3.1E-04	0.10
Minimum	7.28	41.7	35.5	39.9	0.001	0.04	0.4	0.06	0.001	0.01	1.1	0.4	0.9	0.40	1.6E-05	1.9E-04	6.5E-03	5.3E-04	1.3E-05	1.0E-04	0.06
UBC-1-XA: From 16/11/06 to 02/05/08 (18)																					
Average	8.37	322.9	139.9	42.3	0.042	0.36	2.0	0.05	0.007	0.02	1.5	3.4	3.5	0.42	6.6E-04	1.7E-03	3.1E-02	4.1E-04	9.5E-05	1.6E-04	0.08
Maximum	7.91	672.8	294.4	50.6	0.070	0.67	3.1	0.07	0.013	0.02	1.8	7.0	7.3	0.51	1.1E-03	3.2E-03	4.7E-02	6.0E-04	1.7E-04	2.1E-04	0.10
Minimum	7.49	127.5	68.2	30.8	0.023	0.17	1.0	0.01	0.001	0.01	1.2	1.3	1.7	0.31	3.6E-04	8.0E-04	1.6E-02	8.2E-05	1.3E-05	1.0E-04	0.06

* Number of samples evaluated in the sampling period

Loading rates (mg/day) at each sampling period (t) are expressed as mass of the element released per time. Thus, loading rates were obtained through the multiplication of the elemental concentration by flowrate. In particular, the loading rates in the field cells were calculated through Eq. 4.6 by multiplying the elemental concentration (mg/L) by the drained volume (L) and dividing by the sampling period time (i.e. elapsed days between each sampling event).

$$LR_t = \frac{[Xe].V}{t} \qquad \text{Eq. 4.6}$$

where LR_t = loading rates at each sampling time (mg/kg of waste rock),

t = sampling period time (day)

However, for a relative comparison of elemental release from each field cell, the release rates were calculated and normalized on a waste rock mass basis and on a surface area basis at each time of sampling. They also were calculated considering the entire sampling period (T). Normalized release rates are more useful than effluent concentrations in order to compare the behaviour of each sample placed in the field cell because of the variability in their wet waste rock mass (284 – 325 kg), cumulative drained volume (211.0 - 287.5 L), surface area, and the installation time (see Table 4.1). Thus, release rates were obtained through Eq. 4.7 and 4.8 by dividing the loading rates by the dry waste rock mass (kg) or by the total surface area (m^2).

$$RR_m = \frac{LR_t}{m.(1-\omega)} or = \frac{TEP}{m.(1-\omega).T} \qquad \text{Eq. 4.7}$$

$$RR_{SA} = \frac{LR_t}{SA_s} or = \frac{TEP}{SA_s.T} \qquad \text{Eq. 4.8}$$

where RR_m = release rate on a waste rock mass basis (mg/kg/day),

RR_{SA} = release rate on a total surface area basis (mg/m^2/day),

SA_s = surface area of the whole-waste rock placed in the field cell (m^2)

T = total sampling period (day)

In addition, depletion proportions (DP), which are the proportion of the initial amount of the element that was released; and an approach for determining the time to deplete 100% of the elements (DT) were calculated through Eq. 4.9 and Eq. 4.10.

$$DP = 100 - (\frac{SP - CEP}{SP} * 100) \qquad \text{Eq. 4.9}$$

$$DT = \frac{SP \,.\, T}{CEP} * 365 \qquad \text{Eq. 4.10}$$

where DP = depletion proportion (%),

SP = solid phase elemental or initial elemental concentration (mg/kg),

DT = depletion time, to reduce 100% of the element (year)

Finally, based on Eq. 2.8, the neutralization potential (NP) depletion rate was calculated considering that carbonate minerals as the primary neutralizing sources, according to Eq. 4.11 on a mass basis, and Eq.4.12 on surface area basis.

$$NP_{DR} = RR_{m(SO_4)} \,.\, MR_{(Ca+Mg)/SO_4} \qquad \text{Eq. 4.11}$$

$$NP_{DR} = RR_{SA(SO_4)} \,.\, MR_{(Ca+Mg)/SO_4} \qquad \text{Eq. 4.12}$$

where NP_{DR} = neutralization potential depletion rate (mg $CaCO_3$/kg/day),

$RR_{m(SO_4)}$ = release rate of sulphate on a mass basis (mg SO_4/kg/day),

$RR_{SA(SO_4)}$ = release rate of sulphate on a surface area basis (mg SO_4/m^2/day),

$MR_{(Ca+Mg)/SO_4}$ = molar ration of calcium+magnesium by leachate sulphate (mg $CaCO_3$/mg SO_4),

4.4 Geochemical Speciation Calculations

PHREEQC Version 2.15 and MINTEQ.V4.DAT database (Parkhurst et al., 1999) were used to determine the saturation indices (*SI's*) in the drainage data collected from the field cells with respect to relatively reactive minerals such as gypsum and calcite, and to identify possible solubility controls for the weathering products.

Each SOLUTION represents one sampling time of drainage water from the field cells. Data were set and obtained from EQWin and converted to PHREEQC input files using MS Excel macros. In order to obtain the geochemical speciation, an oxidation-reduction potential energy (pe) of 12 was assumed for all solutions. This value is considered representative of oxidizing conditions encountered in materials exposed to the atmosphere and was established in EQUILIBRIUM-PHASE with respect to the partial pressure of atmospheric oxygen (pO_2 = 0.21 atm = $10^{-0.68}$). The alkalinity values were set as mg/L of calcium carbonate ($CaCO_3$). Likewise, the following parameters were considered: pH, temperature, sulphate (SO_4), chlorine (Cl), nitrate as N (N-NO_3), ammonia as N (N-NH_3), fluoride (F), and metals (Al, Sb, As, Ba, B, Cd, Ca, Cr, Co, Cu, Fe, Pb, Mg, Hg, Mo, Ni, K, Se, Si, Ag, Na, Sr, Zn) in mg/L. This list includes all major ions and selected trace metals that showed frequent "hits" above detection limit. If concentrations were found to be below the detection limit, the results were multiplied by 10^{-20}.

A SELECTED OUTPUT file was used to print out the saturation indices for the following minerals in all solutions: Sulphates including anglesite [$PbSO_4$], anhydrite [$CaSO_4$], celestite [$SrSO_4$], gypsum [$CaSO_4$:$2H_2O$], larnakite [PbO:$PbSO_4$], zincosite [$ZnSO_4$], and barite [$BaSO_4$]; barium arsenate [$Ba_3(AsO_4)_2$]; carbonate minerals such as aragonite (amorphous calcite) [$CaCO_3$], calcite [$CaCO_3$], cerrusite [$PbCO_3$], dolomite [$CaMg(CO_3)_2$], magnesite [$MgCO_3$], otavite [$CdCO_3$], smithsonite [$ZnCO_3$], and malachite [$Cu_2(OH)_2CO_3$]; oxides minerals such as birnessite [MnO_2], bixbyite [Mn_2O_3], hausmannite [Mn_3O_4], nsutite [MnO_2], pyrolusite [MnO_2], manganite [MnOOH], tenorite [CuO], and plattnerite [PbO_2]; hydroxide minerals including spertiniite [$Cu(OH)_2$], and wülfingite [$Zn(OH)_2$]; molybdate minerals such as powelite [$CaMoO_4$], cadmium-molybdate [$CdMoO_4$], and wulfenite [$PbMoO_4$]; fluorite mineral [CaF_2]; and the quartz [SiO_2] as representative of the silicate minerals. These phases were chosen based on preliminary screening to identify possible solubility controls (Mayer, 2007).

The potential for mineral precipitation or secondary mineral formation was assessed using the saturation index (SI) calculated according to Eq. 4.13.

$$SI = \log \frac{IAP}{K_{sp}} \qquad \text{Eq. 4.13}$$

where, IAP (ion activity product) is the product of a solution's calculated ion activities (or concentrations) in a dissolution reaction and K_{sp} (solubility product) is the equilibrium constant for the mineral dissolution reaction (Sherlock et al., 1995). If *SI*>0, the solution is supersaturated with respect to a particular mineral phase, and the mineral will tend to precipitate. If *SI*<0, the solution is undersaturated, which then implies a driving force for mineral dissolution or suggesting that mineral phase is absent. Finally, when *SI* values are close to zero "0," it indicates that the solution is in equilibrium with respect to the mineral in question. Therefore, based on the above assumptions, the reported conservative *SI* values of between 0.5 and -0.5 were considered to be in equilibrium with the solution.

Mineral stability was evaluated for a limited number of geochemically-credible mineral phases that are known to precipitate/dissolve without significant kinetic impediments under ambient conditions at mining sites and in concordance with the Antamina's geology and mineralogy.

Geochemical speciation modeling conducted for all field cell samples indicates that the leachate solutions were undersaturated with respect to almost all secondary mineral phases such as zincosite [$ZnSO_4$] and wülfingite [$Zn(OH)_2$] (Table 4.7 and Appendix D5, Figure D5.1 to Figure D5.4). Duplicate samples show similar behaviour and therefore their results were grouped.

The solutions from all field cells remained undersaturated with respect to most of the sulphate minerals including anglesite [$PbSO_4$], anhydrite [$CaSO_4$], celestite [$SrSO_4$], gypsum [$CaSO_4$:$2H_2O$], larnakite [PbO:$PdSO_4$] and zincosite [$ZnSO_4$]. The only exception was barite [$BaSO_4$], which has a low solubility, but its SI was close to equilibrium for all solutions. This indicates that sulphate released from the field cells provided a suitable estimate for sulfide weathering rates.

On the other hand, carbonate minerals such as dolomite [$CaMg(CO_3)_2$], magnesite [$MgCO_3$], otavite [$CdCO_3$] and smithsonite [$ZnCO_3$], remained soluble in the solutions indicating that carbonates weather

rapidly in response to sulfide oxidation. However, the aragonite, calcite [$CaCO_3$], and cerrusite [$PbCO_3$] were near equilibrium with the solutions, maintaining the leachates from field cells under circumneutral pH conditions through the dissolution of carbonate minerals. In addition, malachite [$Cu_2(OH)_2CO_3$] remained in equilibrium or supersaturated, indicating that copper release could be controlled by this mineral.

Table 4.7 Mineral stability evaluated in the drainage water from all the field cells

Mineral	UBC-1-0A/0B	UBC-1-1A	UBC-1-2A/2B	UBC-1-3A	UBC-1-4A	UBC-1-XA
Anglesite [$PbSO_4$]	U	U	U	U	U	U
Anhydrite [$CaSO_4$]	U	U	U	U	U	U
Celestite [$SrSO_4$]	U	U	U	U	U	U
Gypsum [$CaSO_4:2H_2O$] *	U	U	U	U	U	U
Larnakite [$PbO:PbSO_4$] *	U	U	U	U	U	U
Zincosite [$ZnSO_4$]	U	U	U	U	U	U
Barite [$BaSO_4$]	E	E	E	E	E	E
Barium arsenate [$Ba_3(AsO_4)_2$]	S	S	S	S	S	S
Aragonite [$CaCO_3$]	E	E	E	E	E	E
Calcite [$CaCO_3$]	E	E	E	E	E	E
Cerrusite [$PbCO_3$]	E	E	E	E	E	E
Dolomite [$CaMg(CO_3)_2$]	U	U	U	U	U	U
Magnesite [$MgCO_3$]	U	U	U	U	U	U
Otavite [$CdCO_3$] *	U	U	U	U	U	U
Smithsonite [$ZnCO_3$]	U	U	E	E	E	E
Malachite [$Cu_2(OH)_2CO_3$]	E	E	S	S	S	S
Birnessite [MnO_2]	S	S	S	S	S	S
Bixbyite [Mn_2O_3]	S	S	S	S	S	S
Hausmannite [Mn_3O_4]	S	S	S	S	S	S
Nsutite [MnO_2]	S	S	S	S	S	S
Pyrolusite [MnO_2]	S	S	S	S	S	S
Manganite [MnOOH]	S	S	S	S	S	S
Tenorite [CuO]	E	E	E	E	E	E
Plattnerite [PbO_2]	U	U	U	U	U	U
Spertiniite [$Cu(OH)_2$]	U	U	E	E	E	E
Wülfingite [$Zn(OH)_2$]	U	U	U	U	U	U
Powellite [$CaMoO_4$]	U	U	U	U	U	U
Cadmium-molybdate [$CdMoO_4$]	E	E	E	E	E	E
Wulfenite [$PbMoO_4$]	S	S	S	S	S	S
Fluorite [CaF_2]	E	E	E	E	E	E
Quartz [SiO_2]	E	E	E	E	E	E

U: Undersaturated or mineral formed or precipitated. **E:** Solution in equilibrium with respect to determined mineral. **S:** Mineral supersaturated
* Solution in equilibrium with respect to minerals at the first flushing, the accumulated concentration during the dry season was flushed out.

Most of the oxide minerals such as birnessite [MnO_2], hausmannite [Mn_3O_4], manganite [MnOOH], and tenorite [CuO] remained in equilibrium or supersaturated, indicating that manganese mobilization could be controlled by these minerals, although copper in tenorite was present in both solid and leachate phases. However, all solutions remained undersaturated with respect to plattnerite [PbO_2], which indicates that lead mobilization was taking place all leachates.

Most of the solutions with respect to molybdate minerals were present in the three phases. The solutions were undersaturated with respect to powelite [$CaMoO_4$], indicating that either Ca and Mo mobilization was occurring, or that the mineral was never formed. With respect to cadmium-molydbate [$CdMoO_4$], the solutions were in equilibrium, suggesting that the dissolution of this specific mineral could be occurring slowly. However, the solutions from all samples remained supersaturated with respect to wulfenite

[$PbMoO_4$], which indicates that the mobilization of Pb and Mo are controlled by the formation of this particular mineral.

As it is commonly understood, silicate minerals weather slowly, and this was confirmed by the fact that the solutions from all the field cells were in equilibrium with respect to quartz.

4.5 Hydrologic Budget at the Field Cells

A hydrologic budget, water budget, or water balance is a measurement of the continuity of the water flow, holds true for any time interval, and applies to any sized area ranging from any drainage area to the earth as a whole (Todd and Mays, 2005).

In an open system, such as the field cells, exposure to the atmosphere, the water balance equation (Eq. 4.14) can be expressed as in a surface water system in units of volume per unit time.

$$P + Q_{in} - Q_{out} + Q_g - E_s - T_s - I = \Delta S_s \qquad \text{Eq. 4.14}$$

where P = precipitation (m/day),

Q_{in} = surface water flow into the system (m^3/day),

Q_{out} = surface water flow out of the system (m^3/day),

Q_g = groundwater flow into the stream (m^3/day),

E_s = surface evaporation (m/day),

T_s = transpiration of the system (m/day),

I = infiltration into the system (m^3/day), and

ΔS_s = change in water storage of the surface water system (m^3/day)

Considering the field cell as a system, the flowrates in Q_g, T_s, and I do not occur, therefore these were assumed to be zero "0". The Q_{in}, and E_s were transformed by multiplying the precipitation data by the surface area of the top of the field cell according to Eq. 4.15 and Eq. 4.16, respectively.

$$Q_{in-fc} = P \;\; x \;\; A_{fc} \qquad \text{Eq. 4.15}$$

$$E_p = E_s \;\; x \;\; A_{fc} \qquad \text{Eq. 4.16}$$

where A_{fc} = surface area of the top of field cell (m^2),

Q_{in-fc} = water inflow to the field cell (L/day),

E_p = pan evaporation data (L/day),

By substituting Eq. 4.15 and Eq. 4.16 in Eq. 4.14, it becomes:

$$Q_{in-fc} - Q_{out-fc} - E_p = \Delta S_{fc}$$ Eq. 4.17

where Q_{out-fc} = water outflow of the field cell (L/day),

ΔS_{fc} = change in water storage within the field cell (L/day)

The evaluated precipitation and pan evaporation data (2006 - 2008) were obtained from the Yanacancha meteorological station (C-YA), which is located half kilometre from the field cells area at the mine.

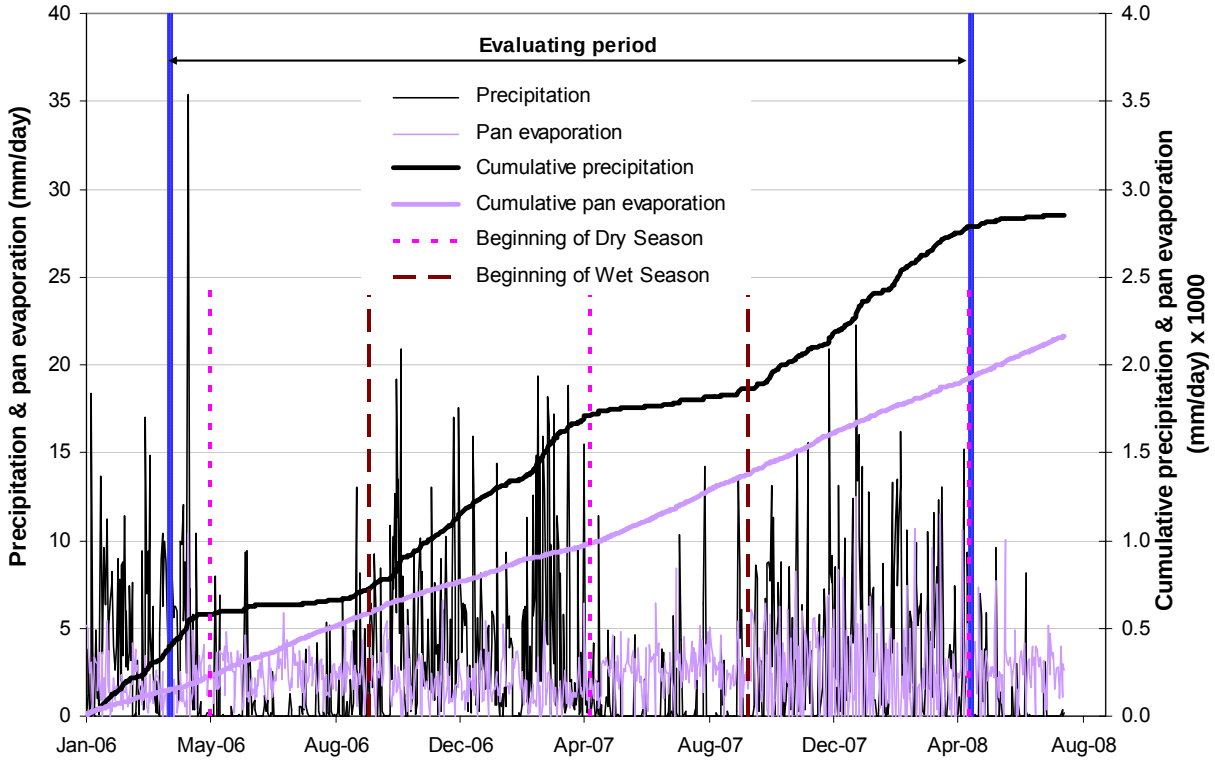

Figure 4.5 Precipitation and pan evaporation at the field cells area (2006-2008)

The Antamina mine is located at an average of 4,200 meters above sea level and has a remarkably mild climate for a site at this elevation. At the Yanacancha camp (where the field cells are located), the annual temperatures range from -8 to 28°C and with approximately 1,235 mm of annual average precipitation (Golder Associates, 2007a). Two well defined seasons exist; the dry season is from May to September, and the wet season is from October to April. Pan evaporation measurements are commonly used to define “potential evaporation.” The potential evaporation is usually higher during the dry season, in contrast with the wet season, when it is lower (Figure 4.5).

The data provided was used to compute changes in the water storage in the field cells according to Eq. 4.17. The field cells were operated under site conditions (seasonal cycles), therefore with undersaturated flow. In general, in all the field cells, the inflow was higher than the pan evaporation and outflow; therefore changes seasonally in water storage may exist. For instance, during the wet season,

the inflow in the field cell containing the black marble sample reached approximately 40% (Figure 4.6). However, during the dry season the storage was negligible, remaining at zero percent. At the end of the evaluated period (May 2008), there was not water reported in any of the field cells, suggesting that the 2008 dry season had started, and the evaporation had reduced the water which had been present within the waste rock placed in the field cells. All plots related to water budget for all field cells, are shown in Appendix D6 (Figure D6.1 and Figure D6.2).

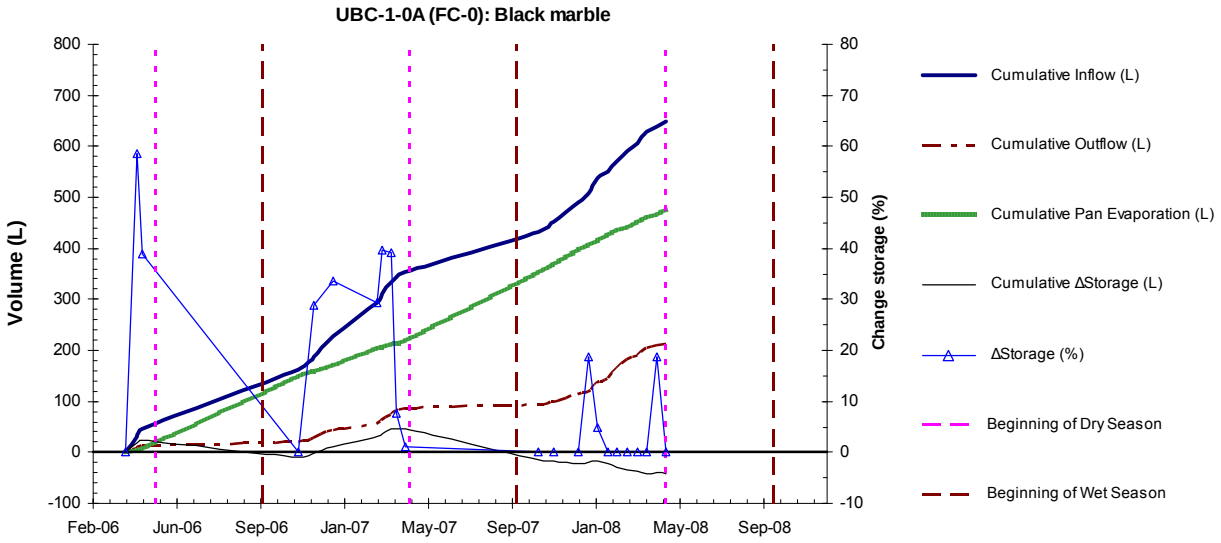

Figure 4.6 Water balance considering change in water storage and pan evaporation data in the field cell with Class B black marble waste rock material (2006-2008)

However, as the potential evaporation was significantly higher than the actual evaporation (evaporation) from the waste rock (Corazao Gallegos, 2007), the evaporation in the field cell (E_{fc}) was calculated considering that the change in water storage was insignificant (ΔS_{fc} = 0), and replacing E_{fc} with E_p. Then, Eq. 4.17 becomes:

$$Q_{in-fc} - Q_{out-fc} = E_{fc} \qquad \text{Eq. 4.18}$$

where ET_{fc} = evaporation in the field cell (L/day),

Figure 4.7 shows that pan evaporation (potential evaporation) was higher than evaporation from the all the field cells (Appendix D6, Figure D6.3 and Figure D6.4). However, in field cell UBC-1-1A, which contained one of the diopside marble samples, a significant difference was found compared with the other field cells, and the evaporation was close to the higher outflow rate (Table 4.8). This suggests that there was a relatively less water retention within the waste rock content in that field cell when compared to the other field cells, and indicates that the material allowed for a rapid flux of water.

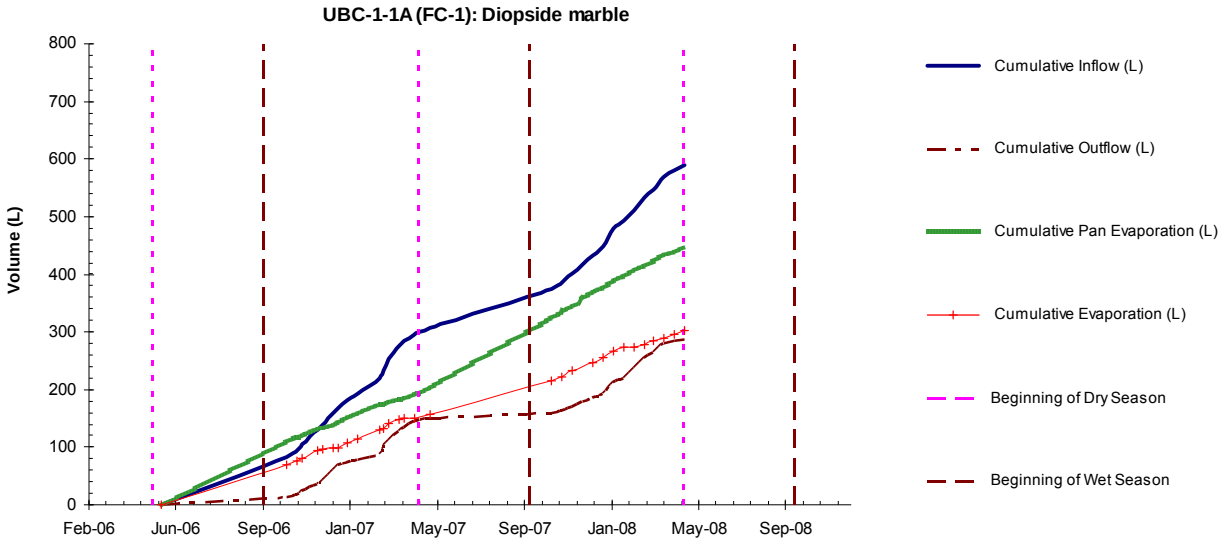

Figure 4.7 Water balance considering ΔS=0 and estimated evaporation in all field cell with Class B diopside marble waste rock (2006-2008)

Table 4.8 shows the variation of outflow rates which took place during the 2007 water year. If assumptions of inflow (precipitation) and pan evaporation in that year would have occurred similarly in all field cells, then water retention could have been evaluated for each cell. However, the water retention was higher in the field cell containing the black marble sample than in other field cells. This was evidenced by the lower cumulative outflow from that field cell.

At the end of the evaluated period (May 2, 2008), water retention in this field cell sample was found to be similar to that of the other field cells.

Table 4.8 Flow rates in the field cells

Field cell code	Flow rates in L/year (2007)				Flow rates in L/year (up to May 2, 2008)				Starting date
	$Q_{in\text{-}fc}$	$Q_{out\text{-}fc}$	E_{fc}	E_p	$Q_{in\text{-}fc}$	$Q_{out\text{-}fc}$	E_p	E_{fc}	
UBC-1-0A	277	84	193	234	648.3	213.5	477.6	434.8	21/03/2006
UBC-1-0B	277	67	210	234	627.3	208.8	462.6	418.5	21/03/2006
UBC-1-1A	277	143	134	234	589.8	287.5	448.7	302.3	12/05/2006
UBC-1-2A	277	108	169	234	579.7	238.8	419.7	340.9	29/06/2006
UBC-1-2B	277	98	179	234	579.7	238.0	419.7	341.7	29/06/2006
UBC-1-3A	277	100	177	234	579.0	217.0	414.3	362.0	07/07/2006
UBC-1-4A	277	130	147	234	579.0	253.5	414.3	325.5	07/07/2006
UBC-1-XA	277	100	177	234	648.3	211.0	477.6	437.3	21/03/2006

5 INTERGRATION OF RESULTS AND DISCUSSION

5.1 Introduction

All results from the physical (PSA, density, SA, moisture content), chemical (assay, ABA) and mineralogical (mineral abundance, exposure or availability) characterizations of the waste rock are integrated in such a way as to provide the necessary information to understand the geochemical properties of the Class B material.

Subsequently, the concentrations of the leachates and their release rates from the field cells are analyzed and discussed, taking into account the waste rock characterization. This information is integrated in order to interpret and explain the geochemical behavior of Class B waste rock. The resulting conclusions are the operation of field kinetic cells is more suitable than static tests for predicting neutral rock drainage and metal leaching.

Finally, conclusions and recommendations will be discussed; in particular on those which could to be incorporated as a component of the current waste rock management program at the Antamina mine.

5.2 Integration of Laboratory Test Results

5.2.1 Weight Elemental Distribution in Class B Material

Solid phase concentrations of S-total Cu, Pb, Zn, Sb, As, and Mo increased with decreasing particle size, exhibiting relatively higher grades and therefore a higher elemental distribution in the fine particles rather than in the coarse particles, as shown in Appendix E1 (Figure E1.1 to Figure E1.9). This finding suggests that the presence of the specific element (and consequently mineral) is in fine sizes, but that it has not necessarily been liberated. As such it could contribute to increasing the free surface area available for chemical reactions (i.e. leaching) and therefore to increasing the mobilization of specific elements from the fine particles. Even though the weight elemental distribution of these elements shows that higher proportions are present in the coarse size fractions of the diopside marble samples (FC-1, FC-2 and FC-3), it does not give any indication regarding their liberation. This does not necessarily imply that the mineral is coarse and free; most of the minerals remain locked or enclosed within either rock particles or other minerals. However, the availability of Cu, Pb and Zn minerals was reported in higher proportions in the coarse size fractions of samples FC-2 and FC-3, suggesting an increase in the level of release and mobilization of these elements from the coarse particles. In addition, solid Ca and Fe concentrations remained stable throughout all of the size fractions.

As mentioned previously, particle or mineral grain size affects liberation, and therefore the availability for leaching. Thus, the cumulative retained elemental distribution was compared to the particle size distribution and plotted in Figure E1.10. Calcium distribution in all samples followed the mass distribution trend, indicating that Ca is likely present as fine particles, but also constituting almost the whole rock particle in the coarse size fractions. In the diopside marble samples, iron distribution tends to follow the mass distribution, indicating that the iron minerals such as pyrite, ferric oxides and ferric oxyhydroxides are likely fine, whereas in the black marble and gray hornfels samples, there is no significant correlation between iron and mass distribution. Sulfur-total, Cu, Pb, and Zn distributions do not follow the mass

distribution either, suggesting that sulfide or other minerals containing the elements mentioned above are most probably locked in the coarse particle sizes.

On the other hand, Figure E1.1 and Figure E1.2 demonstrate that there is a good correlation between S and Fe in all samples. This is a strong indication that most of the sulfide minerals present in the waste rock are pyrite and pyrrhotite, as was confirmed by the MLA analysis summarized in Table 3.12. However, there also is a relatively good correlation of S-total with Cu, Pb and Zn in all samples except in the black marble (Figure E1.11). This indication suggests that besides pyrite and pyrrhotite, there are other sulfide minerals such as chalcopyrite, galena or sphalerite that could be present in the samples, as was evidenced after mineralogy reporting (Table 3.12). In addition, there is a good correlation between S-total and Sb for samples FC-1 and FC-4, suggesting the likelihood that Sb is present as a sulfide mineral (e.g. stibnite or watanabeite). However, watanabeite was reported as the main and most abundant mineral source of Sb in these samples (Table 3.12 and Table C5.7).

The presence of iron sulfide minerals as the most abundant sulfides was verified through the Fe/S molar ratio of pyrite. Theoretically, the Fe/S molar ratio is 1/2. The molar ratio in the Class B waste rock samples ranged from 1/1.6 to 1/2.1 (Figure 5.1), where higher S-total was found for the sample FC-2 (value closer to the theoretical ratio). This suggests that S-total is primarily due to pyrite, although other sulfide minerals could also be present within the waste rock particles. MLA analysis found that the sulfide minerals chalcopyrite, galena and sphalerite were also present. Sample FC-2 reported the highest solid phase iron concentration (Figure E1.2), which could be attributed to the high pyrite, ferric oxide and ferric oxyhydroxides proportions reported by MLA (Table 3.12 and Table C5.3).

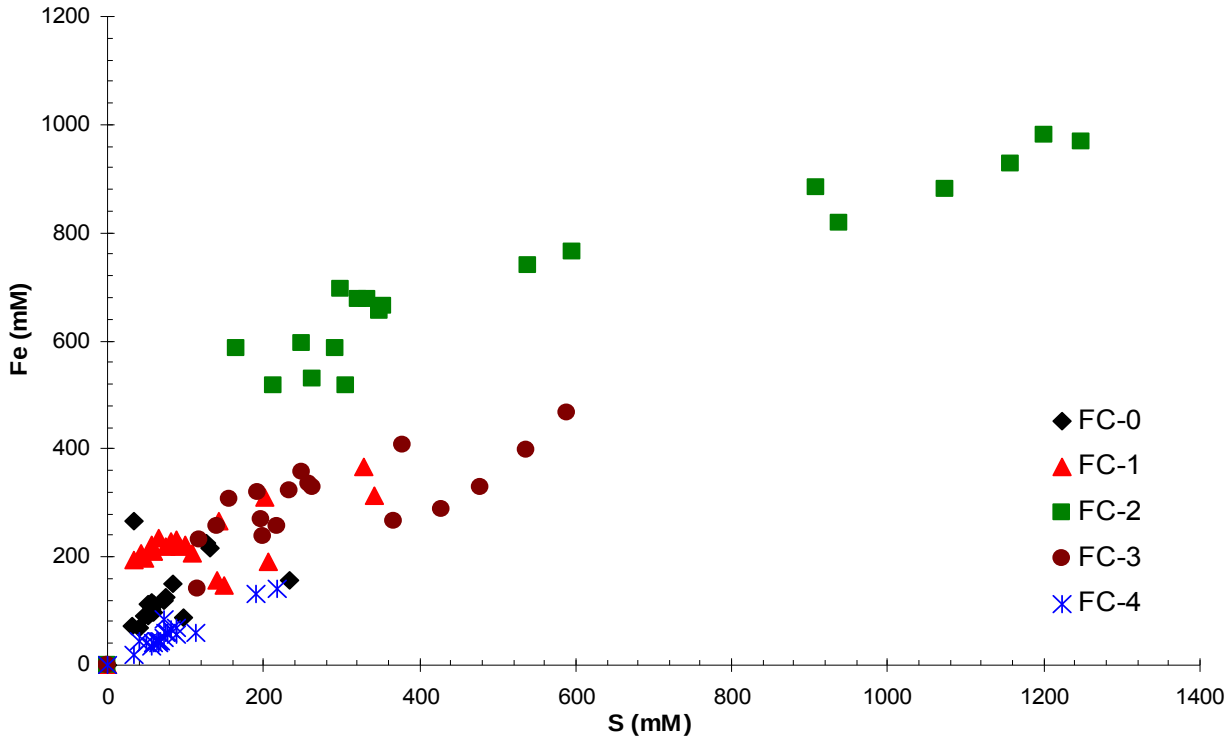

Figure 5.1 Iron/sulfur-total molar ratio in solid phase in all Class B waste rock

Since Cu, Pb and Zn show a poor correlation with S-total concentrations in the black marble sample (Figure E1.11), this may be an indication that these elements do not necessarily occur as sulfide minerals. These elements could be constituents in sulphate, carbonate or oxide minerals as well. After mineralogy reporting, these elements were found in abundance in ferric oxyhydroxide minerals (Table 3.12 and Table C5.6).

5.3 Mineralogy of Class B Waste Rock

5.3.1 Mineral Phases

Table 3.12 shows the different mineral phases found in the Class B samples using MLA. Primary minerals were identified, but some of them were found to be impure, as are named below.

Pyrite [FeS_2] and impure pyrite [FeS_2]Cu was the main and most abundant sulfide mineral found in all samples, with pure and impure chalcopyrite [(Cu,Pb,Zn)FeS_2] and pure and impure sphalerite [(Zn,Cu)S] following in order of abundance. This was particularly true of the diopside marble samples. Galena [PbS], pyrrhotite [$Fe_{(1-x)}S$ (x = 0 to 0.2)] and watanabeite [$(Cu,Zn)_4(As,Sb)_2S_5$] were also found is small proportions. Bornite [Cu_5FeS_4], realgar [AsS], stibnite [Sb_2S_3], molybdenite [MoS_2], chalcocite [Cu_2S], arsenopyrite [FeAsS], enargite [$(Cu,Zn)_3AsS_4$], linnaeite [$(Co,Ni,Cu,Zn)Co_2S_4$], sieginite [$(Ni,Cu,Fe)Co_2S_4$], and tennantite [$(Cu,Zn,Fe)_{12}As_4S_{13}$] were the other sulfide minerals reported in very small amounts, mostly as trace minerals below the detection limit (0.01 wt.%). The oxidation of these sulfide minerals could result in the mobilization of elements such as Fe, Cu, Pb, Zn, Sb, As, and Mo. Sample FC-2 reported the largest sulfide mineral content; this correlates well with the higher solid phase S-total reported in this sample. Sample FC-3 had the next highest sulfide mineral abundance, as determined by MLA. This result was corroborated by the S-total concentration obtained by chemical assay. Sample FC-0, black marble, had the lowest Sulfur-total concentration (Figure E1.1), which is in agreement with MLA results which also showed it to have had the lowest sulfide mineral content. In general, between 30 to 60% of the sulfide mineral content corresponded to the S-total content.

The main and most abundant carbonate mineral was found to be calcite [$CaCO_3$], which comprised almost 99% of the total carbonate minerals. Others carbonate minerals included dolomite [$CaMg(CO_3)_2$], otavite [(Cd,Zn,Cu)CO_3], siderite [(Fe,As,Mn,Zn,Cu)CO_3], smithsonite [$ZnCO_3$], and malachite [$Cu_2CO_3(OH)_2$]. Most of these were found in low proportions, and some of them were present in trace level amounts only (below 0.01 wt.%). The highest amount of carbonate mineral was present in the gray hornfels sample (FC-4). This result was confirmed by ICP analysis, which indicated that the sample had the highest solid phase calcium concentration. Sample FC-2 reported the lowest abundance of carbonate minerals, and this was also confirmed by ICP analysis which indicated that it had the lowest solid phase calcium concentration (Figure E1.3). The amounts of carbonate were sufficient to neutralize any acid generation, even in the sample FC-2, which had the lowest proportion of calcite.

Several silicate minerals including andalusite [Al_2SiO_5], biotite [$K(Mg,Fe)_3(AlSi_3O_{10})(OH)_2$], chlorite [$(Mg,Fe)_3(Si,Al)_4O_{10}(OH)_2$•$(Mg,Fe)_3(OH)_6$], epidote [$Ca_2(Al,Fe)_3O(SiO_4)(Si_2O_7)(OH)$], K-feldspar (e.g. microcline [$KAlSi_3O_8$]), muscovite [$KAl_2(AlSi_3O_{10})(OH)_2$], kaolinite [$Al_2Si_2O_5(OH)_4$], plagioclase (e.g. albite [$NaAlSi_3O_8$]), pyroxene (e.g. diopside [$CaMgSi_2O_6$]), quartz [SiO_2], and zircon [$ZrSiO_4$], among others

were found. In contrast to carbonates, the highest proportion of silicates was reported in sample FC-2, and was associated with diopside content, whereas sample FC-4 contained the lowest proportion of silicate minerals. The major silicates in samples FC-2 and FC-3 were K-feldspar, plagioclase and pyroxene (e.g. diopside). Even though there were high proportions of silicate in all of the samples, it is known that these weather more slowly than carbonates. However, the diopside minerals weather faster than biotite, microcline, albite, muscovite, and much faster than quartz (Figure 2.1). This process will facilitate the neutralization of any acid release once the carbonates have been completely consumed. Clay minerals such as chlorite, kaolinite and mica were found in relatively high proportions in sample FC-0 (Table 3.12), specifically in the finest size fraction (<53 μm), this is shown in Appendix C5, Table C5.1 and Figure C5.1, confirming the observations noted during the visual description of this particular size fraction. The presence of these minerals could play an important role in the adsorption or coating of soluble elements such as Cu, Pb, or Zn.

Apatite [$Ca_5(PO_4)_3(F,Cl,OH)$] was the most abundant phosphate mineral identified. It was present in highest proportions in sample FC-0. Its dissolution could contribute to fluoride mobilization. High amounts of ferric oxyhydroxides [FeO(OH)] or hydrous ferric oxides (HFO) [$FeO(OH)\cdot nH_2O$] were identified in samples FC-0 and FC-2, and these minerals could encapsulate and therefore adsorb any soluble elements present such as Cu, Pb, and Zn, or even other mineral phases, forming minerals with surface complexation. A much higher proportion of Fe oxyhydroxides was noted in the finest size fraction of sample FC-0 (Table C5.1 and Figure C5.1), also confirming observations made during the early visual description of that particular sample.

Ferric sulphate [$(Fe,Cu,As,Mo,Zn)_2(SO_4)_3$] was determined to be the most abundant sulphate mineral, but was present in low proportions. Gypsum [$CaSO_4\cdot 2H_2O$] was found in amounts below the detection limit (0.01 wt.%), indicating that gypsum is not present in the fresh waste rock.

In addition, some other minerals such as fluorite [CaF_2] were also found, but in low proportions.

5.3.2 Mineral Availability for Leaching

As was noted in Figure 3.18, after extrapolation, the availability of sulfide minerals was found to be higher (>98 wt.%) in the fine particle sizes (below 0.6 mm of diameter) for all samples. These start to decrease with increasing particle size, resulting in less than 50 wt.% availability above a particle size of 5 mm. Sample FC-0 had the highest sulfide availability at the coarser particle sizes (50 wt.% @ 25 mm), whereas sample FC-1 had the lowest (50 wt.% @ 5 mm). The extrapolation was done as a function of the mineral availability for leaching calculated for the fines size fractions, which can not represent the true results for the coarse size fractions.

The availability of copper minerals after extrapolation is shown in Figure 3.18 as well. Higher availability (> 94 wt.%) occurred in the fine particles (below 0.3 mm) for all samples. Above this size, in samples FC-0, FC-1 and FC-4, the availability began to decrease with increasing particle size, reaching 50 wt.% of availability between particle sizes of 8 to 20 mm. However, Cu minerals were still available in higher proportions (>80 wt.%) in the coarse size fractions in samples FC-2 and FC-3. The availability of lead minerals for leaching followed the same behavior as did those for Cu.

With extrapolation, the availability of zinc minerals followed the same pattern for samples FC-0, FC-1 and FC-4, but was quite different for samples FC-2 and FC-3. Zinc was still available in much higher proportions (>90 wt.%) in the coarse particle sizes.

The fact that Cu, Pb and Zn minerals were still available in higher proportions in the coarse size fractions indicates that the mobilization of these elements was also occurring at high rates for the coarse particles, particularly for samples FC-2 and FC-3.

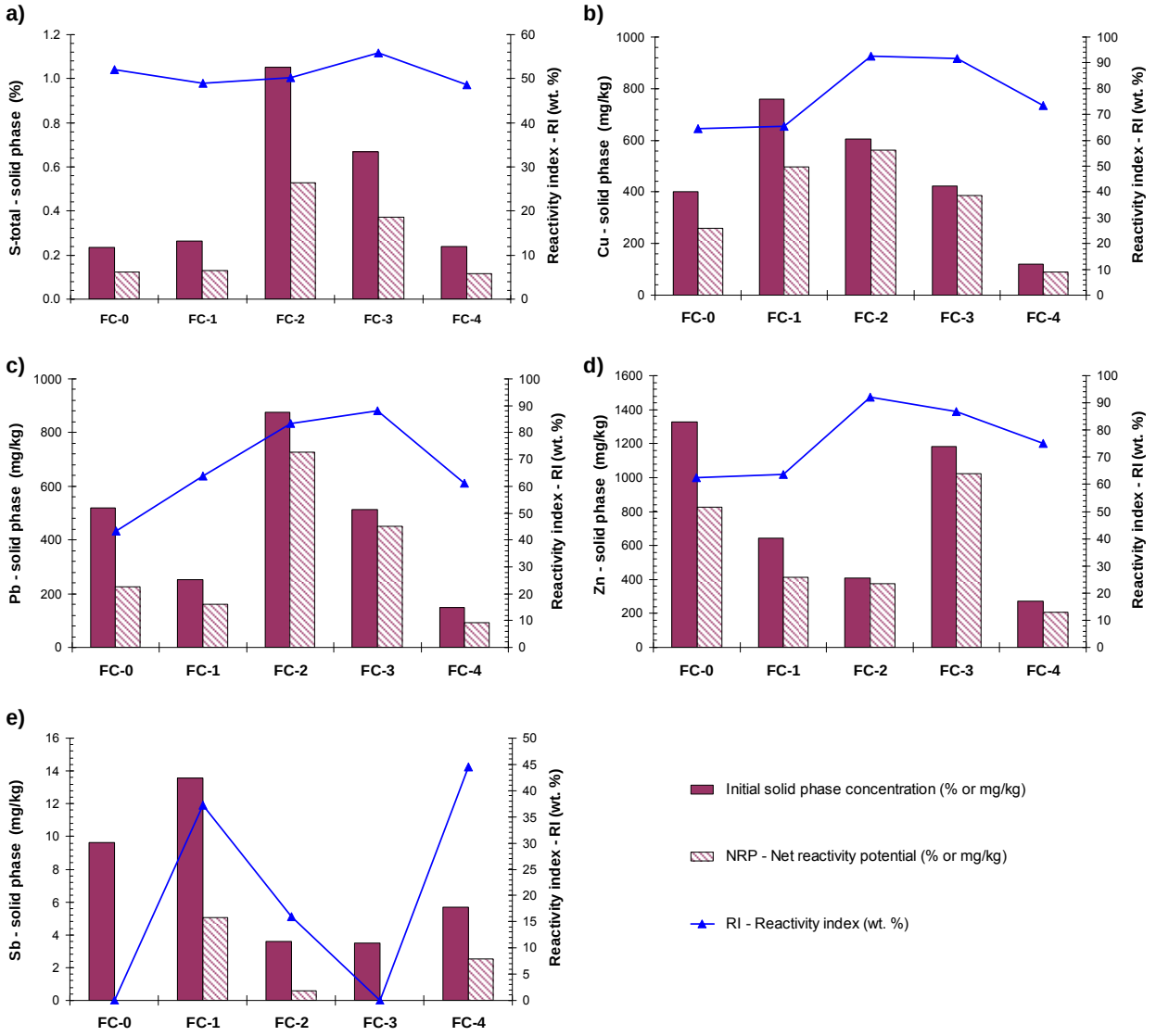

Figure 5.2 Net reactivity potential of a) sulfur-total, b) copper, c) lead, d) zinc, and e) antimony based on availability proportion for leaching (reactivity index) in all Class B waste rock

The net reactivity potential (NRP) for the different Class B waste rock samples, which is the proportion of the initial solid phase elemental concentration that will be available to react or leach, is reported in Figure 5.2 and Table 5.1 to Table 5.5. These were estimated for the reactive elements (of environmental concern) which reported higher grades or solid phase concentrations, i.e. S-total, Cu, Pb and Zn. Other

reactive elements such as Sb, As and Mo which contained low solid concentrations will be further discussed regarding the interpretation of the drainage quality in the field cells section. However, the availability of Sb was assessed as an example.

The reactivity indices of sulfide minerals were around 50 wt.% for all samples (Figure 5.2a), suggesting that sulfide oxidation will take place in only half of the S-total or sulfur-sulfide present in each waste rock type. In sample FC-1, the initial Cu solid phase concentration was higher than in other samples (Figure 5.2b), but samples FC-2 and FC-3 had higher reactivity indices (92 wt.%) for Cu minerals, indicating that even though the Cu concentration was lower in these samples, it will be almost completely available for leaching. Higher reactivity indices for Pb minerals of 80 and 90 wt.% were also obtained for samples FC-2 and FC-3, respectively (Figure 5.2c), suggesting that Pb will be released at relatively higher rates from these samples. This is especially true for sample FC-2, which contained the higher initial solid phase Pb concentration. Samples FC-2 and FC-3 also reported higher reactivity indices for Zn minerals (80 - 90 wt.%) (Figure 5.2d), signifying that as well as Cu and Pb, Zn also will be available for leaching; however the highest initial solid phase Zn concentration was found in sample FC-0, which had the lowest reactivity index (~60 wt.%). This indicates that Zn will be mobilized only at low rates from this particular sample, regardless of its higher solid phase Zn concentration. In addition, the reactivity indices of Sb for three of the samples (FC-0, FC-2, and FC-3) were almost 0 wt.% (Figure 5.2e), but these also had very low solid phase Sb concentrations. Sample FC-1 had the highest solid Sb concentration and a high reactivity index (37 wt.%), showing a good correlation that may be reflected in the mobilization of Sb in the leachate from this sample. Furthermore, even though sample FC-4 did not have a high initial solid phase Sb concentration as did FC-1, it also exhibited a high reactivity index (45 wt.%), suggesting that Sb may be released as well.

Table 5.1 Minerals available for leaching based on their elemental grades by size fraction of the black marble sample (FC-0) Class B waste rock

Project:	Waste Rock Study at Antamina Mine	**Sample Code:**	**FC-0**
Material Type:	Waste rock - Class B	**Sampling Date:**	15-Mar-06
Rock Type:	Black marble	**Sampling by:**	C. Aranda
Location:	Antamina Open Pit	**Testing Date:**	July-2008 and March-2009
	Protective layer in Pile 1	**Testing by:**	C. Aranda / R. Blaskovich
Description:	Field Cell (UBC-1-0A and UBC-1-0B)	**Review by:**	C. Aranda

Sieve		Repres. Size	Weight		Surface area		Grades					Elemental distribution					Mineral availability					Reactivity index				
					SA	Distribution	S-total	Cu	Pb	Zn	Sb	S-total	Cu	Pb	Zn	Sb	Sulfide minerals	Cu minerals	Pb minerals	Zn minerals	Sb minerals	S-total	Cu	Pb	Zn	Sb
(US)	(mm)	(mm)	(kg)	(wt.%)	(m^2)	(wt.%)	(%)	(mg/Kg)	(mg/Kg)	(mg/Kg)	(mg/Kg)	(wt. %)	(wt. %)	(wt. %)	(wt. %)	(wt. %)	(wt. %)	(wt. %)	(wt. %)	(wt. %)	(wt. %)	(wt. %)	(wt. %)	(wt. %)	(wt. %)	(wt. %)
4"	100.0	122.5	0.00	0.00	0.00	0.00	0.00	0.00	0.00	0.00	0.00	0.00	0.00	0.00	0.00	0.00	0.00	0.00	0.00	0.00	0.00	0.00	0.00	0.00	0.00	0.00
3"	75.0	86.6	1.60	1.2	179	0.07	0.31	66	15	39	1.0	1.6	0.2	0.0	0.0	0.1	7.4	0.1	0.0	7.3	0.0	0.12	0.00	0.00	0.00	0.00
2"	50.0	61.2	25.40	19.5	3771	1.46	0.13	167	184	363	4.2	10.8	8.1	6.9	5.3	8.6	15.9	0.7	0.4	15.7	0.0	1.72	0.06	0.03	0.84	0.00
11/2"	37.5	43.3	14.30	11.0	3126	1.21	0.75	395	1750	3610	6.8	35.2	10.8	37.1	29.9	7.8	27.2	3.1	2.0	26.8	0.0	9.57	0.34	0.75	8.02	0.00
1"	25.0	30.6	16.10	12.4	5323	2.06	0.19	191	239	1350	5.3	10.0	5.9	5.7	12.6	6.8	39.8	8.6	6.3	39.2	0.0	3.99	0.51	0.36	4.94	0.00
3/4"	19.0	21.8	9.10	7.0	4413	1.71	0.10	145	162	245	5.8	3.0	2.5	2.2	1.3	4.2	51.8	17.4	13.9	51.1	0.0	1.55	0.44	0.30	0.66	0.00
1/2"	12.5	15.4	10.10	7.8	7092	2.75	0.15	274	207	430	6.3	5.0	5.3	3.1	2.5	5.1	62.8	29.0	24.7	61.9	0.0	3.12	1.54	0.77	1.56	0.00
3/8"	9.50	10.90	4.70	3.6	4572	1.77	0.18	339	201	492	9.2	2.8	3.0	1.4	1.3	3.4	71.9	41.6	37.1	70.9	0.0	2.00	1.27	0.52	0.95	0.00
1/4"	6.30	7.74	5.30	4.1	7305	2.83	0.19	322	203	631	7.3	3.3	3.3	1.6	1.9	3.1	79.0	53.6	49.3	77.9	0.0	2.61	1.75	0.79	1.51	0.00
#4	4.75	5.47	1.84	1.4	1700	0.66	0.18	226	209	364	10.7	1.1	0.8	0.6	0.4	1.6	84.6	64.3	60.4	83.4	0.0	0.92	0.51	0.35	0.32	0.00
#6	3.35	3.99	2.77	2.1	3511	1.36	0.23	323	380	1650	10.3	2.1	1.7	1.6	2.6	2.3	88.5	72.4	69.0	87.2	0.0	1.85	1.24	1.08	2.31	0.00
#8	2.36	2.81	2.31	1.8	3320	1.29	0.17	419	314	758	9.4	1.3	1.8	1.1	1.0	1.7	91.6	79.5	76.8	90.3	0.0	1.18	1.47	0.82	0.91	0.00
#16	1.18	1.67	3.23	2.5	6172	2.39	0.27	782	596	1530	14.4	2.9	4.8	2.9	2.9	3.7	94.8	87.1	85.1	93.5	0.0	2.71	4.21	2.43	2.68	0.00
#30	0.600	0.841	2.31	1.8	5172	2.01	0.42	854	785	1910	19.8	3.2	3.8	2.7	2.6	3.6	97.1	93.0	91.9	96.1	0.0	3.09	3.51	2.47	2.45	0.00
#50	0.300	0.424	2.77	2.1	5719	2.22	0.41	845	733	1740	20.0	3.7	4.5	3.0	2.8	4.4	99.3	96.9	94.7	96.5	0.0	3.70	4.34	2.85	2.69	0.00
#100	0.150	0.212	4.61	3.5	5954	2.31	0.24	471	427	1110	12.8	3.6	4.2	2.9	3.0	4.7	97.8	97.2	96.1	96.2	0.0	3.55	4.04	2.81	2.85	0.00
#140	0.106	0.126	3.23	2.5	4222	1.64	0.19	427	363	1010	9.6	2.0	2.6	1.7	1.9	2.5	99.9	98.2	96.9	97.0	0.0	2.01	2.59	1.68	1.83	0.00
#200	0.075	0.089	2.77	2.1	3943	1.53	0.17	417	368	1010	10.4	1.5	2.2	1.5	1.6	2.3	99.7	98.7	98.2	97.5	0.0	1.54	2.18	1.48	1.58	0.00
#270	0.053	0.063	2.31	1.8	3862	1.50	0.18	544	442	1180	13.6	1.4	2.4	1.5	1.6	2.5	99.3	99.2	98.6	98.9	0.0	1.35	2.38	1.49	1.56	0.00
-#270	-0.053	0.045	15.22	11.7	178514	69.23	0.11	1100	996	2800	26.0	5.5	32.0	22.5	24.7	31.6	99.7	99.9	99.8	99.8	0.0	5.48	32.00	22.44	24.65	0.00
Total			**129.95**	**100.0**	**257873**	**100.0**	**0.23**	**402**	**519**	**1328**	**9.6**	**100.0**	**100.0**	**100.0**	**100.0**	**100.0**	**57.9**	**39.9**	**38.1**	**57.1**	**0.0**	**52.06**	**64.36**	**43.41**	**62.32**	**0.00**

Note: No sample were obtained at + 4 inch size fraction

Table 5.2 Minerals available for leaching based on their elemental grades by size fraction of the diopside marble sample (FC-1) Class B waste rock

Project:	Waste Rock Study at Antamina Mine	**Sample Code:**	**FC-1**
Material Type:	Waste rock - Class B	**Sampling Date:**	12-May-06
Rock Type:	Diopside marble	**Sampling by:**	C. Aranda
Location:	Antamina Open Pit	**Testing Date:**	July-2008 and March-2009
	First tipping phase in Pile 1	**Testing by:**	C. Aranda / R. Blaskovich
Description:	Field Cell (UBC-1-1A)	**Review by:**	C. Aranda

Sieve		Repres. Size	Weight		Surface area		Grades					Elemental distribution					Mineral availability					Reactivity index				
					SA	Distribution	S-total	Cu	Pb	Zn	Sb	S-total	Cu	Pb	Zn	Sb	Sulfide minerals	Cu minerals	Pb minerals	Zn minerals	Sb minerals	S-total	Cu	Pb	Zn	Sb
(US)	(mm)	(mm)	(kg)	(wt.%)	(m^2)	(wt.%)	(%)	(mg/Kg)	(mg/Kg)	(mg/Kg)	(mg/Kg)	(wt. %)	(wt. %)	(wt. %)	(wt. %)	(wt. %)	(wt. %)	(wt. %)	(wt. %)	(wt. %)	(wt. %)	(wt. %)	(wt. %)	(wt. %)	(wt. %)	(wt. %)
4"	100.0	122.5	0.00	0.00	0.00	0.00	0.00	0.00	0.00	0.00	0.00	0.00	0.00	0.00	0.00	0.00	0.00	0.00	0.00	0.00	0.00	0.00	0.00	0.00	0.00	0.00
3"	75.0	86.6	5.70	3.7	340	0.41	0.14	180	114	337	3.4	2.0	0.9	1.7	1.9	0.9	0.0	3.1	3.0	7.2		0.00	0.03	0.05	0.14	0.00
2"	50.0	61.2	27.50	17.8	2139	2.57	0.11	254	142	496	5.9	7.4	5.9	10.0	13.7	7.7	0.0	8.5	8.3	15.4		0.00	0.50	0.83	2.11	0.00
11/2"	37.5	43.3	17.00	11.0	1921	2.30	0.15	292	138	588	3.8	6.2	4.2	6.0	10.0	3.1	0.4	17.3	17.0	26.5		0.02	0.73	1.02	2.65	0.00
1"	25.0	30.6	20.40	13.2	3651	4.38	0.19	522	59	326	4.2	9.5	9.1	3.1	6.7	4.1	1.9	28.8	28.3	38.7		0.18	2.61	0.88	2.58	0.00
3/4"	19.0	21.8	12.20	7.9	3022	3.62	0.18	592	485	634	11.8	5.4	6.1	15.2	7.8	6.8	5.9	41.0	40.2	50.4		0.32	2.51	6.10	3.91	0.00
1/2"	12.5	15.4	14.30	9.2	5800	6.96	0.30	1550	104	478	7.5	10.5	18.8	3.8	6.9	5.1	13.6	52.9	51.9	61.1		1.43	9.96	1.97	4.19	0.00
3/8"	9.50	10.90	7.20	4.7	4065	4.88	0.21	682	229	845	18.3	3.7	4.2	4.2	6.1	6.3	24.5	63.3	62.2	69.9		0.91	2.64	2.63	4.27	0.00
1/4"	6.30	7.74	8.30	5.4	6759	8.11	0.32	812	330	483	14.1	6.5	5.7	7.0	4.0	5.6	36.9	71.9	70.6	76.9		2.40	4.12	4.96	3.09	0.00
#4	4.75	5.47	4.06	2.6	2639	3.16	0.24	838	116	335	21.9	2.4	2.9	1.2	1.4	4.2	49.6	78.7	77.3	82.3		1.18	2.27	0.93	1.12	0.00
#6	3.35	3.99	4.63	3.0	3224	3.87	0.26	1000	619	824	13.5	2.9	3.9	7.4	3.8	3.0	60.1	83.5	82.0	86.0		1.77	3.29	6.03	3.30	0.00
#8	2.36	2.81	3.48	2.2	2563	3.07	0.28	794	356	748	19.3	2.4	2.3	3.2	2.6	3.2	70.1	87.5	85.9	89.1		1.67	2.05	2.73	2.32	0.00
#16	1.18	1.67	5.21	3.4	4833	5.80	0.46	1090	394	972	24.4	5.9	4.8	5.3	5.1	6.1	81.3	91.6	90.0	92.2		4.77	4.43	4.74	4.69	0.00
#30	0.600	0.841	3.48	2.2	2835	3.40	0.65	1510	659	1360	43.4	5.5	4.5	5.9	4.7	7.2	89.0	94.7	93.1	94.4	100.0	4.92	4.22	5.46	4.47	7.18
#50	0.300	0.424	2.32	1.5	2063	2.47	1.05	1590	617	1210	35.2	6.0	3.1	3.7	2.8	3.9	98.2	96.2	93.6	96.2	50.0	5.84	3.01	3.43	2.70	1.94
#100	0.150	0.212	2.61	1.7	1819	2.18	1.10	1760	469	1090	49.4	7.0	3.9	3.1	2.8	6.1	98.4	98.0	97.6	98.1	76.7	6.90	3.82	3.06	2.79	4.70
#140	0.106	0.126	2.32	1.5	1131	1.36	0.66	1330	382	842	29.4	3.7	2.6	2.3	2.0	3.2	99.4	97.1	96.0	96.0	0.0	3.72	2.54	2.18	1.88	0.00
#200	0.075	0.089	2.32	1.5	1008	1.21	0.48	1050	274	809	28.0	2.7	2.1	1.6	1.9	3.1	99.5	95.8	94.0	94.6	99.7	2.71	1.98	1.53	1.78	3.08
#270	0.053	0.063	1.74	1.1	792	0.95	0.45	1200	258	871	28.8	1.9	1.8	1.1	1.5	2.4	99.5	97.4	93.0	95.1	97.4	1.90	1.73	1.07	1.44	2.32
-#270	-0.053	0.045	9.85	6.4	32775	39.31	0.35	1560	567	1450	38.5	8.4	13.1	14.3	14.3	18.1	99.4	99.4	99.2	99.6	100.0	8.38	12.98	14.20	14.26	18.05
Total			**154.60**	**100.0**	**83377**	**100.0**	**0.26**	**761**	**252**	**645**	**13.6**	**100.0**	**100.0**	**100.0**	**100.0**	**100.0**	**28.1**	**47.4**	**46.6**	**53.4**	**13.3**	**49.02**	**65.44**	**63.78**	**63.70**	**37.28**

Note: No sample were obtained at + 4 inch size fraction

Table 5.3 Minerals available for leaching based on their elemental grades by size fraction of the diopside marble sample (FC-2) Class B waste rock

Project:	Waste Rock Study at Antamina Mine	**Sample Code:**	**FC-2**
Material Type:	Waste rock - Class B	**Sampling Date:**	29-Jun-06
Rock Type:	Diopside marble	**Sampling by:**	C. Aranda
Location:	Antamina Open Pit	**Testing Date:**	July-2008 and March-2009
	Second tipping phase in Pile 1	**Testing by:**	C. Aranda / R. Blaskovich
Description:	Field Cell (UBC-1-2A and UBC-1-2B)	**Review by:**	C. Aranda

Sieve		Repres. Size	Weight		Surface area		Grades					Elemental distribution					Mineral availability					Reactivity index				
					SA	Distribution	S-total	Cu	Pb	Zn	Sb	S-total	Cu	Pb	Zn	Sb	Sulfide minerals	Cu minerals	Pb minerals	Zn minerals	Sb minerals	S-total	Cu	Pb	Zn	Sb
(US)	(mm)	(mm)	(kg)	(wt.%)	(m^2)	(wt.%)	(%)	(mg/Kg)	(mg/Kg)	(mg/Kg)	(mg/Kg)	(wt. %)	(wt. %)	(wt. %)	(wt. %)	(wt. %)	(wt. %)	(wt. %)	(wt. %)	(wt. %)	(wt. %)	(wt. %)	(wt. %)	(wt. %)	(wt. %)	(wt. %)
4"	100.0	122.5	0.00	0.00	0.00	0.00	0.00	0.00	0.00	0.00	0.00	0.00	0.00	0.00	0.00	0.00	0.00	0.00	0.00	0.00	0.00	0.00	0.00	0.00	0.00	0.00
3"	75.0	86.6	14.60	9.1	1501	1.31	0.53	275	153	172	1.5	4.6	4.1	1.6	3.9	3.8	3.1	87.2	75.9	87.4	0.0	0.14	3.60	1.21	3.37	0.00
2"	50.0	61.2	36.20	22.6	5002	4.38	0.98	329	351	451	2.5	21.1	12.3	9.1	25.1	15.4	8.7	87.8	77.0	88.0	0.0	1.82	10.75	6.98	22.06	0.00
11/2"	37.5	43.3	20.60	12.8	4027	3.52	0.68	305	231	194	1.9	8.3	6.5	3.4	6.1	6.7	17.8	88.3	78.1	88.5	0.0	1.48	5.71	2.65	5.43	0.00
1"	25.0	30.6	21.40	13.3	6413	5.61	0.84	322	2790	205	3.2	10.7	7.1	42.6	6.7	11.7	29.5	88.9	79.2	89.1	0.0	3.15	6.30	33.70	6.00	0.00
3/4"	19.0	21.8	13.30	8.3	5706	4.99	0.94	379	807	260	2.4	7.4	5.2	7.7	5.3	5.4	42.0	89.4	80.2	89.6	0.0	3.11	4.64	6.14	4.76	0.00
1/2"	12.5	15.4	14.20	8.9	9626	8.43	0.96	762	521	346	3.1	8.1	11.1	5.3	7.5	7.7	54.2	90.0	81.3	90.2	0.0	4.38	10.02	4.29	6.81	0.00
3/8"	9.50	10.90	6.50	4.1	6174	5.40	1.13	853	437	230	2.1	4.4	5.7	2.0	2.3	2.3	64.9	90.6	82.4	90.8	0.0	2.83	5.16	1.67	2.08	0.00
1/4"	6.30	7.74	7.00	4.4	9801	8.58	0.80	488	471	389	2.6	3.3	3.5	2.4	4.2	3.1	73.7	91.1	83.4	91.3	0.0	2.45	3.20	1.96	3.82	0.00
#4	4.75	5.47	3.33	2.1	3500	3.06	1.07	610	574	382	3.2	2.1	2.1	1.4	2.0	1.8	80.7	91.7	84.5	91.9	0.0	1.71	1.92	1.15	1.80	0.00
#6	3.35	3.99	3.33	2.1	4517	3.95	1.03	764	459	408	4.2	2.0	2.6	1.1	2.1	2.4	85.6	92.2	85.5	92.4	0.0	1.74	2.41	0.93	1.93	0.00
#8	2.36	2.81	2.33	1.5	3468	3.04	1.12	625	988	379	4.1	1.6	1.5	1.6	1.4	1.6	89.7	92.7	86.6	92.9	0.0	1.39	1.39	1.42	1.26	0.00
#16	1.18	1.67	3.33	2.1	2939	2.57	1.73	777	858	636	4.9	3.4	2.7	2.0	3.3	2.8	93.9	93.6	88.2	93.8	0.0	3.21	2.49	1.80	3.05	0.00
#30	0.600	0.841	2.00	1.2	2156	1.89	2.91	1075	1225	866	5.9	3.5	2.2	1.7	2.7	2.0	96.3	96.2	95.2	97.3	0.0	3.33	2.13	1.66	2.59	0.00
#50	0.300	0.424	1.67	1.0	2159	1.89	3.85	1590	1490	999	9.3	3.8	2.7	1.8	2.6	2.7	99.7	93.8	84.4	91.8	0.0	3.80	2.56	1.49	2.35	0.00
#100	0.150	0.212	1.67	1.0	2742	2.40	4.00	3080	1775	1195	11.2	4.0	5.3	2.1	3.1	3.2	99.8	96.7	95.9	97.8	0.0	3.95	5.10	2.02	2.99	0.00
#140	0.106	0.126	0.67	0.4	1343	1.18	3.71	3710	2030	1255	10.6	1.5	2.5	1.0	1.3	1.2	99.8	98.2	97.5	98.8	0.0	1.46	2.50	0.94	1.27	0.00
#200	0.075	0.089	0.67	0.4	1469	1.29	3.44	3560	1850	1270	12.1	1.4	2.4	0.9	1.3	1.4	99.9	98.7	98.1	98.9	0.0	1.36	2.41	0.86	1.29	0.00
#270	0.053	0.063	0.67	0.4	1326	1.16	3.01	3330	1525	1270	11.4	1.2	2.3	0.7	1.3	1.3	99.9	98.9	98.4	99.0	0.0	1.19	2.26	0.71	1.29	0.00
-#270	-0.053	0.045	6.90	4.3	40377	35.34	1.91	2560	2390	1700	19.7	7.8	18.2	11.8	18.0	23.4	99.9	99.5	99.3	99.4	68.1	7.81	18.08	11.68	17.91	15.97
Total			**160.37**	**100.0**	**114246**	**100.0**	**1.05**	**606**	**875**	**406**	**3.6**	**100.0**	**100.0**	**100.0**	**100.0**	**100.0**	**38.1**	**89.8**	**80.9**	**90.0**	**2.9**	**50.32**	**92.64**	**83.26**	**92.08**	**15.97**

Note: No sample were obtained at + 4 inch size fraction

Table 5.4 Minerals available for leaching based on their elemental grades by size fraction of the diopside marble sample (FC-3) Class B waste rock

Project:	Waste Rock Study at Antamina Mine	**Sample Code:**	**FC-3**
Material Type:	Waste rock - Class B	**Sampling Date:**	07-Jul-06
Rock Type:	Diopside marble	**Sampling by:**	C. Aranda
Location:	Antamina Open Pit	**Testing Date:**	July-2008 and March-2009
	Third tipping phase in Pile 1	**Testing by:**	C. Aranda / R. Blaskovich
Description:	Field Cell (UBC-1-3A)	**Review by:**	C. Aranda

Sieve		Repres. Size	Weight		Surface area		Grades					Elemental distribution					Mineral availability					Reactivity index				
					SA	Distribution	S-total	Cu	Pb	Zn	Sb	S-total	Cu	Pb	Zn	Sb	Sulfide minerals	Cu minerals	Pb minerals	Zn minerals	Sb minerals	S-total	Cu	Pb	Zn	Sb
(US)	(mm)	(mm)	(kg)	(wt.%)	(m^2)	(wt.%)	(%)	(mg/Kg)	(mg/Kg)	(mg/Kg)	(mg/Kg)	(wt. %)	(wt. %)	(wt. %)	(wt. %)	(wt. %)	(wt. %)	(wt. %)	(wt. %)	(wt. %)	(wt. %)	(wt. %)	(wt. %)	(wt. %)	(wt. %)	(wt. %)
4"	100.0	122.5	0.00	0.00	0.00	0.00	0.00	0.00	0.00	0.00	0.00	0.00	0.00	0.00	0.00	0.00	0.00	0.00	0.00	0.00	0.00	0.00	0.00	0.00	0.00	0.00
3"	75.0	86.6	0.00	0.0	0	0.00	0.00	0	0	0	0.0	0.0	0.0	0.0	0.0	0.0	0.6	84.3	80.7	79.2	0.0	0.00	0.00	0.00	0.00	0.00
2"	50.0	61.2	17.80	12.7	1639	2.34	0.38	204	62	1380	2.2	7.2	6.1	1.5	14.8	7.9	2.5	85.0	81.5	80.2	0.0	0.18	5.22	1.26	11.90	0.00
11/2"	37.5	43.3	16.00	11.4	2106	3.00	0.37	269	26	369	1.4	6.3	7.3	0.6	3.6	4.5	7.5	85.7	82.3	81.1	0.0	0.47	6.24	0.47	2.89	0.00
1"	25.0	30.6	20.10	14.4	3889	5.54	0.45	220	833	1185	2.2	9.7	7.5	23.3	14.4	8.8	15.9	86.4	83.1	82.0	0.0	1.54	6.46	19.36	11.80	0.00
3/4"	19.0	21.8	12.90	9.2	3361	4.79	0.80	313	658	1500	2.7	11.1	6.8	11.8	11.7	7.1	27.1	87.1	83.9	82.9	0.0	2.99	5.94	9.91	9.69	0.00
1/2"	12.5	15.4	16.70	11.9	7017	10.00	0.70	228	627	441	2.8	12.5	6.4	14.6	4.4	9.4	39.7	87.8	84.7	83.8	0.0	4.97	5.65	12.34	3.73	0.00
3/8"	9.50	10.90	8.10	5.8	4936	7.03	0.62	386	225	968	4.4	5.4	5.3	2.5	4.7	7.3	52.1	88.4	85.5	84.7	0.0	2.80	4.68	2.17	4.01	0.00
1/4"	6.30	7.74	8.80	6.3	7779	11.08	0.50	309	186	881	2.7	4.7	4.6	2.3	4.7	4.8	63.0	89.1	86.3	85.6	0.0	2.97	4.10	1.96	4.01	0.00
#4	4.75	5.47	5.37	3.8	4722	6.73	0.63	432	293	1035	2.5	3.6	3.9	2.2	3.4	2.8	72.1	89.8	87.1	86.6	0.0	2.61	3.52	1.90	2.90	0.00
#6	3.35	3.99	4.54	3.2	3649	5.20	0.84	582	687	2290	3.7	4.1	4.5	4.3	6.3	3.4	78.8	90.4	87.8	87.4	0.0	3.22	4.04	3.81	5.49	0.00
#8	2.36	2.81	3.51	2.5	1710	2.44	0.75	556	591	1465	6.2	2.8	3.3	2.9	3.1	4.4	84.6	91.1	88.6	88.3	0.0	2.38	3.01	2.56	2.74	0.00
#16	1.18	1.67	4.95	3.5	2886	4.11	0.83	717	601	1585	4.7	4.4	6.0	4.1	4.7	4.7	90.6	92.2	89.8	89.7	0.0	3.99	5.53	3.72	4.26	0.00
#30	0.600	0.841	2.48	1.8	1761	2.51	1.21	964	1045	1990	6.3	3.2	4.0	3.6	3.0	3.2	94.4	96.1	95.9	95.0	0.0	3.03	3.88	3.45	2.83	0.00
#50	0.300	0.424	2.57	1.8	1827	2.60	1.89	1095	1195	2330	8.8	5.2	4.8	4.3	3.6	4.6	98.4	91.6	87.3	88.1	0.0	5.12	4.35	3.73	3.18	0.00
#100	0.150	0.212	3.43	2.4	1727	2.46	1.72	1195	1260	1820	6.3	6.3	6.9	6.0	3.8	4.4	98.4	95.7	93.7	95.5	0.0	6.21	6.62	5.62	3.59	0.00
#140	0.106	0.126	2.14	1.5	1050	1.50	1.53	1185	827	1730	8.6	3.5	4.3	2.5	2.2	3.7	99.6	98.1	96.7	97.2	0.0	3.49	4.21	2.38	2.18	0.00
#200	0.075	0.089	2.14	1.5	1007	1.44	1.37	1040	560	1480	5.8	3.1	3.8	1.7	1.9	2.5	99.7	98.7	96.5	98.6	0.0	3.13	3.72	1.61	1.89	0.00
#270	0.053	0.063	1.71	1.2	931	1.33	1.18	1035	523	1670	6.8	2.2	3.0	1.2	1.7	2.4	99.4	98.6	97.5	98.3	0.0	2.15	2.95	1.21	1.70	0.00
-#270	-0.053	0.045	6.74	4.8	18181	25.91	0.64	1010	1135	1945	10.2	4.6	11.5	10.6	7.9	13.9	99.6	99.6	99.2	99.3	0.0	4.60	11.47	10.56	7.87	0.00
Total			**139.97**	**100.0**	**70176**	**100.0**	**0.67**	**423**	**514**	**1183**	**3.5**	**100.0**	**100.0**	**100.0**	**100.0**	**100.0**	**43.3**	**88.9**	**86.0**	**85.3**	**0.0**	**55.87**	**91.58**	**88.01**	**86.66**	**0.00**

Note: No sample were obtained at + 4 inch size fraction

Table 5.5 Minerals available for leaching based on their elemental grades by size fraction of the gray hornfels sample (FC-4) Class B waste rock

Project:	Waste Rock Study at Antamina Mine	**Sample Code:**	**FC-4**
Material Type:	Waste rock - Class B	**Sampling Date:**	07-Jul-06
Rock Type:	Gray hornfels	**Sampling by:**	C. Aranda
Location:	Antamina Open Pit	**Testing Date:**	July-2008 and March-2009
	Third/Fourth tipping phase in Pile 1	**Testing by:**	C. Aranda / R. Blaskovich
Description:	Field Cell (UBC-1-4A)	**Review by:**	C. Aranda

Sieve		Repres. Size	Weight		Surface area		Grades					Elemental distribution					Mineral availability					Reactivity index				
					SA	Distribution	S-total	Cu	Pb	Zn	Sb	S-total	Cu	Pb	Zn	Sb	Sulfide minerals	Cu minerals	Pb minerals	Zn minerals	Sb minerals	S-total	Cu	Pb	Zn	Sb
(US)	(mm)	(mm)	(kg)	(wt.%)	(m^2)	(wt.%)	(%)	(mg/Kg)	(mg/Kg)	(mg/Kg)	(mg/Kg)	(wt. %)	(wt. %)	(wt. %)	(wt. %)	(wt. %)	(wt. %)	(wt. %)	(wt. %)	(wt. %)	(wt. %)	(wt. %)	(wt. %)	(wt. %)	(wt. %)	(wt. %)
4"	100.0	122.5	0.00	0.00	0.00	0.00	0.00	0.00	0.00	0.00	0.00	0.00	0.00	0.00	0.00	0.00	0.00	0.00	0.00	0.00	0.00	0.00	0.00	0.00	0.00	0.00
3"	75.0	86.6	1.70	1.2	58	0.12	0.11	18	46	60	1.8	0.6	0.2	0.4	0.3	0.4	0.0	0.1	0.0	0.1	0.0	0.00	0.00	0.00	0.00	0.00
2"	50.0	61.2	15.50	11.2	877	1.88	0.18	23	64	84	0.8	8.5	2.1	4.8	3.4	1.5	0.4	0.7	0.0	0.7	0.0	0.03	0.02	0.00	0.02	0.00
11/2"	37.5	43.3	13.20	9.5	1116	2.39	0.36	73	143	131	1.6	14.4	5.7	9.1	4.5	2.7	2.0	3.1	0.1	3.0	0.0	0.29	0.17	0.01	0.14	0.00
1"	25.0	30.6	19.90	14.3	2323	4.98	0.13	53	59	69	0.9	7.8	6.3	5.7	3.6	2.2	6.3	8.5	0.5	8.4	0.0	0.49	0.53	0.03	0.30	0.00
3/4"	19.0	21.8	10.30	7.4	1737	3.72	0.19	44	39	81	0.8	5.9	2.7	1.9	2.2	1.0	13.9	17.2	2.4	17.0	0.0	0.82	0.46	0.05	0.37	0.00
1/2"	12.5	15.4	13.90	10.0	3482	7.46	0.21	51	46	125	2.5	8.9	4.2	3.0	4.6	4.3	24.6	28.7	7.2	28.3	0.0	2.18	1.20	0.22	1.29	0.00
3/8"	9.50	10.90	6.60	4.7	2584	5.54	0.22	40	45	79	2.9	4.4	1.6	1.4	1.4	2.4	37.0	41.1	15.5	40.7	0.0	1.63	0.65	0.22	0.56	0.00
1/4"	6.30	7.74	7.30	5.3	4028	8.63	0.16	94	134	105	3.2	3.5	4.1	4.7	2.0	3.0	49.2	53.0	26.5	52.4	0.0	1.74	2.15	1.24	1.05	0.00
#4	4.75	5.47	4.10	3.0	1433	3.07	0.24	126	166	251	2.1	3.0	3.1	3.3	2.7	1.1	60.3	63.5	38.9	62.8	0.0	1.80	1.94	1.27	1.70	0.00
#6	3.35	3.99	3.50	2.5	1854	3.97	0.25	110	201	368	4.2	2.7	2.3	3.4	3.4	1.9	68.9	71.5	50.1	70.7	0.0	1.83	1.62	1.69	2.39	0.00
#8	2.36	2.81	2.70	1.9	1520	3.26	0.26	190	159	368	7.4	2.1	3.0	2.1	2.6	2.5	76.6	78.5	61.1	77.7	0.0	1.63	2.38	1.26	2.02	0.00
#16	1.18	1.67	5.00	3.6	3385	7.25	0.28	201	325	604	14.3	4.2	6.0	7.8	7.9	9.0	84.9	86.1	74.3	85.1	0.0	3.60	5.13	5.81	6.74	0.00
#30	0.600	0.841	3.00	2.2	2017	4.32	0.61	473	748	1815	16.1	5.6	8.4	10.8	14.3	6.1	91.9	91.3	82.9	92.8	0.0	5.10	7.68	8.95	13.26	0.00
#50	0.300	0.424	4.30	3.1	2618	5.61	0.70	418	445	936	21.6	9.1	10.7	9.2	10.6	11.7	95.9	96.1	96.9	90.6	0.0	8.76	10.24	8.93	9.56	0.00
#100	0.150	0.212	7.31	5.3	1576	3.38	0.20	136	188	416	6.3	4.4	5.9	6.6	8.0	5.8	91.0	94.9	95.5	95.8	0.0	4.03	5.57	6.31	7.64	0.00
#140	0.106	0.126	3.44	2.5	815	1.75	0.21	117	138	250	7.5	2.2	2.4	2.3	2.3	3.2	99.8	97.5	95.2	96.1	100.0	2.19	2.33	2.17	2.17	3.23
#200	0.075	0.089	4.08	2.9	963	2.06	0.23	169	137	301	10.6	2.8	4.1	2.7	3.2	5.5	97.8	97.4	96.3	96.5	100.0	2.79	3.97	2.58	3.11	5.45
#270	0.053	0.063	4.30	3.1	935	2.00	0.28	180	157	332	12.6	3.7	4.6	3.2	3.7	6.8	98.8	97.1	95.6	96.8	100.0	3.61	4.46	3.10	3.63	6.80
-#270	-0.053	0.045	8.82	6.3	13348	28.60	0.23	439	415	838	26.1	6.2	23.0	17.6	19.4	29.0	99.9	99.4	98.3	99.1	100.0	6.15	22.82	17.33	19.21	29.01
Total			**138.95**	**100.0**	**46669**	**100.0**	**0.24**	**121**	**150**	**274**	**5.7**	**100.0**	**100.0**	**100.0**	**100.0**	**100.0**	**41.5**	**43.3**	**33.6**	**42.9**	**14.9**	**48.66**	**73.33**	**61.18**	**75.17**	**44.49**

Note: No sample were obtained at + 4 inch size fraction

5.3.3 Determining the Reactive Zone

Initially, three reactive zones divided by two particle size cut offs were established based on the fact that only a small proportion of the waste rock material was physically more available for leaching. Particles below 2 mm (sand, silt and clay) in size were located in the "more reactive zone." The region between 2 - 12 mm (medium gravel) was categorized as the "slightly reactive zone"; particles above 12 mm (coarse gravel and stones) were categorized as the "less reactive zone" (Price, 1997). In order to validate the previous assumption, the cumulative weight surface area distribution, in conjunction with the particle size distribution, was analyzed.

If we start from the assumption that most of the reactivity occurs in the fine size fractions where the surface area should supposedly be higher, then the highest surface area proportion should be located in the fine particles. Therefore, if greater than 50 wt.% of the surface area and/or greater than 25 wt.% of the mass (because most of the mass occurs in the coarse particles) are present in the regions defined, then the different reactivity zones will be able to be determined. According to Table 5.6 and Figure 5.3, all samples have higher SA (greater than 50 wt.%) in the more reactive zone, with the exception of FC-2 and FC-3, which had relatively lower SA, at 45 and 40 wt.%, respectively. However, as was expected, all samples had a higher weight percentage (greater than 25 wt.%) in the coarse material, or in the "less reactive zone", although two samples, FC-0 and FC-4, had slightly higher mass (greater than 25 wt.%) in the "more reactive zone". Therefore, for samples FC-0, FC-1, and FC-4, the three reactive zones could remain as initially defined; but for samples FC-2 and FC-3, the "more reactive zone" should include the "slightly reactive zone" as well, becoming only two reactive zones, namely "more reactive" and "less reactive" divided by the 12 cm cut off. This suggested that the weathering in samples FC-2 and FC-3 was occurring widely in the particles which are less than 12 mm in diameter.

Table 5.6 Cumulative weight surface area and particle size distribution in the different reactive zones of the Class B waste rock samples

Sample ID	**FC-0**			**FC-1**			**FC-2**			**FC-3**			**FC-4**		
(mm)	<2	2-12	>12	<2	2-12	>12	<2	2-12	>12	<2	2-12	>12	<2	2-12	>12
wt.% SA	**82**	8	10	**55**	23	22	45	25	30	**40**	35	25	**52**	20	28
wt.%*	**28**	12	60	18	20	**62**	10	15	**75**	18	22	**60**	**28**	20	52
wt.% S	22	10	**68**	40	18	42	25	15	**60**	32	20	48	38	17	45
wt.% Cu	**55**	10	35	35	20	**45**	38	15	47	42	20	38	**65**	12	23
wt.% Pb	38	7	**55**	36	22	42	22	8	**70**	35	12	**53**	**58**	20	22
wt.% Zn	40	8	**52**	35	20	45	34	20	**56**	28	25	47	**68**	14	18

* weight percentage from the particle size distribution

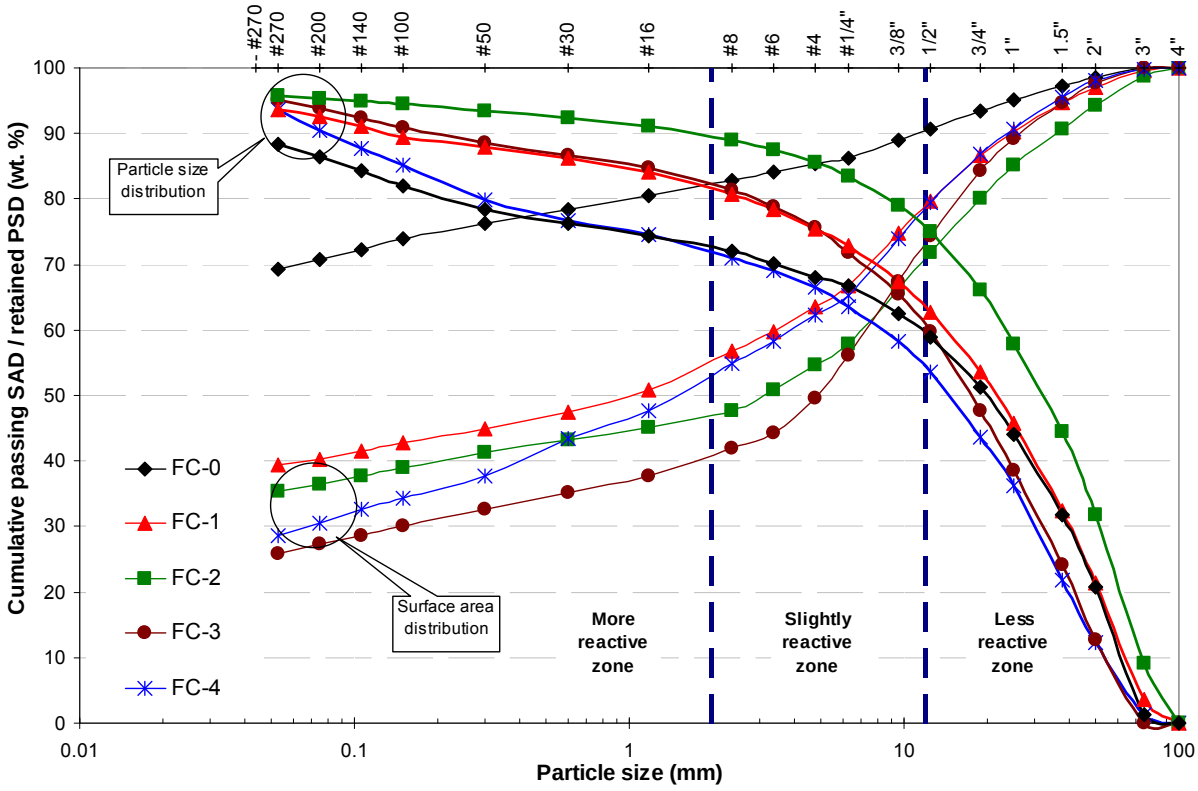

Figure 5.3 Cumulative surface area and particle size distribution curves for determining the reactive zone for all Class B waste rock

The cumulative weight elemental distributions for S-total, Cu, Pb, and Zn were analyzed using the same methodology that was used for the weight surface area distribution. According to Table 5.6, Figures E1.1, E1.4, E1.5, and E1.6 (Appendix E1), the highest weight percentages of elements occurred in the "less reactive zone" for most of the samples, with the exception of the gray hornfels sample, where the highest distribution occurred in the "more reactive zone".

Therefore, to define the reactive zones, in which greater than 50 wt.% of the elemental distribution must be within the "more reactive zone", the particle size cut off should be moved up towards 12 mm. The more reactive zone then would include particles above 2 mm but below 12 mm, for samples FC-2 and FC-3.

In order to validate these findings, the availability of sulfide, copper, lead, and zinc minerals was evaluated as well. As previously mentioned, for sulfide minerals, more than 80 wt.% of mineral availability for leaching occurred in waste rock particles below 1 mm (Figure 3.18). After assessing the availability of sulfide for leaching, Cu, Pb and Zn minerals curves with the intersection at the particles cut offs, it was found that these minerals were still available in high proportions in particles less than 12 mm in diameter. Availability greater than 50 wt.% was still present for particles below 3 - 25 mm in diameter in samples FC-0, FC-1, and FC-4. The opposite is true with samples FC-2 and FC-3, where >50 wt.% of availability was occurring at coarse particle sizes (>100 mm in diameter).

In addition, the partial reactivity indices, defined as the RI at each size fraction, show higher values at the finest size fraction (<53 μm) for Cu, Pb, Zn, and Sb in almost all samples, suggesting that the most

reactive zone is present in the finest particles. However, relatively high partial reactivity indices for sulfide minerals were also distributed in coarse particle sizes of all the samples. This effect was also seen for the RI of Cu, Pb, and Zn minerals in samples FC-2 and FC-3 (Table 5.1 to Table 5.5).

Consequently, only two reactive areas and one particle size cut off were defined for Class B waste rock material. Those which were equal or less than 12 mm (1/2 inch) were categorized in the "more reactive zone", whereas those which were greater than 12 mm were categorized in the "less reactive zone". For practical purposes, Class B material passing the US St. ½ inch (12.5 mm) screen, will be considered the more reactive material.

5.4 Geochemistry of the Field Cells

Trends for concentrations, elemental production, and release rates on a mass and surface area basis for parameters such as SO_4, Ca, alkalinity, Cu, Pb, Zn, Sb, As, Mo, and fluoride present in the leachate from all field cells are discussed below and can be seen plotted in Appendix E2, (Figure E2.1 to Figure E2.10). In general, the cumulative elemental production (mg/kg) given on a weekly or bi-weekly basis are 1 to 2 orders of magnitude higher than the elemental release rates on a waste rock mass basis (mg/kg/day), which are also 4 to 5 orders of magnitude higher than the elemental rates on a surface area basis ($mg/m^2/day$) because surface area results provide much larger values than do mass values.

a. Sulphate (SO_4)

Since most of the samples contain sulfur corresponding to sulfide and some sulphate minerals (Table 3.11 and Table 3.12), leachate sulphate concentrations from field cells were evaluated as part of the sulfide oxidation and sulphate mineral dissolution processes. Relatively high leachate sulphate concentrations ranging from 25 to 860 mg/L (0.3 to 9 mmol/L) were reported from the field cells UBC-1-1A, -2A/2B and -3A which contained diopside marble material. Higher values were reported at the beginning of the wet seasons, after which they subsequently decreased to approximately 120 mg/L. Cumulative sulphate production reached up to 185 mg/kg, and release rates were up to 10 mg/kg/day and $2x10^{-3}$ $mg/m^2/day$ (Figure E2.1). Solid-phase S-total ranged from 0.30 to 1.2% (Table 3.10), which is consistent with the leachate sulphate release reported. Most of the sulfur content in these samples exists as sulfide (Table 3.11).

In the leachate from the field cells containing gray hornfels and black marble samples, sulphate ranging from 40 to 740 mg/L (0.4 to 7.7 mmol/L) was found, with SO_4 production reaching up to 185 mg/kg, and release rates up to 12 mg/kg/day and $2x10^{-3}$ $mg/m^2/day$. S-total concentrations in the solid phase were approximately 0.25%, lower than in other samples, but some of the sulfur content was present as sulphate ($S\text{-}SO_4$) minerals, although mineralogy tests reported relatively more sulfide than sulphate minerals (Table 3.12). However at the end of the evaluated period, this sample reported similar cumulative sulphate production and release rates to other field cells containing diopside marble samples. All of the samples which were studied showed similar sulphate trends to those of previous Class B field cells (Golder Associates, 2008).

Coarse and grainy disseminated sulfide minerals were observed in the diopside marble samples, particularly in samples FC-2 and FC-3. However, very finely disseminated sulfide minerals were observed

in the black marble and gray hornfels samples. Large sulphate release rates were observed as high concentrations in the leachate from the field cells, and were probably the result of sulfide mineral (from 0.48 to 5.53 wt.% in Table 3.12) oxidation (Figure 5.5). However, this was likely also due to sulphate mineral (from 0.04 to .035 in Table 3.12) dissolution, although most of sulphate minerals were shown to be iron sulphate minerals that are generally formed as secondary mineral products after the weathering process. The most abundant sulfide minerals reported by MLA analysis included galena, sphalerite, chalcopyrite, pyrrhotite, and pyrite. Other sulfide minerals including bornite, realgar, watanabeite, molybdenite, among others, were present in low concentrations. Iron sulphate was found to be the most abundant sulphate mineral, particularly in samples FC-0 and FC-2, affecting the release of sulphate due to its dissolution.

b. Calcium (Ca)

High calcium concentrations were found in most of the samples. Calcium is present in calcite [$CaCO_3$], the main component of marble, in calcium magnesium silicates minerals (diopside), and in the calcium silicate minerals of hornfels.

The highest calcium concentrations were reported in the first samplings at the beginning of the wet season, and were considered to be part of the flushing effect. Peaks between 320 and 435 mg/L (8 to 11 mmol/L) detected in some marble samples were immediately depleted to 30 mg/L (0.7 mmol/L). In general, the average calcium concentrations ranged from 50 to 140 mg/L (1.2 to 3.5 mmol/L). Cumulative Ca production reached values from 45 to 100 mg/kg, and release rates from 3 to 5 mg/kg/day, and $2x10^{-4}$ to $9x10^{-4}$ mg/m^2/day (Figure E2.2).

High solid phase calcium concentrations were found to range between 18 and 35% (Table 3.10 and Figure 5.5). These concentrations provide a high neutralization potential (Table 3.11), and therefore are able to neutralize any potential acid generation if most of the Ca is a component of the carbonate minerals such as calcite. This was confirmed after MLA analysis, where the main source of Ca was found to be calcite, which was found in higher proportions in the black marble and gray hornfels samples, but in lower proportions in one of the diopside marble samples (FC-2). This explains why the lowest solid phase calcium concentration was detected in sample FC-2. This may reduce its buffering capacity in the long term, although it reported a high NP value, and may be the reason that the leachate from this sample still remained under circumneutral pH conditions.

Thus, calcium concentrations found in the leachate resulted from calcite and plagioclase dissolution, but according to the mineralogy data, calcite was responsible for most of the Ca release.

c. Alkalinity (Alk)

High alkalinity results, reported as calcium carbonate ($CaCO_3$), ranging from 30 to 60 mg/L (0.3 to 0.6 mmol/L) were found. In all the samples, cumulative alkalinity production reached values of up to 27 to 50 mg/kg, and release rates of 2 to 4 mg/kg/day and $1x10^{-4}$ to $1x10^{-3}$ mg/m^2/day (Figure E2.3). The leachate from field cell UBC-1-1A shows the highest release rates, thus demonstrating a strong relationship with its high pH values (Figure 4.4). As mentioned in previous sections, most of the samples contained abundant carbonate minerals, particularly calcite. These were able to provide a high long-term

buffer capacity, with sample FC-2 being the exception. The alkalinity was controlled by dolomite, magnesite, otavite, and smithsonite dissolution, or by the absence of these minerals. However, calcite and aragonite dissolution contributed widely to high alkalinity results. The dissolution of these minerals was evidenced after geochemical speciation calculations, where these minerals remained in equilibrium with the solutions (Table 4.7).

In addition to the field cell UBC-1-1A, high alkalinity results were observed in the leachate from the field cell containing gray hornfels (Figure 5.4), suggesting initially that carbonate mineral dissolution was occurring faster in these samples than in others. However, based on MLA results, the highest carbonate mineral content (90.8 wt.%) was found in this particular sample (Table 3.12), therefore resulting in being the main source of higher alkalinity results.

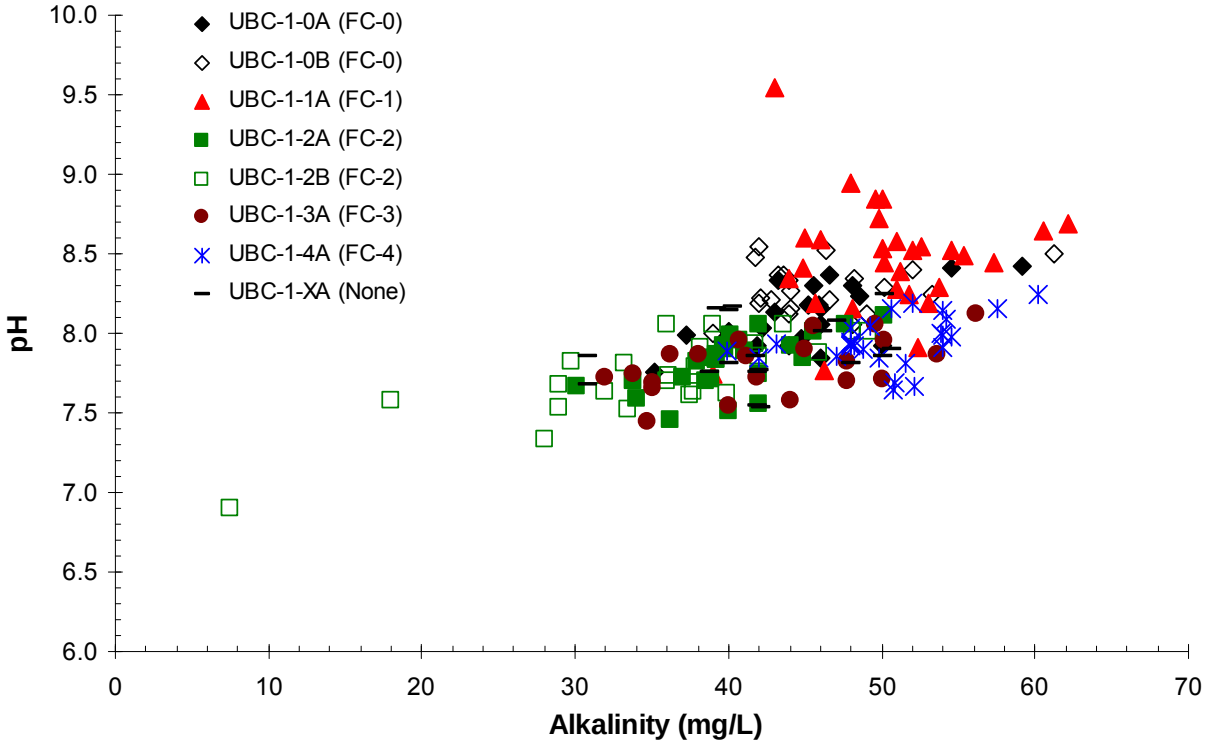

Figure 5.4 pH as a function of alkalinity in the leachate from waste rock samples placed in the field cells

d. Copper (Cu)

Two diopside marble samples (UBC-1-2A/B and -3A) and the gray hornfels sample showed relatively high copper (one of the ores mined by Antamina) concentrations, ranging between 0.03 and 0.3 mg/L ($5x10^{-4}$ to $9x10^{-3}$ mmol/L). Cumulative copper production reached up to 0.1 mg/kg and had a release rate of up to $9x10^{-2}$ mg/kg/day and $1x10^{-2}$ mg/m^2/day for these samples.

The other samples showed concentrations from <0.001 to 0.07 mg/L ($2x10^{-5}$ to $1x10^{-3}$ mmol/L), but most of them were below the analytical detection limit (0.001 mg/L). The cumulative Cu production for these

samples reached maximum values of 0.001 mg/kg and release rates of $1x10^{-4}$ mg/kg/day and $1x10^{-8}$ mg/m^2/day (Figure E2.4).

Solid phase copper concentrations for all samples ranged from 160 to 820 mg/kg (Table 3.10). The sample with the highest copper grade was one of the diopside marble (UBC-1-1A) samples. That with the lowest copper grade was the gray hornfels (UBC-1-4A) sample. There were no demonstrable relationships between the solid phase copper and production or release rates. For instance, while the lower release rates occurred in the leachate from field cell UBC-1-1A containing the diopside marble sample; this field cell was also found to have the highest solid phase copper concentration (Figure 5.5).

Besides chalcopyrite, Cu was associated with iron oxyhydroxide, iron sulphate and apatite minerals in UBC-1-2A/B, -3A and -4A field cells. This was true even in coarse particles (Table C5.6), which would have enhanced the source Cu that may be released in a solution. Moreover, Cu minerals were found to have a high reactivity index which determines the availability of copper for leaching, particularly for the UBC-1-2A/B, and -3A field cells. This explains why relatively high Cu concentrations were found in the leachates from these samples.

In contrast, low Cu concentrations were found in the leachate from the black marble and one of the diopside marble (UBC-1-1A) samples, whose Cu sources were chalcopyrite, iron oxyhydroxide, apatite and Cu silicates. The explanation may be that Cu had co-precipitated as part of the ferric precipitates such as copper iron oxyhydroxide, or had been adsorbed on iron oxyhydroxide. Sorption of Cu on iron oxyhydroxides is common at mine sites (Blowes et al., 2003). Although the geochemical speciation results did not show any iron oxyhydroxide mineral formation, they remained undersaturated with respect to the solutions. However, MLA analysis found that copper, associated with Fe oxyhydroxide minerals, was also present in low amounts in samples placed in the field cells UBC-1-0A/0B and -1A, with chalcopyrite being the main source of Cu in these samples (Table C5.6). Another explanation may be that Cu had precipitated as carbonate or oxide minerals. This statement was verified using geochemical speciation calculations, where the solutions from these samples were found to be in equilibrium with malachite and tenorite (Table 4.7), indicating the formation of these minerals. No copper hydroxide mineral formation was reported using geochemical calculations; for instance the solutions remained undersaturated with respect to spertiniite.

However, other additional explanations could be also given: 1) chalcopyrite may oxidise at a much lower rate than pyrite at a neutral pH. 2) As relatively high proportions of clay minerals, particularly in black marble, were reported by MLA, these could have adsorbed or encapsulated the Cu, forming silicate minerals with surface complexation. Coincidently, MLA found very high FeCu silicate minerals (Table C5.6), indicating the existence of undetected Cu sinks. 3) A low Cu reactivity index was reported in sample FC-0 which was placed in the field cell UBC-1-0A/0B, suggesting low levels of Cu available for leaching.

Besides chalcopyrite, other Cu minerals including enargite, bornite, and watanabeite, among others were reported by MLA.

e. Lead (Pb)

Relatively high lead concentrations were detected in the leachate from some field cells. Lead ranged from 0.2 to 4.0 mg/L ($9x10^{-4}$ to $2x10^{-2}$ mmol/L) in five field cells (UBC-1-2A/2B, -3A, -4A and -XA), but the highest concentrations were reported in the UBC-1-2A/2B field cells. Cumulative lead production in the leachates from these field cells reached values ranging between 0.2 and 0.4 mg/kg, and release rates up to $3x10^{-2}$ and $5x10^{-6}$ mg/m^2/day (Figure E2.5) were also reported. The solid phase lead concentrations in these samples ranged from 160 to 840 mg/kg (Table 3.10). The highest concentrations were found in the diopside marble sample placed in the UBC-1-2A/2B field cell.

The leachates from other field cells showed very low Pb concentrations, most of them below the analytical detection limit (0.01 mg/L). Their cumulative Pb production reached up to 0.01 mg/kg, and release rates of $1x10^{-3}$ mg/kg/day and $1x10^{-7}$ mg/m^2/day were found. Their solid phase concentrations ranged from 310 to 540 mg/kg.

In samples FC-2 and FC-3, there was an apparent relationship between the solid phase concentration and the concentrations registered in the leachate from the field cells. In sample FC-4, low solid phase Pb concentration reported a relatively high release of Pb in its leachate (Figure 5.5). The main source of Pb was galena, but a relatively high proportion of Pb was also present in association with Fe oxyhydroxide, chalcopyrite and Fe/Cu silicates, particularly for samples placed in -2A/2B and -3A field cells (Table C5.6). This, associated with their high reactivity indices, has contributed a high Pb availability for leaching, as observed later on in the leachates from these particular field cells.

Even though the sample in UBC-1-0A/0B field cell did not have the highest solid phase Pb concentration, its result was almost the same as that found in the -3A field cell. As with Cu, very low Pb concentrations were found in its leachate. In addition, one of the diopside marble (UBC-1-1A) samples also reported low concentrations in its leachate. Although Pb mobilization is not well understood under circumneutral pH conditions, it has the same ionic charge as Cu (+2), and therefore may display a similar geochemical behaviour. Therefore, a similar explanation may be also given for Pb behaviour. Thus, Pb could have co-precipitated with iron oxyhydroxide. Although the geochemical speciation results did not show any iron oxyhydroxide or oxide (plattnerite) mineral formation, they remained undersaturated. However, other results have shown that the solutions were in equilibrium with cerrusite (lead carbonate) and were supersaturated with respect to wulfenite (lead molybdate), reducing the Pb mobilization in the leachate.

Additionally, other explanations could also be given: 1) Galena may oxidise at a much lower rate than pyrite at a neutral pH. 2) Soluble lead may have been adsorbed or coated by clay minerals, which were detected with MLA, essentially in the black marble sample. Therefore, undetected sinks for Pb could exist. 3) Low Pb reactivity indices were reported in these samples, indicating low Pb availability for leaching.

In conclusion, in the early stage, lead was also identified as a product of the neutral rock drainage. This phenomenon was not previously well defined.

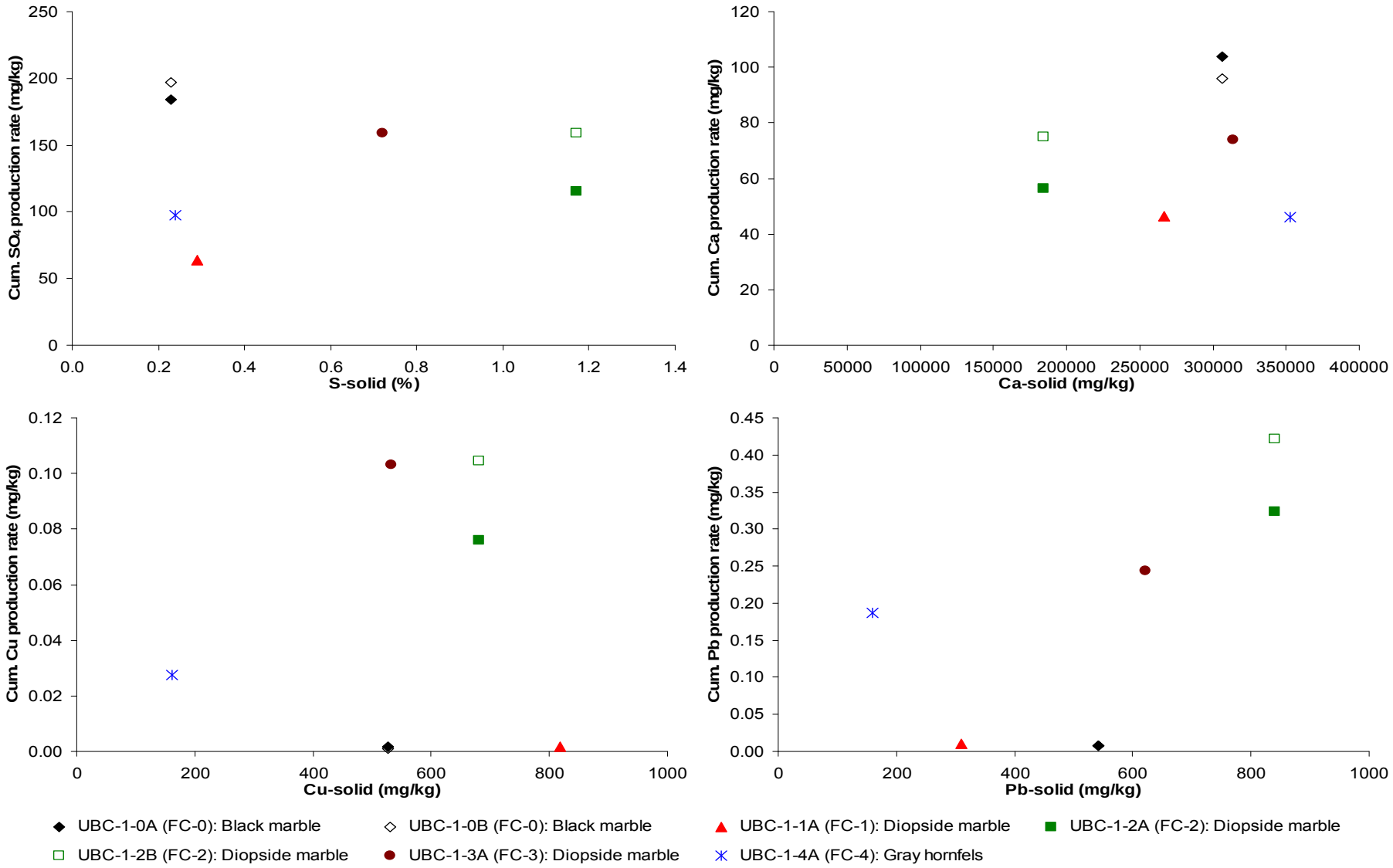

Figure 5.5 Cumulative elemental production rates related to solid phase S-SO_4, Ca, Cu, and Pb concentrations (ICP-MS) of the Class B waste rock samples

f. Zinc (Zn)

Zinc (another product extracted by Antamina) was selected as the most important element of environment concern since it may rapidly mobilize under circumneutral pH condition. Furthermore, solid phase zinc concentrations are currently widely used in the waste rock classification system.

The same field cells (UBC-1-2A/B, -3A, -4A and -XA) that reported high copper and lead concentrations in the leachate from the field cells also reported elevated zinc concentrations, ranging from 0.4 to 17 mg/L ($7x10^{-3}$ to 0.26 mmol/L). On January 11th, 2008 during the last rainy season, a peak of 17 mg/L in the leachate from the UBC-1-2A field cell was reported as a consequence of the flushing effect associated with a heavy rain event at that time. It eventually decreased to 5-6 mg/L (Figure 5.9) after the rains subsided. Cumulative zinc production reached up to from 1 to 3.6 mg/kg, and release rates from 0.08 to 0.25 mg/kg/day and $2x10^{-5}$ to $3x10^{-5}$ mg/m^2/day (Figure E2.6) were detected. Solid phase zinc concentrations ranged from 400 to 1270 mg/kg (Table 3.10).

Very low zinc concentrations ranging from 0.004 to 0.17 mg/L ($6x10^{-5}$ to $3x10^{-3}$ mmol/L) were reported in the leachate from the field cells containing the black marble (UBC-1-0A/B) and the diopside marble (UBC-1-1A) samples. These results are more consistent with the previous Class B field cell drainage results, where most of the concentrations were below 0.1 mg/L (Golder Associates, 2007b). Their cumulative Zn production reached up to 0.05 mg/kg, and release rates were up to $5x10^{-3}$ mg/kg/day and $3x10^{-7}$ mg/m^2/day, with solid phase zinc concentrations of 650 and 1360 mg/kg for UBC-1-1A and UBC-1-0A/B, respectively.

Surprisingly, there was no evidence of a relationship between solid phase zinc concentrations and the leachate from the field cells, except in the UBC-1-3A field cell. For instance, the highest solid phase zinc concentration occurred in the black marble sample, but the production or release rates in the leachate from field cell UBC-1-0A/0B, which contained this sample, were the lowest ones. The opposite was true for field cells UBC-1-2A/2B containing one of the diopside marble samples. These cells displayed the lowest solid zinc concentrations, but the highest cumulative Zn production rates in the leachate from the field cells (Figure 5.6).

Sphalerite is the primary mineral contributor of Zn for mobilization; however low proportions of Zn in association with Fe oxyhydroxide, Fe sulphate, and apatite were also identified (Table C5.6), particularly in the black marble sample placed in the -0A/0B field cell. The reasons for the high release rates of Zn from the -2A/2B and -3A field cells are because these have high Zn mineral reactivity indices, which correspond to more Zn being available for leaching. Secondary Zn mineral formations such as zincosite (zinc sulphate) or wülfingite (zinc hydroxide), which remained undersaturated with the solutions, were reported. The above reasons, which are associated with a high capability for Zn mobilization under circumneutral pH conditions, could have contributed to the high concentrations of Zn found in these samples.

On the other hand, the low Zn concentrations found in the leachate from the black marble and one of the diopside marble (UBC-1-1A) samples may be explained in a manner which is similar to that which was discussed with regard to the behaviours of Cu and Pb. Zinc was not present in the leachate because these samples showed low reactivity indices for Zn minerals (62.3 and 63.7 wt.% for UBC-1-0A/0B and -1A field cells, respectively); therefore limited amounts of Zn were available for leaching. Another reason

may be because Zn was likely to have co-precipitated with ferric oxyhydroxide (Stromberg and Banwart, 1999a). Although the geochemical speciation results did not show any ferric oxyhydroxide mineral formation, zincosite, wülfingite, or smithsonite (zinc carbonate), all them remained undersaturated. Likewise, sphalerite may oxidise at a much lower rate than pyrite at a neutral pH. However, the most feasible explanation may be that Zn was trapped or adsorbed by clay minerals, as were detected in the black marble sample, although MLA also found some clay minerals (altered mica) in association with Zn (Table C5.6), indicating that sorption of Zn may be taking place. In addition, iron oxyhydroxide minerals may have also encapsulated it into their structure. These reasons have contributed to the presence of undetected Zn in the leachate from these samples.

g. Antimony (Sb)

Relatively high antimony concentrations were detected in some of the samples. The field cell containing one of the diopside marble (UBC-1-1A) samples showed the higher antimony concentrations, ranging from 0.02 to 0.25 mg/L ($2x10^{-4}$ to $3x10^{-3}$ mmol/L) that the other field cells. Cumulative antimony production reached up to 0.2 mg/kg, and release rates were up to 0.01 mg/kg/day and $2x10^{-6}$ mg/m^2/day (Figure E2.7). Sb(V) is the most soluble form, and its presence is probably due to the oxidation of stibnite and watanabeite, which were identified by MLA as the source of Sb (Table C5.7). The higher release rate was also consistent with the high Sb solid phase concentration of 16.5 mg/kg (Table 3.10) present in this sample.

The gray hornfels (UBC-1-4A) sample was found to release antimony between 0.06 and 0.17 mg/L ($5x10^{-4}$ to $1x10^{-3}$ mmol/L). Cumulative antimony production was reached up to 0.1 mg/kg, and release rates up to 0.008 mg/kg/day and $2x10^{-6}$ mg/m^2/day were notes as having a solid phase antimony concentration of 6 mg/kg.

Other samples showed concentrations below 0.1 mg/L (<$9x10^{-4}$ mmol/L), and most of them were below the analytical detection limit. Their cumulative Sb production reached values from 0.01 to 0.02 mg/kg; as well as release rates of $7x10^{-4}$ to $3x10^{-3}$ mg/kg/day, and $2x10^{-8}$ to $2x10^{-7}$ mg/m^2/day. These showed low solid phase antimony concentrations ranging from 3.5 to 11 mg/kg. In general, the relationship between the solid phase antimony concentration and the concentrations in the leachate was observed for all the samples (Figure 5.6).

Approximately 40 to 45 wt.% of reactive index for Sb minerals were reported from the samples placed in UBC-1-1A and -4A field cells, which explains why Sb was being released from these samples. The availability for leaching of Sb minerals was not reported for any of the other samples.

h. Arsenic (As)

In general, arsenic, currently an element used as part of the waste rock classification system too, showed very low concentrations in the leachates from all field cells (Figure E2.8). The concentrations ranged from 0.001 mg/L to 0.0036 mg/L ($1x10^{-5}$ to $5x10^{-4}$ mmol/L), reaching a maximum cumulative arsenic production of 0.02 mg/kg, and release rates of $2x10^{-3}$ mg/kg/day, and $2x10^{-7}$ mg/m^2/day. This behaviour was also seen in other Class B field cells (Golder Associates, 2007b). Arsenic concentrations in the solid phase ranged between 20 and 120 mg/kg (Table 3.10). The highest solid phase concentration was present in

black marble, and the lowest was present in gray hornfels. However, the highest arsenic concentrations were found in the leachate from the field cell containing black marble, and one of the diopside marble samples (UBC-1-0A/0B and -2A/2B), indicating a suitable relationship between them (Figure 5.6). Arsenic minerals such as arsenopyrite, enargite, realgar, tennantite, and watanabeite were identified in low proportions by MLA analysis, and only some in trace quantities for some of the samples.

i. Molybdenum (Mo)

Most of the Class B marble and hornfels samples showed molybdenum (another metal extracted by Antamina) concentrations below 0.06 mg/L ($6x10^{-4}$ mmol/L), with many of them below the analytical detection limit (0.01 mg/L). However, a slightly increasing trend for relatively high concentrations was observed in the leachate from the field cell (UBC-1-1A) which contained one of the diopside samples (Figure E2.9). Future observations will be necessary to verify if this increase is still on-going. Previous field cells containing Class B material have also shown molybdenum concentrations of less than 0.13 mg/L (Golder Associates, 2007b), indicating that current field cell samples are cleaner with respect to molybdenum than were previous ones. Cumulative Mo production reached maximum values of 0.03 mg/kg, as well as release rates of $3x10^{-3}$ mg/kg/day and $3x10^{-7}$ mg/m^2/day. Solid phase molybdenum concentrations ranged between 5 to 92 mg/kg (Table 3.10). The highest solid phase concentration was present in the UBC-1-1A sample, indicating that there was a strong correlation with the concentration found in the leachate from this field cell (Figure 5.6). However, the molybdenum concentration in the leachate could be controlled by wulfenite precipitation, which was determined after geochemical speciation calculations (Table 4.7). Molybdenite was identified by MLA as the primary mineral containing Mo in almost all samples. However, molybdenum, in association with iron sulphate, was identified in higher proportion in the black marble samples (Table C5.7).

j. Fluoride (F)

As was reported in previous Class B field cells (Golder Associates, 2008), fluoride was also discussed as another element of environmental concern. In most of the leachate from the field cells, fluoride concentrations ranged from 0.3 to 2.2 mg/L (0.02 to 0.11 mmol/L). A peak of 3.1 mg/L in the black marble sample was detected at the beginning of the 2008 wet season as consequence of the flushing effect, but this decreased immediately to 1.0 mg/L. Cumulative fluoride production reached values up to 1.1 mg/kg, and release rates were up to 0.1 mg/kg/day and $2x10^{-5}$ mg/m^2/day (Figure E2.10)

The primary source of fluoride is fluorite, which occurs in intrusions and along dykes in the waste rock, as well as in association with pyrite in the ore (Golder Associates, 2008).

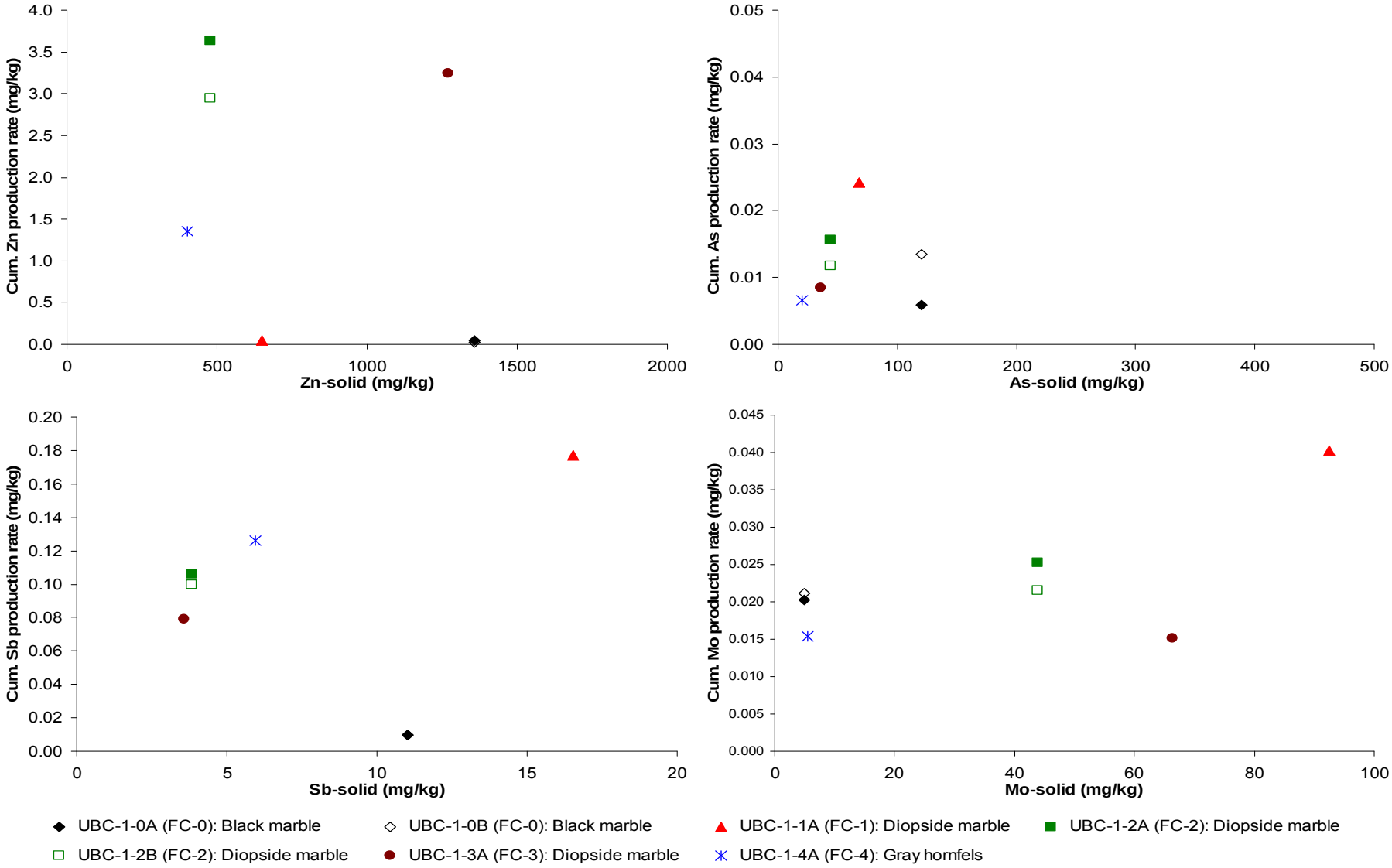

Figure 5.6 Cumulative elemental production rates related to the solid phase Zn, Sb, As, and Mo concentrations (ICP-MS) of the Class B waste rock samples

5.5 Verifying the Sulfide Oxidation and Neutralization Potential

As previously mentioned, all samples displayed a high neutralization potential (NP). However, in order to observe whether the major contribution of NP is primarily due to carbonate minerals such as calcite and dolomite, the inorganic carbon (CO_2) content in the waste rock was plotted as a function of NP. Figure 5.7a shows a direct positive correlation, assuming then that NP is mainly attributed to carbonate minerals. Then, calcium and calcium/magnesium-bearing was examined through plotting Ca vs NP in Figure 5.7b and Ca+Mg vs NP in Figure 5.7c. A positive correlation was found in both plots, even though Mg was present in very low concentrations (Table 3.11) when compared with Ca, suggesting that only Ca could be used as an indicator for neutralization potential. However, both elements were considered for molar examination.

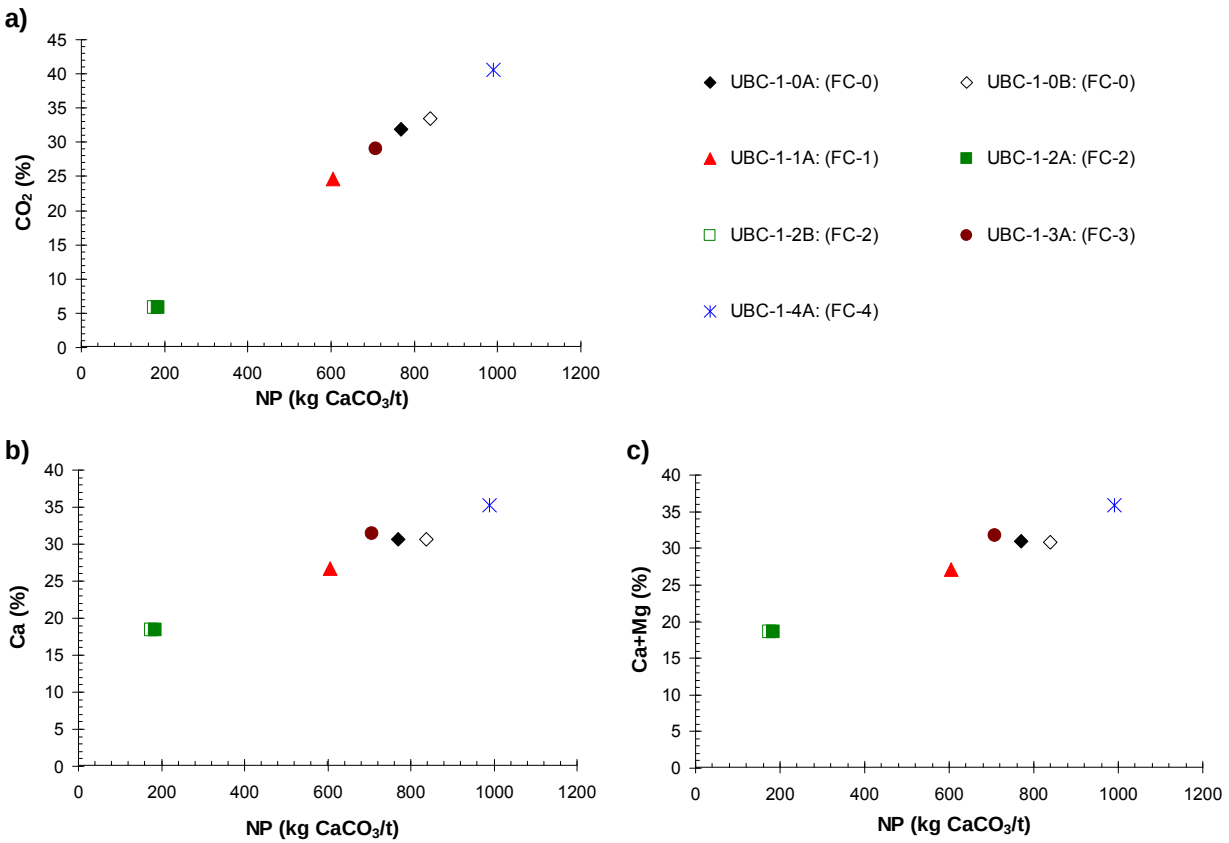

Figure 5.7 a) CO_2 concentration with respect to NP, b) Ca solid-phase concentration versus NP, and c) Ca and Mg solid-phase concentrations in the whole waste rock as a function of NP

When a mole of sulfide (pyrite) mineral is oxidized in the presence of carbonate (calcite) mineral dissolution, some of the products will result in one mole of sulphate and one mole of calcium (Eq. 2.8). But carbonate minerals also contain magnesium; therefore a molar ratio 1:1 of calcium+magnesium/sulphate verifies that sulfide oxidation is taking place. After plotting calcium according to leachate sulphate concentrations for all field cells (Figure 5.8), the molar ratio (Ca+Mg)/SO_4 of the samples was found to range from 1:0.8 to 1:1.2, with an average of 1:1, indicating that sulfide

oxidation is occurring in most of the samples placed in the field cells, but that they are also potentially being neutralized by carbonate dissolution, and therefore becoming oxidation reactions under circumneutral pH conditions. However, in some samples sulphate concentrations were relatively higher than Ca and Mg, and this could have been because other carbonates were present in the sample, and that they were not being taken into account as part of the molar ratio. Perhaps also, sulfide oxidation was occurring more rapidly than carbonate dissolution. This could furthermore have been the result of primary sulphates, or from sulphates that had accumulated earlier and which were being flushed. Despite the occurrence of sulfide oxidation in most field cells, as was shown by elevated sulphate concentrations especially in UBC-1-2A/B field cell, any acid release was neutralized by carbonate mineral dissolution during the time period studied.

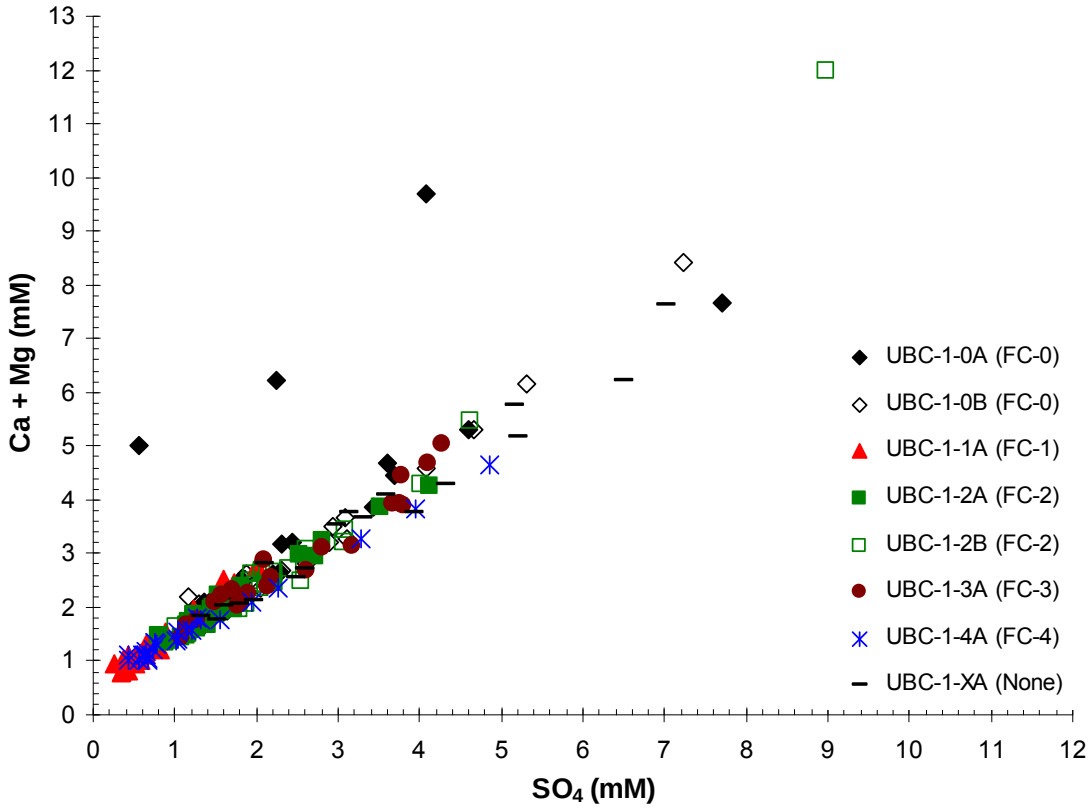

Figure 5.8 Molar ratio between calcium and sulphate in the leachate from the field cells

Other crossing plots between the main parameters with respect to leachate sulphate concentrations are presented in Appendix E3 (Figure E3.1 and Figure E3.2). Molar leachate sulphate with calcium showed a good linear correlation, similar to $Ca+Mg/SO_4$ (Figure 5.8), indicating that most of the carbonate was present as calcite. There was also a slight linear correlation between Cu, Pb, and Zn, particularly for field cells UBC-1-2A/2B and -3A, where the sulphate molarities were higher than for Cu, Pb, and Zn. This suggests that the oxidation of sulfide minerals containing these elements (e.g. chalcopyrite, galena, and sphalerite) was occurring, although those could also be part of overall sulfide oxidation. In contrast, no a

direct molar ratio relationship was found between Sb, As and Mo with sulphate, indicating that not only the sulfide minerals contained the elements mentioned above, although elements such as As and Mo were not present in high solid phase concentrations, which may have been reflected in the leachate from the field cells. Additionally, no molar relationship was found between Ca and F, indicating that the source of fluoride found in the leachate was due to fluorite dissolution, even though the geochemical speciation calculation had shown that the leachates were in equilibrium with respect to fluorite. In reality, Ca molarities were mostly found to be influenced by calcite dissolution rather than by fluorite. Calcite was present in much higher proportion than was fluorite in all the samples (Table 3.12).

In a similar manner, Ca, Cu, Pb, and Zn were plotted with respect to alkalinity concentrations and are shown in Appendix E3 (Figure E3.3). Under controlled acidic conditions where only pyrite oxidation and calcite dissolution occur, Ca concentration would be controlled by gypsum precipitation, and therefore Ca molarities should be lower than alkalinity results. However, as in this case, at specific-sites where the leachate was occurring into circumneutral pH conditions, very high Ca values with respect to alkalinity were reported, indicating that gypsum precipitation or formation was not taking place. This result was also indicated by geochemical speciation calculations. This could also suggest that calcite dissolution was occurring slowly. In addition, malachite precipitation was also determined by geochemical speciation calculations, resulting in alkalinity consumption and therefore lower alkalinity concentrations were found in the leachate from the field cells.

Furthermore, Cu, Pb and Zn were observed occurring in relatively high concentrations where alkalinity concentrations were lower, indicating that they were more mobile under acid conditions.

5.6 Release and Neutralization Potential Rates of Main Elements

Up to May 2, 2008, the total amounts of different elements produced, which were calculated through Eq. 4.5, are shown in Table 5.7. Very low amounts (<0.1 g) of Cu, Pb, Zn, Sb, As, and Mo were produced in all field cells, except in field cells UBC-1-2A/2B and -3A, which released approximately 1 g of Zn. However, in these cells, Ca and sulphate were produced in larger quantities. Amounts from 13.5 to 27.4 g Ca^{2+} were calculated; the black marble sample (UBC-1-0A/0B field cell) released the highest amount of Ca, whereas one of the diopside marble samples (UBC-1-1A) released the lowest amount. Sulphate quantities ranging from 18.4 to 52.1 g were released, where coincidentally the highest and lowest amounts were found in the same fields cells which had released the highest and lowest amounts of Ca, suggesting that sulfide oxidation and carbonate dissolution were consistent in these field cells. However, despite that UBC-1-1A field cell was installed early as compared to the last field cells, the diopside marble sample placed in that cell had released the lowest amounts of SO_4^{2-} and Ca^{2+}, indicating that gypsum precipitation could be taking place. However, the geochemical speciation calculation indicated that the leachates remained relatively undersaturated with respect to gypsum (i.e. gypsum precipitation does not exist). Alternatively, this may also indicate that sulfide mineral oxidation and calcite dissolution rates were slower in this particular sample because low levels of leachate sulphate and calcium were released. Finally, almost 0.3 g of F was released from every field cell.

Release rates on a mass basis were calculated through Eq. 4.7 and are shown in Table 5.7 and Appendix E2 (Figure E2.1 to Figure E2.10). Elements such as Cu, Pb, Zn, Sb, As, Mo, and F had low

release rates ($2x10^{-6}$ – $2x10^{-3}$ mg/kg/day), whereas Ca and SO_4 showed relatively high release rates (0.1 – 0.3 mg/kg/day). In fact, Cu, Pb, and Zn had 1 to 2 orders of magnitude higher release rates in the UBC-2A/2B and -3A field cells (both containing diopside marble) than in the other cells, and this was evidenced by the higher concentrations and elemental production amounts found in the leachate from those field cells. Calcium and SO_4 release rates were almost the same in all samples, suggesting that carbonate (e.g. calcite) dissolution and sulfide mineral oxidation rates were almost the same in all field cells. However, there were some exceptions in the UBC-1-0A/0B and UBC-1-1A field cells, which had relatively higher and lower Ca release rates, respectively compared with the other samples. This was not necessarily associated with their solid content, for instance, the UBC-1-4A field cell had the highest Ca concentration (Table 3.10). Also, relatively high sulphate release rates were observed from field cells UBC-1-0A/0B, -2A/2B, and -3A, suggesting that sulfide oxidation was occurring rapidly in these samples. This was also evidenced by the higher level of sulphate production and by the fact that less sulfur remained in the black marble sample (Table 5.7).

Low release rates on a surface area basis calculated according to Eq. 4.8 were found for Cu, Pb, Zn, Sb, As, Mo, and F ($4x10^{-12}$ – $3x10^{-8}$ mg/m^2/day) in comparison with the relatively high release rates for Ca and SO_4 ($7x10^{-7}$ – $2x10^{-6}$ mg/m^2/day). However, despite the higher surface area in the UBC-1-0A/0B field cell which contained the black marble sample (Figure 5.10) and in which theoretically, the weathering could have occurred faster and adopted a high release rate early on, surprisingly, the release rates for most of the elements in this sample were 1 to 2 orders of magnitude lower than in other samples. As such, a longer time would have been necessary to fully deplete the elements in this sample. Therefore, elements such as Cu, Pb, and Zn remained in the sample, perhaps forming secondary minerals (precipitates), being adsorbed or even locked, encapsulated or sunk within carbonate or silicate minerals such as clay particles (as explained above). However, Ca and SO_4 were released in the highest proportion from this sample when compared to the other samples, indicating that carbonate dissolution and sulfide oxidation were taking place rapidly. The opposite was true for elements such as Cu, Pb, Zn, even Ca, and SO_4 present in the diopside marble samples in UBC-1-2A/2B and -3A field cells, which had higher release rates as are showed in Appendix E2 (Figure E2.1 to Figure E2.6), suggesting that these elements were being released in the absence of any control processes such as sorption or precipitation.

Therefore, according to the concentrations observed in the leachates from the field cells, the release rates on a surface area basis were more consistent and accurate. Nevertheless, in order to calculate weathering rates, which include release rates calculated only with the drainage data (collected in the bottom of the field cells) and oxidation rates occurring in the pore water (within the whole waste rock), other geochemical processes or factors such as the presence of oxygen, bacterial activity, sorption, precipitation, among others should be considered. The aforementioned geochemical processes are not discussed in this thesis.

As indicated in Table 5.7, most of the elements have only been depleted by less than 3% in all samples, which were calculated using Eq. 4.9 and therefore, S-SO_4 (<1 – 3%), Ca (<0.1%), Cu (<0.1%), Pb (<0.1%), Zn (<0.01 – 0.7%), Sb (<1 – 3%), As (<0.1%), and Mo (<0.4%). At an early point in the evaluation (800 days), more than 99.5% of most of the elements still remained within the field cells. Only antimony and S-total had been reduced to 97 - 99%.

Overall, the time required to deplete almost 100% of most of the elements present ranged roughly between 5,000 and 900,000 years, except for Sb and S-SO_4, which would be completely reduced in 70 to 300 years. However, this could change if these elements, which constitute the minerals, become exposed, therefore accelerating their release rates.

Table 5.7 Elemental production and release rates determined in the leachate from the field cells containing Class B waste rock samples

Field Cell	Parameter	Units	S-SO_4*	Ca	Cu	Pb	Zn	Sb	As	Mo	F	T (day)	m (kg)	SA (m^2)
	CEP	mg/kg	190.6	100.0	0.001	0.008	0.033	0.01	0.01	0.021	0.8			
	SP	mg/kg	6891	306000	526	542	1358	11.04	120.0	5.0	ND			
	TEP	g	52.1	27.4	0.0004	0.002	0.009	0.003	0.003	0.006	0.2			
UBC-1-0A/0B	RR_m	mg/kg/day	6E-07	3E-07	4E-12	2E-11	1E-10	3E-11	3E-11	7E-11	3E-09	759.0	273.6	542822
	RR_{SA}	mg/m^2/day	6E-07	3E-07	4E-12	2E-11	1E-10	3E-11	3E-11	7E-11	3E-09			
	DP	(%)	2.8	0.03	0.0003	0.001	0.002	0.1	0.01	0.4	ND			
	DT	(year)	75	6,370	838,467	146,027	106,695	2,296	30,865	502	ND			
	CEP	mg/kg	63.5	46.5	0.002	0.011	0.043	0.177	0.024	0.040	1.2			
	SP	mg/kg	8688	267000	819	309	649	16.54	68.0	92.5	ND			
	TEP	g	18.4	13.5	0.0005	0.003	0.01	0.05	0.01	0.01	0.4			
UBC-1-1A	RR_m	mg/kg/day	0.09	0.07	2E-06	2E-05	6E-05	3E-04	4E-05	6E-05	2E-03	688	289.9	156256
	RR_{SA}	mg/m^2/day	9E-07	6E-07	2E-11	1E-10	6E-10	2E-09	3E-10	5E-10	2E-08			
	DP	(%)	0.7	0.02	0.0002	0.003	0.007	1.1	0.04	0.0	ND			
	DT	(year)	258	10,833	908,561	55,425	28,767	176	5,307	4,334	ND			
	CEP	mg/kg	137.3	65.6	0.09	0.37	3.3	0.103	0.01	0.02	1.0			
	SP	mg/kg	35052	184000	680	840	479	3.84	44.0	43.8	ND			
	TEP	g	44.5	21.3	0.03	0.1	1.1	0.03	0.004	0.01	0.3			
UBC-1-2A/2B	RR_m	mg/kg/day	0.22	0.10	1E-04	6E-04	5E-03	2E-04	2E-05	4E-05	2E-03	628	324.3	230902
	RR_{SA}	mg/m^2/day	2E-06	7E-07	1E-09	4E-09	4E-08	1E-09	2E-10	3E-10	1E-08			
	DP	(%)	0.4	0.04	0.0133	0.044	0.687	2.7	0.03	0.1	ND			
	DT	(year)	451	4,921	13,271	3,947	253	64	5,637	3,242	ND			
	CEP	mg/kg	158.7	73.9	0.103	0.244	3.246	0.079	0.008	0.015	1.0			
	SP	mg/kg	21570	314000	532	622	1271	3.59	36.0	66.4	ND			
	TEP	g	51.4	23.9	0.03	0.1	1.1	0.03	0.003	0.005	0.3			
UBC-1-3A	RR_m	mg/kg/day	0.25	0.12	2E-04	4E-04	5E-03	1E-04	1E-05	2E-05	2E-03	628	324.1	162374
	RR_{SA}	mg/m^2/day	2E-06	1E-06	2E-09	4E-09	5E-08	1E-09	1E-10	2E-10	2E-08			
	DP	(%)	0.7	0.02	0.0194	0.039	0.255	2.2	0.02	0.0	ND			
	DT	(year)	234	7,313	8,862	4,393	674	78	7,351	7,563	ND			
	CEP	mg/kg	97.2	46.1	0.027	0.187	1.350	0.126	0.007	0.015	1.2			
	SP	mg/kg	7190	353000	162	160	401	5.95	20.0	5.5	ND			
	TEP	g	31.6	15.0	0.01	0.1	0.4	0.04	0.002	0.005	0.4			
UBC-1-4A	RR_m	mg/kg/day	0.15	0.07	4E-05	3E-04	2E-03	2E-04	1E-05	2E-05	2E-03	628	324.8	109133
	RR_{SA}	mg/m^2/day	2E-06	1E-06	6E-10	4E-09	3E-08	3E-09	2E-10	4E-10	3E-08			
	DP	(%)	1.4	0.01	0.0169	0.117	0.337	2.1	0.03	0.3	ND			
	DT	(year)	127	13,171	10,188	1,475	511	81	5,232	615	ND			

CEP: Cumulative elemental production in the leachate from the field cell

SP: Solid phase concentration

TEP: Total elemental production

RR_m: Release rate on a mass basis

RR_{SA}: Release rate on a surface area basis

DP: Depletion proportion

DT: Time to deplete 100% of the element

T: Entire sampling period

m: dry mass of waste rock [m.(1-ω)]

SA: total surface area of waste rock placed in the field cell

* Sulfur as sulphate solid phase was obtained by dividing sulfur concentration (%) by sulfur molecular weight and multiplying by sulphate molecular weight times 10000

ND: No data

The neutralization potential depletion rates calculated according to Eq. 4.11 and Eq. 4.12, and shown in Table 5.8 are almost similar to the sulphate release rates. The black marble and two diopside marble (-2A/2B and -3A) samples showed similar high NP depletion rates on a mass basis. However, field cell UBC-1-1A had the lowest NP depletion rate, suggesting that the solution was in equilibrium with respect calcite, or calcite dissolution was occurring slowly even though it had shown higher alkalinity concentrations when compared to other field cells. In addition, the NP depletion rates on a surface area basis for all samples were in the same order of magnitude, indicating that the calcite dissolution rates were in the same order of magnitude as the sulfide mineral oxidations rates for all the samples. It is known, that at circumneutral pH conditions, carbonate dissolution rates are orders of magnitude higher than sulfide oxidation rates. This was observed only in the first three samples, with the last two samples demonstrating a slightly inverse relationship.

Table 5.8 Neutralization potential depletion rates determined in the leachate from the field cells containing Class B waste rock samples

Field Cell	$RR_{(SO_4)}$		MR	NP_{DR}	
	mg SO_4/kg/day	mg SO_4/m^2/day	Mg $CaCO_3$/mg SO_4	mg $CaCO_3$/kg/day	mg $CaCO_3$/m^2/day
UBC-1-0A/0B	0.25	6E-07	1.011	0.25	6.E-07
UBC-1-1A	0.09	9E-07	1.183	0.11	1.E-06
UBC-1-2A/2B	0.22	2E-06	1.096	0.24	2.E-06
UBC-1-3A	0.25	2E-06	0.974	0.25	2.E-06
UBC-1-4A	0.15	2E-06	0.810	0.13	2.E-06

$RR_{(SO_4)}$: Sulphate release rate on a mass and surface area basis
MR: Molar ratio of Ca+Mg by sulphate
NP_{DR}: Neutralization potential depletion rate

5.7 Release Rates Related to Rainfall

No samples were collected during the dry seasons even though Figure 4.5 shows low rainfall events during dry seasons. The outflow from the field cells was controlled by the occurrence of high rates of evaporation. However, during the wet seasons, release rates during sampling times were controlled by rainfall events, indicating that higher release rates were associated with heavy rainfall events. For instance, the samples collected in January 2008 showed higher Zn release rates (0.04 mg/kg/day) from field cells UBC-1-2A/2B and -3A, which experienced almost 120 mm/day of rainfall in the period before sampling (Figure 5.9). A similar shape was distinguished for sulphate release rates from field cells UBC-1-0A/0B and -3A. Even though the outflow was higher in UBC-1-1A field cell, it was not releasing high concentrations of Zn, but a faster transport of the sulphate produced by sulfide mineral oxidation was evidenced.

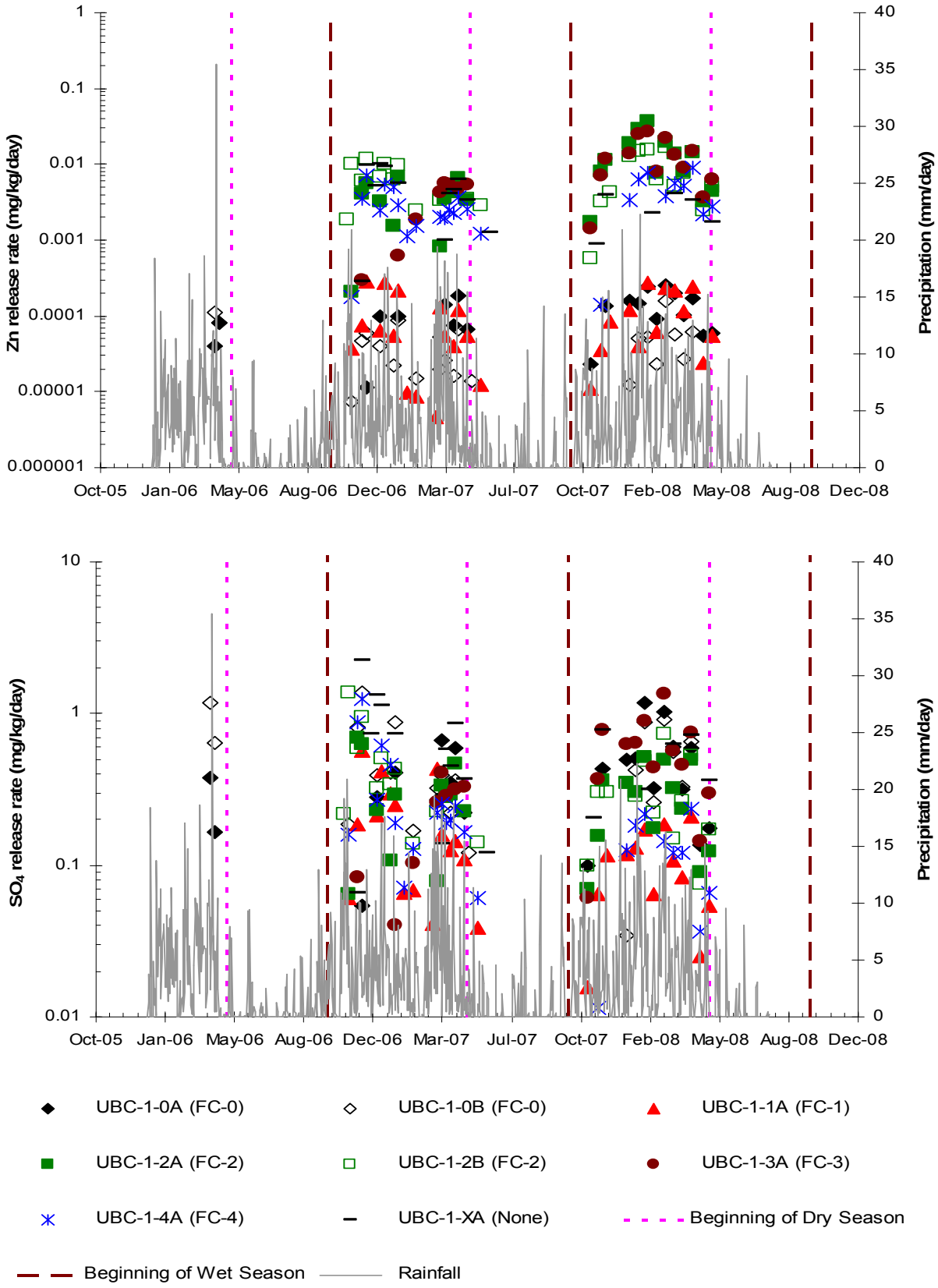

Figure 5.9 Zinc and sulphate mass loading rates in the leachate from the field cells related to site-specific rainfall data

5.8 pH Dependence

Appendix E4 (Figure E4.1 and Figure E4.2) shows the pH dependence on the solubilisation of elements such as SO_4, Ca, Cu, Pb, Zn, Sb, As, and Mo. As mentioned previously, the leachates from the field cells are draining under circumneutral pH conditions. The UBC-1-1A field cell is an exception, with drainage occurring under relatively alkaline conditions. In this sample, relatively high Sb concentrations were found between pH 8 - 9.5, indicating that the minerals containing Sb (e.g. watanabeite or stibnite) could be oxidizing and therefore releasing Sb in that range of pH. In general, Sb, As and Mo mobilization were observed in more alkaline pH conditions, with the pH above 8.5 (Figure E4.2).

The mobilization of Cu, Pb, and Zn under neutral pH conditions (pH 7.5 - 8.0) was particularly observed and confirmed in UBC-1-2A/2B and -3A field cells, even though the lowest solid Zn concentration was obtained from the UBC-1-2A/2B field cell of the diopside marble sample; here, mobilization was enhanced due to the higher reactivity indices of the minerals containing these elements. On the other hand, very low Cu, Pb, and Zn concentrations were detected when the pH ranged from 7.5 to 9.0, especially in field cells UBC-1-0A/0B and -1A. This was despite the fact that their solid phases showed relatively high concentrations particularly with regard to the sample content in the UBC-1-0A/0B field cell. This suggests that the solubility of the minerals may have been controlled by other geochemical processes such as sorption or co-precipitation as was mentioned previously, or that the mobilization of these elements was not taking place because they had been coated or encapsulated within the minerals and so were not available for leaching. This explanation could be confirmed after an assessment of the reactivity index; black marble had a low RI, indicating that Cu, Pb and Zn minerals are not available for leaching.

5.9 Integrating Laboratory Results with Field Results

Since the specific surface area in the black marble (FC-0) sample was higher at the finest size fractions (<53 μm) compared with other samples (Table 3.8), a higher average weight SSA calculated through Eq. 3.16 for the FC-0 waste rock sample was expected. Therefore, the surface area calculated through Eq. 3.17 of the whole-waste rock placed in the field cells (UBC-1-0A/0B) was found to be higher than in the other field cells (Figure 5.10). Thus, SA of 542,822; 156,256; 230,902; 162,374; and 109,133 m^2 were found for UBC-1-0A/0B, UBC-1-1A, UBC-1-2A/2B, UBC-1-3A, and UBC-1-4A, respectively.

Based on the assumption that the weathering process would occur over the entire surface area, it was thought that higher release rates, and therefore higher weathering rates, would occur in the black marble sample and lower release and weathering rates would occur in the gray hornfels sample. However, a greater amount of surface area can create more surface availability through which to adsorb soluble elements. As was previously mentioned, clay minerals found in relatively high proportions at the finest size fraction (<53 μm) of sample FC-0 (Table C5.1 and Figure C5.1) were primarily responsible for the increase in the surface area of this sample. The soluble elements which are most likely to be adsorbed are Cu, Pb and Zn, considerably reducing their mobilization in the leachate from the black marble sample. Zinc may be noted in particular, since it represents the highest solid phase concentration of all the samples.

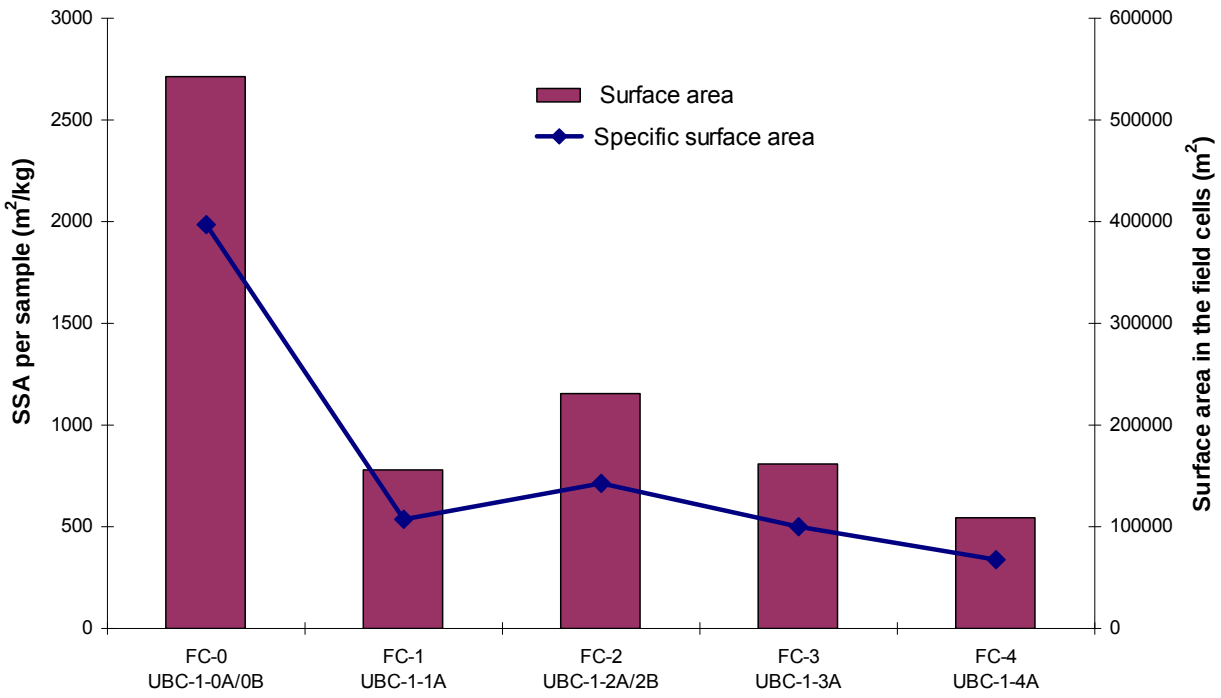

Figure 5.10 Surface area of Class B whole-waste rock samples placed in the field cells

Metal leaching for Cu, Pb and Zn have an excellent relationship with mineral availability, and are expressed as a reactivity index for all Class B samples (Figure 5.11). This indicates that mineral dissolution is directly related to mineral exposure in the particles. Sulfide oxidation, expressed as sulphate formation, also is given as the same relationship. The FC-2 and FC-3 samples have the highest reactivity indices; therefore they reported the highest levels of metal leaching found in the leachate from the field cells. The diopside marble samples are therefore considered to be the dirtiest samples, and the black marble (FC-0) samples are considered to be the cleanest ones.

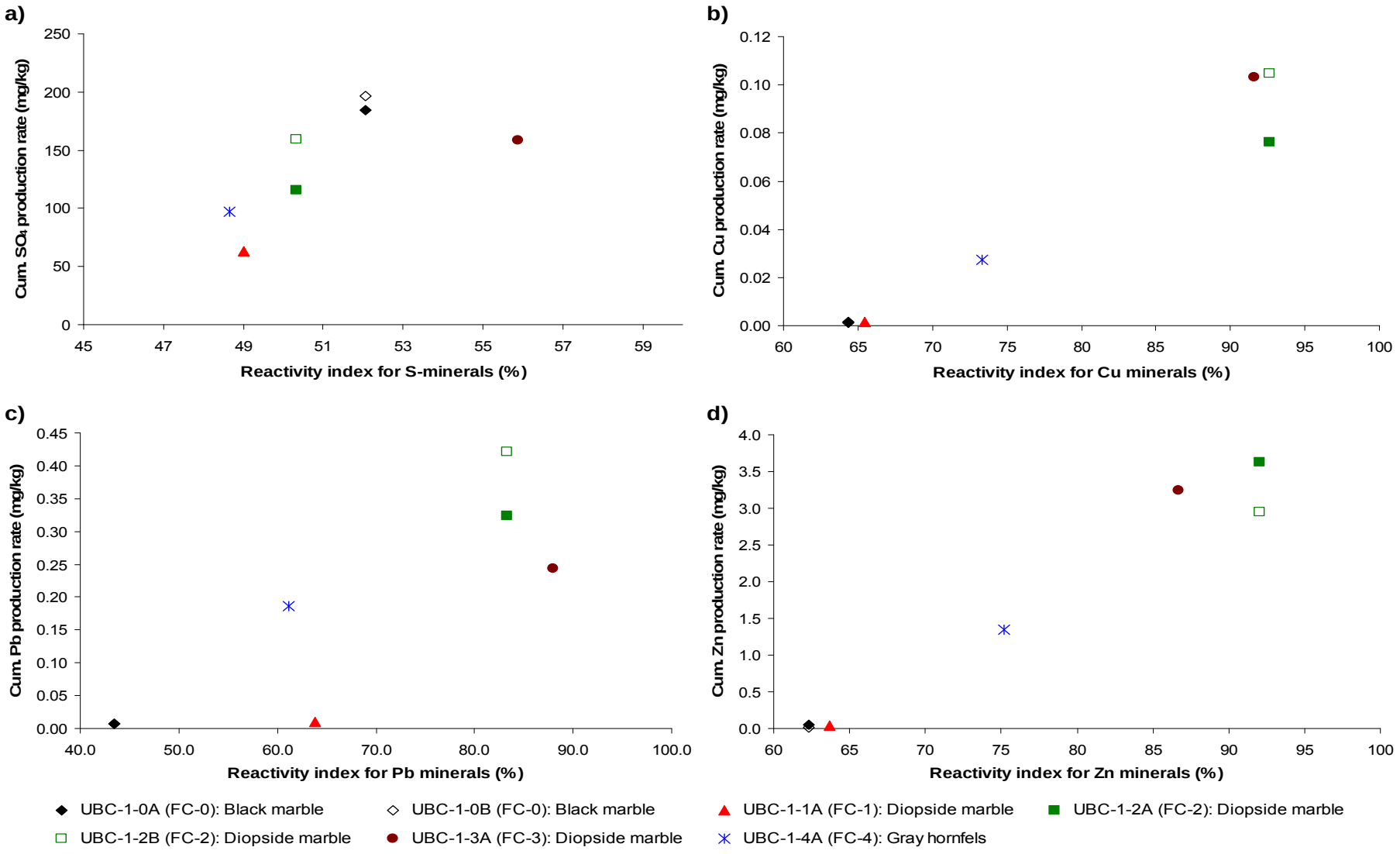

Figure 5.11 Relationship between a) sulfide, b) copper, c) lead, and d) zinc mineral availability for leaching and cumulative elemental production rates of the Class B waste rock samples

5.10 Stoichiometry of Class B Waste Rock

Based on the minerals found by MLA as being the primary constituents of different Class B waste rock, the geochemical speciation calculation results, and the elements found in the leachate from the field cells, some geochemical processes that could be occurring in the field cells are summarized in Table 5.9.

Table 5.9 Important geochemical processes that are probably occurring in the Class B waste rock material at the Antamina mine

Process	Reaction	Equation
Pyrite weathering	$FeS_{2(s)} + 15/4O_{2(g)} + 7/2H_2O_{(l)} \rightarrow 4H^+_{(aq)} + 2SO_4^{2-}{}_{(aq)} + Fe(OH)_{3(s)}$	Eq. 5.1
Pyrrhotite weathering	$Fe_{1-x}S_{(s)} + (2-x/2)O_{2(g)} + xH_2O_{(l)} \rightarrow 2xH^+_{(aq)} + SO_4^{2-}{}_{(aq)} + 1-xFe^{2+}{}_{(aq)}$	Eq. 5.2
Chalcopyrite weathering	$CuFeS_{2(s)} + 17/4O_{2(g)} + 5/2H_2O_{(l)} \rightarrow 2H^+_{(aq)} + 2SO_4^{2-}{}_{(aq)} + Cu^{2+}{}_{(aq)} + Fe(OH)_{3(s)}$	Eq. 5.3
Galena weathering	$PbS_{(s)} + 2O_{2(g)} + H_2O_{(l)} \rightarrow H_2O_{(aq)} + SO_4^{2-}{}_{(aq)} + Pb^{2+}{}_{(aq)}$	Eq. 5.4
Sphalerite weathering	$ZnS_{(s)} + 2O_{2(g)} + H_2O_{(l)} \rightarrow H_2O_{(aq)} + SO_4^{2-}{}_{(aq)} + Zn^{2+}{}_{(aq)}$	Eq. 5.5
Stibnite weathering	$Sb_2S_{3(s)} + 6O_{2(g)} + 2H_2O_{(l)} \rightarrow 4H^+_{(aq)} + 2SO_4^{2-}{}_{(aq)} + (SbO)_2SO_{4(s)}$	Eq. 5.6
Realgar weathering	$As_2S_{2(s)} + 7O_{2(g)} + 2H_2O_{(l)} \rightarrow 4H^+_{(aq)} + 2SO_4^{2-}{}_{(aq)} + 2AsO_4^{3-}{}_{(aq)}$	Eq. 5.7
Molybdenite weathering	$MoS_{(s)} + 4O_{2(g)} + H_2O_{(l)} \rightarrow H_2O_{(aq)} + SO_4^{2-}{}_{(aq)} + MoO_4^{2-}{}_{(aq)}$	Eq. 5.8
Calcite dissolution	$CaCO_{3(S)} + CO_{2(g)} + H_2O_{(l)} \rightarrow Ca^{2+}{}_{(aq)} + 2HCO_3^-{}_{(aq)}$	Eq. 5.9
Plagioclase weathering	$CaAl_2Si_2O_{8(S)} + 2H^+_{(aq)} + 6H_2O_{(l)} \rightarrow Ca^{2+}{}_{(aq)} + 2H_4SiO_{4(s)} + 2Al(OH)_{3(s)}$	Eq. 5.10
Fluorite dissolution	$CaF_{2(s)} \leftrightarrow Ca^{2+}{}_{(aq)} + 2F^-{}_{(aq)}$	Eq. 5.11

5.11 Waste Rock Management

Based on the current waste rock classification system at Antamina and the assay results obtained by ICP-MS, only two samples placed in field cells UBC-1-0A/0B (black marble) and UBC-1-3A (diopside marble) met the criteria, according to their solid phase Zn concentrations (700-1500 mg/kg), for being classified as Class B material. The other three samples from field cells UBC-1-1A (diopside marble), UBC-1-2A/2B (diopside marble), and UBC-1-4A (gray hornfels) corresponded to Class C material (< 700 mg/kg Zn) (Figure 5.12). However, this inconsistency could have occurred because the material within of the polygon was heterogeneous, and the samples could have been taken from locations with low Zn content. However, according to As (<400 mg/kg) content, all samples met the criteria for being classified as Class B material.

Although none of the samples met the criteria for being classified as Class A (reactive material), most of them had high leaching rates for some elements of environmental concern, including Cu, Pb, Zn, Sb, and/or F. This suggests that the waste rock classification system which was based on assay, should be revised, taking into consideration, and possibly including, other aspects such as mineralogy and liberation of reactive minerals in order to determine the availability that these elements have for leaching.

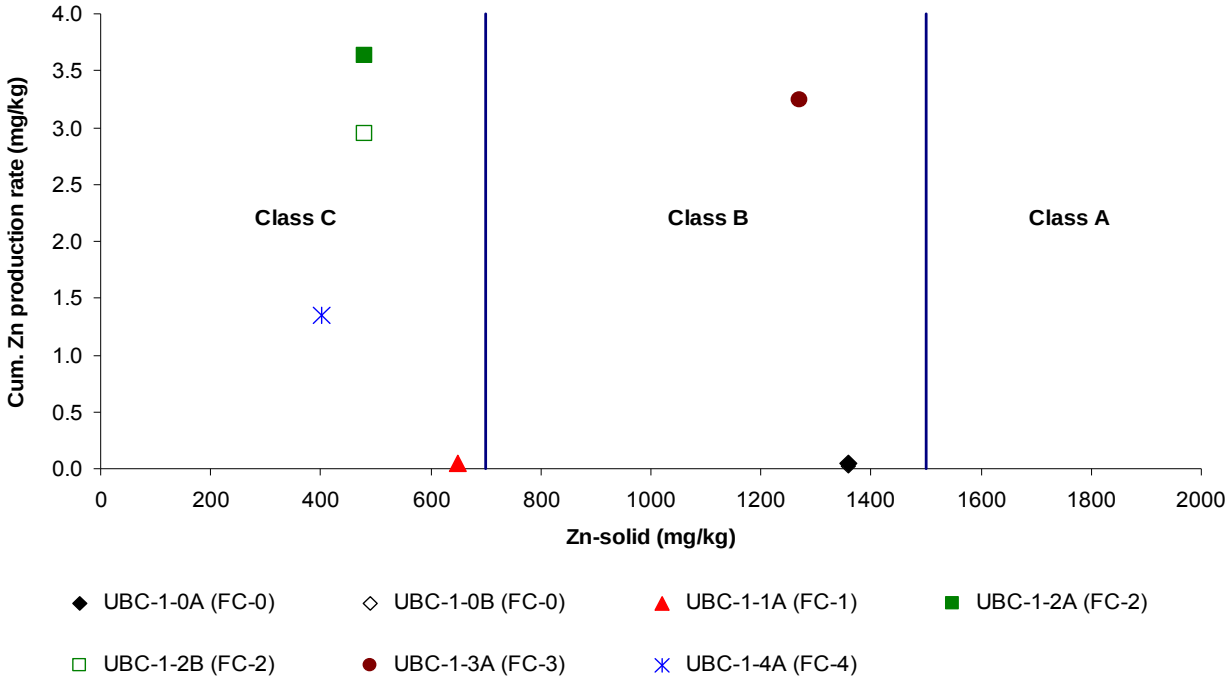

Figure 5.12 Solid phase Zn concentration as criteria of the current waste rock classification system compared for all Class B waste rock samples

Despite the occurrence of weak (economically removable) mineralization in the diopside exoskarn host (Lipten and Smith, 2004), both coarse and finely disseminated sulfide, sulphate, and oxides/hydroxide minerals that contain elements of environmental concern may be present in elevated concentrations and thus may be available for leaching. This was observed in samples FC-1, FC-2, and FC-3. Therefore, the diopside waste rock type should be carefully evaluated for the availability of trace or minor elements for leaching, which could generate long-term environmental impacts. It is therefore recommended that waste rock types in contact with diopside skarn which are likely to include diopside marble or diopside hornfels as shown in Figure 5.13 (Class B taken from that polygon), should be grouped into Class A material, regardless of their solid phase Zn concentrations (i.e. even if Zn is less than 1,500 mg/kg or 0.15%).

The neutralization potential ratio (NPR=NP/AP) was plotted against sulfur-sulfide (Figure 5.14a) and S-total (Figure 5.14b) for all samples. If the cut offs of NPR and S-S_2 or S-total content for potential acid generation are determined, then the data distribution may be divided into four quadrants. Samples with NPR<3 (Table 2.1) are considered uncertainly and potentially acid generating (Brodie et al., 1991). Samples containing less than 0.3% S-S_2 are generally considered to be incapable of sustaining acid generation (Price, 1997). Thus, the lines NPR = 3 and S-S_2 = 0.3% are superimposed on Figure 5.14a, dividing it into four quadrants. The two upper quadrants (NPR>3, S-S_2<0.3% and NPR>3, S-S_2>0.3%) are considered non-acid generating; whereas the bottom right-hand quadrant (NPR<3, S-S_2>0.3) is considered potentially acid generating (Downing and Mills, 1998). As was determined by ABA results, all Class B waste rock samples were considered non-acid generating, even though one of the diopside marble samples (UBC-1-2A/2B=FC-2) was close to the boundary line. However, even though the upper right-hand quadrant was considered not to be acid generating, and if the S-S_2 contents had been

distributed in that quadrant, it could have been considered as potentially metal leaching generating, which then should be verified through kinetic testing. Diopside marble waste rock samples which were placed in field cells UBC-1-2A/2B and -3A have confirmed that high concentrations of Cu, Pb and Zn were being released, supporting the assumption described above. Cumulative zinc production rates as a function of S-total content determined by ICP-MS (Table 3.10) are plotted in Figure 5.15, showing the correlation of the metal leaching as a function of sulfur content, where samples with S-total above 0.3% have reported higher cumulative Zn production. As a result, it is recommended that additional samples with similar S-S_2 content (>0.3%) should be evaluated through static and kinetic tests to confirm this statement. If results prove it to be true, then it is recommended that the S-S_2=0.3% cut off should be included in the waste rock classification system. Samples containing S-S_2<0.3% should be considered as non-reactive material.

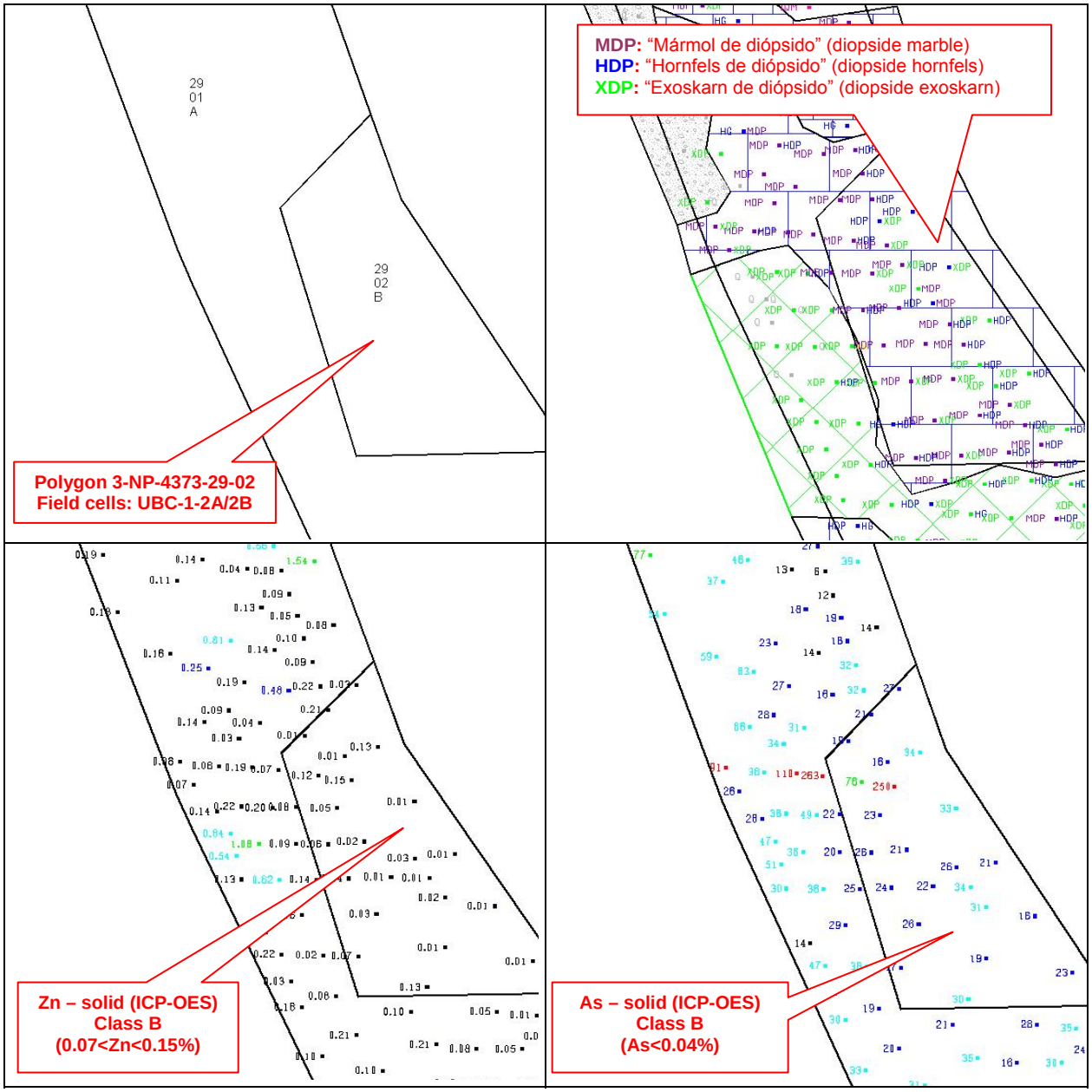

Figure 5.13 Rock types and assay (Zn and As) in the waste rock classification system at the block model of Antamina mine

In addition, it is important to note that the cut off should be established for the sulfur-sulfide rather than S-total, despite the fact that in this case, the S-total plot (Figure 5.14b) showed almost the same distribution as S-S_2. However, the values for the duplicates of the black marble and gray hornfels samples had moved slightly towards the right-hand quadrant, suggesting that the sulfur contents in these samples were also present as sulphate minerals (confirmed by MLA mineralogy data in Table 3.12). Therefore, it is important to keep this in mind and avoid ensuing mistakes during interpretation.

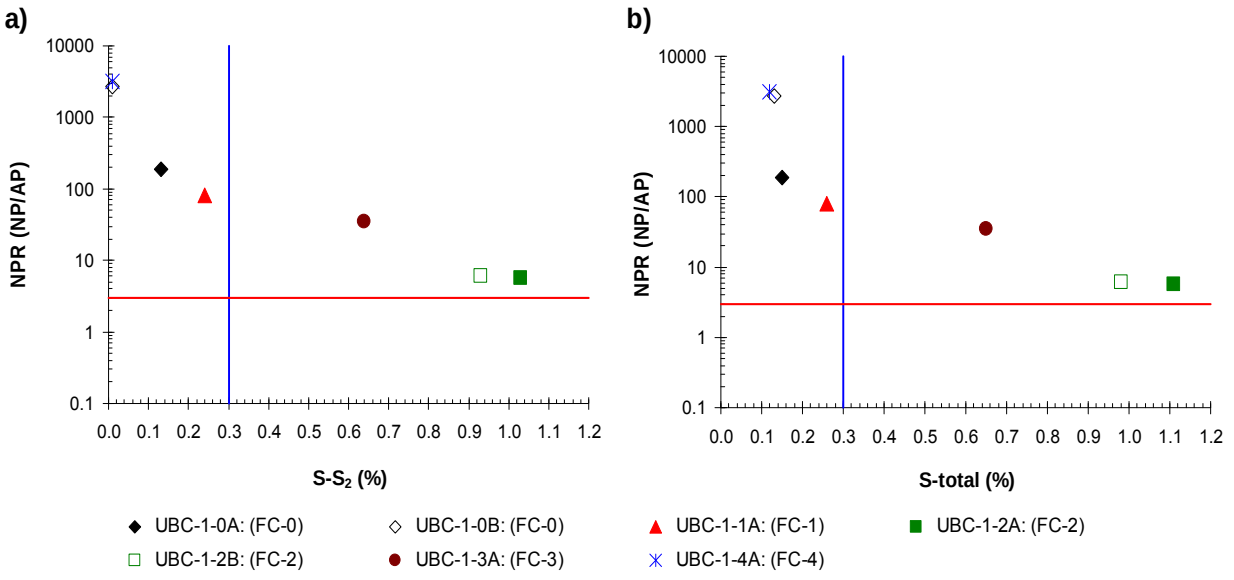

Figure 5.14 a) NRP against sulfur-sulfide content, and b) NPR in function of sulfur-total content of waste rock samples

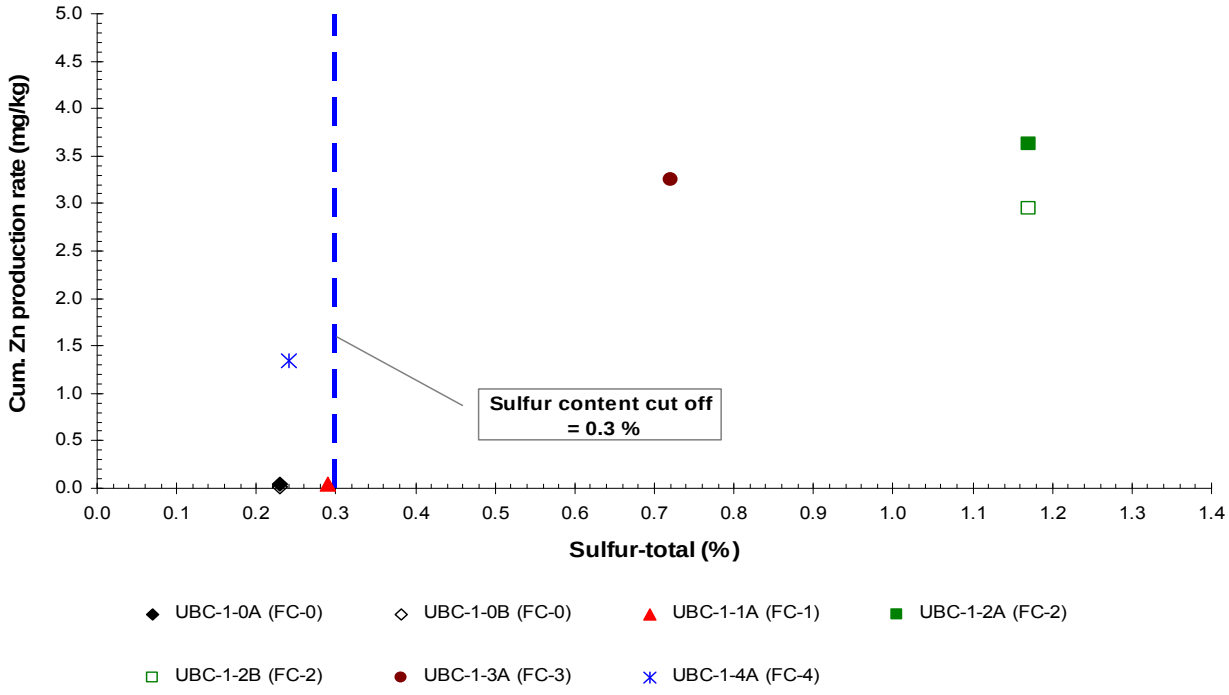

Figure 5.15 Cumulative zinc production as a function of sulfur-total content of waste rock samples

6 CONCLUSIONS AND RECOMMENDATIONS

The determination of metal release rates under circumneutral pH conditions which are based on field kinetics tests are more accurate than laboratory testing (ABA and humidity cells), since kinetic testing is operated under site-conditions. This means that carbonate and sulfide mineral content determination in a sample, through ABA, is not a sufficient indicator for predicting metal release rates. Class B waste rock samples have been identified as non-acid generating, but never-the-less, they do release relatively high rates of Sb, Cu, Pb, Zn, and F, which are elements of environmental concern. Although ABA results could be used during the initial stages of the prediction of leaching behaviour, kinetic tests must also be conducted. Subsequently, data from both tests should be integrated in order to understand the geochemical behaviour of waste rock, and to determine the evaluation criteria which will allow for the identification of the reactive material in the non-reactive waste rock. After assessment of other Class B samples with similar characteristics, a sulfur-sulfide cut off of 0.3% is recommended as an additional criterion of the waste rock classification system. Waste rock containing below 0.3% $S\text{-}S_2$ can be considered non-reactive material and will produce low metal release rates; however other non-sulfide minerals should be evaluated.

As has been observed in field cells containing diopside marble samples Sb, Cu, and Zn are the most likely to be mobile under circumneutral pH conditions. However, although Pb mobilization is generally known to occur under acidic conditions, this element was also found in relatively high concentrations in the leachate from the diopside marble samples.

The main sources of Cu, Pb, and Zn identified include chalcopyrite, galena and sphalerite for all samples. MLA also reported that iron oxyhydroxide, iron sulphate and apatite had these elements within their structure, particularly in the coarse particles of samples FC-2 and FC-3. This, associated with the higher reactivity indices determined for Cu, Pb and Zn minerals in these samples, has resulted in these elements being available for leaching, as was observed in the leachates from the corresponding field cells. The absence of secondary mineral formation including copper hydroxide, lead oxide, zinc sulphate, and zinc hydroxide has also contributed to the mobilization of these elements, and the solutions were found to remain undersaturated with respect to these minerals after geochemical speciation calculations.

Despite the relatively high solid phase concentrations found in the black marble and in one of the diopside marble samples (UBC-1-1A), low leachate Cu, Pb, and Zn concentrations were reported in the leachate from the field cells. Several reasons could be given: 1) Cu, Pb, and Zn may have co-precipitated with iron oxyhydroxide or may have been adsorbed on iron oxyhydroxide. Sorption of Cu and Zn on iron oxyhydroxides is common at mine sites (Blowes et al., 2003). Although geochemical speciation results did not show any iron oxyhydroxide mineral formation, the samples remained undersaturated. 2) These elements may have also precipitated as carbonate, hydroxide or oxide minerals. The geochemical speciation calculations determined that solutions from these samples were in equilibrium or supersaturated with respect to malachite and tenorite for Cu, and cerrusite and wulfenite for Pb, thus

controlling the mobilization of these elements. 3) Cu, Pb and Zn minerals in these samples have low reactivity indices that render these elements unavailable for leaching. 4) Chalcopyrite, galena and sphalerite may oxidise at a much lower rate than pyrite at neutral pH. 5) The most likely reason is that Cu, Pb and Zn may have been trapped or adsorbed on clay minerals, forming silicate minerals with surface complexation. MLA reported relatively high proportions of clay minerals, particularly in the black marble sample. However, in order to verify some of the possible reasons mentioned above, further assessments on weathered samples are recommended. This work could determine if, for example, sorption processes are taking place.

High neutralization potential (NP) was found to be present in the samples. After evaluation of the correlation between calcium and CO_2 concentrations present in the whole rock, carbonate minerals were found to be the main mineral source for neutralizing acid generation. This conclusion was confirmed by MLA results, where calcite was identified as the primary neutralizing mineral. However, as three of the samples are primarily composed by diopside, high silicate mineral contents were reported; these minerals weather or dissolve at much slower rates than do carbonate minerals under circumneutral pH conditions. Based on the alkalinity concentrations found in the leachate from the field cells, the NP depletion rates on a surface area basis are more consistent than on a mass basis, suggesting that the release rates, and therefore the weathering rates, are proportional to the surface area of the waste rock particles. It was also supported that at circumneutral pH conditions, carbonate mineral leaching rates are orders of magnitude faster than sulfide mineral leaching rates; this is more consistent determining release rates on a surface area basis.

The leachates from the field cells remain undersaturated with respect to all sulphate minerals of relevance, indicating that sulphate release is a suitable indicator of sulfide oxidation or sulphate mineral dissolution. These mineral phases were reported by MLA, with most of the sulfur-sulfide content being found in the diopside marble samples, whereas most of the sulfur-sulphate content was in the black marble and gray hornfels samples. This suggests that greater sulfide oxidation is occurring in the diopside samples, generating metal release which can impact the environment.

According to the mass content, surface area distribution, elemental distribution, and availability of minerals for leaching, some samples (black marble and gray hornfels) showed higher reactivity in the fine particles (below 2 mm), whereas others, such as the diopside marble samples, showed higher reactivity in the coarse particles (below 12 mm). As a consequence, a particle size cut off of 12 mm was determined. Particles below this size will be present in the “more reactive zone.”

As was observed in the studied samples, despite the weak ore mineralization (economically extractible) occurring in the diopside host, coarse grain and finely disseminated sulfide minerals available for metal leaching are more likely to be associated with the diopside marble than with either the black marble or gray hornfels. This could generate elevated metal concentrations in its drainage. Therefore, the evaluation of additional diopside marble or hornfels samples is recommended. However, waste rock types

in contact with diopside skarn (reactive material) which are most likely to be diopside marble or diopside hornfels, should be carefully evaluated, and it is recommended that the material should be grouped into either a the reactive or non-reactive category based on its sulfur-sulfide content (cutoff of 0.3%), regardless of its solid phase metal concentration (e.g. zinc).

Solid phase element content is not a rigorous enough criterion for classifying the waste rock material. The reactive minerals and elements present in the black marble and gray hornfels samples were mostly available in the fine particles, therefore almost half of their content would be able to leach. The opposite is true in the diopside marble samples; the reactive minerals reported higher reactivity indices particularly, for samples FC-2 and FC-3, indicating the reactivity of the minerals present in the coarse particles, and therefore almost 100% of the total solid phase found by assay was available for leaching. Despite the fact that sulfide minerals are the main source of reactive elements, other mineral phases such as iron oxyhydroxides, oxides, and sulphates may also contribute to element mobilization. It is therefore recommended that mineralogical and availability information to be included as part of the criteria for the classification system. A reactivity index or factor that combines mineralogy data, texture, rock type (lithology), availability and solid phase concentrations should be developed and applied to the waste rock classification system.

REFERENCES

Akcil, A. and Koldas, S., 2006. Acid Mine Drainage (AMD): causes, treatment and case studies. Journal of Cleaner Production, 14(12-13): pp. 1139-1145.

Alarcón, L.E., Rate, A.W., Hinz, C. and Campbell, G.D., 2004. Weathering of sulphide minerals at circum-neutral-pH in semi-arid/arid environments: influence of water content. Proceedings of Third Australian New Zealand Soils Conference, 5 – 9 December 2004, Sydney, Australia.

American Public Health Association. et al., 1998. Standard methods for the examination of water and wastewater. American Public Health Association, 1st version, Washington, DC, USA

Antamina, 2000. "Control de Calidad y Procedimientos de Caracterización para Materiales de Construcción de la Presa de Relaves", Compañía Minera Antamina S.A., Geology Department, Yanacancha, Peru.

Antamina, 2001. "Geología de Antamina", Compañía Minera Antamina S.A., Geology Department. Yanacancha, Peru.

Antamina, 2004. 2004 Life of Mine Plan, Compañía Minera Antamina S.A., Mine Engineering Department. Yanacancha, Peru.

Antamina, 2007. Ore Control Procedure Manual, Compañía Minera Antamina S.A., Geology Department, Yanacancha, Peru.

Appelo, C.A.J. and Postma, D., 2005. Geochemistry, groundwater and pollution. Balkema, Leiden, The Netherlands ; New York, NY, xviii, 649 p. pp.

Aranda, C.A., Klein, B., Beckie, R.D. and Mayer, K.U., 2009. Assessment of waste rock weathering characteristics at the Antamina mine based on field cells experiment, Securing the Future and 8th ICARD, June 23-26, 2009, Skelleftea, Sweden.

Bartram, J., Ballance, R., United Nations Environment Program and World Health Organization, 1996. Water quality monitoring: a practical guide to the design and implementation of freshwater quality studies and monitoring programs. E & FN Spon, London; New York, xii, 383 p. pp.

Bay, D.S., Beckie, R.D. and Mayer, K.U., 2009. Assessment of Environmental Loadings in Neutral pH Drainage from Three Experimental Waste-Rock Piles at the Antamina Mine, Peru, Securing the Future and 8th ICARD, June 23-26, 2009, Skellefteå, Sweden.

Blowes, D.W., Ptacek, C.J., Jambor, J.L. and Weisener, C.G., 2003. The Geochemistry of Acid Mine Drainage - Treatise on Geochemistry. Elsevier, pp. p.149-204.

Brantley, S.L. and Mellott, N.P., 2000. Surface area and porosity of primary silicate minerals. American Mineralogist, 85(11-12): 1767-1783.

British Columbia Acid Mine Drainage Task Force, 1990. Draft acid rock drainage technical guide, Vol. II: British Columbia Acid Mine Drainage Task Force report. The Task Force, Victoria.

Brodie, M.J., L.M., B. and Robertson, A.M., 1991. A Conceptual Rock Classification System for Waste Management and a Laboratory Method for ARD Prediction From Rock Piles, In Second International Conference on the Abatement of Acid Drainage, Conference Proceedings, September 16, 17, and 18, 1991, Montreal, Canada.

Broughton, L.M. and Robertson, A.M., 1992. Acid Rock Drainage from Mines - Where Are We Now, Steffen, Roberston and Kirsten. IMM Minerals, Metals and the Environment Conference, Vancouver, B.C.

Carter, M.R., Gregorich, E.G. and Canadian Society of Soil Science, 2008. Soil sampling and methods of analysis. CRC Press, Boca Raton, FL, 1224 p. pp.

Corazao Gallegos, J.C., 2007. The design, construction, instrumentation and initial response of a field-scale waste rock test pile, University of British Columbia. The Faculty of Graduate Studies. (Mining Engineering). Thesis. M.A.Sc., 2007. University of British Columbia, Vancouver, Canada.

Dana, J.D., Klein, C. and Hurlbut, C.S., 1993. Manual of mineralogy (after James D. Dana). Wiley, New York, xii, 681 p.pp.

Dietrich, R.V. and Skinner, B.J., 1979. Rocks and rock minerals. Wiley, New York, xi, 319 p. pp.

Dogan, A.U. et al., 2006. Baseline studies of The Clay Minerals Society source clays: Specific surface area by the Brunauer Emmett Teller (BET) method. Clays and Clay Minerals, 54(1): 62-66.

Downing, B.W. and Mills, C., 1998. Quality Assurance / Quality Control for Acid Rock Drainage Studies. Paper published on ARD Web site www.enviromine.com/ard.

Eaton, A.D., Franson, M.A.H., American Public Health Association, American Water Works Association, and Water Environment Federation, 2005. Standard methods for the examination of water & wastewater. American Public Health Association, Washington, DC, USA.

Fandrich, R., Gu, Y., Burrows, D. and Moellr, K., 2006. Modern SEM-based mineral liberation analysis. Elsevier B.V., International Journal of Mineral Processing.

Ferguson, K.D. and Morin, K.A., 1991. The Prediction of Acid Rock Drainage - Lessons From the Database, In Second International Conference on the Abatement of Acid Drainage. Conference Proceedings, September 16, 17, and 18, 1991, Montreal, Canada.

Figura, L.O. and Teixeira, A.A., 2007. Food Physics: Physical Properties - Measurement and Applications, Berlin.

Fritz, S.J., 1994. A survey of charge-balance errors on published analyses of potable ground and surface waters. Ground Water, 32(4): 539-546.

Frostad, S., Klein, B. and Lawrence, R.W., 2002. Evaluation of kinetic test methods for measuring rates of weathering, Mine Water and the Environment.

Frostad, S., Klein, B. and Lawrence, R.W., 2005. Determining the weathering characteristics of a waste rock dump with field cells. Mining, Reclamation and Environment.

Golder Associates, 2003. Waste Rock and Tailings Geochemistry and Disposal Plan - Phase 1, Antamina Mine Peru, January 2003, Golder Associates Ltd. Mississauga, Canada.

Golder Associates, 2004. Waste Rock Geochemistry - Phase 2, Antamina Mine Peru, Final Version 4.0, December 2004, Golder Associates Ltd. Mississauga, Canada.

Golder Associates, 2007a. "Estudio de Impacto Ambiental - Proyecto de Expansión del Tajo Abierto y Optimización del Procesamiento", Mina Antamina, Julio 2007, Golder Associates Peru S.A., Lima, Peru.

Golder Associates, 2007b. Waste Rock and Tailings Geochemistry, Field Cell Monitoring 2002 to 2006, Antamina Mine Peru, Version 4.0, February 2007, Golder Associates Ltd. Mississauga, Canada.

Golder Associates, 2008. Waste Rock and Tailings Geochemistry, Field Cell Monitoring December 2002 to May 2007, Antamina Mine Peru, Version 3.0, March 2008, Golder Associates Ltd. Mississauga, Canada.

Gormely Process Engineering, 1989. Draft acid rock drainage technical guide, Vol. 1: British Columbia Acid Mine Drainage Task Force report. Energy, Mines and Resources; Victoria: Ministry of Energy, Mines and Petroleum Resources, Ottawa.

Greenberg, A.E. et al., 1992. Standard methods for the examination of water and wastewater. American Public Health Association, 1st version, Washington, DC, USA.

Helgeson, H.C., Murphy, W.M. and Aagaard, P., 1984. 1. Thermodynamic and kinetic constraints on reaction-rates among minerals and aqueous-solutions. 2. Rate constants, effective surface area, and the hydrolysis of feldspar. Geochimica Et Cosmochimica Acta, 48(12): 2405-2432.

King, R.P., 2001. Modeling and Simulation of Mineral Processing Systems. Butterworth-Heinemann, Great Britain, 403 pp.

Klein, C., Hurlbut, C.S. and Dana, J.D., 2002. The 22nd edition of the manual of mineral science: (after James D. Dana). J. Wiley, New York, xii, 641 p. pp.

Klohn-Crippen, S.S.A., 1998. "Antamina Environmental Impact Assessment", March 1998, Klohn Crippen - SVS S.A., Lima, Peru.

Langmuir, D., 1997. Aqueous environmental geochemistry. Prentice Hall, Upper Saddle River, N.J., viii, 600 p. pp.

Lapakko, K., 1993. Mine Waste Drainage Quality Prediction: A Literature Review. Draft Paper. Minnesota Department of Natural Resources, Division of Minerals, St. Paul, Minnesota, USA.

Lipten, E.J. and Smith, S.W., 2004. The Geology of the Antamina Copper-Zinc Deposit, Peru, South America. PGC Publishing: 17.

Lowell, S., 2004. Characterization of porous solids and powders: surface area, pore size and density. Particle technology series. Kluwer Academic Publishers, Dordrecht, Boston, xiv, 347 p. pp.

Malmstrom, M.E., Destouni, G., Banwart, S.A. and Stromberg, B.H.E., 2000. Resolving the scale-dependence of mineral weathering rates. Environmental Science & Technology, 34(7): 1375-1378.

Manahan, S.E., 2005. Environmental chemistry. CRC Press, Boca Raton, Fla., 783 p. pp.

Mayer, K.U., 2007. Interpretation of Geochemical Tests of Huckleberry Mine Waste Rock, November, 2007.

MEND (Canada), 1996. Annual report 1995. MEND Secretariat, Ottawa, Canada.

MEND (Canada), 2000. MEND Manual Report 5.4.2 - 2000, Mine Environment Neutral Drainage, Ottawa, Canada.

Morris, D.A. and Johnson, A.I., 1967. Summary of hydrologic and physical properties of rock and soil materials, as analyzed by the hydrologic laboratory of the U.S. Geological Survey 1948-60. Geological Survey water-supply paper. Washington, D.C., USA, iv, 42 p. pp.

Murray, K. and Wade, P., 1996. Checking anion-cation charge balance of water quality analyses: Limitations of the traditional method for non-potable waters. Water Sa, 22(1): 27-32.

Parkhurst, D.L., Appelo, C.A.J. and Geological Survey (U.S.), 1999. User's guide to PHREEQC, Version 2: a computer program for speciation, batch-reaction, one-dimensional transport, and inverse geochemical calculations. Water-resources investigations report. U.S. Geological Survey : Earth Science Information Center, Open-File Reports Section, Denver, Colorado, USA, xiv, 312 p. pp.

Price, W.A., 1997. Guidelines and Recommended Methods for the Prediction of Metal Leaching and Acid Rock Drainage at Minesites in British Columbia - Draft, Smithers, British Columbia, Canada.

Price, W.A., 2003. Challenges posed by metal leaching and acid rock drainage at closed mines, Environment Section, CANMET, Natural Resources Canada, Smithers, British Columbia, Canada.

Price, W.A., Errington, J.C. and British Columbia. Ministry of Energy & Mines, 1998. Guidelines for metal leaching and acid rock drainage at minesites in British Columbia. Ministry of Energy & Mines, Victoria, Canada.

Robertson, A.M. and Broughton, L.M., 1992. Reability of Acid Rock Drainage Testing, Steffen, Roberston and Kirsten. Internal Paper, Vancouver, British Columbia, Canada.

Sherlock, E.J., Lawrence, R.W. and Poulin, R., 1995. On the neutralization of acid rock drainage by carbonate and silicate minerals. Environmental Geology, 25(1): 43-54.

Skousen, J., Simmons, J., McDonald, L.M. and Ziemkiewicz, P., 2002. Acid-base accounting to predict post-mining drainage quality on surface mines. Journal of Environmental Quality, 31(6): 2034-2044.

Sobek, A.A., Schuller, W.A., Freeman, J.R. and Smith, R.M., 1978. Field and Laboratory Methods Applicable to Overburden and Minesoils.

Stromberg, B. and Banwart, S., 1999a. Weathering kinetics of waste rock from the Aitik copper mine, Sweden: scale dependent rate factors and pH controls in large column experiments. Journal of Contaminant Hydrology, 39(1-2): 59-89.

Stromberg, B. and Banwart, S.A., 1999b. Experimental study of acidity-consuming processes in mining waste rock: some influences of mineralogy and particle size. Applied Geochemistry, 14(1): 1-16.

Sutherland, D., 2007. Estimation of mineral grain size using automated mineralogy, pp. 452-460.

Todd, D.K. and Mays, L.W., 2005. Groundwater hydrology. Wiley, Hoboken, NJ, USA, xvii, 636 pp.

Treat, W.J., Engler, C.R. and Soltes, E.J., 1987. Measurement of callus growth with an Air-Comparison Pycnometer.

USEPA, 1994. Acid Mine Drainage - Technical Report, U.S. Environmental Protection Agency (USEPA), Washington, USA.

White, A.F. and Brantley, S.L., 2003. The effect of time on the weathering of silicate minerals: why do weathering rates differ in the laboratory and field?. pp. 479-506.

Wills, B.A., Napier-Munn, T. and Julius Kruttschnitt Mineral Research Centre, 2006. Wills' mineral processing technology: an introduction to the practical aspects of ore treatment and mineral recovery. Elsevier/Butterworth-Heinemann, Amsterdam, The Netherlands, viii, 444 p. pp.

Zhonghua, H. and Vansant, E.F., 1995. Carbon molecular sieves produced from walnut shell. Elsevier Science Ltd., Vol. 33, No 5: pp. 561-567.

APPENDICES

Appendix A

Waste Rock Classification System at the Antamina Mine

Table A1.1 Antamina waste rock/ore classification system

Material Classification for Dispatch Polygons and Field Stakes - March 2007

ESTACAS DE MADERA

Código	Color de estaca	Clasificación de rocas	Límites de metal / Restricciones	Destino
X	ESTACAS COLOR NARANJA CON CINTA AZUL		NO CARGAR	NO CARGAR
A	NARANJA	Zonas de oxidación/ desmonte	• Hornfels/Calizas/Skarn/Intrusivo • > 1500 ppm (0.15%) Zn & > 400 ppm (0.04%) As • > 3 % sulfuros; Oxidos visuales > 10%	Dentro límites del tajo ó botaderos
B	AZUL	Material para construcción en el valle de Antamina. Hornfels/Calizas y Mármol	• Hornfels/Calizas 700 - 1500 ppm Zn • < 2-3 % sulfuros; Óxidos visuales < 10% • Donde se controla el drenaje • Los niveles de metales cambiaran en otros tipos de rocas, skarns e intrusitos.	STOCKPILE PADS & CONSTRUCTION MATERIAL
C	VERDE	Hornfels Calizas y mármol	• Hornfels/Calizas • < 700 ppm (0.07%) Zn & < 400 ppm (0.04%) As • < 2-3% de sulfuros totales; mínimo de óxidos • < 20 % finos cuando se utiliza en el dique-represa	PARA CUALQUIER LUGAR REQUERIDO

PIN STAKES

Código	Color de Banderín	Clasificación de rocas	VPHRM K$/h	% Cu	% Zn	ppm Bi	Destino
M1	FUCCIA	Cu Bajo Bismuto	≥ $20	NA	< 0.9	< 25	Chancadora primaria y Stockpile de M1
M2	AMARILLO	Cu Alto Bismuto	≥ $20	NA	< 0.5	25-115	Chancadora primaria y Stockpile de M2
M2A	VERDE ESMERALDA	Cu MUY Alto Bismuto	≥ $20	NA	< 0.5	≥ 115	Chancadora primaria y Stockpile de M2A
M3	MORADO	Cu-Zn Bajo Bismuto	≥ $20	NA	≥ 0.9	< 25	Chancadora primaria y Stockpile de M3
M4	VERDE	Cu-Zn Alto Bismuto	≥ $20	NA	≥ 0.5	25-115	Chancadora primaria y Stockpile de M4
M4A	NARANJA	Cu-Zn Muy Alto Bismuto	≥ $20	NA	≥ 0.5	≥ 115	Chancadora primaria y Stockpile de M4A
M5	CELESTE	Bornita Bajo Zinc	≥ $20	NA	< 0.5	NA	Chancadora primaria y Stockpile de M5
M6	AZUL	Bornita Alto Zinc	≥ $20	NA	≥ 0.5	NA	Chancadora primaria y Stockpile de M6
MP	NARANJA Y BLANCO EN CUADROS	Mineral de Picos	≥ $20	NA	%Pb >=0.3%	NA	LO DECIDE CORTO PLAZO
M?OX	ROSADA CINTA NARANJA	Mineral Oxidado	≥ $20	DE ACUERDO A PRUEBAS METALURGICAS O >40% RATIO CUAC >CUTOT			Lo decide Corto Plazo
LM	Fucsia con Cinta Amarilla	Mineral Ley Media	VPHRM=$7.0 - $20.0				Stock pile de Ley Media
BL	Franja Verde	Mineral Baja Ley	VPHRM= $1.5 - $7.0				Stock pile de baja Ley
ML	Franja Azul	Mineral Marginal	VPHRM = $0.00 - $1.5				Stock pile de Mineral Marginal

Nota: Desde el 2006, el mineral marginal en toda la mina se esta llevando a los botaderos y no se esta guardando en los stockpiles.

Appendix B

List of Mineral Phases

Table B1.1 Equilibrium constants and enthalpies of selected reactions at 25°C and 1 bar pressure

Mineral	Reaction	ΔH_r^0 (kcal/mol)	Log K
	I Fluoride Species		
Cryolite	$Na_3AlF_6 = 3Na^+ + Al^{3+} + 6F^-$	9.09	-33.84
Fluorite	$CaF_2 = Ca^{2+} + 2F^-$	4.69	-10.6
	II Oxide and Hydroxide Species		
Portlandite	$Ca(OH)_2 + 2H^+ = Ca^{2+} + 2H_2O$	-31.0	22.8
Brucite	$Mg(OH)_2 + 2H^+ = Mg^{2+} + 2H_2O$	-27.1	16.84
Pyrolusite	$MnO_2 + 4H^+ + 2e^- = Mn^{2+} + 2H_2O$	-65.11	41.38
Hausmanite	$Mn_3O_4 + 8H^+ + 2e^- = 3Mn^{2+} + 4H_3O$	-100.64	61.03
Manganite	$MnOOH + 3H^+ + e^- = Mn^{2+} + 2H_2O$	-	25.34
Pyrochroite	$Mn(OH)_2 + 2H^+ = Mn^{2+} + 2H_2O$	-	15.2
Gibbsite (crystalline)	$Al(OH)_3 + 3H^+ = Al^{3+} + 3H_2O$	-22.8	8.11
Gibbsite (microcrystalline)	$Al(OH)_3 + 3H^+ = Al^{3+} + 3H_2O$	(-24.5)	9.35
Al $(OH)_3$ (amorphous)	$Al(OH)_3 + 3H^+ = Al^{3+} + 3H_2O$	(-26.5)	10.8
Goethite	$FeOOH + 3H^+ = Fe^{3+} + 2H_2O$	-	-1.0
Ferrihydrite (amorphous to microcrystalline)	$Fe(OH)_3 + 3H^+ = Fe^{3+} + 3H_2O$	-	3.0 to 5.0
	III Carbonate Species		
Calcite	$CaCO_3 = Ca^{2+} + CO_3^{2-}$	-2.297	-8.48
Aragonite	$CaCO_3 = Ca^{2+} + CO_3^{2-}$	-2.589	-8.336
Dolomite (ordered)	$CaMg(CO_3)_2 = Ca^{2+} + Mg^{2+} + 2\ CO_3^{2-}$	-9.436	-17.09
Dolomite (disordered)	$CaMg(CO_3)_2 = Ca^{2+} + Mg^{2+} + 2\ CO_3^{2-}$	-11.09	-16.54
Strontianite	$SrCO_3 = Sr^{2+} + CO\ CO_3^{2-}$	-0.40	-9.271
Siderite (crystalline)	$FeCO_3 = Fe^{2+} + CO_3^{2-}$	-2.48	-10.89
Siderite (precipitated)	$FeCO_3 = Fe^{2+} + CO_3^{2-}$	-	-10.45
Witherite	$BaCO_3 = Ba^{2+} + CO_3^{2-}$	0.703	-8.562
Rhodocrosite (crystalline)	$MnCO_3 = Mn^{2+} + CO_3^{2-}$	-1.43	-11.13
Rhodocrosite (synthetic)	$MnCO_3 = Ba^{2+} + CO_3^{2-}$	-	-10.39
	IV Silicate Species		
Kaolinite	$Al_2Si_2O_5(OH)_4 + 6H^+ = 2Al^{3+} + 2Si(OH)_4^0 + H_2O$	-35.3	7.435
Chrysotile	$Mg_3Si_2O_5(OH)_4 + 6H^+ = 3Mg^{2+} + 2Si(OH)_4^0 + H_2O$	-46.8	32.20
Sepiolite	$Mg_2Si_3O_{7.5}(OH) \cdot 3H_2O + 4H^+ + 0.5H_2O = 2Mg^{2+} + 3Si(OH)_4^0$	-10.7	15.76
Kerolite	$Mg_3Si_4O_{10}(OH)_2 \cdot H_2O + 6H^+ + 3H_2O = 3Mg^{2+} + 4Si(OH)_4^0$	-	25.79
Quartz	$SiO_2 + 3H_2O = Si(OH)_4^0$	5.99	-3.98
Chalcedony	$SiO_2 + 3H_2O = Si(OH)_4^0$	4.72	-3.55
Amorphous silica	$SiO_2 + 3H_2O = Si(OH)_4^0$	3.34	-2.71
	V Sulphate Species		
Gypsum	$CaSO_4 \cdot 2H_2O = Ca^{2+} + SO_4^{2-} + 2H_2O$	-0.109	-4.58
Anhydrite	$CaSO_4 = Ca^{2+} + SO_4^{2-}$	-1.71	-4.36
Celestile	$SrSO_4 = Sr^{2+} + SO_4^{2-}$	-1.037	-6.63
Barite	$BaSO_4 = Sr^{2+} + SO_4^{2-}$	6.35	-9.97
Radium sulfate	$RaSO_4 = Ra^{2+} + SO_4^{2-}$	9.40	-10.26
Melanterite	$FeSO_4 \cdot 7H_2O = Fe^{2+} + SO_4^{2-} + 7H_2O$	4.91	-2.209
Alunite	$KAl_3(SO_4)_2(OH)_6 + 6H^+ = K^+ + 3Al^{3+} + 2SO_4^{2-} + 6H_2O$	-50.25	-1.4

Source: Reprinted with permission from Nordstrom et al. Chemical Modelling of Aqueous Systems II. © 1990 American Chemical Society

Appendix C

Appendix C1

Particle Size Analysis Results

Table C1.1 Particle size analysis by the Elutriation method for fine size fraction of Class B waste rock samples

Project:	Waste Rock Study at Antamina Mine	**Sample code:**	**FC-0 to FC-4**
Material type:	Waste Rock - Class B	**Sampling date:**	March 2006 to July 2006
Rock type:	Marble and hornfels	**Sampling by:**	C. Aranda
Location:	Antamina open pit. Field cells	**Testing date:**	27/08/2008 to 10/09/2008
Test type	Particle size analysis by the Elutriation method (-#270 or -53 μm)	**Testing by:**	C. Aranda
		Review by:	C. Aranda

Date	**27/08/2008**	**28/08/2008**	**08/09/2008**	**02/09/2008**	**01/09/2008**	**Average**	**Repr. Size**
Sample Code	**FC-0**	**FC-1**	**FC-2**	**FC-3**	**FC-4**	**(μm)**	**(μm)**
Sample net weight (g)	100.00	100.00	100.00	100.00	100.00		
Flow rate (mm)	180	180	180	180	180		
(mL/min)	11.6	11.6	11.6	11.6	11.6		
Water Temp. (°C)	19	18.2	18.20	17.90	18.10		
Particle Sp. Gr.	2.72	2.86	3.04	2.84	2.77		
Elutration time (min)	20	20	20	20	20		
Corr. Factor (Flow - f_1)	1.00	1.00	1.00	1.00	1.00		
Corr. Factor (Temp - f_2)	1.015	1.025	1.025	1.027	1.025		
Corr. Factor (SG - f_3)	0.97	0.94	0.90	0.94	0.96		
Corr. Factor (Time - f_4)	0.955	0.955	0.955	0.955	0.955		
Overall Corr. Factor	0.940	0.920	0.881	0.922	0.940		
Limiting Particle Separation Size (d_l in μm)							
Cyclone N° 1	41.70	41.70	41.70	41.70	41.70		
Cyclone N° 2	30.50	30.50	30.50	30.50	30.50		
Cyclone N° 3	21.70	21.70	21.70	21.70	21.70		
Cyclone N° 4	15.80	15.80	15.80	15.80	15.80		
Cyclone N° 5	11.30	11.30	11.30	11.30	11.30		
Residual	-11.30	-11.30	-11.30	-11.30	-11.30		
Effective Particle Separation Size (d_e in μm)							
Cyclone N° 1	39.2	38.4	36.7	38.4	39.2	38	46
Cyclone N° 2	28.7	28.1	26.9	28.1	28.7	28	33
Cyclone N° 3	20.4	20.0	19.1	20.0	20.4	20	24
Cyclone N° 4	14.9	14.5	13.9	14.6	14.8	15	17
Cyclone N° 5	10.6	10.4	10.0	10.4	10.6	10	12
Residual	-10.6	-10.4	-10.0	-10.4	-10.6		9
Dry sample weight (g)							
Cyclone N° 1	3.21	4.15	4.21	2.49	2.69		
Cyclone N° 2	9.74	15.16	16.46	11.30	16.19		
Cyclone N° 3	8.60	16.94	17.17	16.66	16.27		
Cyclone N° 4	6.37	14.01	14.74	14.59	16.63		
Cyclone N° 5	3.94	8.71	9.21	8.77	10.36		
Residual *	68.14	41.03	38.21	46.19	37.86		
Bucket	37.60	23.60	27.10	25.30	16.60		
Lost	30.54	17.43	11.11	20.89	21.26		
Retained (wt.%)							
Cyclone N° 1	3.2	4.2	4.2	2.5	2.7		
Cyclone N° 2	9.7	15.2	16.5	11.3	16.2		
Cyclone N° 3	8.6	16.9	17.2	16.7	16.3		
Cyclone N° 4	6.4	14.0	14.7	14.6	16.6		
Cyclone N° 5	3.9	8.7	9.2	8.8	10.4		
Residual	68.1	41.0	38.2	46.2	37.9		
Cumulative retained (wt.%)							
Cyclone N° 1	3.2	4.2	4.2	2.5	2.7		
Cyclone N° 2	13.0	19.3	20.7	13.8	18.9		
Cyclone N° 3	21.6	36.3	37.8	30.5	35.2		
Cyclone N° 4	27.9	50.3	52.6	45.0	51.8		
Cyclone N° 5	31.9	59.0	61.8	53.8	62.1		
Residual	100.0	100.0	100.0	100.0	100.0		
Cumulative passing (wt.%)							
Cyclone N° 1	96.8	95.9	95.8	97.5	97.3		
Cyclone N° 2	87.1	80.7	79.3	86.2	81.1		
Cyclone N° 3	78.5	63.8	62.2	69.6	64.9		
Cyclone N° 4	72.1	49.7	47.4	55.0	48.2		
Cyclone N° 5	68.1	41.0	38.2	46.2	37.9		
Residual	0.0	0.0	0.0	0.0	0.0		

Note: * Mostly clay minerals mixed with hydrous ferric oxides or ferric oxyhydroxide in FC-0 sample

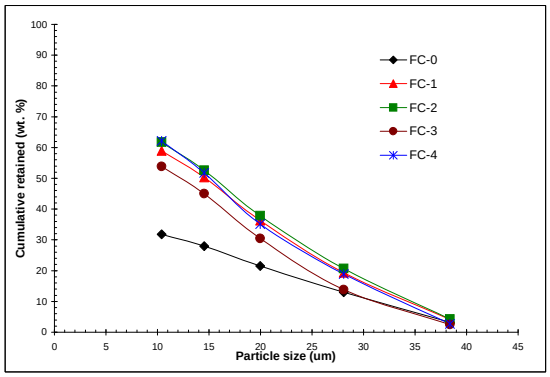

Figure C1.1 Cumulative weight retained obtained by Elutriation method

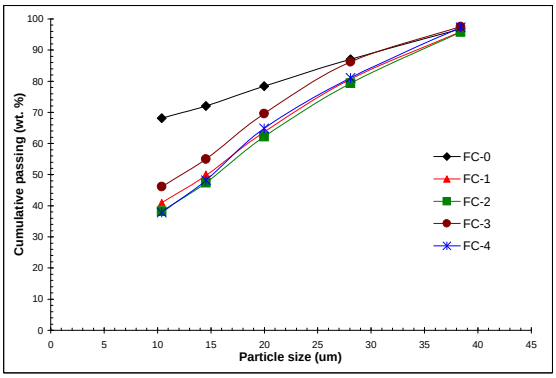

Figure C1.2 Cumulative weight passing obtained by Elutriation method

Table C1.2 Particle size analysis data for all Class B waste rock samples placed in the field cells

Project: Waste Rock Study at Antamina Mine
Material type: Waste Rock - Class B
Rock type: Marble and hornfels
Location: Antamina open pit. Field cells
Test type Particle size analysis
Sieving and Elutriation Methods

Sample code: FC-0 to FC-4
Sampling date: 07-Jul-06
Sampling by: C. Aranda
Testing date: May 26 to July 17, 2008
Testing by: C. Aranda
Review by: C. Aranda

Size fraction			Representative size	FC-0: Black marble				FC-1: Diopside marble				FC-2: Diopside marble				FC-3: Diopside marble				FC-4: Gray hornfels				Method	Particle type	Comments
Sieve/mesh	Opening			Weight (wt)	Retained	Cumulative retained	Cumulative passing	Weight (wt)	Retained	Cumulative retained	Cumulative passing	Weight (wt)	Retained	Cumulative retained	Cumulative passing	Weight (wt)	Retained	Cumulative retained	Cumulative passing	Weight (wt)	Retained	Cumulative retained	Cumulative passing			
(US)	(in)	(mm)	(mm)	(kg)	(wt.%)	(wt.%)	(wt.%)	(kg)	(wt.%)	(wt.%)	(wt.%)	(kg)	(wt.%)	(wt.%)	(wt.%)	(kg)	(wt.%)	(wt.%)	(wt.%)	(kg)	(wt.%)	(wt.%)	(wt.%)			
4"	4	100.0	122.5	0.00	0.0	0.0	100.0	0.0	0.0	0.0	100.0	0.0	0.0	0.0	100.0	0.0	0.0	0.0	100.0	0.0	0.0	0.0	100.0	Sieving	Cobble	
3"	3	75.0	86.6	1.60	1.2	1.2	98.8	5.7	3.7	3.7	96.3	14.6	9.1	9.1	90.9	0.0	0.0	0.0	100.0	1.7	1.2	1.2	98.8	Sieving	Cobble	
2"	2	50.0	61.2	25.40	19.5	20.8	79.2	27.5	17.8	21.5	78.5	36.2	22.6	31.7	68.3	17.8	12.7	12.7	87.3	15.5	11.2	12.4	87.6	Sieving	Gravel	Above 64 mm is cobble
11/2"	1.5	37.5	43.3	14.30	11.0	31.8	68.2	17.0	11.0	32.5	67.5	20.6	12.8	44.5	55.5	16.0	11.4	24.1	75.9	13.2	9.5	21.9	78.1	Sieving	Gravel	
1"	1	25.0	30.6	16.10	12.4	44.2	55.8	20.4	13.2	45.7	54.3	21.4	13.3	57.9	42.1	20.1	14.4	38.5	61.5	19.9	14.3	36.2	63.8	Sieving	Gravel	
3/4"	0.75	19.0	21.8	9.10	7.0	51.2	48.8	12.2	7.9	53.6	46.4	13.3	8.3	66.2	33.8	12.9	9.2	47.7	52.3	10.3	7.4	43.6	56.4	Sieving	Gravel	
1/2"	0.5	12.5	15.4	10.10	7.8	58.9	41.1	14.3	9.2	62.8	37.2	14.2	8.9	75.0	25.0	16.7	11.9	59.7	40.3	13.9	10.0	53.6	46.4	Sieving	Gravel	
3/8"	0.375	9.50	10.9	4.70	3.6	62.6	37.4	7.2	4.7	67.5	32.5	6.5	4.1	79.1	20.9	8.1	5.8	65.4	34.6	6.6	4.7	58.4	41.6	Sieving	Gravel	
1/4"	0.265	6.30	7.74	5.30	4.1	66.6	33.4	8.3	5.4	72.8	27.2	7.0	4.4	83.4	16.6	8.8	6.3	71.7	28.3	7.3	5.3	63.6	36.4	Sieving	Gravel	
#4	0.188	4.75	5.47	1.84	1.4	68.1	31.9	4.06	2.6	75.5	24.5	3.33	2.1	85.5	14.5	5.37	3.8	75.6	24.4	4.10	3.0	66.6	33.4	Sieving	Gravel	
#6	0.133	3.35	3.99	2.77	2.1	70.2	29.8	4.63	3.0	78.5	21.5	3.33	2.1	87.6	12.4	4.54	3.2	78.8	21.2	3.50	2.5	69.1	30.9	Sieving	Gravel	
#8	0.094	2.36	2.81	2.31	1.8	72.0	28.0	3.48	2.2	80.7	19.3	2.33	1.5	89.0	11.0	3.51	2.5	81.3	18.7	2.70	1.9	71.0	29.0	Sieving	Gravel	
#16	0.047	1.18	1.67	3.23	2.5	74.4	25.6	5.21	3.4	84.1	15.9	3.33	2.1	91.1	8.9	4.95	3.5	84.9	15.1	5.00	3.6	74.6	25.4	Sieving	Sand	Above 2 mm is gravel
#30	0.023	0.600	0.84	2.31	1.8	76.2	23.8	3.48	2.2	86.3	13.7	2.00	1.2	92.4	7.6	2.48	1.8	86.6	13.4	3.00	2.2	76.8	23.2	Sieving	Sand	
#50	0.012	0.300	0.42	2.77	2.1	78.4	21.6	2.32	1.5	87.8	12.2	1.67	1.0	93.4	6.6	2.57	1.8	88.5	11.5	4.30	3.1	79.9	20.1	Sieving	Sand	
#100	0.0059	0.150	0.21	4.61	3.5	81.9	18.1	2.61	1.7	89.5	10.5	1.67	1.0	94.4	5.6	3.43	2.4	90.9	9.1	7.31	5.3	85.1	14.9	Sieving	Sand	
#140	0.0041	0.106	0.13	3.23	2.5	84.4	15.6	2.32	1.5	91.0	9.0	0.67	0.4	94.9	5.1	2.14	1.5	92.4	7.6	3.44	2.5	87.6	12.4	Sieving	Sand	
#200	0.0029	0.075	0.09	2.77	2.1	86.5	13.5	2.32	1.5	92.5	7.5	0.67	0.4	95.3	4.7	2.14	1.5	94.0	6.0	4.08	2.9	90.6	9.4	Sieving	Sand	
#270	0.0021	0.053	0.06	2.31	1.8	88.3	11.7	1.74	1.1	93.6	6.4	0.67	0.4	95.7	4.3	1.71	1.2	95.2	4.8	4.30	3.1	93.7	6.3	Sieving	Silt	Above 62 μm is sand
C-1	0.0015	0.038	0.045	0.49	0.4	88.7	11.3	0.41	0.3	93.9	6.1	0.29	0.2	95.9	4.1	0.17	0.1	95.3	4.7	0.24	0.2	93.8	6.2	Elutriation	Silt	
C-2	0.0011	0.028	0.033	1.48	1.1	89.8	10.2	1.49	1.0	94.9	5.1	1.14	0.7	96.6	3.4	0.76	0.5	95.8	4.2	1.43	1.0	94.8	5.2	Elutriation	Silt	
C-3	0.0008	0.020	0.024	1.31	1.0	90.8	9.2	1.67	1.1	95.9	4.1	1.18	0.7	97.3	2.7	1.12	0.8	96.7	3.3	1.44	1.0	95.9	4.1	Elutriation	Silt	
C-4	0.0006	0.015	0.017	0.97	0.7	91.6	8.4	1.38	0.9	96.8	3.2	1.02	0.6	98.0	2.0	0.98	0.7	97.4	2.6	1.47	1.1	96.9	3.1	Elutriation	Silt	
C-5	0.0004	0.010	0.012	0.60	0.5	92.0	8.0	0.86	0.6	97.4	2.6	0.64	0.4	98.4	1.6	0.59	0.4	97.8	2.2	0.91	0.7	97.6	2.4	Elutriation	Silt	
C-6	-0.0004	-0.010	0.009	10.37	8.0	100.0	0.0	4.04	2.6	100.0	0.0	2.64	1.6	100.0	0.0	3.11	2.2	100.0	0.0	3.34	2.4	100.0	0.0	Elutriation	Clay	Below 4 μm is clay
Total				**129.95**	**100.00**			**154.60**	**100.00**			**160.37**	**100.00**			**139.97**	**100.00**			**138.95**	**100.00**					
Total weight of head or whole sample (kg)				**129.95**				**154.60**				**160.37**				**139.97**				**138.95**						
Finest fraction (kg)	**<0.010 mm**			**10.37**	**8.0 %**			**4.04**	**2.6 %**			**2.64**	**1.6 %**			**3.11**	**2.2 %**			**3.34**	**2.4 %**					

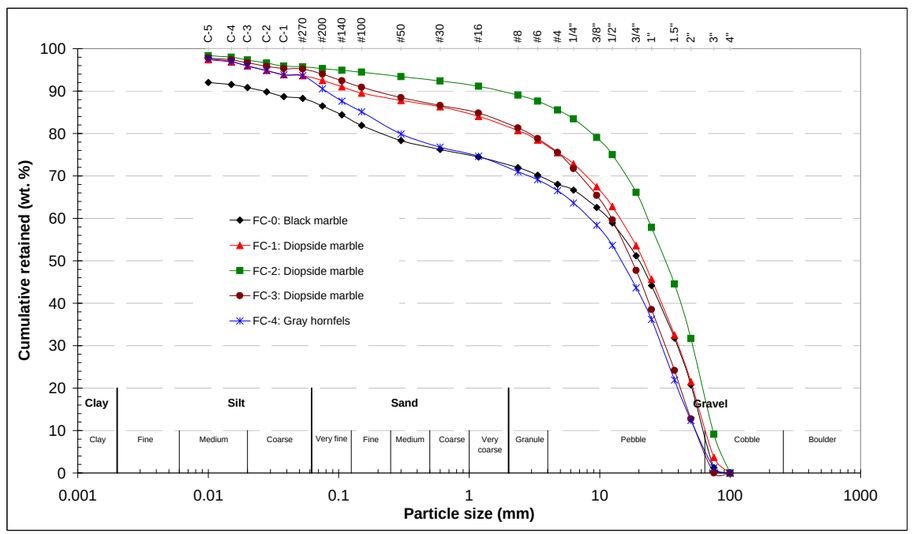

Figure C1.3 Cumulative weight retained for all Class B waste rock samples placed in the field cells

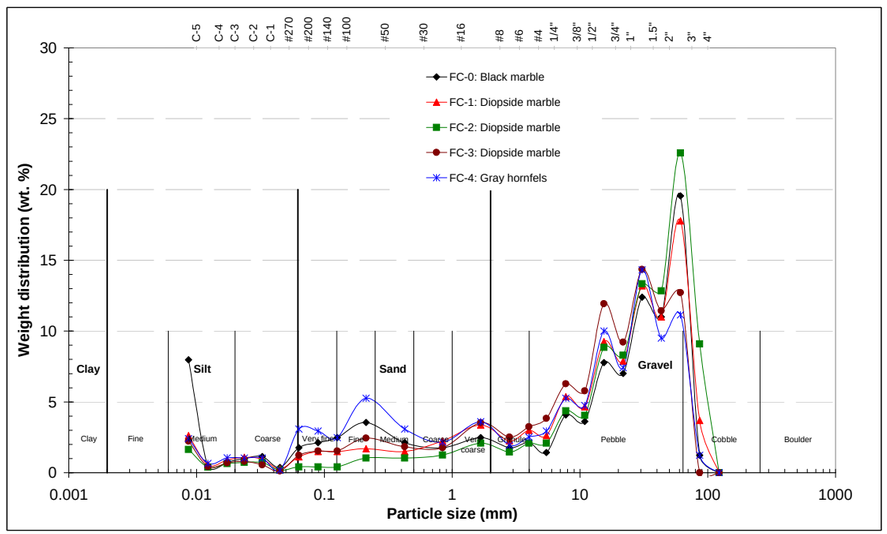

Figure C1.4 Particle size weight distribution for all Class B waste rock samples placed in the field cells

Appendix C2

Density Determination Results

University of British Columbia
Department of Mining Engineering
"Assessment of waste rock weathering characteristics at the Antamina mine based on field cells experiment"

Project:	Waste Rock Study at Antamina Mine	**Sample code:**	**Balls bearing**
Material type:	Waste Rock - Class B	**Sampling date:**	October, 2008
Rock type:	Marble and Hornfels	**Sampling by:**	C. Haupt
Location:	Antamina Open Pit. Field Cells	**Testing date:**	06-Oct-08
Test type	Calibration of Air Pycnometer	**Testing by:**	C. Aranda
	Beckman Model 930	**Review by:**	C. Aranda

Table C2.1 Volume values of balls bearing used for calibration of the air-pycnometer

Ball bearing			Quantity	Volume	
Fraction	Decimal	Decimal		Unit	Total
(in)	(in)	(cm)		cm^3	cm^3
13/16	0.81250	2.06375	1	4.60	4.60
1/2	0.50000	1.27000	1	1.07	1.07
3/8	0.37500	0.95250	1	0.45	0.45
5/16	0.31250	0.79375	5	0.26	1.31
9/32	0.28125	0.71438	2	0.19	0.38
1/4	0.25000	0.63500	5	0.13	0.67
7/32	0.21875	0.55563	5	0.09	0.45
3/16	0.18750	0.47625	5	0.06	0.28

Table C2.2 Specifications of balls bearing used for calibration of the air-pycnometer

Ball bearing	Quantity	Total volume	
Fraction		True	Measured
(in)		cm^3	cm^3
5/16	5	1.31	0.25
13/16	1	4.60	3.64
13/16; 1/2; 3/8	1; 1; 1	6.12	5.35
13/16; 1/2; 3/8; 5/16	1; 1; 1; 5	7.43	6.39
13/16; 1/2; 3/8; 5/16; 9/32	1; 1; 1; 5; 2	7.81	6.75
13/16; 1/2; 3/8; 5/16; 9/32; 1/4	1; 1; 1; 5; 2; 5	8.48	7.54
13/16; 1/2; 3/8; 5/16; 9/32; 1/4; 7/32	1; 1; 1; 5; 2; 5; 5	8.93	7.97
13/16; 1/2; 3/8; 5/16; 9/32; 1/4; 7/32; 3/16	1; 1; 1; 5; 2; 5; 5; 5	9.21	8.25

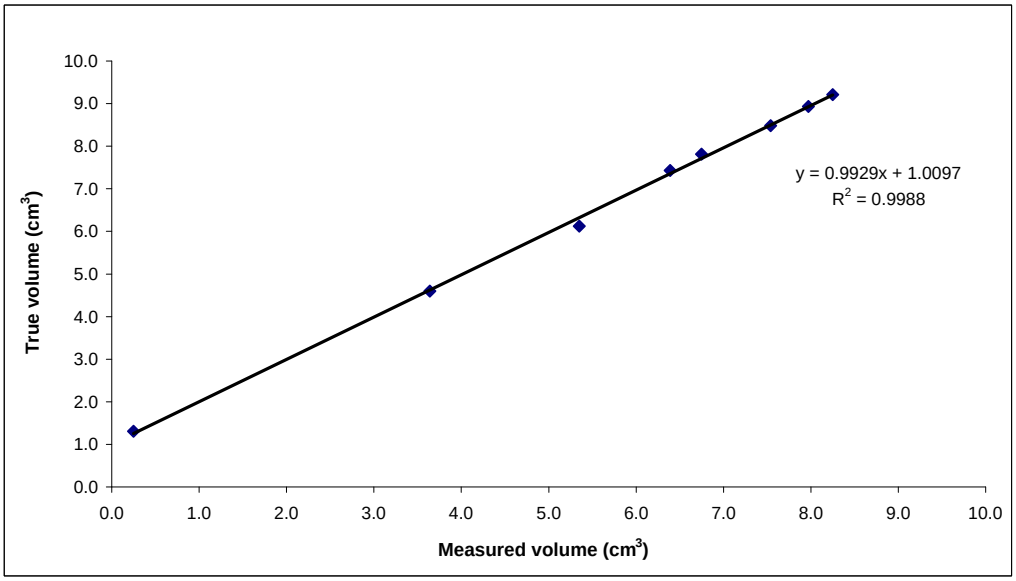

Figure C2.1 Air-pycnometer calibration curve

University of British Columbia
Department of Mining Engineering
"Assessment of waste rock weathering characteristics at the Antamina mine based on field cells experiment"

Table C2.3 Particle density determination data by using the air-pycnometer of the black marble (FC-0) sample

Project:	Waste Rock Study at Antamina Mine	**Sample Code:**	**FC-0**
Material Type:	Waste Rock - Class B	**Sampling Date:**	15-Mar-06
Rock Type:	Black marble	**Sampling by:**	C. Aranda
Location:	Antamina Open Pit	**Testing Date:**	13-Aug-08
	Pretective layer in the Pile 1	**Testing by:**	C. Aranda
Description:	Field Cell (UBC-1-0A and UBC-1-0B)	**Review by:**	C. Aranda

Samples ID	Size fraction		Mass					Volume (cc)			Density				
	Mesh	d_{pi}	Total	Sub sample	Testing (g)			Volume Testing			Test 1	Test 2	Test 3	Average	(kg/m^3)
	(US)	(mm)	(kg)	(kg)	Test 1	Test 2	Test 3	Test 1	Test 2	Test 3	(g/cc)	(g/cc)	(g/cc)	(g/cc)	
FC-0-A	4"	122.5	0.00	No sample											
FC-0-B	3"	86.6	1.60	0.12	42.70	67.30	49.00	15.19	24.65	17.36	2.81	2.73	2.82	2.79	2787.89
FC-0-C	2"	61.2	25.40	0.41	45.80	58.60	63.30	16.55	21.31	22.98	2.77	2.75	2.75	2.76	2757.06
FC-0-D	11/2"	43.3	14.30	0.39	57.20	52.40	65.20	20.47	18.78	23.45	2.79	2.79	2.78	2.79	2788.18
FC-0-E	1"	30.6	16.10	0.44	51.10	60.10	59.70	18.24	21.66	21.60	2.80	2.77	2.76	2.78	2780.03
FC-0-F	3/4"	21.8	9.10	0.28	58.40	57.40	61.20	21.11	20.72	22.27	2.77	2.77	2.75	2.76	2761.93
FC-0-G	1/2"	15.4	10.10	0.33	58.00	51.10	56.60	21.02	18.41	20.48	2.76	2.78	2.76	2.77	2766.57
FC-0-H	3/8"	10.9	4.70	0.27	51.10	55.10	54.00	18.43	19.91	19.51	2.77	2.77	2.77	2.77	2769.46
FC-0-I	1/4"	7.74	5.30	0.33	49.80	56.80	57.60	17.96	20.55	20.83	2.77	2.76	2.77	2.77	2767.52
FC-0-J	#4	5.47	1.84	0.11	49.80	52.10		18.14	18.82		2.75	2.77		2.76	2756.86
FC-0-K	#6	3.99	2.77	0.16	47.40	49.00	55.00	16.95	17.63	19.80	2.80	2.78	2.78	2.78	2784.94
FC-0-L	#8	2.81	2.31	0.11	51.90	61.40		18.72	22.21		2.77	2.76		2.77	2768.37
FC-0-M	#16	1.67	3.23	0.17	61.60	61.90	65.30	22.26	22.28	23.51	2.77	2.78	2.78	2.77	2774.61
FC-0-N	#30	0.84	2.31	0.13	59.80	60.10		21.26	21.49		2.81	2.80		2.80	2804.19
FC-0-O	#50	0.42	2.77	0.15	56.80	57.70		20.21	20.63		2.81	2.80		2.80	2803.57
FC-0-P	#100	0.21	4.61	0.26	59.50	59.30		21.56	21.55		2.76	2.75		2.76	2755.39
FC-0-Q	#140	0.13	3.23	0.20	59.80	58.30		21.81	21.22		2.74	2.75		2.74	2744.88
FC-0-R	#200	0.089	2.77	0.14	57.90	59.30		21.17	21.58		2.74	2.75		2.74	2741.58
FC-0-S	#270	0.063	2.31	0.12	57.00	56.30		20.75	20.40		2.75	2.76		2.75	2753.42
FC-0-T	-#270	0.044	15.22	0.82	61.12	58.67	62.67	22.55	21.48	23.10	2.71	2.73	2.71	2.72	2718.23
															2767.61

Table C2.4 Particle density determination data by using the air-pycnometer of the diopside marble (FC-1) sample

Project:	Waste Rock Study at Antamina Mine	**Sample Code:**	**FC-1**
Material Type:	Waste Rock - Class B	**Sampling Date:**	12-May-06
Rock Type:	Marble diopside	**Sampling by:**	C. Aranda
Location:	Antamina Open Pit	**Testing Date:**	14-Aug-08
	First dumping in the Pile 1	**Testing by:**	C. Aranda
Description:	Field Cell (UBC-1-1A)	**Review by:**	C. Aranda

Samples ID	Size fraction		Mass					Volume (cc)			Density				
	Mesh	d_{pi}	Total	Sub sample	Testing (g)			Volume Testing			Test 1	Test 2	Test 3	Average	(kg/m^3)
	(US)	(mm)	(kg)	(kg)	Test 1	Test 2	Test 3	Test 1	Test 2	Test 3	(g/cc)	(g/cc)	(g/cc)	(g/cc)	
FC-1-A	4"	122.5	0.00	No sample											
FC-1-B	3"	86.6	5.70	0.25	65.80	71.50	74.20	22.31	24.27	25.29	2.95	2.95	2.93	2.94	2943.24
FC-1-C	2"	61.2	27.50	0.46	65.90	67.70		22.34	23.03		2.95	2.94		2.94	2944.80
FC-1-D	11/2"	43.3	17.00	0.45	69.43	74.23	74.15	23.92	25.52	25.54	2.90	2.91	2.90	2.90	2904.70
FC-1-E	1"	30.6	20.40	0.32	69.20	69.60		23.76	23.80		2.91	2.92		2.92	2918.79
FC-1-F	3/4"	21.8	12.20	0.19	67.80	71.90		23.02	24.63		2.94	2.92		2.93	2932.04
FC-1-G	1/2"	15.4	14.30	0.13	69.30	69.30		23.75	23.85		2.92	2.91		2.91	2912.17
FC-1-H	3/8"	10.9	7.20	0.10	64.70			22.01			2.94			2.94	2939.64
FC-1-I	1/4"	7.74	8.30	0.11	66.30			22.64			2.93			2.93	2929.08
FC-1-J	#4	5.47	4.06	0.18	62.40	64.00		21.13	21.91		2.95	2.92		2.94	2937.37
FC-1-K	#6	3.99	4.63	0.20	62.60	63.30		21.55	21.71		2.90	2.92		2.91	2909.99
FC-1-L	#8	2.81	3.48	0.16	61.20	64.90		21.02	22.26		2.91	2.92		2.91	2913.91
FC-1-M	#16	1.67	5.21	0.24	63.50	62.50		21.71	21.41		2.92	2.92		2.92	2921.69
FC-1-N	#30	0.84	3.48	0.16	63.20	62.20		21.54	21.17		2.93	2.94		2.94	2936.21
FC-1-O	#50	0.42	2.32	0.11	61.90			20.95			2.96			2.96	2955.06
FC-1-P	#100	0.21	2.61	0.12	61.60			21.22			2.90			2.90	2903.58
FC-1-Q	#140	0.13	2.32	0.11	61.70			21.21			2.91			2.91	2909.65
FC-1-R	#200	0.089	2.32	0.11	61.50			21.81			2.82			2.82	2819.68
FC-1-S	#270	0.063	1.74	0.08	59.60			21.15			2.82			2.82	2818.54
FC-1-T	-#270	0.044	9.85	0.44	63.70			22.31			2.86			2.86	2855.55
															2910.83

University of British Columbia
Department of Mining Engineering
"Assessment of waste rock weathering characteristics at the Antamina mine based on field cells experiment"

Table C2.5 Particle density determination data by using the air-pycnometer of the diopside marble (FC-2) sample

Project:	Waste Rock Study at Antamina Mine	**Sample Code:**	**FC-2**
Material Type:	Waste Rock - Class B	**Sampling Date:**	29-Jun-06
Rock Type:	Marble diopside	**Sampling by:**	C. Aranda
Location:	Antamina Open Pit	**Testing Date:**	16-Aug-08
	Second dumping in the Pile 1	**Testing by:**	C. Aranda
Description:	Field Cell (UBC-1-2A and UBC-1-2B)	**Review by:**	C. Aranda

Samples ID	Size fraction		Mass					Volume (cc)			Density				
	Mesh	d_{pi}	Total	Sub sample	Testing (g)			Volume Testing			Test 1	Test 2	Test 3	Average	(kg/m^3)
	(US)	(mm)	(kg)	(kg)	Test 1	Test 2	Test 3	Test 1	Test 2	Test 3	(g/cc)	(g/cc)	(g/cc)	(g/cc)	
FC-0-A	4"	122.5	0.00	No sample											
FC-0-B	3"	86.6	14.60	0.22	69.30	72.90		21.64	23.00		3.20	3.17		3.19	3185.66
FC-0-C	2"	61.2	36.20	0.26	69.30	74.40		22.42	24.10		3.09	3.09		3.09	3089.00
FC-0-D	11/2"	43.3	20.60	0.21	70.10	73.50		22.26	23.42		3.15	3.14		3.14	3143.94
FC-0-E	1"	30.6	21.40	0.19	70.50	74.20		22.44	23.75		3.14	3.12		3.13	3133.40
FC-0-F	3/4"	21.8	13.30	0.24	67.30	72.90		21.31	23.04		3.16	3.16		3.16	3160.62
FC-0-G	1/2"	15.4	14.20	0.20	68.30	74.40		21.39	23.36		3.19	3.18		3.19	3188.72
FC-0-H	3/8"	10.9	6.50	0.19	66.70	72.20		21.01	22.61		3.18	3.19		3.18	3184.56
FC-0-I	1/4"	7.74	7.00	0.23	68.00	68.20		21.37	21.60		3.18	3.16		3.17	3169.24
FC-0-J	#4	5.47	3.33	0.12	65.90	68.10		20.80	21.61		3.17	3.15		3.16	3159.76
FC-0-K	#6	3.99	3.33	0.12	65.50	67.70		20.57	21.36		3.18	3.17		3.18	3176.57
FC-0-L	#8	2.81	2.33	0.19	69.30	68.00		22.09	21.57		3.14	3.15		3.14	3144.73
FC-0-M	#16	1.67	3.33	0.25	68.50	68.90		21.67	21.63		3.16	3.19		3.17	3172.91
FC-0-N	#30	0.84	2.00	0.16	68.10			21.46			3.17			3.17	3172.84
FC-0-O	#50	0.42	1.67	0.13	67.90			21.36			3.18			3.18	3178.22
FC-0-P	#100	0.21	1.67	0.12	65.90			21.07			3.13			3.13	3128.22
FC-0-Q	#140	0.13	0.67	0.06	54.10			17.55			3.08			3.08	3082.37
FC-0-R	#200	0.089	0.67	0.05	46.00			14.94			3.08			3.08	3078.96
FC-0-S	#270	0.063	0.67	0.04	39.90			13.04			3.06			3.06	3058.96
FC-0-T	-#270	0.044	6.90	0.26	58.50			19.26			3.04			3.04	3037.51
															3139.27

Table C2.6 Particle density determination data by using the air-pycnometer of the diopside marble (FC-3) sample

Project:	Waste Rock Study at Antamina Mine	**Sample Code:**	**FC-3**
Material Type:	Waste Rock - Class B	**Sampling Date:**	07-Jul-06
Rock Type:	Marble diopside	**Sampling by:**	C. Aranda
Location:	Antamina Open Pit	**Testing Date:**	18-Aug-08
	Third dumping in the Pile 1	**Testing by:**	C. Aranda
Description:	Field Cell (UBC-1-3A)	**Review by:**	C. Aranda

Samples ID	Size fraction		Mass					Volume (cc)			Density				
	Mesh	d_{pi}	Total	Sub sample	Testing (g)			Volume Testing			Test 1	Test 2	Test 3	Average	(kg/m^3)
	(US)	(mm)	(kg)	(kg)	Test 1	Test 2	Test 3	Test 1	Test 2	Test 3	(g/cc)	(g/cc)	(g/cc)	(g/cc)	
FC-1-A	4"	122.5	0.00	No sample											
FC-1-B	3"	86.6	0.00	No sample											
FC-1-C	2"	61.2	17.80	0.15	74.50	76.40		25.51	26.27		2.92	2.91		2.91	2914.14
FC-1-D	11/2"	43.3	16.00	0.20	64.90	74.50		23.00	26.47		2.82	2.81		2.82	2818.10
FC-1-E	1"	30.6	20.10	0.19	68.90	77.40		23.28	26.23		2.96	2.95		2.96	2955.23
FC-1-F	3/4"	21.8	12.90	0.18	67.10	76.26		22.65	25.80		2.96	2.96		2.96	2958.68
FC-1-G	1/2"	15.4	16.70	0.16	69.80	74.24		22.75	25.73		3.07	2.89		2.98	2976.29
FC-1-H	3/8"	10.9	8.10	0.24	64.90	68.30		22.03	23.25		2.95	2.94		2.94	2941.81
FC-1-I	1/4"	7.74	8.80	0.14	62.80	71.30		21.39	24.41		2.94	2.92		2.93	2928.03
FC-1-J	#4	5.47	5.37	0.18	64.70	62.40		22.10	21.59		2.93	2.89		2.91	2908.82
FC-1-K	#6	3.99	4.54	0.15	64.80	65.10		22.15	22.25		2.93	2.93		2.93	2925.91
FC-1-L	#8	2.81	3.51	0.12	65.90	66.30		22.55	22.75		2.92	2.91		2.92	2918.35
FC-1-M	#16	1.67	4.95	0.14	66.40			22.63			2.93			2.93	2934.79
FC-1-N	#30	0.84	2.48	0.15	64.30			21.76			2.95			2.95	2954.79
FC-1-O	#50	0.42	2.57	0.16	64.50			21.92			2.94			2.94	2942.49
FC-1-P	#100	0.21	3.43	0.22	66.40			23.17			2.87			2.87	2865.62
FC-1-Q	#140	0.13	2.14	0.15	64.80			22.96			2.82			2.82	2821.97
FC-1-R	#200	0.089	2.14	0.12	61.80			21.78			2.84			2.84	2837.31
FC-1-S	#270	0.063	1.71	0.10	64.40			22.82			2.82			2.82	2821.63
FC-1-T	-#270	0.044	6.74	0.19	62.60			22.03			2.84			2.84	2841.66
															2903.65

University of British Columbia
Department of Mining Engineering
"Assessment of waste rock weathering characteristics at the Antamina mine based on field cells experiment"

Table C2.7 Particle density determination data by using the air-pycnometer of the gray hornfels (FC-4) sample

Project:	Waste Rock Study at Antamina Mine	**Sample Code:**	**FC-4**
Material Type:	Waste Rock - Class B	**Sampling Date:**	07-Jul-06
Rock Type:	Gray Hornfels	**Sampling by:**	C. Aranda
Location:	Antamina Open Pit	**Testing Date:**	18-Aug-08
	Third/Fourth dumping in the Pile 1	**Testing by:**	C. Aranda
Description:	Field Cell (UBC-1-4A)	**Review by:**	C. Aranda

Samples ID	Size fraction		Mass					Volume (cc)			Density				
	Mesh	d_{pi}	Total	Sub sample	Testing (g)			Volume Testing			Test 1	Test 2	Test 3	Average	(kg/m^3)
	(US)	(mm)	(kg)	(kg)	Test 1	Test 2	Test 3	Test 1	Test 2	Test 3	(g/cc)	(g/cc)	(g/cc)	(g/cc)	
FC-0-A	4"	122.5	0.00	No sample											
FC-0-B	3"	86.6	1.70	0.15	72.00	71.70		26.31	26.26		2.74	2.73		2.73	2733.60
FC-0-C	2"	61.2	15.50	0.18	69.90	74.80		25.60	27.38		2.73	2.73		2.73	2730.93
FC-0-D	11/2"	43.3	13.20	0.16	67.50	74.40		24.61	27.05		2.74	2.75		2.75	2746.40
FC-0-E	1"	30.6	19.90	0.14	63.70	73.30		23.18	26.79		2.75	2.74		2.74	2742.24
FC-0-F	3/4"	21.8	10.30	0.16	68.10	69.70		24.95	25.52		2.73	2.73		2.73	2730.17
FC-0-G	1/2"	15.4	13.90	0.10	67.20			24.48			2.74			2.74	2744.89
FC-0-H	3/8"	10.9	6.60	0.21	64.60	67.80		23.58	24.74		2.74	2.74		2.74	2740.15
FC-0-I	1/4"	7.74	7.30	0.21	60.80	71.30		22.10	26.11		2.75	2.73		2.74	2741.00
FC-0-J	#4	5.47	4.10	0.24	63.90	64.10		23.31	23.31		2.74	2.75		2.75	2745.58
FC-0-K	#6	3.99	3.50	0.18	62.60	64.30		22.83	23.43		2.74	2.74		2.74	2742.99
FC-0-L	#8	2.81	2.70	0.35	65.60	65.30		23.87	23.70		2.75	2.76		2.75	2752.11
FC-0-M	#16	1.67	3.70	0.48	66.70			24.22			2.75			2.75	2753.50
FC-0-N	#30	0.84	1.60	0.40	66.90			24.35			2.75			2.75	2747.12
FC-0-O	#50	0.42	2.33	0.19	65.60			23.83			2.75			2.75	2753.23
FC-0-P	#100	0.21	10.98	0.83	64.20			23.31			2.75			2.75	2754.16
FC-0-Q	#140	0.13	8.65	0.65	62.20			22.56			2.76			2.76	2757.63
FC-0-R	#200	0.089	4.33	0.32	62.80			22.81			2.75			2.75	2752.72
FC-0-S	#270	0.063	1.66	0.14	60.80			22.12			2.75			2.75	2748.80
FC-0-T	-#270	0.044	7.00	0.50	59.00			21.26			2.77			2.77	2774.53
															2746.93

Table C2.8 Comparison of particle density determination data by using the air-pycnometer and water displacement method

Samples ID	Size fraction		Mass								Volume						Density					Differential error
	Mesh	d_{pi}	Testing (g)			Volumetric method testing (g)					Air-pycnometer testing (cc)			VM testing (mL or cc)			AP (g/cc)				VM (g/cc)	
	(US)	(mm)	Test 1	Test 2	Test 3	Flask	Flask+Sp	Fl+Sp+Water	Sample	Water	Test 1	Test 2	Test 3	Flask	Water	Sample	Test 1	Test 2	Test 3	Average		
FC-0-E	1"	30.6	69.41	69.40	69.30	82.69	152.05	326.69	69.36	174.64	25.21	25.19	25.18	200.00	174.64	25.36	2.75	2.76	2.75	2.75	2.74	0.01
FC-0-I	1/4"	7.74	65.37	65.35	65.32	81.21	146.55	322.42	65.34	175.87	23.83	23.84	23.89	200.00	175.87	24.13	2.74	2.74	2.73	2.74	2.71	0.01
FC-0-N	#30	0.84	62.43	62.40	62.50	80.82	143.28	320.71	62.46	177.43	22.38	22.31	22.28	200.00	177.43	22.57	2.79	2.80	2.81	2.80	2.77	0.01
FC-0-S	#270	0.063	59.49	59.49	59.49	79.73	139.20	317.22	59.47	178.02	21.54	21.65	21.64	200.00	178.02	21.98	2.76	2.75	2.75	2.75	2.71	0.02
FC-2-E	1"	30.6	66.50	66.45	66.47	81.27	147.84	326.32	66.57	178.48	21.22	21.36	21.35	200.00	178.48	21.52	3.13	3.11	3.11	3.12	3.09	0.01
FC-2-I	1/4"	7.74	70.35	70.33	70.33	80.14	150.56	328.02	70.42	177.46	22.35	22.30	22.27	200.00	177.46	22.54	3.15	3.15	3.16	3.15	3.12	0.01
FC-2-N	#30	0.84	72.06	72.06	72.06	78.15	150.31	327.13	72.16	176.82	22.94	23.05	22.99	200.00	176.82	23.18	3.14	3.13	3.13	3.13	3.11	0.01
FC-2-R	#200	0.089	45.93	45.92	45.91	80.86	126.84	311.35	45.98	184.51	15.22	15.12	15.16	200.00	184.51	15.49	3.02	3.04	3.03	3.03	2.97	0.02

Appendix C3

Surface Area Determination Results

University of British Columbia
Department of Mining Engineering
"Assessment of waste rock weathering characteristics at the Antamina mine based on field cells experiment"

Table C3.1 Surface area determination by using both GE and BET methods of the black marble (FC-0) sample

Project: Waste Rock Study at Antamina Mine
Material type: Waste Rock - Class B
Rock type: Black marble
Location: Antamina Open Pit
Protective layer in the Pile 1
Description: Field cell (UBC-1-0A and UBC-1-0B)

Sample code: FC-0
Sampling date: 15-Mar-06
Sampling by: C. Aranda
Testing date: Aug 16 to Aug 24, 2008
Testing by: C. Aranda
Review by: C. Aranda

Samples ID	Mesh		Mass	Geometric diameter (d)	BET measurments							$A_v = 6/d$	Particle density (ρ)	Specific surface area				Lamda		Final specific surface area (SSA_i)	Surface Area (SA)		Method	Observation
	(US)	(mm)	Total (wt)		Cell	Cell + sample 1	Sample 1	Cell + sample 1 (reweighed)	Sample 1 (rewt.)	Outgassing test	Outgassing time			$A_m = A_v / \rho$	SSA_{BET}	SSA_{GE}	SSA_{BET}	$\lambda = SSA_{BET}/SSA_{GE}$			BET (in cell)	$SA_i = SSA_i \cdot wt$		
			(kg)	(m)	(g)	(g)	(g)	(g)	(g)	(micro/min)	(h)	(m^{-1})	(kg/m^3)	(m^2/kg)	(m^2/g)	(m^2/kg)	(m^2/kg)	Initial	Final (adj.)	(m^2/kg)	(m^2)	(m^2)		
FC-0-A	4"	100.0	0.00																				GE	
FC-0-B	3"	75.0	1.60	0.07408								81.0	2787.9	0.029		0.029			3857	112		179.3	GE	
FC-0-C	2"	50.0	25.40	0.05855								102.5	2757.1	0.037		0.037			3994	148		3770.9	GE	
FC-0-D	11/2"	37.5	14.30	0.04133								145.2	2788.2	0.052		0.052			4198	219		3125.7	GE	
FC-0-E	1"	25.0	16.10	0.02879								208.4	2780.0	0.075		0.075			4409	331		5322.6	GE	
FC-0-F	3/4"	19.0	9.10	0.02062								290.9	2761.9	0.105		0.105			4604	485		4413.4	GE	
FC-0-G	1/2"	12.5	10.10	0.01482								404.9	2766.6	0.146		0.146			4798	702		7092.5	GE	
FC-0-H	3/8"	9.50	4.70	0.01106								542.3	2769.5	0.196		0.196			4968	973		4572.3	GE	
FC-0-I	1/4"	6.30	5.30	0.00810								740.6	2767.5	0.268		0.268			5151	1378		7304.8	GE	
FC-0-J	#4	4.75	1.84	0.00601	22.3315	29.0411	6.7096	29.0271	6.6956	4.00	24.56	998.7	2756.9	0.362	0.9214	0.362	921	2543	2543	921	6.2	1699.7	GE and BET	Test passed, above 1m^2
FC-0-K	#6	3.35	2.77	0.00399	22.9015	30.1148	7.2133	30.1065	7.2050	44.20	23.28	1504.1	2784.9	0.540	1.2690	0.540	1269	2350	2350	1269	9.1	3511.4	BET	Test passed, above 1m^2
FC-0-L	#8	2.36	2.31	0.00281	17.3625	25.8954	8.5329	25.8791	8.5166	41.93	5.72	2133.9	2768.4	0.771	1.4400	0.771	1440	1868	1868	1440	12.3	3320.4	BET	Test passed, above 1m^2 From duplicate
FC-0-M	#16	1.18	3.23	0.00167	17.3608	24.3272	6.9664	24.3113	6.9505	47.20	23.00	3595.5	2774.6	1.296	1.9120	1.296	1912	1475	1475	1912	13.3	6172.3	BET	Test passed, above 1m^2
FC-0-N	#30	0.600	2.31	0.00084	17.0412	25.2287	8.1875	25.2020	8.1608	29.48	9.36	7130.7	2804.2	2.543	2.2430	2.543	2243	882	882	2243	18.3	5172.0	BET	Test passed, above 1m^2 From duplicate
FC-0-O	#50	0.300	2.77	0.00042	16.6501	25.5630	8.9129	25.5350	8.8849	44.33	45.22	14142.1	2803.6	5.044	2.0670	5.044	2067	410	410	2067	18.4	5719.4	BET	Test passed, above 1m^2 From duplicate
FC-0-P	#100	0.150	4.61	0.00021	16.6490	23.3533	6.7043	23.3452	6.6962	36.30	42.72	28284.3	2755.4	10.265	1.2910	10.265	1291	126	126	1291	8.6	5953.7	BET	Test passed, above 1m^2
FC-0-Q	#140	0.106	3.23	0.00013	17.0396	24.0613	7.0217	24.0439	7.0043	17.50	5.95	47583.1	2744.9	17.335	1.3080	17.335	1308	75	75	1308	9.2	4222.5	BET	Test passed, above 1m^2
FC-0-R	#200	0.075	2.77	0.00009	17.6373	25.7494	8.1121	25.7282	8.0909	34.36	40.40	67292.7	2741.6	24.545	1.4250	24.545	1425	58	58	1425	11.5	3943.0	BET	Test passed, above 1m^2 From duplicate
FC-0-S	#270	0.053	2.31	0.00006	17.6809	23.9400	6.2591	23.9210	6.2401	34.50	20.95	95526.1	2753.4	34.694	1.6750	34.694	1675	48	48	1675	10.5	3862.3	BET	Test passed, above 1m^2 From duplicate
FC-0-T	-#270	0.044	15.22	0.00004	17.3617	20.1469	2.7852	20.1065	2.7448	12.92	21.50	135605.1	2718.2	49.887	11.7300	49.887	11730			11730	32.2	178514.4	BET	Test passed, above 1m^2
			129.95																	**1984**		**257872.6**		

Duplicates

FC-0-J	#4	4.75	1.84		22.3315	29.0411	6.7096	29.0271	6.6956	4.00	24.56				0.9214						6.2		GE and BET	Test passed, above 1m^2
FC-0-J(D1)	#4	4.75	1.84		22.3308	29.0370	6.7062	29.0267	6.6959	9.89	18.49				0.8509						5.7		GE and BET	Test passed, above 1m^2
FC-0-K	#6	3.35	2.77		22.9015	30.1148	7.2133	30.1065	7.2050	44.20	23.28				1.2690						9.1		BET	Test passed, above 1m^2
FC-0-K(D1)	#6	3.35	2.77		22.9021	30.0969	7.1948	30.0808	7.1787	20.63	22.18				1.3450						9.7		BET	Test passed, above 1m^2
FC-0-L	#8	2.36	2.31		17.7301	25.3835	7.6534	25.3624	7.6323	8.93	23.83				1.8720						14.3		BET	Test passed, above 1m^2
FC-0-L(D1)	#8	2.36	2.31		17.8890	26.0078	8.1188	25.9864	8.0974	11.65	14.32				1.6010						13.0		BET	Test passed, above 1m^2
FC-0-L(D2)	#8	2.36	2.31		17.3625	25.8954	8.5329	25.8791	8.5166	41.93	5.72				1.4400						12.3		BET	Test passed, above 1m^2
FC-0-M	#16	1.18	3.23		17.3608	24.3272	6.9664	24.3113	6.9505	47.20	23.00				1.9120						13.3		BET	Test passed, above 1m^2
FC-0-M(D1)	#16	1.18	3.23		17.7290	26.0404	8.3114	26.0129	8.2839	6.56	17.23				2.1100						17.5		BET	Test passed, above 1m^2
FC-0-N	#30	0.600	2.31		17.8888	25.2393	7.3505	25.2168	7.3280	9.60	22.75				2.3890						17.5		BET	Test passed, above 1m^2
FC-0-N(D1)	#30	0.600	2.31		17.0412	25.2287	8.1875	25.2020	8.1608	29.48	9.36				2.2430						18.3		BET	Test passed, above 1m^2
FC-0-O	#50	0.300	2.77		17.6791	24.4128	6.7337	24.3908	6.7117	15.20	7.93				2.2360						15.0		BET	Test passed, above 1m^2
FC-0-O(D1)	#50	0.300	2.77		16.6501	25.5630	8.9129	25.5350	8.8849	44.33	45.22				2.0600						18.3		BET	Test passed, above 1m^2
FC-0-P	#100	0.150	4.61		16.6490	23.3533	6.7043	23.3452	6.6962	36.30	42.72				1.2910						8.6		BET	Test passed, above 1m^2
FC-0-P(D1)	#100	0.150	4.61		17.6804	26.1387	8.4583	26.1190	8.4386	9.66	23.85				1.4800						12.5		BET	Test passed, above 1m^2
FC-0-P(D2)	#100	0.150	4.61		17.6375	24.4760	6.8385	24.4610	6.8235	40.00	47.90				1.3700						9.3		BET	Test passed, above 1m^2
FC-0-P(D3)	#100	0.150	4.61		17.3622	24.8762	7.5140	24.8571	7.4949	9.83	22.20				1.4760						11.1		BET	Test passed, above 1m^2
FC-0-Q	#140	0.106	3.23		17.0396	24.0613	7.0217	24.0439	7.0043	17.50	5.95				1.3080						9.2		BET	Test passed, above 1m^2
FC-0-Q(D1)	#140	0.106	3.23		16.9516	25.5951	8.6435	25.5742	8.6226	48.00	6.00				1.2820						11.1		BET	Test passed, above 1m^2
FC-0-R	#200	0.075	2.77		17.7311	23.7418	6.0107	23.7358	6.0047	24.50	7.47				1.1840						7.1		BET	Test passed, above 1m^2
FC-0-R(D1)	#200	0.075	2.77		17.6373	25.7494	8.1121	25.7282	8.0909	34.36	40.40				1.4250						11.5		BET	Test passed, above 1m^2
FC-0-S	#270	0.053	2.31		17.6809	23.9400	6.2591	23.9210	6.2401	34.50	20.95				1.6750						10.5		BET	Test passed, above 1m^2
FC-0-S(D1)	#270	0.053	2.31		17.6373	25.6008	7.9635	25.5793	7.9420	5.15	18.00				2.0090						16.0		BET	Test passed, above 1m^2
FC-0-T	-#270	0.044	15.22		17.3617	20.1469	2.7852	20.1065	2.7448	12.92	21.50				11.7300						32.2		BET	Test passed, above 1m^2
FC-0-T(D1)	-#270	0.044	15.22		17.3630	21.2242	3.8612	21.1726	3.8096	12.25	20.15				11.7500						44.8		BET	Test passed, above 1m^2

Notes:

A_v: Specific surface area based on volume (m^{-1})

A_m: Specific surface area based on mass (m^2/kg)

GE: Geometrical Estimation method

BET: Brunauer-Emmett-Teller method

Table C3.2 Surface area determination by using both GE and BET methods of the diopside marble (FC-1) sample

Project: Waste Rock Study at Antamina Mine
Material type: Waste Rock - Class B
Rock type: Diopside marble
Location: Antamina Open Pit
First tipping phase in the Pile 1
Description: Field cell (UBC-1-1A)

Sample code: FC-1
Sampling date: 12-May-06
Sampling by: C. Aranda
Testing date: Aug 24 to Aug 31, 2008
Testing by: C. Aranda
Review by: C. Aranda

Samples ID	Mesh		Mass	Geometric diameter (d)	BET measurments							$A_v = 6/d$	Particle density (ρ)	Specific surface area				Lamda		Final specific surface area (SSA_i)	Surface Area (SA)		Method	Observation
	(US)	(mm)	Total (wt)		Cell	Cell + sample 1	Sample 1	Cell + sample 1 (reweighed)	Sample 1 (rewt.)	Outgassing test	Outgassing time			$A_m = A_v / \rho$	SSA_{BET}	SSA_{GE}	SSA_{BET}	$\lambda = SSA_{BET}/SSA_{GE}$			BET (in cell)	$SA_i = SSA_i wt$		
			(kg)	(m)	(g)	(g)	(g)	(g)	(g)	(micro/min)	(h)	(m^{-1})	(kg/m^3)	(m^2/kg)	(m^2/g)	(m^2/kg)	(m^2/kg)	Initial	Final (adj.)	(m^2/kg)	(m^2)	(m^2)		
FC-1-A	4"	100.0	0.00																				GE	
FC-1-B	3"	75.0	5.70	0.07717								77.8	2943.2	0.026		0.026			2255	60		339.6	GE	
FC-1-C	2"	50.0	27.50	0.06121								98.0	2944.8	0.033		0.033			2336	78		2138.6	GE	
FC-1-D	11/2"	37.5	17.00	0.04471								134.2	2904.7	0.046		0.046			2447	113		1921.4	GE	
FC-1-E	1"	25.0	20.40	0.02975								201.7	2918.8	0.069		0.069			2590	179		3650.7	GE	
FC-1-F	3/4"	19.0	12.20	0.02224								269.8	2932.0	0.092		0.092			2692	248		3021.7	GE	
FC-1-G	1/2"	12.5	14.30	0.01444								415.5	2912.2	0.143		0.143			2843	406		5800.0	GE	
FC-1-H	3/8"	9.50	7.20	0.01066								562.8	2939.6	0.191		0.191			2949	565		4065.2	GE	
FC-1-I	1/4"	6.30	8.30	0.00770								778.7	2929.1	0.266		0.266			3063	814		6759.2	GE	
FC-1-J	#4	4.75	4.06	0.00534	22.9028	28.6204	5.7176	28.6151	5.7123	27.65	5.44	1124.5	2937.4	0.383	0.6507	0.383	651	1700	1700	651	3.72	2638.7	GE and BET	Test passed, above 1m^2
FC-1-K	#6	3.35	4.63	0.00399	22.3302	29.9054	7.5752	29.9005	7.5703	4.72	19.36	1504.1	2910.0	0.517	0.6957	0.517	696	1346	1346	696	5.27	3224.2	BET	Test passed, above 1m^2
FC-1-L	#8	2.36	3.48	0.00281	16.6494	25.5393	8.8899	25.5315	8.8821	4.13	25.49	2133.9	2913.9	0.732	0.7373	0.732	737	1007	1007	737	6.55	2562.8	BET	Test passed, above 1m^2
FC-1-M	#16	1.18	5.21	0.00167	17.7299	25.6970	7.9671	25.6879	7.9580	3.89	42.25	3595.5	2921.7	1.231	0.9269	1.231	927	753	753	927	7.38	4832.7	BET	Test passed, above 1m^2
FC-1-N	#30	0.600	3.48	0.00084	17.3636	25.3711	8.0075	25.3642	8.0006	6.94	46.35	7130.7	2936.2	2.429	0.8156	2.429	816	336	336	816	6.53	2834.9	BET	Test passed, above 1m^2
FC-1-O	#50	0.300	2.32	0.00042	17.6800	25.1604	7.4804	25.1490	7.4690	4.85	17.73	14142.1	2955.1	4.786	0.8901	4.786	890	186	186	890	6.65	2062.6	BET	Test passed, above 1m^2
FC-1-P	#100	0.150	2.61	0.00021	16.6494	23.8786	7.2292	23.8691	7.2197	18.16	20.24	28284.3	2903.6	9.741	0.6976	9.741	698	72	72	698	5.04	1818.6	BET	Test passed, above 1m^2
FC-1-Q	#140	0.106	2.32	0.00013	17.6376	25.4370	7.7994	25.4300	7.7924	12.90	4.70	47583.1	2909.7	16.354	0.4881	16.354	488	30	30	488	3.80	1131.0	BET	Test passed, above 1m^2
FC-1-R	#200	0.075	2.32	0.00009	17.4474	24.4274	6.9800	24.4241	6.9767	21.70	4.40	67292.7	2819.7	23.865	0.4350	23.865	435	18	18	435	3.03	1008.0	BET	Test passed, above 1m^2
FC-1-S	#270	0.053	1.74	0.00006	17.8890	25.9034	8.0144	25.9000	8.0110	3.83	18.30	95526.1	2818.5	33.892	0.4559	33.892	456	13	13	456	3.65	792.3	BET	Test passed, above 1m^2
FC-1-T	-#270	0.044	9.85	0.00004	17.6804	21.4483	3.7679	21.4322	3.7518	17.16	23.05	135605.1	2855.6	47.488	3.3280	47.488	3328			3328	12.49	32775.1	BET	Test passed, above 1m^2
			154.60																	**539**		**83377.3**		

Duplicates

FC-1-L	#8	2.36	3.48		17.0423	24.9895	7.9472	24.9799	7.9376	4.78	19.45				0.6183						4.91		BET	Test passed, above 1m^2
FC-1-L(D1)	#8	2.36	3.48		16.6494	25.5393	8.8899	25.5315	8.8821	4.13	25.49				0.7373						6.55		BET	Test passed, above 1m^2
FC-1-P	#100	0.150	2.61		16.6494	23.8786	7.2292	23.8691	7.2197	18.16	20.24				0.6976						5.04		BET	Test passed, above 1m^2
FC-1-P(D1)	#100	0.150	2.61		17.7200	24.6550	6.9350	24.6458	6.9258	4.18	17.07				0.4559						3.16		BET	Test passed, above 1m^2
FC-1-S	#270	0.053	1.74		17.8890	25.9034	8.0144	25.9000	8.0110	3.83	18.30				0.5096						4.08		BET	Test passed, above 1m^2
FC-1-S(D1)	#270	0.053	1.74		17.0414	24.8645	7.8231	24.8597	7.8183	10.53	6.97				0.4559						3.56		BET	Test passed, above 1m^2

Notes:
A_v: Specific surface area based on volume (m^{-1})
A_m: Specific surface area based on mass (m^2/kg)
GE: Geometrical Estimation method
BET: Brunauer-Emmett-Teller method

Table C3.3 Surface area determination by using both GE and BET methods of the diopside marble (FC-2) sample

Project: Waste Rock Study at Antamina Mine
Material type: Waste Rock - Class B
Rock type: Diopside marble
Location: Antamina Open Pit
Second tipping phase in the Pile 1
Description: Field cell (UBC-1-2A and UBC-1-2B)

Sample code: FC-2
Sampling date: 29-Jun-06
Sampling by: C. Aranda
Testing date: Sept 1 to Sept 8, 2008
Testing by: C. Aranda
Review by: C. Aranda

Samples ID	Mesh		Mass	Geometric diameter (d)	BET measurments							A_v = 6/d	Particle density (ρ)	Specific surface area				Lamda		Final specific surface area (SSA_i)	Surface Area (SA)		Method	Observation
	(US)	(mm)	Total (wt)		Cell	Cell + sample 1	Sample 1	Cell + sample 1 (reweighed)	Sample 1 (rewt.)	Outgassing test	Outgassing time			$A_m = A_v / \rho$	SSA_{BET}	SSA_{GE}	SSA_{BET}	$\lambda = SSA_{BET}/SSA_{GE}$			BET (in cell)	$SA_i = SSA_i \cdot wt$		
			(kg)	(m)	(g)	(g)	(g)	(g)	(g)	(micro/min)	(h)	(m^{-1})	(kg/m^3)	(m^2/kg)	(m^2/g)	(m^2/kg)	(m^2/kg)	Initial	Final (adj.)	(m^2/kg)	(m^2)	(m^2)		
FC-2-A	4"	100.0	0.00																				GE	
FC-2-B	3"	75.0	14.60	0.07700								77.9	3185.7	0.024		0.024			4205	103		1501.5	GE	
FC-2-C	2"	50.0	36.20	0.06121								98.0	3089.0	0.032		0.032			4354	138		5001.7	GE	
FC-2-D	11/2"	37.5	20.60	0.04454								134.7	3143.9	0.043		0.043			4562	195		4026.8	GE	
FC-2-E	1"	25.0	21.40	0.03070								195.4	3133.4	0.062		0.062			4805	300		6412.8	GE	
FC-2-F	3/4"	19.0	13.30	0.02220								270.3	3160.6	0.086		0.086			5017	429		5705.9	GE	
FC-2-G	1/2"	12.5	14.20	0.01468								408.8	3188.7	0.128		0.128			5287	678		9626.0	GE	
FC-2-H	3/8"	9.50	6.50	0.01088								551.7	3184.6	0.173		0.173			5483	950		6173.9	GE	
FC-2-I	1/4"	6.30	7.00	0.00772								777.5	3169.2	0.245		0.245			5707	1400		9800.8	GE	
FC-2-J	#4	4.75	3.33	0.00564	22.9038	29.6226	6.7188	29.6100	6.7062	5.76	8.86	1064.1	3159.8	0.337	1.0500	0.337	1050	3118	3118	1050	7.0	3500.4	GE and BET	Test passed, above $1m^0$
FC-2-K	#6	3.35	3.33	0.00399	22.3288	30.0969	7.7681	30.0896	7.7608	14.01	21.60	1504.1	3176.6	0.474	1.3550	0.474	1355	2862	2862	1355	10.5	4517.2	BET	Test passed, above $1m^1$
FC-2-L	#8	2.36	2.33	0.00281	17.2353	27.5435	10.3082	27.5304	10.2951	42.08	88.04	2133.9	3144.7	0.679	1.4860	0.679	1486	2190	2190	1486	15.3	3467.8	BET	Test passed, above $1m^2$. From duplicate
FC-2-M	#16	1.18	3.33	0.00167	16.6532	26.2746	9.6214	26.2605	9.6073	28.18	24.00	3595.5	3172.9	1.133	0.8817	1.133	882	778	778	882	8.5	2939.4	BET	Test passed, above $1m^2$
FC-2-N	#30	0.600	2.00	0.00084	17.4645	26.5120	9.0475	26.4807	9.0162	8.01	20.00	7130.7	3172.8	2.247	1.0780	2.247	1078	480	480	1078	9.7	2156.3	BET	Test passed, above $1m^2$
FC-2-O	#50	0.300	1.67	0.00042	17.7288	26.9871	9.2583	26.9721	9.2433	38.08	6.50	14142.1	3178.2	4.450	1.2950	4.450	1295	291	291	1295	12.0	2158.6	BET	Test passed, above $1m^2$
FC-2-P	#100	0.150	1.67	0.00021	17.0402	25.2070	8.1668	25.1913	8.1511	18.14	48.36	28284.3	3128.2	9.042	1.6450	9.042	1645	182	182	1645	13.4	2742.0	BET	Test passed, above $1m^2$
FC-2-Q	#140	0.106	0.67	0.00013	17.6360	26.0796	8.4436	26.0586	8.4226	14.36	62.51	47583.1	3082.4	15.437	2.0140	15.437	2014	130	130	2014	17.0	1342.8	BET	Test passed, above $1m^2$
FC-2-R	#200	0.075	0.67	0.00009	16.6487	25.7736	9.1249	25.7506	9.1019	9.24	23.27	67292.7	3079.0	21.856	2.2030	21.856	2203	101	101	2203	20.1	1468.9	BET	Test passed, above $1m^2$
FC-2-S	#270	0.053	0.67	0.00006	17.3621	25.3773	8.0152	25.3480	7.9859	37.70	7.95	95526.1	3059.0	31.228	1.9890	31.228	1989	64	64	1989	15.9	1326.2	BET	Test passed, above $1m^2$
FC-2-T	-#270	0.044	6.90	0.00004	17.4471	22.4211	4.9740	22.3888	4.9417	34.15	21.97	135605.1	3037.5	44.644	5.8510	44.644	5851			5851	28.9	40377.0	BET	Test passed, above $1m^2$
			160.37																	**712**		**114246.0**		

Duplicates

FC-2-L	#8	2.36	2.33		17.3616	26.9437	9.5821	26.9382	9.5766	5.63	21.00				0.6439						6.2		BET	Test passed, above $1m^2$
FC-2-L(D1)	#8	2.36	2.33		17.3627	25.6836	8.3209	25.6753	8.3126	8.04	7.58				0.6989						5.8		BET	Test passed, above $1m^2$
FC-2-L(D2)	#8	2.36	2.33		17.2353	27.5435	10.3082	27.5304	10.2951	42.08	88.04				1.4860						15.3		BET	Test passed, above $1m^2$

Notes:
A_v: Specific surface area based on volume (m^{-1})
A_m: Specific surface area based on mass (m^2/kg)
GE: Geometrical Estimation method
BET: Brunauer-Emmett-Teller method

University of British Columbia
Department of Mining Engineering
"Assessment of waste rock weathering characteristics at the Antamina mine based on field cells experiment"

Table C3.4 Surface area determination by using both GE and BET methods of the diopside marble (FC-3) sample

Project: Waste Rock Study at Antamina Mine
Material type: Waste Rock - Class B
Rock type: Diopside marble
Location: Antamina Open Pit
Third tipping phase in the Pile 1
Description: Field cell (UBC-1-3A)

Sample code: FC-3
Sampling date: 07-Jul-06
Sampling by: C. Aranda
Testing date: Sept 8 to Sept 15, 2008
Testing by: C. Aranda
Review by: C. Aranda

Samples ID	Mesh		Mass	Geometric diameter (d)	BET measurments							$A_v = 6/d$	Particle density (ρ)	Specific surface area				Lamda		Final specific surface area (SSA_i)	Surface Area (SA)		Method	Observation
	(US)	(mm)	Total (wt)		Cell	Cell + sample 1	Sample 1	Cell + sample 1 (reweighed)	Sample 1 (rewt.)	Outgassing test	Outgassing time			$A_m = A_v / \rho$	SSA_{BET}	SSA_{GE}	SSA_{BET}	$\lambda = SSA_{BET}/SSA_{GE}$			BET (in cell)	$SA_i = SSA_i wt$		
			(kg)	(m)	(g)	(g)	(g)	(g)	(g)	(micro/min)	(h)	(m^{-1})	(kg/m^3)	(m^2/kg)	(m^2/g)	(m^2/kg)	(m^2/kg)	Initial	Final (adj.)	(m^2/kg)	(m^2)	(m^2)		
FC-3-A	4"	100.0	0.00																				GE	
FC-3-B	3"	75.0	0.00																				GE	
FC-3-C	2"	50.0	17.80	0.05706								105.2	2914.1	0.036		0.036			2552	92		1639.2	GE	
FC-3-D	11/2"	37.5	16.00	0.04304								139.4	2818.1	0.049		0.049			2661	132		2105.9	GE	
FC-3-E	1"	25.0	20.10	0.02946								203.6	2955.2	0.069		0.069			2807	193		3888.5	GE	
FC-3-F	3/4"	19.0	12.90	0.02264								265.0	2958.7	0.090		0.090			2909	261		3360.6	GE	
FC-3-G	1/2"	12.5	16.70	0.01475								406.7	2976.3	0.137		0.137			3075	420		7016.6	GE	
FC-3-H	3/8"	9.50	8.10	0.01071								560.5	2941.8	0.191		0.191			3198	609		4935.6	GE	
FC-3-I	1/4"	6.30	8.80	0.00771								778.4	2928.0	0.266		0.266			3325	884		7778.7	GE	
FC-3-J	#4	4.75	5.37	0.00531	22.3312	27.8041	5.4729	27.8015	5.4703	4.58	74.00	1129.6	2908.8	0.388	0.8799	0.388	880	2266	2266	880	4.8	4721.7	GE and BET	Test passed, above 1m^2
FC-3-K	#6	3.35	4.54	0.00399	22.9024	29.6883	6.7859	29.6788	6.7764	4.05	87.12	1504.1	2925.9	0.514	0.8036	0.514	804	1563	1563	804	5.4	3648.8	BET	Test passed, above 1m^2
FC-3-L	#8	2.36	3.51	0.00281	17.4484	25.8617	8.4133	25.8511	8.4027	3.35	92.53	2133.9	2918.3	0.731	0.4875	0.731	488	667	667	488	4.1	1710.5	BET	Test passed, above 1m^2
FC-3-M	#16	1.18	4.95	0.00167	17.6800	25.5262	7.8462	25.5179	7.8379	11.30	7.36	3595.5	2934.8	1.225	0.5826	1.225	583	476	476	583	4.6	2885.8	BET	Test passed, above 1m^2
FC-3-N	#30	0.600	2.48	0.00084	17.3668	26.4965	9.1297	26.4804	9.1136	5.63	18.56	7130.7	2954.8	2.413	0.7110	2.413	711	295	295	711	6.5	1760.9	BET	Test passed, above 1m^2
FC-3-O	#50	0.300	2.57	0.00042	16.6450	25.8641	9.2191	25.8510	9.2060	15.54	17.53	14142.1	2942.5	4.806	0.7112	4.806	711	148	148	711	6.5	1827.0	BET	Test passed, above 1m^2
FC-3-P	#100	0.150	3.43	0.00021	17.6365	26.2053	8.5688	26.1994	8.5629	11.02	7.50	28284.3	2865.6	9.870	0.5041	9.870	504	51	51	504	4.3	1726.6	BET	Test passed, above 1m^2
FC-3-Q	#140	0.106	2.14	0.00013	17.7280	26.4198	8.6918	26.4146	8.6866	9.49	20.56	47583.1	2822.0	16.862	0.4907	16.862	491	29	29	491	4.3	1050.4	BET	Test passed, above 1m^2
FC-3-R	#200	0.075	2.14	0.00009	17.0408	25.1851	8.1443	25.1716	8.1308	7.48	20.20	67292.7	2837.3	23.717	0.4705	23.717	471	20	20	471	3.8	1007.2	BET	Test passed, above 1m^2
FC-3-S	#270	0.053	1.71	0.00006	17.8889	25.5068	7.6179	25.4981	7.6092	8.13	23.62	95526.1	2821.6	33.855	0.5439	33.855	544	16	16	544	4.1	931.5	BET	Test passed, above 1m^2
FC-3-T	-#270	0.044	6.74	0.00004	17.4479	23.0474	5.5995	23.0235	5.5756	15.77	46.35	135605.1	2841.7	47.720	2.6970	47.720	2697			2697	15.0	18180.6	BET	Test passed, above 1m^2
			139.97																	**501**		**70176.2**		

Duplicates

FC-3-L	#8	2.36	3.51		17.4478	25.9129	8.4651	25.9030	8.4552	17.22	21.75				0.6534						5.5		BET	Test passed, above 1m^2
FC-3-L(D1)	#8	2.36	3.51		17.4484	25.8617	8.4133	25.8511	8.4027	3.35	92.53				0.4875						4.1		BET	Test passed, above 1m^2

Notes:
A_v: Specific surface area based on volume (m^{-1})
A_m: Specific surface area based on mass (m^2/kg)
GE: Geometrical Estimation method
BET: Brunauer-Emmett-Teller method

Table C3.5 Surface area determination by using both GE and BET methods of gray the hornfels (FC-4) sample

Project: Waste Rock Study at Antamina Mine
Material type: Waste Rock - Class B
Rock type: Gray hornfels
Location: Antamina Open Pit
Third/fourth tipping phase in the Pile 1
Description: Field cell (UBC-1-4A)

Sample code: FC-4
Sampling date: 07-Jul-06
Sampling by: C. Aranda
Testing date: Sept 16 to Sept 23, 2008
Testing by: C. Aranda
Review by: C. Aranda

Samples ID	Mesh		Mass	Geometric diameter (d)	BET measurments							$A_v = 6/d$	Particle density (ρ)	Specific surface area				Lamda		Final specific surface area (SSA_i)	Surface Area (SA)		Method	Observation
	(US)	(mm)	Total (wt)		Cell	Cell + sample 1	Sample 1	Cell + sample 1 (reweighed)	Sample 1 (rewt.)	Outgassing test	Outgassing time			$A_m = A_v / \rho$	SSA_{BET}	SSA_{GE}	SSA_{BET}	$\lambda = SSA_{BET}/SSA_{GE}$			BET (in cell)	$SA_i = SSA_i wt$		
			(kg)	(m)	(g)	(g)	(g)	(g)	(g)	(micro/min)	(h)	(m^{-1})	(kg/m^3)	(m^2/kg)	(m^2/g)	(m^2/kg)	(m^2/kg)	Initial	Final (adj.)	(m^2/kg)	(m^2)	(m^2)		
FC-4-A	4"	100.0	0.00																				GE	
FC-4-B	3"	75.0	1.70	0.09056								66.3	2733.6	0.024		0.024			1399	34		57.7	GE	
FC-4-C	2"	50.0	15.50	0.05818								103.1	2730.9	0.038		0.038			1498	57		876.7	GE	
FC-4-D	11/2"	37.5	13.20	0.04075								147.3	2746.4	0.054		0.054			1577	85		1116.0	GE	
FC-4-E	1"	25.0	19.90	0.03074								195.2	2742.2	0.071		0.071			1640	117		2322.7	GE	
FC-4-F	3/4"	19.0	10.30	0.02230								269.1	2730.2	0.099		0.099			1711	169		1737.0	GE	
FC-4-G	1/2"	12.5	13.90	0.01562								384.1	2744.9	0.140		0.140			1790	251		3482.1	GE	
FC-4-H	3/8"	9.50	6.60	0.01050								571.2	2740.2	0.208		0.208			1878	392		2584.4	GE	
FC-4-I	1/4"	6.30	7.30	0.00772								776.9	2741.0	0.283		0.283			1947	552		4027.6	GE	
FC-4-J	#4	4.75	4.10	0.00547	22.3312	28.2036	5.8724	28.2016	5.8704	3.47	18.21	1097.4	2745.6	0.400	0.3496	0.400	349.6	874.7	875	350	2.1	1433.4	GE and BET	Test passed, above 1m^2
FC-4-K	#6	3.35	3.50	0.00399	22.9020	29.2456	6.3436	29.2431	6.3411	6.79	22.27	1504.1	2743.0	0.548	0.5296	0.548	529.6	965.8	966	530	3.4	1853.6	BET	Test passed, above 1m^2
FC-4-L	#8	2.36	2.70	0.00281	17.0421	25.4590	8.4169	25.4541	8.4120	96.64	3.15	2133.9	2752.1	0.775	0.5630	0.775	563.0	726.1	726	563	4.7	1520.1	BET	Test passed, above 1m^2
FC-4-M	#16	1.18	5.00	0.00167	16.6495	24.7091	8.0596	24.7030	8.0535	5.83	8.21	3595.5	2753.5	1.306	0.6770	1.306	677.0	518.5	518	677	5.5	3385.0	BET	Test passed, above 1m^2
FC-4-N	#30	0.600	3.00	0.00084	16.6489	25.3857	8.7368	25.3827	8.7338	11.42	5.12	7130.7	2747.1	2.596	0.6724	2.596	672.4	259.0	259	672	5.9	2017.2	BET	Test passed, above 1m^2
FC-4-O	#50	0.300	4.30	0.00042	17.3622	25.4790	8.1168	25.4735	8.1113	3.64	25.29	14142.1	2753.2	5.137	0.6090	5.137	609.0	118.6	119	609	4.9	2618.1	BET	Test passed, above 1m^2
FC-4-P	#100	0.150	7.31	0.00021	17.0411	24.7546	7.7135	24.7497	7.7086	4.60	23.34	28284.3	2754.2	10.270	0.2156	10.270	215.6	21.0	21	216	1.7	1575.7	BET	Test passed, above 1m^2
FC-4-Q	#140	0.106	3.44	0.00013	17.7282	25.7401	8.0119	25.7300	8.0018	3.53	20.66	47583.1	2757.6	17.255	0.2370	17.255	237.0	13.7	14	237	1.9	815.1	BET	Test passed, above 1m^2
FC-4-R	#200	0.075	4.08	0.00009	17.8895	25.4888	7.5993	25.4808	7.5913	17.91	19.39	67292.7	2752.7	24.446	0.2359	24.446	235.9	9.6	10	236	1.8	963.4	BET	Test passed, above 1m^2
FC-4-S	#270	0.053	4.30	0.00006	17.6376	25.4565	7.8189	25.4545	7.8169	6.70	6.40	95526.1	2748.8	34.752	0.2176	34.752	217.6	6.3	6	218	1.7	935.5	BET	Test passed, above 1m^2
FC-4-T	-#270	0.044	8.82	0.00004	17.6796	23.5991	5.9195	23.5859	5.9063	4.09	42.81	135605.1	2774.5	48.875	1.5130	48.875	1513.0			1513	8.9	13347.8	BET	Test passed, above 1m^2
			138.95																	**336**		**46669.1**		
Duplicates																								
FC-4-K	#6	3.35	3.50		22.9020	29.2456	6.3436	29.2431	6.3411	6.79	22.27				0.5296						3.4		BET	Test passed, above 1m^2
FC-4-K(D1)	#6	3.35	3.50		22.9011	30.0272	7.1261	30.0186	7.1175	3.92	18.98				0.5634						4.0		BET	Test passed, above 1m^2
FC-4-L	#8	2.36	2.70		17.3629	24.6477	7.2848	24.6460	7.2831	6.77	5.39				0.4719						3.4		BET	Test passed, above 1m^2
FC-4-L(D1)	#8	2.36	2.70		17.0421	25.4590	8.4169	25.4541	8.4120	96.64	3.15				0.5630						4.7		BET	Test passed, above 1m^2

Notes:
A_v: Specific surface area based on volume (m^{-1})
A_m: Specific surface area based on mass (m^2/kg)
GE: Geometrical Estimation method
BET: Brunauer-Emmett-Teller method

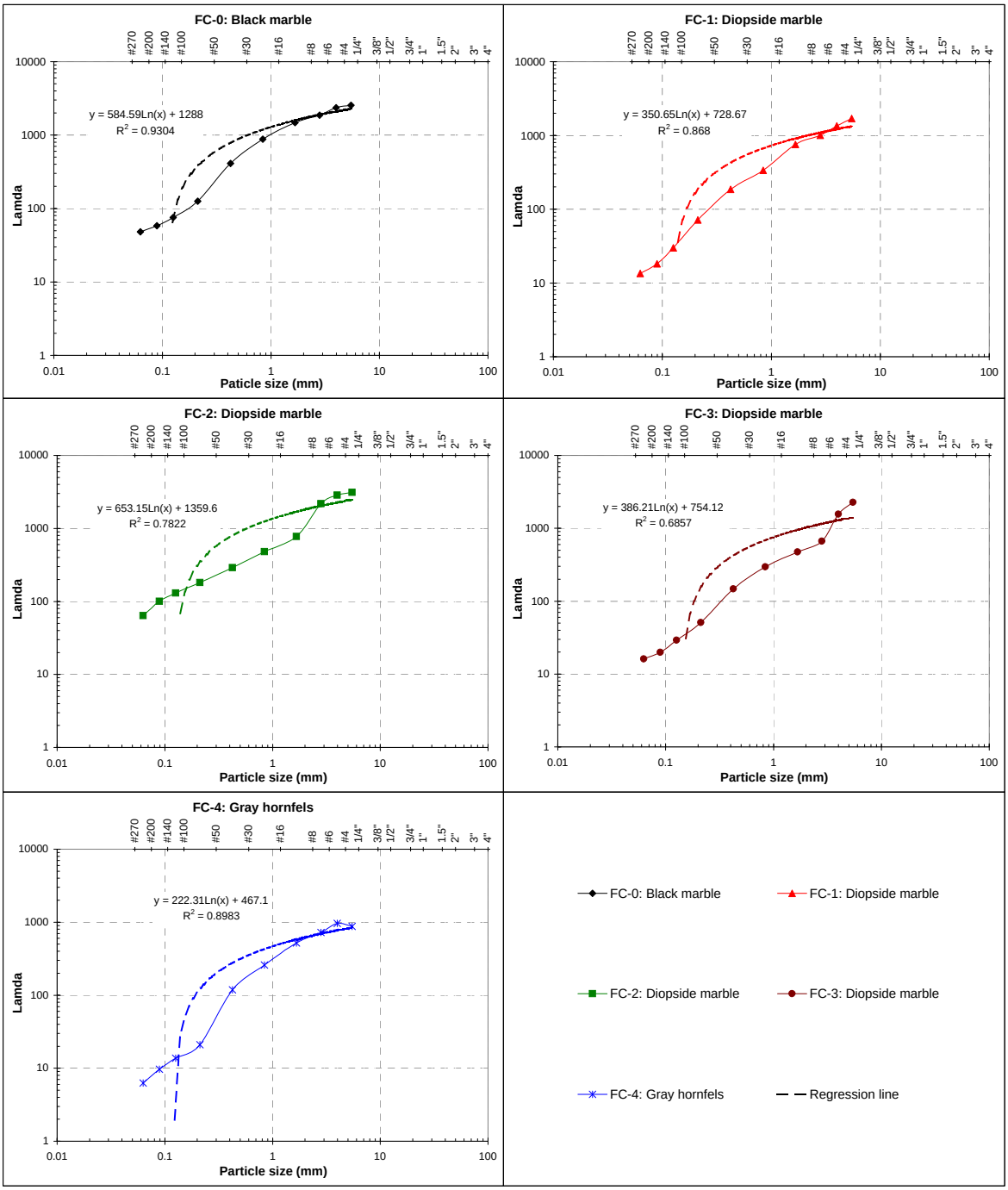

Figure C3.1 Logarithmic regression lines after plotting of lamda against the representative particle size of size fractions for all Class B waster rock samples

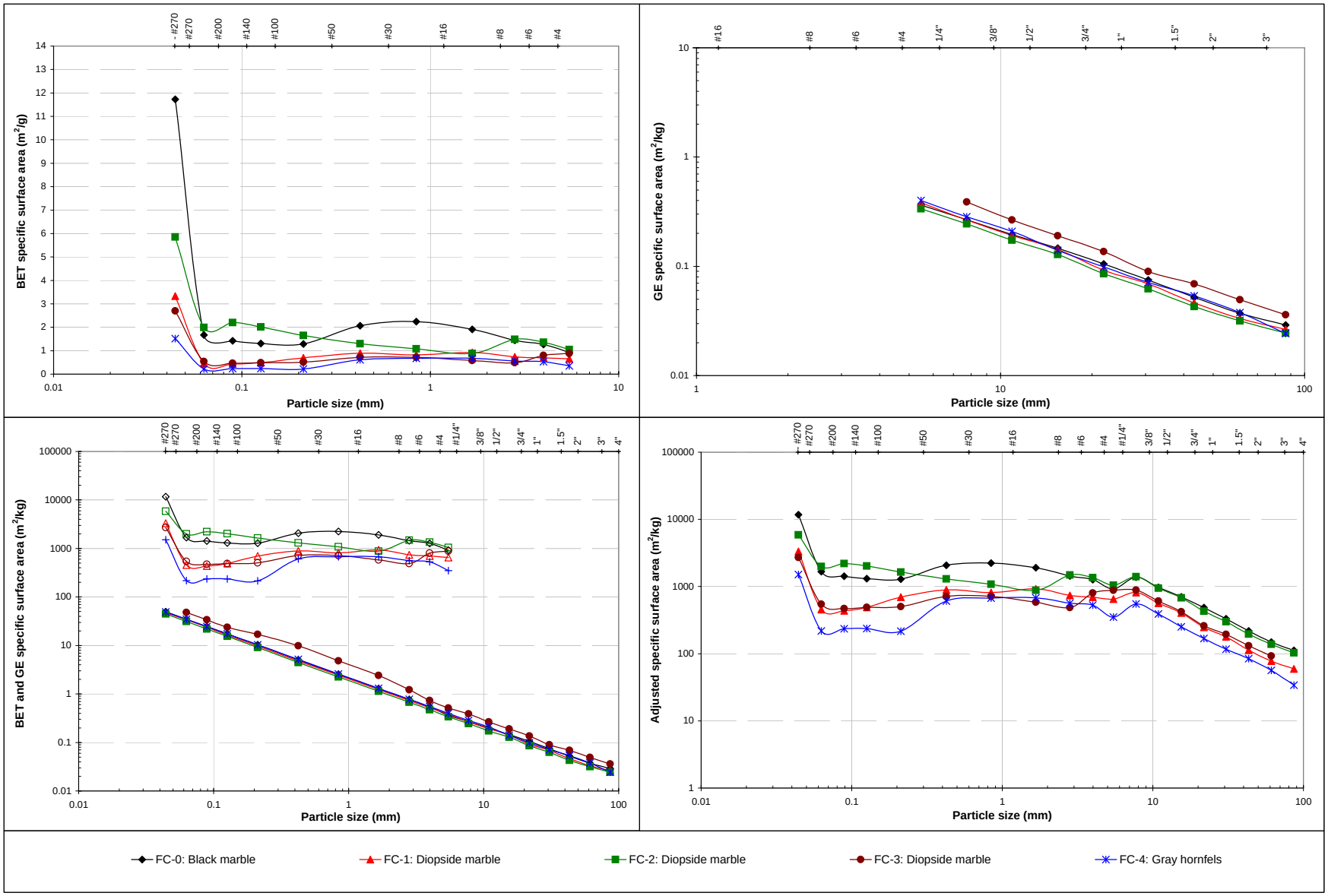

Figure C3.2 Specific surface area plots by using both GE and BET methods for all Class B waste rock samples

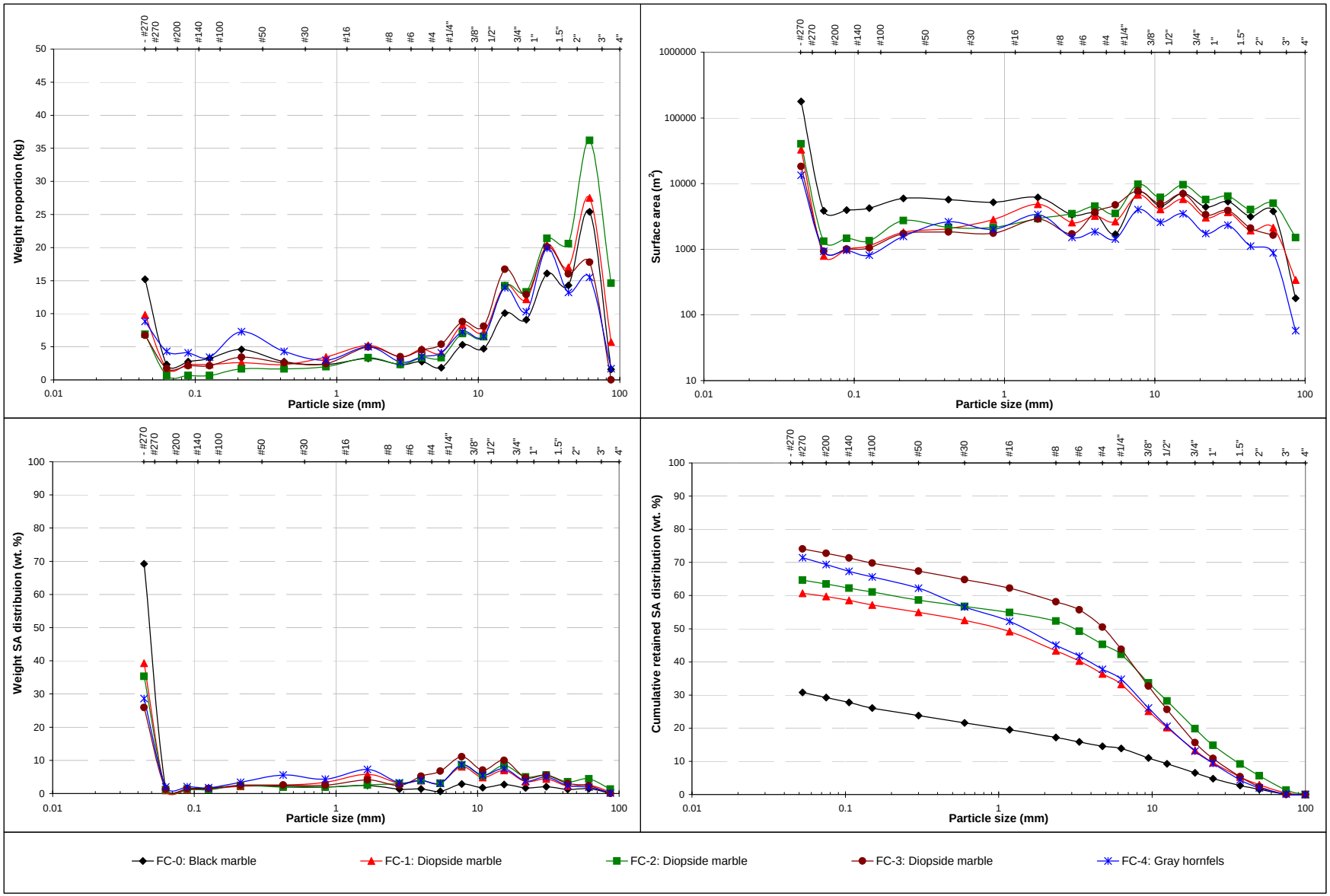

Figure C3.3 Surface area plots for all Class B waste rock samples

Appendix C4

Chemical Assay Results

University of British Columbia
Department of Mining Engineering
"Assessment of waste rock weathering characteristics at the Antamina mine based on field cells experiment"

Table C4.1 Sample preparation data and assay results of the black marble (FC-0) sample

Project:	Waste Rock Study at Antamina Mine	**Sample Code:**	**FC-0**
Material Type:	Waste rock - Class B	**Sampling Date:**	15-Mar-06
Rock Type:	Black marble	**Sampling by:**	C. Aranda
Location:	Antamina Open Pit	**Testing Date:**	25-Jul-08
	Protective layer in Pile 1	**Testing by:**	C. Aranda
Description:	Field Cell (UBC-1-0A and UBC-1-0B)	**Review by:**	C. Aranda

Samples ID	Size		Mass		Crusher			Sample Mass*	Observation	Total Metals by ICP-MS																																												ICP-MS	Leco
	(US)	(mm)	Total (wt.)	Sub sample	Primary	Secondary	Tertiary			Ag	Al	As	Ba	Be	Bi	Ca	Cd	Ce	Co	Cr	Cs	Cu	Fe	Ga	Ge	Hf	In	K	La	Li	Mg	Mn	Mo	Na	Nb	Ni	P	Pb	Rb	Re	Sb	Sc	Se	Sn	Sr	Ta	Te	Th	Ti	Tl	U	V	W	Y	Zn	Zr	S	S
			(kg)	(kg)	(Y/N)	(Y/N)	(Y/N)	(g)		ppm	%	ppm	ppm	ppm	ppm	%	ppm	ppm	ppm	ppm	ppm	ppm	%	ppm	ppm	ppm	ppm	%	ppm	ppm	%	ppm	ppm	ppm	ppm	ppm	ppm	ppm	ppm	ppm	ppm	ppm	ppm	ppm	ppm	ppm	ppm	%	ppm	ppm	ppm	ppm	ppm	ppm	ppm	%	%
FC-0-A	4"	+100.0	0.00					54.95	Duplicate (FC-0-D)																																																						
FC-0-B	3"	75.0 - 100.0	1.60	1.60	Y	Y	Y	49.52		0.26	0.93	22	40	0.34	0.3	28.8	0.13	9.7	1.9	10	2.72	66	0.49	2.58	0.07	0.2	0.005	0.47	4.3	12	0.68	123	0.78	0.11	3	0.2	310	15.3	33.3	0.006	0.95	1.5	2	0.4	755	0.18	0.05	1.9	0.05	0.28	1.5	9	0.4	4.6	39	3.9	0.31	0.28
FC-0-C	2"	50.0 - 75.0	25.40	6.60	Y	Y	Y	58.07		0.86	0.99	44	50	0.39	1.19	28.8	1.42	11.95	2	9	5.55	167	0.38	2.77	0.07	0.2	0.011	0.42	5.6	12.2	0.61	223	1.3	0.09	2.9	0.2	210	183.5	30.9	0.003	4.23	1.8	2	0.4	821	0.17	0.12	2	0.049	0.24	1	10	1.6	5.4	363	4.3	0.13	0.13
FC-0-D	11/2"	37.5 - 50.0	14.30	3.60	Y	Y	Y	57.50		8.52	1.49	70	80	0.5	20	27	10.05	16.3	2.7	16	5.06	395	0.87	4.41	0.09	0.3	0.436	0.76	8.2	29.3	0.7	329	0.86	0.11	4.6	7.1	260	1750	49.5	0.003	6.8	2.9	8	1.3	857	0.27	1.28	3.1	0.077	0.5	1	21	26.6	7.4	3610	7.5	0.75	0.66
FC-0-E	1"	25.0 - 37.5	16.10	2.00	Y	Y	Y	57.13		1.62	1.3	75	80	0.45	2.59	27.1	4.24	17.75	2.6	12	5.94	191	0.63	3.61	0.06	0.3	0.187	0.59	8.8	13.4	0.66	336	0.91	0.11	4.1	4.5	280	239	39.4	0.003	5.28	2.2	2	0.7	859	0.25	0.18	3	0.068	0.37	1.2	15	4.2	6.6	1350	8.5	0.19	0.15
FC-0-F	3/4"	19.0 - 25.0	9.10	1.30	Y	Y	Y	63.53		1.02	1.04	64	60	0.38	1.28	28.3	1.05	11.8	1.9	9	4.23	144.5	0.4	2.81	0.05	0.2	0.006	0.48	5.5	11.8	0.56	224	1.94	0.09	3.1	0.2	210	161.5	33.6	0.002	5.8	1.8	2	0.4	849	0.18	0.09	2.3	0.052	0.26	0.9	10	1.6	5.6	245	5.2	0.1	0.08
FC-0-G	1/2"	12.5 - 19.0	10.10	1.391	N	Y	Y	55.52		1.33	1.36	66	80	0.44	1.31	28.1	1.41	16.9	2.2	12	5.67	274	0.5	3.51	0.06	0.3	0.018	0.63	8.3	12.8	0.63	255	0.68	0.11	4	2.4	230	207	41.9	0.002	6.3	2.2	2	0.6	890	0.24	0.12	3	0.068	0.37	1.1	15	3	6.6	430	6.5	0.15	0.15
FC-0-H	3/8"	9.5 - 12.5	4.70	1.141	N	Y	Y	51.75		1.91	1.36	72	70	0.45	3.21	28.3	1.71	20.3	2.5	13	5.66	339	0.65	3.65	0.06	0.3	0.033	0.61	10.6	11.7	0.61	291	2.48	0.11	4.2	5.8	250	201	40.5	0.003	9.17	2.2	2	0.9	905	0.25	0.13	3.3	0.07	0.36	1.2	14	3	6.9	492	8.5	0.18	0.16
FC-0-I	1/4"	6.3 - 9.5	5.30	1.277	N	N	Y	60.93		1.6	1.37	75	70	0.47	1.97	27.5	2.28	16.3	2.6	15	5.72	322	0.62	3.59	0.05	0.3	0.045	0.64	8	12.1	0.63	299	7.34	0.1	4.1	9.8	250	203	42.4	0.004	7.28	2.2	2	0.8	864	0.25	0.14	2.9	0.07	0.36	1.1	15	17.7	6.8	631	8	0.19	0.2
FC-0-J	#4	4.75 - 6.30	1.84	0.096	N	N	Y	44.22		1.32	1.41	89	80	0.44	2.08	27.1	1.64	17.1	2.3	21	6.39	226	0.54	3.6	0.06	0.3	0.028	0.68	8.7	12.3	0.65	283	1.09	0.12	4.2	28.7	260	209	45.9	0.003	10.65	2.2	2	1	859	0.25	0.1	3.2	0.07	0.4	1.2	16	2.4	6.7	364	7.7	0.18	0.15
FC-0-K	#6	3.35 - 4.75	2.77	0.162	N	N	Y	51.77		2.48	1.52	89	80	0.48	5.2	26.8	4.79	18.25	2.6	17	6.95	323	0.66	4.01	0.07	0.4	0.105	0.69	9.4	14.6	0.69	376	1.64	0.1	4.5	17.2	280	380	47	0.002	10.25	2.3	3	1.4	847	0.26	0.22	3.3	0.077	0.39	1.3	18	5.3	7.3	1650	9.9	0.23	0.16
FC-0-L	#8	2.36 - 3.35	2.31	0.123	N	N	N	47.44		1.92	1.51	96	80	0.53	3.74	26.5	2.63	18.7	2.4	19	6.74	419	0.63	3.91	0.07	0.3	0.076	0.68	9.4	14.3	0.68	343	1.66	0.1	4.6	21.8	290	314	48.3	0.002	9.4	2.2	2	1.2	835	0.27	0.18	3.3	0.077	0.43	1.3	17	4.8	7.1	758	10.1	0.17	0.17
FC-0-M	#16	1.18 - 2.36	3.23	0.176	N	N	N	52.41		3.75	1.76	146	80	0.64	13.85	26.7	4.23	21.4	3	17	8.38	782	0.84	4.61	0.06	0.4	0.116	0.75	10.9	15.9	0.77	421	10.15	0.1	5.1	16.7	310	596	52	0.007	14.35	2.5	3	1.9	828	0.31	0.47	3.6	0.086	0.49	1.4	21	7.7	7.7	1530	12	0.27	0.23
FC-0-N	#30	0.60 - 1.18	2.31	0.129	N	N	N	48.35		3.97	2.02	192	80	0.8	13.95	24	4.59	21.6	3.5	25	9.52	854	1.21	5.26	0.06	0.5	0.155	0.75	11	18.5	1.01	511	5.38	0.1	5.8	30.7	350	785	53.5	0.003	19.8	3.1	3	2.4	727	0.35	0.53	3.9	0.099	0.54	1.6	27	18	7.9	1910	14.7	0.42	0.31
FC-0-O	#50	0.30 - 0.60	2.77	0.147	N	N	N	50.25		3.97	1.82	190	70	0.71	11.95	24.3	3.92	20.6	3.9	20	9.99	845	1.26	4.64	0.06	0.5	0.141	0.62	11.1	18.1	1.01	488	7.5	0.1	4.6	20.5	270	733	44	0.003	19.95	2.9	3	1.4	724	0.27	0.53	3.1	0.078	0.49	1.4	24	12.8	6.7	1740	13.7	0.41	0.37
FC-0-P	#100	0.15 - 0.30	4.61	0.275	N	N	N	69.16		1.88	1.19	124	70	0.41	7.05	27.6	2.62	14.35	2.6	12	6.6	471	0.7	2.75	0.05	0.3	0.09	0.52	7.2	11.1	0.63	323	6.27	0.07	2.9	10.3	190	427	33.5	0.003	12.75	1.9	2	0.8	813	0.17	0.3	1.9	0.048	0.37	1	13	63.2	5.9	1110	7.9	0.24	0.21
FC-0-Q	#140	0.106 - 0.15	3.23	0.194	N	N	N	57.76		2.59	1.04	85	70	0.35	4.52	29	2.64	15.6	2.4	8	4.89	427	0.54	2.36	0.06	0.2	0.077	0.52	7.8	8.7	0.51	296	3.52	0.06	2.7	1	160	363	32.2	0.002	9.56	1.6	3	0.7	873	0.16	0.21	1.9	0.046	0.34	0.9	10	6.2	6	1010	7.2	0.19	0.13
FC-0-R	#200	0.075 - 0.106	2.77	0.143	N	N	N	52.82		1.7	1.05	94	70	0.32	6.58	28.9	2.66	15.25	2.5	8	4.84	417	0.51	2.35	0.06	0.3	0.086	0.53	7.3	8.4	0.53	309	8.9	0.06	3.1	0.6	160	368	32.8	0.015	10.4	1.6	3	0.7	887	0.18	0.23	2	0.052	0.35	1	10	26.8	6.1	1010	7.1	0.17	0.13
FC-0-S	#270	0.053 - 0.075	2.31	0.132	N	N	N	52.67		1.52	1.18	105	70	0.37	7.67	28.4	3.09	17	3.2	12	5.54	544	0.58	2.71	0.06	0.3	0.106	0.56	7.7	9.1	0.6	363	9.93	0.07	3.8	18.2	200	442	36.1	0.007	13.6	1.8	3	3	883	0.23	0.24	2.4	0.063	0.43	1	13	20.1	6.5	1180	9.8	0.18	0.14
FC-0-T	-#270	-0.053	15.22	0.800	N	N	N	56.37		4.08	2.98	199	120	1.07	13.35	21.9	3.78	37.1	6.3	20	27.2	1100	1.48	7	0.07	1.3	0.14	1.12	17.3	24.8	0.85	761	11.6	0.08	9.7	11.9	1690	996	74.2	0.003	26	4.2	2	1.6	519	0.62	0.57	7.2	0.165	1.65	2.7	33	26.9	12.1	2800	37.7	0.11	0.09
Total			**129.95**						**Average (based on wt%)**	**2.64**	**1.47**	**91**	**75**	**0.52**	**6.40**	**27.0**	**3.40**	**18.2**	**2.9**	**13**	**8.28**	**402**	**0.70**	**3.84**	**0.07**	**0.4**	**0.116**	**0.64**	**8.8**	**15.9**	**0.67**	**350**	**3.67**	**0.10**	**4.5**	**6.9**	**410**	**519**	**43.3**	**0.003**	**9.6**	**2.4**	**3**	**0.9**	**807**	**0.27**	**0.35**	**3.2**	**0.075**	**0.51**	**1.3**	**17**	**12.4**	**7.0**	**1328**	**10.8**	**0.23**	**0.21**
									Max	**8.52**	**2.98**	**199**	**120**	**1.07**	**20.00**	**29.0**	**10.05**	**37.1**	**6.3**	**25**	**27.2**	**1100**	**1.48**	**7.00**	**0.09**	**1.3**	**0.436**	**1.12**	**17.3**	**29.3**	**1.01**	**761**	**11.60**	**0.12**	**9.7**	**30.7**	**1690**	**1750**	**74.2**	**0.015**	**26**	**4.2**	**8**	**3**	**905**	**0.62**	**1.28**	**7.2**	**0.165**	**1.65**	**2.7**	**33**	**63.2**	**12.1**	**3610**	**37.7**	**0.75**	**0.66**
									Min	**0.26**	**0.93**	**22**	**40**	**0.32**	**0.30**	**21.9**	**0.13**	**9.7**	**1.9**	**8**	**2.72**	**66**	**0.38**	**2.35**	**0.05**	**0.2**	**0.005**	**0.42**	**4.3**	**8.4**	**0.51**	**123**	**0.68**	**0.06**	**2.7**	**0.2**	**160**	**15.3**	**30.9**	**0.002**	**0.95**	**1.5**	**2**	**0.4**	**519**	**0.16**	**0.05**	**1.9**	**0.046**	**0.24**	**0.9**	**9**	**0.4**	**4.6**	**39**	**3.9**	**0.10**	**0.08**

QA/QC

Duplicates at the same laboratory										Ag	Al	As	Ba	Be	Bi	Ca	Cd	Ce	Co	Cr	Cs	Cu	Fe	Ga	Ge	Hf	In	K	La	Li	Mg	Mn	Mo	Na	Nb	Ni	P	Pb	Rb	Re	Sb	Sc	Se	Sn	Sr	Ta	Te	Th	Ti	Tl	U	V	W	Y	Zn	Zr	S	S
FC-0-D	11/2"	37.5	14.30	3.60	Y	Y	Y	57.50	a	8.52	1.49	60	80	0.5	20	27	10.05	16.3	2.7	16	5.06	395	0.87	4.41	0.09	0.3	0.436	0.76	8.2	29.3	0.7	329	0.86	0.11	4.6	7.1	260	1750	49.5	0.003	6.8	2.9	8	1.3	857	0.27	1.28	3.1	0.077	0.5	1	21	14.7	7.4	3350	7.5	0.75	0.66
FC-0-D (D1)	11/2"	37.5	14.30	3.60	Y	Y	Y	54.12	Duplicate same lab (FC-0-A) b	8.24	1.58	74	90	0.53	18.4	26.9	10.25	16.85	2.5	17	5.06	381	0.84	4.7	0.13	0.4	0.463	0.79	8.8	24.7	0.72	342	0.97	0.12	4.7	5	250	1690	49.7	0.003	8.15	2.8	7	1.3	847	0.29	1.28	3.1	0.08	0.49	1	21	34	7.4	3610	8.7	0.67	0.5
FC-0-D (D2)	11/2"	37.5	14.30	3.60	Y	Y	Y	54.12	Reanalysis of FC-0-A. c	10	1.7	70	90	0.44	19.7	31.4	10.5	15.8	2.1	16	5.49	461	0.96	4.25	0.06	0.3	0.461	0.84	7.7	21.8	0.74	366	0.8	0.12	4.3	21.9	270	1945	49.3	0.004	7.08	2.5	8	1.3	971	0.29	1.54	3.3	0.08	0.75	1.1	20	26.6	7	3690	7.5	0.77	
									% of variability (a&b)	3.3	-5.9	-20.9	-11.8	-5.8	8.3	0.4	-2.0	-3.3	7.7	-6.1	0.0	3.6	3.5	-6.4	-36.4	-28.6	-6.0	-3.9	-7.1	17.0	-2.8	-3.9	-12.0	-8.7	-2.2	34.7	3.9	3.5	-0.4	0.0	-18.1	3.5	13.3	0.0	1.2	-7.1	0.0	0.0	-3.8	2.0	0.0	0.0	-79.3	0.0	-7.5	-14.8	11.3	27.6
									% of variability (a&c)	-16.0	-13.2	-15.4	-11.8	12.8	1.5	-15.1	-4.4	3.1	25.0	0.0	-8.2	-15.4	-9.8	3.7	40.0	0.0	-5.6	-10.0	6.3	29.4	-5.6	-10.6	7.2	-8.7	6.7	-102.1	-3.8	-10.6	0.4	-28.6	-4.0	14.8	0.0	0.0	-12.5	-7.1	-18.4	-6.2	-3.8	-40.0	-9.5	4.9	-57.6	5.6	-9.7	0.0	-2.6	

Notes:

* Sample mass sent to the laboratory for metal by ICP-MS and total sulfur by Leco analysis

Table C4.2 Sample preparation data and assay results of the diopside marble (FC-1) sample

Project:	Waste Rock Study at Antamina Mine	**Sample Code:**	**FC-1**
Material Type:	Waste rock - Class B	**Sampling Date:**	12-May-06
Rock Type:	Diopside marble	**Sampling by:**	C. Aranda
Location:	Antamina Open Pit	**Testing Date:**	25-Jul-08
	First tipping phase in Pile 1	**Testing by:**	C. Aranda
Description:	Field Cell (UBC-1-1A)	**Review by:**	C. Aranda

Samples ID	Size (US)	Size (mm)	Mass Total (wt.) (kg)	Mass Sub sample (kg)	Crusher Primary (Y/N)	Crusher Secondary (Y/N)	Crusher Tertiary (Y/N)	Sample Mass* (g)	Observation
FC-1-A	4"	+100.0	0.00					48.93	Duplicate (FC-1-E)
FC-1-B	3"	75.0 - 100.0	5.70	5.70	Y	Y	Y	49.50	
FC-1-C	2"	50.0 - 75.0	27.50	7.30	Y	Y	Y	50.76	
FC-1-D	11/2"	37.5 - 50.0	17.00	3.60	Y	Y	Y	49.91	
FC-1-E	1"	25.0 - 37.5	20.40	2.40	Y	Y	Y	56.17	
FC-1-F	3/4"	19.0 - 25.0	12.20	1.50	Y	Y	Y	48.17	
FC-1-G	1/2"	12.5 - 19.0	14.30	0.963	N	Y	Y	47.82	
FC-1-H	3/8"	9.5 - 12.5	7.20	0.412	N	Y	Y	46.90	
FC-1-I	1/4"	6.3 - 9.5	8.30	0.461	N	N	Y	48.30	
FC-1-J	#4	4.75 - 6.30	4.06	0.156	N	N	Y	51.00	
FC-1-K	#6	3.35 - 4.75	4.63	0.197	N	N	N	52.83	
FC-1-L	#8	2.36 - 3.35	3.48	0.151	N	N	N	54.95	
FC-1-M	#16	1.18 - 2.36	5.21	0.209	N	N	N	54.67	
FC-1-N	#30	0.60 - 1.18	3.48	0.148	N	N	N	51.22	
FC-1-O	#50	0.30 - 0.60	2.32	0.102	N	N	N	43.21	
FC-1-P	#100	0.15 - 0.30	2.61	0.105	N	N	N	45.90	
FC-1-Q	#140	0.106 - 0.15	2.32	0.093	N	N	N	39.48	
FC-1-R	#200	0.075 - 0.106	2.32	0.098	N	N	N	48.04	
FC-1-S	#270	0.053 - 0.075	1.74	0.077	N	N	N	47.93	
FC-1-T	-#270	-0.053	9.85	0.412	N	N	N	50.33	
Total			**154.60**						

Total Metals by ICP-MS

Samples ID	Ag ppm	Al %	As ppm	Ba ppm	Be ppm	Bi ppm	Ca %	Cd ppm	Ce ppm	Co ppm	Cr ppm	Cs ppm	Cu ppm	Fe %	Ga ppm	Ge ppm	Hf ppm
FC-1-A																	
FC-1-B	0.55	2.65	35	40	0.9	1.88	27.2	0.82	37.5	6.1	24	4.35	179.5	1.16	6.46	0.07	1.8
FC-1-C	1.02	2.52	32	30	0.86	2.96	27.3	1.18	34.5	4.3	19	2.25	254	1.08	6.25	0.07	1.4
FC-1-D	1.26	2.55	47	30	0.89	3.92	26.4	1.33	32.3	4.4	19	2.89	292	1.1	6.22	0.07	1.2
FC-1-E	0.5	3.09	51	80	1.02	2.41	23.5	0.71	33.2	4.4	21	2.83	522	1.18	7.34	0.08	1.5
FC-1-F	3.65	3.16	64	80	1.03	13.45	24	1.31	38.8	5.5	23	3.34	592	1.25	7.67	0.07	1.5
FC-1-G	2.42	3.14	53	100	0.99	5.56	22.5	1.39	35.1	4.4	27	3.74	1550	1.22	7.63	0.06	1.4
FC-1-H	2.77	3.35	85	130	1	11.55	22.5	1.95	34.9	4.2	27	3.51	682	1.31	7.9	0.08	1.4
FC-1-I	4.62	3.24	61	110	1.02	17.1	22.6	1.32	41	4.1	24	4.07	812	1.24	7.94	0.07	1.3
FC-1-J	1.83	3.19	91	100	1.16	5.48	22.7	0.79	37.5	3.9	23	3.95	838	1.23	7.72	0.07	1.3
FC-1-K	3.76	3.29	56	110	1.05	13.55	22.9	2.08	36.3	4.2	25	4.62	1000	1.27	7.99	0.08	1.3
FC-1-L	4.17	3.49	83	140	1.14	12.15	22	1.75	36.9	4.6	28	4.85	794	1.29	8.23	0.07	1.3
FC-1-M	4.75	3.49	94	130	0.99	14.15	21.1	2.25	35.9	6	23	4.92	1090	1.48	8.6	0.08	1.3
FC-1-N	7.74	3.71	127	130	1.05	22.6	21	3.23	41	6.3	21	5.57	1510	1.73	9	0.08	1.3
FC-1-O	8.05	3.48	103	120	1.11	29.3	19.95	2.86	40.6	6.9	23	5.09	1590	2.04	8.63	0.09	1.2
FC-1-P	6.38	2.57	116	90	0.86	22.9	21.3	2.73	29.2	7.2	15	4.37	1760	1.75	6.44	0.07	0.9
FC-1-Q	5.08	1.63	70	70	0.52	16.05	23.8	2.18	21.5	4.2	13	2.95	1330	1.06	4.07	0.06	0.5
FC-1-R	3.58	1.42	72	60	0.45	12.2	25.2	2.17	19.95	3.7	9	2.42	1050	0.83	3.54	0.06	0.5
FC-1-S	3.46	1.68	84	70	0.51	13.75	27.8	2.53	20.3	3.3	9	2.63	1200	0.88	4.12	0.05	0.5
FC-1-T	6.13	2.68	128	110	0.95	32.9	25.1	3.81	36	5.1	16	10.35	1560	1.15	7.07	0.07	0.8
Average (based on wt%)	**2.67**	**2.90**	**63**	**78**	**0.95**	**9.68**	**24.4**	**1.57**	**34.9**	**4.7**	**21**	**3.80**	**761**	**1.21**	**7.08**	**0.07**	**1.3**
Max	**8.05**	**3.71**	**128**	**140**	**1.16**	**32.90**	**27.8**	**3.81**	**41**	**7.2**	**28**	**10.35**	**1760**	**2.04**	**9.00**	**0.09**	**1.8**
Min	**0.50**	**1.42**	**32**	**30**	**0.45**	**1.88**	**19.95**	**0.71**	**19.95**	**3.3**	**9**	**2.25**	**179.5**	**0.83**	**3.54**	**0.05**	**0.5**

Samples ID	In ppm	K %	La ppm	Li ppm	Mg %	Mn ppm	Mo ppm	Na %	Nb ppm	Ni ppm	P ppm	Pb ppm	Rb ppm	Re ppm	Sb ppm	Sc ppm
FC-1-A																
FC-1-B	0.033	0.21	18.7	6.6	1.23	625	19.65	0.03	8.4	33.8	410	114	18.5	0.003	3.43	4.3
FC-1-C	0.029	0.22	17.3	7.6	1.15	698	11.5	0.03	8.1	15.8	300	141.5	20.4	0.003	5.89	4.1
FC-1-D	0.045	0.28	16.2	9.9	1.12	718	27.5	0.04	7.9	14.2	330	138	27	0.006	3.84	4.1
FC-1-E	0.069	0.83	16.6	11.7	1.13	634	91.6	0.1	8	24	380	59.3	40.9	0.015	4.19	4.3
FC-1-F	0.052	0.83	19.6	12.1	1.18	753	148.5	0.08	8	30.7	400	485	44.6	0.035	11.75	4.3
FC-1-G	0.129	1.14	17.7	12.4	1.1	692	60.5	0.11	8.2	44.5	390	103.5	54.7	0.017	7.51	4.1
FC-1-H	0.128	1.28	17.3	14.1	1.12	834	100	0.11	8.1	52.5	400	229	58	0.018	18.3	4.3
FC-1-I	0.08	1.21	20.6	15.4	1.1	714	85.9	0.12	7.9	42.1	390	330	59.9	0.013	14.05	4.2
FC-1-J	0.076	1.14	19	13.2	1.06	694	97.4	0.12	7.6	28.2	400	115.5	54.3	0.022	21.9	4.1
FC-1-K	0.131	1.26	17.8	16	1.12	773	95.9	0.11	8.1	30.6	400	619	64.4	0.029	13.45	4.3
FC-1-L	0.109	1.41	18.7	15.8	1.08	759	78.6	0.12	8.1	30.2	390	356	69.3	0.017	19.3	4.3
FC-1-M	0.205	1.43	18.2	15.9	1.04	758	91.3	0.11	7.9	27.2	380	394	73.1	0.015	24.4	4.3
FC-1-N	0.222	1.45	20.8	16.7	1.02	802	96.5	0.11	8.6	22.9	370	659	75.6	0.024	43.4	4.2
FC-1-O	0.259	1.3	20.8	16.9	0.93	762	147.5	0.11	8	31.2	330	617	67.8	0.045	35.2	3.9
FC-1-P	0.242	1.02	14.7	13.9	0.73	624	232	0.1	6.1	13.7	310	469	54.5	0.067	49.4	3.2
FC-1-Q	0.173	0.71	10.7	9.3	0.52	497	189.5	0.07	4.3	16.6	250	382	37.2	0.044	29.4	2.3
FC-1-R	0.164	0.66	10.1	7.4	0.46	470	153	0.06	3.7	10.2	200	274	32.6	0.037	28	2
FC-1-S	0.208	0.76	10.1	9	0.52	528	147	0.07	3.4	9	200	258	37.1	0.037	28.8	2.5
FC-1-T	0.295	1.23	17.3	24.6	1.24	761	177	0.1	5.4	11	420	567	74.7	0.05	38.5	4.5
Average (based on wt%)	**0.101**	**0.81**	**17.5**	**12.3**	**1.10**	**703**	**81.1**	**0.08**	**7.7**	**26**	**360**	**252**	**44.4**	**0.0**	**13.6**	**4.1**
Max	**0.295**	**1.45**	**20.8**	**24.6**	**1.24**	**834**	**232.0**	**0.12**	**8.6**	**52.5**	**420**	**659.0**	**75.6**	**0.067**	**49.4**	**4.5**
Min	**0.029**	**0.21**	**10.1**	**6.6**	**0.46**	**470**	**11.5**	**0.03**	**3.4**	**9**	**200**	**59.3**	**18.5**	**0.003**	**3.43**	**2**

Samples ID	Se ppm	Sn ppm	Sr ppm	Ta ppm	Te ppm	Th ppm	Ti %	Tl ppm	U ppm	V ppm	W ppm	Y ppm	Zn ppm	Zr ppm	ICP-MS S %	Leco S %
FC-1-A																
FC-1-B	2	1.1	1340	0.51	0.12	6.5	0.139	0.1	1.4	27	4.2	13.5	337	53.8	0.14	0.09
FC-1-C	2	1.1	1210	0.47	0.11	6	0.134	0.12	1.2	26	7	12.1	496	44.1	0.11	0.12
FC-1-D	2	1.1	1110	0.47	0.19	5.7	0.133	0.17	1.2	29	6.6	11.4	588	36.7	0.15	0.15
FC-1-E	2	1.4	878	0.5	0.08	6.4	0.139	0.45	1.3	29	6.8	11.5	326	43.2	0.19	0.14
FC-1-F	3	1.7	901	0.5	0.27	6.7	0.14	0.34	1.3	30	9.1	12	634	46.6	0.18	0.14
FC-1-G	2	1.9	806	0.53	0.14	6.3	0.133	0.4	1.3	30	6.4	11.1	478	39.8	0.3	0.25
FC-1-H	2	2.1	833	0.52	0.21	6.6	0.139	0.42	1.3	32	7.7	11.9	845	41.9	0.21	0.19
FC-1-I	3	2.1	858	0.5	0.29	6.4	0.133	0.45	1.3	32	8.7	11.3	483	37.4	0.32	0.27
FC-1-J	2	2.2	883	0.47	0.12	6.5	0.132	0.42	1.4	33	6.6	11.3	335	39	0.24	0.17
FC-1-K	4	3.3	851	0.51	0.4	6.6	0.137	0.54	1.4	33	9.7	11.5	824	39.6	0.26	0.2
FC-1-L	3	3.7	816	0.5	0.27	6.4	0.137	0.53	1.4	34	11.9	11.4	748	39.5	0.28	0.23
FC-1-M	3	4.5	752	0.5	0.29	6.2	0.134	0.59	1.3	35	13.1	11.2	972	37.6	0.46	0.34
FC-1-N	4	4.5	717	0.52	0.52	6.6	0.14	0.64	1.5	35	19.2	11.6	1360	39.6	0.65	0.51
FC-1-O	5	3.4	639	0.48	0.68	6.2	0.133	0.61	1.4	34	29.1	11.1	1210	37.1	1.05	0.82
FC-1-P	4	2.9	686	0.36	0.63	4.8	0.099	0.54	1.1	24	24.1	9.3	1090	25.9	1.1	0.93
FC-1-Q	4	2	831	0.27	0.46	3.1	0.071	0.36	0.8	15	46.9	7.5	842	15.7	0.66	0.64
FC-1-R	3	1.9	917	0.23	0.29	2.9	0.062	0.3	0.7	13	29.8	7	809	14.2	0.48	0.43
FC-1-S	3	1.9	1045	0.15	0.23	3.4	0.069	0.37	0.8	15	23.4	7.3	871	15.3	0.45	0.44
FC-1-T	4	3.4	937	0.32	0.49	5.8	0.115	1.01	1.3	29	37.8	10.6	1450	22.7	0.35	0.34
Average (based on wt%)	**3**	**2.0**	**960**	**0.47**	**0.22**	**6.1**	**0.131**	**0.38**	**1.3**	**29**	**11.4**	**11.4**	**645**	**39.2**	**0.26**	**0.23**
Max	**5**	**4.5**	**1340**	**0.53**	**0.68**	**6.7**	**0.14**	**1.01**	**1.5**	**35**	**46.9**	**13.5**	**1450**	**53.8**	**1.1**	**0.93**
Min	**2**	**1.1**	**639**	**0.15**	**0.08**	**2.9**	**0.062**	**0.1**	**0.7**	**13**	**4.2**	**7**	**326**	**14.2**	**0.11**	**0.09**

QA/QC

Duplicates at the same laboratory

Samples ID	Size (US)	Size (mm)	Total (kg)	Sub sample (kg)	Primary	Secondary	Tertiary	Sample Mass* (g)	Observation
FC-1-E	1"	25.0	20.40	2.40	Y	Y	Y	56.17	a
FC-1-E (D1)	1"	25.0	20.40	2.40	Y	Y	Y	48.69	Duplicate same lab (FC-1-A) b
FC-1-E (D2)	1"	25.0	20.40	2.40	Y	Y	Y	48.69	Reanalysis of FC-1-A. c

Samples ID	Ag	Al	As	Ba	Be	Bi	Ca	Cd	Ce	Co	Cr	Cs	Cu	Fe	Ga	Ge	Hf
FC-1-E (a)	0.5	3.09	51	80	1.02	2.41	23.5	0.71	33.2	4.4	21	2.83	522	1.18	7.34	0.08	1.5
FC-1-E (D1) (b)	0.58	3.09	55	90	0.97	2.03	23.2	0.58	31.9	4.3	21	3.14	875	1.13	7.34	0.07	1.5
FC-1-E (D2) (c)	0.62	3.37	53	90	0.87	2.07	25.9	0.68	35.3	4.4	21	2.88	387	1.18	7.67	0.08	1.4
% of variability (a & b)	-14.8	0.0	-7.5	-11.8	5.0	17.1	1.3	20.2	4.0	2.3	0.0	-10.4	-50.5	4.3	0.0	13.3	0.0
% of variability (a & c)	-21.4	-8.7	-3.8	-11.8	15.9	15.2	-9.7	4.3	-6.1	0.0	0.0	-1.8	29.7	0.0	-4.4	0.0	6.9

Samples ID	In	K	La	Li	Mg	Mn	Mo	Na	Nb	Ni	P	Pb	Rb	Re	Sb	Sc
FC-1-E (a)	0.069	0.83	16.6	11.7	1.13	634	91.6	0.1	8	24	380	59.3	40.9	0.015	4.19	4.3
FC-1-E (D1) (b)	0.088	0.88	15.9	12	1.13	614	80.9	0.1	7.9	28.7	350	65.5	43.5	0.014	4.6	4.4
FC-1-E (D2) (c)	0.048	0.88	17.1	13.9	1.27	684	83.1	0.11	7.8	34.1	430	75.5	41.5	0.014	4.14	4.4
% of variability (a & b)	-24.2	-5.8	4.3	-2.5	0.0	3.2	12.4	0.0	1.3	-17.8	8.2	-9.9	-6.2	6.9	-9.3	-2.3
% of variability (a & c)	35.9	-5.8	-3.0	-17.2	-11.7	-7.6	9.7	-9.5	2.5	-34.8	-12.3	-24.0	-1.5	6.9	1.2	-2.3

Samples ID	Se	Sn	Sr	Ta	Te	Th	Ti	Tl	U	V	W	Y	Zn	Zr	S	S
FC-1-E (a)	2	1.4	878	0.5	0.08	6.4	0.139	0.45	1.3	29	6.8	11.5	326	43.2	0.22	0.14
FC-1-E (D1) (b)	2	1.4	880	0.49	0.09	6.3	0.138	0.58	1.3	30	6.8	11.5	257	43.6	0.19	0.15
FC-1-E (D2) (c)	2	1.4	977	0.53	0.09	6.5	0.151	0.57	1.4	32	6.1	11.5	287	43.8	0.16	
% of variability (a & b)	0.0	0.0	-0.2	2.0	-11.8	1.6	0.7	-25.2	0.0	-3.4	0.0	0.0	23.7	-0.9	14.6	-6.9
% of variability (a & c)	0.0	0.0	-10.7	-5.8	-11.8	-1.6	-8.3	-23.5	-7.4	-9.8	10.9	0.0	12.7	-1.4	31.6	

Notes:

* Sample mass sent to the laboratory for metal by ICP-MS and total sulfur by Leco analysis

University of British Columbia
Department of Mining Engineering
"Assessment of waste rock weathering characteristics at the Antamina mine based on field cells experiment"

Table C4.3 Sample preparation data and assay results of the diopside marble (FC-2) sample

Project:	Waste Rock Study at Antamina Mine	**Sample Code:**	**FC-2**
Material Type:	Waste rock - Class B	**Sampling Date:**	29-Jun-06
Rock Type:	Diopside marble	**Sampling by:**	C. Aranda
Location:	Antamina Open Pit	**Testing Date:**	25-Jul-08
	Second tipping phase in Pile 1	**Testing by:**	C. Aranda
Description:	Field Cell (UBC-1-2A and UBC-1-2B)	**Review by:**	C. Aranda

Samples ID	Size		Mass		Crusher			Sample Mass*	Observation
	(US)	(mm)	Total (wt.)	Sub sample	Primary	Secondary	Tertiary		
			(kg)	(kg)	(Y/N)	(Y/N)	(Y/N)	(g)	
FC-2-A	4"	+100.0	0.00					35.10	Duplicate (FC-2-P)
FC-2-B	3"	75.0 - 100.0	14.60	10.00	Y	Y	Y	51.82	
FC-2-C	2"	50.0 - 75.0	36.20	8.60	Y	Y	Y	55.42	
FC-2-D	11/2"	37.5 - 50.0	20.60	5.50	Y	Y	Y	55.22	
FC-2-E	1"	25.0 - 37.5	21.40	2.90	Y	Y	Y	51.49	
FC-2-F	3/4"	19.0 - 25.0	13.30	1.90	Y	Y	Y	54.89	
FC-2-G	1/2"	12.5 - 19.0	14.20	0.962	N	Y	Y	51.02	
FC-2-H	3/8"	9.5 - 12.5	6.50	0.362	N	Y	Y	51.53	
FC-2-I	1/4"	6.3 - 9.5	7.00	0.456	N	N	Y	55.63	
FC-2-J	#4	4.75 - 6.30	3.33	0.124	N	N	Y	46.44	
FC-2-K	#6	3.35 - 4.75	3.33	0.131	N	N	N	51.16	
FC-2-L	#8	2.36 - 3.35	2.33	0.160	N	N	N	52.63	
FC-2-M	#16	1.18 - 2.36	3.33	0.230	N	N	N	55.37	
FC-2-N	#30	0.60 - 1.18	2.00	0.161	N	N	N	55.43	
FC-2-O	#50	0.30 - 0.60	1.67	0.125	N	N	N	51.15	
FC-2-P	#100	0.15 - 0.30	1.67	0.111	N	N	N	34.87	
FC-2-Q	#140	0.106 - 0.15	0.67	0.053	N	N	N	46.00	
FC-2-R	#200	0.075 - 0.106	0.67	0.047	N	N	N	39.24	
FC-2-S	#270	0.053 - 0.075	0.67	0.040	N	N	N	35.05	
FC-2-T	-#270	-0.053	6.90	0.250	N	N	N	50.55	
Total			**160.37**						

Total Metals by ICP-MS

Samples ID	Ag	Al	As	Ba	Be	Bi	Ca	Cd	Ce	Co	Cr	Cs	Cu	Fe	Ga	Ge	Hf
	ppm	%	ppm	ppm	ppm	ppm	%	ppm	ppm	ppm	ppm	ppm	ppm	%	ppm	ppm	ppm
FC-2-A																	
FC-2-B	1.27	6.34	19	150	1.96	8.23	18.1	0.38	64.8	5.8	71	1.06	275	3.28	16.8	0.12	2
FC-2-C	4.1	6.05	27	290	1.94	42.8	15.6	1.3	72.9	8.4	75	1.74	329	2.89	15.5	0.17	1.7
FC-2-D	2.21	6.24	17	280	1.72	13.25	16.7	0.43	74.3	7.1	65	1.46	305	2.88	16.6	0.15	1.9
FC-2-E	18.5	5.98	33	240	2.24	45	16.7	0.59	98.1	7.5	60	1.56	322	2.96	16.25	0.17	1.7
FC-2-F	4.5	5.8	22	160	1.92	20.9	18.4	0.7	87.6	7.1	68	1.34	379	3.28	16.05	0.13	2
FC-2-G	4.07	6.49	29	180	2.1	21.6	18.65	0.92	79.3	7.1	70	2.63	762	3.88	18.25	0.13	2.4
FC-2-H	4.29	6.45	21	180	1.85	20.1	18.05	0.46	71.6	6.7	65	1.68	853	3.71	17.3	0.12	2.1
FC-2-I	3.18	6.42	31	190	2.28	16.7	17.8	1.01	88.3	6.5	74	2.62	488	3.32	17.25	0.15	2.2
FC-2-J	6.29	6.41	44	180	2.22	24.9	17.65	1.01	87.7	7.3	75	2.99	610	3.78	17.95	0.14	2.1
FC-2-K	4.59	6.55	57	200	1.86	22	17.9	0.99	76	7.7	75	3.62	764	3.78	17.95	0.13	2.2
FC-2-L	5.11	6.39	64	200	2.11	24.7	17.2	0.99	80.7	7.6	70	3.72	625	3.65	17.55	0.13	2.1
FC-2-M	6.44	6.27	62	200	2	28	16.85	1.68	79.2	9.3	70	3.66	777	4.13	17.45	0.14	2.1
FC-2-N	8.27	5.97	92	210	2.03	36.5	16.1	2.49	76.6	12.4	66	4.24	1075	4.94	16.85	0.15	2
FC-2-O	9.42	5.67	107	180	1.79	44.8	15.3	2.94	72.8	16.1	63	4.05	1590	5.47	16	0.16	1.9
FC-2-P	13.5	5.24	129	160	1.32	63.1	14.3	3.63	55.7	15.8	64	4.5	3080	5.41	14.85	0.15	1.7
FC-2-Q	15.65	4.96	139	180	1.33	77.6	13.6	3.82	52.4	14.8	81	4.89	3710	5.18	14.05	0.15	1.4
FC-2-R	16.1	4.96	156	210	1.31	88.8	13.3	3.92	52.2	13.8	76	5.28	3560	4.91	14.25	0.14	1.3
FC-2-S	14.4	5.03	164	220	1.39	85.3	13.5	3.82	50.7	13.4	79	5.62	3330	4.56	14.3	0.12	1.2
FC-2-T	17.2	4.78	306	210	1.62	125	15.8	5.35	72.3	15.9	43	14.55	2560	4.27	13.9	0.14	1.4
Average (based on wt%)	**6.55**	**6.09**	**44**	**225**	**1.96**	**33.23**	**16.9**	**1.13**	**78.3**	**8.1**	**68**	**2.51**	**606**	**3.34**	**16.40**	**0.15**	**1.9**
Max	**18.50**	**6.55**	**306**	**290**	**2.28**	**#####**	**18.7**	**5.35**	**98.1**	**16.1**	**81**	**14.55**	**3710**	**5.47**	**18.25**	**0.17**	**2.4**
Min	**1.27**	**4.78**	**17**	**150**	**1.31**	**8.23**	**13.3**	**0.38**	**50.7**	**5.8**	**43**	**1.06**	**275**	**2.88**	**13.9**	**0.12**	**1.2**

Samples ID	In	K	La	Li	Mg	Mn	Mo	Na	Nb	Ni	P	Pb	Rb	Re	Sb	Sc	Se	Sn	Sr	Ta	Te	Th	Ti	Tl	U	V	W	Y	Zn	Zr	ICP-MS S	Leco S
	ppm	%	ppm	ppm	%	ppm	ppm	%	ppm	ppm	ppm	ppm	ppm	ppm	ppm	ppm	ppm	ppm	ppm	ppm	ppm	ppm	%	ppm	ppm	ppm	ppm	ppm	ppm	ppm	%	%
FC-2-A																																
FC-2-B	0.086	2.07	26.1	7.4	1.61	2040	8.35	0.25	12.8	142.5	630	152.5	62	0.003	1.51	9.9	2	3.7	122.5	0.79	0.32	11.9	0.288	0.29	2.6	109	27.4	22	172	55.8	0.53	0.45
FC-2-C	0.096	2.71	35.5	9.4	1.56	1915	20.4	0.25	15.5	151.5	710	351	74.1	0.002	2.46	9.9	4	3.5	162.5	1.09	1.11	12.5	0.3	0.4	2.3	100	18.2	22.4	451	43.2	0.98	0.82
FC-2-D	0.078	2.43	33.2	7.3	1.64	2060	12.65	0.25	16	120	710	231	66.7	0.002	1.9	10.3	3	3.3	138	1.17	0.59	13.7	0.313	0.32	2.4	104	12.3	22.3	194	46.7	0.68	0.75
FC-2-E	0.091	2.58	44.8	9.3	1.67	1975	10.6	0.2	14.7	105	690	2790	75.7	0.002	3.16	9.7	11	3.8	137	1.09	3.57	12.8	0.292	0.52	3.3	103	16.7	22.1	205	41.5	0.84	0.96
FC-2-F	0.114	2.07	40.3	7.6	1.73	2140	11.65	0.16	13.4	132.5	670	807	64.2	0.003	2.35	10.3	4	3.8	114.5	0.84	0.92	10.7	0.291	0.33	2.6	109	17.2	22.7	260	52.4	0.94	0.8
FC-2-G	0.235	2.11	36	10	1.62	2240	23.7	0.22	15.4	122.5	700	521	68	0.005	3.14	10.9	3	6.1	121	1.02	0.82	11.7	0.321	0.4	2.9	112	15.5	25.2	346	62.9	0.96	0.72
FC-2-H	0.181	2.14	31.4	7.6	1.61	2130	14.1	0.22	14.2	113	680	437	67.7	0.004	2.05	10.3	3	5.4	121.5	0.88	0.75	11.8	0.307	0.36	2.6	107	46	22.8	230	54.6	1.13	0.94
FC-2-I	0.166	2.34	38.7	10	1.68	2060	13.4	0.21	15	149.5	710	471	75.4	0.003	2.6	10.8	3	4.9	129.5	0.95	0.64	13.3	0.319	0.38	3.2	111	25.2	24.6	389	57.3	0.8	0.64
FC-2-J	0.334	2.2	38.4	11	1.53	2130	13.6	0.25	14.2	162.5	680	574	73.9	0.005	3.19	10.4	4	5	122.5	0.9	1.07	12.5	0.307	0.5	3.2	107	21	24.2	382	58	1.07	0.97
FC-2-K	0.19	2.29	34.2	11.7	1.6	2310	33.8	0.23	13.9	164.5	720	459	77.1	0.007	4.16	10.3	3	7.3	123.5	0.89	0.78	12.2	0.303	0.56	2.8	109	14.1	24.1	408	59.1	1.03	0.8
FC-2-L	0.183	2.49	36.3	12.7	1.57	2090	25.5	0.22	14.5	118.5	680	988	83.6	0.007	4.05	10.3	4	6.5	130	0.9	1.15	12.1	0.307	0.59	2.8	106	25.6	23.4	379	56.9	1.12	1.06
FC-2-M	0.236	2.37	35.9	12	1.46	2040	33	0.2	14.1	112.5	660	858	82.3	0.008	4.88	10.2	5	7.1	124	0.87	1.2	12.9	0.294	0.59	2.7	107	18.4	23.8	636	55	1.73	1.64
FC-2-N	0.214	2.33	34.5	13.1	1.39	1950	49.9	0.21	13.7	102	620	1225	83.6	0.017	5.89	9.6	7	7.9	123	0.86	1.71	12.4	0.287	0.91	2.7	100	27.4	22.7	866	52	2.91	2.33
FC-2-O	0.26	2.08	33	13.1	1.2	1845	123	0.2	13	99.1	570	1490	75.6	0.045	9.32	8.8	8	5.2	112	0.81	1.98	11.7	0.273	0.74	2.5	93	39.9	21.6	999	49.3	3.85	3.22
FC-2-P	0.332	1.87	25.8	13.4	1	1750	243	0.21	11.6	109.5	560	1775	71.1	0.09	11.15	7.9	9	7.4	113.5	0.71	2.65	8.4	0.242	0.87	1.9	83	46.6	19.2	1195	46.4	4	3.14
FC-2-Q	0.372	2.06	24.5	13.9	0.88	1635	323	0.24	9.9	217	560	2030	76.2	0.103	10.6	6.8	9	36.4	120.5	0.58	2.89	8.3	0.208	0.97	1.8	74	67.8	16.9	1255	38.1	3.71	2.97
FC-2-R	0.372	2.46	24.3	14.4	0.94	1635	354	0.25	9.1	229	560	1850	86.4	0.113	12.05	6.6	8	27.6	127	0.57	2.68	8.2	0.195	1.17	1.8	70	98.6	16.1	1270	34.2	3.44	2.65
FC-2-S	0.36	2.76	23.7	14.5	1.05	1705	359	0.27	8.9	207	530	1525	95.6	0.113	11.35	6.8	7	77	133.5	0.54	2.37	8.2	0.191	1.28	1.7	69	90.7	15.7	1270	32.1	3.01	2.52
FC-2-T	0.316	2.69	33.4	25.3	1.71	2550	289	0.22	12.1	36.4	870	2390	106	0.096	19.7	9.4	7	64.5	146.5	0.83	4.08	12.9	0.256	2.58	2.1	79	100	19.7	1700	34.3	1.91	1.61
Average (based on wt%)	**0.142**	**2.40**	**35.7**	**9.8**	**1.60**	**2055**	**35.8**	**0.23**	**14.5**	**128**	**693**	**875**	**72.7**	**0.010**	**3.6**	**10.0**	**5**	**7.4**	**136**	**0.99**	**1.40**	**12.3**	**0.298**	**0.52**	**2.6**	**103**	**24.3**	**22.6**	**406**	**49.0**	**1.05**	**0.93**
Max	**0.372**	**2.76**	**44.8**	**25.3**	**1.73**	**2550**	**359.0**	**0.27**	**16**	**229**	**870**	**2790**	**106**	**0.113**	**19.7**	**10.9**	**11**	**77**	**162.5**	**1.17**	**4.08**	**13.7**	**0.321**	**2.58**	**3.3**	**112**	**100**	**25.2**	**1700**	**62.9**	**4.00**	**3.22**
Min	**0.078**	**1.87**	**23.7**	**7.3**	**0.88**	**1635**	**8.4**	**0.16**	**8.9**	**36.4**	**530**	**152.5**	**62**	**0.002**	**1.51**	**6.6**	**2**	**3.3**	**112**	**0.54**	**0.32**	**8.2**	**0.191**	**0.29**	**1.7**	**69**	**12.3**	**15.7**	**172**	**32.1**	**0.53**	**0.45**

QA/QC

Duplicates at the same laboratory

Samples ID	(US)	(mm)	Total (wt.)	Sub sample	Primary	Secondary	Tertiary	Sample Mass*	Observation	
FC-2-P	#100	0.150	1.67	0.111	N	N	N	34.87		a
FC-2-P (D1)	#100	0.150	1.67	0.111	N	N	N	34.18	Duplicate same lab (FC-2-A)	b
FC-2-P (D2)	#100	0.150	1.67	0.111	N	N	N	34.18	Reanalysis of (FC-2-A)	c

Samples ID	Ag	Al	As	Ba	Be	Bi	Ca	Cd	Ce	Co	Cr	Cs	Cu	Fe	Ga	Ge	Hf
FC-2-P (a)	13.5	5.24	129	160	1.32	63.1	14.3	3.63	55.7	15.8	64	4.5	3080	5.41	14.85	0.15	1.7
FC-2-P (D1) (b)	12.85	5.18	122	160	1.56	54	14.2	3.43	59.1	15.2	65	4.51	2900	5.39	15.1	0.15	1.7
FC-2-P (D2) (c)	14.05	5.2	114	170	1.39	72.2	14.25	3.22	60.2	15.8	66	4.27	2940	5.3	13.85	0.14	1.6
% of variability (a & b)	4.9	1.2	5.6	0.0	-16.7	15.5	0.7	5.7	-5.9	3.9	-1.6	-0.2	6.0	0.4	-1.7	0.0	0.0
% of variability (a & c)	-4.0	0.8	12.3	-6.1	-5.2	-13.5	0.4	12.0	-7.8	0.0	-3.1	5.2	4.7	2.1	7.0	6.9	6.1

Samples ID	In	K	La	Li	Mg	Mn	Mo	Na	Nb	Ni	P	Pb	Rb	Re	Sb	Sc	Se	Sn	Sr	Ta	Te	Th	Ti	Tl	U	V	W	Y	Zn	Zr	S	S
FC-2-P (a)	0.332	1.87	25.8	13.4	1	1750	243	0.21	11.6	109.5	560	1775	71.1	0.09	11.15	7.9	9	7.4	113.5	0.71	2.65	8.4	0.242	0.87	1.9	83	40.3	19.2	1195	46.4	4	3.14
FC-2-P (D1) (b)	0.314	1.82	26.5	14.2	0.98	1720	196	0.21	11.2	104	530	1915	70.2	0.067	8.42	7.9	9	12.1	112	0.7	2.48	10.2	0.236	0.83	2.1	82	178.5	19.2	1125	46.1	3.8	3.13
FC-2-P (D2) (c)	0.321	1.91	27.1	14.7	1	1720	274	0.21	11.8	114	570	1795	66.4	0.076	8.2	6.4	9	7	116	0.8	3.2	9	0.233	0.84	2	80	46.6	18.3	1095	40.6	3.64	
% of variability (a & b)	5.6	2.7	-2.7	-5.8	2.0	1.7	21.4	0.0	3.5	5.2	5.5	-7.6	1.3	29.3	27.9	0.0	0.0	-48.2	1.3	1.4	6.6	-19.4	2.5	4.7	-10.0	1.2	-126.3	0.0	6.0	0.6	5.1	0.3
% of variability (a & c)	3.4	-2.1	-4.9	-9.3	0.0	1.7	-12.0	0.0	-1.7	-4.0	-1.8	-1.1	6.8	16.9	30.5	21.0	0.0	5.6	-2.2	-11.9	-18.8	-6.9	3.8	3.5	-5.1	3.7	-14.5	4.8	8.7	13.3	9.4	

Notes:

* Sample mass sent to the laboratory for metal by ICP-MS and total sulfur by Leco analysis

University of British Columbia
Department of Mining Engineering
"Assessment of waste rock weathering characteristics at the Antamina mine based on field cells experiment"

Table C4.4 Sample preparation data and assay results of the diopside marble (FC-3) sample

Project:	Waste Rock Study at Antamina Mine	**Sample Code:**	**FC-3**
Material Type:	Waste rock - Class B	**Sampling Date:**	07-Jul-06
Rock Type:	Diopside marble	**Sampling by:**	C. Aranda
Location:	Antamina Open Pit	**Testing Date:**	25-Jul-08
	Third tipping phase in Pile 1	**Testing by:**	C. Aranda
Description:	Field Cell (UBC-1-3A)	**Review by:**	C. Aranda

Samples ID	Size (US)	Size (mm)	Mass Total (wt.) (kg)	Mass Sub sample (kg)	Crusher Primary (Y/N)	Crusher Secondary (Y/N)	Crusher Tertiary (Y/N)	Sample Mass* (g)	Observation	Total Metals by ICP-MS Ag ppm	Al %	As ppm	Ba ppm	Be ppm	Bi ppm	Ca %	Cd ppm	Ce ppm	Co ppm	Cr ppm	Cs ppm	Cu ppm	Fe %	Ga ppm	Ge ppm	Hf ppm	In ppm	K %	La ppm	Li ppm	Mg %	Mn ppm	Mo ppm	Na %	Nb ppm	Ni ppm	P ppm	Pb ppm	Rb ppm	Re ppm	Sb ppm	Sc ppm	Se ppm	Sn ppm	Sr ppm	Ta ppm	Te ppm	Th ppm	Ti %	Tl ppm	U ppm	V ppm	W ppm	Y ppm	Zn ppm	Zr ppm	ICP-MS S %	Leco S %
FC-3-A	4"	+100.0	0.00					--	There is no sample																																																		
FC-3-B	3"	75.0 - 100.0	0.00					48.38	Duplicate (FC-3-N)																																																				
FC-3-C	2"	50.0 - 75.0	17.80	9.30	Y	Y	Y	49.00		0.92	2.83	33	30	0.85	35.4	31.8	3.18	34.9	3.7	26	1.54	204	1.3	6.98	0.06	1.2	0.58	0.34	17.4	6.4	1.08	849	47.5	0.09	7.6	14.4	430	62.4	19.1	0.01	2.19	5.4	3	1.8	932	0.43	0.33	6.3	0.152	0.21	2	34	20.2	13.6	1380	35.3	0.38	0.33
FC-3-D	11/2"	37.5 - 50.0	16.00	3.10	Y	Y	Y	49.82		0.45	1.69	22	50	0.54	5.12	32.6	1.07	19.9	2.4	15	2.7	269	0.79	4.16	0.06	0.6	0.176	0.45	10.3	7.3	0.86	374	9.77	0.12	3.4	2.8	280	25.6	22.9	0.01	1.38	3	3	1	1435	0.15	0.15	3.1	0.073	0.23	2	20	3.1	7	369	18.1	0.37	0.36
FC-3-E	1"	25.0 - 37.5	20.10	3.00	Y	Y	Y	60.51		8.04	3.02	33	30	1.04	44	30.7	3.15	41.1	3.8	24	1.61	220	1.43	7.35	0.08	1.2	0.295	0.29	20.8	7.4	1.13	774	188	0.06	7	11.2	510	833	20.6	0.119	2.15	5.4	7	1.9	706	0.39	0.91	6.4	0.144	0.24	2	33	50	13.7	1185	38.5	0.45	0.51
FC-3-F	3/4"	19.0 - 25.0	12.90	1.50	Y	Y	Y	54.79		6.05	3.2	38	40	1.08	29.8	26.3	4.13	43.6	4.7	28	2.21	313	1.99	8.34	0.09	1.3	0.762	0.55	21.6	8.3	1.14	1025	22.1	0.08	7.4	20.8	470	658	28.8	0.021	2.71	5.7	5	3.6	738	0.42	0.81	6.7	0.147	0.26	2.4	39	9.3	13.8	1500	42.1	0.8	0.71
FC-3-G	1/2"	12.5 - 19.0	16.70	1.176	N	Y	Y	48.48		8.93	2.57	35	40	0.87	51.9	31.2	1.34	35.1	4.9	24	3.19	228	1.43	6.5	0.08	0.9	0.27	0.42	17.4	8.4	1.02	666	24.4	0.11	5.9	12.5	370	627	26.5	0.009	2.75	4.5	6	2.4	972	0.32	0.85	5.3	0.12	0.41	2	30	11.6	11.8	441	29.1	0.7	0.56
FC-3-H	3/8"	9.5 - 12.5	8.10	0.498	N	Y	Y	62.87		2.6	2.83	38	40	0.89	57.8	30.3	2.54	36.3	3.9	25	2.38	386	1.78	7.42	0.07	1.2	0.481	0.45	18.1	8	1.09	856	38.9	0.1	6.5	17.6	460	225	26.9	0.016	4.42	5	4	3.6	693	0.35	0.48	5.4	0.13	0.3	1.9	34	11.2	12.2	968	36.8	0.62	0.49
FC-3-I	1/4"	6.3 - 9.5	8.80	0.276	N	N	Y	53.13		1.69	2.79	33	50	0.77	17.95	27.4	2.26	31.8	3.9	25	2.47	309	1.71	7.55	0.07	1.1	0.412	0.51	15.6	8.1	1.06	826	69.5	0.1	6.4	20.6	410	185.5	28.8	0.045	2.69	4.9	4	3.6	849	0.34	0.3	5.3	0.131	0.26	1.8	34	16.9	12	881	36.9	0.5	0.44
FC-3-J	#4	4.75 - 6.30	5.37	0.162	N	N	Y	53.64		2.28	2.5	31	50	0.89	51.9	29.5	2.8	34.3	3.5	22	2.95	432	1.5	6.65	0.08	1	0.391	0.49	17.7	9.8	1.03	693	44.9	0.11	5.9	7.9	410	293	30.9	0.018	2.54	4.7	4	2.7	781	0.31	0.69	5	0.122	0.31	1.9	32	12.7	11.3	1035	31.5	0.63	0.56
FC-3-K	#6	3.35 - 4.75	4.54	0.155	N	N	Y	52.69		6.93	2.83	56	60	0.86	36.6	30.5	6.31	34	4.8	25	3.08	582	1.84	7.38	0.09	1.1	0.785	0.58	16.7	9.4	1.07	788	69.3	0.13	6.5	15.7	440	687	33.3	0.014	3.67	4.8	6	3.3	817	0.35	0.73	5.2	0.129	0.4	2	35	39.6	12.3	2290	34	0.84	0.68
FC-3-L	#8	2.36 - 3.35	3.51	0.103	N	N	N	50.03		5.29	2.81	34	60	0.95	36.5	30	3.97	35.9	4.5	27	3.21	556	1.81	7.54	0.09	1.1	0.533	0.66	17.9	9.7	1.06	753	75.4	0.13	6.3	39.2	410	591	36.3	0.024	6.17	4.7	6	3.6	806	0.33	0.67	5.2	0.127	0.37	2.2	35	24.8	12	1465	32.5	0.75	0.59
FC-3-M	#16	1.18 - 2.36	4.95	0.142	N	N	N	49.52		5.92	2.81	50	60	0.99	55.3	26.4	4.36	36	4.2	24	2.97	717	1.88	7.59	0.09	1	0.683	0.67	17.7	9.5	1.03	781	76.6	0.12	6.2	15.9	420	601	37.2	0.021	4.7	4.7	6	3.8	758	0.32	1.25	5.3	0.127	0.4	2.2	35	44.9	11.7	1585	32.6	0.83	0.71
FC-3-N	#30	0.60 - 1.18	2.48	0.150	N	N	N	49.43		9.23	3.03	48	70	1.01	67.6	25.8	5.34	38	5.9	24	3.98	964	2.28	8.3	0.1	1.1	0.768	0.71	19.1	10.8	1.04	834	88.1	0.13	6.6	16.4	410	1045	40.1	0.027	6.3	4.9	8	4.8	775	0.36	1.23	5.7	0.135	0.46	2.3	42	46.1	12.3	1990	34.6	1.21	1.01
FC-3-O	#50	0.30 - 0.60	2.57	0.154	N	N	N	48.06		9.76	2.67	119	60	0.87	55.4	25.6	6.4	32.2	7.7	23	3.8	1095	2.6	7.16	0.1	0.9	0.813	0.59	16.6	9.2	0.88	755	77.1	0.12	5.7	19.2	330	1195	32.8	0.023	8.79	4	9	4	801	0.29	1.47	4.4	0.115	0.46	1.8	33	38.5	10.5	2330	29.1	1.89	1.35
FC-3-P	#100	0.15 - 0.30	3.43	0.210	N	N	N	54.73		11.7	1.78	43	50	0.55	57.7	33.7	4.97	25.8	7.2	15	2.55	1195	2.22	4.97	0.09	0.6	0.617	0.45	13.9	8	0.74	595	113	0.1	4.2	30.1	260	1260	23.4	0.044	6.34	2.6	10	2.8	1225	0.27	1.31	3.6	0.078	0.4	1.7	22	54.5	8.2	1820	20.3	1.72	1.39
FC-3-Q	#140	0.106 - 0.15	2.14	0.144	N	N	N	52.47		9.14	1.32	51	40	0.42	52.4	35.2	4.65	19.6	5.5	10	2.04	1185	1.84	3.83	0.08	0.4	0.625	0.43	10.7	7	0.69	489	79.1	0.09	3.1	19.6	220	827	21.8	0.026	8.59	2.1	8	2.3	1245	0.21	1.08	2.8	0.057	0.44	1.7	16	25.2	7	1730	14.3	1.53	1.19
FC-3-R	#200	0.075 - 0.106	2.14	0.111	N	N	N	52.65		6.57	1.13	46	40	0.35	40.8	31.5	4.02	15.4	5	9	1.8	1040	1.61	3.27	0.08	0.3	0.559	0.41	8	5.6	0.61	429	86.1	0.08	2.7	14.5	190	560	20.1	0.031	5.75	1.9	7	2	1050	0.17	0.82	2.3	0.05	0.32	1.4	15	40.1	6.3	1480	11.6	1.37	1.09
FC-3-S	#270	0.053 - 0.075	1.71	0.099	N	N	N	49.39		7.13	1.18	33	50	0.34	46.9	31.8	4.67	16.35	4.5	11	2.03	1035	1.48	3.48	0.09	0.4	0.66	0.47	8.4	5.9	0.64	450	88.7	0.08	2.9	14.2	210	523	23.1	0.03	6.79	2.1	7	2.1	1005	0.18	0.81	2.4	0.053	0.36	1.6	15	40.9	6.8	1670	11.7	1.18	0.98
FC-3-T	-#270	-0.053	6.74	0.188	N	N	N	50.35		11.35	1.66	51	70	0.55	86.4	30.8	5.53	22.2	5	21	7.69	1010	1.33	4.92	0.12	0.5	0.685	0.7	11.1	17.4	1.16	681	133	0.1	4.5	17.2	490	1135	44.4	0.04	10.15	3	9	2.7	919	0.3	1.67	4	0.082	0.84	2.3	23	53.4	8.5	1945	16.4	0.64	0.53
Total			**139.97**						**Average (based on wt%)**	**5.36**	**2.56**	**37**	**44**	**0.83**	**40.65**	**30.3**	**3.16**	**33.2**	**4.2**	**23**	**2.67**	**423**	**1.53**	**6.61**	**0.08**	**1.0**	**0.473**	**0.46**	**16.7**	**8.4**	**1.03**	**731**	**70.05**	**0.10**	**6.0**	**15**	**407**	**514**	**26.6**	**0.0**	**3.5**	**4.5**	**5**	**2.6**	**915**	**0.33**	**0.72**	**5.2**	**0.121**	**0.33**	**2.0**	**31**	**25.0**	**11.5**	**1183**	**31.1**	**0.67**	**0.58**
									Max	**11.70**	**3.20**	**119**	**70**	**1.08**	**86.40**	**35.2**	**6.4**	**43.6**	**7.7**	**28**	**7.69**	**1195**	**2.6**	**8.34**	**0.12**	**1.3**	**0.813**	**0.71**	**21.6**	**17.4**	**1.16**	**1025**	**188.0**	**0.13**	**7.6**	**39.2**	**510**	**1260**	**44.4**	**0.119**	**10.15**	**5.7**	**10**	**4.8**	**1435**	**0.43**	**1.67**	**6.7**	**0.152**	**0.84**	**2.4**	**42**	**54.5**	**13.8**	**2330**	**42.1**	**1.89**	**1.39**
									Min	**0.45**	**1.13**	**22**	**30**	**0.34**	**5.12**	**25.6**	**1.07**	**15.4**	**2.4**	**9**	**1.54**	**204**	**0.79**	**3.27**	**0.06**	**0.3**	**0.176**	**0.29**	**8**	**5.6**	**0.61**	**374**	**9.77**	**0.06**	**2.7**	**2.8**	**190**	**25.6**	**19.1**	**0.009**	**1.38**	**1.9**	**3**	**1**	**693**	**0.15**	**0.15**	**2.3**	**0.05**	**0.21**	**1.4**	**15**	**3.1**	**6.3**	**369**	**11.6**	**0.37**	**0.33**

QA/QC

Duplicates at the same laboratory										Ag ppm	Al %	As ppm	Ba ppm	Be ppm	Bi ppm	Ca %	Cd ppm	Ce ppm	Co ppm	Cr ppm	Cs ppm	Cu ppm	Fe %	Ga ppm	Ge ppm	Hf ppm	In ppm	K %	La ppm	Li ppm	Mg %	Mn ppm	Mo ppm	Na %	Nb ppm	Ni ppm	P ppm	Pb ppm	Rb ppm	Re ppm	Sb ppm	Sc ppm	Se ppm	Sn ppm	Sr ppm	Ta ppm	Te ppm	Th ppm	Ti %	Tl ppm	U ppm	V ppm	W ppm	Y ppm	Zn ppm	Zr ppm	S %	S %
FC-3-N	#30	0.600	2.48	0.150	N	N	N	49.43	a	9.23	3.03	48	70	1.01	67.6	25.8	5.34	38	5.9	24	3.98	964	2.28	8.3	0.1	1.1	0.768	0.71	19.1	10.8	1.04	834	88.1	0.13	6.6	16.4	410	1045	40.1	0.027	6.3	4.9	8	4.8	775	0.36	1.23	5.7	0.135	0.46	2.3	42	46.1	12.3	1990	34.6	1.21	1.01
FC-3-N (D1)	#30	0.600	2.48	0.150	N	N	N	37.93	Duplicate same lab (FC-3-B) b	10.55	3.07	54	70	0.94	71.3	26.1	5.18	36.2	5.6	26	3.44	960	2.28	8.13	0.09	1.1	0.709	0.73	18	11.5	1.06	858	99.6	0.13	6.5	18.1	400	1225	40.8	0.033	5.88	4.8	9	3.9	766	0.35	1.33	5.6	0.137	0.46	2.2	39	44.7	12.2	2010	33.8	1.2	1.11
FC-3-N (D2)	#30	0.600	2.48	0.150	N	N	N	37.93	Reanalysis of (FC-3-B) c	10.45	3.02	48	80	0.94	76.3	27.1	5.32	35.1	5.8	24	3.35	1060	2.25	7.63	0.08	0.9	0.677	0.75	17.2	11.1	1.08	856	88.8	0.14	6.8	33.8	420	1290	38.3	0.034	10.35	4.1	9	3.9	772	0.44	1.59	5.2	0.134	0.46	2.2	36	38.2	11.3	2030	28.4	1.17	
									% of variability (a & b)	-13.3	-1.3	-11.8	0.0	7.2	-5.3	-1.2	3.0	4.9	5.2	-8.0	14.6	0.4	0.0	2.1	10.5	0.0	8.0	-2.8	5.9	-6.3	-1.9	-2.8	-12.3	0.0	1.5	-9.9	2.5	-15.9	-1.7	-20.0	6.9	2.1	-11.8	20.7	1.2	2.8	-7.8	1.8	-1.5	0.0	4.4	7.4	3.1	0.8	-1.0	2.3	0.8	-9.4
									% of variability (a & c)	-12.4	0.3	0.0	-13.3	7.2	-12.1	-4.9	0.4	7.9	1.7	0.0	17.2	-9.5	1.3	8.4	22.2	20.0	12.6	-5.5	10.5	-2.7	-3.8	-2.6	-0.8	-7.4	-3.0	-69.3	-2.4	-21.0	4.6	-23.0	-48.6	17.8	-11.8	20.7	0.4	-20.0	-25.5	9.2	0.7	0.0	4.4	15.4	18.7	8.5	-2.0	19.7	3.4	

Notes:

* Sample mass sent to the laboratory for metal by ICP-MS and total sulfur by Leco analysis

University of British Columbia
Department of Mining Engineering
"Assessment of waste rock weathering characteristics at the Antamina mine based on field cells experiment"

Table C4.5 Sample preparation data and assay results of the gray hornfels (FC-4) sample

Project:	Waste Rock Study at Antamina Mine	**Sample Code:**	**FC-4**
Material Type:	Waste rock - Class B	**Sampling Date:**	07-Jul-06
Rock Type:	Gray hornfels	**Sampling by:**	C. Aranda
Location:	Antamina Open Pit	**Testing Date:**	25-Jul-08
	Third/Fourth tipping phase in Pile 1	**Testing by:**	C. Aranda
Description:	Field Cell (UBC-1-4A)	**Review by:**	C. Aranda

Samples ID	Size		Mass		Crusher			Sample Mass*	Observation
	(US)	(mm)	Total (wt.)	Sub sample	Primary	Secondary	Tertiary		
			(kg)	(kg)	(Y/N)	(Y/N)	(Y/N)	(g)	
FC-4-A	4"	+100.0	0.00					58.16	Duplicate (FC-4-M)
FC-4-B	3"	75.0 - 100.0	1.70	1.00	Y	Y	Y	50.13	
FC-4-C	2"	50.0 - 75.0	15.50	7.70	Y	Y	Y	50.73	
FC-4-D	11/2"	37.5 - 50.0	13.20	2.70	Y	Y	Y	44.73	
FC-4-E	1"	25.0 - 37.5	19.90	2.30	Y	Y	Y	46.16	
FC-4-F	3/4"	19.0 - 25.0	10.30	1.30	Y	Y	Y	50.30	
FC-4-G	1/2"	12.5 - 19.0	13.90	0.835	N	Y	Y	44.08	
FC-4-H	3/8"	9.5 - 12.5	6.60	0.438	N	Y	Y	50.58	
FC-4-I	1/4"	6.3 - 9.5	7.30	0.440	N	N	Y	51.09	
FC-4-J	#4	4.75 - 6.30	4.10	0.281	N	N	Y	50.62	
FC-4-K	#6	3.35 - 4.75	3.50	0.212	N	N	Y	53.37	
FC-4-L	#8	2.36 - 3.35	2.70	0.351	N	N	N	49.14	
FC-4-M	#16	1.18 - 2.36	5.00	0.442	N	N	N	52.60	
FC-4-N	#30	0.60 - 1.18	3.00	0.393	N	N	N	62.77	
FC-4-O	#50	0.30 - 0.60	4.30	0.190	N	N	N	50.92	
FC-4-P	#100	0.15 - 0.30	7.31	0.819	N	N	N	59.47	
FC-4-Q	#140	0.106 - 0.15	3.44	0.641	N	N	N	58.76	
FC-4-R	#200	0.075 - 0.106	4.08	0.311	N	N	N	55.06	
FC-4-S	#270	0.053 - 0.075	4.30	0.130	N	N	N	50.83	
FC-4-T	-#270	-0.053	8.82	0.553	N	N	N	48.33	
Total			**138.95**						

Total Metals by ICP-MS

Samples ID	Ag	Al	As	Ba	Be	Bi	Ca	Cd	Ce	Co	Cr	Cs	Cu	Fe	Ga	Ge	Hf	In	K	La	Li	Mg	Mn	Mo	Na	Nb	Ni
	ppm	%	ppm	ppm	ppm	ppm	%	ppm	ppm	ppm	ppm	ppm	ppm	%	ppm	ppm	ppm	ppm	%	ppm	ppm	%	ppm	ppm	%	ppm	ppm
FC-4-A																											
FC-4-B	0.59	0.24	5	40	0.11	0.64	34.6	0.26	3.52	0.9	3	0.71	17.8	0.1	0.65	0.13	0.1	0.011	0.07	1.8	11.2	0.53	125	0.43	0.02	0.5	0.2
FC-4-C	0.44	0.38	7	30	0.14	0.91	35	0.36	4.5	1.1	3	2.57	22.5	0.2	1.01	0.11	0.1	0.013	0.14	2.3	15.8	0.68	136	1.22	0.04	0.9	0.2
FC-4-D	1.83	0.35	13	20	0.14	13.05	33.7	0.63	4.49	1.1	4	1.97	72.5	0.33	1.07	0.08	0.1	0.062	0.13	2.3	18.6	0.82	142	1.3	0.04	0.9	0.2
FC-4-E	0.6	0.57	5	50	0.2	1.22	33.4	0.3	5.83	1.2	5	2.65	53.2	0.24	1.74	0.11	0.1	0.009	0.29	2.9	18.6	0.69	165	1.22	0.11	1	0.2
FC-4-F	0.41	0.41	7	30	0.17	2.43	35	0.36	5.42	1	4	2	43.9	0.23	1.15	0.1	0.1	0.028	0.22	2.8	13.3	0.72	138	1.17	0.05	0.9	0.2
FC-4-G	0.61	0.56	17	30	0.16	1.89	35.1	0.58	5.11	1.1	5	2.53	51	0.23	1.46	0.12	0.2	0.036	0.24	2.5	15.1	0.74	146	2	0.07	1.2	4.1
FC-4-H	0.67	0.47	22	30	0.12	1.68	35.8	0.61	4.59	1.1	5	2.47	40.1	0.25	1.23	0.12	0.1	0.015	0.2	2.3	15.2	0.72	162	1.05	0.05	1.2	0.2
FC-4-I	0.97	0.52	21	30	0.15	3.47	35.4	0.61	5.22	1	5	2.21	93.7	0.23	1.33	0.12	0.1	0.03	0.24	2.6	12.4	0.73	179	1.7	0.06	1.2	2.1
FC-4-J	1.61	0.5	10	40	0.1	5.96	34.8	1	4.98	1.2	11	2.53	126	0.33	1.35	0.1	0.1	0.106	0.22	2.4	12.7	0.73	182	1.77	0.06	1.1	6.4
FC-4-K	1.74	0.61	26	40	0.13	8.65	34.4	1.4	5.78	1.3	6	2.82	109.5	0.34	1.7	0.11	0.2	0.214	0.3	2.9	13.5	0.73	213	4.99	0.08	1.3	6.4
FC-4-L	1.99	0.54	20	40	0.12	9.33	33.6	1.51	5.5	1.3	7	2.76	189.5	0.36	1.59	0.12	0.1	0.18	0.28	2.7	12.8	0.71	224	4.22	0.06	1.2	7.4
FC-4-M	3.37	0.66	27	60	0.19	9.67	33.7	1.8	6.26	1.3	6	3.25	201	0.38	1.79	0.05	0.2	0.233	0.36	3.1	15.1	0.74	238	11.15	0.08	1.4	8.4
FC-4-N	6.31	0.77	32	60	0.19	29.4	31.9	5.66	6.96	2.2	9	3.73	473	0.73	2.52	0.08	0.2	0.596	0.42	3.3	15.9	0.75	294	20.6	0.08	1.6	19
FC-4-O	4.62	0.54	42	40	0.13	17.65	32.5	2.71	5.04	2.4	6	2.28	418	0.79	1.5	0.07	0.1	0.278	0.24	2.6	11.5	0.6	235	11.8	0.09	1	11.2
FC-4-P	1.49	0.21	12	20	0.08	4.67	35.6	1.4	3.94	1	3	0.72	135.5	0.25	0.58	0.07	0.1	0.106	0.08	2	4.3	0.45	152	7.61	0.03	0.5	1.9
FC-4-Q	1.24	0.17	16	20	0.06	4.4	35.7	1.09	4.12	1.1	3	0.69	117	0.24	0.53	0.11	0.1	0.084	0.07	2	3.7	0.46	149	6.01	0.02	0.5	2.1
FC-4-R	1.57	0.18	28	20	0.05	6.77	35.8	1.25	4.6	1.1	3	0.79	168.5	0.28	0.6	0.12	0.1	0.125	0.09	2.5	4.2	0.49	158	18.2	0.02	0.5	1.7
FC-4-S	1.58	0.2	30	20	0.06	5.07	36.4	1.38	4.49	1.3	4	0.85	180	0.32	0.65	0.09	0.1	0.123	0.1	2.2	4.4	0.52	168	13.05	0.02	0.5	2.5
FC-4-T	4.79	0.59	58	60	0.18	21	34.5	2.65	6.55	1.7	12	7.69	439	0.47	1.91	0.09	0.1	0.342	0.35	3.2	24.2	1.09	319	24.1	0.04	1.4	7.7
Average (based on wt%)	**1.53**	**0.46**	**18**	**35**	**0.15**	**6.30**	**34.6**	**1.01**	**5.1**	**1.2**	**5**	**2.56**	**121**	**0.30**	**1.31**	**0.10**	**0.1**	**0.095**	**0.22**	**2.6**	**14.5**	**0.71**	**175**	**5.35**	**0.06**	**1.0**	**2.9**
Max	**6.31**	**0.77**	**58**	**60**	**0.20**	**29.40**	**36.4**	**5.66**	**6.96**	**2.4**	**12**	**7.69**	**473**	**0.79**	**2.52**	**0.13**	**0.2**	**0.596**	**0.42**	**3.3**	**24.2**	**1.09**	**319**	**24.10**	**0.11**	**1.6**	**19**
Min	**0.41**	**0.17**	**5**	**20**	**0.05**	**0.64**	**31.9**	**0.26**	**3.52**	**0.9**	**3**	**0.69**	**17.8**	**0.1**	**0.53**	**0.05**	**0.1**	**0.009**	**0.07**	**1.8**	**3.7**	**0.45**	**125**	**0.43**	**0.02**	**0.5**	**0.2**

Samples ID	P	Pb	Rb	Re	Sb	Sc	Se	Sn	Sr	Ta	Te	Th	Ti	Tl	U	V	W	Y	Zn	Zr	S (ICP-MS)	S (Leco)
	ppm	ppm	ppm	ppm	ppm	ppm	ppm	ppm	ppm	ppm	ppm	ppm	%	ppm	ppm	ppm	ppm	ppm	ppm	ppm	%	%
FC-4-A																						
FC-4-B	120	46.3	5.8	0.002	1.77	0.5	3	0.2	6250	0.05	0.07	0.3	0.009	0.11	0.4	3	0.3	2.6	60	2.2	0.11	0.09
FC-4-C	120	64.4	19.4	0.005	0.77	0.9	3	0.2	1965	0.05	0.17	0.6	0.018	0.22	1.4	10	0.9	2.9	84	2.9	0.18	0.12
FC-4-D	90	142.5	15.3	0.004	1.62	0.7	4	0.2	1655	0.05	0.83	0.5	0.018	0.18	1.2	9	0.9	2.5	131	3.8	0.36	0.29
FC-4-E	140	59.2	24	0.002	0.86	0.9	3	0.2	1770	0.06	0.11	0.8	0.023	0.29	0.8	8	12.4	3	69	2.7	0.13	0.09
FC-4-F	100	38.9	17.7	0.003	0.8	0.7	3	0.2	1665	0.05	0.17	0.6	0.019	0.22	1.1	8	0.8	2.7	81	3.1	0.19	0.14
FC-4-G	110	45.5	22.1	0.005	2.47	0.9	3	0.2	1775	0.07	0.18	1.2	0.024	0.26	1.5	12	1.1	3	125	5.7	0.21	0.19
FC-4-H	130	45	20.4	0.005	2.86	0.8	3	0.2	2030	0.06	0.16	0.9	0.023	0.25	1.3	11	25.4	2.9	79	4.6	0.22	0.16
FC-4-I	110	133.5	20.6	0.004	3.23	0.8	3	0.3	1775	0.07	0.2	1	0.023	0.29	1.2	10	0.9	2.8	105	4.1	0.16	0.13
FC-4-J	130	166	20.4	0.004	2.11	0.8	3	0.6	1860	0.06	0.26	0.9	0.022	0.29	1.3	11	3.7	2.9	251	4.8	0.24	0.22
FC-4-K	130	201	26	0.005	4.22	0.9	3	0.5	1555	0.08	0.28	1.1	0.027	0.32	1.4	11	1.8	3	368	5.3	0.25	0.24
FC-4-L	140	159	23.9	0.005	7.44	0.8	3	0.7	1475	0.07	0.3	1	0.024	0.31	1.4	11	4.1	2.8	368	5.2	0.26	0.2
FC-4-M	130	325	27.8	0.007	14.25	0.9	3	0.8	1465	0.08	0.35	1.2	0.028	0.34	1.5	12	7.7	3	604	5.9	0.28	0.2
FC-4-N	150	748	33.2	0.011	16.05	0.9	5	1.8	1395	0.1	0.87	1.5	0.034	0.4	1.6	13	9.2	3	1815	6.5	0.61	0.57
FC-4-O	110	445	19.8	0.006	21.6	0.6	5	1	2090	0.05	1.13	0.7	0.02	0.25	1.1	9	11.2	2.5	936	4	0.7	0.44
FC-4-P	60	188	5.9	0.004	6.34	0.5	3	0.3	2370	0.05	0.3	0.3	0.008	0.09	0.7	3	3.2	2.4	416	1.7	0.2	0.2
FC-4-Q	70	138	5.6	0.003	7.45	0.5	3	0.3	1930	0.05	0.18	0.4	0.008	0.1	0.8	4	12.5	2.5	250	1.7	0.21	0.11
FC-4-R	70	136.5	6.3	0.006	10.6	0.5	3	0.3	1735	0.05	0.21	0.4	0.009	0.1	0.8	5	7.3	2.6	301	1.7	0.23	0.18
FC-4-S	70	157	7.1	0.005	12.55	0.6	3	0.6	1650	0.05	0.21	0.4	0.01	0.11	0.9	5	5.3	2.7	332	2	0.28	0.18
FC-4-T	190	415	33.3	0.009	26.1	0.9	4	1.1	1435	0.08	0.58	1.2	0.029	0.5	2.1	18	14.7	3.1	838	4.9	0.23	0.14
Average (based on wt%)	**116**	**150**	**19.7**	**0.005**	**5.7**	**0.8**	**3**	**0.4**	**1833**	**0.06**	**0.32**	**0.8**	**0.020**	**0.25**	**1.2**	**10**	**6.2**	**2.8**	**274**	**3.7**	**0.24**	**0.18**
Max	**190**	**748.0**	**33.3**	**0.011**	**26.1**	**0.9**	**5**	**1.8**	**6250**	**0.10**	**1.13**	**1.5**	**0.034**	**0.5**	**2.1**	**18**	**25.4**	**3.1**	**1815**	**6.5**	**0.7**	**0.57**
Min	**60**	**38.9**	**5.6**	**0.002**	**0.77**	**0.5**	**3**	**0.2**	**1395**	**0.05**	**0.07**	**0.3**	**0.008**	**0.09**	**0.4**	**3**	**0.3**	**2.4**	**60**	**1.7**	**0.11**	**0.09**

QA/QC

Duplicates at the same laboratory

Samples ID	Size (US)	(mm)	Total (kg)	Sub sample (kg)	Primary	Secondary	Tertiary	Sample Mass (g)	Observation
FC-4-M	#16	1.18	3.70	0.442	N	N	N	52.60	a
FC-4-M (D1)	#16	1.18	3.70	0.442	N	N	N	56.43	Duplicate same lab (FC-4-A) b
FC-4-M (D2)	#16	1.18	3.70	0.442	N	N	N	56.43	Reanalysis of (FC-4-A) c

	Ag	Al	As	Ba	Be	Bi	Ca	Cd	Ce	Co	Cr	Cs	Cu	Fe	Ga	Ge	Hf	In	K	La	Li	Mg	Mn	Mo	Na	Nb	Ni
FC-4-M (a)	3.37	0.66	27	60	0.19	9.67	33.7	1.8	6.26	1.3	6	3.25	201	0.38	1.79	0.05	0.2	0.233	0.36	3.1	15.1	0.74	238	11.15	0.08	1.4	8.4
FC-4-M (D1) (b)	3.15	0.67	31	50	0.27	11.5	33.1	1.78	5.45	1.7	7	3.35	233	0.42	2.59	0.08	0.2	0.302	0.36	2.6	46.6	0.75	241	6.03	0.08	1.4	0.4
FC-4-M (D2) (c)	2.28	0.66	21	50	0.24	8.61	33.9	1.68	5.39	1.1	7	3.38	253	0.39	1.7	0.05	0.2	0.231	0.34	2.7	15.3	0.76	240	9.7	0.08	1.2	9.6
% of variability (a & b)	6.7	-1.5	-13.8	18.2	-34.8	-17.3	1.8	1.1	13.8	-26.7	-15.4	-3.0	-14.7	-10.0	-36.5	-46.2	0.0	-25.8	0.0	17.5	-102.1	-1.3	-1.3	59.6	0.0	0.0	181.8
% of variability (a & c)	38.6	0.0	25.0	18.2	-23.3	11.6	-0.6	6.9	14.9	16.7	-15.4	-3.9	-22.9	-2.6	5.2	0.0	0.0	0.9	5.7	13.8	-1.3	-2.7	-0.8	13.9	0.0	15.4	-13.3

	P	Pb	Rb	Re	Sb	Sc	Se	Sn	Sr	Ta	Te	Th	Ti	Tl	U	V	W	Y	Zn	Zr	S	S
FC-4-M (a)	130	325	27.8	0.007	14.25	0.9	3	0.8	1465	0.08	0.35	1.2	0.028	0.34	1.5	12	7.7	3	604	5.9	0.28	0.2
FC-4-M (D1) (b)	140	291	35.8	0.006	13.75	1.4	5	1	1465	0.08	0.36	1	0.031	0.39	1.3	13	4.7	3.4	618	6	0.27	0.23
FC-4-M (D2) (c)	130	225	27.9	0.006	12.85	0.9	3	0.8	1625	0.07	0.35	1	0.028	0.36	1.3	13	7.4	2.8	621	5.2	0.24	
% of variability (a & b)	-7.4	11.0	-25.2	15.4	3.6	-43.5	-50.0	-22.2	0.0	0.0	-2.8	18.2	-10.2	-13.7	14.3	-8.0	48.4	-12.5	-2.3	-1.7	3.6	-14.0
% of variability (a & c)	0.0	36.4	-0.4	15.4	10.3	0.0	0.0	0.0	-10.4	13.3	0.0	18.2	0.0	-5.7	14.3	-8.0	4.0	6.9	-2.8	12.6	15.4	

Notes:

* Sample mass sent to the laboratory for metal by ICP-MS and total sulfur by Leco analysis

Table C4.6 Chemical assay results carried out at different laboratories by using different analytical methods for all Class B waste rock samples

Project: Waste Rock Study at Antamina Mine
Material Type: Waste Rock - Class B
Rock Type: Marble and Hornfels
Location: Antamina Open Pit. Field Cells
Test Type **Chemical Assay: Metal by ICP-MS, by ICP-OES and Sulfur by Leco**

Sample Code: FC-0 to FC-4
Sampling Date: March 2006 to July 2006
Sampling by: C. Aranda
Testing Date: February 2008 to September 2008
Testing by: ALS Chemex-Canadá, ALS Chemex-Peru and Antamina Labs
Review by: C. Aranda

Laboratory	Samples	Analytical method	Digestion type	Total Metals by ICP-MS																																																	ICP-MS	Leco
				Ag	Al	As	Ba	Be	Bi	Ca	Cd	Ce	Co	Cr	Cs	Cu	Fe	Ga	Ge	Hf	In	K	La	Li	Mg	Mn	Mo	Na	Nb	Ni	P	Pb	Rb	Re	Sb	Sc	Se	Sn	Sr	Ta	Te	Th	Ti	Tl	U	V	W	Y	Zn	Zr	S	S
				ppm	%	ppm	ppm	ppm	ppm	%	ppm	ppm	ppm	ppm	ppm	ppm	%	ppm	ppm	ppm	ppm	%	ppm	ppm	%	ppm	ppm	%	ppm	ppm	ppm	ppm	ppm	ppm	ppm	ppm	ppm	ppm	ppm	ppm	ppm	ppm	%	ppm	ppm	ppm	ppm	ppm	ppm	ppm	%	%
Sample: FC-0. Field Cell: UBC-1-0A and UBC-1-0B. Rock type: Black marble. Location in the pile: Protective layer. Location in the open pit: 3-SP-4358-12-02																																																						
ALS - Canada	Both FC	ICP-MS	Four acids	2.64	1.47	91	75	0.52	6.40	27.0	3.40	18.2	2.9	13.4	8.28	402	0.70	3.84	0.07	0.40	0.12	0.64	8.84	15.9	0.67	350	3.7	0.1	4.5	6.9	410	519	43.3	0.003	9.63	2.4	2.8	0.9	807	0.27	0.35	3.2	0.075	0.51	1.3	16.7	12.4	7.0	1328	11	0.23	0.21
ALS - Peru	FC: UBC-1-0A	ICP-MS	Four acids	3.57	2.42	194	100	0.59	9.66	31.6	3.82	23.8	4.1	16	12.15	845	1.06	5.17	0.06	0.6	0.112	0.79	11.7	17.1	1.09	589	9.75	0.1	5.3	7.4	700	852	50.3	<0.002	12.55	3	2	1.4	807	0.36	0.42	3.9	0.111	0.76	1.6	26	23.8	7.6	2220	17	0.25	0.15
		ICP-OES	Two acids	<4.0	1.05	142	13.1	<1.0	<40	33.2	3.8		<4.0	6.5		709	0.8					0.16		9.8	0.41	422	<8.0	0.04		<10	550	740			<20		<5.0	<10	587				0.04	<100		11.9			2010			
	FC: UBC-1-0B	ICP-MS	Four acids	1.11	1.96	74	100	0.51	3.23	33.1	1.26	18.6	2.6	12	8.33	331	0.67	4.05	0.05	0.3	0.028	0.81	9	13.1	0.78	348	1.55	0.14	4.3	4.3	460	255	47.5	<0.002	10.95	2.2	2	0.8	1105	0.29	0.17	3.3	0.085	0.55	1.1	18	4.9	6.7	525	8.6	0.22	0.12
		ICP-OES	Two acids	<4.0	0.74	72	8	<1.0	<40	32.7	<1.0		<4.0	<4.0		322	0.51					0.09		7	0.25	262	<8.0	0.06		<10	400	208			<20		<4.0	<10	766				0.02	<100		6			492			
Antamina	Entire polygon	ICP-OES	Two acids	4.18		97.87			12.00				3.00			430	0.59										10.0					400																	1040			
Average ICP-MS				2.44	1.95	120	92	0.54	6.43	30.6	2.83	20.2	3.2	13.8	9.59	526	0.81	4.35	0.06	0.43	0.09	0.75	9.85	15.4	0.85	429	5.0	0.1	4.7	6.2	523	542	47.0	0.003	11.04	2.5	2.3	1.0	906	0.31	0.31	3.5	0.090	0.61	1.3	20.2	13.7	7.1	1358	12	0.23	0.16
Minimum ICP-MS				1.11	1.47	74	75	0.51	3.23	27.0	1.26	18.2	2.6	12.0	8.28	331	0.67	3.84	0.05	0.30	0.03	0.64	8.84	13.1	0.67	348	1.6	0.1	4.3	4.3	410	255	43.3	0.003	9.63	2.2	2.0	0.8	807	0.27	0.17	3.2	0.075	0.51	1.1	16.7	4.9	6.7	525	9	0.22	0.12
Maximum ICP-MS				3.57	2.42	194	100	0.59	9.66	33.1	3.82	23.8	4.1	16.0	12.15	845	1.06	5.17	0.07	0.60	0.12	0.81	11.70	17.1	1.09	589	9.8	0.1	5.3	7.4	700	852	50.3	0.003	12.55	3.0	2.8	1.4	1105	0.36	0.42	3.9	0.111	0.76	1.6	26.0	23.8	7.6	2220	17	0.25	0.21
Sample: FC-1. Field Cell: UBC-1-1A. Rock type: Diopside marble. Location in the pile: First tipping phase. Location in the open pit: 3-SP-4343-22-02																																																						
ALS - Canada	All FC	ICP-MS	Four acids	2.67	2.90	63	78	0.95	9.68	24.4	1.57	34.9	4.7	21.3	3.80	761	1.21	7.08	0.07	1.31	0.10	0.81	17.45	12.3	1.10	703	81.1	0.1	7.7	25.7	360	252	44.4	0.019	13.59	4.1	2.6	2.0	960	0.47	0.22	6.1	0.131	0.38	1.3	28.9	11.4	11.4	645	39	0.26	0.23
ALS - Peru	UBC-1-1A	ICP-MS	Four acids	4.72	3.8	73	120	0.96	13.25	29.1	1.4	36.1	5.1	15	4.41	878	1.33	8.57	0.07	1.3	0.097	1.13	17.9	16.3	1.36	836	104	0.11	7.8	6.1	450	366	53.7	0.018	19.5	4.8	3	2	1100	0.53	0.28	5.9	0.147	0.49	1.2	34	17.4	11	653	37.5	0.32	0.26
		ICP-OES	Two acids	<4.0	1.04	63	18.3	<1.0	<40	25.2	<1.0		<4.0	7		709	0.60					0.14		5.8	0.36	421	75.3	<0.04		<10	340	229			<20		<4.0	<10	802				0.07	<100		13.4			468			
Antamina	Entire polygon	ICP-OES	Two acids	2.49		40.12			9.14				3.01			340	0.63										10.0					290																	650			
Average ICP-MS				3.70	3.35	68	99	0.95	11.47	26.7	1.48	35.5	4.9	18.1	4.11	819	1.27	7.82	0.07	1.30	0.10	0.97	17.68	14.3	1.23	770	92.5	0.1	7.7	15.9	405	309	49.1	0.018	16.54	4.5	2.8	2.0	1030	0.50	0.25	6.0	0.139	0.44	1.2	31.5	14.4	11.2	649	38	0.29	0.24
Minimum ICP-MS				2.67	2.90	63	78	0.95	9.68	24.4	1.40	34.9	4.7	15.0	3.80	761	1.21	7.08	0.07	1.30	0.10	0.81	17.45	12.3	1.10	703	81.1	0.1	7.7	6.1	360	252	44.4	0.018	13.59	4.1	2.6	2.0	960	0.47	0.22	5.9	0.131	0.38	1.2	28.9	11.4	11.0	645	38	0.26	0.23
Maximum ICP-MS				4.72	3.80	73	120	0.96	13.25	29.1	1.57	36.1	5.1	21.3	4.41	878	1.33	8.57	0.07	1.31	0.10	1.13	17.90	16.3	1.36	836	104.0	0.1	7.8	25.7	450	366	53.7	0.019	19.50	4.8	3.0	2.0	1100	0.53	0.28	6.1	0.147	0.49	1.3	34.0	17.4	11.4	653	39	0.32	0.26
Sample: FC-2. Field Cell: UBC-1-2A and UBC-1-2B. Rock type: Diopside marble. Location in the pile: Second tipping phase. Location in the open pit: 3-NP-4373-29-02																																																						
ALS - Canada	Both FC	ICP-MS	Four acids	6.55	6.09	44.00	224.6	1.96	33.23	16.92	1.13	78.30	8.07	68.02	2.51	606	3.34	16.40	0.15	1.90	0.14	2.40	35.69	9.85	1.60	2055	35.8	0.23	14.54	128.1	693.5	875	72.69	0.01	3.62	10.04	4.76	7.43	136	0.99	1.40	12.33	0.30	0.52	2.64	103.4	24.27	22.58	406	48.96	1.05	0.93
ALS - Peru	FC: UBC-1-2A	ICP-MS	Four acids	8.06	7.25	41	220	2.03	36.7	18.9	1.59	79.9	10.4	36	2.59	824	3.51	17.9	0.13	2.1	0.152	2.39	37	12.3	1.71	2240	43	0.33	15.8	19.7	760	1010	75.9	0.009	3.71	9.9	5	4.5	175	1.1	1.38	11.6	0.305	0.62	2.3	99	36.2	21.7	590	49	1.37	1.11
		ICP-OES	Two acids	6.2	1.51	36.9	5.6	1.12	<40	9.82	1.32		4.9	20.9		719	1.94					0.07		6.7	0.24	808	52.9	<0.02		<5.0	569	825			<10		<4.0	<5.0	37.8				0.13	<50		47.5			524			
	FC: UBC-1-2B	ICP-MS	Four acids	5.68	7.36	47	200	2.45	25	19.5	1.19	87.9	8.6	37	2.31	610	3.58	18	0.14	2.2	0.13	2.19	38.3	10.6	1.76	2360	52.6	0.2	15.7	18.6	710	634	68.8	0.009	4.18	10.2	4	4.3	136	1.1	1.07	11.9	0.3	0.58	2.7	110	34	23.5	440	54.7	1.10	0.98
		ICP-OES	Two acids	4.3	1.59	40	6.4	1.48	<40	9.93	0.82		4.4	19.7		614	1.93					0.06		5.9	0.02	758	49.6	<0.02		<5.0	567	560			<10		<2.0	<5.0	34				0.12	<50		52.8			332			
Antamina	Entire polygon	ICP-OES	Two acids	5.57		36.66			39.28				9.93			630	3.30								0.21		20.0					770																	440			
Average ICP-MS				6.76	6.90	44	215	2.15	31.64	18.4	1.30	82.0	9.0	47.0	2.47	680	3.48	17.43	0.14	2.07	0.14	2.33	37.00	10.9	1.69	2218	43.8	0.3	15.3	55.5	721	840	72.5	0.009	3.84	10.0	4.6	5.4	149	1.06	1.28	11.9	0.301	0.57	2.5	104.1	31.5	22.6	479	51	1.17	1.01
Minimum ICP-MS				5.68	6.09	41	200	1.96	25.00	16.9	1.13	78.3	8.1	36.0	2.31	606	3.34	16.40	0.13	1.90	0.13	2.19	35.69	9.8	1.60	2055	35.8	0.2	14.5	18.6	693	634	68.8	0.009	3.62	9.9	4.0	4.3	136	0.99	1.07	11.6	0.298	0.52	2.3	99.0	24.3	21.7	406	49	1.05	0.93
Maximum ICP-MS				8.06	7.36	47	225	2.45	36.70	19.5	1.59	87.9	10.4	68.0	2.59	824	3.58	18.00	0.15	2.20	0.15	2.40	38.30	12.3	1.76	2360	52.6	0.3	15.8	128.1	760	1010	75.9	0.010	4.18	10.2	5.0	7.4	175	1.10	1.40	12.3	0.305	0.62	2.7	110.0	36.2	23.5	590	55	1.37	1.11
Sample: FC-3. Field Cell: UBC-1-3A. Rock type: Diopside marble. Location in the pile: Third tipping phase. Location in the open pit: 3-SP-4328-21-01 and 3-SP-4328-21-06																																																						
ALS - Canada	All FC	ICP-MS	Four acids	5.36	2.56	37.46	44.0	0.83	40.65	30.25	3.16	33.21	4.21	22.76	2.67	423	1.53	6.61	0.08	0.99	0.47	0.46	16.67	8.37	1.03	731	70.0	0.10	6.00	14.7	407.0	514	26.62	0.03	3.50	4.54	5.40	2.55	915	0.33	0.72	5.22	0.12	0.33	2.02	30.8	24.96	11.49	1183	31.14	0.67	0.58
ALS - Peru	UBC-1-3A	ICP-MS	Four acids	5.93	2.88	34	50	0.83	34.4	32.6	3.34	30.1	4.6	13	2.53	642	1.57	6.77	0.08	1	0.417	0.49	15.4	10.1	1.20	762	62.8	0.12	5.8	6.8	460	730	25.3	0.011	3.68	4	6	2.5	907	0.38	0.75	4.4	0.117	0.3	1.7	30	27	10.8	1360	27.6	0.78	0.65
		ICP-OES	Two acids	<5.0	1.18	30	11.7	<1.0	<40	26.8	2.7		<4.0	6.5		491	1.08					0.11		5	0.40	422	57	0.06		<10	380	511			<20		<8.0	<10	710				0.07	<100		14.7			1030			
Antamina	Entire polygon	ICP-OES	Two acids	4.40		23.83			14.23				4.52			250	1.77										50.0					340																	1160			
Antamina	Entire polygon	ICP-OES	Two acids	4.07		17.03			17.56				3.03			200	0.35										10.0					300																	800			
Average ICP-MS				5.64	2.72	36	47	0.83	37.53	31.4	3.25	31.7	4.4	17.9	2.60	532	1.55	6.69	0.08	0.99	0.45	0.47	16.04	9.2	1.11	747	66.4	0.1	5.9	10.8	434	622	26.0	0.022	3.59	4.3	5.7	2.5	911	0.35	0.74	4.8	0.119	0.31	1.9	30.4	26.0	11.1	1271	29	0.72	0.61
Minimum ICP-MS				5.36	2.56	34	44	0.83	34.40	30.3	3.16	30.1	4.2	13.0	2.53	423	1.53	6.61	0.08	0.99	0.42	0.46	15.40	8.4	1.03	731	62.8	0.1	5.8	6.8	407	514	25.3	0.011	3.50	4.0	5.4	2.5	907	0.33	0.72	4.4	0.117	0.30	1.7	30.0	25.0	10.8	1183	28	0.67	0.58
Maximum ICP-MS				5.93	2.88	37	50	0.83	40.65	32.6	3.34	33.2	4.6	22.8	2.67	642	1.57	6.77	0.08	1.00	0.47	0.49	16.67	10.1	1.20	762	70.0	0.1	6.0	14.7	460	730	26.6	0.034	3.68	4.5	6.0	2.6	915	0.38	0.75	5.2	0.121	0.33	2.0	30.8	27.0	11.5	1360	31	0.78	0.65
Sample: FC-4. Field Cell: UBC-1-4A. Rock type: Gray hornfels. Location in the pile: Third/fourth tipping phase. Location in the open pit: 3-SP-4328-21-08																																																						
ALS - Canada	All FC	ICP-MS	Four acids	1.53	0.46	17.92	35.3	0.15	6.30	34.56	1.01	5.14	1.22	5.18	2.56	121	0.30	1.31	0.10	0.12	0.10	0.22	2.57	14.52	0.71	175	5.4	0.06	1.00	2.9	116.1	150	19.72	0.00	5.71	0.79	3.26	0.40	1833	0.06	0.32	0.79	0.02	0.25	1.21	9.5	6.23	2.82	274	3.74	0.24	0.18
ALS - Peru	UBC-1-4A	ICP-MS	Four acids	1.36	0.46	23	30	0.11	9.58	36.1	1.51	4.19	1.2	3	1.88	203	0.29	1.08	0.05	0.1	0.235	0.19	2.2	9.6	0.78	205	5.69	0.04	0.8	1.3	110	170	14	<0.002	6.19	0.6	2	0.5	1810	<0.05	0.31	0.6	0.017	0.18	0.9	8	3.8	2.3	528	4.2	0.25	0.11
		ICP-OES	Two acids	<4.0	2.58	47	22.5	<1.0	<40	30.4	<1.0		<4.0	<4.0		286	0.34					0.12		8.3	0.54	187	10.5	<0.04		<10	<100	185			<20		<4.0	<10	1330				0.02	<100		10.2			325			
Antamina	Entire polygon	ICP-OES	Two acids	2.17		29.19			26.46				4.88			150	1.14										10.0					160																	1050			
Average ICP-MS				1.44	0.46	20	33	0.13	7.94	35.3	1.26	4.7	1.2	4.1	2.22	162	0.29	1.20	0.08	0.11	0.17	0.20	2.39	12.1	0.74	190	5.5	0.0	0.9	2.1	113	160	16.9	0.005	5.95	0.7	2.6	0.4	1821	0.06	0.31	0.7	0.019	0.22	1.1	8.8	5.0	2.6	401	4	0.24	0.15
Minimum ICP-MS				1.36	0.46	18	30	0.11	6.30	34.6	1.01	4.2	1.2	3.0	1.88	121	0.29	1.08	0.05	0.10	0.10	0.19	2.20	9.6	0.71	175	5.4	0.0	0.8	1.3	110	150	14.0	0.005	5.71	0.6	2.0	0.4	1810	0.06	0.31	0.6	0.017	0.18	0.9	8.0	3.8	2.3	274	4	0.24	0.11
Maximum ICP-MS				1.53	0.46	23	35	0.15	9.58	36.1	1.51	5.1	1.2	5.2	2.56	203	0.30	1.31	0.10	0.12	0.24	0.22	2.57	14.5	0.78	205	5.7	0.1	1.0	2.9	116	170	19.7	0.005	6.19	0.8	3.3	0.5	1833	0.06	0.32	0.8	0.020	0.25	1.2	9.5	6.2	2.8	528	4	0.25	0.18

Appendix C5

Mineralogy and Mineral Availability Data

Table C5.1 Mineral phases by size fractions of the black marble (FC-0) sample

Mineral group	Mineral name	Representative size of each size fraction (μm)									Weight average (wt.%)
		840	420	210	130	90	60	35	20	10	
Weight distribution (wt. %)		**1.77**	**2.13**	**3.55**	**2.48**	**2.13**	**1.77**	**1.52**	**1.75**	**8.44**	**25.55**
Sulfide	Bornite	0.0	0.0	0.0	0.0	0.0	0.0	0.0	0.0	0.0	0.00
	Galena	0.0	0.3	0.0	0.0	0.0	0.0	0.0	0.0	0.0	0.03
	Sphalerite	0.0	0.0	0.0	0.1	0.0	0.0	0.1	0.0	0.1	0.05
	Chalcopyrite	0.1	0.0	0.1	0.2	0.1	0.0	0.2	0.0	0.2	0.11
	Pyrrotite	0.3	0.2	0.3	0.1	0.1	0.1	0.1	0.1	0.0	0.11
	Realgar-Orpiment	0.0	0.0	0.0	0.0	0.0	0.0	0.0	0.0	0.0	0.00
	Stibnite	0.0	0.0	0.0	0.0	0.0	0.0	0.0	0.0	0.0	0.00
	Watanabeite	0.0	0.0	0.0	0.0	0.0	0.0	0.0	0.0	0.0	0.00
	Pyrite	0.0	0.3	0.1	0.2	0.2	0.2	0.3	0.0	0.2	0.19
	Molybdenite	0.0	0.0	0.0	0.0	0.0	0.0	0.0	0.0	0.0	0.00
	Enargite	0.0	0.0	0.0	0.0	0.0	0.0	0.0	0.0	0.0	0.00
	Others	0.0	0.0	0.0	0.0	0.0	0.0	0.0	0.0	0.0	0.00
	Subtotal	**0.4**	**0.9**	**0.5**	**0.5**	**0.3**	**0.3**	**0.8**	**0.1**	**0.5**	**0.48**
Carbonate	Calcite	70.9	62.2	74.6	81.7	82.7	80.8	76.9	72.4	14.5	55.22
	Otavite	0.0	0.0	0.0	0.0	0.0	0.0	0.0	0.0	0.0	0.00
	Siderite	0.0	0.0	0.0	0.0	0.0	0.0	0.0	0.0	0.0	0.01
	Dolomite	0.0	0.0	0.0	0.0	0.0	0.0	0.0	0.0	0.1	0.04
	Others	0.1	0.2	0.1	0.0	0.0	0.0	0.1	0.1	0.9	0.36
	Subtotal	**71.0**	**62.3**	**74.7**	**81.7**	**82.7**	**80.9**	**77.0**	**72.6**	**15.5**	**55.63**
Silicate	Biotite	0.3	0.5	0.4	0.3	0.2	0.3	0.3	1.3	4.0	1.60
	Chlorite	0.0	0.0	0.1	0.0	0.0	0.0	0.0	0.1	0.8	0.30
	K_Feldspar	1.1	1.7	2.3	2.0	1.9	1.9	1.8	3.3	13.0	5.66
	Kaolinite	0.3	0.0	0.1	0.0	0.0	0.0	0.1	0.1	1.5	0.53
	Muscovite	0.0	0.0	0.0	0.2	0.1	0.2	0.1	0.3	2.9	1.01
	Plagioclase	3.0	4.7	2.8	2.2	2.0	2.5	2.7	4.9	9.6	5.21
	Pyroxene	5.0	6.8	4.2	3.7	3.8	4.4	6.4	6.0	14.1	7.94
	Quartz	6.6	7.2	4.2	1.9	2.1	2.3	2.2	2.7	17.6	8.30
	Talc	0.0	0.0	0.0	0.0	0.0	0.0	0.0	0.0	0.0	0.00
	Mica	2.7	2.0	2.5	2.1	2.0	1.9	2.0	2.5	7.8	4.06
	Titanite	0.2	0.4	0.8	0.5	0.4	0.4	0.7	0.5	0.5	0.49
	Others	8.0	12.0	6.2	4.2	3.9	4.4	5.4	4.7	5.5	5.89
	Subtotal	**27.1**	**35.3**	**23.6**	**17.1**	**16.5**	**18.4**	**21.6**	**26.4**	**77.2**	**41.00**
Phosphate		0.1	0.6	0.3	0.3	0.1	0.1	0.2	0.4	2.6	**1.04**
Oxides	FeOxyhydroxides	1.4	0.9	0.8	0.3	0.3	0.3	0.4	0.3	2.1	1.09
	Others	0.0	0.0	0.0	0.1	0.0	0.0	0.0	0.0	0.3	0.10
	Subtotal	**1.4**	**0.9**	**0.8**	**0.4**	**0.3**	**0.3**	**0.4**	**0.4**	**2.4**	**1.19**
Sulphates	FeSulphate	0.0	0.0	0.1	0.0	0.1	0.1	0.1	0.2	0.8	0.32
	Barite	0.0	0.0	0.0	0.0	0.0	0.0	0.0	0.0	0.0	0.00
	Gypsum	0.0	0.0	0.0	0.0	0.0	0.0	0.0	0.0	0.0	0.01
	Others	0.0	0.0	0.0	0.0	0.0	0.0	0.0	0.0	0.0	0.00
	Subtotal	**0.0**	**0.0**	**0.1**	**0.0**	**0.1**	**0.1**	**0.1**	**0.2**	**0.8**	**0.33**
Others		0.0	0.0	0.0	0.0	0.0	0.0	0.0	0.0	1.0	0.35
	Total	**100.0**	**100.0**	**100.0**	**100.0**	**100.0**	**100.0**	**100.0**	**100.0**	**100.0**	**100.0**

NOTE: For each sample, the vertical list of mineral phases are the SumTotal of all phases determined by this MLA method; a value of ZERO means that there is "trace" (i.e. <0.01 wt. %)

Table C5.2 Mineral phases by size fractions of the diopside marble (FC-1) sample

Mineral group	Mineral name	Representative size of each size fraction (μm)									Weight average (wt.%)
		840	420	210	130	90	60	35	20	10	
Weight distribution (wt. %)		**2.25**	**1.50**	**1.69**	**1.50**	**1.50**	**1.12**	**1.23**	**1.97**	**3.17**	**15.93**
Sulfide	Bornite	0.0	0.0	0.2	0.0	0.0	0.0	0.0	0.0	0.0	0.02
	Galena	0.2	0.2	0.0	0.1	0.1	0.0	0.0	0.0	0.0	0.08
	Sphalerite	0.4	0.6	0.3	0.2	0.2	0.3	0.4	0.0	0.2	0.26
	Chalcopyrite	0.2	0.5	0.7	0.4	0.4	0.3	0.5	0.3	1.7	0.65
	Pyrrotite	0.0	0.1	0.2	0.1	0.1	0.1	0.3	0.2	0.3	0.15
	Realgar-Orpiment	0.0	0.0	0.0	0.0	0.0	0.0	0.0	0.0	0.0	0.00
	Stibnite	0.0	0.0	0.0	0.0	0.0	0.0	0.0	0.0	0.0	0.00
	Watanabeite	0.0	0.0	0.0	0.0	0.0	0.0	0.1	0.0	0.0	0.01
	Pyrite	0.2	1.1	1.4	0.9	0.6	0.3	0.9	0.3	0.9	0.72
	Molybdenite	0.0	0.0	0.1	0.0	0.0	0.0	0.0	0.0	0.1	0.04
	Enargite	0.0	0.0	0.0	0.0	0.0	0.0	0.0	0.0	0.0	0.01
	Others	0.0	0.0	0.0	0.0	0.0	0.0	0.1	0.0	0.0	0.03
	Subtotal	**1.0**	**2.6**	**2.9**	**1.7**	**1.4**	**1.1**	**2.3**	**0.9**	**3.2**	**1.98**
Carbonate	Calcite	37.6	36.4	45.6	65.2	71.4	69.9	64.9	54.4	22.0	47.47
	Otavite	0.0	0.0	0.0	0.0	0.0	0.0	0.0	0.0	0.0	0.00
	Siderite	0.0	0.0	0.0	0.0	0.0	0.0	0.0	0.0	0.0	0.00
	Dolomite	0.0	0.0	0.0	0.0	0.0	0.0	0.0	0.0	0.1	0.03
	Others	0.0	0.0	0.0	0.0	0.0	0.0	0.0	0.1	0.2	0.05
	Subtotal	**37.6**	**36.4**	**45.6**	**65.2**	**71.4**	**69.9**	**64.9**	**54.5**	**22.3**	**47.54**
Silicate	Biotite	0.6	0.6	0.3	0.2	0.3	0.3	0.4	2.8	4.5	1.50
	Chlorite	0.0	0.0	0.2	0.1	0.0	0.0	0.0	0.0	0.0	0.04
	K_Feldspar	7.3	5.5	4.0	2.7	2.9	3.7	3.2	5.9	16.8	7.06
	Kaolinite	0.0	0.0	0.1	0.1	0.0	0.1	0.1	0.2	0.9	0.23
	Muscovite	0.1	0.7	0.6	0.4	0.2	0.2	0.2	0.3	2.6	0.77
	Plagioclase	4.7	2.1	2.6	2.1	1.5	1.4	1.3	2.6	5.3	3.06
	Pyroxene	4.9	4.6	4.4	2.8	2.7	3.0	5.4	9.7	18.6	7.63
	Quartz	6.6	12.7	13.7	10.4	8.3	7.7	5.0	5.5	9.0	8.73
	Talc	0.0	0.0	0.0	0.0	0.0	0.0	0.0	0.0	0.0	0.00
	Mica	2.6	6.5	4.1	2.3	2.0	2.5	2.1	4.3	2.2	3.12
	Titanite	0.2	0.2	0.6	0.3	0.1	0.1	0.2	0.3	0.8	0.36
	Others	33.6	27.2	19.7	11.3	9.1	9.8	14.4	12.7	11.9	17.05
	Subtotal	**60.6**	**60.1**	**50.3**	**32.5**	**27.1**	**28.8**	**32.2**	**44.2**	**72.5**	**49.57**
Phosphate		0.1	0.1	0.7	0.3	0.1	0.1	0.1	0.2	0.9	**0.35**
Oxides	FeOxyhydroxides	0.8	0.7	0.4	0.1	0.1	0.1	0.3	0.1	0.3	0.35
	Others	0.0	0.1	0.0	0.0	0.0	0.0	0.1	0.0	0.1	0.04
	Subtotal	**0.8**	**0.8**	**0.4**	**0.1**	**0.1**	**0.1**	**0.4**	**0.1**	**0.4**	**0.39**
Sulphates	FeSulphate	0.0	0.0	0.1	0.0	0.0	0.0	0.1	0.1	0.2	0.06
	Barite	0.0	0.0	0.0	0.0	0.0	0.0	0.0	0.0	0.0	0.00
	Gypsum	0.0	0.0	0.0	0.0	0.0	0.0	0.0	0.0	0.0	0.00
	Others	0.0	0.0	0.0	0.0	0.0	0.0	0.0	0.0	0.0	0.00
	Subtotal	**0.0**	**0.0**	**0.1**	**0.0**	**0.0**	**0.0**	**0.1**	**0.1**	**0.2**	**0.07**
Others		0.0	0.0	0.1	0.1	0.0	0.0	0.0	0.0	0.5	0.13
	Total	**100.0**	**100.1**	**100.0**	**100.0**	**100.0**	**100.0**	**100.0**	**100.0**	**100.0**	**100.0**

NOTE: For each sample, the vertical list of mineral phases are the SumTotal of all phases determined by this MLA method; a value of ZERO means that there is "trace" (i.e. <0.01 wt. %)

Table C5.3 Mineral phases by size fractions of the diopside marble (FC-2) sample

Mineral group	Mineral name	Representative size of each size fraction (μm)									Weight average (wt.%)
		840	420	210	130	90	60	35	20	10	
Weight distribution (wt. %)		**1.25**	**1.04**	**1.04**	**0.42**	**0.42**	**0.42**	**0.89**	**1.37**	**2.04**	**8.88**
Sulfide	Bornite	0.0	0.0	0.0	0.0	0.0	0.0	0.0	0.0	0.0	0.00
	Galena	0.0	0.1	0.3	0.2	0.1	0.1	0.1	0.1	0.0	0.08
	Sphalerite	0.0	0.0	0.1	0.2	0.2	0.1	0.2	0.1	0.3	0.15
	Chalcopyrite	0.3	0.1	0.6	1.4	1.1	0.9	1.3	0.6	1.3	0.79
	Pyrrotite	0.0	0.0	0.0	0.0	0.1	0.0	0.0	0.0	0.0	0.02
	Realgar-Orpiment	0.0	0.0	0.0	0.0	0.0	0.0	0.0	0.0	0.0	0.00
	Stibnite	0.0	0.0	0.0	0.0	0.0	0.0	0.0	0.0	0.0	0.00
	Watanabeite	0.0	0.0	0.0	0.0	0.0	0.0	0.0	0.0	0.0	0.00
	Pyrite	0.1	6.8	5.1	3.8	3.5	3.5	5.6	2.4	2.5	3.42
	Molybdenite	0.0	0.0	0.0	0.1	0.1	0.0	0.1	0.0	0.1	0.05
	Enargite	0.0	0.0	0.0	0.0	0.0	0.0	0.0	0.0	0.0	0.00
	Others	0.0	0.0	0.0	0.0	0.0	0.0	0.0	0.0	0.0	0.01
	Subtotal	**0.4**	**7.0**	**6.2**	**5.7**	**5.1**	**4.6**	**7.3**	**3.2**	**4.3**	**4.53**
Carbonate	Calcite	11.9	8.2	8.0	10.8	11.5	13.7	12.9	18.0	5.2	10.51
	Otavite	0.0	0.0	0.0	0.0	0.0	0.0	0.0	0.0	0.0	0.00
	Siderite	0.0	0.0	0.0	0.0	0.0	0.0	0.0	0.2	0.0	0.04
	Dolomite	0.0	0.0	0.0	0.0	0.0	0.0	0.0	0.0	0.0	0.01
	Others	0.1	0.0	0.1	0.2	0.2	0.1	0.2	0.5	1.4	0.48
	Subtotal	**12.1**	**8.2**	**8.1**	**11.0**	**11.7**	**13.9**	**13.2**	**18.6**	**6.6**	**11.04**
Silicate	Biotite	0.7	0.2	0.4	0.5	0.5	0.4	0.3	0.7	0.7	0.54
	Chlorite	0.1	0.0	0.0	0.1	0.0	0.0	0.0	0.1	0.1	0.06
	K_Feldspar	8.8	8.8	9.7	8.7	9.9	13.0	9.4	13.5	25.9	13.86
	Kaolinite	0.0	0.0	0.2	0.1	0.1	0.2	0.0	0.3	0.8	0.28
	Muscovite	0.1	0.7	0.7	0.8	1.0	1.1	1.2	0.6	1.3	0.83
	Plagioclase	4.1	3.2	3.0	3.2	2.7	2.9	2.1	3.1	4.0	3.33
	Pyroxene	18.1	11.3	9.8	8.4	8.8	9.5	13.4	16.5	22.9	15.43
	Quartz	8.6	8.7	14.0	19.0	18.6	14.3	9.0	7.0	6.5	9.78
	Talc	0.0	0.0	0.0	0.0	0.0	0.0	0.0	0.0	0.0	0.00
	Mica	3.5	4.9	5.8	6.9	7.6	7.8	6.9	7.5	2.2	5.16
	Titanite	0.4	0.2	0.8	0.7	0.5	0.5	0.5	0.9	1.9	0.88
	Others	42.2	46.5	40.4	33.1	32.0	29.9	34.4	26.5	17.3	32.09
	Subtotal	**86.5**	**84.5**	**84.9**	**81.4**	**81.7**	**79.7**	**77.3**	**76.6**	**83.8**	**82.23**
Phosphate		0.1	0.0	0.1	0.2	0.3	0.2	0.3	0.2	1.3	**0.43**
Oxides	FeOxyhydroxides	0.9	0.2	0.6	1.5	1.1	1.4	1.5	1.0	2.1	1.21
	Others	0.0	0.0	0.0	0.0	0.1	0.1	0.1	0.1	0.2	0.08
	Subtotal	**0.9**	**0.2**	**0.7**	**1.5**	**1.2**	**1.5**	**1.7**	**1.1**	**2.3**	**1.29**
Sulphates	FeSulphate	0.1	0.0	0.0	0.1	0.1	0.1	0.2	0.2	1.2	0.35
	Barite	0.0	0.0	0.0	0.0	0.0	0.0	0.0	0.0	0.0	0.00
	Gypsum	0.0	0.0	0.0	0.0	0.0	0.0	0.0	0.0	0.0	0.00
	Others	0.0	0.0	0.0	0.0	0.0	0.0	0.0	0.0	0.0	0.00
	Subtotal	**0.1**	**0.0**	**0.0**	**0.1**	**0.1**	**0.1**	**0.2**	**0.2**	**1.2**	**0.35**
Others		0.0	0.0	0.0	0.0	0.0	0.0	0.1	0.1	0.5	0.14
	Total	**100.0**	**100.0**	**100.0**	**100.0**	**100.0**	**100.0**	**100.0**	**100.0**	**100.0**	**100.0**

NOTE: For each sample, the vertical list of mineral phases are the SumTotal of all phases determined by this MLA method; a value of ZERO means that there is "trace" (i.e. <0.01 wt. %)

Table C5.4 Mineral phases by size fractions of the diopside marble (FC-3) sample

Mineral group	Mineral name	Representative size of each size fraction (μm)									Weight average (wt.%)
		840	420	210	130	90	60	35	20	10	
Weight distribution (wt. %)		**1.77**	**1.84**	**2.45**	**1.53**	**1.53**	**1.22**	**0.66**	**1.50**	**2.65**	**15.15**
Sulfide	Bornite	0.0	0.0	0.0	0.0	0.0	0.0	0.0	0.0	0.0	0.00
	Galena	0.2	0.0	0.1	0.1	0.0	0.0	0.1	0.1	0.0	0.06
	Sphalerite	0.2	0.1	0.3	0.2	0.3	0.4	0.4	0.3	0.3	0.24
	Chalcopyrite	0.0	0.4	0.1	0.5	0.6	0.5	0.5	0.3	0.7	0.38
	Pyrrotite	0.0	0.7	0.1	0.1	0.2	0.2	0.5	0.3	0.4	0.25
	Realgar-Orpiment	0.0	0.0	0.0	0.0	0.0	0.0	0.0	0.0	0.0	0.00
	Stibnite	0.0	0.0	0.0	0.0	0.0	0.0	0.0	0.0	0.0	0.00
	Watanabeite	0.0	0.0	0.0	0.0	0.0	0.0	0.0	0.0	0.0	0.00
	Pyrite	1.3	2.7	1.7	1.9	1.6	1.4	2.2	0.4	0.9	1.49
	Molybdenite	0.0	0.0	0.0	0.0	0.0	0.0	0.0	0.0	0.0	0.01
	Enargite	0.0	0.0	0.0	0.0	0.0	0.0	0.0	0.0	0.0	0.00
	Others	0.0	0.0	0.0	0.0	0.0	0.0	0.0	0.0	0.0	0.00
	Subtotal	**1.7**	**3.8**	**2.2**	**2.7**	**2.6**	**2.5**	**3.6**	**1.4**	**2.2**	**2.44**
Carbonate	Calcite	57.6	53.0	66.9	77.7	79.6	79.1	76.6	76.3	47.8	65.50
	Otavite	0.0	0.0	0.0	0.0	0.0	0.0	0.0	0.0	0.0	0.00
	Siderite	0.0	0.0	0.0	0.0	0.0	0.0	0.0	0.0	0.1	0.02
	Dolomite	0.0	0.0	0.0	0.0	0.0	0.1	0.0	0.0	0.3	0.06
	Others	0.0	0.0	0.0	0.0	0.0	0.0	0.0	0.1	0.4	0.09
	Subtotal	**57.6**	**53.0**	**66.9**	**77.7**	**79.7**	**79.2**	**76.7**	**76.4**	**48.5**	**65.67**
Silicate	Biotite	0.6	0.1	0.3	0.1	0.1	0.1	0.1	0.6	6.9	1.42
	Chlorite	0.1	0.0	0.0	0.0	0.1	0.0	0.0	0.0	0.1	0.04
	K_Feldspar	2.7	2.6	1.3	1.2	1.1	1.4	1.4	2.0	5.9	2.50
	Kaolinite	0.0	0.0	0.0	0.0	0.0	0.0	0.0	0.0	0.3	0.06
	Muscovite	0.0	0.4	0.1	0.1	0.1	0.1	0.1	0.1	0.4	0.17
	Plagioclase	3.9	5.5	3.2	2.5	2.3	2.2	2.9	2.4	6.4	3.78
	Pyroxene	4.0	5.3	4.4	2.7	2.7	3.2	3.1	5.0	13.0	5.52
	Quartz	3.6	4.1	3.3	2.5	2.2	1.9	1.4	1.4	3.5	2.91
	Talc	0.0	0.0	0.0	0.0	0.0	0.0	0.0	0.0	0.0	0.00
	Mica	1.1	1.5	1.3	1.1	1.1	1.3	1.0	1.9	1.3	1.31
	Titanite	0.6	0.2	0.2	0.1	0.1	0.1	0.1	0.3	0.8	0.34
	Others	22.8	23.4	16.5	8.7	7.6	7.2	8.8	7.8	7.8	12.92
	Subtotal	**39.6**	**43.0**	**30.5**	**19.0**	**17.4**	**17.7**	**19.0**	**21.6**	**46.3**	**30.96**
Phosphate		0.9	0.1	0.1	0.1	0.1	0.1	0.1	0.1	0.8	**0.30**
Oxides	FeOxyhydroxides	0.0	0.0	0.2	0.3	0.2	0.3	0.3	0.1	0.7	0.25
	Others	0.0	0.0	0.0	0.0	0.0	0.0	0.0	0.0	0.1	0.03
	Subtotal	**0.0**	**0.1**	**0.2**	**0.3**	**0.2**	**0.3**	**0.3**	**0.1**	**0.9**	**0.28**
Sulphates	FeSulphate	0.2	0.0	0.0	0.2	0.1	0.1	0.2	0.2	0.5	0.17
	Barite	0.0	0.0	0.0	0.0	0.0	0.0	0.0	0.0	0.0	0.00
	Gypsum	0.0	0.0	0.0	0.0	0.0	0.0	0.0	0.0	0.0	0.01
	Others	0.0	0.0	0.0	0.0	0.0	0.0	0.0	0.0	0.0	0.00
	Subtotal	**0.2**	**0.0**	**0.0**	**0.2**	**0.1**	**0.2**	**0.2**	**0.2**	**0.5**	**0.18**
Others		0.0	0.0	0.0	0.0	0.0	0.0	0.1	0.1	0.9	0.17
	Total	**100.0**	**100.0**	**100.0**	**100.0**	**100.0**	**100.0**	**100.0**	**100.0**	**100.0**	**100.0**

NOTE: For each sample, the vertical list of mineral phases are the SumTotal of all phases determined by this MLA method; a value of ZERO means that there is "trace" (i.e. <0.01 wt. %)

Table C5.5 Mineral phases by size fractions of the gray hornfels (FC-4) sample

Mineral group	Mineral name	Representative size of each size fraction (μm)									Weight average (wt.%)
		840	420	210	130	90	60	35	20	10	
Weight distribution (wt. %)		**2.16**	**3.09**	**5.26**	**2.48**	**2.94**	**3.09**	**1.20**	**2.09**	**3.06**	**25.37**
Sulfide	Bornite	0.0	0.0	0.0	0.0	0.0	0.0	0.0	0.0	0.0	0.00
	Galena	0.0	0.0	0.0	0.0	0.0	0.1	0.0	0.0	0.0	0.01
	Sphalerite	0.0	0.0	0.0	0.1	0.1	0.1	0.2	0.0	0.1	0.04
	Chalcopyrite	0.0	0.2	0.0	0.0	0.0	0.0	0.1	0.1	0.2	0.07
	Pyrrotite	0.2	0.0	0.0	0.0	0.0	0.0	0.0	0.1	0.0	0.03
	Realgar-Orpiment	0.0	0.0	0.0	0.0	0.0	0.0	0.0	0.0	0.0	0.00
	Stibnite	0.0	0.0	0.0	0.0	0.0	0.0	0.0	0.0	0.0	0.00
	Watanabeite	0.0	0.0	0.0	0.0	0.0	0.0	0.0	0.0	0.0	0.01
	Pyrite	1.5	0.9	0.3	0.3	0.3	0.5	0.6	0.1	0.4	0.49
	Molybdenite	0.0	0.0	0.0	0.0	0.0	0.0	0.0	0.0	0.0	0.00
	Enargite	0.0	0.0	0.0	0.0	0.0	0.0	0.0	0.0	0.0	0.00
	Others	0.0	0.0	0.0	0.0	0.0	0.0	0.0	0.0	0.0	0.01
	Subtotal	**1.7**	**1.2**	**0.3**	**0.5**	**0.4**	**0.6**	**0.9**	**0.4**	**0.7**	**0.67**
Carbonate	Calcite	84.7	85.5	94.5	96.7	97.1	96.4	96.5	92.9	72.3	90.61
	Otavite	0.0	0.0	0.0	0.0	0.0	0.0	0.0	0.0	0.2	0.03
	Siderite	0.0	0.0	0.0	0.0	0.0	0.0	0.0	0.0	0.0	0.00
	Dolomite	0.2	0.5	0.0	0.0	0.0	0.0	0.0	0.1	0.3	0.12
	Others	0.0	0.0	0.0	0.0	0.0	0.0	0.0	0.0	0.1	0.02
	Subtotal	**84.9**	**86.1**	**94.5**	**96.8**	**97.1**	**96.4**	**96.5**	**93.0**	**72.9**	**90.78**
Silicate	Biotite	0.2	0.3	0.2	0.0	0.1	0.1	0.0	0.6	9.6	1.32
	Chlorite	0.6	0.1	0.2	0.0	0.0	0.0	0.0	0.0	0.0	0.11
	K_Feldspar	0.3	0.5	0.2	0.1	0.1	0.1	0.2	0.5	1.2	0.36
	Kaolinite	0.1	0.0	0.0	0.0	0.0	0.0	0.0	0.0	0.2	0.04
	Muscovite	0.0	0.0	0.0	0.0	0.0	0.0	0.0	0.0	0.2	0.04
	Plagioclase	6.1	3.6	1.5	0.9	0.7	1.0	0.8	1.1	2.5	1.99
	Pyroxene	1.7	1.0	0.7	0.6	0.6	0.6	0.6	2.7	4.7	1.43
	Quartz	1.7	3.2	1.1	0.4	0.4	0.4	0.3	0.7	2.5	1.27
	Talc	0.0	0.0	0.0	0.0	0.0	0.0	0.0	0.0	0.0	0.00
	Mica	1.8	0.5	0.1	0.2	0.1	0.1	0.1	0.4	0.9	0.42
	Titanite	0.0	0.6	0.1	0.0	0.0	0.0	0.0	0.1	0.3	0.15
	Others	0.5	2.8	0.7	0.3	0.3	0.3	0.3	0.2	1.8	0.87
	Subtotal	**12.9**	**12.5**	**4.8**	**2.7**	**2.3**	**2.8**	**2.4**	**6.4**	**24.0**	**8.01**
Phosphate		0.0	0.2	0.1	0.0	0.0	0.0	0.0	0.1	0.3	**0.09**
Oxides	FeOxyhydroxides	0.5	0.1	0.3	0.1	0.2	0.1	0.2	0.1	1.3	0.33
	Others	0.0	0.0	0.0	0.0	0.0	0.0	0.0	0.0	0.0	0.01
	Subtotal	**0.5**	**0.1**	**0.3**	**0.1**	**0.2**	**0.1**	**0.2**	**0.1**	**1.4**	**0.34**
Sulphates	FeSulphate	0.0	0.0	0.0	0.0	0.0	0.0	0.0	0.0	0.3	0.04
	Barite	0.0	0.0	0.0	0.0	0.0	0.0	0.0	0.0	0.0	0.00
	Gypsum	0.0	0.0	0.0	0.0	0.0	0.0	0.0	0.0	0.0	0.00
	Others	0.0	0.0	0.0	0.0	0.0	0.0	0.0	0.0	0.0	0.00
	Subtotal	**0.0**	**0.0**	**0.0**	**0.0**	**0.0**	**0.0**	**0.0**	**0.0**	**0.3**	**0.05**
Others		0.0	0.0	0.0	0.0	0.0	0.0	0.0	0.0	0.5	0.07
	Total	**100.0**	**100.0**	**100.0**	**100.0**	**100.0**	**100.0**	**100.0**	**100.0**	**100.0**	**100.0**

NOTE: For each sample, the vertical list of mineral phases are the SumTotal of all phases determined by this MLA method; a value of ZERO means that there is "trace" (i.e. <0.01 wt. %)

Table C5.6 Copper, lead, and zinc distribution by mineral in all Class B waste rock samples

Sample ID	FC-0									FC-1									FC-2									FC-3									FC-4								
Representative size (µm)	840	420	210	130	90	60	35	20	10	840	420	210	130	90	60	35	20	10	840	420	210	130	90	60	35	20	10	840	420	210	130	90	60	35	20	10	840	420	210	130	90	60	35	20	10
Mineral					Cu (%)									Cu (%)									Cu (%)									Cu (%)									Cu (%)				
TrampMetal	0.5	0.1	0.0	0.6	0.7	0.1	0.0	0.8	54.3	1.2	0.5	0.4	0.6	0.2	5.2	1.6	4.5	18.6	0.0	1.8	0.0	0.6	0.0	0.3	1.3	2.4	12.6	0.0	0.0	0.0	0.2	0.1	0.1	1.9	17.8	40.8	0.9	2.3	0.0	0.0	0.8	4.6	1.0	5.4	45.4
PyriteCu	0.4	6.1	0.1	0.1	0.0	0.1	0.6	0.3	0.0	0.4	0.2	2.1	1.9	0.1	2.3	0.1	0.5	0.4	0.3	31.1	2.2	1.1	1.4	0.4	2.6	4.8	4.5	2.1	0.4	0.9	0.8	0.9	0.4	0.7	1.0	3.6	0.9	0.1	0.3	1.2	5.3	0.2	4.8	1.5	0.2
Chalcocite	0.0	0.0	0.6	0.0	0.0	0.0	0.0	0.0	0.0	0.0	0.0	0.0	0.0	0.0	0.3	1.6	0.0	0.0	0.0	0.0	0.0	0.0	0.0	0.0	0.0	0.0	0.0	0.0	0.0	0.0	0.0	0.0	0.0	0.0	0.0	0.0	0.0	0.0	0.0	0.0	0.0	0.0	0.0	0.0	0.0
Bornite	0.0	0.0	1.5	0.0	0.0	0.8	0.0	0.1	0.0	0.0	2.7	26.1	1.3	1.4	0.4	3.3	0.0	0.7	0.0	0.0	0.0	0.0	0.0	0.0	0.2	0.3	0.0	0.0	0.0	0.0	0.1	0.0	0.0	0.0	0.0	0.0	0.0	0.0	0.2	0.0	0.0	0.0	0.0	0.0	0.0
Chalcopyrite	40.4	0.0	7.1	48.1	10.8	0.4	17.9	5.1	2.2	8.6	41.2	20.7	68.1	28.2	43.8	28.4	23.1	5.6	65.6	24.2	43.3	26.1	36.9	41.8	33.9	24.6	12.4	8.6	61.1	14.9	41.9	32.7	22.5	54.7	26.7	6.1	8.5	75.4	2.3	45.9	8.3	8.8	32.1	14.7	1.9
ChalcopyritePb	0.8	0.5	3.9	0.0	27.0	0.0	18.0	0.2	4.4	17.0	11.4	12.4	12.8	22.7	12.2	14.0	35.1	49.2	2.4	3.1	14.1	29.6	27.5	15.2	23.9	22.9	29.2	1.3	4.5	32.1	31.9	21.0	37.0	8.0	16.2	17.6	0.0	0.8	1.1	0.0	28.8	0.8	8.4	15.6	10.5
ChalcopyriteZn	2.9	0.0	3.0	0.0	6.6	10.8	1.1	2.5	2.8	32.0	11.4	18.6	0.6	26.2	7.1	19.4	5.4	6.6	0.2	2.2	14.7	24.0	10.4	18.6	11.0	2.1	10.1	1.4	22.2	10.4	4.4	25.4	15.2	14.5	10.0	9.9	1.1	0.1	0.0	0.0	0.0	0.0	3.9	17.8	3.3
Enargite	0.0	0.0	0.0	0.0	0.0	0.0	0.0	0.0	0.0	0.6	1.7	1.0	0.0	3.3	1.0	0.0	6.6	0.0	2.4	0.3	0.0	0.0	0.0	0.0	0.5	0.1	0.0	0.0	0.0	0.1	0.0	0.0	0.5	0.0	0.0	0.0	0.0	0.0	0.0	0.2	1.2	17.8	1.7	8.7	0.0
EnargiteZn	0.0	0.0	0.0	0.0	0.0	1.8	0.0	0.0	0.0	0.0	4.7	0.0	0.0	1.1	0.3	0.0	0.0	0.0	0.3	0.0	0.0	0.0	0.0	0.1	0.0	0.0	0.0	0.0	0.0	0.0	0.0	0.0	0.0	1.4	1.9	0.0	0.0	0.0	0.0	0.0	0.0	0.0	0.0	0.0	0.0
TennantiteZnFe	0.0	0.0	0.0	0.0	0.0	0.0	0.0	0.0	0.0	0.0	0.0	0.0	0.0	0.5	0.0	3.4	0.1	1.7	0.9	0.5	0.0	0.0	0.0	0.0	0.7	0.1	0.0	0.0	0.0	0.5	0.0	0.0	0.0	0.0	0.0	1.0	0.0	0.0	0.0	0.0	0.1	0.6	4.4	0.0	2.4
WatanabeiteZn	0.0	0.0	0.1	0.0	0.0	0.0	4.2	0.0	0.0	0.1	0.0	0.4	0.2	2.9	9.0	12.7	1.9	0.0	0.2	0.0	0.0	0.0	0.0	0.0	0.5	0.0	0.0	0.0	0.0	0.0	0.0	0.0	0.0	0.0	0.0	0.0	0.0	0.0	1.7	25.5	6.8	20.9	1.1	14.0	0.0
SphaleriteCu	0.0	0.3	1.1	2.0	0.1	0.9	2.4	0.2	0.3	11.3	8.3	2.0	2.9	3.4	6.0	4.7	0.8	0.6	0.1	0.0	1.6	1.4	1.7	0.6	1.0	0.7	1.5	9.6	2.1	12.8	3.2	3.2	7.0	4.5	5.1	1.2	0.0	0.1	0.1	10.5	7.8	7.9	9.5	0.9	0.9
FeOxyhydroxCuPbZnS	36.7	15.0	13.4	6.5	8.7	8.1	5.5	5.2	8.8	17.4	6.6	2.1	1.4	0.9	1.7	3.1	1.1	0.9	13.8	3.0	5.8	6.1	5.4	7.9	5.9	5.7	6.6	0.8	0.7	5.3	2.5	1.2	3.5	3.1	1.2	2.4	21.8	2.8	19.2	9.3	16.7	12.9	8.5	3.3	8.1
Cuprite	0.0	0.0	0.0	0.0	1.4	0.0	0.0	0.6	0.0	0.0	3.6	0.0	0.0	0.0	0.0	0.0	0.4	0.0	0.0	1.3	1.3	0.5	2.1	0.6	1.1	0.0	0.0	0.0	0.0	0.0	1.3	8.3	0.0	0.0	0.0	0.0	0.0	0.6	13.6	0.0	1.1	0.1	0.0	0.3	0.0
SideriteAsMnZnCu	0.0	0.0	0.0	0.1	0.1	0.0	0.0	0.0	0.0	0.0	0.0	0.0	0.0	0.0	0.0	0.0	0.0	0.0	0.0	0.0	0.0	0.0	0.0	0.0	0.0	0.2	0.0	0.0	0.0	0.0	0.0	0.0	0.0	0.0	0.0	0.1	0.0	0.0	0.0	0.0	0.0	0.0	0.0	0.0	0.0
GruneritePbCuZn	0.0	0.5	0.0	0.0	0.0	0.4	0.4	2.4	1.8	0.0	0.3	0.0	0.3	0.1	0.0	0.4	0.9	0.7	2.5	0.4	0.7	1.0	1.0	0.9	0.7	2.3	3.3	0.5	0.0	0.7	0.1	0.0	0.1	0.0	0.8	0.2	0.2	0.0	0.0	0.0	0.0	0.0	0.0	0.1	0.1
Malachite	0.0	0.0	0.0	0.0	0.0	0.0	0.0	0.0	0.0	0.0	0.0	0.0	0.0	0.0	0.0	0.0	0.0	0.0	0.0	0.0	0.0	0.0	0.0	0.0	0.0	4.9	4.6	0.0	0.0	0.0	0.0	0.0	0.0	0.0	0.0	0.0	0.0	0.0	0.0	0.0	0.0	0.0	0.0	0.0	1.4
OtaviteZnCu	0.0	0.0	0.0	0.0	0.0	0.0	0.0	0.0	0.0	0.0	0.0	0.0	0.0	0.0	0.0	0.0	0.0	0.0	0.0	0.0	0.0	0.0	0.0	0.0	0.0	0.0	0.0	0.0	0.0	0.0	0.0	0.0	0.0	0.0	0.0	0.1	0.0	0.0	0.0	0.0	0.0	0.0	0.0	0.0	4.2
FeSulphateCuAsMoZn	0.8	0.3	2.7	1.0	6.6	4.6	2.5	0.8	0.5	0.3	0.3	0.8	0.0	0.2	0.0	1.6	1.5	0.1	0.2	0.2	0.6	0.4	0.3	1.7	1.5	0.6	0.1	21.1	0.8	0.8	4.4	1.2	3.9	4.2	3.3	0.8	1.1	0.2	0.5	0.8	5.2	2.3	0.6	1.6	0.5
JarositeCu	0.0	0.0	0.0	0.0	1.0	0.0	0.0	0.0	0.0	0.0	0.0	0.0	0.0	0.0	0.0	0.0	0.0	0.0	0.0	0.0	0.0	0.0	0.0	0.0	0.0	0.0	0.1	0.0	0.0	0.0	0.0	0.0	0.0	0.0	0.0	0.0	0.0	0.0	0.0	0.0	0.0	0.0	0.0	0.0	0.0
MolybdofornaciteZn	0.1	0.2	0.0	0.0	0.0	0.0	0.0	0.0	0.0	0.4	1.8	1.2	0.3	1.2	0.0	0.2	0.0	0.0	0.0	0.1	0.1	0.0	0.1	0.0	0.2	0.0	0.0	0.0	0.1	0.1	0.4	0.2	0.2	0.3	0.3	0.0	0.0	0.0	0.0	0.0	0.0	0.1	0.1	0.0	0.0
ApatiteCuPbZn	1.2	4.3	2.5	2.9	1.0	1.4	1.6	3.1	6.6	0.9	0.5	2.0	2.6	0.9	0.6	0.7	1.3	1.7	0.8	0.3	0.4	0.6	1.0	0.8	0.6	0.8	2.3	22.0	0.7	3.1	0.4	0.3	0.6	0.6	0.7	1.9	0.5	2.0	5.4	0.4	3.0	1.9	0.5	1.1	1.2
FornaciteCa	0.0	0.2	0.0	0.0	0.0	0.0	0.0	0.0	2.8	0.0	0.0	0.0	0.0	0.0	0.0	0.0	0.0	0.5	0.0	0.0	0.0	0.0	0.0	0.0	0.0	0.0	0.1	0.0	0.0	0.0	0.0	0.0	0.0	0.0	0.0	0.0	0.0	0.0	0.0	0.0	0.0	0.0	0.0	0.0	0.0
TyrolitePb	0.0	0.0	0.0	0.0	0.0	0.0	0.0	0.0	0.2	0.0	0.0	0.0	0.0	0.0	0.0	0.0	0.0	0.0	0.0	0.0	0.0	0.0	0.0	0.0	0.0	0.0	0.0	0.0	0.0	0.0	0.0	0.0	0.0	0.0	0.0	0.0	0.0	0.0	0.0	0.0	0.0	0.0	0.0	0.0	0.0
MicaAlteredCuZn	1.9	16.9	13.0	5.2	3.2	12.3	6.5	16.3	13.3	5.3	1.4	2.0	2.0	2.4	2.7	1.4	8.9	10.3	0.1	0.9	3.1	0.4	0.8	1.0	1.0	1.4	3.9	1.5	1.3	10.7	3.0	3.0	2.1	1.4	2.3	8.9	57.8	1.1	4.9	4.3	3.3	8.0	0.2	7.0	13.4
FeCuSilicate	8.3	49.2	35.1	23.3	21.2	47.8	30.1	54.4	0.0	0.4	0.9	5.0	1.0	2.4	5.4	1.7	3.4	0.0	4.2	27.1	4.4	5.2	8.7	6.8	11.3	20.3	2.5	5.7	2.9	0.7	4.2	1.7	5.3	3.1	9.9	2.0	6.2	1.1	44.1	1.6	6.1	11.9	21.1	5.7	4.1
TitaniteMixPbCu	6.1	6.4	16.1	10.2	11.6	10.5	9.3	8.3	2.1	4.1	2.5	3.2	4.0	2.0	2.0	1.9	4.2	2.4	6.0	3.6	7.7	3.0	2.9	3.2	2.1	5.7	6.1	25.5	3.4	7.0	1.3	0.9	1.5	1.4	3.0	3.4	1.1	13.4	6.7	0.3	5.5	1.3	2.0	2.2	2.5
Total	100.0	100.0	100.0	100.0	100.0	100.0	100.0	100.0	100.0	100.0	100.0	100.0	100.0	100.0	100.0	100.0	100.0	100.0	100.0	100.0	100.0	100.0	100.0	100.0	100.0	100.0	100.0	100.0	100.0	100.0	100.0	100.0	100.0	100.0	100.0	100.0	100.0	100.0	100.0	100.0	100.0	100.0	100.0	100.0	100.0
Mineral					Pb (%)									Pb (%)									Pb (%)									Pb (%)									Pb (%)				
ChalcopyritePb	0.4	0.1	2.0	0.0	16.3	0.0	15.2	0.1	3.9	3.1	4.0	16.4	6.1	8.5	12.1	20.7	30.1	52.4	1.8	1.5	3.8	19.6	21.8	12.0	20.9	14.7	18.2	0.2	11.3	5.6	16.5	37.0	29.8	9.2	13.3	20.7	0.0	0.7	0.7	0.0	6.3	0.2	8.4	26.3	14.3
GalenaSe	0.2	78.5	0.0	18.4	6.6	0.2	0.0	3.0	0.0	74.2	67.0	5.5	69.2	76.2	63.1	25.3	29.7	0.0	1.7	72.7	72.1	40.6	32.9	32.7	29.3	24.2	1.7	68.4	12.2	78.4	65.5	34.8	42.7	52.4	53.8	1.6	0.0	2.0	0.0	86.9	65.0	84.4	32.5	11.3	0.0
FeOxyhydroxCuPbZnS	78.7	11.2	34.6	22.9	26.0	33.1	23.1	22.5	37.6	15.5	11.5	13.8	3.3	1.7	8.4	22.7	4.8	4.9	50.8	7.4	7.6	20.0	21.1	30.7	25.6	17.9	20.2	0.5	8.2	4.6	6.3	10.5	13.9	17.7	4.7	14.1	90.4	11.9	57.8	12.1	17.9	11.7	42.0	27.7	54.7
PbMoOxide	0.0	0.0	0.0	0.0	0.0	0.0	0.0	0.0	0.2	0.3	0.0	0.0	0.0	0.3	0.0	0.0	0.0	8.1	0.2	0.0	0.0	0.0	0.0	0.1	0.0	0.2	1.3	0.0	0.0	0.0	0.8	0.0	0.0	0.0	0.0	17.1	0.0	0.0	0.0	0.0	0.0	0.0	0.0	0.0	0.0
PbOxideZn	0.0	0.0	0.0	0.0	0.0	0.0	0.0	0.0	0.0	0.0	0.0	0.0	0.0	0.0	0.0	0.0	0.0	0.0	0.0	0.0	0.0	0.0	0.0	0.0	1.7	1.1	0.8	0.0	0.0	0.0	0.0	0.0	0.0	0.0	0.0	5.5	0.0	0.0	0.0	0.0	0.0	0.0	0.0	0.0	0.0
GruneritePbCuZn	0.0	0.5	0.0	0.1	0.1	1.9	2.2	13.6	9.9	0.0	0.6	0.1	0.8	0.3	0.0	3.6	5.0	4.7	12.0	1.2	1.3	4.1	4.9	4.7	4.0	9.5	13.0	0.4	0.2	0.8	0.4	0.1	0.5	0.3	4.0	1.4	0.9	0.2	0.0	0.0	0.0	0.0	0.0	1.1	0.4
MolybdofornaciteZn	0.4	0.4	0.0	0.5	0.0	0.0	0.0	0.0	0.0	1.0	10.1	24.4	2.3	6.7	0.1	4.4	0.5	0.0	0.1	0.6	0.5	0.2	0.7	0.0	3.2	0.0	0.0	0.1	2.4	0.1	3.0	4.4	2.1	5.8	4.4	0.0	0.0	0.0	0.1	0.0	0.0	0.2	0.9	0.6	0.0
Powellite_trans	0.0	0.0	0.0	0.0	0.0	0.0	0.0	0.0	0.0	0.0	0.0	0.0	0.0	0.0	0.0	0.0	0.0	0.1	0.0	0.0	0.0	0.0	0.0	0.0	0.0	0.0	0.0	0.0	0.0	0.0	0.0	0.0	0.0	0.0	0.0	0.0	0.0	0.0	0.0	0.0	0.0	0.0	0.0	0.0	0.0
Wulfenite_trans	0.0	0.0	0.0	0.0	0.0	0.0	0.0	0.0	0.0	0.1	0.0	0.0	0.0	0.0	0.0	0.0	0.5	1.8	0.0	3.6	0.0	0.0	0.0	0.0	0.7	3.4	10.8	0.0	0.3	0.0	1.7	0.0	0.3	0.6	0.5	2.9	0.5	0.0	0.0	0.0	0.0	0.5	0.0	0.0	0.0
ApatiteCuPbZn	2.1	2.6	5.2	8.1	2.5	4.7	5.3	10.8	22.7	0.7	0.7	10.7	5.0	1.3	2.4	3.9	4.5	7.0	2.2	0.6	0.4	1.6	3.0	2.4	2.1	2.1	5.7	10.1	7.0	2.1	0.9	2.0	2.0	2.8	2.3	8.8	1.7	6.9	13.1	0.5	2.6	1.4	2.1	7.6	6.4
FornaciteCa	0.0	0.1	0.0	0.0	0.0	0.0	0.0	0.0	12.9	0.0	0.0	0.0	0.0	0.0	0.0	0.0	0.0	2.6	0.0	0.0	0.0	0.0	0.0	0.0	0.0	0.0	0.4	0.0	0.0	0.0	0.0	0.0	0.0	0.0	0.0	0.0	0.0	0.0	0.0	0.0	0.0	0.0	0.0	0.0	0.0
TyrolitePb	0.0	0.0	0.0	0.0	0.0	0.0	0.0	0.0	0.5	0.0	0.0	0.0	0.0	0.0	0.0	0.0	0.0	0.0	0.0	0.0	0.0	0.0	0.0	0.0	0.0	0.0	0.0	0.0	0.0	0.0	0.0	0.0	0.0	0.0	0.0	0.1	0.0	0.0	0.0	0.0	0.0	0.0	0.0	0.0	0.0
MoSilicate	0.0	0.0	0.0	0.0	0.0	0.0	0.0	0.0	0.0	0.0	0.0	0.0	0.0	0.0	0.0	0.0	0.0	0.6	0.0	0.0	0.0	0.0	0.0	0.0	0.0	0.0	0.3	0.0	0.0	0.0	0.0	0.0	0.0	0.0	0.0	0.1	0.0	0.0	0.0	0.0	0.0	0.0	0.0	0.0	0.8
TitaniteMixPbCu	18.3	6.7	58.2	50.0	48.6	60.0	54.2	50.0	12.4	5.2	6.0	29.2	13.2	5.0	13.9	19.4	25.0	17.8	31.2	12.3	14.3	13.9	15.8	17.4	12.6	25.3	26.2	20.4	58.5	8.4	4.6	11.2	8.6	11.2	17.2	27.9	6.4	78.4	28.4	0.5	8.2	1.7	14.1	25.4	23.4
Total	100.0	100.0	100.0	100.0	100.0	100.0	100.0	100.0	100.0	100.0	100.0	100.0	100.0	100.0	100.0	100.0	100.0	100.0	100.0	100.0	100.0	100.0	100.0	100.0	100.0	100.0	100.0	100.0	100.0	100.0	100.0	100.0	100.0	100.0	100.0	100.0	100.0	100.0	100.0	100.0	100.0	100.0	100.0	100.0	100.0
Mineral					Zn (%)									Zn (%)									Zn (%)									Zn (%)									Zn (%)				
TrampMetal	1.5	0.1	0.0	0.2	2.1	0.1	0.0	1.1	33.7	0.1	0.1	0.1	0.2	0.0	0.7	0.3	3.5	12.4	0.1	12.3	0.0	0.3	0.0	0.3	0.9	2.1	5.7	0.0	0.0	0.0	0.1	0.0	0.0	0.3	2.7	17.0	0.9	4.4	0.0	0.0	0.1	0.5	0.1	4.0	17.9
AgSulphosalt	0.0	0.0	0.0	0.0	2.5	0.0	0.0	0.0	0.0	0.0	0.0	0.0	0.0	0.0	0.0	0.0	0.0	0.0	0.3	0.0	0.0	0.0	0.0	0.0	0.0	0.0	0.0	0.0	0.0	0.0	0.0	0.0	0.0	0.0	0.0	0.8	0.0	0.0	0.0	0.0	0.0	0.0	0.0	0.0	2.2
ChalcopyriteZn	1.5	0.0	0.3	0.0	3.0	1.2	0.1	0.6	0.3	0.4	0.2	1.1	0.0	0.9	0.2	0.5	0.7	0.7	0.1	2.3	1.1	2.0	0.8	3.1	1.1	0.3	0.7	0.0	1.3	0.1	0.2	0.9	0.3	0.4	0.2	0.6	0.2	0.0	0.0	0.0	0.0	0.0	0.1	2.0	0.2
EnargiteZn	0.0	0.0	0.0	0.0	0.0	1.5	0.0	0.0	0.0	0.0	0.5	0.0	0.0	0.3	0.0	0.0	0.0	0.0	0.9	0.0	0.0	0.0	0.0	0.1	0.0	0.0	0.0	0.0	0.0	0.0	0.0	0.0	0.0	0.3	0.3	0.0	0.0	0.0	0.0	0.0	0.0	0.0	0.0	0.0	0.0
TennantiteZnFe	0.0	0.0	0.0	0.0	0.0	0.0	0.0	0.0	0.0	0.0	0.0	0.0	0.0	0.1	0.0	0.5	0.1	0.9	2.0	3.0	0.0	0.0	0.0	0.0	0.4	0.1	0.0	0.0	0.0	0.0	0.0	0.0	0.0	0.0	0.0	0.3	0.0	0.0	0.0	0.0	0.0	0.1	0.3	0.0	0.8
WatanabeiteZn	0.0	0.0	0.0	0.0	0.0	0.0	0.7	0.0	0.0	0.0	0.0	0.1	0.0	0.3	0.6	1.1	0.8	0.0	0.3	0.0	0.0	0.0	0.0	0.0	0.2	0.0	0.0	0.0	0.0	0.0	0.0	0.0	0.0	0.0	0.0	0.0	0.0	0.0	1.6	1.0	0.3	1.1	0.1	5.3	0.0
Sphalerite	0.0	30.1	0.0	0.0	0.0	0.0	0.1	0.0	11.5	0.6	0.4	0.1	0.0	0.5	2.0	2.0	5.0	26.2	1.9	21.6	1.6	0.2	0.6	2.4	9.3	5.0	0.6	1.2	1.0	1.4	0.5	9.7	4.2	9.1	1.6	11.7	0.0	55.9	0.0	0.0	26.6	0.0	0.1	0.5	3.5
SphaleriteCu	9.0	30.6	78.5	90.6	44.9	76.1	92.8	35.5	22.6	97.5	98.0	93.7	95.9	96.0	95.6	94.4	74.3	44.8	49.4	20.0	91.9	93.0	94.0	81.9	81.6	76.9	81.5	91.4	95.9	96.5	96.8	87.9	94.5	88.6	93.7	59.5	3.3	19.0	30.9	98.0	71.1	95.8	98.8	76.3	40.7
FeOxyhydroxCuPbZnS	63.9	6.5	4.3	1.3	13.6	3.2	1.0	4.1	2.9	0.7	0.3	0.4	0.2	0.1	0.1	0.3	0.5	0.3	21.0	10.7	1.4	1.8	1.4	4.4	2.1	2.6	1.6	0.0	0.1	0.2	0.3	0.2	0.2	0.3	0.1	0.5	12.0	2.8	18.2	0.4	0.7	0.7	0.4	1.3	1.7
PbOxideZn	0.0	0.0	0.0	0.0	0.0	0.0	0.0	0.0	0.0	0.0	0.0	0.0	0.0	0.0	0.0	0.0	0.0	0.0	0.0	0.0	0.0	0.0	0.0	0.0	0.1	0.1	0.1	0.0	0.0	0.0	0.0	0.0	0.0	0.0	0.0	0.2	0.0	0.0	0.0	0.0	0.0	0.0	0.0	0.0	0.0
SideriteAsMnZnCu	0.2	0.0	0.0	1.1	3.8	0.1	0.1	0.9	0.0	0.0	0.0	0.0	0.0	0.0	0.0	0.0	0.2	0.0	1.2	4.0	0.5	0.1	0.1	0.9	0.5	3.8	0.0	0.0	0.0	0.0	0.2	0.0	0.1	0.1	0.1	0.6	0.0	0.5	0.8	0.0	0.0	0.1	0.0	0.1	0.2
GruneritePbCuZn	0.1	0.8	0.0	0.0	0.1	0.5	0.3	7.2	2.2	0.0	0.1	0.0	0.2	0.1	0.0	0.1	1.4	0.9	14.4	4.9	0.7	1.0	0.9	2.0	1.0	4.1	3.0	0.1	0.0	0.1	0.1	0.0	0.0	0.0	0.2	0.2	0.4	0.1	0.0	0.0	0.0	0.0	0.0	0.2	0.0
OtaviteZnCu	0.0	0.0	0.0	0.0	0.0	0.0	0.0	0.0	0.0	0.0	0.0	0.0	0.0	0.0	0.0	0.0	0.0	0.0	0.0	0.0	0.0	0.0	0.0	0.0	0.0	0.0	0.0	0.0	0.0	0.0	0.0	0.0	0.0	0.0	0.0	0.4	0.0	0.0	0.0	0.0	0.0	0.0	0.0	0.0	23.9
FeSulphateCuAsMoZn	0.8	0.1	0.5	0.1	5.6	1.0	0.2	0.3	0.1	0.0	0.0	0.1	0.0	0.0	0.0	0.1	0.3	0.0	0.2	0.4	0.1	0.1	0.0	0.5	0.3	0.2	0.0	0.5	0.1	0.0	0.3	0.1	0.1	0.2	0.2	0.1	0.3	0.1	0.3	0.0	0.1	0.1	0.0	0.3	0.1
MolybdofornaciteZn	0.1	0.1	0.0	0.0	0.0	0.0	0.0	0.0	0.0	0.0	0.1	0.3	0.1	0.2	0.0	0.0	0.0	0.0	0.0	0.3	0.0	0.0	0.0	0.0	0.1	0.0	0.0	0.0	0.0	0.0	0.1	0.0	0.0	0.0	0.0	0.0	0.0	0.0	0.0	0.0	0.0	0.0	0.0	0.0	0.0
Wulfenite_trans	0.0	0.0	0.0	0.0	0.0	0.0	0.0	0.0	0.0	0.0	0.0	0.0	0.0	0.0	0.0	0.0	0.0	0.1	0.0	3.6	0.0	0.0	0.0	0.0	0.0	0.4	0.6	0.0	0.0	0.0	0.0	0.0	0.0	0.0	0.0	0.1	0.1	0.0	0.0	0.0	0.0	0.0	0.0	0.0	0.0
ApatiteCuPbZn	14.6	13.1	5.7	4.1	11.5	4.0	1.9	17.3	15.4	0.3	0.2	3.0	2.7	0.8	0.3	0.4	3.9	4.2	8.1	8.2	0.7	1.3	1.7	3.1	1.5	2.8	3.9	6.5	1.0	0.7	0.4	0.3	0.3	0.4	0.4	3.0	2.0	14.4	36.3	0.1	0.9	0.7	0.2	3.1	1.8
MicaAlteredCuZn	8.4	18.7	10.7	2.6	12.9	12.4	2.9	32.9	11.3	0.5	0.2	1.1	0.7	0.8	0.5	0.3	9.4	9.4	0.4	8.6	2.0	0.3	0.5	1.4	0.9	1.7	2.4	0.2	0.6	0.9	1.1	0.9	0.3	0.3	0.5	5.1	81.0	2.8	11.8	0.5	0.3	1.1	0.0	6.9	7.2
Total	100.0	100.0	100.0	100.0	100.0	100.0	100.0	100.0	100.0	100.0	100.0	100.0	100.0	100.0	100.0	100.0	100.0	100.0	100.0	100.0	100.0	100.0	100.0	100.0	100.0	100.0	100.0	100.0	100.0	100.0	100.0	100.0	100.0	100.0	100.0	100.0	100.0	100.0	100.0	100.0	100.0	100.0	100.0	100.0	100.0

Table C5.7 Antimony, arsenic and molybdenum distribution by mineral in all Class B waste rock samples

Sample ID	FC-0									FC-1									FC-2									FC-3									FC-4								
Representive size (µm)	840	420	210	130	90	60	35	20	10	840	420	210	130	90	60	35	20	10	840	420	210	130	90	60	35	20	10	840	420	210	130	90	60	35	20	10	840	420	210	130	90	60	35	20	10
Mineral					**Sb%**									**Sb%**									**Sb%**									**Sb%**								
Stibnite	0.0	0.0	0.0	0.0	0.0	0.0	0.0	0.0	0.0	0.0	100.0	24.0	0.0	22.0	0.0	10.7	55.6	100.0	0.0	0.0	0.0	0.0	0.0	0.0	0.0	0.0	100.0	100.0	0.0	0.0	0.0	0.0	0.0	0.0	0.0	0.0	0.0	0.0	45.3	0.0	58.8	36.2	0.0	0.0	100.0
WatanabeiteZn	0.0	0.0	100.0	0.0	0.0	0.0	100.0	0.0	0.0	100.0	0.0	76.0	100.0	78.0	100.0	89.3	44.4	0.0	100.0	0.0	0.0	0.0	0.0	0.0	100.0	0.0	0.0	0.0	0.0	0.0	0.0	0.0	0.0	0.0	0.0	0.0	0.0	0.0	54.7	100.0	41.2	63.8	100.0	100.0	0.0
Total	0.0	0.0	100.0	0.0	0.0	0.0	100.0	0.0	0.0	100.0	100.0	100.0	100.0	100.0	100.0	100.0	100.0	100.0	100.0	0.0	0.0	0.0	0.0	0.0	100.0	0.0	100.0	100.0	0.0	0.0	0.0	0.0	0.0	0.0	0.0	0.0	0.0	0.0	100.0	100.0	100.0	100.0	100.0	100.0	100.0
Mineral					**As (%)**									**As (%)**									**As (%)**									**As (%)**								
Arsenopyrite	0.0	0.0	0.0	0.0	0.0	0.0	0.0	0.0	0.0	0.0	0.0	0.0	0.0	0.0	0.0	0.0	0.0	23.6	0.0	0.0	0.0	0.0	0.0	0.0	0.0	0.0	0.0	0.0	0.0	0.0	0.0	0.0	0.0	0.0	0.0	0.0	0.0	0.0	0.0	0.0	0.0	0.0	0.0	0.0	0.0
RealgarOrpiment	0.0	0.0	0.0	0.0	0.0	0.0	0.0	0.0	0.0	0.0	0.0	0.0	0.0	0.0	0.0	0.0	0.0	0.0	0.0	0.0	0.0	0.0	71.6	0.0	0.0	0.0	0.0	0.0	0.0	0.0	0.0	0.0	0.0	0.0	0.0	0.0	0.0	0.0	0.0	0.0	0.0	0.0	0.0	0.0	0.0
Enargite	0.0	0.0	0.0	0.0	0.0	0.0	0.0	0.0	0.0	6.7	15.4	22.0	0.4	38.3	10.2	0.0	51.1	0.0	21.7	8.0	0.0	0.0	0.0	0.2	5.5	0.9	0.0	0.0	0.0	1.2	0.0	0.3	3.7	0.0	0.0	0.0	0.0	0.0	0.0	0.9	4.4	37.0	12.3	33.5	0.0
EnargiteZn	0.0	0.0	0.0	0.0	0.0	12.0	0.0	0.0	0.0	0.0	51.3	0.8	0.0	15.6	3.4	0.1	0.0	0.0	2.9	0.0	0.0	0.0	0.0	0.7	0.0	0.0	0.0	0.0	0.0	0.0	0.0	0.0	0.0	11.5	18.9	0.0	0.0	0.0	0.0	0.0	0.0	0.0	0.0	0.0	0.0
TennantiteZnFe	0.0	0.0	0.0	0.0	0.0	0.0	0.0	0.0	0.0	0.0	0.2	0.1	0.0	7.1	0.0	20.4	0.8	38.1	9.3	20.0	0.0	0.0	0.0	0.0	9.4	1.3	0.0	0.0	0.0	10.5	0.0	0.1	0.0	0.0	0.0	21.3	0.0	0.0	0.0	0.0	0.2	1.4	40.4	0.0	35.7
WatanabeiteZn	0.0	0.0	0.4	0.0	0.0	0.0	26.1	0.0	0.0	0.5	0.0	8.0	17.0	26.9	76.8	50.9	11.8	0.0	1.4	0.0	0.0	0.0	0.0	0.0	4.6	0.0	0.0	0.0	0.0	0.0	0.0	0.0	0.0	0.0	0.0	0.0	0.0	0.0	11.7	75.2	19.2	35.2	6.7	43.5	0.0
FeOxyhydroxCuPbZnS	88.3	84.5	46.5	39.6	17.9	20.4	19.7	48.9	28.6	85.4	26.9	22.2	75.0	4.8	8.4	7.1	4.1	8.0	56.7	42.9	52.3	72.2	21.3	40.8	30.6	34.5	81.7	0.7	12.6	42.6	8.6	14.9	12.6	9.7	4.4	20.6	77.7	63.6	74.2	15.7	27.2	12.4	29.4	5.9	45.2
SideriteAsMnZnCu	0.2	0.1	0.0	26.9	4.1	0.3	2.4	8.5	0.0	0.0	0.3	0.4	0.0	0.0	0.0	0.7	1.3	0.0	2.6	13.3	14.6	2.5	1.3	6.5	5.7	41.3	0.0	0.0	0.0	7.3	4.3	2.4	2.6	4.2	4.1	17.8	0.2	10.0	2.8	0.0	0.0	1.0	0.0	0.5	4.0
FeSulphateCuAsMoZn	11.4	10.2	53.1	33.6	78.1	67.3	51.8	42.6	10.2	7.5	5.9	46.5	7.5	7.3	1.2	20.8	31.0	5.3	5.4	15.8	33.1	25.3	5.9	51.7	44.2	22.1	8.6	99.3	87.4	38.4	87.1	82.4	81.1	74.7	72.6	39.4	22.1	26.5	11.4	8.3	49.0	13.0	11.2	16.5	15.1
FornaciteCa	0.0	5.2	0.0	0.0	0.0	0.0	0.0	0.0	57.1	0.0	0.0	0.0	0.0	0.0	0.0	0.0	0.0	24.4	0.0	0.0	0.0	0.0	0.0	0.0	0.0	9.7	0.0	0.0	0.0	0.0	0.0	0.0	0.0	0.0	0.0	0.0	0.0	0.0	0.0	0.0	0.0	0.0	0.0	0.0	0.0
TyrolitePb	0.0	0.0	0.0	0.0	0.0	0.0	0.0	0.0	4.2	0.0	0.0	0.0	0.0	0.0	0.0	0.0	0.0	0.6	0.0	0.0	0.0	0.0	0.0	0.0	0.0	0.0	0.0	0.0	0.0	0.0	0.0	0.0	0.0	0.0	0.0	1.0	0.0	0.0	0.0	0.0	0.0	0.0	0.0	0.0	0.0
Total	100.0	100.0	100.0	100.0	100.0	100.0	100.0	100.0	100.0	100.0	100.0	100.0	100.0	100.0	100.0	100.0	100.0	100.0	100.0	100.0	100.0	100.0	100.0	100.0	100.0	100.0	100.0	100.0	100.0	100.0	100.0	100.0	100.0	100.0	100.0	100.0	100.0	100.0	100.0	100.0	100.0	100.0	100.0	100.0	100.0
Mineral					**Mo (%)**									**Mo (%)**									**Mo (%)**									**Mo (%)**								
Molybdenite	64.5	0.0	0.0	0.0	0.0	4.1	0.0	0.0	72.0	95.2	23.7	96.0	68.1	67.7	99.8	93.9	89.9	24.4	96.6	6.8	19.0	92.3	98.4	90.6	90.5	76.1	30.3	4.3	70.1	86.9	32.7	95.7	60.8	0.0	86.3	20.6	0.0	0.0	94.6	98.7	0.0	10.4	0.0	0.0	8.8
PbMoOxide	0.0	0.0	0.0	0.0	0.0	0.0	0.2	0.0	6.0	1.3	0.3	0.0	0.0	3.7	0.0	0.0	0.0	4.7	1.0	0.3	0.0	0.0	0.0	0.3	0.0	0.7	1.4	0.0	0.0	0.0	7.3	0.0	0.0	0.0	0.0	28.5	0.0	0.0	0.0	0.0	0.0	0.0	0.0	0.0	0.0
PbOxideZn	0.0	0.0	0.0	0.0	0.0	0.0	0.0	0.0	0.0	0.0	0.0	0.0	0.0	0.0	0.0	0.0	0.0	0.0	0.0	0.0	0.0	0.0	0.0	0.0	0.6	1.0	0.2	0.0	0.0	0.0	0.0	0.0	0.0	0.0	0.0	2.2	0.0	0.0	0.0	0.0	0.0	0.0	0.0	0.0	0.0
FeSulphateCuAsMoZn	31.4	47.0	100.0	86.5	100.0	16.8	99.9	100.0	22.0	0.3	0.9	1.0	0.6	1.8	0.2	4.9	5.7	0.1	1.3	1.7	8.4	0.5	0.7	7.4	2.7	2.2	0.1	70.1	19.6	4.4	29.6	3.4	20.3	60.3	9.3	2.3	64.7	100.0	5.3	1.3	9.1	4.8	83.1	97.4	1.6
MoCaSulphate	0.0	0.0	0.0	0.0	0.0	0.0	0.0	0.0	0.0	0.6	0.1	0.0	5.8	5.1	0.0	0.0	2.1	5.5	0.6	10.6	23.6	1.1	0.0	0.0	3.4	0.0	0.0	13.5	4.9	7.3	3.7	0.0	15.1	23.1	0.9	0.0	0.0	0.0	0.0	0.0	91.0	59.7	0.0	0.0	3.7
MolybdofornaciteZn	4.1	53.0	0.0	7.6	0.0	0.0	0.0	0.0	0.0	0.7	13.7	3.0	16.1	17.7	0.1	1.2	0.3	0.0	0.1	1.5	3.3	0.1	0.3	0.0	0.9	0.0	0.0	0.3	3.0	0.5	5.2	1.0	1.8	9.5	1.9	0.0	0.0	0.0	0.2	0.0	0.0	0.3	16.9	2.6	0.0
Powellite_trans	0.0	0.0	0.0	0.0	0.0	0.0	0.0	0.0	0.0	1.1	6.7	0.0	0.0	0.0	0.0	0.0	0.0	3.9	0.0	0.0	0.0	0.0	0.0	0.0	0.0	0.0	0.0	0.0	0.0	0.0	0.0	0.0	0.0	0.0	0.0	0.0	0.0	0.0	0.0	0.0	0.0	19.4	0.0	0.0	0.0
Wulfenite_trans	0.0	0.0	0.0	0.0	0.0	0.0	0.0	0.0	0.0	0.4	0.1	0.0	2.1	0.8	0.0	0.0	2.0	1.5	0.0	60.3	0.2	0.0	0.1	0.0	1.4	17.8	16.7	0.1	2.4	0.9	21.4	0.0	2.0	7.1	1.5	6.7	35.3	0.0	0.0	0.0	0.0	5.4	0.0	0.0	0.0
CaMoSilicate	0.0	0.0	0.0	0.0	0.0	79.1	0.0	0.0	0.0	0.1	39.3	0.0	7.4	3.3	0.0	0.0	0.0	37.6	0.3	0.0	2.1	6.0	0.1	1.7	0.0	2.1	32.8	7.9	0.0	0.0	0.2	0.0	0.0	0.0	0.0	29.4	0.0	0.0	0.0	0.0	0.0	0.0	0.0	0.0	0.6
MoSilicate	0.0	0.0	0.0	5.9	0.0	0.0	0.0	0.0	0.0	0.3	15.1	0.0	0.0	0.0	0.0	0.0	0.0	22.3	0.2	18.8	43.5	0.1	0.4	0.0	0.6	0.0	18.5	3.8	0.0	0.0	0.0	0.0	0.0	0.0	0.0	10.4	0.0	0.0	0.0	0.0	0.0	0.0	0.0	0.0	85.3
Total	100.0	100.0	100.0	100.0	100.0	100.0	100.0	100.0	100.0	100.0	100.0	100.0	100.0	100.0	100.0	100.0	100.0	100.0	100.0	100.0	100.0	100.0	100.0	100.0	100.0	100.0	100.0	100.0	100.0	100.0	100.0	100.0	100.0	100.0	100.0	100.0	100.0	100.0	100.0	100.0	100.0	100.0	100.0	100.0	100.0

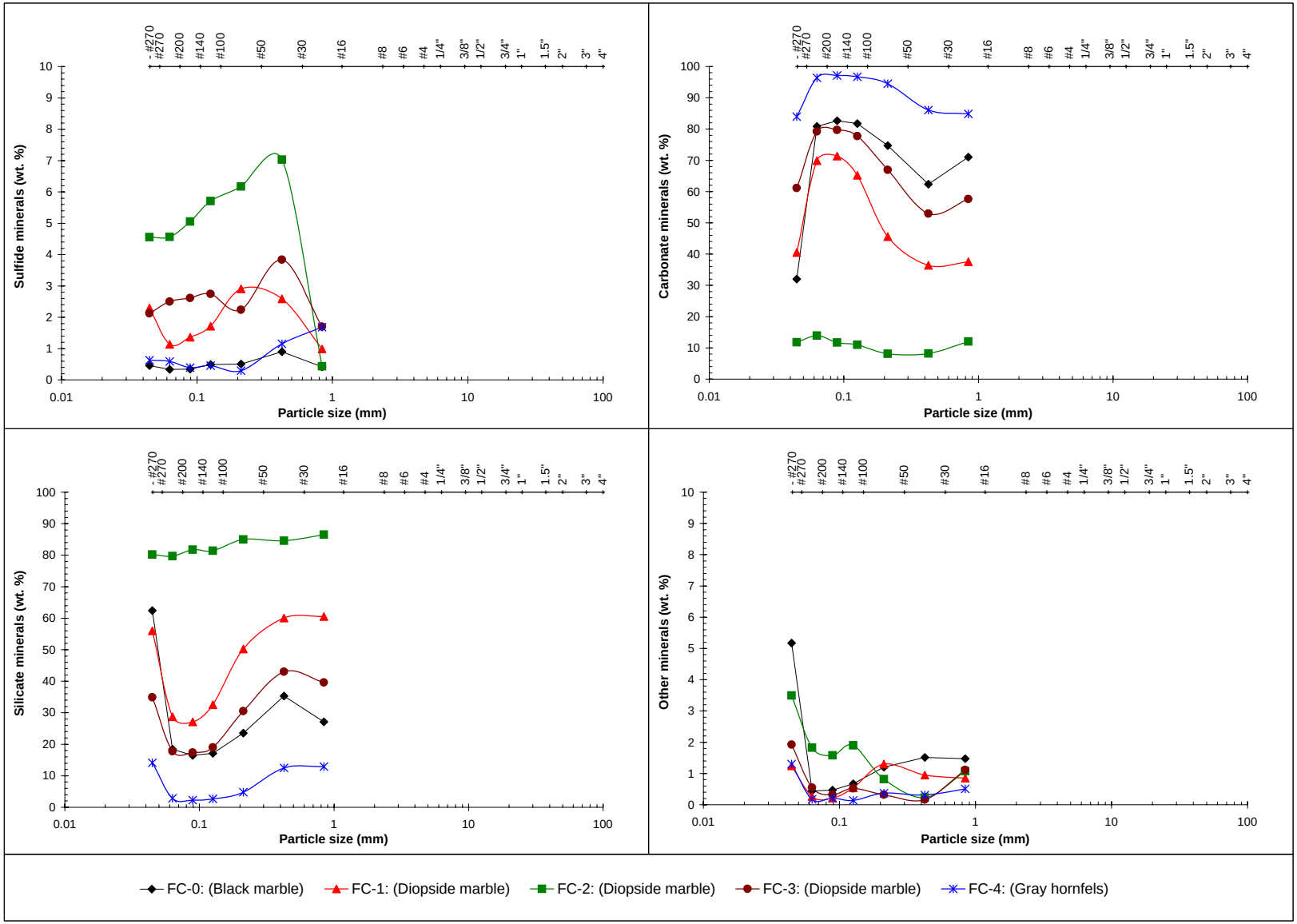

Figure C5.1 Mineral phase proportions by size fractions of Class B waste rock samples

Table C5.8 Mineral liberation by free surface of the black marble (FC-0) sample

Rep. size (μm)	Distribution of mineral (wt.%)									
	0% (barren)	0% (not exposed)	0% < x <= 30%	30% < x <= 50%	50% < x <= 70%	70% < x <= 90%	90% < x < 100%	100%	Availability (wt.%)	Sum
Composition of particle surface (% total sulfide minerals)										
840	0.0	2.9	40.4	0.0	21.2	33.4	0.0	2.1	97.1	100.0
420	0.0	0.7	5.3	0.0	7.0	21.1	24.0	42.0	99.3	100.0
210	0.0	2.2	8.7	5.3	52.0	0.0	14.5	17.4	97.8	100.0
130	0.0	0.1	3.0	11.8	1.9	34.3	0.0	48.9	99.9	100.0
90	0.0	0.4	0.6	0.0	0.8	4.0	8.3	85.9	99.7	100.0
60	0.0	0.7	10.3	11.3	5.6	8.4	6.6	57.1	99.3	100.0
35	0.0	0.2	6.5	8.9	3.1	0.7	9.8	71.0	99.8	100.0
20	0.0	0.0	31.3	15.5	10.9	16.2	0.0	26.2	100.0	100.0
10	0.0	0.3	0.0	0.0	0.3	28.5	0.0	70.9	99.7	100.0
Composition of particle surface (% Cu minerals)										
840	0.0	7.0	20.8	0.1	0.0	68.5	0.0	3.7	93.0	100.0
420	0.0	3.1	19.5	0.0	5.7	11.3	16.1	44.4	96.9	100.0
210	0.0	2.8	13.5	6.7	18.0	0.4	11.1	47.4	97.2	100.0
130	0.0	1.8	16.1	5.2	0.1	10.6	9.5	56.8	98.2	100.0
90	0.0	1.3	16.7	3.3	9.4	11.6	3.3	54.4	98.7	100.0
60	0.0	0.9	14.6	7.7	7.0	10.8	12.2	46.9	99.2	100.0
35	0.0	0.6	4.9	3.5	5.3	15.3	12.0	58.5	99.4	100.0
20	0.0	0.2	4.9	4.2	7.0	11.1	10.4	62.2	99.8	100.0
10	0.0	0.0	1.4	0.3	5.3	6.1	1.1	85.8	100.0	100.0
Composition of particle surface (% Pb minerals)										
840	0.0	8.1	12.0	0.1	0.0	77.2	0.0	2.6	91.9	100.0
420	0.0	5.3	15.0	0.0	10.1	0.5	22.9	46.2	94.7	100.0
210	0.0	3.9	15.5	12.2	17.7	0.0	9.3	41.5	96.1	100.0
130	0.0	3.2	18.9	7.0	1.7	2.0	4.7	62.5	96.9	100.0
90	0.0	1.9	17.9	4.0	5.9	15.9	3.3	51.2	98.2	100.0
60	0.0	1.4	22.4	9.1	9.9	11.5	4.6	41.1	98.6	100.0
35	0.0	0.8	6.0	2.5	9.3	18.1	8.1	55.3	99.2	100.0
20	0.0	0.3	6.4	9.9	6.6	6.8	4.4	65.6	99.7	100.0
10	0.0	0.1	2.0	0.3	1.4	2.1	1.6	92.5	99.9	100.0
Composition of particle surface (% Zn minerals)										
840	0.0	3.9	5.7	0.1	0.0	86.6	0.0	3.7	96.1	100.0
420	0.0	3.5	16.5	0.0	0.0	5.8	24.1	50.1	96.5	100.0
210	0.0	3.8	10.1	17.6	25.8	0.8	2.2	39.7	96.2	100.0
130	0.0	3.0	14.5	4.1	1.3	2.0	10.7	64.4	97.0	100.0
90	0.0	2.5	9.6	0.5	2.1	26.4	2.1	56.9	97.5	100.0
60	0.0	1.1	11.2	5.2	6.7	13.9	5.3	56.7	98.9	100.0
35	0.0	1.1	7.2	1.5	6.9	12.1	18.8	52.4	98.9	100.0
20	0.0	0.2	5.9	9.4	6.9	9.4	7.2	61.0	99.8	100.0
10	0.0	0.0	2.5	0.7	5.3	5.7	1.4	84.4	100.0	100.0

NOTE: for each sample - a value of ZERO means that there is "trace" (i.e. <0.01 wt.%)
+/- 5% tolerance
Availability is summation of liberation composition greater than 0% of middling class

Table C5.9 Mineral liberation by free surface of the diopside marble (FC-1) sample

Rep. size (μm)	Distribution of mineral (wt.%)									
	0% (barren)	0% (not exposed)	0% < x <= 30%	30% < x <= 50%	50% < x <= 70%	70% < x <= 90%	90% < x < 100%	100%	Availability (wt.%)	Sum
Composition of particle surface (% total sulfide minerals)										
840	0.0	11.0	88.7	0.0	0.0	0.0	0.0	0.3	89.0	100.0
420	0.0	1.8	24.8	7.3	18.6	10.0	5.7	31.8	98.2	100.0
210	0.0	1.6	3.8	4.6	3.0	5.9	10.8	70.4	98.4	100.0
130	0.0	0.7	1.7	0.0	2.7	17.4	2.0	75.5	99.4	100.0
90	0.0	0.5	3.4	4.4	1.3	9.2	2.2	79.1	99.5	100.0
60	0.0	0.5	1.6	4.5	5.9	4.2	1.2	82.2	99.5	100.0
35	0.0	0.0	1.1	0.9	3.1	2.2	3.5	89.3	100.0	100.0
20	0.0	0.3	1.5	4.5	9.8	5.2	2.5	76.2	99.7	100.0
10	0.0	0.9	1.1	1.1	0.2	1.9	0.0	94.7	99.1	100.0
Composition of particle surface (% Cu minerals)										
840	0.0	5.3	48.3	0.0	0.0	0.0	0.0	46.3	94.7	100.0
420	0.0	3.8	36.7	4.7	18.4	1.5	0.8	34.1	96.2	100.0
210	0.0	2.1	9.9	3.3	2.6	10.8	16.1	55.3	98.0	100.0
130	0.0	2.9	13.8	3.9	0.1	9.0	1.8	68.6	97.1	100.0
90	0.0	4.2	17.3	4.6	6.3	6.9	5.0	55.7	95.8	100.0
60	0.0	2.6	13.3	2.2	7.4	4.2	0.0	70.3	97.4	100.0
35	0.0	1.4	7.4	2.0	5.0	7.3	7.2	69.8	98.7	100.0
20	0.0	0.4	7.6	7.3	4.9	10.9	4.3	64.6	99.6	100.0
10	0.0	0.4	1.9	1.9	2.0	1.0	2.0	90.9	99.6	100.0
Composition of particle surface (% Pb minerals)										
840	0.0	6.9	30.7	0.0	0.0	0.0	62.1	0.2	93.1	100.0
420	0.0	6.4	32.6	7.9	2.9	0.0	0.0	50.3	93.6	100.0
210	0.0	2.4	10.4	4.6	1.8	5.9	8.3	66.6	97.6	100.0
130	0.0	4.0	13.2	3.9	7.4	0.0	2.8	68.7	96.0	100.0
90	0.0	6.1	25.1	10.9	8.1	20.5	0.3	29.1	94.0	100.0
60	0.0	7.0	25.4	4.2	9.4	0.8	4.0	49.3	93.0	100.0
35	0.0	2.9	14.8	2.8	0.3	10.8	23.5	44.9	97.1	100.0
20	0.0	0.7	10.8	5.2	6.6	22.6	7.3	46.7	99.3	100.0
10	0.0	0.1	2.6	3.2	1.5	1.6	0.0	90.9	99.9	100.0
Composition of particle surface (% Zn minerals)										
840	0.0	5.6	22.7	0.0	0.0	0.0	71.2	0.5	94.4	100.0
420	0.0	3.8	43.2	2.4	0.1	3.3	0.0	47.2	96.2	100.0
210	0.0	2.0	10.7	2.4	2.1	14.8	16.4	51.7	98.1	100.0
130	0.0	4.0	19.2	2.2	0.1	0.4	4.6	69.5	96.0	100.0
90	0.0	5.4	19.4	2.9	11.3	11.2	3.6	46.2	94.6	100.0
60	0.0	4.9	15.2	0.5	4.3	1.4	4.8	68.9	95.1	100.0
35	0.0	1.5	7.8	1.6	3.1	4.7	29.9	51.3	98.5	100.0
20	0.0	0.5	9.6	9.4	5.1	9.4	2.8	63.2	99.5	100.0
10	0.0	0.0	2.4	1.1	3.6	0.4	3.5	89.0	100.0	100.0

NOTE: for each sample - a value of ZERO means that there is "trace" (i.e. <0.01 wt.%)
+/- 5% tolerance
Availability is summation of liberation composition greater than 0% of middling class

Table C5.10 Mineral liberation by free surface of the diopside marble (FC-2) sample

Rep. size (μm)	Distribution of mineral (wt.%)									
	0% (barren)	0% (not exposed)	0% < x <= 30%	30% < x <= 50%	50% < x <= 70%	70% < x <= 90%	90% < x < 100%	100%	Availability (wt.%)	Sum
Composition of particle surface (% total sulfide minerals)										
840	0.0	3.7	95.8	0.0	0.0	0.0	0.0	0.5	96.3	100.0
420	0.0	0.3	2.8	0.2	0.0	20.0	36.5	40.3	99.7	100.0
210	0.0	0.2	3.9	1.6	0.7	17.1	20.8	55.7	99.8	100.0
130	0.0	0.2	1.5	1.3	1.9	10.1	10.1	74.8	99.8	100.0
90	0.0	0.1	1.3	2.6	2.1	6.8	7.7	79.5	99.9	100.0
60	0.0	0.2	1.2	2.8	1.4	4.4	7.2	82.8	99.9	100.0
35	0.0	0.2	1.1	1.8	2.4	4.3	5.7	84.6	99.8	100.0
20	0.0	0.0	1.9	1.7	2.8	10.0	4.7	78.8	100.0	100.0
10	0.0	0.1	2.1	2.6	0.8	5.5	3.4	85.5	99.9	100.0
Composition of particle surface (% Cu minerals)										
840	0.0	3.8	52.8	0.2	0.0	0.5	40.2	2.5	96.2	100.0
420	0.0	6.2	20.8	0.1	22.0	0.0	33.0	17.9	93.8	100.0
210	0.0	3.3	15.3	8.8	2.6	6.4	2.5	61.0	96.7	100.0
130	0.0	1.9	7.6	4.5	2.0	6.4	10.8	67.0	98.2	100.0
90	0.0	1.3	7.6	3.8	2.6	9.0	6.0	69.9	98.7	100.0
60	0.0	1.2	8.2	5.2	5.6	10.3	6.7	63.0	98.9	100.0
35	0.0	0.6	6.8	3.0	5.8	8.5	13.1	62.2	99.4	100.0
20	0.0	0.6	7.2	4.8	9.4	11.8	7.7	58.5	99.4	100.0
10	0.0	0.4	2.9	2.8	3.9	3.2	5.3	81.6	99.6	100.0
Composition of particle surface (% Pb minerals)										
840	0.0	4.8	40.9	0.3	0.0	0.7	50.4	2.9	95.2	100.0
420	0.0	15.6	38.6	1.9	0.0	0.0	0.0	44.0	84.4	100.0
210	0.0	4.1	12.4	3.2	0.0	6.4	11.9	62.1	95.9	100.0
130	0.0	2.5	11.4	3.4	2.4	6.0	13.0	61.4	97.5	100.0
90	0.0	1.9	10.3	3.8	1.1	10.7	6.9	65.3	98.1	100.0
60	0.0	1.6	10.9	3.2	5.5	11.2	11.2	56.5	98.4	100.0
35	0.0	0.9	10.4	6.7	7.9	9.3	9.4	55.4	99.1	100.0
20	0.0	1.0	10.0	5.8	5.8	14.1	7.7	55.7	99.0	100.0
10	0.0	0.4	3.4	2.4	4.0	4.1	5.5	80.3	99.6	100.0
Composition of particle surface (% Zn minerals)										
840	0.0	2.7	28.6	0.0	0.0	0.0	68.6	0.1	97.3	100.0
420	0.0	8.2	35.6	0.0	0.0	0.0	0.0	56.3	91.8	100.0
210	0.0	2.3	16.1	8.2	0.0	11.4	6.1	56.0	97.8	100.0
130	0.0	1.2	4.3	5.0	2.9	4.6	20.0	61.9	98.8	100.0
90	0.0	1.1	5.9	2.3	2.2	10.9	5.4	72.2	98.9	100.0
60	0.0	1.0	5.0	5.6	7.0	8.6	10.7	62.1	99.0	100.0
35	0.0	0.5	4.8	5.6	7.3	13.9	10.0	58.0	99.5	100.0
20	0.0	0.9	10.5	5.5	9.3	12.7	6.2	55.0	99.1	100.0
10	0.0	0.4	3.3	3.1	3.4	4.7	5.7	79.3	99.6	100.0

NOTE: for each sample - a value of ZERO means that there is "trace" (i.e. <0.01 wt.%)
+/- 5% tolerance
Availability is summation of liberation composition greater than 0% of middling class

Table C5.11 Mineral liberation by free surface of the diopside marble (FC-3) sample

Rep. size (μm)	Distribution of mineral (wt.%)									
	0% (barren)	0% (not exposed)	0% < x <= 30%	30% < x <= 50%	50% < x <= 70%	70% < x <= 90%	90% < x < 100%	100%	Availability (wt.%)	Sum
Composition of particle surface (% total sulfide minerals)										
840	0.0	5.6	54.2	1.1	0.7	0.0	0.0	38.5	94.4	100.0
420	0.0	1.6	25.5	1.0	0.8	22.7	16.2	32.2	98.4	100.0
210	0.0	1.6	10.6	7.8	6.6	22.1	7.0	44.3	98.4	100.0
130	0.0	0.4	4.0	3.3	13.0	8.5	8.1	62.7	99.6	100.0
90	0.0	0.3	4.2	3.4	6.9	10.8	11.4	63.0	99.7	100.0
60	0.0	0.7	3.2	5.1	5.8	7.5	4.4	73.5	99.4	100.0
35	0.0	0.3	4.5	7.1	4.6	11.7	5.0	66.8	99.7	100.0
20	0.0	0.6	7.5	8.7	11.5	5.1	2.6	64.1	99.4	100.0
10	0.0	0.3	1.0	8.0	4.3	0.0	10.7	75.8	99.7	100.0
Composition of particle surface (% Cu minerals)										
840	0.0	3.9	13.6	0.1	0.0	0.0	74.1	8.3	96.1	100.0
420	0.0	8.5	39.9	0.0	4.1	0.0	24.9	22.7	91.6	100.0
210	0.0	4.3	14.8	8.2	1.9	24.5	0.0	46.3	95.7	100.0
130	0.0	1.9	15.4	6.0	9.1	15.1	5.8	46.7	98.1	100.0
90	0.0	1.3	13.6	4.2	3.9	8.2	19.6	49.2	98.7	100.0
60	0.0	1.4	9.1	7.0	0.3	10.1	6.9	65.1	98.6	100.0
35	0.0	0.9	8.7	9.5	7.8	10.6	4.4	58.1	99.1	100.0
20	0.0	0.4	7.9	12.4	11.2	11.6	6.2	50.3	99.6	100.0
10	0.0	0.2	2.0	1.2	1.7	0.0	4.7	90.2	99.8	100.0
Composition of particle surface (% Pb minerals)										
840	0.0	4.1	10.8	0.1	0.0	0.0	84.8	0.2	95.9	100.0
420	0.0	12.7	49.5	0.0	2.2	0.0	6.6	29.1	87.3	100.0
210	0.0	6.3	18.9	5.3	2.4	7.0	0.0	60.1	93.7	100.0
130	0.0	3.3	23.1	7.8	1.4	12.0	3.8	48.8	96.7	100.0
90	0.0	3.5	25.8	3.2	6.5	1.4	0.0	59.6	96.5	100.0
60	0.0	2.5	14.7	8.7	1.2	12.9	0.9	59.2	97.5	100.0
35	0.0	2.2	16.4	17.3	9.1	10.0	1.8	43.4	97.9	100.0
20	0.0	0.8	13.9	16.7	16.2	5.6	3.9	43.0	99.2	100.0
10	0.0	0.4	2.8	0.9	3.8	0.0	0.0	92.1	99.6	100.0
Composition of particle surface (% Zn minerals)										
840	0.0	5.0	79.4	0.2	0.0	0.0	3.7	11.7	95.0	100.0
420	0.0	11.9	43.5	0.0	0.0	0.0	8.9	35.7	88.1	100.0
210	0.0	4.6	10.9	11.4	3.2	23.1	0.0	46.9	95.5	100.0
130	0.0	2.8	18.0	13.8	6.7	11.3	3.8	43.6	97.2	100.0
90	0.0	1.4	15.3	7.1	5.5	12.3	18.4	40.0	98.6	100.0
60	0.0	1.8	9.0	9.6	2.8	11.8	4.2	60.9	98.3	100.0
35	0.0	1.1	9.9	11.8	7.0	4.0	9.4	56.8	99.0	100.0
20	0.0	0.8	11.9	20.0	5.5	3.2	3.0	55.7	99.2	100.0
10	0.0	0.5	0.8	0.2	3.5	0.0	0.0	95.0	99.5	100.0

NOTE: for each sample - a value of ZERO means that there is "trace" (i.e. <0.01 wt.%)
+/- 5% tolerance
Availability is summation of liberation composition greater than 0% of middling class

Table C5.12 Mineral liberation by free surface of the gray hornfels (FC-4) sample

Rep. size (μm)	Distribution of mineral (wt.%)									
	0% (barren)	0% (not exposed)	0% < x <= 30%	30% < x <= 50%	50% < x <= 70%	70% < x <= 90%	90% < x < 100%	100%	Availability (wt.%)	Sum
Composition of particle surface (% total sulfide minerals)										
840	0.0	8.1	32.5	0.0	0.0	0.0	0.0	59.4	91.9	100.0
420	0.0	4.1	9.5	0.6	3.9	64.1	17.8	0.1	95.9	100.0
210	0.0	9.0	19.7	10.9	0.0	35.4	0.0	25.0	91.0	100.0
130	0.0	0.3	12.3	1.5	0.0	13.9	0.0	72.1	99.8	100.0
90	0.0	2.2	11.1	2.6	3.7	3.4	0.9	76.0	97.8	100.0
60	0.0	1.2	4.3	4.3	0.5	10.9	0.0	78.8	98.8	100.0
35	0.0	0.3	1.6	5.1	11.0	8.0	2.6	71.3	99.7	100.0
20	0.0	0.3	5.8	7.0	2.0	21.6	1.0	62.4	99.7	100.0
10	0.0	0.0	0.7	0.3	1.7	4.2	0.0	93.2	100.0	100.0
Composition of particle surface (% Cu minerals)										
840	0.0	8.7	20.6	20.3	0.0	0.0	0.1	50.3	91.3	100.0
420	0.0	3.9	16.4	0.1	0.0	18.9	46.9	13.9	96.1	100.0
210	0.0	5.1	10.6	2.3	0.7	18.9	12.8	49.6	94.9	100.0
130	0.0	2.5	9.4	13.4	5.8	0.0	1.1	67.9	97.5	100.0
90	0.0	2.6	9.2	4.2	2.8	0.0	0.0	81.2	97.4	100.0
60	0.0	2.9	9.7	3.1	0.6	12.0	2.6	69.2	97.1	100.0
35	0.0	1.5	7.4	2.4	11.0	6.4	8.9	62.4	98.5	100.0
20	0.0	0.9	10.9	4.0	6.1	15.4	3.6	59.1	99.1	100.0
10	0.0	0.1	1.6	2.1	6.5	0.6	0.0	89.1	99.9	100.0
Composition of particle surface (% Pb minerals)										
840	0.0	17.2	35.3	47.5	0.0	0.0	0.0	0.0	82.9	100.0
420	0.0	3.1	18.6	0.0	0.0	0.0	61.2	17.1	96.9	100.0
210	0.0	4.5	14.7	0.0	0.0	0.0	16.6	64.2	95.5	100.0
130	0.0	4.8	16.8	16.3	8.7	0.0	0.0	53.4	95.2	100.0
90	0.0	3.7	8.9	2.5	7.4	0.0	0.0	77.6	96.3	100.0
60	0.0	4.5	10.6	4.2	0.0	28.8	0.0	52.0	95.6	100.0
35	0.0	3.3	13.7	3.5	0.0	5.4	4.0	70.0	96.7	100.0
20	0.0	3.0	14.7	0.0	10.0	19.6	7.4	45.3	97.0	100.0
10	0.0	0.1	2.0	3.0	10.4	0.0	0.0	84.5	99.9	100.0
Composition of particle surface (% Zn minerals)										
840	0.0	7.2	18.2	21.4	0.0	0.0	0.1	53.1	92.8	100.0
420	0.0	9.4	44.9	0.0	0.0	0.0	0.0	45.7	90.6	100.0
210	0.0	4.2	18.2	2.8	1.1	0.0	18.6	55.2	95.8	100.0
130	0.0	3.9	15.4	21.0	18.3	0.0	0.0	41.4	96.1	100.0
90	0.0	3.6	9.0	1.9	6.6	0.0	0.0	79.0	96.5	100.0
60	0.0	3.2	11.9	2.6	0.0	12.4	0.0	69.9	96.8	100.0
35	0.0	2.8	13.7	1.8	0.0	4.7	4.9	72.1	97.2	100.0
20	0.0	1.0	13.1	0.2	8.4	5.7	4.6	66.9	99.0	100.0
10	0.0	0.1	2.2	1.6	9.4	0.0	0.0	86.6	99.9	100.0

NOTE: for each sample - a value of ZERO means that there is "trace" (i.e. <0.01 wt.%)
+/- 5% tolerance
Availability is summation of liberation composition greater than 0% of middling class

Appendix C6

Figures of Equipment and Instrumentation for Waste Rock Characterization

Figure C6.1 The US Standard Sieve Trays (45 cm x 65 cm) for wet particle size analysis of coarse size fractions

Figure C6.2 Eight-inch standard round Gilson stainless steel cloth sieves in vibrating shakers (ro-taps) for dry particle size analysis of fine size fractions

Figure C6.3 Pressure filter for filtration of finest particles during the particle size analysis

Figure C6.4 Laboratory scale (Mettler PC 4400) using for particle size analysis and sample preparation for assay

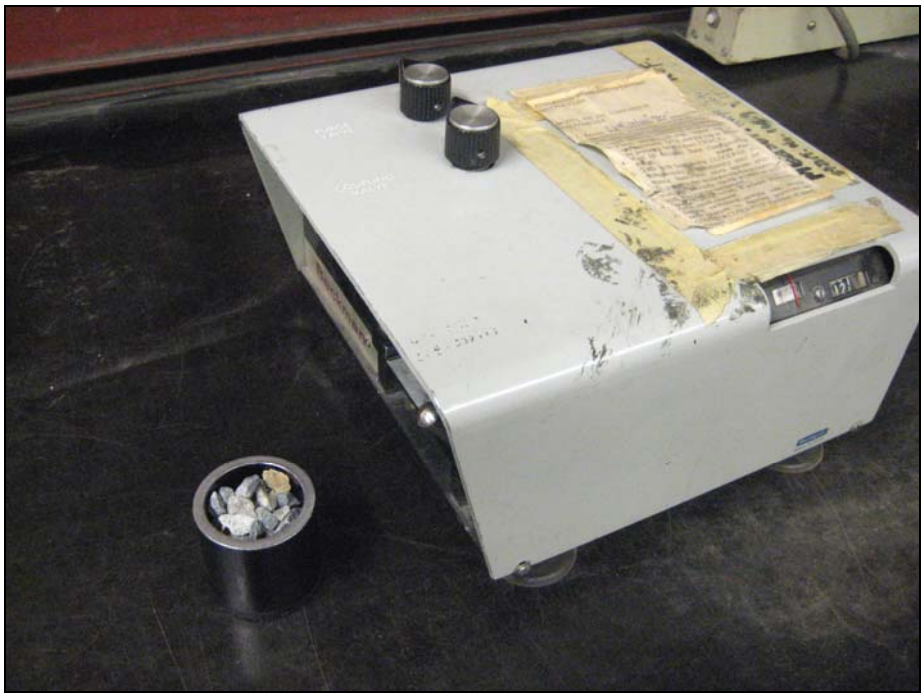

Figure C6.5 Air comparison pycnometer in determining volume and density particle of waste rock material

Figure C6.6 Autosorb-1 Surface Area Analyzer (Quantachrome Instruments Corporation) for determining specific surface area by using the BET method

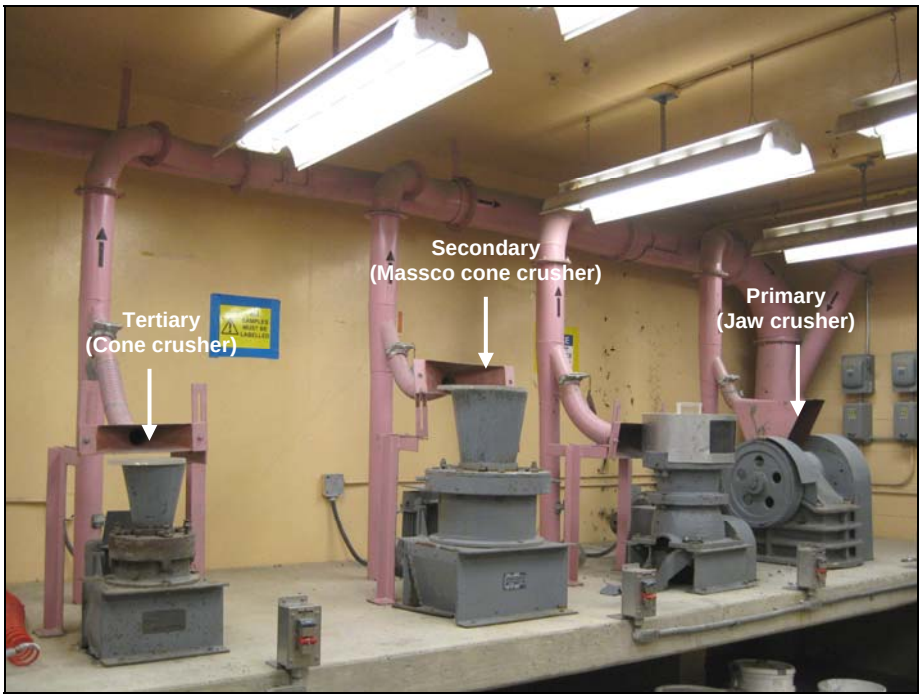

Figure C6.7 Crushers used during the coarse size fractions grinding for preparing samples for assay

Figure C6.8 Ring mill pulveriser using a carbon steel (chrome free) ring set (TM Engineering Ltd.) for preparing samples for assay

Figure C6.9 Rotary micro riffler with 3 inch turntable, 15mm OD x 8 tubes (*Quantachrome* Instruments Corporation) for preparing samples to analyze with MLA

Figure C6.10 Struers Tegra polisher system for polishing mounts to analyze with MLA

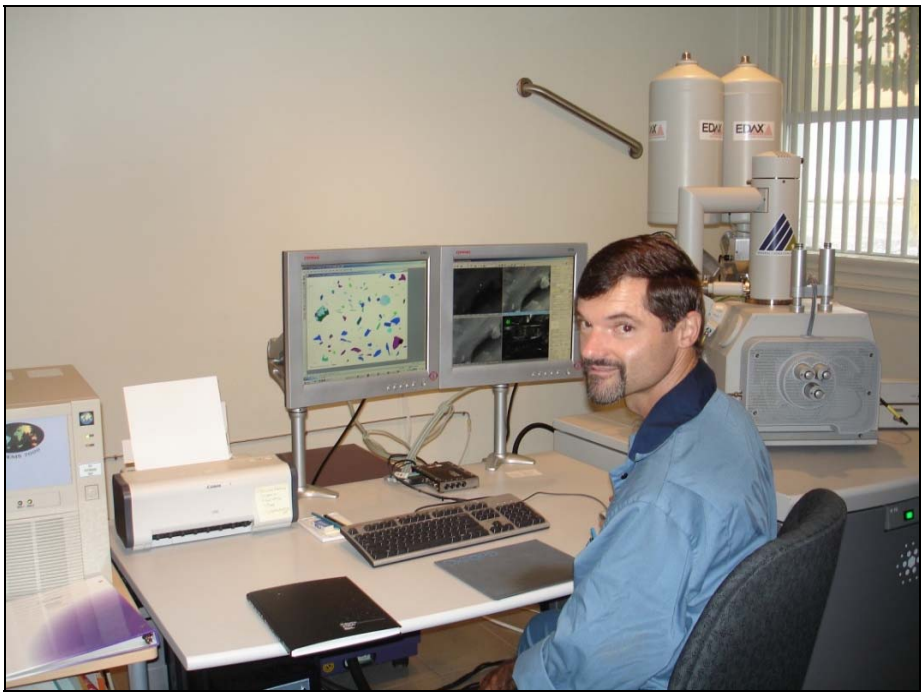

Figure C6.11 Bruker-AXS XFlash 4010 Mineral Liberation Analyzer (MLA) of Teck's ART group at Trail, B.C.

Figure C6.12 FEI Quanta600-SEM Mineral Liberation Analyzer (MLA) of Teck's ART group at Trail, B.C.

Appendix D

Appendix D1

Field Cell Installation

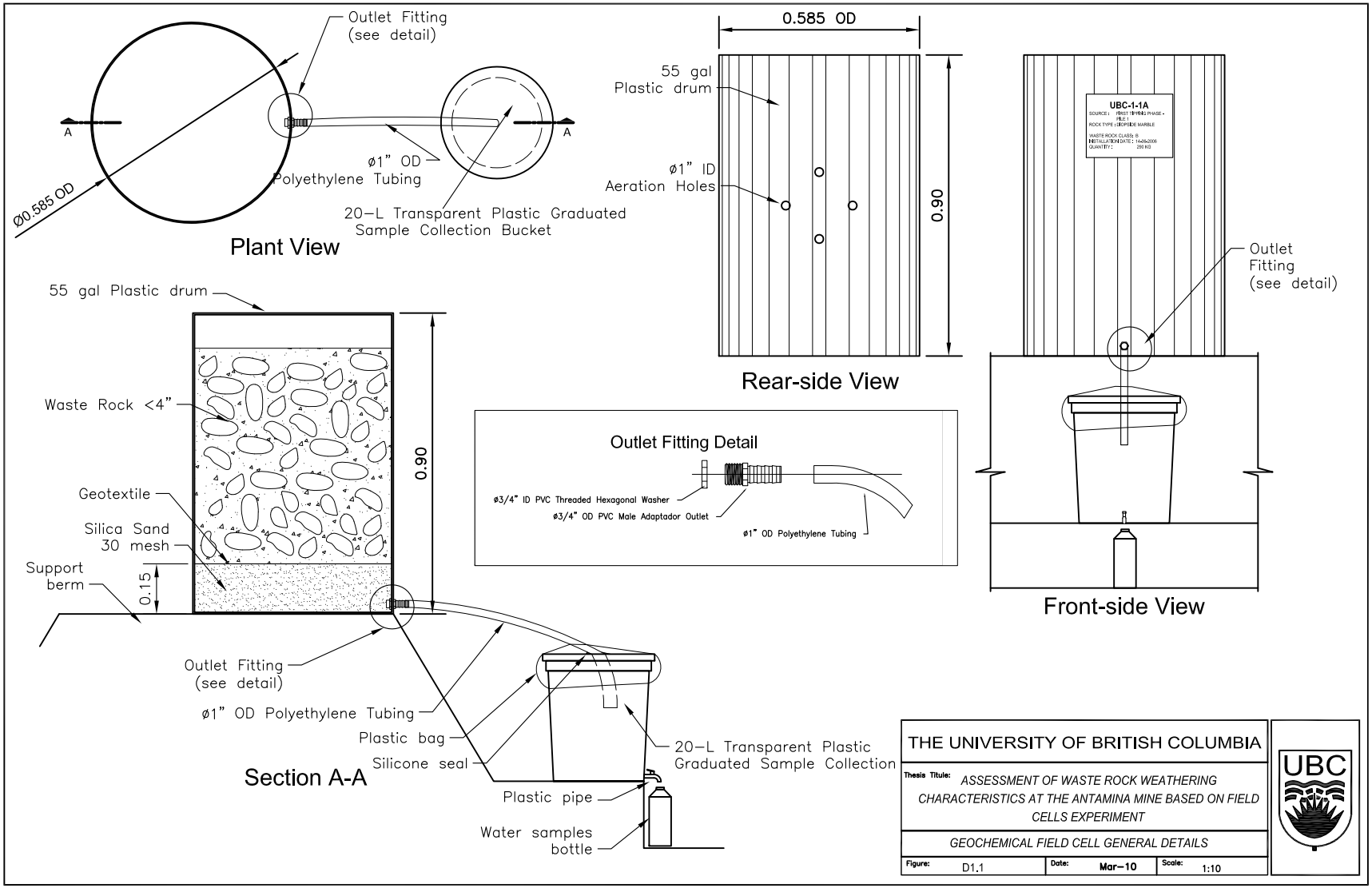

Figure D1.1 Geochemical field cell general details

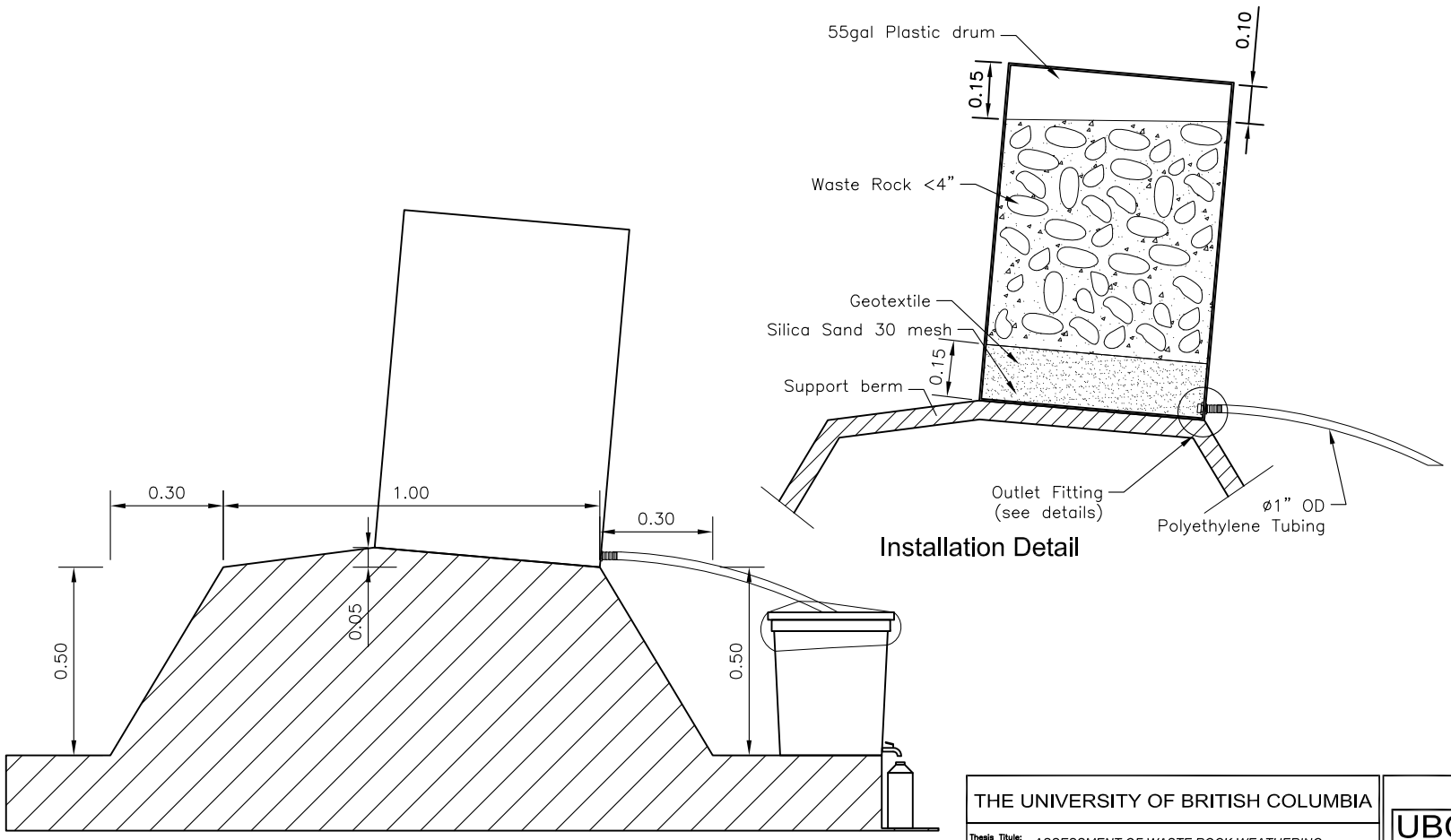

Figure D1.2 Geochemical field cell placement details

Appendix D2

Figures of Waste Rock Materials in the Field Cells

Figure D2.1 Field cell UBC-1-0A containing Class B black marble waste rock material

Figure D2.2 Field cell UBC-1-0B (duplicate of -0A) containing Class B black marble waste rock material

Figure D2.3 Field cell UBC-1-1A containing Class B diopside marble waste rock material

Figure D2.4 Field cell UBC-1-2A containing Class B diopside marble waste rock material

Figure D2.-5 Field cell UBC-1-2B (duplicate of -2A) containing Class B diopside marble waste rock material

Figure D2.6 Field cell UBC-1-3A containing Class B diopside marble waste rock material

Figure D2.7 Field cell UBC-1-4A containing Class B gray hornfels waste rock material

Figure D2.8 Field cell UBC-1-XA containing Class C black marble waste rock material

Appendix D3

Block Model of the Antamina Mine

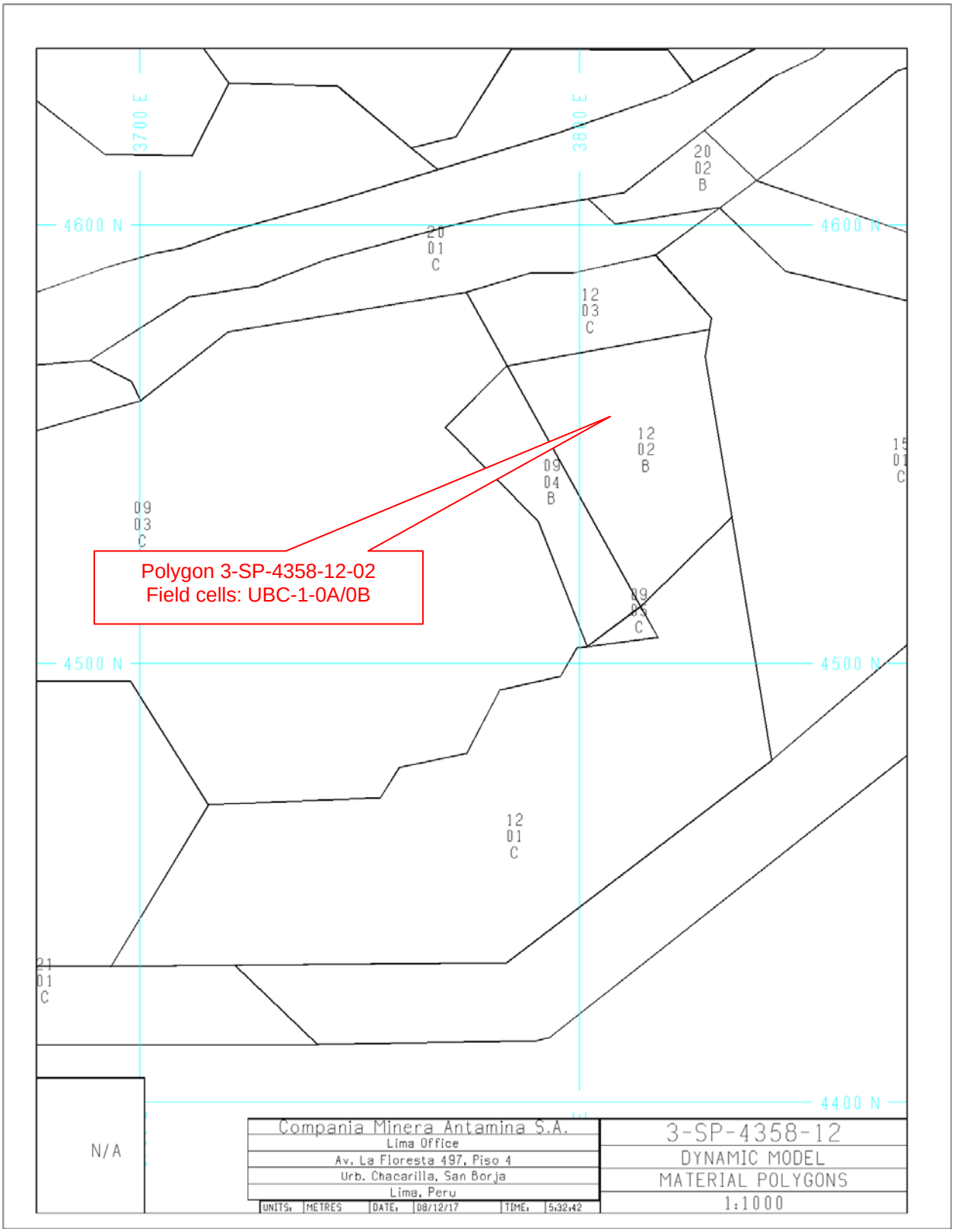

Figure D3.1 Polygons of waste rock classes. Class B material within 3-SP-4358-12 mesh from block model

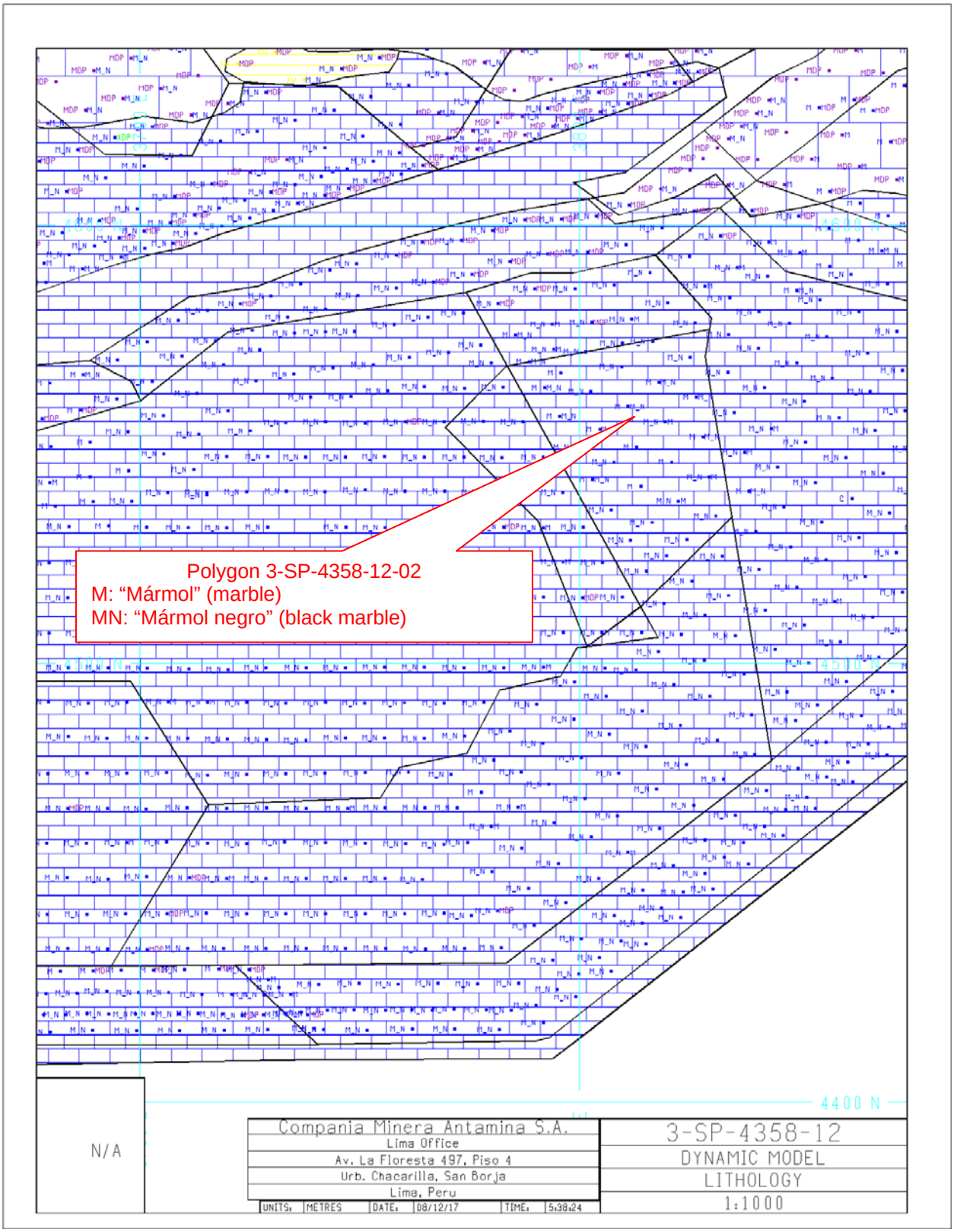

Figure D3.2 Lithology of waste rock classes within 3-SP-4358-12 mesh. Class B black marble material from block model (FC: UBC-1-0A/0B)

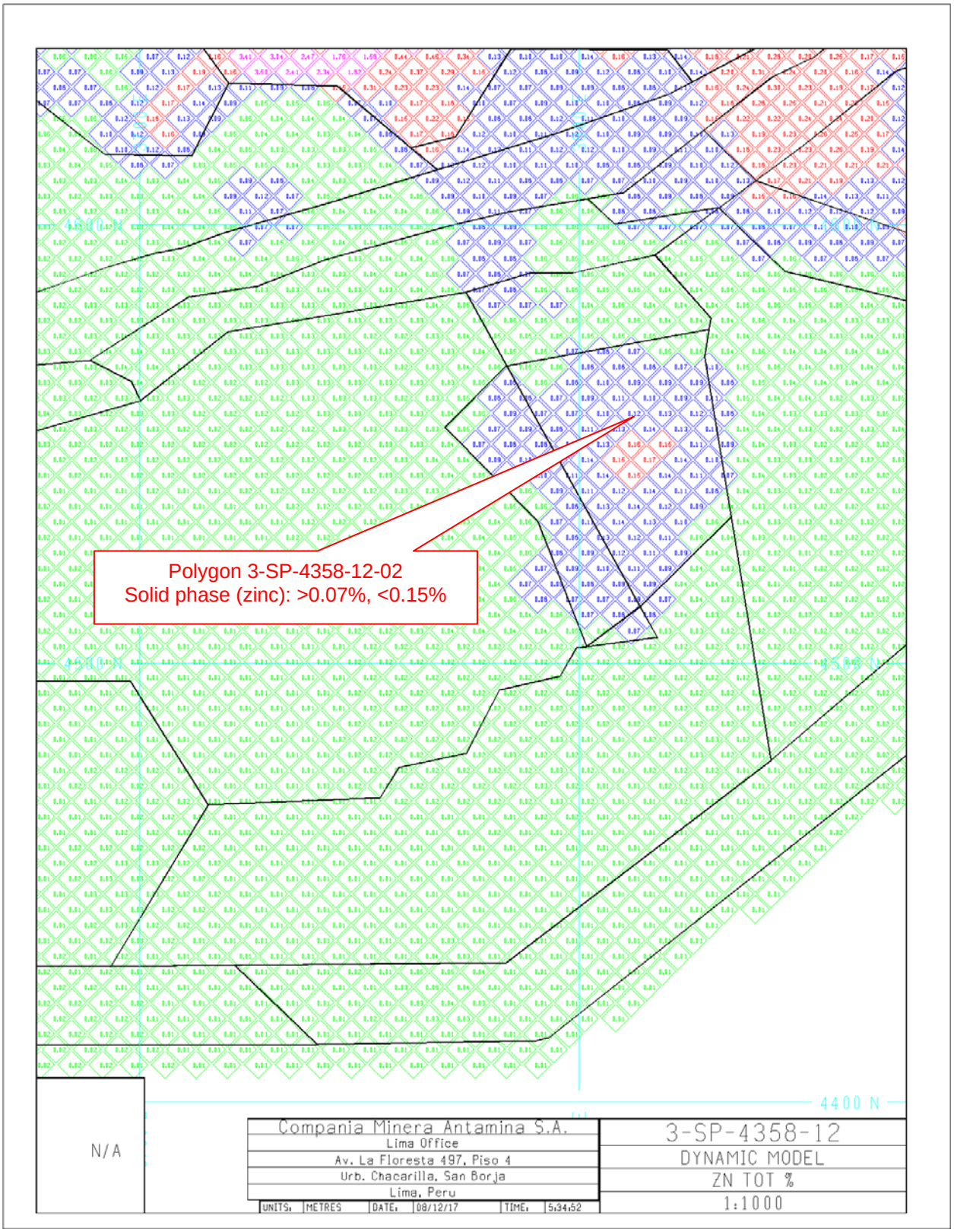

Figure D3.3 Solid phase zinc concentration in the waste rock classes. Class B black marble material from block model

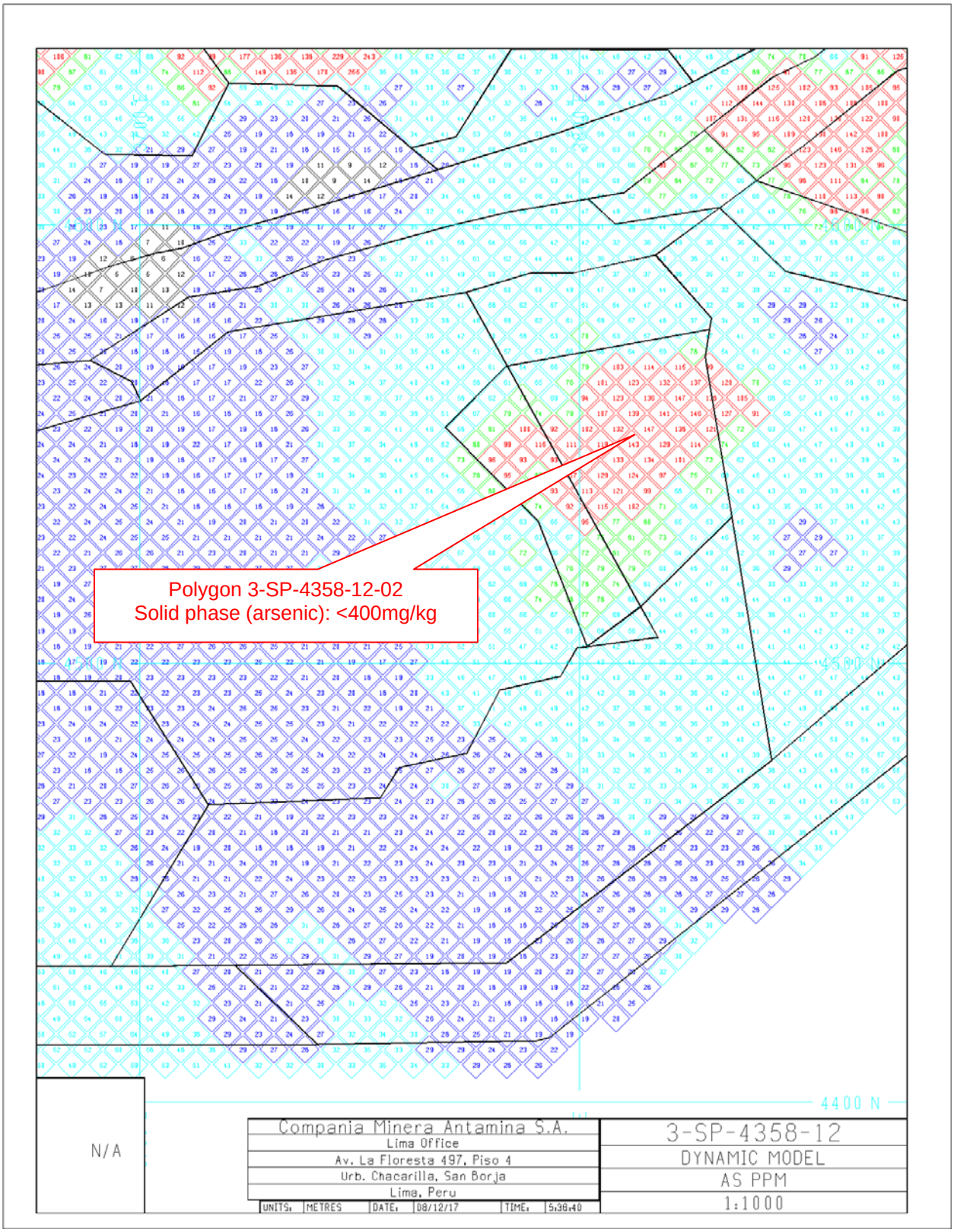

Figure D3.4 Solid phase arsenic concentration in the waste rock classes. Class B black marble material from block model

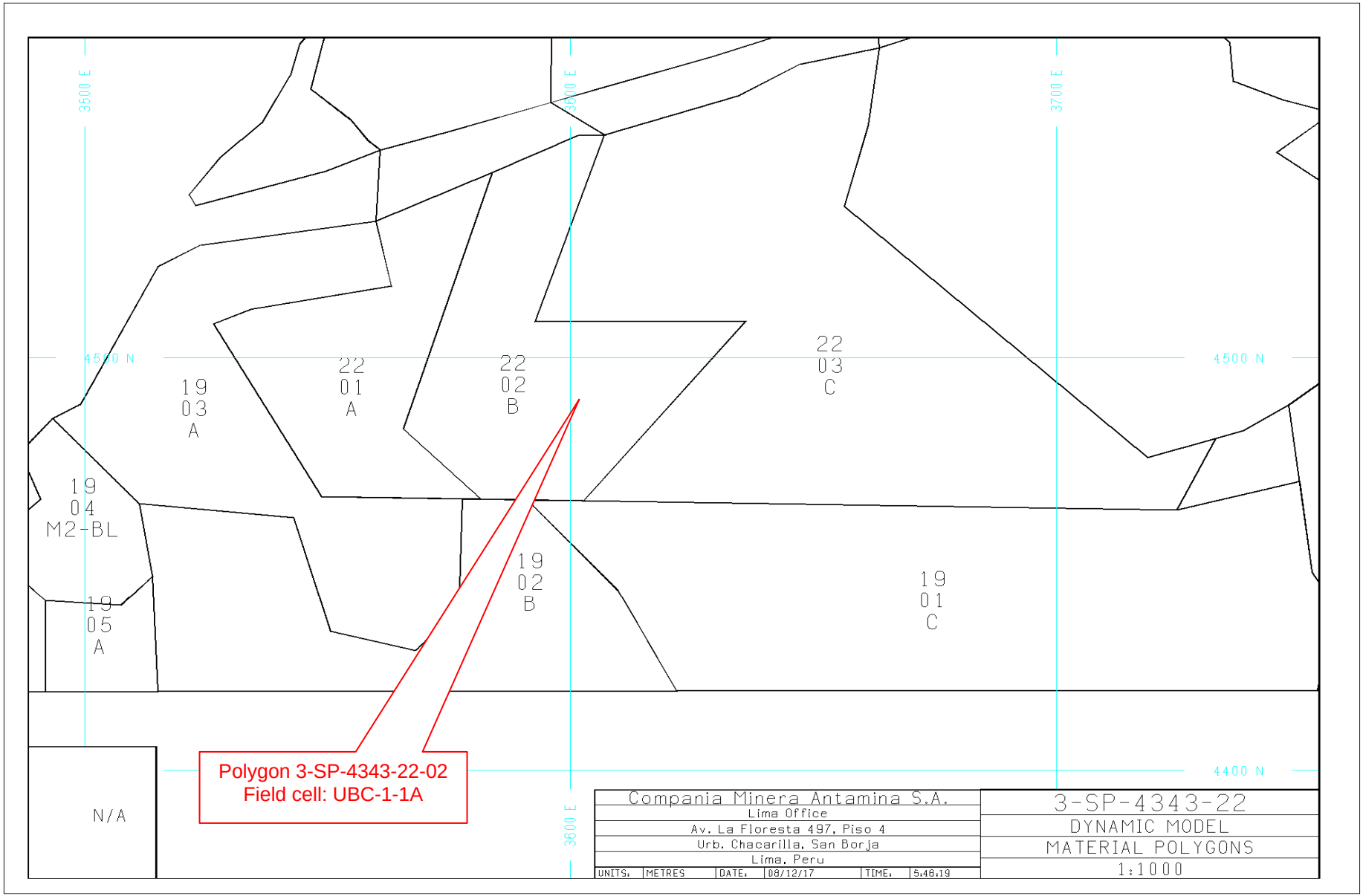

Figure D3.5 Polygons of waste rock classes. Class B material within 3-SP-4343-22 mesh from block model

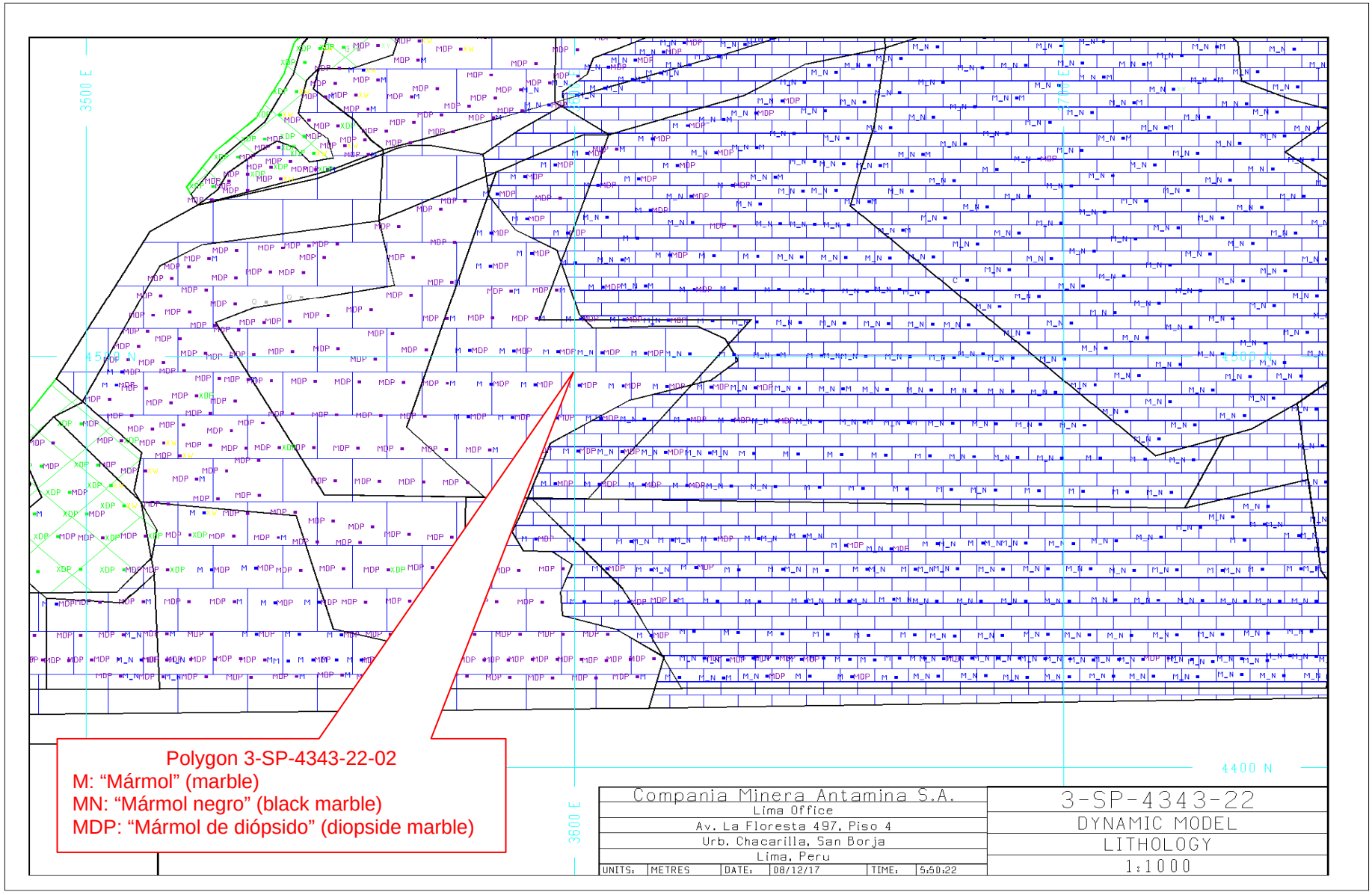

Figure D3.6 Lithology of waste rock classes within 3-SP-4358-22 mesh. Class B black marble material from block model (FC: UBC-1-1A)

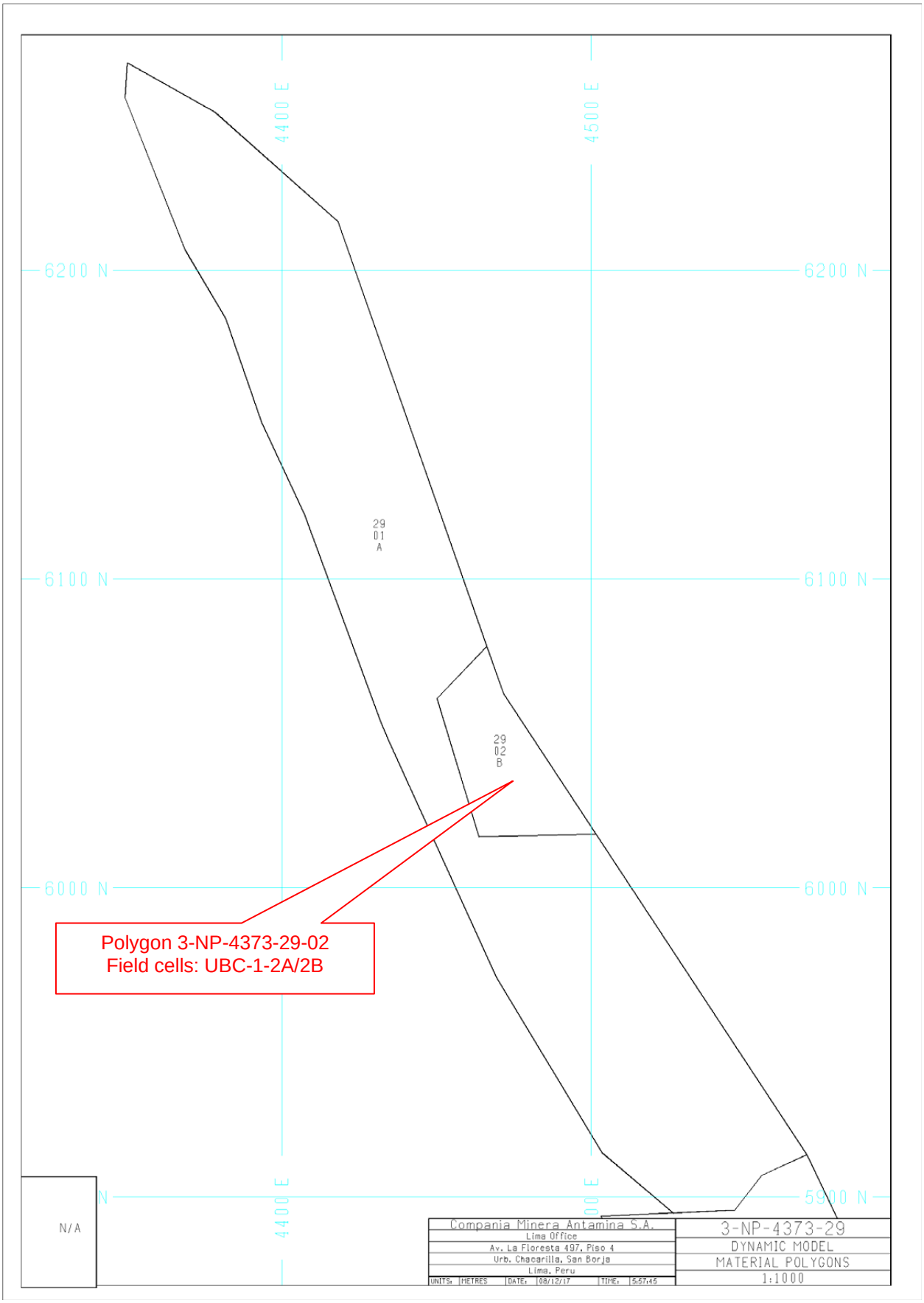

Figure D3.7 Polygons of waste rock classes. Class B material within 3-NP-4373-29 mesh from block model

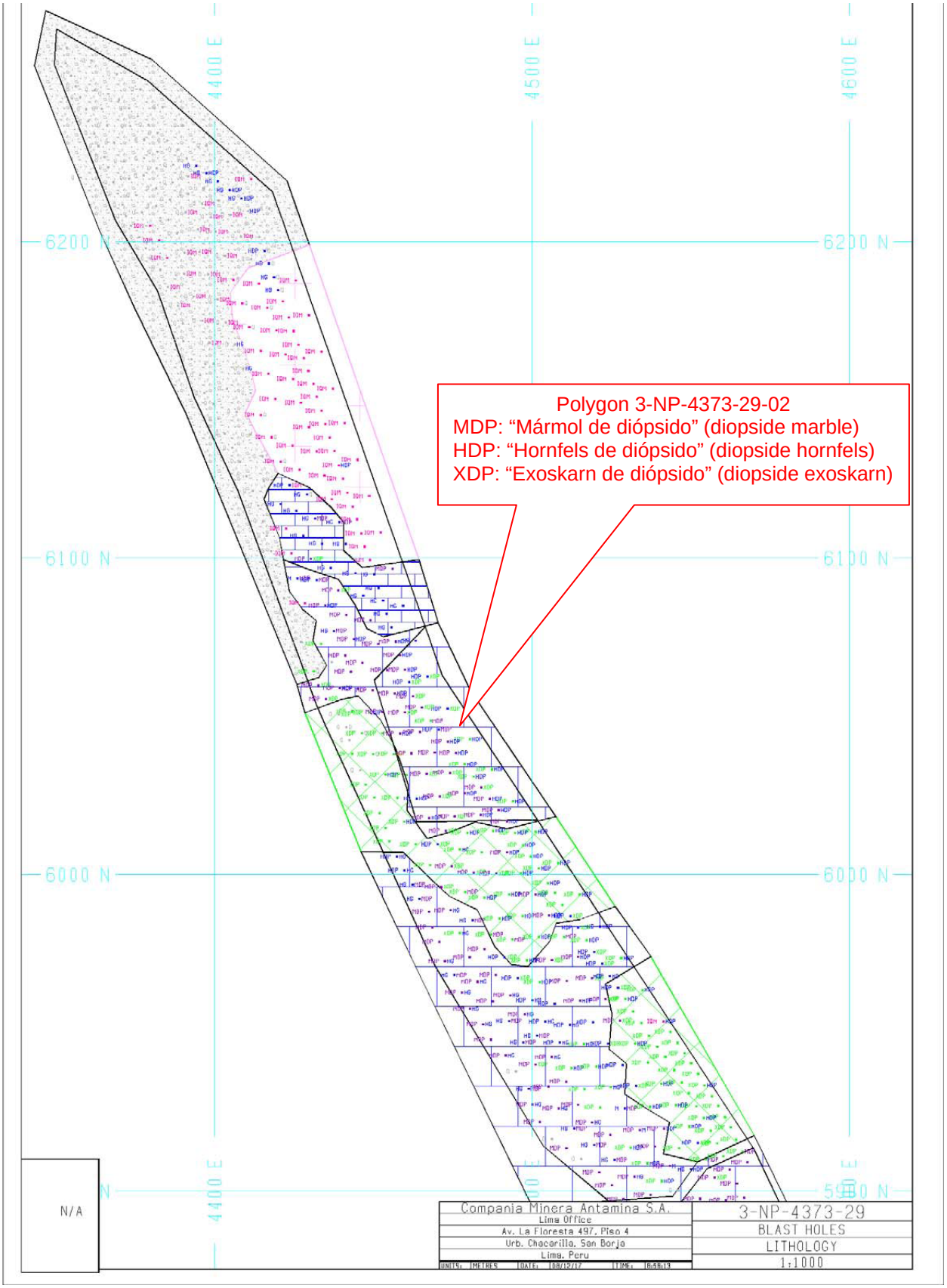

Figure D3.8 Lithology of waste rock classes within 3-NP-4373-29 mesh. Class B black marble material from block model (FC: UBC-1-2A/2B)

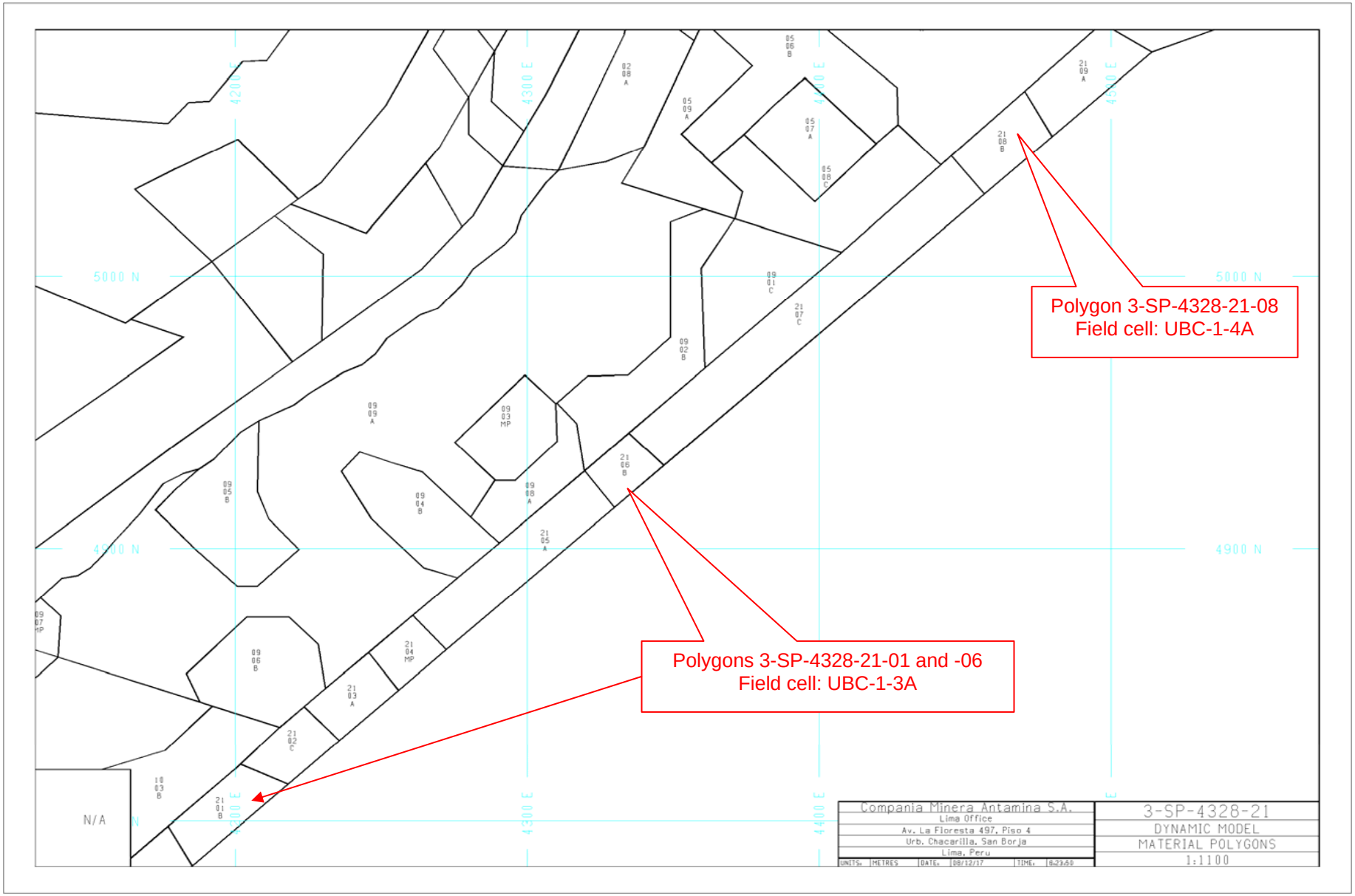

Figure D3.9 Polygons of waste rock classes. Class B material within 3-SP-4328-21 mesh from block model

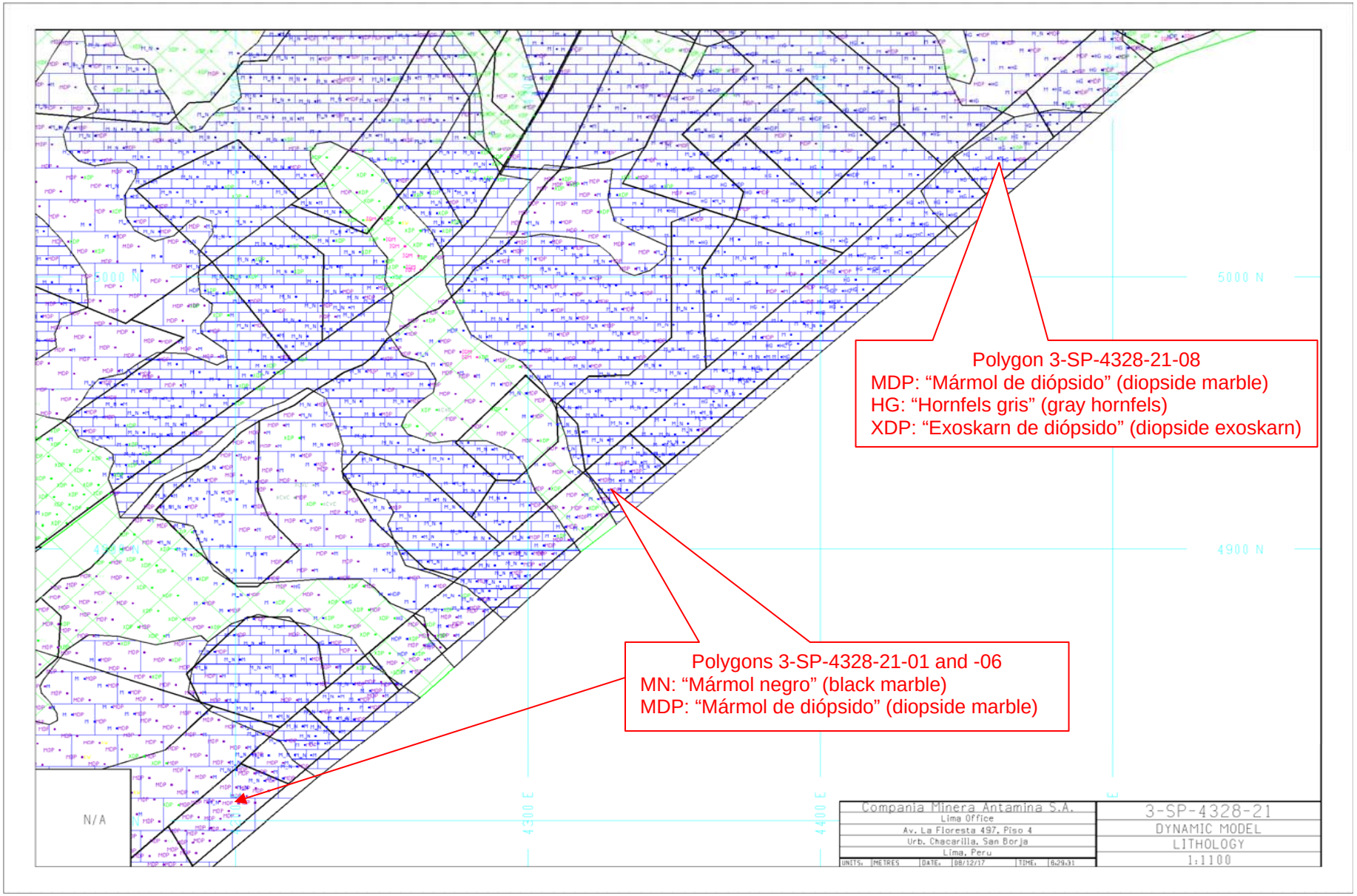

Figure D3.10 Lithology of waste rock classes within 3-SP-4328-21 mesh. Class B black marble material from block model (FC: UBC-1-3A and -4A)

Appendix D4

Leachate Results from the Field Cells

Table D4.1 Summary of water drainage data from the field cells containing Class B waste rock material

Station Name:		UBC-1-0A: Protective layer - Pile 1 (Black marble - Class B)				UBC-1-0B: Protective layer (D) - Pile 1 (Black marble - Class B)				UBC-1-1A: First tipping phase - Pile 1 (Diopside marble - Class B)				UBC-1-2A: Second tipping phase - Pile 1 (Diopside marble - Class B)				UBC-1-2B: Second tipping phase (D) - Pile 1 (Diopside marble - Class B)				UBC-1-3A: Third tipping phase - Pile 1 (Diopside marble - Class B)				UBC-1-4A: Third/fourth tipping phase - Pile 1 (Gray hornfels - Class B)				UBC-1-XA: Base of Pile 1 (Crushed material) - Black marble - Class C			
Sampling Period (dd/mm/yy)		From 06/04/06 to 02/05/08				From 06/04/06 to 02/05/08				From 26/10/06 to 02/05/08				From 26/10/06 to 02/05/08				From 12/10/06 to 02/05/08				From 26/10/06 to 02/05/08				From 02/11/06 to 02/05/08				From 16/11/06 to 02/05/08			
Parameter	Units	Samples Number	Average	Minimum	Maximum	Samples Number	Average	Minimum	Maximum	Samples Number	Average	Minimum	Maximum	Samples Number	Average	Minimum	Maximum	Samples Number	Average	Minimum	Maximum	Samples Number	Average	Minimum	Maximum	Samples Number	Average	Minimum	Maximum	Samples Number	Average	Minimum	Maximum
Aluminum - Dissolved	mg/L	22	0.04	0.02	0.09	22	0.04	0.02	0.09	29	0.03	0.02	0.07	25	0.03	0.02	0.08	25	0.03	0.02	0.08	21	0.03	0.02	0.08	26	0.03	0.02	0.07	18	0.04	0.02	0.09
Aluminum - Total	mg/L	22	0.05	0.02	0.12	22	0.05	0.02	0.13	29	0.05	0.02	0.13	25	0.06	0.02	0.17	25	0.05	0.02	0.14	21	0.05	0.02	0.11	26	0.05	0.02	0.11	18	0.06	0.02	0.13
Antimony - Dissolved	mg/L	22	0.014	0.01	0.041	22	0.047	0.01	0.067	29	0.186	0.02	0.252	25	0.053	0.021	0.106	25	0.047	0.017	0.088	21	0.055	0.038	0.079	26	0.127	0.064	0.166	18	0.05	0.01	0.073
Antimony - Total	mg/L	22	0.015	0.01	0.041	22	0.05	0.028	0.068	29	0.203	0.02	0.255	25	0.056	0.024	0.107	25	0.05	0.018	0.094	21	0.058	0.039	0.081	26	0.133	0.065	0.17	18	0.058	0.01	0.157
Arsenic - Dissolved	mg/L	22	0.007	0.001	0.022	22	0.017	0.001	0.026	29	0.024	0.012	0.035	25	0.02	0.001	0.036	25	0.014	0.001	0.028	21	0.012	0.001	0.022	26	0.008	0.001	0.016	18	0.007	0.001	0.013
Arsenic - Total	mg/L	22	0.008	0.001	0.022	22	0.019	0.001	0.027	29	0.025	0.012	0.035	25	0.022	0.001	0.041	25	0.017	0.001	0.03	21	0.013	0.001	0.022	26	0.009	0.001	0.017	18	0.008	0.001	0.013
Barium - Dissolved	mg/L	22	0.016	0.006	0.04	22	0.016	0.008	0.038	29	0.025	0.014	0.05	25	0.043	0.026	0.066	25	0.042	0.02	0.068	21	0.035	0.016	0.076	26	0.062	0.039	0.101	18	0.037	0.021	0.049
Barium - Total	mg/L	22	0.02	0.008	0.066	22	0.019	0.008	0.048	29	0.027	0.018	0.059	25	0.046	0.029	0.075	25	0.045	0.02	0.075	21	0.04	0.017	0.079	26	0.066	0.041	0.101	18	0.041	0.023	0.066
Boron - Dissolved	mg/L	22	0.03	0.03	0.04	22	0.04	0.03	0.06	29	0.04	0.03	0.11	25	0.03	0.03	0.06	25	0.04	0.03	0.08	21	0.03	0.03	0.07	26	0.04	0.03	0.1	18	0.03	0.03	0.03
Boron - Total	mg/L	22	0.04	0.03	0.1	22	0.04	0.03	0.08	29	0.05	0.03	0.11	25	0.04	0.03	0.09	25	0.04	0.03	0.11	21	0.04	0.03	0.11	26	0.04	0.03	0.13	18	0.04	0.03	0.13
Cadmium - Dissolved	mg/L	22	0.003	0.003	0.003	22	0.003	0.003	0.003	29	0.003	0.003	0.003	25	0.021	0.003	0.066	25	0.022	0.005	0.092	21	0.019	0.004	0.049	26	0.012	0.00	0.036	18	0.014	0.00	0.029
Cadmium - Total	mg/L	22	0.003	0.003	0.003	22	0.003	0.003	0.003	29	0.003	0.003	0.005	25	0.023	0.003	0.072	25	0.024	0.005	0.107	21	0.02	0.004	0.053	26	0.013	0.00	0.041	18	0.016	0.00	0.038
Calcium - Dissolved	mg/L	22	137.92	62.81	373.5	22	122.31	63.53	323.8	29	47.6	29.78	103	25	78.39	49.9	158.1	25	108.85	59.7	434.5	21	110.35	54.86	194.3	26	59.09	35.51	161.9	18	139.93	68.16	294.4
Calcium - Total	mg/L	22	150.82	68.37	373.9	22	126.6	67.07	326.8	29	50.58	31.76	117.6	25	83.11	52.9	167.2	25	114.11	62.27	450.2	21	116.34	55.1	203.9	26	62.74	36.82	193.8	18	149.62	70.53	295.3
Chromium - Dissolved	mg/L	22	0.002	0.002	0.002	22	0.002	0.002	0.002	29	0.002	0.002	0.002	25	0.002	0.002	0.002	25	0.002	0.002	0.002	21	0.002	0.002	0.002	26	0.002	0.002	0.002	18	0.002	0.002	0.002
Chromium - Total	mg/L	22	0.002	0.002	0.002	22	0.002	0.002	0.002	29	0.002	0.002	0.002	25	0.002	0.002	0.002	25	0.002	0.002	0.002	21	0.002	0.002	0.002	26	0.002	0.002	0.002	18	0.002	0.002	0.003
Cobalt - Dissolved	mg/L	22	0.005	0.005	0.005	22	0.005	0.005	0.005	29	0.005	0.005	0.005	25	0.005	0.005	0.01	25	0.006	0.005	0.015	21	0.005	0.005	0.005	26	0.005	0.005	0.011	18	0.005	0.005	0.008
Cobalt - Total	mg/L	22	0.005	0.005	0.005	22	0.005	0.005	0.005	29	0.005	0.005	0.005	25	0.005	0.005	0.01	25	0.006	0.005	0.016	21	0.005	0.005	0.006	26	0.005	0.005	0.012	18	0.006	0.005	0.012
Copper - Dissolved	mg/L	22	0.003	0.001	0.011	22	0.001	0.001	0.008	29	0.002	0.001	0.009	25	0.097	0.032	0.208	25	0.138	0.084	0.256	21	0.149	0.037	0.308	26	0.035	0.001	0.072	18	0.042	0.023	0.07
Copper - Total	mg/L	22	0.006	0.001	0.017	22	0.004	0.001	0.018	29	0.007	0.001	0.018	25	0.111	0.046	0.222	25	0.156	0.087	0.265	21	0.166	0.055	0.328	26	0.044	0.022	0.081	18	0.051	0.031	0.077
Iron - Dissolved	mg/L	22	0.005	0.001	0.068	22	0.003	0.001	0.039	29	0.001	0.001	0.001	25	0.001	0.001	0.004	25	0.001	0.001	0.001	21	0.001	0.001	0.001	26	0.001	0.001	0.001	18	0.001	0.001	0.001
Iron - Total	mg/L	22	0.028	0.001	0.1	22	0.029	0.001	0.114	29	0.036	0.001	0.096	25	0.036	0.001	0.185	25	0.035	0.001	0.142	21	0.039	0.001	0.108	26	0.034	0.001	0.12	18	0.031	0.001	0.1
Lead - Dissolved	mg/L	22	0.01	0.01	0.01	22	0.01	0.01	0.01	29	0.011	0.01	0.016	25	0.448	0.178	1.153	25	0.652	0.16	3.994	21	0.395	0.01	0.875	26	0.238	0.039	0.635	18	0.361	0.165	0.665
Lead - Total	mg/L	22	0.012	0.01	0.027	22	0.01	0.01	0.02	29	0.014	0.01	0.036	25	0.49	0.198	1.202	25	0.772	0.166	4.569	21	0.441	0.01	0.878	26	0.277	0.148	0.796	18	0.413	0.177	0.864
Magnesium - Dissolved	mg/L	22	4.031	2.27	8.794	22	2.992	1.635	7.806	29	1.85	1.08	5.548	25	3.559	1.987	7.837	25	4.913	2.099	27.77	21	3.202	2.014	6.986	26	5.25	2.771	14.480	18	3.95	1.8	7.447
Magnesium - Total	mg/L	22	4.498	2.318	8.972	22	3.114	1.661	7.979	29	1.976	1.092	6.049	25	3.794	2.102	9.294	25	5.299	2.203	30.76	21	3.457	2.067	9.977	26	5.612	2.844	18.06	18	4.269	1.85	10.18
Manganese - Dissolved	mg/L	22	0.026	0.001	0.232	22	0.029	0.001	0.283	29	0.009	0.001	0.063	25	0.228	0.02	0.925	25	0.382	0.001	2.688	21	0.066	0.017	0.365	26	0.173	0.023	1.077	18	0.157	0.005	0.48
Manganese - Total	mg/L	22	0.033	0.001	0.232	22	0.032	0.001	0.286	29	0.012	0.001	0.069	25	0.241	0.024	0.934	25	0.409	0.028	3.033	21	0.073	0.019	0.436	26	0.184	0.026	1.236	18	0.174	0.006	0.598
Mercury - Dissolved	mg/L	22	0.0002	0.0002	0.0002	22	0.0002	0.0002	0.0002	29	0.0002	0.0002	0.000	25	0.0002	0.0002	0.0002	25	0.0002	0.0002	0.0002	21	0.0002	0.0002	0.0002	26	0.0002	0.0002	0.0002	18	0.0002	0.0002	0.0002
Mercury - Total	mg/L	22	0.0002	0.0002	0.0002	22	0.0002	0.0002	0.0002	29	0.0002	0.0002	0.0002	25	0.0002	0.0002	0.0002	25	0.0002	0.0002	0.0002	21	0.0002	0.0002	0.0002	26	0.0002	0.0002	0.0002	18	0.0002	0.0002	0.0002
Molybdenum - Dissolved	mg/L	22	0.03	0.02	0.04	22	0.03	0.02	0.03	29	0.04	0.01	0.06	25	0.03	0.01	0.05	25	0.03	0.01	0.04	21	0.02	0.01	0.03	26	0.02	0.01	0.03	18	0.01	0.01	0.02
Molybdenum - Total	mg/L	22	0.03	0.02	0.04	22	0.03	0.02	0.04	29	0.04	0.01	0.07	25	0.04	0.02	0.06	25	0.03	0.01	0.05	21	0.02	0.01	0.03	26	0.020	0.01	0.03	18	0.02	0.01	0.03
Nickel - Dissolved	mg/L	22	0.001	0.001	0.001	22	0.001	0.001	0.001	29	0.001	0.001	0.002	25	0.003	0.001	0.009	25	0.004	0.001	0.02	21	0.003	0.001	0.007	26	0.002	0.001	0.01	18	0.002	0.001	0.006
Nickel - Total	mg/L	22	0.001	0.001	0.001	22	0.001	0.001	0.001	29	0.001	0.001	0.01	25	0.004	0.001	0.009	25	0.005	0.001	0.022	21	0.004	0.001	0.007	26	0.002	0.001	0.012	18	0.003	0.001	0.008
Potassium - Dissolved	mg/L	22	1.34	0.69	2.65	22	1.61	0.83	2.87	29	2.48	1.08	7.77	25	4.48	2.45	12.1	25	6.25	2.38	28.2	21	2	1.15	5.53	26	2.32	0.650	8.37	18	4.29	2.69	6.51
Potassium - Total	mg/L	22	1.5	0.72	3.06	22	1.7	0.9	3	29	2.7	1.18	8.22	25	4.72	2.62	13.25	25	6.57	2.62	30.88	21	2.14	1.21	6.77	26	2.53	0.83	8.76	18	4.61	2.77	7.44
Selenium - Dissolved	mg/L	22	0.002	0.002	0.004	22	0.003	0.002	0.007	29	0.004	0.002	0.009	25	0.003	0.002	0.007	25	0.004	0.002	0.012	21	0.007	0.002	0.011	26	0.003	0.002	0.012	18	0.002	0.002	0.008
Selenium - Total	mg/L	22	0.003	0.002	0.011	22	0.003	0.002	0.008	29	0.005	0.002	0.014	25	0.004	0.002	0.011	25	0.005	0.002	0.012	21	0.007	0.002	0.011	26	0.003	0.002	0.012	18	0.003	0.002	0.009
Silicon - Dissolved	mg/L	20	3.09	2.45	3.73	20	5.48	4.46	6.62	29	4.38	3.39	6.87	25	7.6	6.51	9.23	25	6.98	6.02	7.99	21	4.67	3.48	6.34	26	2.96	1.93	4.49	18	3.19	2.58	4.03
Silicon - Total	mg/L	20	3.29	2.8	4.59	20	5.65	4.49	6.66	29	4.63	3.61	7.16	25	7.93	6.97	9.93	25	7.31	6.32	8.34	21	4.95	4.01	7.4	26	3.12	2.12	5.04	18	3.38	2.58	4.83
Silver - Dissolved	mg/L	22	0.01	0.01	0.01	22	0.01	0.01	0.01	29	0.01	0.01	0.01	25	0.01	0.01	0.01	25	0.01	0.01	0.01	21	0.01	0.01	0.01	26	0.010	0.010	0.01	18	0.01	0.010	0.01
Silver - Total	mg/L	22	0.01	0.01	0.01	22	0.01	0.01	0.01	29	0.01	0.001	0.01	25	0.01	0.01	0.01	25	0.01	0.01	0.01	21	0.01	0.01	0.01	26	0.010	0.001	0.01	18	0.01	0.010	0.01
Sodium - Dissolved	mg/L	22	0.98	0.02	3.48	22	2.21	0.66	4.7	29	1.64	0.14	10.01	25	4.35	1.23	16.27	25	6.41	0.99	55.99	21	1.11	0.26	7.78	26	2.43	0.02	16.55	18	2.69	0.23	7.82
Sodium - Total	mg/L	22	1.16	0.02	4.23	22	2.44	0.66	4.99	29	1.93	0.16	12.13	25	4.61	1.24	16.82	25	6.83	1.14	60.7	21	1.31	0.26	9.46	26	2.74	0.02	19.55	18	3.07	0.27	9.3
Strontium - Dissolved	mg/L	22	0.73	0.352	2.025	22	0.702	0.389	1.76	29	0.422	0.271	0.918	25	0.178	0.09	0.496	25	0.249	0.095	1.388	21	1.325	0.849	2.213	26	3.154	2.168	5.125	18	1.293	0.719	2.317
Strontium - Total	mg/L	22	0.822	0.381	2.254	22	0.733	0.406	1.76	29	0.448	0.284	1.04	25	0.186	0.091	0.523	25	0.257	0.096	1.425	21	1.394	0.883	2.578	26	3.351	2.19	5.184	18	1.375	0.751	2.508
Tungsten - Dissolved	mg/L	12	0.2	0.2	0.2	8	0.2	0.2	0.2	13	0.2	0.2	0.2	13	0.2	0.2	0.2	13	0.2	0.2	0.2	13	0.2	0.2	0.2	10	0.2	0.2	0.2	6	0.2	0.2	0.2
Tungsten - Total	mg/L	12	0.2	0.2	0.2	8	0.2	0.2	0.2	13	0.2	0.2	0.20	13	0.2	0.2	0.2	13	0.2	0.2	0.2	13	0.2	0.2	0.2	10	0.2	0.2	0.2	6	0.2	0.2	0.2
Zinc - Dissolved	mg/L	22	0.064	0.023	0.173	22	0.024	0.009	0.102	29	0.041	0.004	0.117	25	4.378	0.886	16.89	25	4.127	2.215	9.595	21	4.737	1.326	13.94	26	1.786	0.428	4.42	18	2.014	1.016	3.097
Zinc - Total	mg/L	22	0.076	0.034	0.178	22	0.035	0.013	0.115	29	0.066	0.02	0.129	25	4.566	0.974	17.5	25	4.353	2.318	9.635	21	4.953	1.441	14.22	26	1.874	0.463	4.73	18	2.149	1.112	3.773
Acidity - Total	mg/L	21	2	2	2	21	2	2	2	26	2	2	2	23	2	2	2	21	2	2	2	19	2	2	2	23	2	2	2	16	2	2	2
Alkalinity - Total	mg/L	22	45.2	35.2	59.2	22	45.8	39	61.2	28	50.4	39	62.2	25	40.1	30.1	50.2	25	35.5	7.5	49.1	21	42.8	32	56.2	26	50.4	39.900	60.2	18	42.3	30.800	50.6
Alkalinity - Carbonate	mg/L	20	0.3	0.1	1	21	0.3	0.1	0.7	27	0.7	0.1	2.300	23	0.1	0.1	0.200	23	0.100	0.1	0.1	19	0.1	0.1	0.3	24	0.200	0.100	0.600	18	0.1	0.100	0.3
Alkalinity - Bicarbonate	mg/L	20	44.8	35.1	58.7	21	45.6	39.2	60.7	27	49.2	38.7	61.300	23	40	30.1	50.100	23	35.000	7.5	49	19	42.9	32	56	24	50.100	39.8	59.900	18	42.2	30.7	50.3
Sulphate	mg/L	22	240	53.2	739.7	22	251.9	111.3	694.2	29	67.4	25.7	192.2	25	162.6	77.6	395.5	25	231.7	96.9	863.1	21	238.5	102.8	410	26	126.3	41.7	467.40	18	322.9	127.5	672.8
Chloride	mg/L	22	2	1	7	22	2	1	6	29	3	1	16	25	13	4	45	25	20	1	202	21	2	1	9	26	2.00	1	14	18	2	1	4
Nitrate	mg/L	22	18.73	0.1	133.84	22	2.4	0.1	10.46	29	1.747	0.01	10.82	25	1.77	0.25	6.390	25	2.97	0.32	16.6	21	1.03	0.1	9.35	26	1.230	0.21	7.630	18	0.21	0.1	0.71
Ammonia	mg/L	22	0.19	0.01	2.37	22	0.03	0.01	0.13	29	0.08	0.01	1.22	25	0.61	0.01	3.75	25	0.51	0.01	4.55	21	0.24	0.01	3.72	26	1.4	0.01	8.85	18	0.03	0.01	0.1
Phosphate	mg/L	10	0.053	0.007	0.333	13	0.165	0.007	0.969	15	0.011	0.007	0.04	12	0.016	0.007	0.045	10	0.012	0.007	0.054	8	0.013	0.007	0.027	15	0.021	0.007	0.141	11	0.01	0.007	0.035
Fluoride	mg/L	22	1.14	0.54	3.1	22	0.92	0.58	1.16	29	1.27	0.96	1.57	25	1.4	0.31	2.16	25	1.55	0.96	2.2	21	1.45	1.12	1.87	26	1.53	1.12	1.86	18	1.51	1.16	1.84
Hardness - Total	mg/L	11	433.8	186.7	960	15	348.4	168.7	820	18	142.5	82.3	306.7	14	229.6	136	473.3	14	350.5	164.6	1180	10	255.8	138	460	18	193	100.4	533.3	13	341.5	188.8	650
Total Suspended Solids	mg/L	11	2	1	7	15	2	1	15	18	2	1	6	14	1	1	3	14	2	1	5	10	2	1	7	18	1	1	4	13	1	1	2
Total Dissolved Solids	mg/L	11	525	275	1405	15	480	219	1015	18	219	100	419	14	363	202	685	14	547	275	1830	10	386	235	602	18	312	156	750	13	491	281	785
Electrical Cond. - Lab	µS/cm	11	764	407	1894	15	661	374	1281	18	308.5	169.7	600	14	510	294	882	14	739	370	2246	10	520	332	803	18	432	239.8	935	13	657	388	950
Electrical Cond. - Field	µS/cm	53	752	382	2210	63	528	55	1321	58	286	158	673	64	490	242	899	56	591	301	2060	60	639	326	1254	57	378	222	1002	51	773	362	1612
pH - Lab	pH unit	11	7.7	6.9	8.2	15	7.8	7.4	8	18	8.1	7.1	8.8	14	7.3	6.7	7.7	14	7.2	6.6	7.6	10	7.4	7.1	7.8	18	7.5	7	8.1	13	7.4	6.8	7.9
pH - Field	pH unit	53	8.15	7.74	8.63	63	8.28	7.55	8.74	58	8.43	7.45	9.54	64	7.84	7.23	8.71	56	7.73	6.82	8.19	60	7.79	7.11	8.26	57	7.93	7.28	8.34	51	7.91	7.49	8.37
Temperature	°C	53	9.36	2.3	22.2	63	10.86	2.9	27.7	58	10.08	3.9	27.7	64	9.28	1.6	28.1	56	9.55	3.2	22	60	9.51	1.1	28.6	57	10.28	2	26.8	51	8.99	3.9	17.1
Turbidity	NTU	27	2.00	0	5	31	2	0	5	35	2	0	5	36	1.00	0	5	31	1.00	0	4	34	1.00	0.00	3.00	34	1.00	0.00	4	29	1.00	0.00	3.00
Volume	L	25	8.54	1.5	19	25	8.35	0.5	17	34	8.46	1	20	30	8.41	0.5	20	29	8.55	0.5	20	25	8.68	1	20	31	8.18	0.50	15	26	8.12	0.50	20

Appendix D5

Geochemical Speciation Calculation Plots

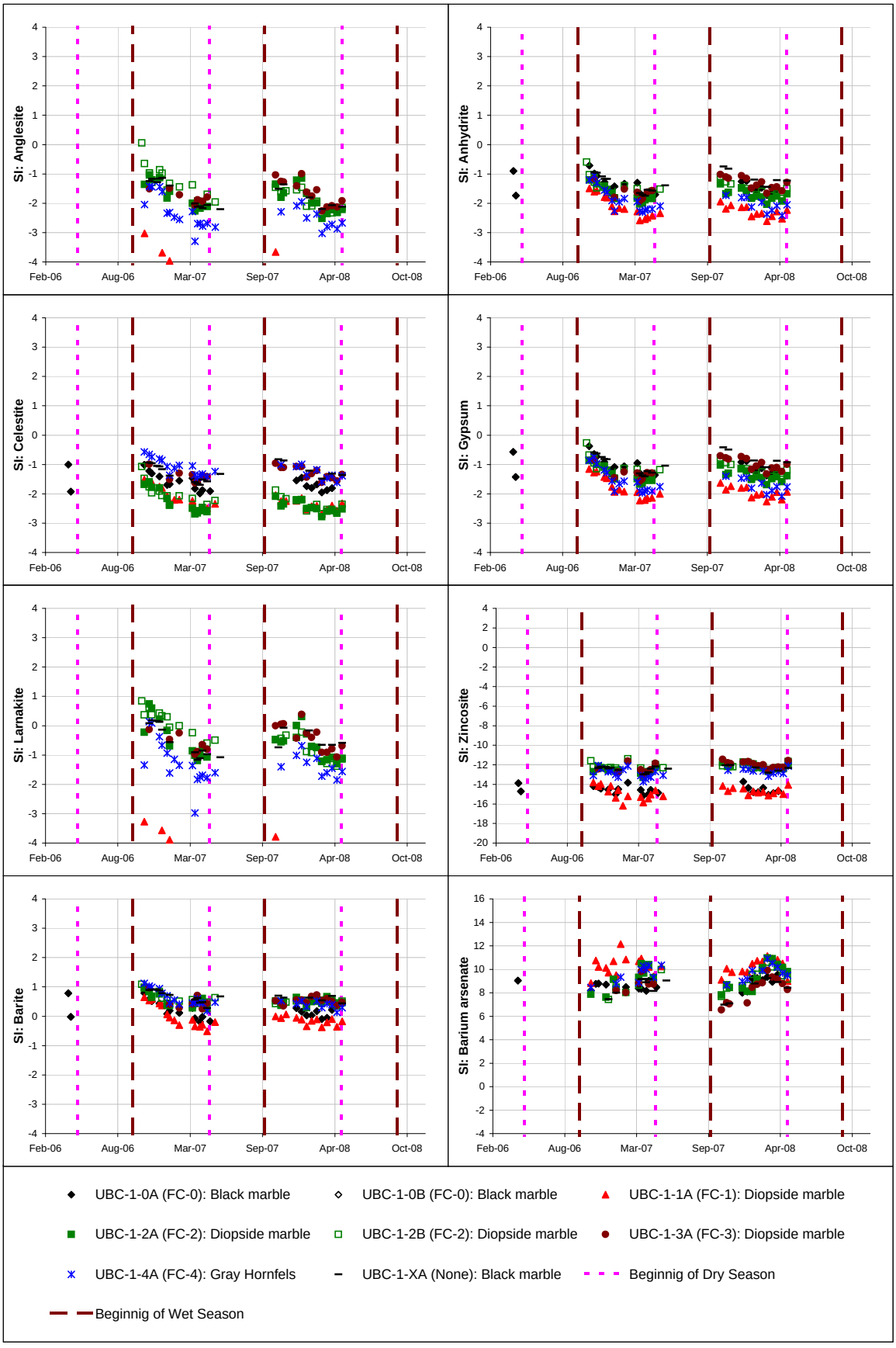

Figure D5.1 Saturation indices of sulphate and arsenate minerals in the leachate from the field cells containing Class B waste rock material

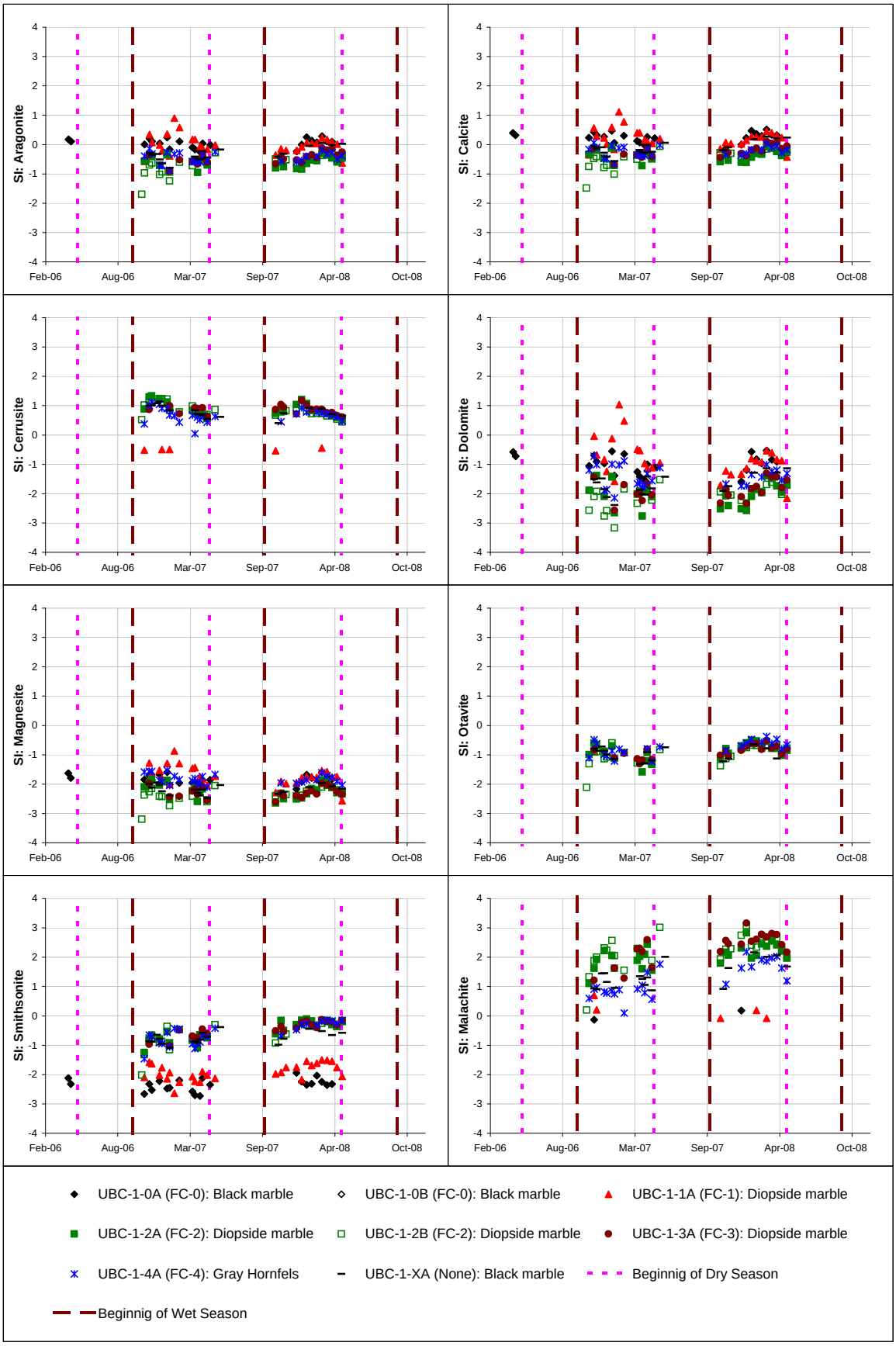

Figure D5.2 Saturation indices of carbonate minerals in the leachate from the field cells containing Class B waste rock material

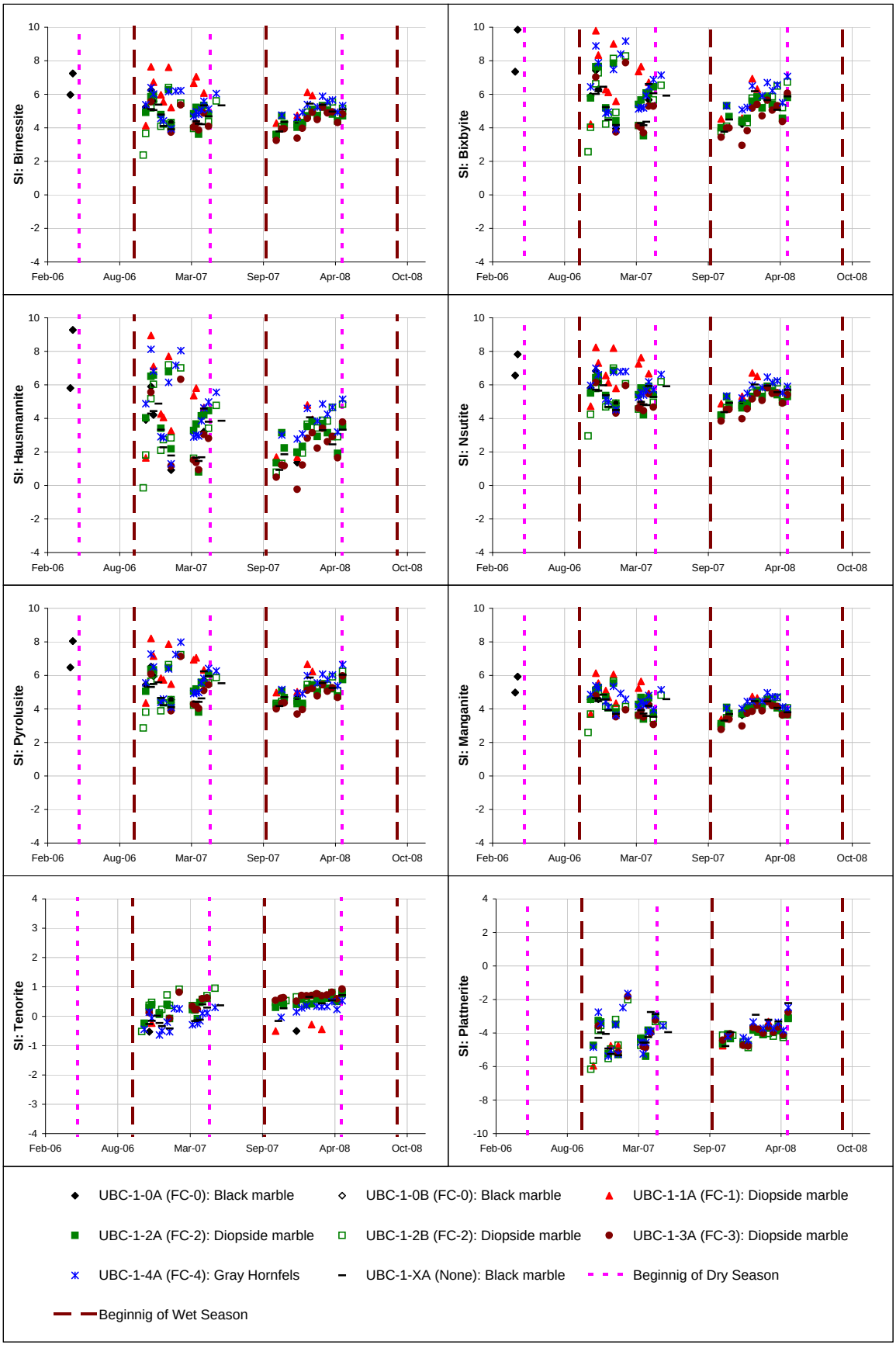

Figure D5.3 Saturation indices of oxide minerals in the leachate from the field cells containing Class B waste rock material

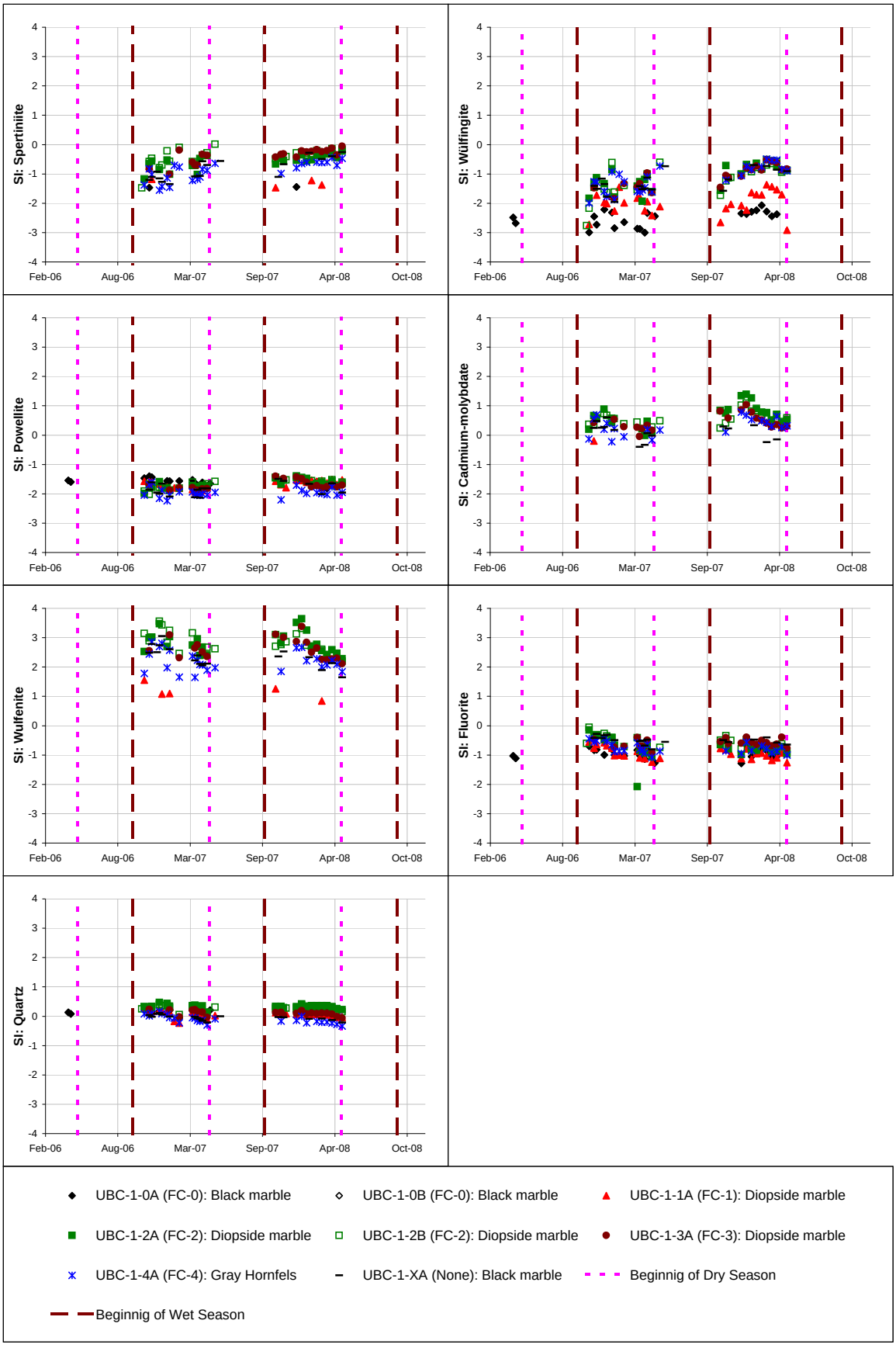

Figure D5.4 Saturation indices of hydroxide, molybdate, fluorite, and silicate minerals in the leachate from the field cells containing Class B waste rock material

Appendix D6

Water Balance at the Field Cells

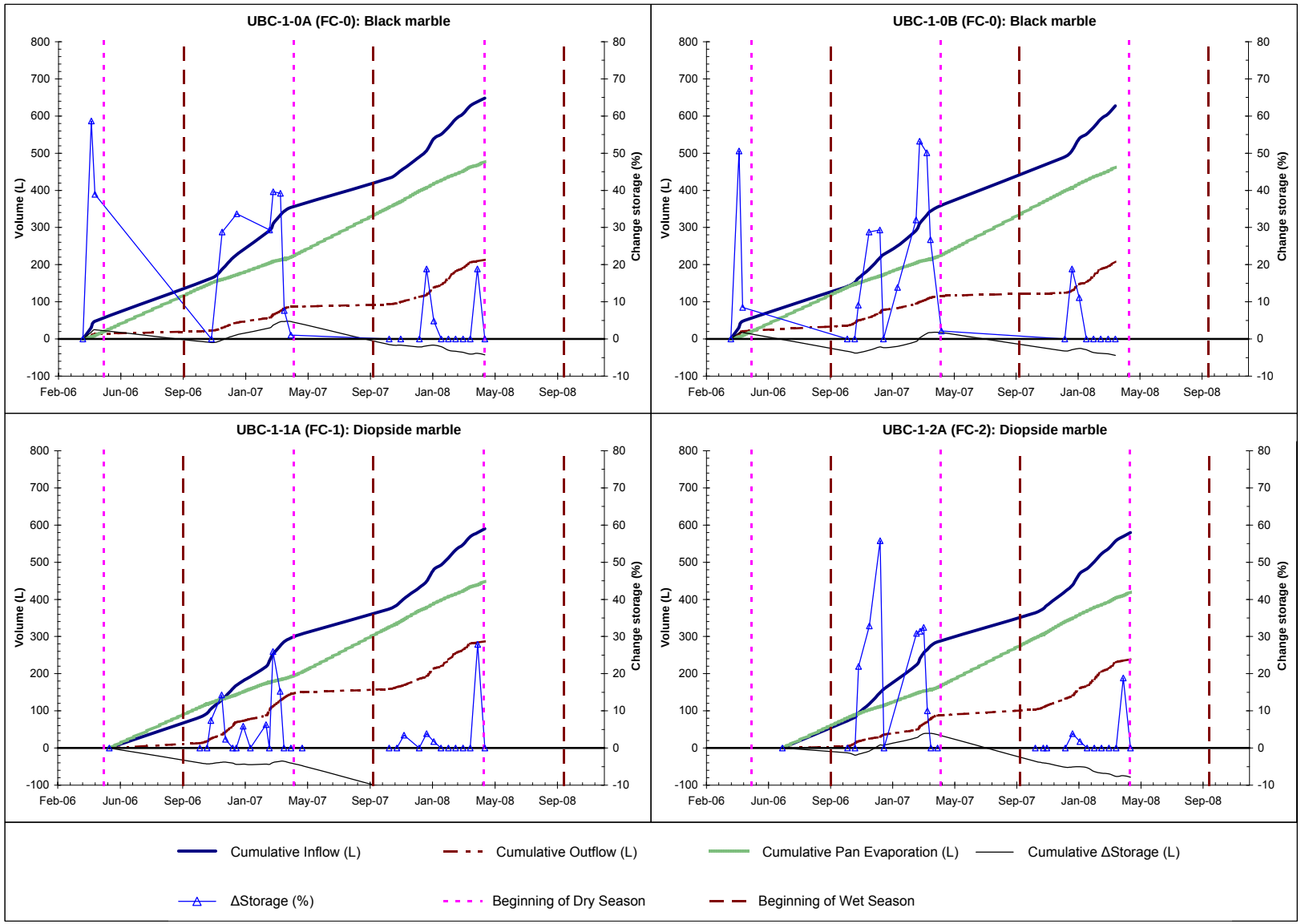

Figure D6.1 Water balance considering the change in water storage and pan evaporation data at field cells UBC-1-0A, -0B, -1A and -2A containing Class B waster rock material

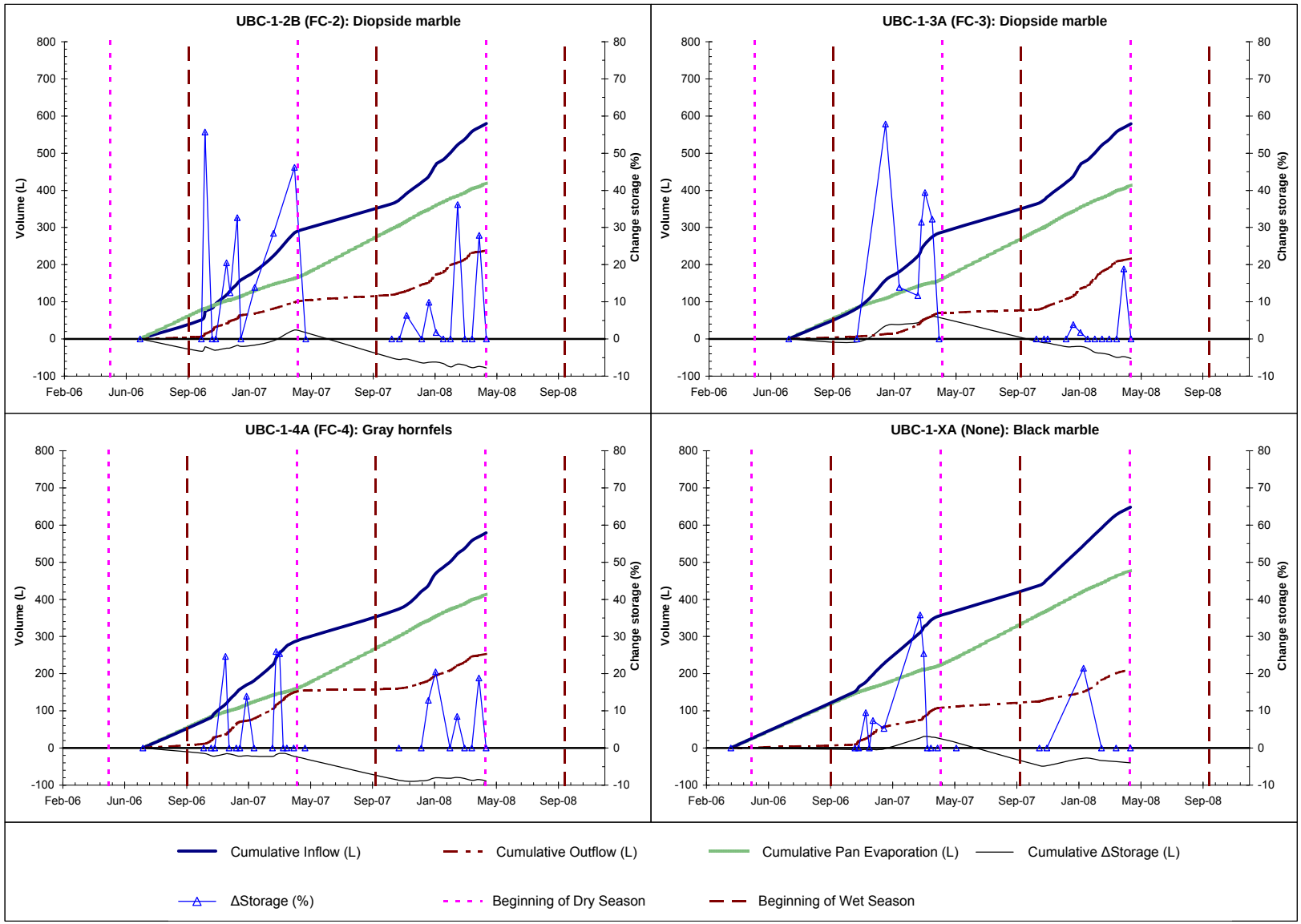

Figure D6.2 Water balance considering the change in water storage and pan evaporation data at field cells UBC-1-2B, -3A, -4A and -XA containing Class B and C waster rock material

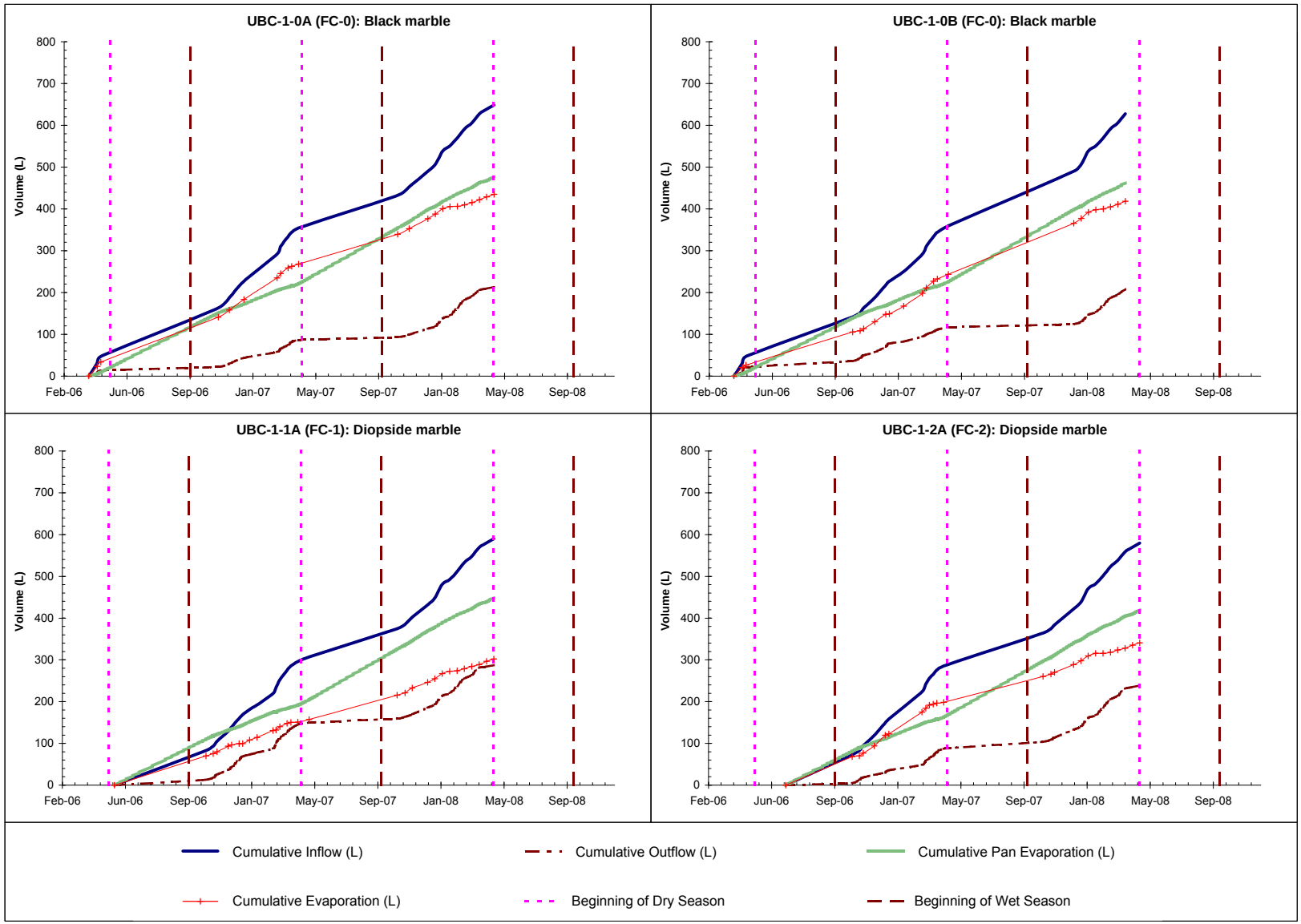

Figure D6.3 Water balance considering ΔS=0 and estimated evaporation at field cells UBC-1-0A, -0B, -1A and -2A containing Class B waster rock material

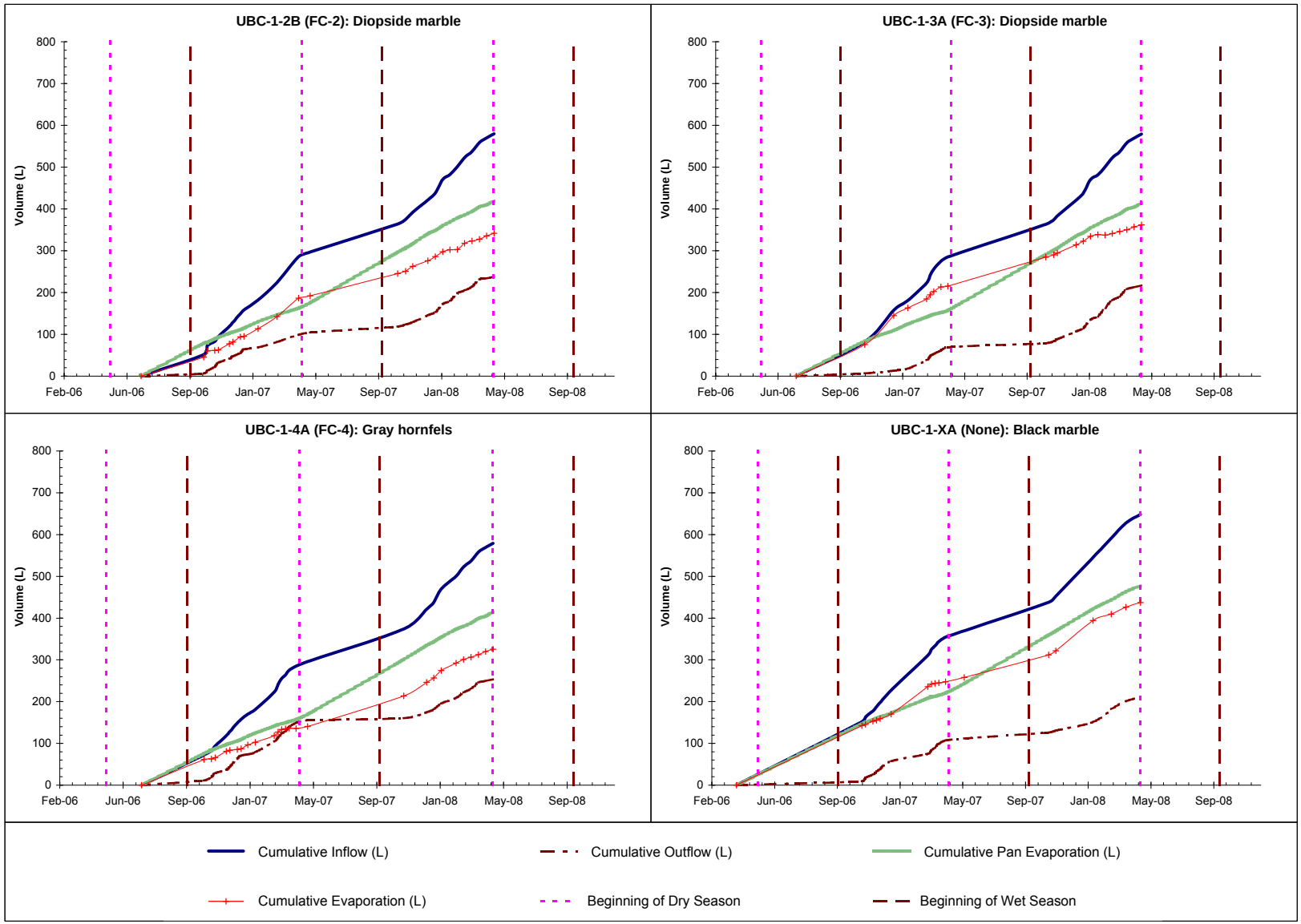

Figure D6.4 Water balance considering ΔS=0 and estimated evaporation at field cells UBC-1-2B, -3A, -4A and -XA containing Class B and C waster rock material

Appendix E

Appendix E1

Elemental Distribution

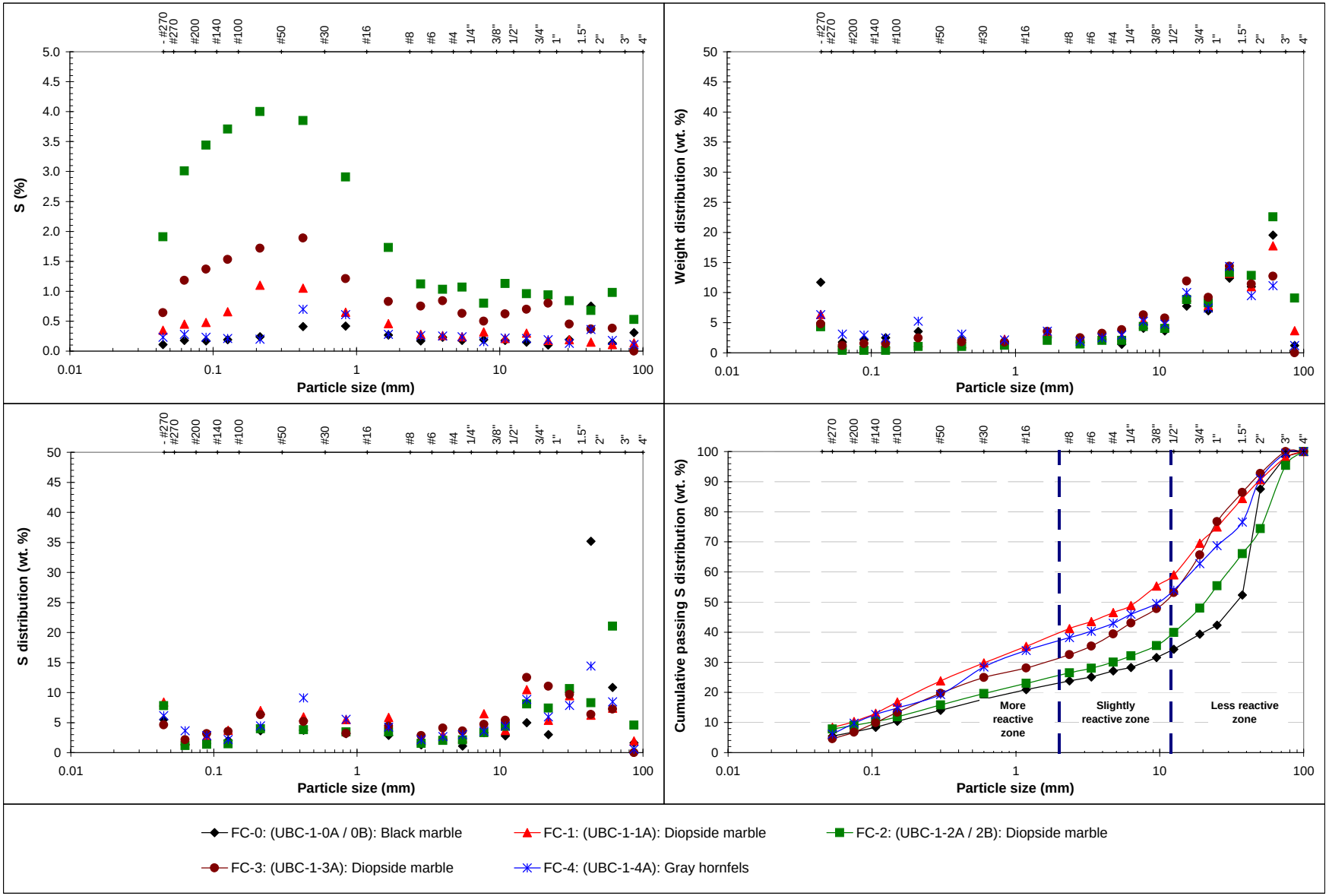

Figure E1.1 Solid phase sulfur-total concentrations and distribution at different size fractions of Class B waste rock samples

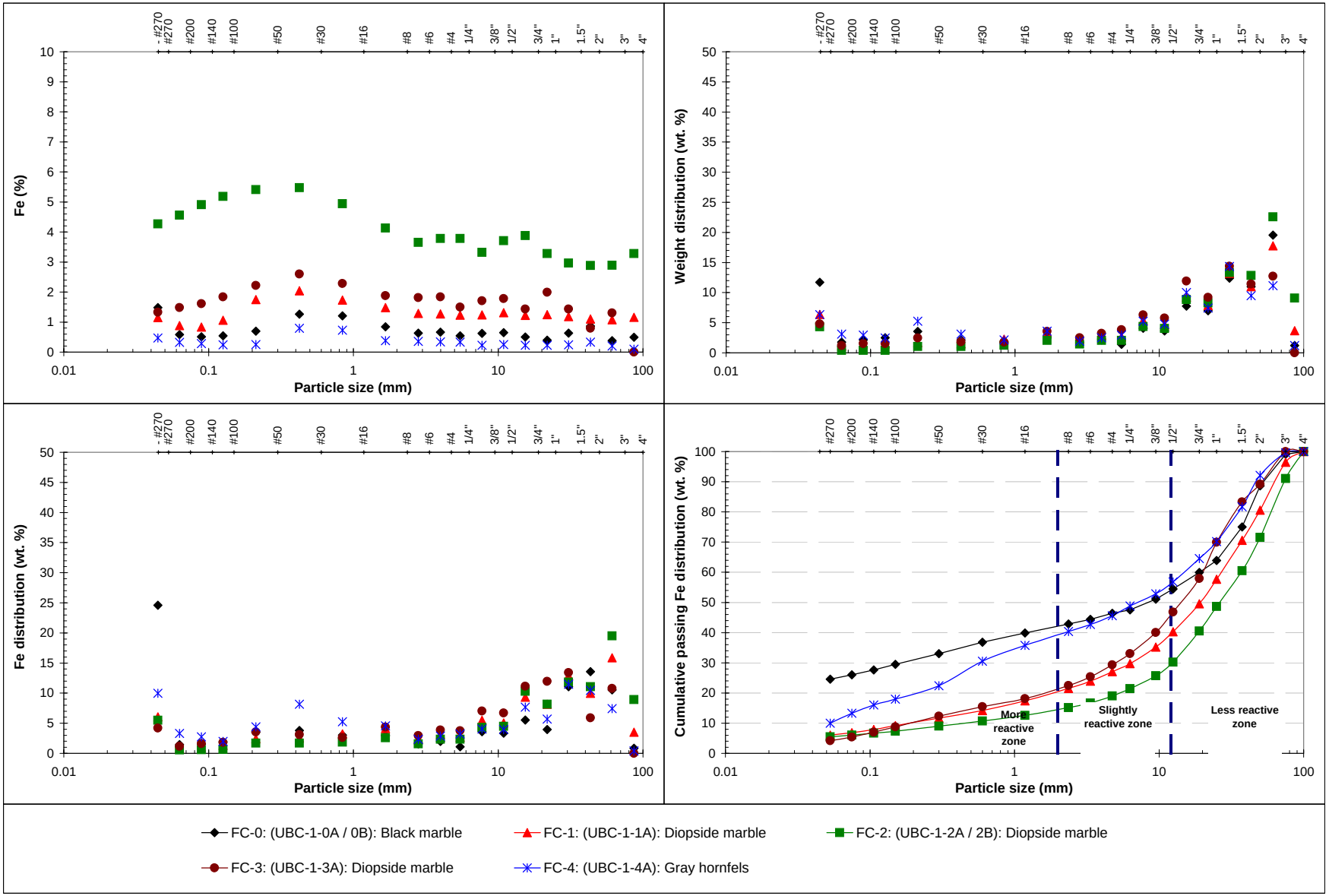

Figure E1.2 Solid phase iron concentrations and distribution at different size fractions of Class B waste rock samples

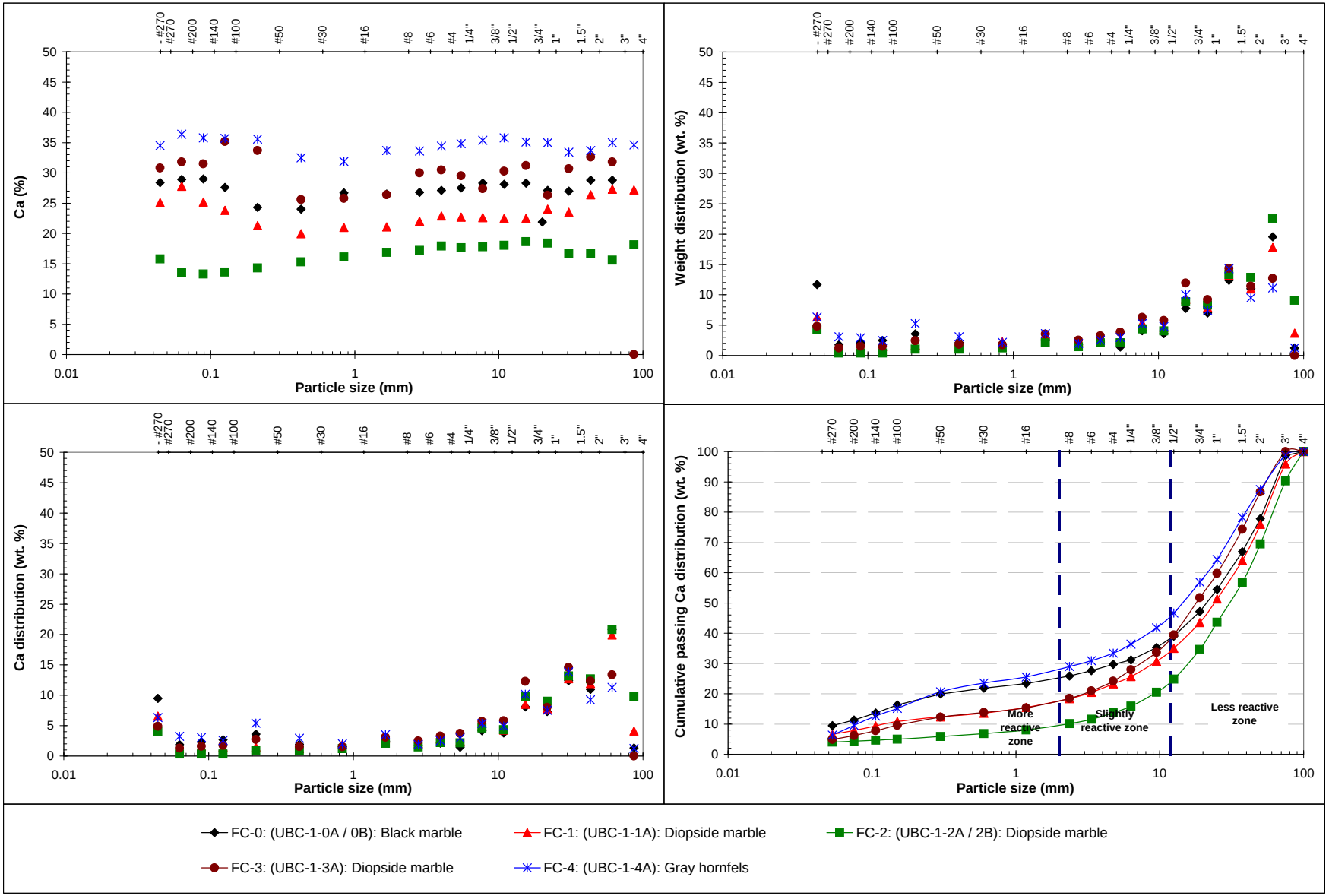

Figure E1.3 Solid phase calcium concentrations and distribution at different size fractions of Class B waste rock samples

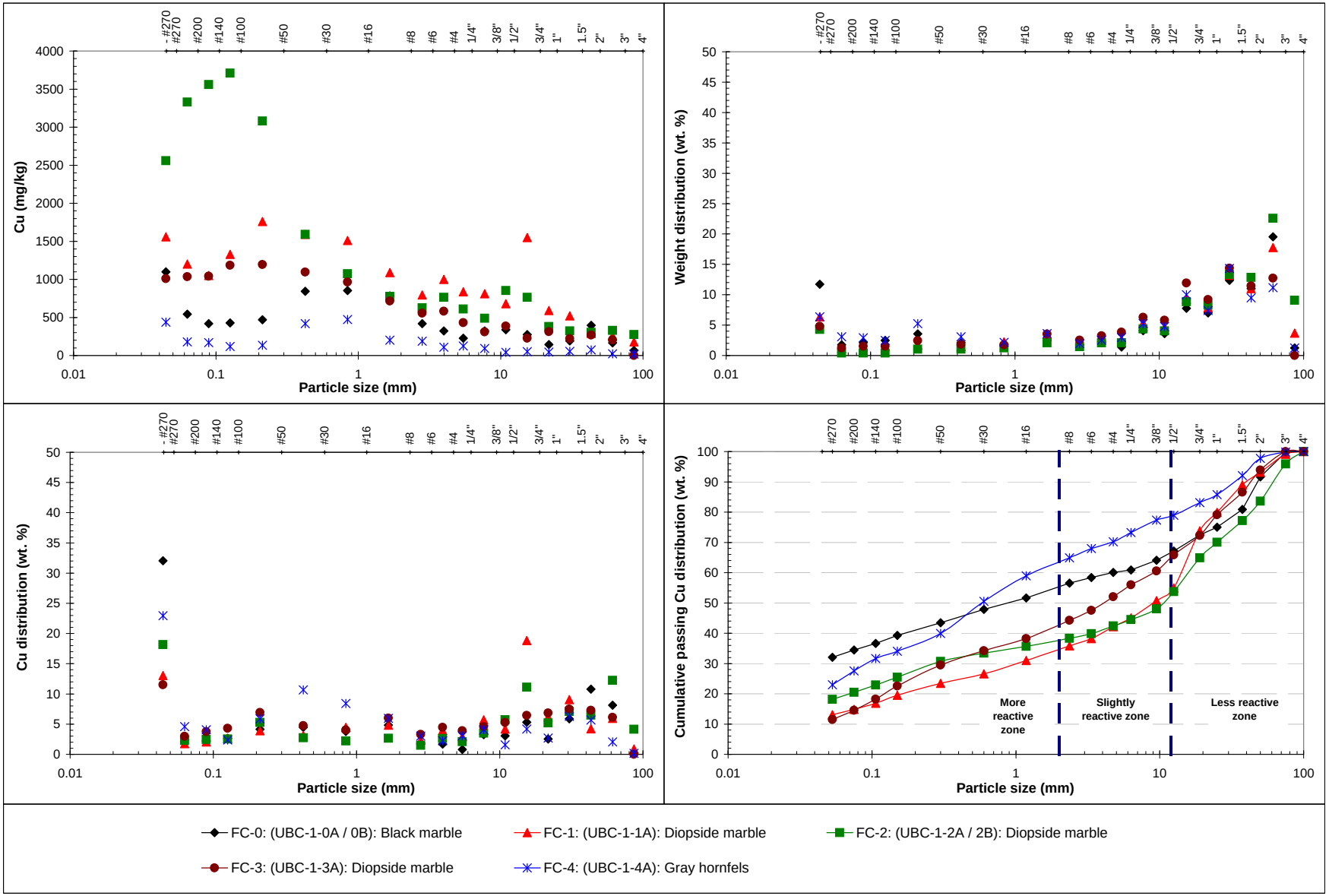

Figure E1.4 Solid phase copper concentrations and distribution at different size fractions of Class B waste rock samples

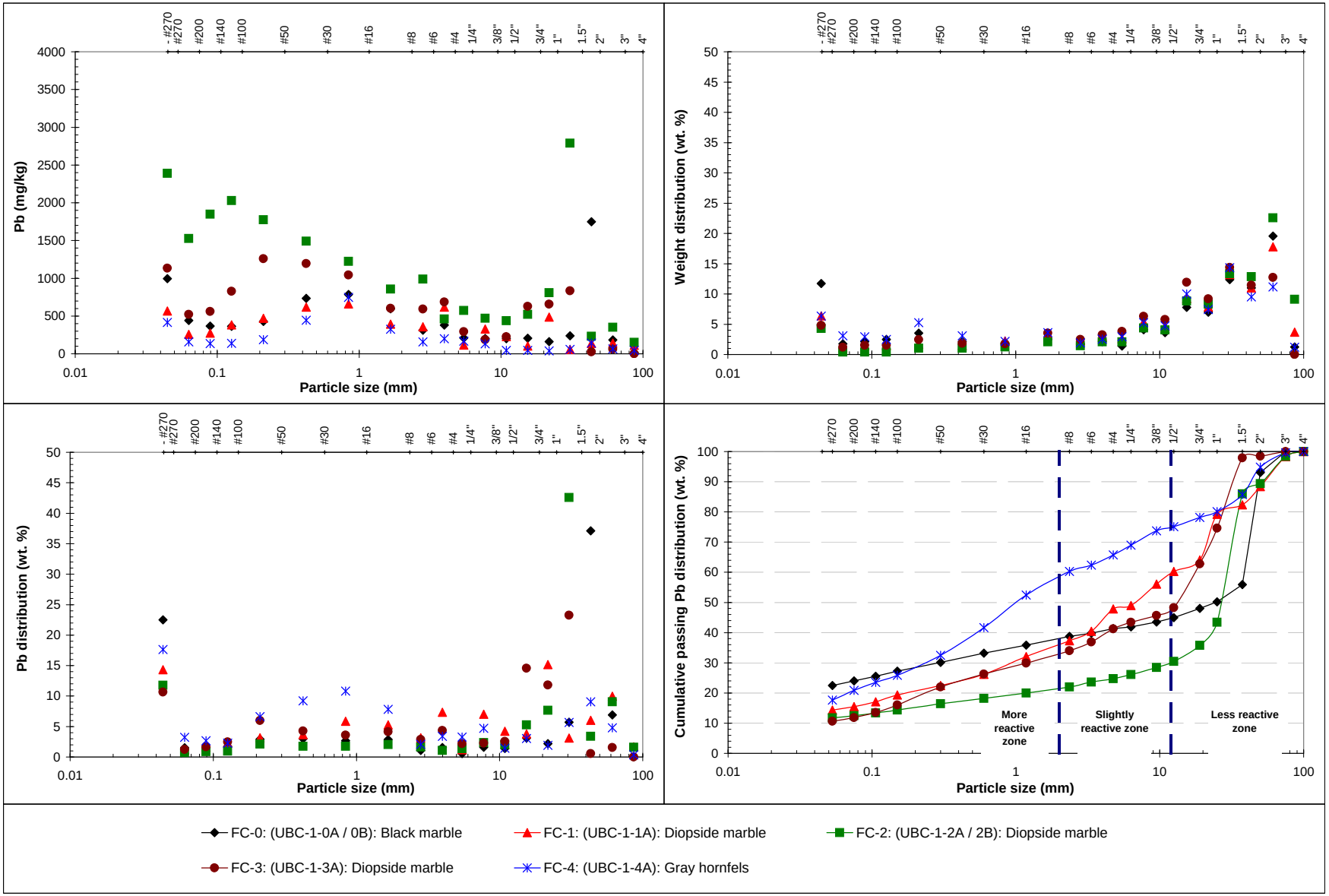

Figure E1.5 Solid phase lead concentrations and distribution at different size fractions of Class B waste rock samples

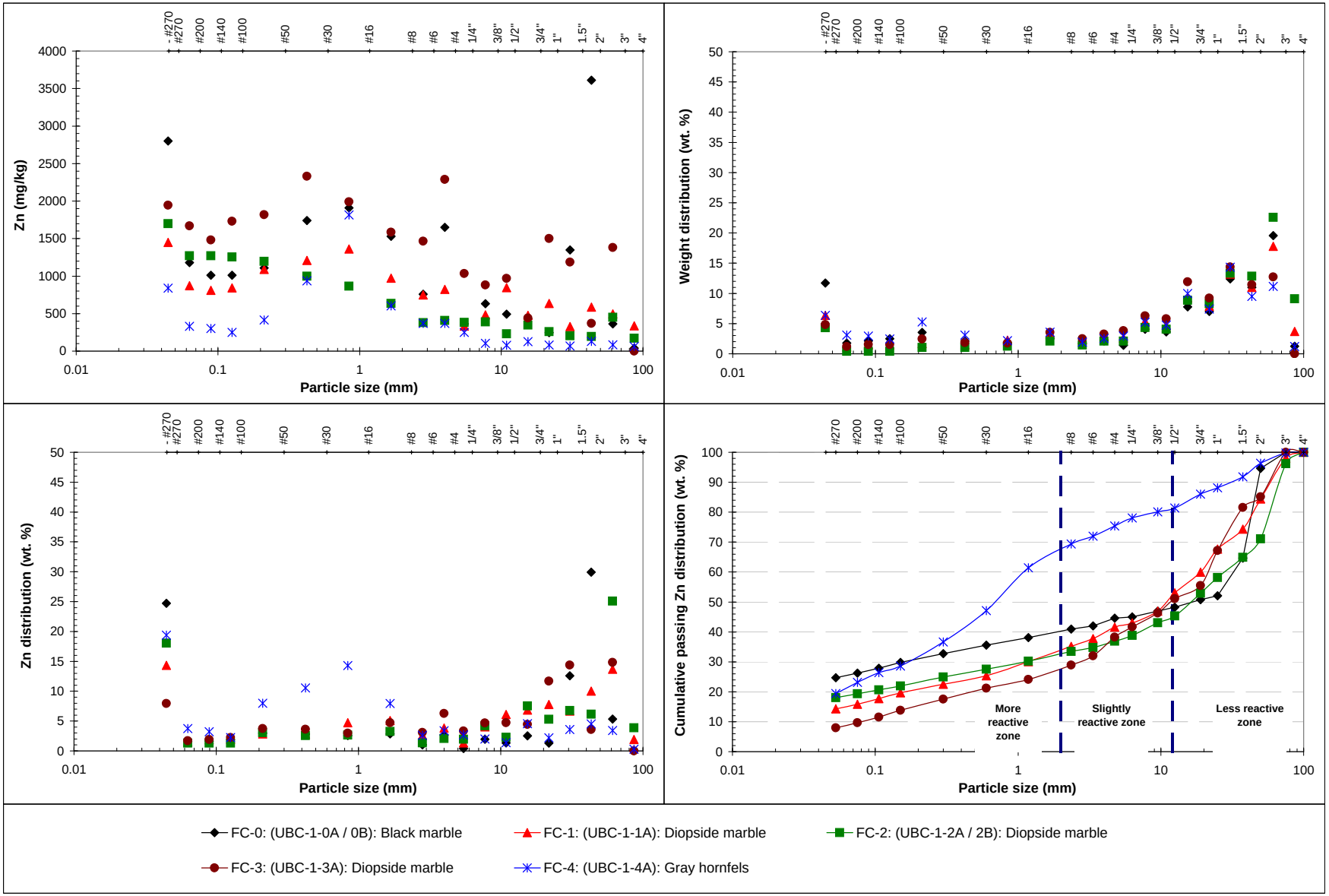

Figure E1.6 Solid phase zinc concentrations and distribution at different size fractions of Class B waste rock samples

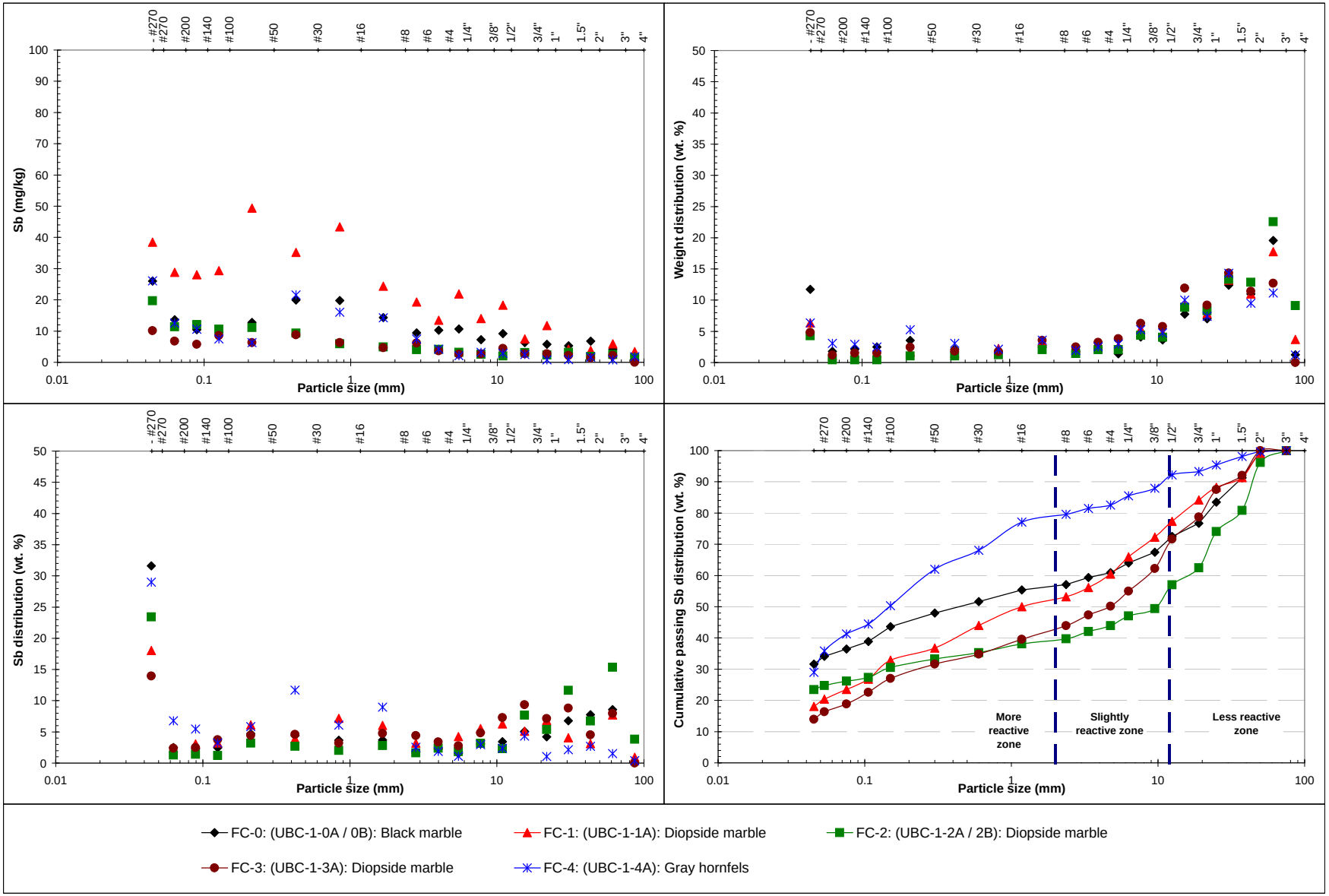

Figure E1.7 Solid phase antimony concentrations and distribution at different size fractions of Class B waste rock samples

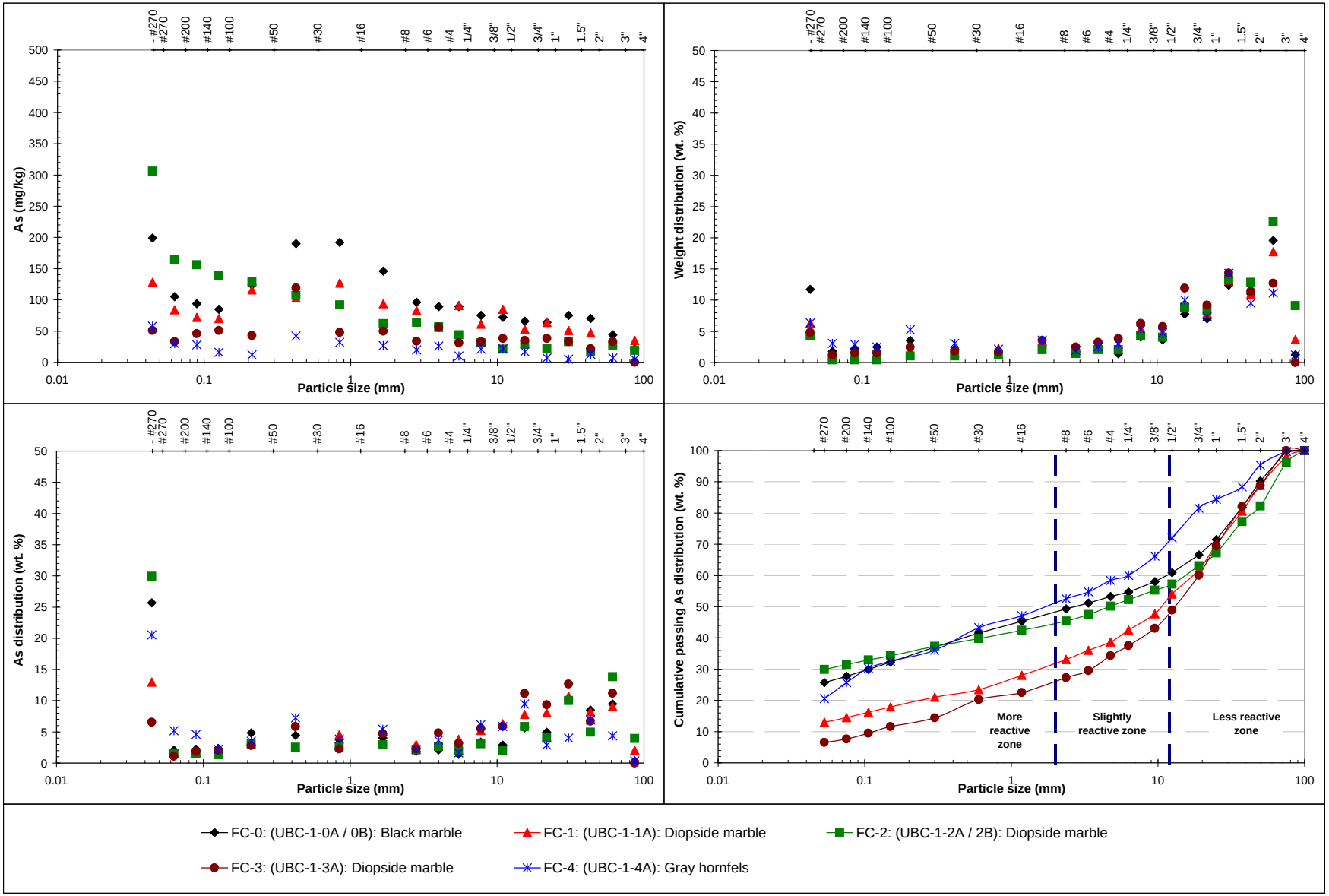

Figure E1.8 Solid phase arsenic concentrations and distribution at different size fractions of Class B waste rock samples

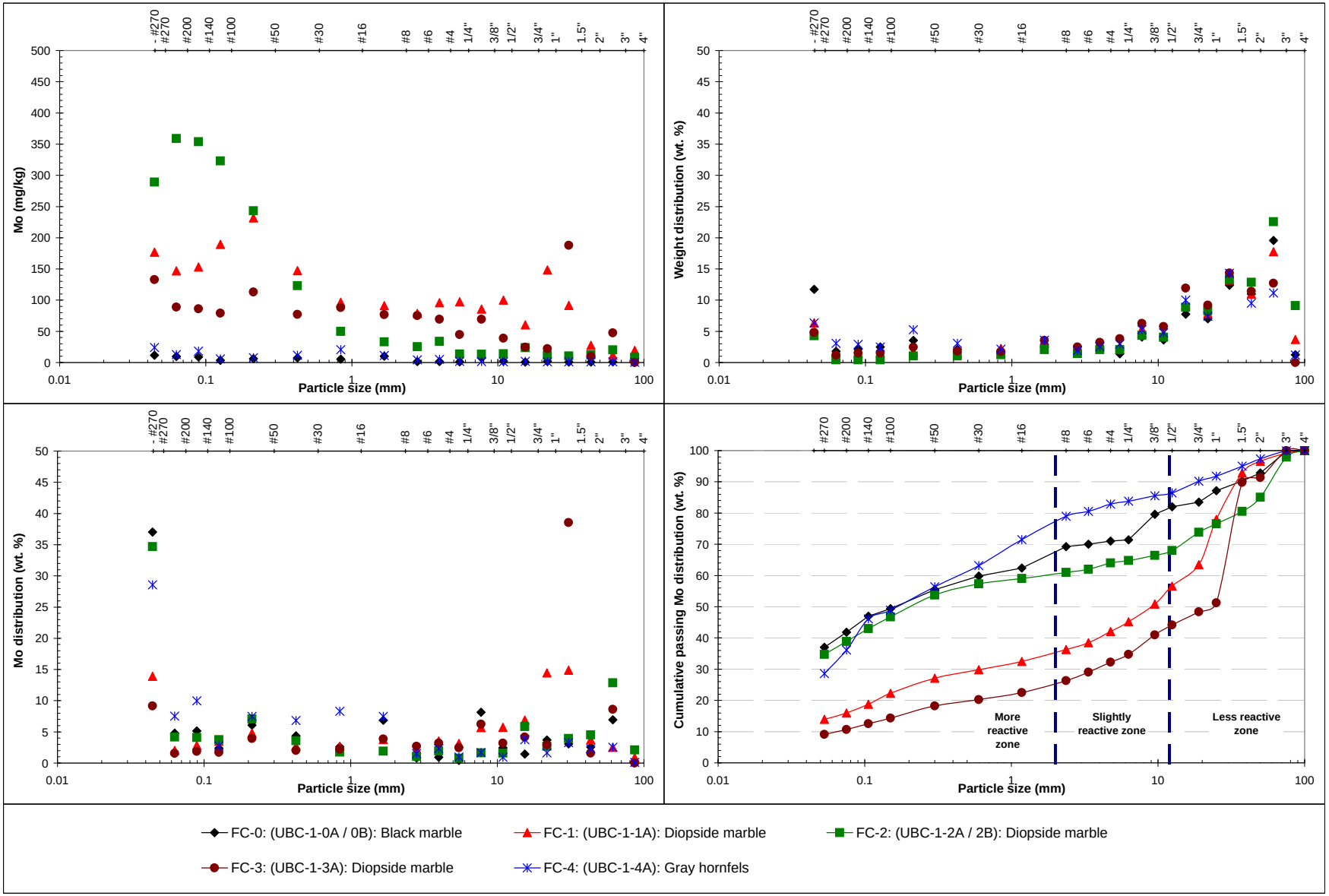

Figure E1.9 Solid phase molybdenum concentrations and distribution at different size fractions of Class B waste rock samples

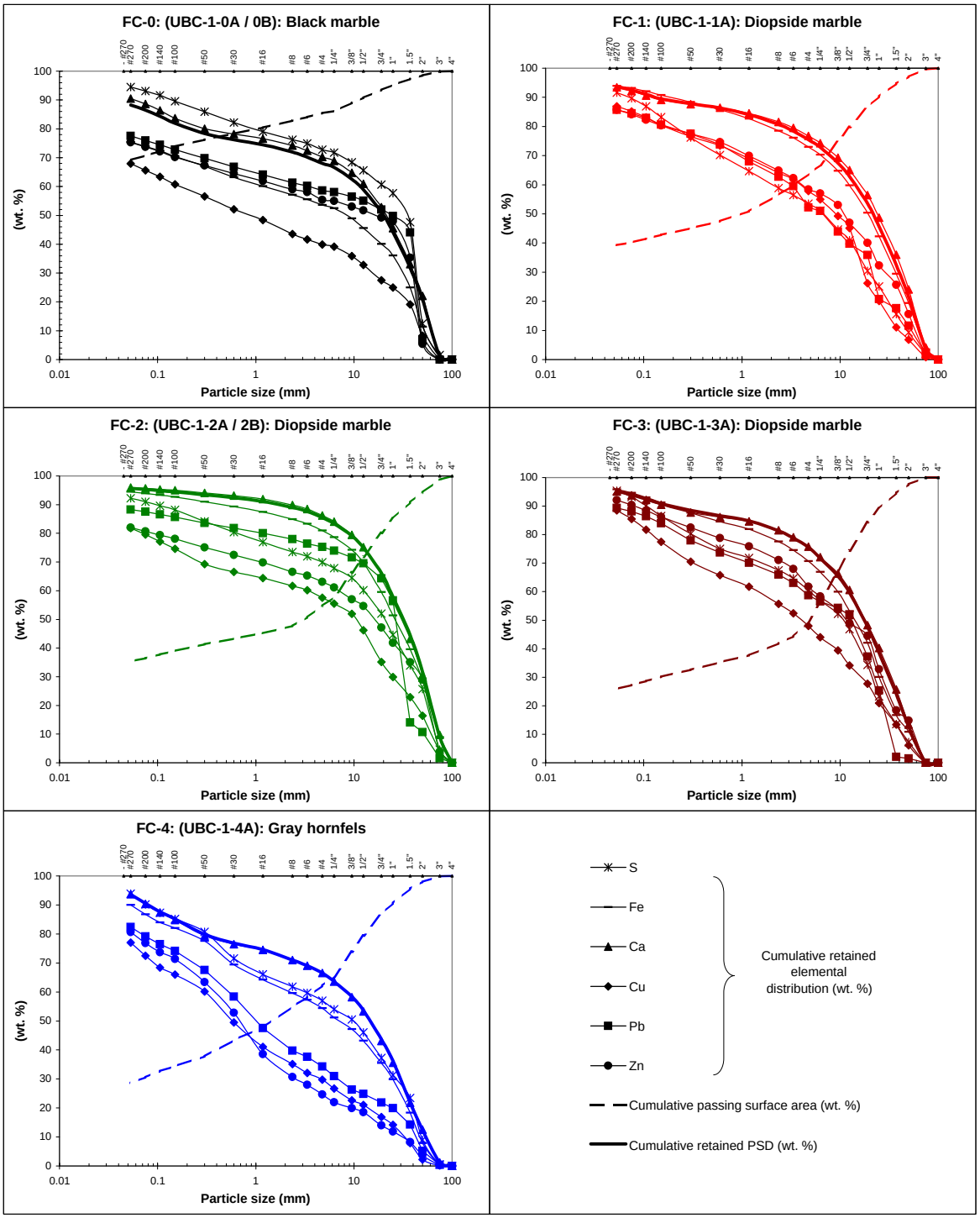

Figure E1.10 Weight elemental (S-total, Fe, Ca, Cu, Pb, and Zn) distribution in comparison with particle size distribution in Class B waste rock samples

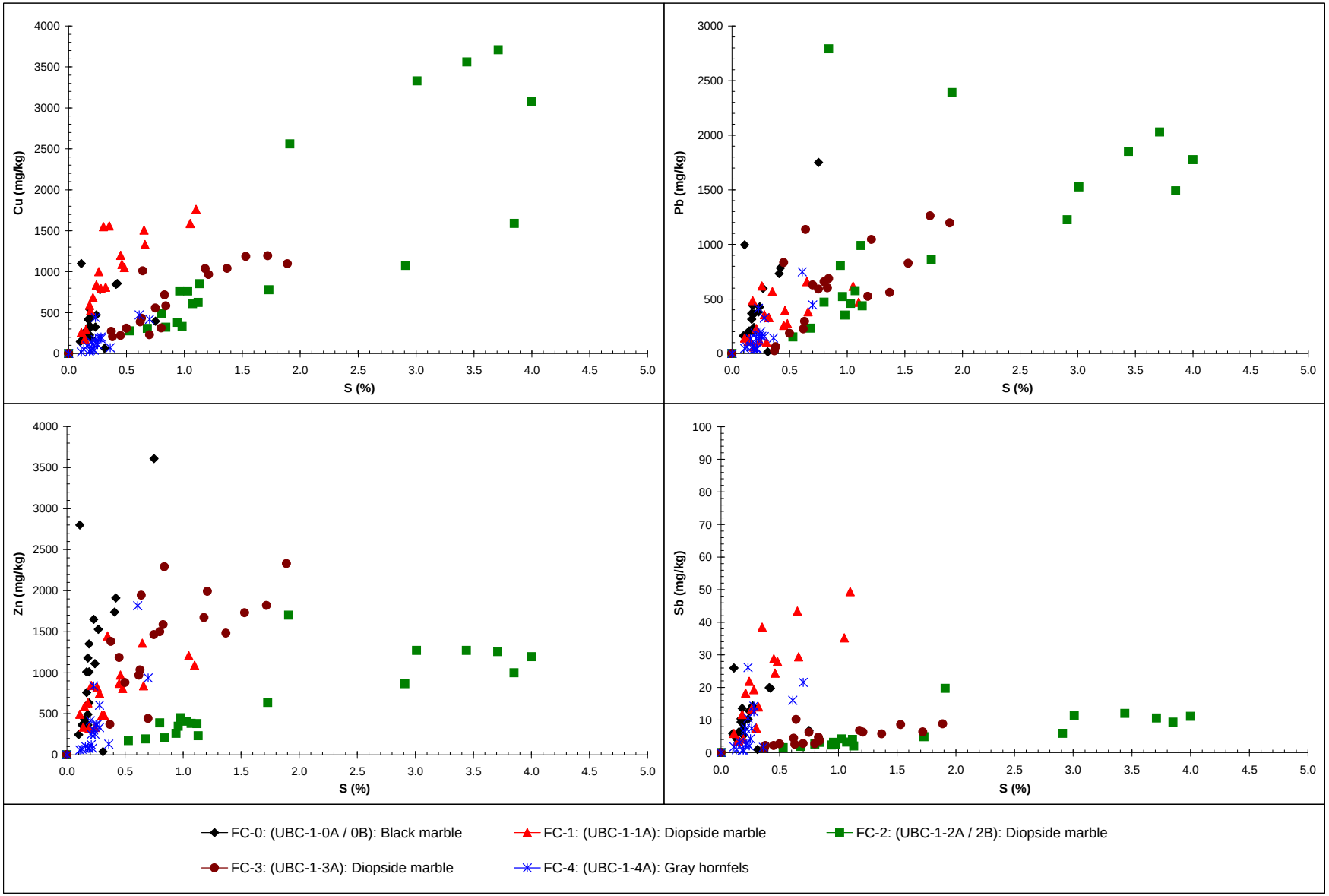

Figure E1.11 Sulfide minerals correlation determining by elemental concentrations (Cu, Pb, Zn and Sb) in function of Sulfur-total in all Class B waste rock samples

Appendix E2

Geochemical Plots at the Field Cells

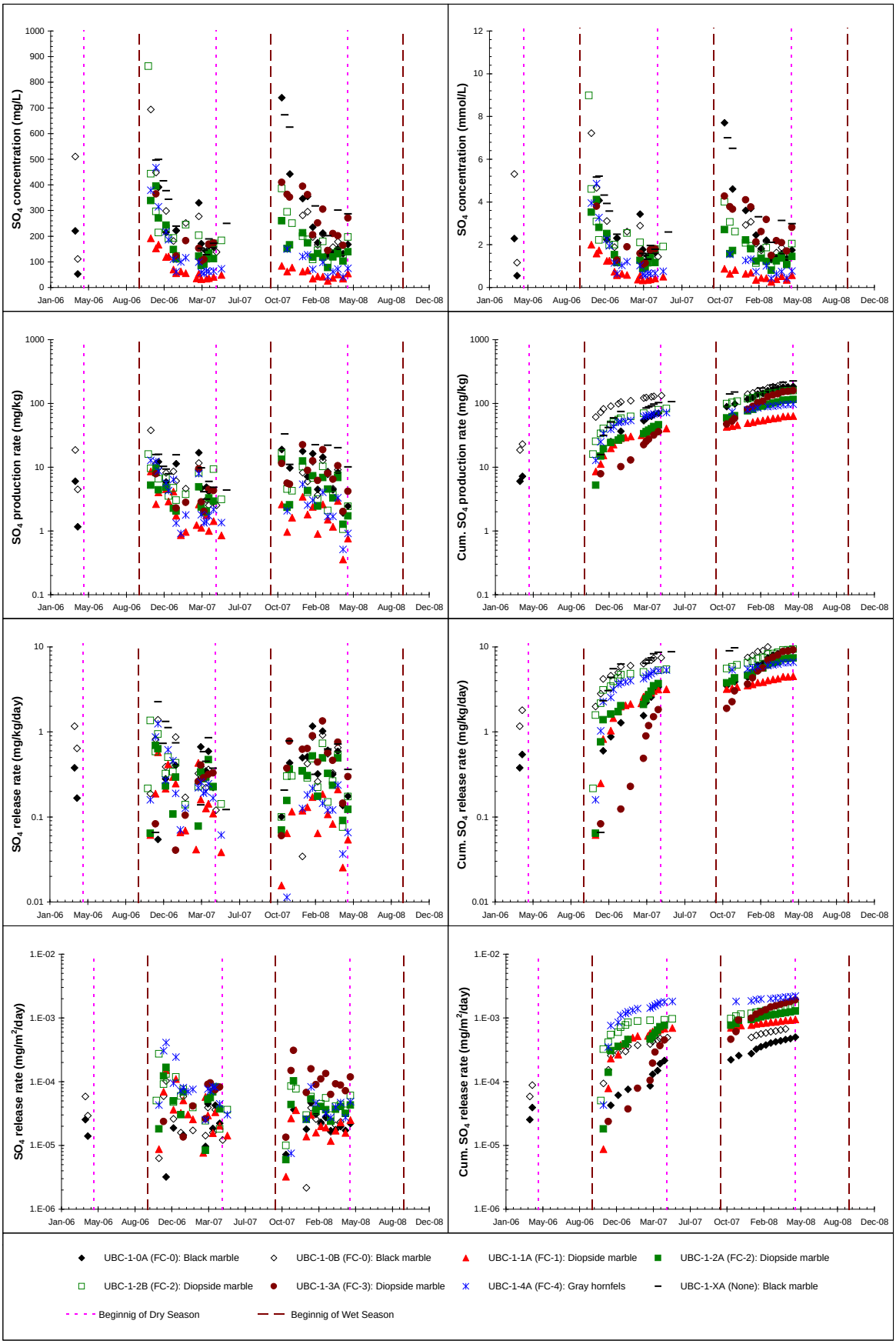

Figure E2.1 Sulphate concentrations, production and release rates found in the leachate from the field cells

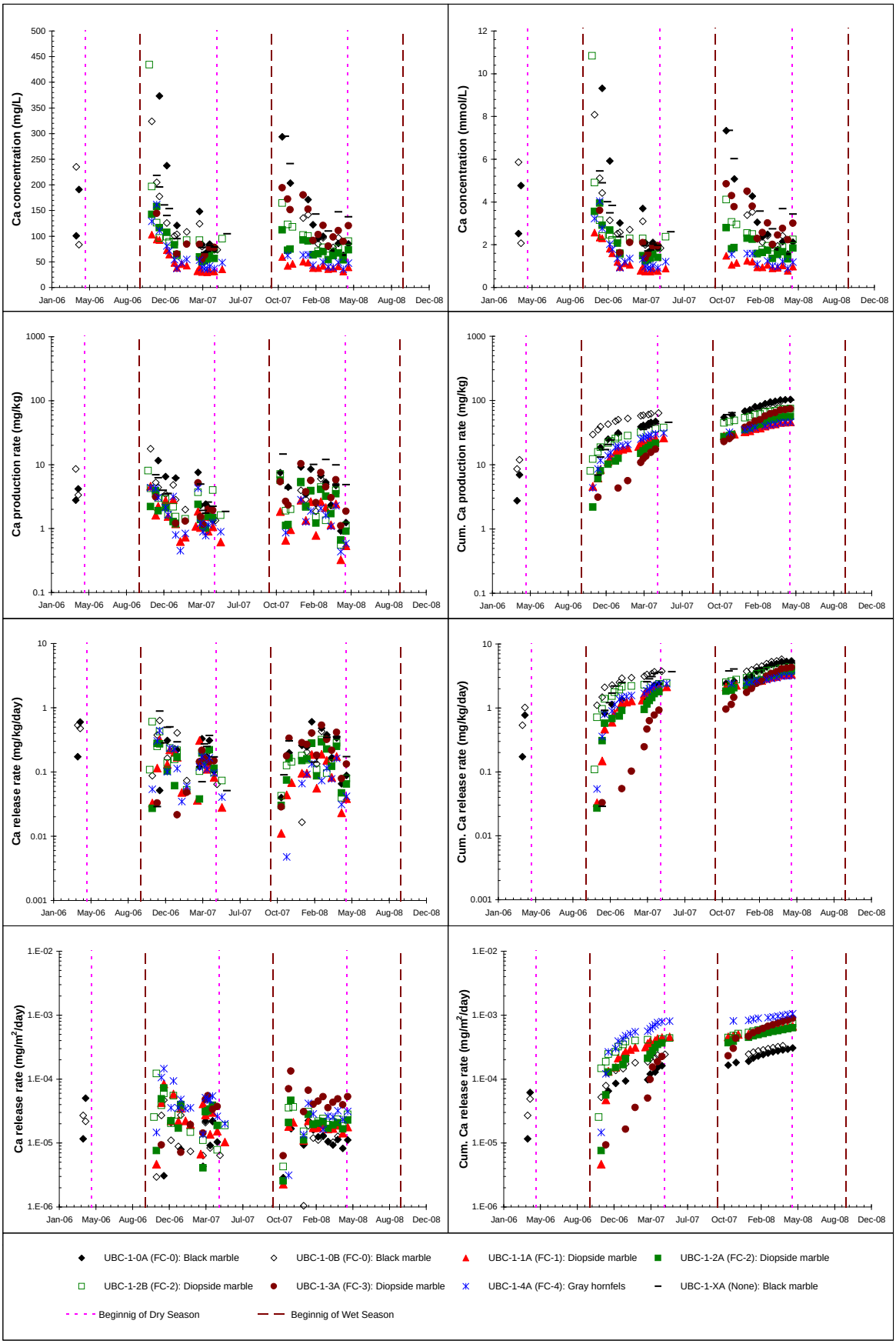

Figure E2.2 Calcium concentrations, production and release rates found in the leachate from the field cells

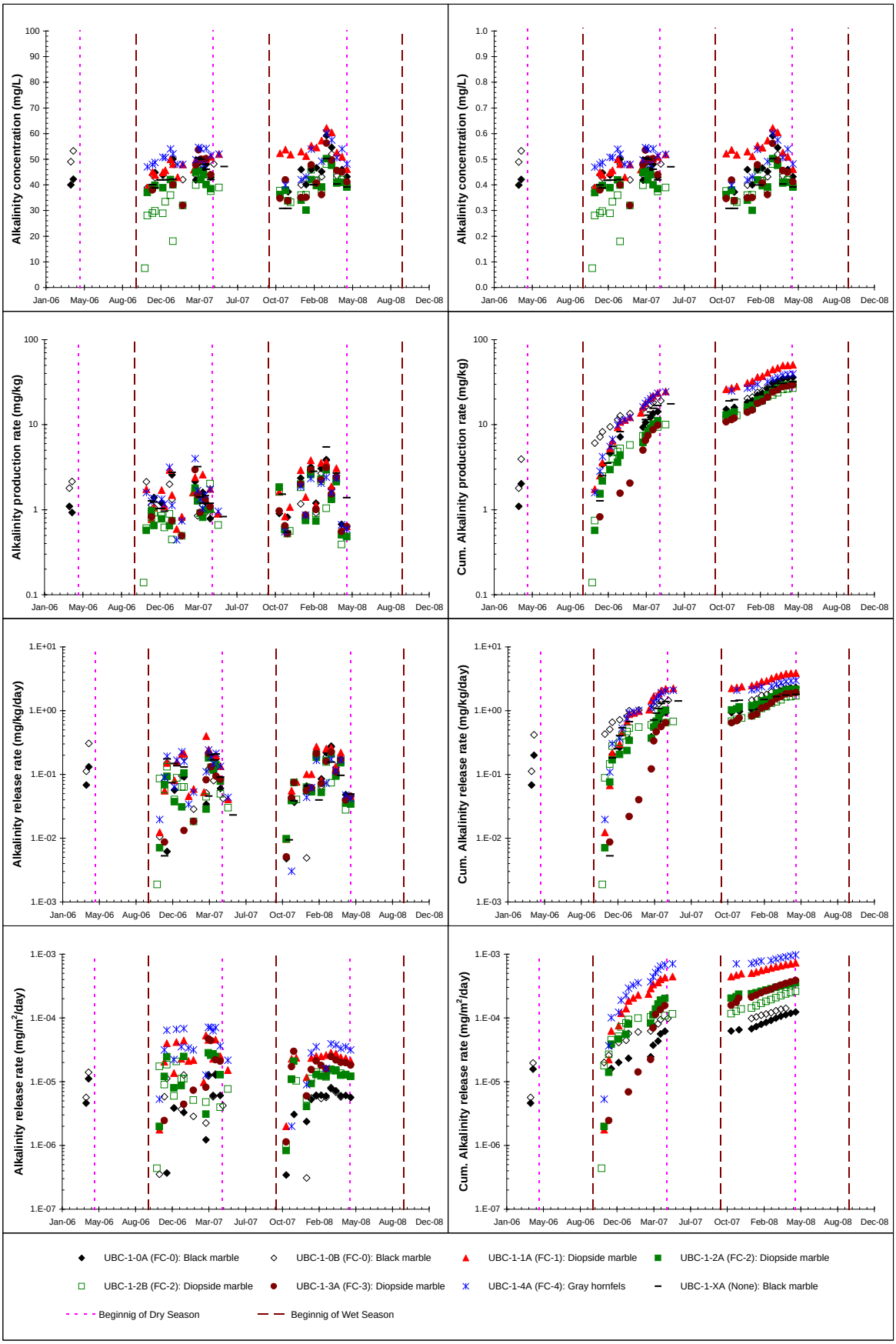

Figure E2.3 Alkalinity concentrations, production and release rates found in the leachate from the field cells

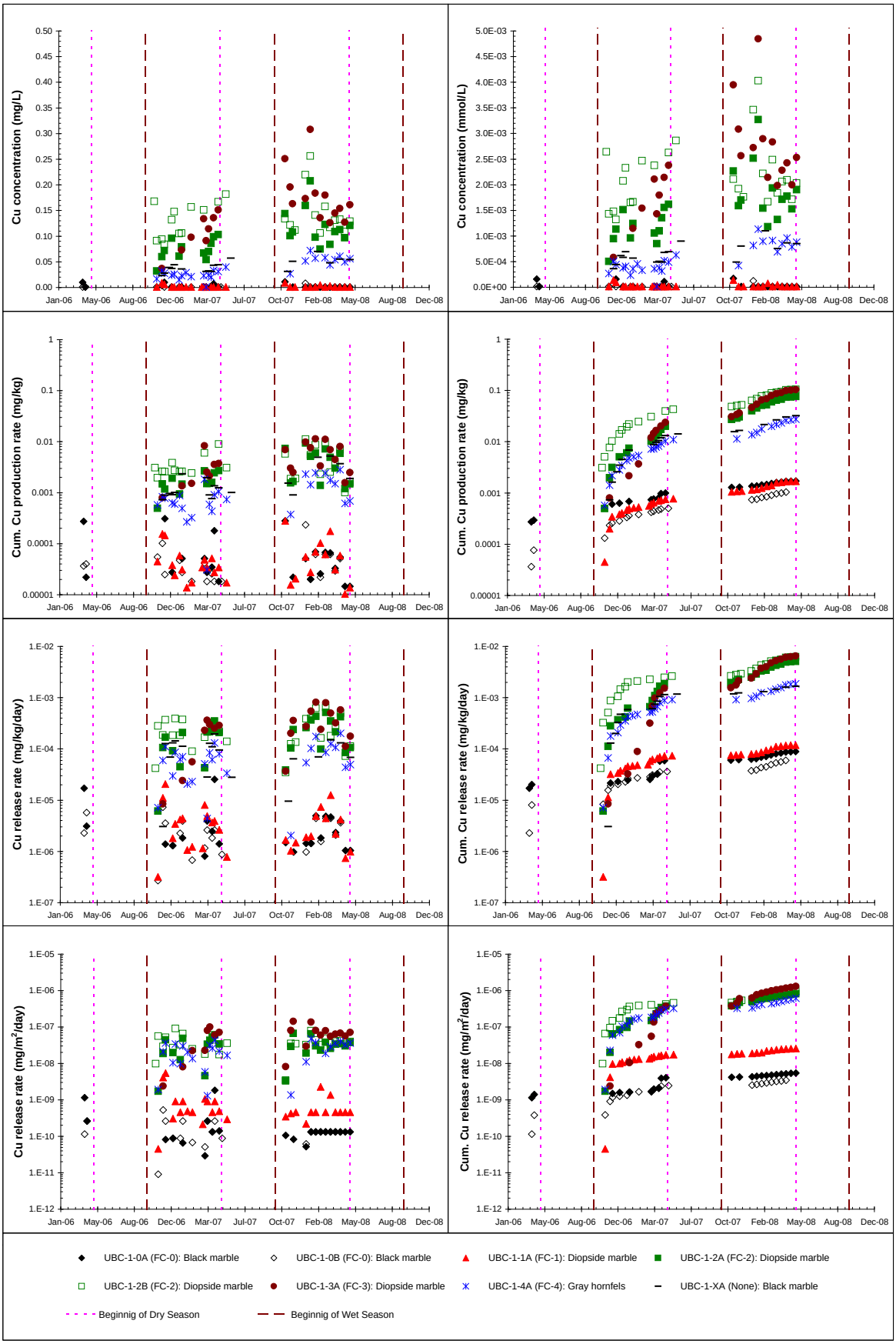

Figure E2.4 Copper concentrations, production and release rates found in the leachate from the field cells

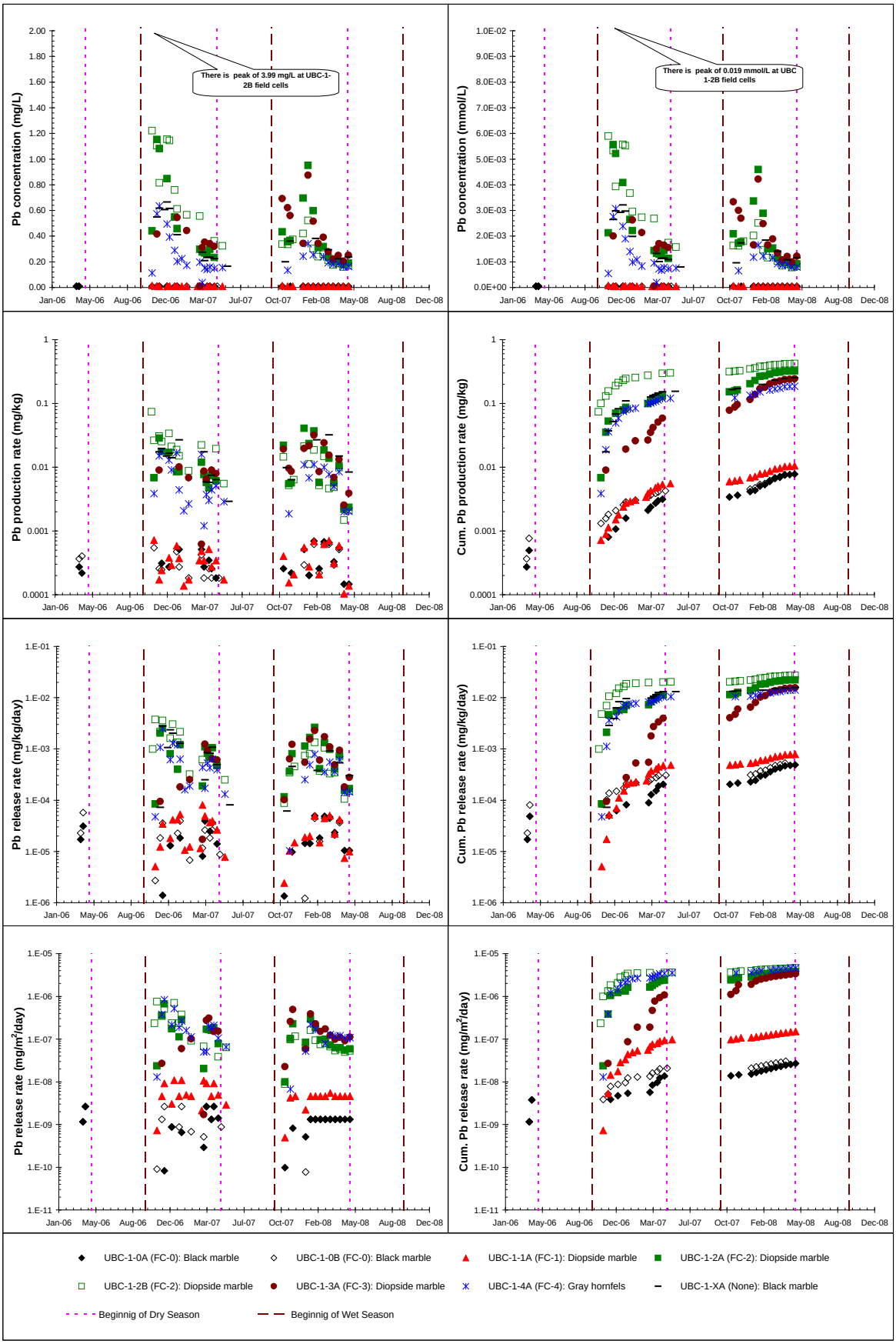

Figure E2.5 Lead concentrations, production and release rates found in the leachate from the field cells

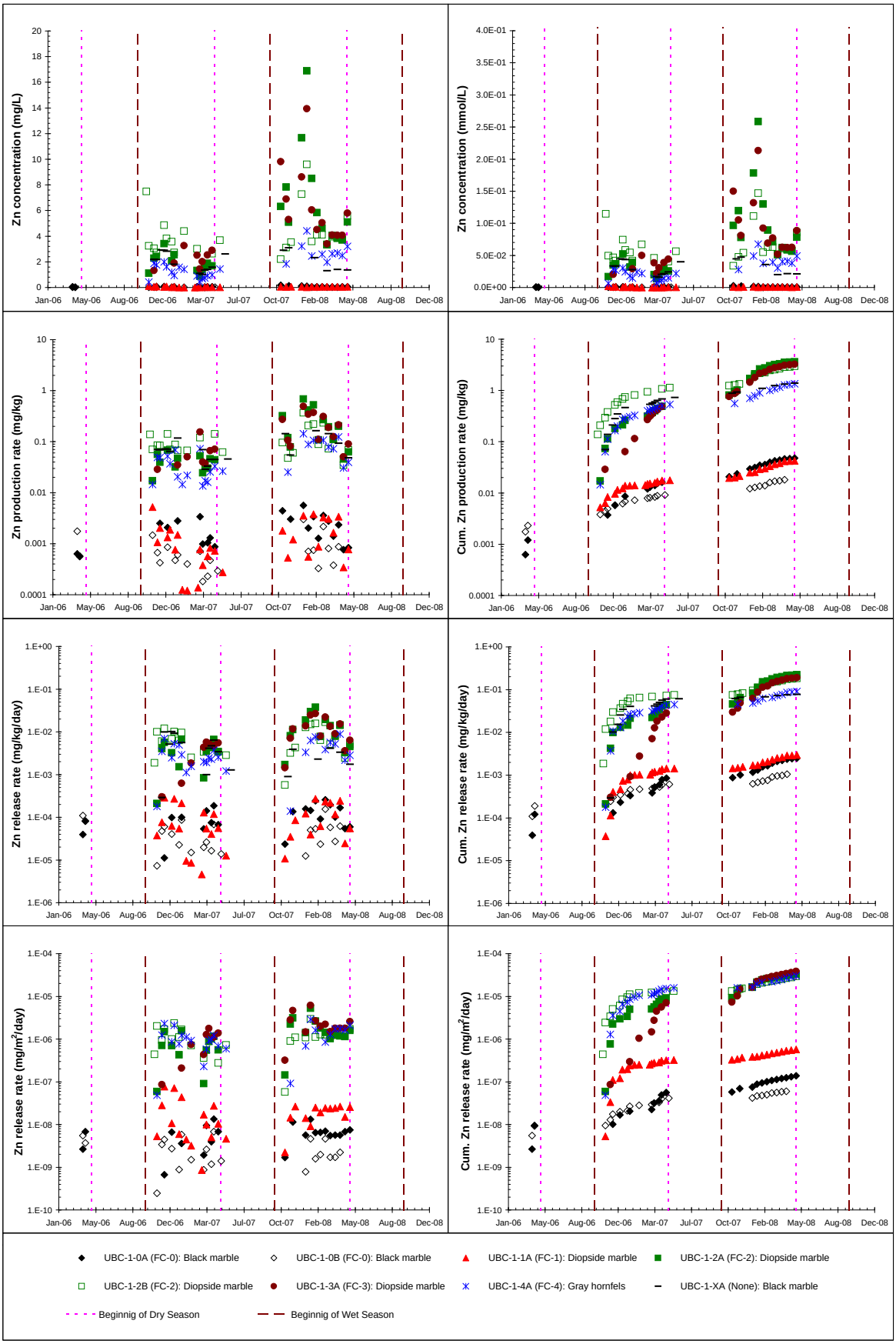

Figure E2.6 Zinc concentrations, production and release rates found in the leachate from the field cells

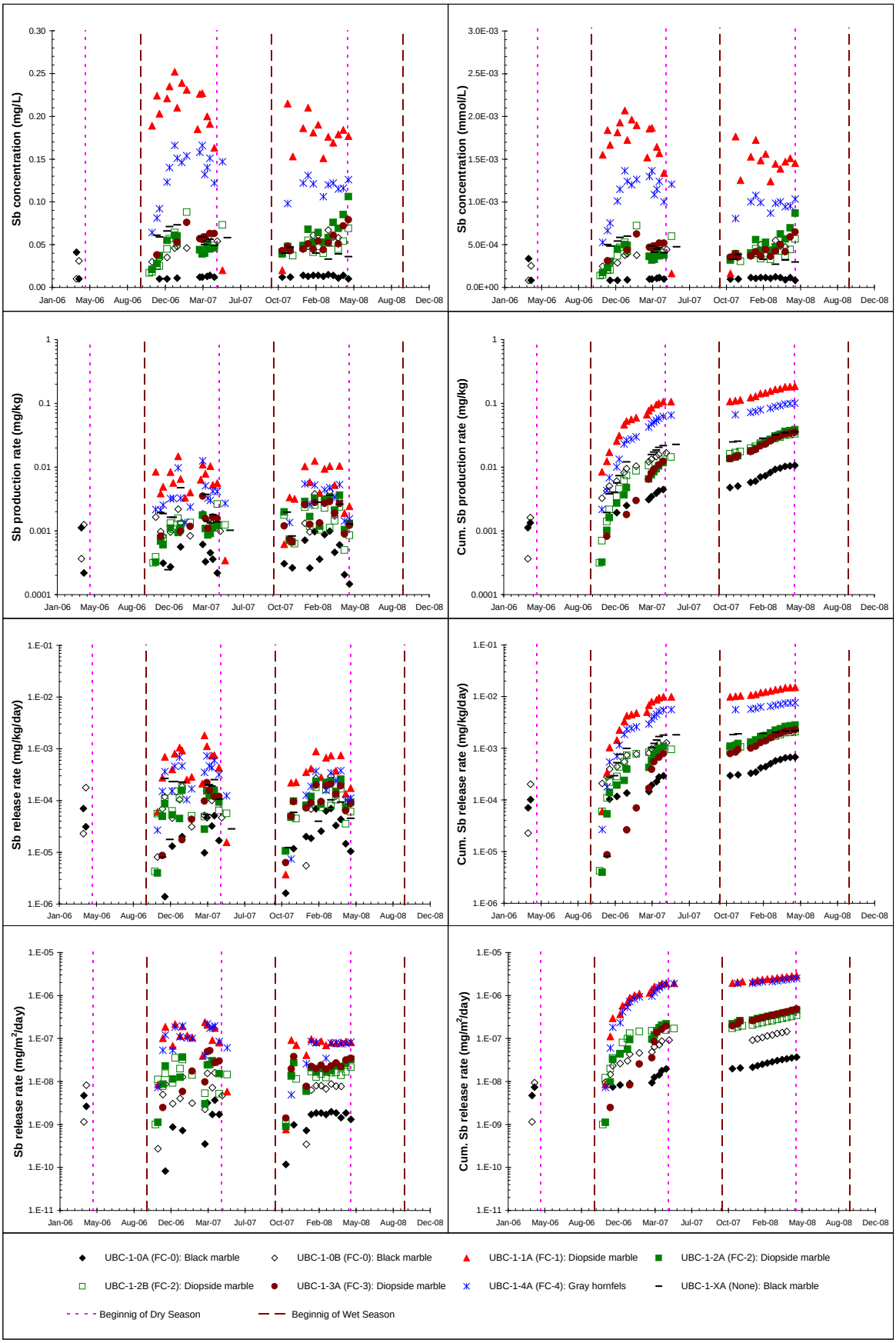

Figure E2.7 Antimony concentrations, production and release rates found in the leachate from the field cells

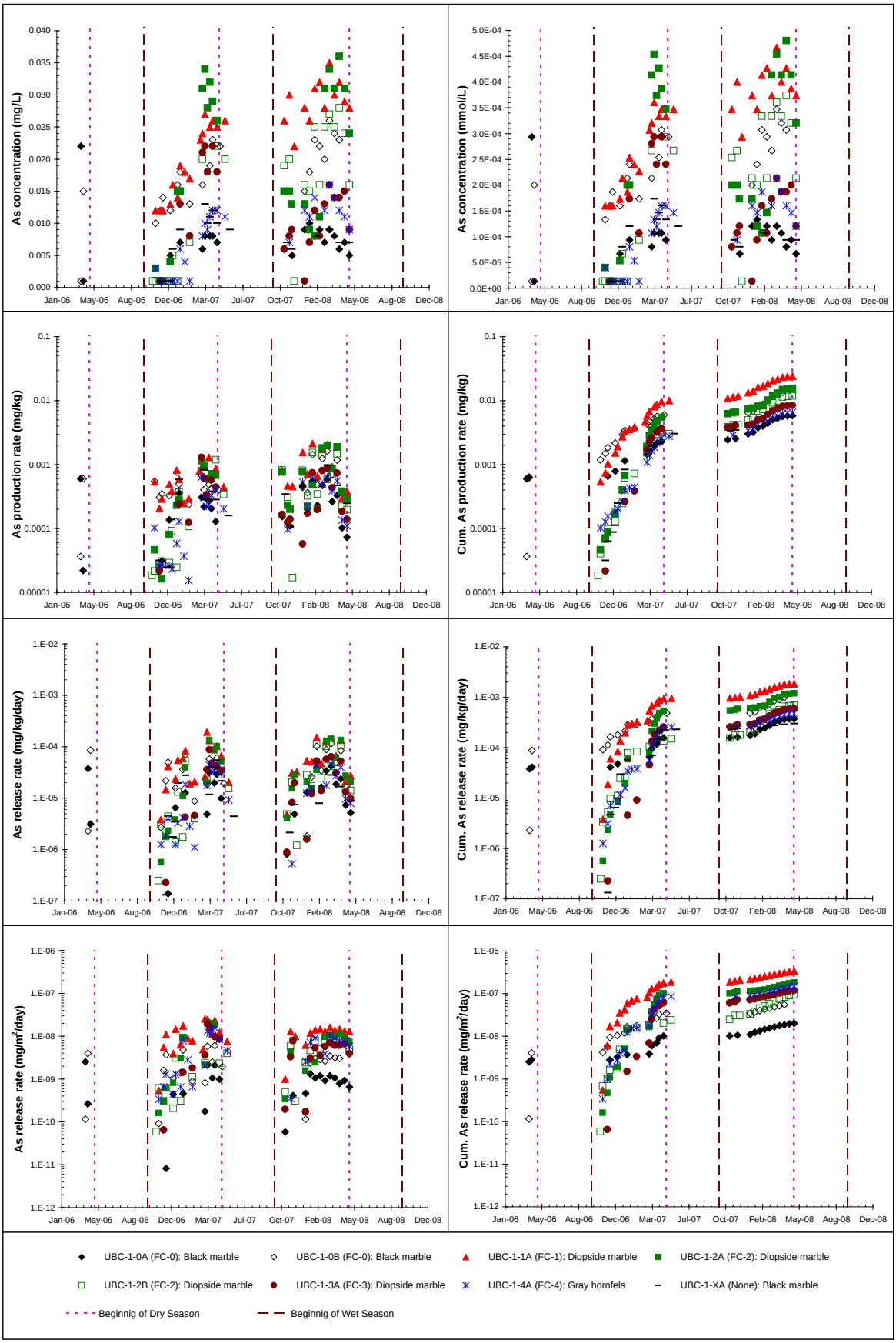

Figure E2.8 Arsenic concentrations, production and release rates found in the leachate from the field cells

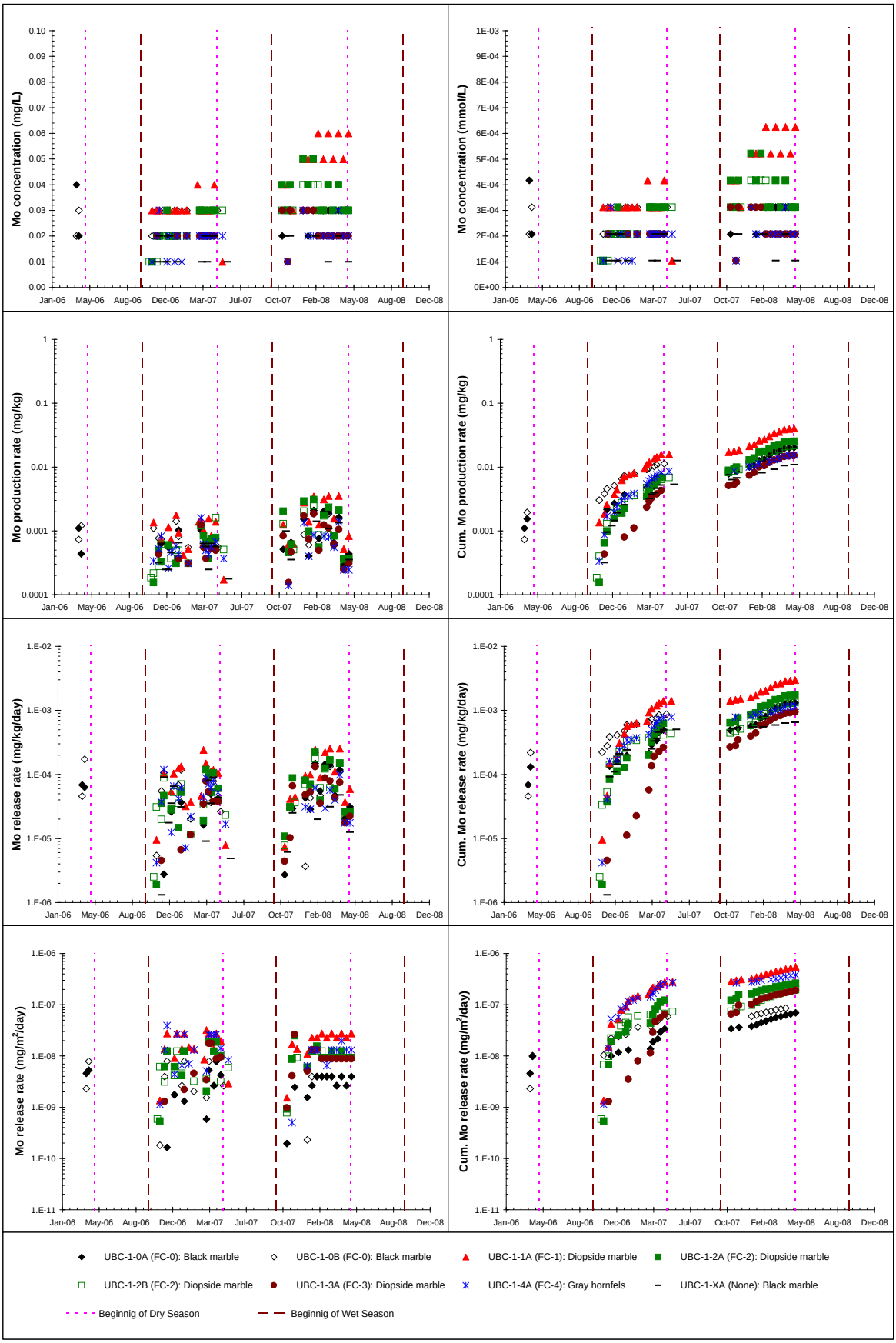

Figure E2.9 Molybdenum concentrations, production and release rates found in the leachate from the field cells

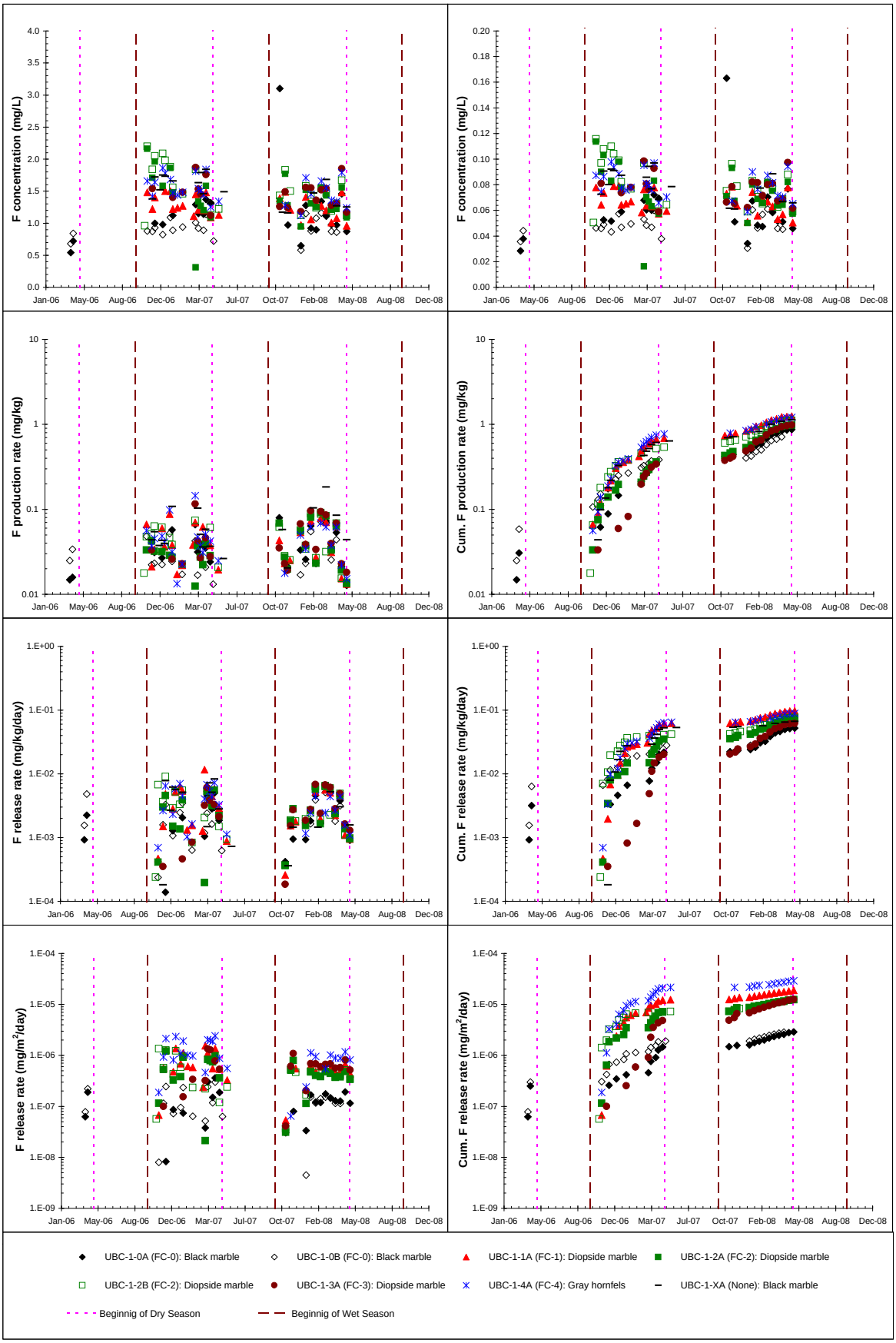

Figure E2.10 Fluoride concentrations, production and release rates found in the leachate from the field cells

Appendix E3

Crossing Plots

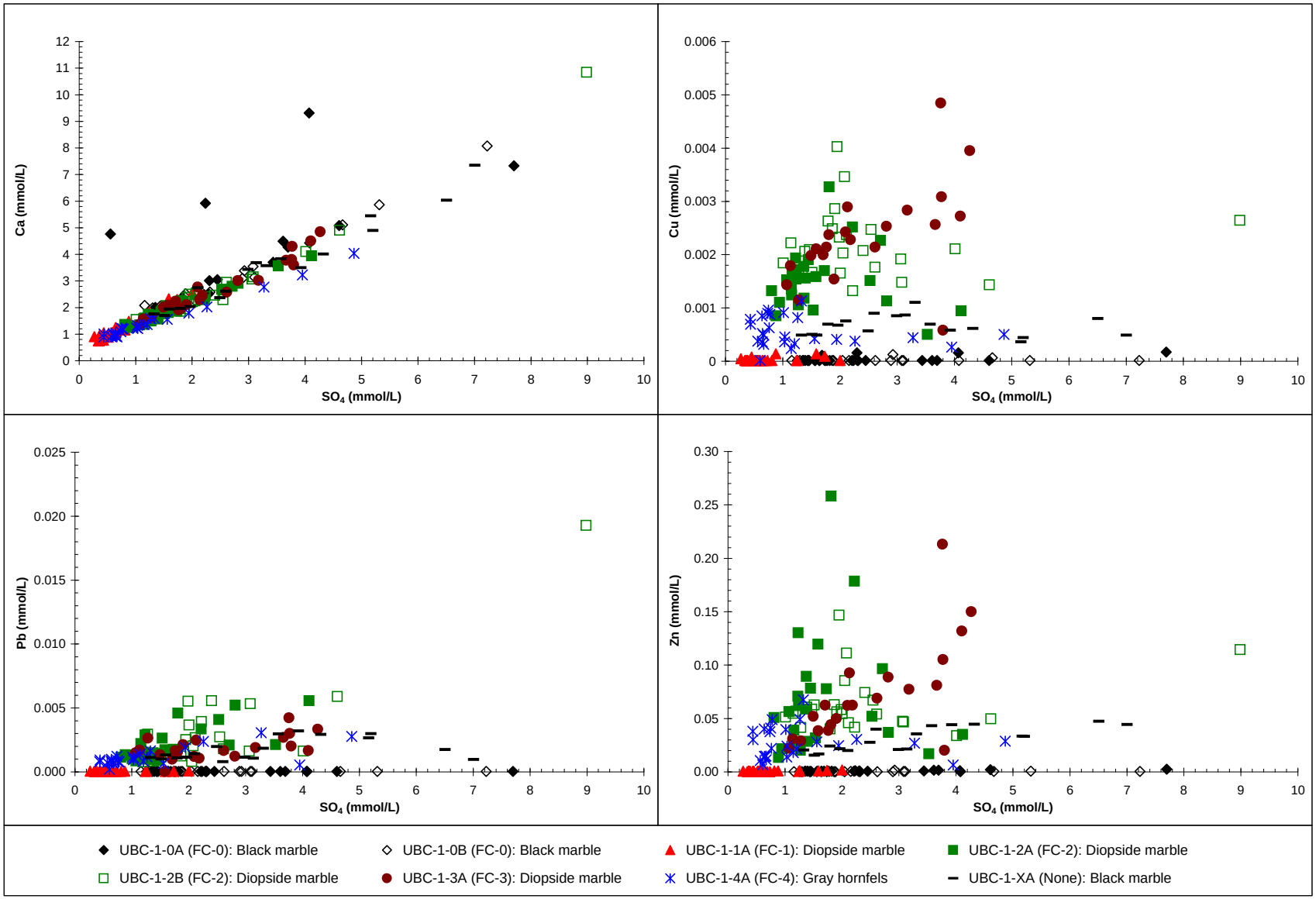

Figure E3.1 Crossing plots of Ca, Cu, Pb, and Zn according to leachate sulphate concentration from the field cells containing Class B waste rock

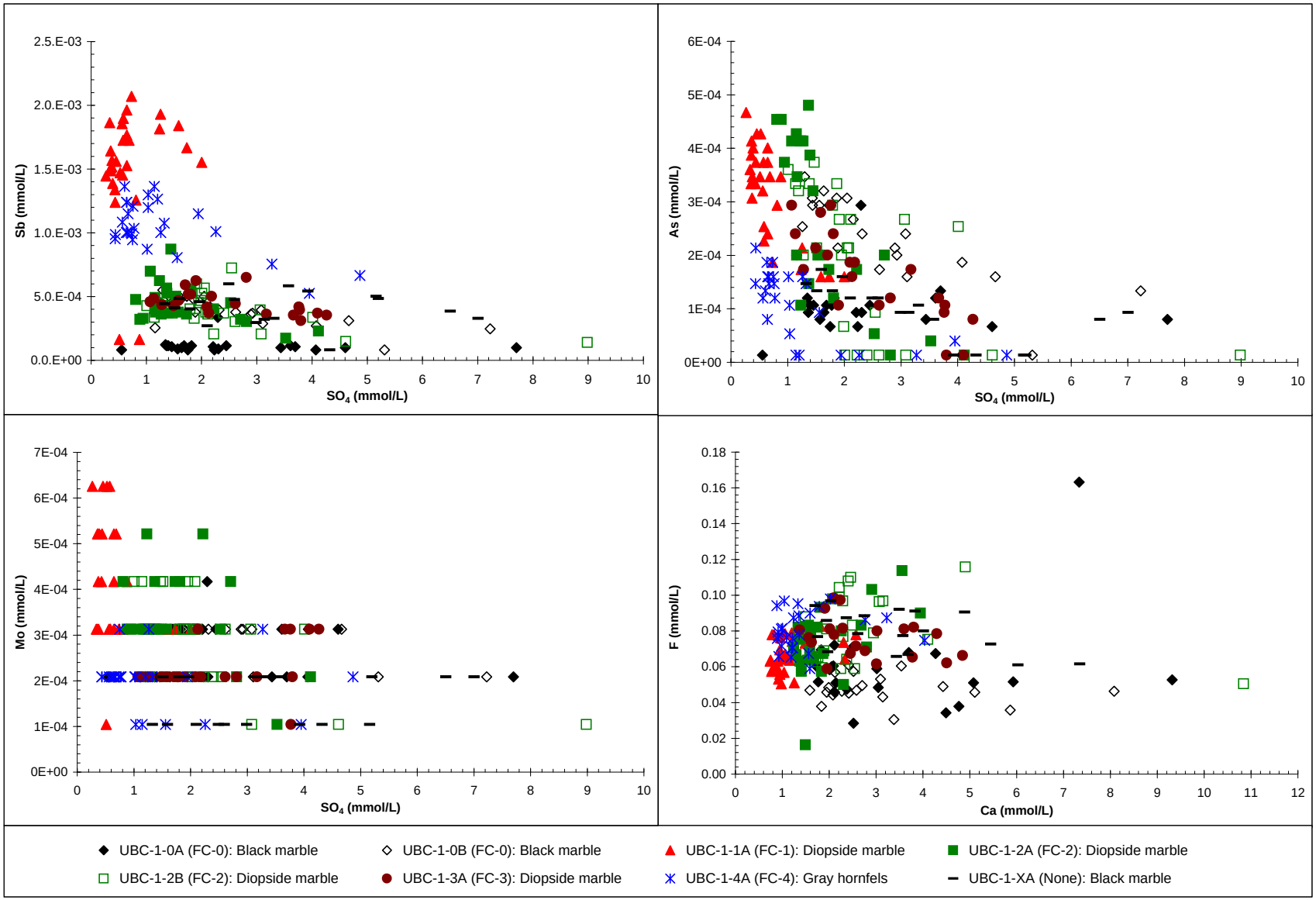

Figure E3.2 Crossing plots of Sb, As and Mo according to leachate sulphate concentration and F-Ca from the field cells containing Class B waste rock

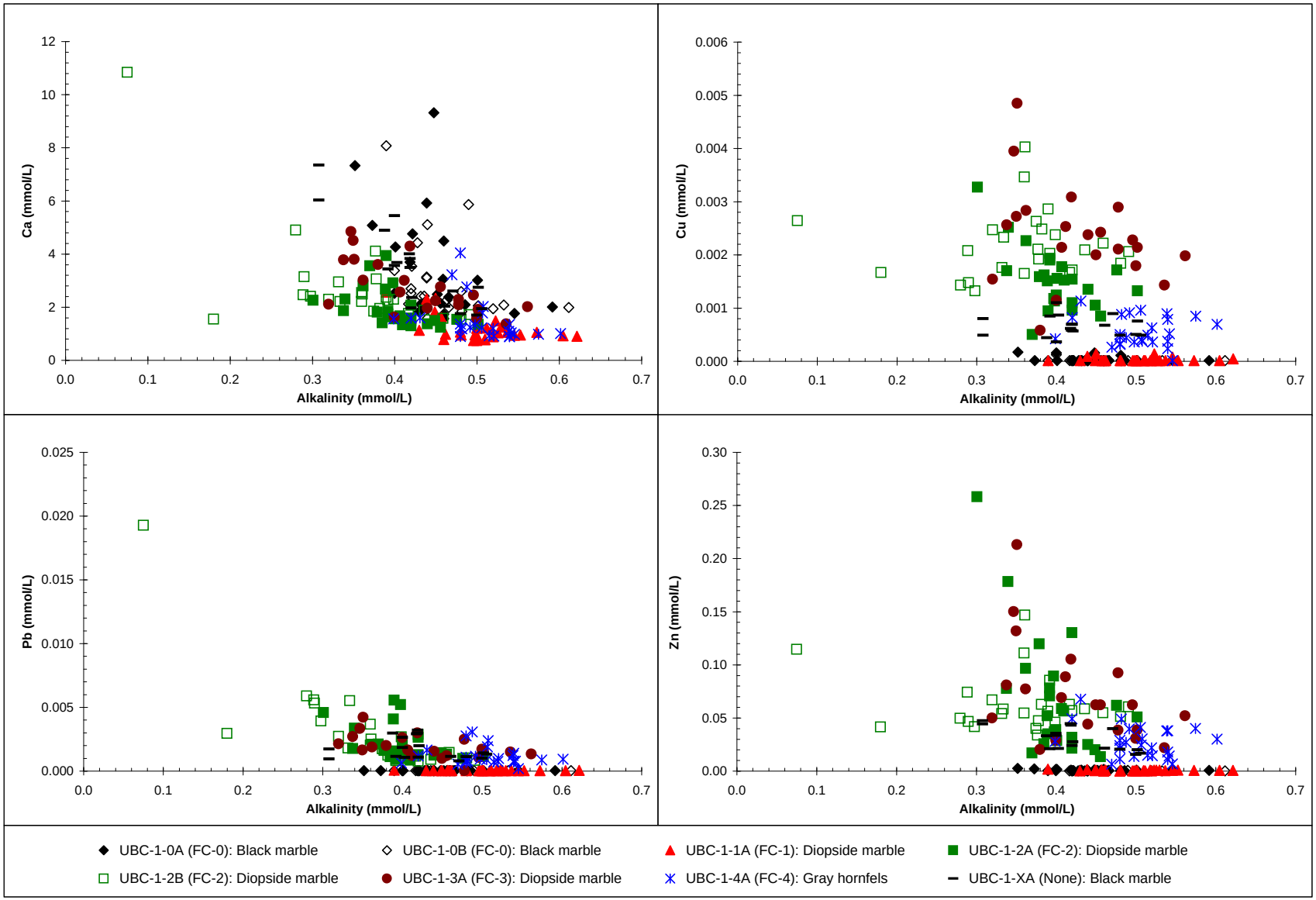

Figure E3.3 Crossing plots of Ca, Cu, Pb, and Zn according to alkalinity in the leachate from the field cells containing Class B waste rock

Appendix E4

pH Dependence

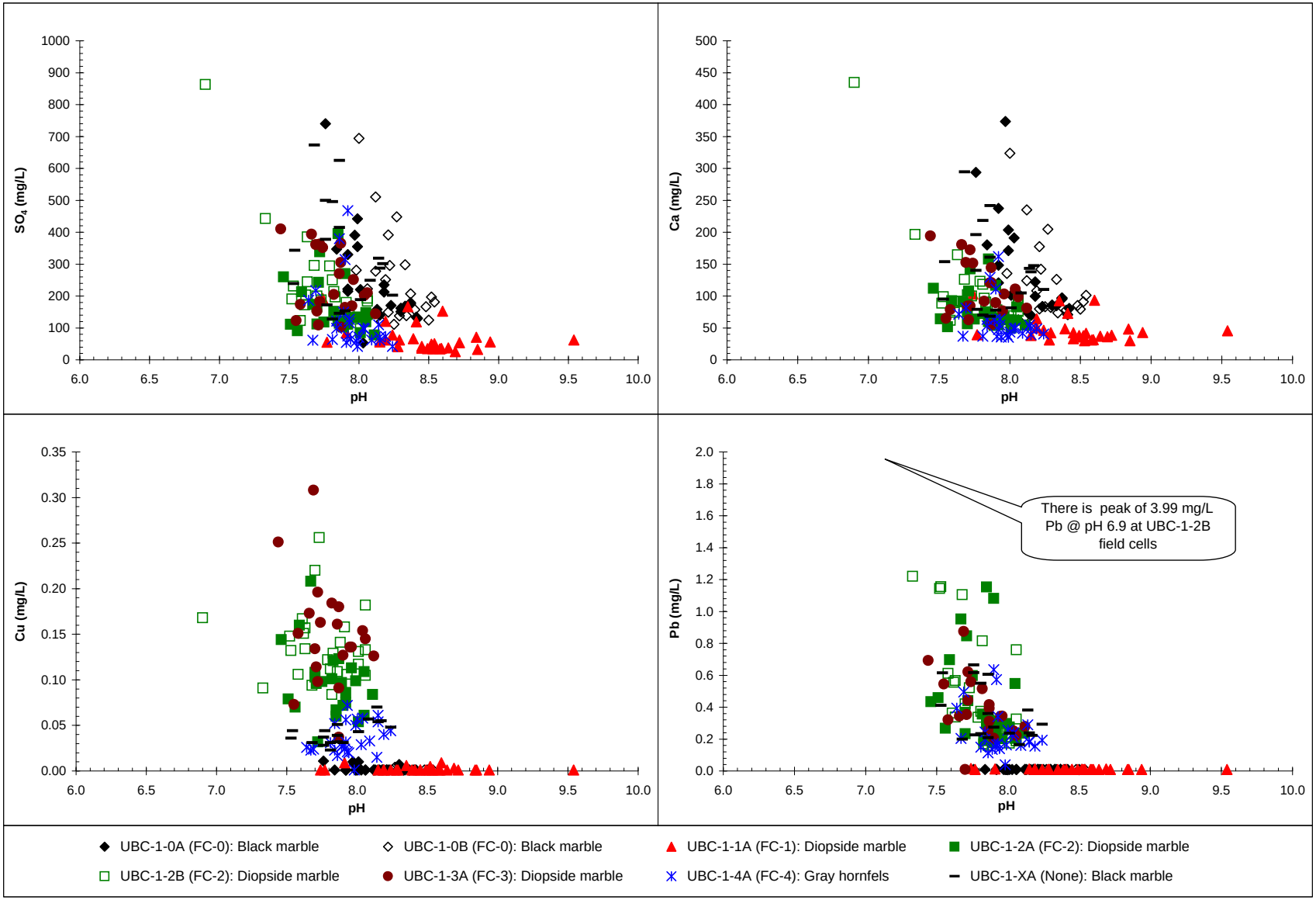

Figure E4.1 pH dependence of SO_4, Ca, Cu and Pb concentrations in the leachate from the field cells containing Class B waste rock

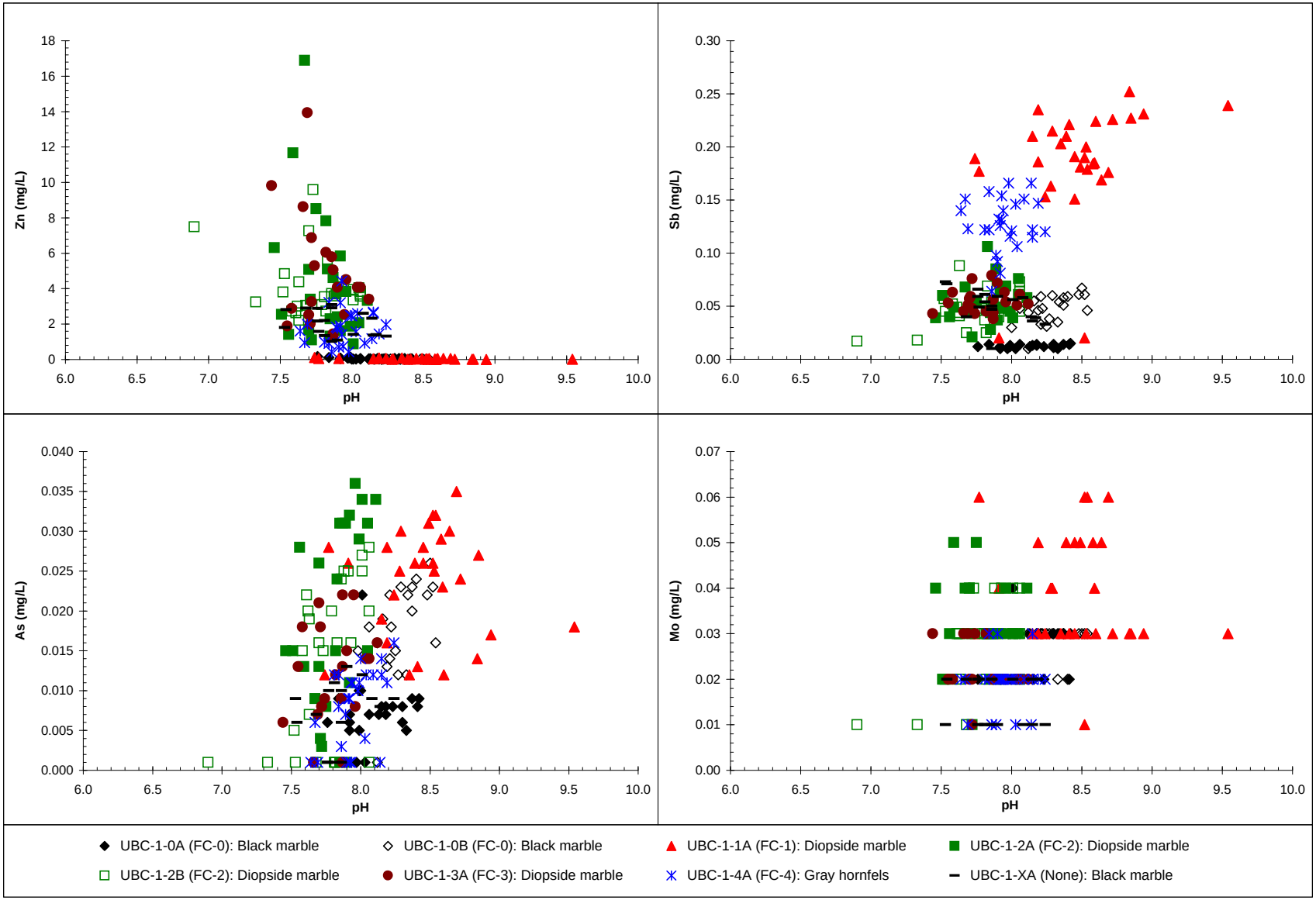

Figure E4.2 pH dependence of Zn, Sb, As, and Mo concentrations in the leachate from the field cells containing Class B waste rock